THE ANALYSIS OF EMBANKMENT DAMS BY NONLINEAR FINITE ELEMENT METHOD

by

MAMDOUH MOUSTAFA ABDEL FATTAH HAMZA

B.Sc.(Cairo), M.Sc.(London), D.I.C.,

M.Sc.(Wales), F.G.S.

A Thesis submitted to the

University of London

for the degree of

Doctor of Philosophy in the Faculty of Engineering

Department of Civil Engineering

Imperial College of Science and Technology

May 1976

ABSTRACT

This thesis examines the undrained behaviour of embankment dams and their foundations, during and immediately after construction, using finite element analysis predictions and field observations.

Techniques for the solution of nonlinear simultaneous equations are examined and compared. A new numerical technique has been developed and is used for the research in order to allow the inclusion of nonlinearities for the soil model. Provision is also made for the addition of further complexities. The stability of the technique at failure loads was proved to be satisfactory. The real soil behaviour under different loading conditions is briefly reviewed in the light of existing mathematical constitutive laws. An arithmetic model utilising the isotropic elastic equations for relating stress and strain increments, was employed.

Empingham trial bank and main embankment were analysed and they were also used exclusively as vehicles for developing the techniques. A back analysis was used to estimate the in-situ stress-strain and strength characteristics and initial stresses from trial bank field observations. A systematic back analysis technique was developed from this, which emphasised the need for direct field measurement of strains.

The back figured soil properties were then used to predict the main dam behaviour, thus bypassing the need for laboratory testing. This exercise uncovered a special

difficulty due to the important effect of undrained shear strength discontinuities at low factors of safety .

During the examination of the finite element results, some general aspects of the behaviour of embankment dams were studied, especially with regard to the simulations of construction sequence. The manner in which finite element could be employed to improve embankment dam engineering is discussed. Finally, a parametric study was made to examine the effect of the different variables involved.

INDEX

		Page
	Abstract	i
	Index	iii
Chapter 1	The Finite Element Methods	
1.1	The Stress Analysis of a Continuum	1
1.2	Outline of the Finite Element Method	3
1.3	The Displacement Formulation of the Method	6
1.4	The Overall Structural Stiffness Matrix Equation	10
1.5	Interpolation Formulae and Shape Functions	12
1.6	Isoparametric Elements and Numerical Integration	15
Chapter 2	Non-linear Solution Techniques	
2.1	Introduction	19
2.2	Step and Iterative Techniques	21
2.2.1	Approximate Step Techniques	23
2.2.1.1	The Quasi Runge-Kutta One-Step Technique	26
2.2.2	Iteration Techniques Using the Residual Force Concept.	30
2.2.2.1	Newton-Raphson Method	34
2.2.2.2	Constant Stiffness Method	37
2.3	Acceleration techniques	39
2.3.1	Alpha-Constant Stiffness Matrix	40

		Page
2.3.1.1	The Structure of Alpha Iterative Process	41
2.3.1.2	Summary of Simplified Algorithm Comparison with Nayak's	45
2.3.2	Comparison between Alpha-Constant Stiffness Matrix and Conjugate-Newton Techniques	46
2.4	Discussion and Conclusions	49
Chapter 3	The Representation of Soil Properties for Static Non-Time-Dependent Stress-Strain Solutions	
3.1	General	51
3.2	Discussion on the Isotropic Elastic Model	54
3.3	Review of the Models Using Isotropic Elasticity	65
3.4	Concepts in Plasticity	79
3.5	Review of the Development of Plasticity Models as Applied to Soil Mechanics Solutions	83
3.6	The Stress-Strain Model Used in this Work	93
Chapter 4	Programmes	
4.1	General	100
4.2	Programmes SAN2 and SAN3	101

			Page
	4.2.1	General Descriptions	101
	4.2.2	Input of Geometry	104
	4.2.3	Input of Material Properties	105
	4.2.4	Input of Initial Stresses	108
	4.2.5	Dealing with the Construction Sequence	110
	4.2.6	Non-linear Programme - SAN2	112
	4.2.7	Non-linear Programme - SAN3	114
	4.2.8	Shear Unloading	116
	4.2.9	Poisson's Ratio ν Varying With Stress	116
	4.2.10	Strain Loading	117
	4.3	The Graphics Programmes EASY and HANDY	118
Chapter 5		Stability of Non-linear Solution Techniques	120
Chapter 6		ANALYSIS OF EMPINGHAM TRIAL BANK	
	6.1	Introduction	124
	6.2	Purpose and Brief Description of the Trial Bank	124
	6.3	Aims of the Finite Element Analysis	128
	6.4	Schedule and Results of the Analysis	131
	6.4.1	Stage 1: Primary analyses before Completion of the Trial Bank Construction	132
	6.4.2	Stage 2: Analysis after the Construction of the Trial Bank	136

		Page
6.4.2.1	The Meshes	136
6.4.2.2	The Initial Stresses	137
6.4.2.3	Summary and Aims of Stage 2 Analyses	138
6.4.2.4	Material Properties for Stage 2	139
6.4.2.5	Findings of Stage 2 Analyses	140
6.4.3	Stage 3: Final Non-linear Analyses	143
6.4.3.1	Field Performance	145
6.4.3.2	Preliminary Non-linear Solutions: Cases 2a, 2c, 2d.	145
6.4.3.3	Effect of Strength: Cases 3a, 3b	146
6.4.3.4	Effect of Fill Non-linearity: Case 3c	148
6.4.3.5	Effect of K_o: Cases 3d, 3e.	149
6.4.3.6	Effect of the Swelling of the Toe: Case 3f	150
6.4.3.7	Interim Conclusions	151
6.4.4	Systematic Back Analysis	151
6.4.4.1	The Use of Systematic Back Analysis for the Trial Bank - Case 4A	154
6.4.5	Modelling of Shear Unloading: Case 4au	156
6.4.6	Shear Strength Parameters in Terms of Effective Stress	157
6.4.7	Inspection of Stresses	158
6.4.8	Vertical Settlements of Fill and Foundation	159
6.4.9	Comparison of the Deduced Stress-Strain Curves with those from Laboratory Triaxial Tests	160
6.5	Conclusion	161

		Page
Chapter 7	Analysis and Prediction of Empingham Main Dam Behaviour	163
7.1	Introduction	163
7.2	Analyses Before Completion of Construction, Taken from the Original Report	165
7.2.1	Soil and Structural Model	165
7.2.2	Soil Properties Used in the Solutions	166
7.2.2.1	Undrained, Saturated Clays in the Foundation	166
7.2.2.2	Undrained, Unsaturated Clays as Fill	167
7.2.2.3	Partly Drained, Saturated Clays in the Sand Drain Zone	168
7.2.3	Solutions Obtained	171
7.2.4	Discussion of the Results	172
7.2.4.1	Main Section	172
7.2.4.2	North Section	174
7.2.4.3	General Pattern of Movements	178
7.2.4.4	Possible Errors in the Solutions	179
7.2.4.5	Summary	183
7.3	Comparison with Field Observation	184
7.4	Analyses After the Completion of the Trial Bank Back Analysis	188
7.4.1	Solutions Obtained	188
7.4.2	Comparison With Field Observation	189
7.5	General Conclusion	190

		Page
Chapter 8	Final Review of Engineering Analysis of Embankment Dams	
8.1	Introduction	193
8.2	The Design Criteria and Procedure	195
8.3	The Advantages and Role of the Finite Element Method in Design	199
8.4	Partial Analyses	202
8.5	Analysis of Construction Phase	203
8.5.1	Layered Analysis	205
8.5.2	Three-dimensional Effects	221
8.5.3	Soil Non-linearity	224
8.5.4	Progressive Failure	227
8.5.5	Anisotropy	229
8.5.6	Stress Path	230
8.6	Local Failure and Strength Discontinuities	239
References	.....	241
Appendix	.....	259
Acknowledgements	.....	

CHAPTER 1

THE FINITE ELEMENT METHODS

1.1. The Stress Analysis of a Continuum

The aim in performing an engineering stress analysis of a real continuous structure is to study the response of that structure to a given set of loading conditions. From this response, the following information may be obtained:-

i) the mechanism of behaviour,

ii) the magnitude and direction (where applicable) of displacements, stresses and/or pore water pressures (directly or inferred) at selected points,

iii) the stability (or the margin of safety) of the structure. This is an active current area of of research. To date (1975), there is no reliable method of defining the stability of a continuum using stress-strain analysis only.

Such solutions involve a knowledge of the following:

i) the loads applied to the structure,

ii) the relevant material properties,

iii) the geometry and appropriate boundary conditions.

There are two well-tried methods for solving a continuum. Firstly there is a model analysis, which involves the application of scaled values of the real applied loads to a model exhibiting all the features of the prototype structure. The response of the model is measured and used to interpret or predict the behaviour of the prototype. For this method a detailed knowledge of the material properties is not always necessary.

The second method is the direct solution of the structure's governing equations. The closed form solution of these equations is only possible for a limited number of simple problems. However, numerical techniques enable the governing equations of a complex problem to be approximated by a system comprising a finite number of variables, whose solution provides an approximation to the true solution of the problem.

Finite difference methods provided the solutions to some problems slightly more complex than those which could be solved in closed form (Bishop 1952), but even for these approximate methods solution time was prohibitive for all but the simplest cases until the advent of the digital computer. The arrival of these machines heralded a great advance in the solution of continuous structures by numerical methods; complex geometries and material behaviour can now be accommodated in such solutions with relative ease.

Problems involving elasticity are governed by linear differential equations, Washizu(1968). More complex material behaviour can often be approximated by a sequence of elastic response increments.

The finite element method (FEM) is a particular numerical technique which can be used to approximate linear differential equations by a system of simultaneous equations (Zienkiewicz, 1971). This approximation is the most important and revealing feature of the method. Use of FEM

in this way, and also in conjunction with incremental procedures of the type just mentioned, can provide approximate solutions to a wide variety of real problems.

The FEM is well suited for use on a digital computer once it is programmed for a particular type of material stress-strain law: Compact input data can produce quick and economic analyses to a variety of problems involving that law.

1.2 Outline of the Finite Element Method

A qualitative outline of the use of the FEM for continuum stress analysis is given in this section. Although the FEM can be explained in terms of mathematical processes (i.e. using variational principles) the application of these to stress analysis has a physical significance which can make their understanding easier; therefore a physical rather than a mathematical explanation is given.

In the closed form solution of stress analysis problems three conditions should be satisfied throughout the structure, Timoshenko and Goodier (1951). These conditions are (i) equilibrium of forces, (ii) compatibility of displacements, and (iii) the material stress-strain laws. In the FEM a structure is approximated by an assemblage of elements of the structure, interconnected at a finite number of joints or nodal points replacing infinite numbers of the element boundary points. This process is called idealisation or discretisation; it involves the evaluation of the element characteristics independently from the rest of the structure

and will be discussed in detail in section 1.3. Once the element characteristics are established, the general procedures of assembly and solution will follow a pattern for which the structural analogy provides a convenient basis (see section 1.4). During the solution, the three conditions listed above are satisfied within each element and at the nodes, while in general only one of the first two conditions can be satisfied at the element interfaces depending on the approach followed, (discussed further in section 1.5). This satisfaction will allow the structure to be approximated by a finite set of primary variables inter-related by a system of simultaneous equations, These primary variables always appear in pairs and are called the nodal variables. In the case of plane stress, plane strain, axisymmetric and three dimensional stress analysis they are the corresponding nodal components of force and displacement. The greater the number of elements the greater are the number of nodes and primary variables and hence the closer is the convergence of the solution to that for a true continuum.

Once the primary variables have been evaluated the secondary variables, strains and stresses are uniquely defined within each element using the definition of strains and the material stress-strain laws.

As mentioned before, the finite element idealisation cannot in general satisfy fully both equilibrium and

compatibility at the element interfaces. The two most common idealisations satisfy either compatibility or equilibrium across each interface of a finite element.* In the present work, the formulation satisfying compatibility throughout is used, it is commonly referred to as the "displacement approach". Thus the unknown primary variables are the displacements at the nodes which are interrelated to the known nodal forces by a set of equations representing the stiffness of the structure. These equations can be obtained either by the virtual work principle or by minimising the strain energy of the finite element idealisation. The strain energy of a displacement idealisation is always less than the structure's true strain energy, Zienkiewicz, (1971), therefore a displacement formulation overestimates a structure's stiffness, and hence underestimates the displacements.

To summarise, the displacement approach of the finite element stress analysis of a continuum involves three basic steps:-

1. From the applied loads, the equivalent nodal forces are calculated $\{F\}$. These are called the known primary variables.

2. From the element characteristics, the overall structural stiffness matrix is assembled $[K]$. Inversion of the stiffness matrix solves for the displacements at the nodes $\{\delta\}$. These are called the unknown primary variables.

* Both can be satisfied in some elements.

3. From the displacements at the nodes, the strains are calculated. Using the material stress-strain laws, the stresses are also calculated, thus the secondary variables are found.

1.3 The Displacement Formulation of the Method

The individual element characteristics, namely the element stiffness matrices and the equivalent nodal force vectors, are now considered. It is important to note that the derivation is carried out independently for each element utilising the principle of virtual displacements (often referred to as the principle of virtual work). This principle does not depend on the mechanical properties of the material and is therefore valid for any state of the body such as solid, liquid, elastic or inelastic. The principle of virtual displacement states:-

"For a body in equilibrium, the sum of work, for any system of virtual displacements, of all external and internal forces acting on the body must be zero".

This means that the forces in equilibrium do not show any tendency to displace the body by doing work on it. The term virtual displacement signifies a small imaginary displacement from the position of equilibrium, which does not violate the geometrical conditions or constraints imposed on the movements or deformations of the body. Subject to the above restriction, the virtual displacements are quite arbitrary.

In the displacement approach of the FEM, the unknown primary variables are the displacements at the nodes, which constitute the element displacement vector $\{\delta\}^e$ in the form:

$$\{\delta\}^e = \begin{Bmatrix} \{\delta\}_1 \\ \vdots \\ \{\delta\}_i \\ \vdots \\ \{\delta\}_n \end{Bmatrix}$$

when n denotes the total number of the nodes around the element. The size of the vector $\{\delta\}_i$ depends on the number of degrees of freedom considered at each node. These displacements may be induced by a loading system consisting of distributed body forces $\{p\}$ (force/unit volume) and/or surface pressure $\{g\}$ (force/unit area) applied to the structure, and constrained by some boundary conditions.

The basic step of any finite element analysis is to describe uniquely the unknown function $\{f\}$, which is the displacement field in this case, within the element in terms of the value of this function at the nodes and a set of n parameters in the form:-

$$\{f\} = \sum_{i=1}^{n} (N_i [I] \{\delta\}_i) = [N] \{\delta\}^e \qquad (1.1)$$

where N_i is a scalar parameter which is a function of the position of the point considered in relation to node i, and will be discussed in detail in section 1.5. $[I]$ is an identity matrix of order equal to the number of displacement components at each node. N_i is called the shape function

of node i, and $[N]$ is the shape function matrix of the element.

With the displacements known at all points within the element, the strains at any point can be determined, resulting in a relationship of the form:-

$$\{\varepsilon\} = \sum_{i=1}^{n} ([B]_i \{\delta\}_i) = [B] \{\delta\}^e \qquad (1.2)$$

$[B]$, being generally composed of derivatives of the shape function at node i . $[B]$ is called the strain matrix of the element.

Assuming strains to be related to stresses by a modulus matrix $[D]$, containing the relevant material properties, then the stresses are uniquely defined as follows:-

$$\{\sigma\} = [D] (\{\varepsilon\} - \{\varepsilon_o\}) + \{\sigma_o\} \qquad (1.3)$$

where $\{\varepsilon_o\}$ and $\{\sigma_o\}$ denote the initial strains and initial stresses respectively.

If virtual displacements $d\{\delta\}^e$ are applied at the nodes, this will result in a system of corresponding displacement ($d\{f\}$) and strain ($d\{\varepsilon\}$) fields within each element defined as follows:-

$$d\{f\} = \sum_{i=1}^{n} [N]_i d\{\delta\}_i = [N] d\{\delta\}^e$$

$$d\{\varepsilon\} = \sum_{i=1}^{n} [B]_i d\{\delta\}_i = [B] d\{\delta\}^e$$

and the sum of the work done dW, by the stresses, distributed

body forces and distributed surface forces over the whole element Ω and its externally loaded boundary Γ will be:

$$dW = (d\{\delta\}^e)^T(\int [B]^T\{\sigma\}d\Omega - \int [N]^T\{p\}d\Omega - \int [N]^T\{g\}d\Gamma)$$

In order to put the element into equilibrium, and hence reduce the virtual work (dW) to zero, a system of nodal forces $\{F\}^e$ statically equivalent to the actual element boundary stresses and any boundary distributed forces must be added to the above equation, taking the form:-

$$(d\{\delta\}^e)^T\{F\}^e = (d\{\delta\}^e)^T(\int[B]^T\{\sigma\}d\Omega-\int[N]^T\{p\}d\Omega-\int[N]^T\{g\}d\Gamma) \quad (1.4)$$

As mentioned before, this relationship is valid for any value of virtual displacement $d\{\delta\}^e$, thus it can be eliminated from both sides of equation (1.4). Substituting Equation (1.2) and Equation (1.3) into Equation (1.4), the element characteristic equation is obtained in the form

$$\{F\}^e = (\int[B]^T[D][B]d\Omega)\{\delta\}^e - \int[B]^T[D]\{\varepsilon_o\}d\Omega + \int[B]^T\{\sigma_o\}d\Omega$$
$$- \int[N]^T\{p\}d\Omega - \int[N]^T\{g\}d\Gamma \quad (1.5)$$

Equation 1.5 is in the form FORCE=STIFFNESS x DISPLACEMENT hence by analogy:

the element stiffness matrix $[K]^e = \int[B]^T[D][B]d\Omega$

and the element equivalent nodal force vectors are:

due to distributed body force $\{F\}^e_p = - \int[N]^T\{p\}d\Omega$

due to distributed surface force $\{F\}^e_g = -\int[N]^T\{g\}d\Gamma$

due to initial stress $\{F\}^e_{\sigma_o} = \int[B]^T\{\sigma_o\}d\Omega$

due to initial strain $\{F\}^e_{\varepsilon o} = -\int[B]^T[D]\{\varepsilon_o\}d\Omega$

Thus equation 1.5 may be rewritten in the form

$$\{F\}^e = [K]^e\{\delta\}^e + \{F\}^e_p + \{F\}^e_g + \{F\}^e_{\sigma_o} + \{F\}^e_{\varepsilon_o} \qquad (1.6)$$

1.4 The Overall Structural Stiffness Matrix Equation

The overall structural stiffness matrix equation, the solution of which provides a solution to the problem, is represented in this section. The basis of the assembly of the overall stiffness matrix and the overall load vector is also given.

After evaluating the force-displacement relationship for each element in the form of equation (1.6) the problem reduces to one of a conventional structural type, which may be readily solved numerically using standard structural analysis techniques (Timoshenko and Young, 1965; Przemieniecki 1968).

Assuming a single notation to each unknown component of the displacements at each node, regardless of its connections with the neighbouring elements, results in the displacement vector for the whole structure in the form:

$$\{\delta\} = \begin{Bmatrix} \{\delta\}_1 \\ \{\delta\}_i \\ \{\delta\}_m \end{Bmatrix}$$

where m denotes the total number of nodes in the whole domain.

This assumption automatically satisfies the displacement compatibility requirements at the nodes.

Proceeding with the solution, requires the satisfaction of the equilibrium condition. Equilibrium is satisfied within the element as explained in the preceding section. The equilibrium condition for each node is established by equating the sum of the equivalent nodal force components, contributed by the elements meeting at that node, to zero. This results in an equation of the form: $\sum_{e=1}^{L} \{F_i\}^e = 0$ for node 'i', where L denotes the number of elements meeting at node i. Substituting for $\{F_i\}^e$ from equation (1,6) the equilibrium equation for node i becomes,

$$\sum_{e=1}^{L}\left\{\left\{\sum_{j=1}^{n}[K_{ij}]^e\{\delta_j\}^e\right\}+\{F_i\}_p^e+\{F_i\}_g^e+\{F_i\}_{\sigma_o}^e+\{F_i\}_{\varepsilon_o}^e\right\}=0$$

If such equations are assembled for all the nodes, the overall structural stiffness matrix equation is obtained in the form

$$[K]\{\delta\} = \{F\} \qquad (1.7)$$

in which the assembled components are

$$[K_{ij}] = \sum_{e=1}^{L}[K_{ij}]^e \qquad \text{See figure (1.1)}$$

and $$\{F_i\} = \sum_{e=1}^{L}\left\{\{F_i\}_g^e+\{F_i\}_p^e+\{F_i\}_{\sigma_o}^e+\{F_i\}_{\varepsilon_o}^e\right\}$$

It is important to note that once a coefficient of the load vector or the stiffness matrix of each element (ie K_{ij}, F_i) is evaluated it could be put immediately in its appropriate location in the storage of the computer. The inversion of

the overall stiffness matrix $[K]$ gives the solution for the unknown displacements vector:

$$\{\delta\} = [K]^{-1}\{F\}$$

It is worth mentioning here that the inversion is only possible if a minimum number of prescribed displacements, to prevent rigid body movements of the structure, are imposed on equation (1.7) otherwise the matrix is singular.

Knowing the displacement vector for each element, the strains and stresses can be calculated using equation (1.2) and equation (1.3).

1.5 Interpolation Formulae and Shape Functions

A finite element solution could be defined as one in which values inside an element are given by an interpolation formula in terms of values at the nodes on the boundary or inside the element. External nodes are not used, partly to reduce the overall stiffness matrix equations bandwidth: see figure (1.1), and partly because in a real engineering structure a sudden change in the material properties usually occurs at a material discontinuity, eg. soft clay lying on top of stiff rock. Such a problem can be handled accurately by introducing an element boundary at the discontinuity, but cannot be handled if strains in the rock depended on nodal movements in the clay (Irons 1968).

In section 1.4, the shape function N_i was defined by equation 1.1. Once these shape functions are found for

the nodes defining an element, the interpolation formula is defined, and hence all element characteristic equations and the overall stiffness matrix equations, equation (1.6) and equation (1.7), could be evaluated and assembled ready for solution. The use of interpolation formulae represents the main approximation in a finite element solution as it limits the infinite number of variables of the true domain to a finite number of nodal variables, and thus the exact solution will never be obtained irrespective of the fineness of the mesh used.* However, the interpolation formula must represent the displacement field within the element and at the sides as closely as possible in order to obtain acceptable solutions. An acceptable solution is one of a series of solutions, each better than or at least as good as the one preceeding it, corresponding to a series of finite element meshes each finer than the one preceding it using the same element type. This is called the convergence test. Convergence conditions can be achieved if the interpolation formula is chosen such that two requirements are satisfied (Bazeley et al 1965):-

1. Continuity of the displacement between adjacent elements must be preserved. This implies that the values of stresses and strains at the element sides are finite. Therefore, the interpolated value of displacement on a side depends only on the value of the displacement at the nodes on that side, and the interpolation formula on the side must be the same for both elements.

* Except in special cases.

2. Constant states of stress and strain can be exactly reproduced. This criterion stems from the fact that if the size of the element reduces to nearly a point, all values of strains inside the element will be the same. An extreme case is that the interpolation formula should produce zero strains if the nodal displacements are caused by rigid body movements.

Assuming, for simplicity, that only one variable is considered at each node, the standard procedure for developing the shape functions is as follows. A square element is used for convenience its sides extending from $\xi = -1$ to $\xi = +1$ and from $\eta = -1$ to $\eta = +1$ (see figure 1.2) where ξ and η are nondimensional curvilinear coordinates. Considering, for example, four corner and four mid-side nodes to define the element. The interpolation formula will be

$$\delta = \sum_{L=1}^{n} N_i \delta_i = N_1\delta_1 + N_2\delta_2 + N_3\delta_3 + \ldots + N_7\delta_7 + N_8\delta_8$$

This interpolation formula must give correct nodal values for all δ_i. Giving any particular δ_i a unit value, the others being zero, N_i will therefore be unity at i and zero at the other nodes. Thus considering each node separately and giving it a unit value for the unknown, the shape function N_i can be determined uniquely if the above two requirements are satisfied (C.F.page 13 and top of this page).

For the element used in all the work reported in this thesis, the 8 - noded quadratic element, Irons and Zienkiewicz (1968) and Irons (1968), the shape

functions are:

corner nodes

$$N_i = \tfrac{1}{4}\,(1+\xi_o)\,(1+\eta_o)\,(\xi_o+\eta_o-1)$$

Mid-side nodes

$$\xi_i = o \quad N_i = \tfrac{1}{2}\,(1-\xi^2)\,(1+\eta_o)$$

$$\eta_i = o \quad N_i = \tfrac{1}{2}\,(1+\xi_o)\,(1-\eta^2)$$

where

$$\xi_o = \xi\xi_i \qquad \eta_o = \eta\eta_i$$

1.6 Isoparametric Elements and Numerical Integration

The preceding section described the square or "parent" element which is the source of the nodal configuration and shape functions N_i and their derivatives, but these simple local dimensionless coordinates become generalized global coordinates in an actual finite element analysis, where the nodes can in principle be in any position, say a curved or distorted shape, to fit a real structure. Therefore a mapping procedure is needed to transform to the new coordinates, allowing for distorting the simple parent element into a more arbitrary shape.

The isoparametric element, Irons and Zienkiewicz, (1968), is a mapped element from a parent one where the global coordinates of any point (x,y) within it are defined by the shape functions N_i which are used also to describe the displacement.

In the two dimensional case the mapping relation is:

$$X = \Sigma N_i X_i$$
$$Y = \Sigma N_i Y_i \qquad (1.8)$$

where (X_i, Y_i) are the global coordinatesof the node i. Equation (1.8) represents a unique relationship between each computation of local coordinates (ξ, η) and its corresponding global coordinate (X,Y), provided that the distortion does not exceed certain limits (Zienkiewicz 1971). If conditions of convergence are satisfied in the parent element, then these conditions are also satisfied in the isoparametric distorted element, Irons (1968).

To establish the element characteristic equations, which include N_i and its derivatives in the global coordinates, two transformations are required; transformation of derivatives and of integration from local to global coordinates. Using rules of partial differentiation, the derivatives in the global coordinates could be defined in terms of derivatives in the local one as follows:

$$\begin{Bmatrix} \frac{\partial N_i}{\partial x} \\ \frac{\partial N_i}{\partial y} \end{Bmatrix} = [J]^{-1} \begin{Bmatrix} \frac{\partial N_i}{\partial \xi} \\ \frac{\partial N_i}{\partial \eta} \end{Bmatrix}, \quad [J] = \begin{bmatrix} \frac{\partial x}{\partial \xi} & \frac{\partial y}{\partial \xi} \\ \frac{\partial x}{\partial \eta} & \frac{\partial y}{\partial \eta} \end{bmatrix}$$

The matrix $[J]$ is called the Jacobian matrix, whose conditions of inversion limit the distortion of the element, (ie $[J]$ must not be singular). To carry out the integration of the element matrices in the local coordinates, thus

keeping simple integration limits, transformation is introduced to the element volume, (see Murnaghan (1951)), as follows:

$$dx\ dy = [J]\, d\xi d\eta$$

and thus, the element stiffness matrix in two dimensions becomes

$$[K]^e = \int\int [B]^T[D][B]\, dxdy = \int_{-1}^{1}\int_{-1}^{1} [B]^T[D][B][J]\, d\xi d\eta$$

In calculating the above integration and the other stiffness equations described in section 1.4 for isoparametric elements many items must be integrated over a domain which may have a curved boundary. Many difficulties arise; not only are the analytic integrals very complicated, but also in certain cases they are ill-conditioned. Taig (1961) has introduced numerical integration for a particular element and Irons (1963) has used it as deliberate policy as a means by which more complicated problems and elements can be implemented.

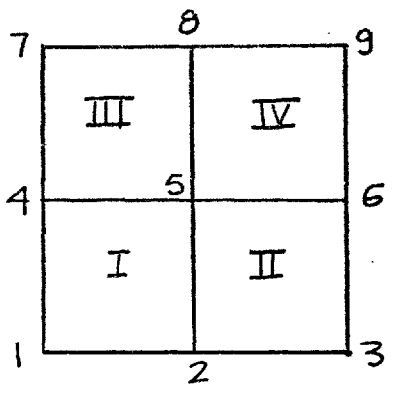
For Gauss quadrature, n sampling integrating points are sufficient to integrate a polynomial of degree (2n-1) exactly. For example if the shape functions are quadratic in x and y, the polynomial of the stiffness matrix will be quartic and 3 Gauss points are needed to integrate $[K]^e$ correctly. But in some cases in which the element type used in this report is one, it was found, (Nayak (1971) and Naylor (1974)), that it is possible to improve the performance

by using a reduced integration rule, say 2 instead of 3 Gauss points. This paradoxical result seems to arrive from neglecting certain badly behaved terms, but no mathematical proof is yet known. Tables with the position of points and weighting coefficients are given in Zienkiewicz (1971).

The isoparametric element combined with numerical integration provides many advantages:-

1. less time is needed for preparing data input.
2. Boundaries can be mapped more accurately and fewer elements are needed to give the required accuracy (Pugh 1976).
3. In nonlinear analysis, it allows the failure zone to spread more smoothly within the element.
4. The stresses at the Gauss points are reliable and there is no need to use approximate averages, which is common practice with simple triangular elements.

Finite element idealization:-



Stiffness matrix of elements I, II, III, IV is:-

$$[K]=\begin{bmatrix} 2 & 0 & -1 & -1 \\ 0 & 2 & -1 & -1 \\ -1 & -1 & 2 & 0 \\ -1 & -1 & 0 & 2 \end{bmatrix}$$

The over-all Stiffness matrix, obtained by adding the contribution of each element at every node, and assuming one degree of freedom per node, is :-

Nodal number →

↓	1	2	3	4	5	6	7	8	9	
1	2	0		-1	-1					I
2	0	4	0	-1	-2	-1				I II
3		0	2		-1	-1				II
4	-1	-1		4	0		-1	-1		I III
5	-1	-2	-1	0	8	0	-1	-2	-1	I II III IV
6		-1	-1		0	4		-1	-1	II IV
7				-1	-1		2	0		III
8				-1	-2	-1	0	4	0	III IV
9					-1	-1		0	2	IV
	I	I II	II	I III	I II III IV	II IV	III	III IV	IV	

Element's Contributions

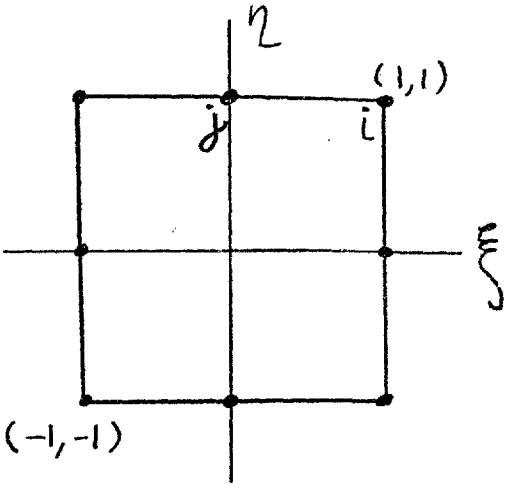
Example:-

Element III contributes to nodes 4, 5, 7 + 8

THE PRINCIPLES OF FINITE ELEMENT ASSEMBLY

Fig. 1.1

The 'parent' square element in the normalized coordinate system (from -1 to +1) with 8 nodes :-



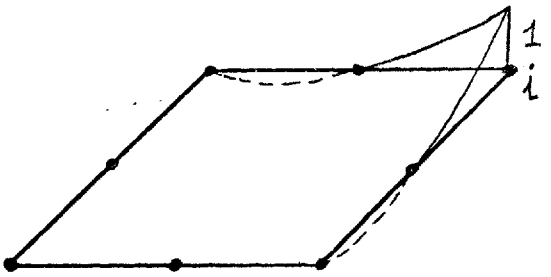
"The Shape Function for any node around the boundary of the element is the equation of the surface passing through a value of 1 at that node and values of zero at the other nodes"

Examples

- Node i :

  Shape Function $N_i =$

  $$\frac{1}{4}(\xi+1)(\eta+1)$$



- Node j :

  Shape Function $N_j =$

  $$\frac{1}{2}(1-\xi^2)(1+\eta)$$

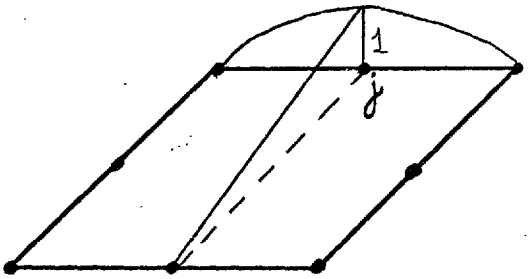


ILLUSTRATION OF THE MEANING AND CALCULATION OF ELEMENT SHAPE FUNCTION

Fig. 1.2

CHAPTER 2

NON-LINEAR SOLUTION TECHNIQUES

2.1 Introduction

In Chapter 1, the displacement approach of finite element formulation yielded the general finite element stiffness equation in the form of a load-displacement relationship as follows:

$$[K]\{\delta\} = \{F\}$$

which represents a system of simultaneous equation, and its solution is the final and most important stage of the analysis. The size of the equation depends on the problem and can in some cases be as large as 10,000 unknowns, thus an economic and reliable algorithm is needed.

As mentioned before, the sub-matrix of $[K]$ is:

$$[K]^e = \int [B]^T [D][B]\, d\Omega$$

which is a function of geometry $[B]$ and material properties $[D]$. If the evaluation of both the strain matrix $[B]$ and modulus matrix $[D]$ is independent of the primary variables $\{\delta\}$ or the secondary variables $\{\sigma\}$ and $\{\varepsilon\}$, the system is a linear one which can be solved using one of the well-tried methods of solution. Recently, it has been shown that no method exists which requires fewer arithmetical operations than the direct Gauss elimination method, Klyuyev, Kokovkin - Sherbak (1965), which has thus become the standard method for finite element linear solutions (Irons 1970, 1971, Rashid 1970, Melosh and Bamford 1969).

Non-linearity appears when either $[B]$ or $[D]$ is dependent (directly or indirectly), on the displacement vector $\{\delta\}$. The work described in this thesis is based on the assumption that displacements are sufficiently small for the problem geometry to be unchanged and that the theory of infinitesimal strains is valid. Thus the matrix $[B]$ is evaluated directly, and nonlinearity is only due to material properties being dependent on the unknown required results. Assuming that stress-strain relationship is written in the nonlinear form:

$$\Delta\{\sigma\} = [D_t(\{\sigma\})] \cdot \Delta\{\varepsilon\} \tag{2.1}$$

where $[D_t(\{\sigma\})] \equiv [D_t]$ is a function of $\{\sigma\}$. This notation will appear frequently in the text. The overall structural stiffness equation may be written in one of the forms:

$$[K(\{\delta\})]\{\delta\} = \{f(\{\delta\})\} = \{F\} \tag{2.2a}$$

$$\text{or } \{R(\{\delta\})\} = \{F\} - \{f(\{\delta\})\} = o \tag{2.2b}$$

or in more general form:

$$f_r(\delta_i) = o \qquad (r,i = 1,\cdots,m) \tag{2.2c}$$

where m denotes the total number of degrees of freedom.

The solution of simultaneous nonlinear equations of the above form is usually a very difficult problem and no very satisfactory methods of functional iteration (which can proved by mathematics only) are known for this problem (Ralston 1965, Broyden 1965).

One important factor (which is stated in much of the literature on the subject, Traub, 1964) is that a good initial estimate is necessary for the success of any iteration method. In a stress analysis of a continuum an initial value of the unknown can be estimated by using a stiffness matrix corresponding to the tangential (or secant) properties of the material at the start of the load increment. However, from the author's experience, this could be dangerous where an increase of external loading requires an increase in stiffness to model non-linear behaviour. Such a situation arises when the increase in load causes a decrease in shear strain and stress in part of the domain.

In this chapter, the most common finite element nonlinear algorithm, the tangential stiffness method, is described. A new method developed during the course of the work is also given; finally a quantitative assessment of some acceleration techniques is made and the best is compared with the present form of the Conjugate-Newton method proposed by Irons (1973). The Alpha-Constant stiffness matrix, Nayak (1971) and Nayak and Zienkiewicz (1972), has proved to be the best acceleration technique, one reason being that it uses only one stiffness matrix during iteration.

2.2 Step and iterative techniques

The methods described in numerical analysis text

books, Householder (1953), Traub (1964), Ostrowski (1966), Wendroff (1966), Saaty and Bram (1964), and some recent papers, Broydon (1969), on the subject of non-linear simultaneous equations are not sufficient for the non-linear finite element analysis for two main reasons:

a. The methods presented are generally not suited for economic computer solution of a large non-linear system.

b. The methods are only tested for very small problems and in non-linear work, a generalisation for larger problems is not always possible.

The advantages of using numerical integration to calculate the residual error after each iteration, and of being able to understand the physical meaning of the different variables and related parameters in equation (2.2) and the symmetric banded nature of the matrix means that the non-linear finite element algorithms take a different form from those of a pure mathematical approach. The available techniques used in solving real non-linear problems can be classified in two main categories:

i. Approximate step techniques

ii. Iteration techniques using the residual force concept.

The basis for classification is that the first category does not give a measure of convergence or of error (it can be inspected manually after the solution as will be shown later), while the second category does give a measure

of convergence. In this section the two categories will be described in general terms as applied to a material governed by a law similar to equation (2.1).

2.2.1. Approximate step techniques

The result after a pre-stated number of steps is considered as a solution for the non-linear problem, i.e. the number of steps are not determined during the marching of the solution as in the iteration methods. Thus the stresses and strains of the solution are not compatible with the nominated stress-strain law, although they can be a good approximation, bearing in mind the uncertainties involved in the selection of basic material parameters defined by equation (2.1).

The most commonly used algorithm of this technique is the tangential stiffness method, usually referred to in soil mechanics literature as the incremental method. Its mathematical basis is the first order Euler-Cauchy step-by-step method, which can be explained geometrically for a single equation, see figure (2.1), as an approximation of the curve by part of a polygon whose first side is tangential to the curve at the initial point and so on. Although the Euler-Cauchy method is used for solving differential equations, Henrici (1962) and Davidenko (1953a, 1953b) converted the problem of simultaneous non-linear equations into a solution of differential equations and Kizner (1964) has used the idea of conversion to give a general method of solution.

The general solution equation for a step J is:

$$\{\delta\}_J = \{\delta\}_{J-1} + \left[K(\{\delta\}_{J-1})\right]^{-1} \cdot \Delta\{F\}_J$$

The Solution Algorithm of the tangential stiffness method for a load vector $\{F\}$ is marched as follows, figure (2.1):

1. Divide the load vector $\{F\}$ into S-steps of loading. (The division could be either equal or unequal steps).

$$F = \sum_{J=1}^{S} \Delta\{F\}_J \qquad S = \text{number of steps.}$$

2. Calculate the tangential matrix $[D_t]$ corresponding to the state of stress at the start of the step:

$$\left[D_t(\{\delta_o\})\right] = \phi\left[E_t(\{\delta_o\}), \nu_t(\{\delta_o\})\right]$$

3. Evaluate the overall stiffness matrix

$$\left[K_t(D_t(\{\delta_o\}))\right]$$

4. Solve to obtain the displacement corresponding to step load $\Delta\{F\}_1$

$$\Delta\{\delta\}_1 = \left[K_t(D_t(\{\delta_o\}))\right]^{-1} \cdot \Delta\{F\}_1$$

5. Compute the strains and stresses corresponding to step displacement $\Delta\{\delta\}_1$:

$$\Delta\{\varepsilon\}_1 = [B] \cdot \Delta\{\delta\}_1$$

$$\Delta\{\sigma\}_1 = \left[D_t(\{\delta_o\})\right] \cdot \Delta\{\varepsilon\}_1$$

6. Accumulate the results to obtain the solution for the first step, which is going to be used to evaluate the properties in the next step

$$\{\delta\}_1 = \{\delta_o\} + \Delta\{\delta\}_1$$

$$\{\varepsilon\}_1 = \{\varepsilon_o\} + \Delta\{\varepsilon\}_1$$

$$\{\sigma\}_1 = \{\sigma_o\} + \Delta\{\sigma\}_1$$

Repeat from 2 to 6 for each step to obtain the final response of the domain to the load vector.

The greater the number of steps, the closer is the approximation to the nominated stress-strain curve at the expense of more computer time. It is worth mentioning that the process is attractive to the soils engineer simulating sequential construction process (e.g. earth/rockfill dam/ embankment and excavation construction) as each step can represent a particular stage of construction. Two steps can also be used for one stage in case of severe non-linearity (i.e. near failure). Early in the application of this method to soil mechanics problems, the material properties for each step were calculated manually from the stresses and strains generated by the previous step. Nowadays the algorithm described above is repeated automatically in the computer once the number of steps have been specified in the input data.

The majority of non-linear finite element analyses in the field of soil mechanics have used this technique. Unfortunately only one documented case showing how well the method succeeded in reproducing the nominated stress-strain curve is available, Al-Hussaini (1972). In figure 13 of this paper, the technique followed the curve very closely using 27 steps, which is very time-consuming. Over-shooting above the failure surface is expected with this technique since the check on stress level is carried out at the start of the step; over-shooting was reported by Dunlop and Duncan (1970) to be of the order of 10% which again could be reduced by using smaller steps near the failure state of stress. Once a point of the domain is above the failure stress a very small value is assigned to the deformation parameter (e.g. E nearly zero). Strain-softening can not be modelled using this technique because the overall stiffness matrix may tend to be non-positive definite.

2.2.1.1. The Quasi Runge-Kutta one-step technique

The second of this category, the Quasi Runge-Kutta one-step technique was developed and implemented in a version of the program FESS (Finite Element System Swansea) by the author (1972). This technique is also used for the majority of applications during the course of research in embankment dams.

In this technique the load vector $\{F\}$ is applied directly in one step and the marching of the solution, which

is described below, is performed. This technique has the same general limitation as the other method with regard to post-peak modelling and stress-strain compatibility with the material law. Two main advantages gained from using this technique are:-

a. The size of the step does not influence the results greatly because the non-linearity is dealt with during the step, thus closer reproduction of the nominated stress-strain curve is achieved for the same computer time.

b. To avoid serious 'overshooting' the risk of local failure during any loading step is examined by an iterative technique, as described in Chapter 4 subsequently.

The technique is an approximation to the fourth order Runge-Kutte method which uses for each step four auxiliary quantities to arrive at the solution. In this approximation one auxiliary vector $\Delta\{\overset{*}{\delta}\}$ is used instead of four. It has a simple geometrical interpretation; for a single equation, see figure (2.2), the curve is approximated by a straight line whose slope corresponds to the tangent of the curve at some intermediate point between the starting point and the final solution. The position of the intermediate point is arrived at by an iterative process to avoid over-shooting. The general solution equation for a vector case is

$$\{\delta\} = \{\delta_o\} + \left[K(\{\delta_o\} + \Delta\{\overset{*}{\delta}\})\right]^{-1} \{F\}$$

where the auxiliary vector is

$$\Delta\{\overset{*}{\delta}\} = \lceil\gamma_1\rfloor \left[K(\{\delta_o\})\right]^{-1} \cdot \{F\}$$

The components of the diagonal matrix $\lceil\gamma_1\rfloor$ are a function of stress level and could also be a function of the non-linearity of the stress-strain curve; they are evaluated using the stress vectors at the Gauss points. $\lceil\gamma_1\rfloor$ need not have space in the core or be stored as it is evaluated inside the Gauss-loop for each point independently. At present the only criterion for evaluating $\lceil\gamma_1\rfloor$ is the position with respect to the failure stress and its components lie between 0.5 and zero. The choice of 0.5 as a limit is arbitrary; the limit should be selected to suit the rate of change of the curvature of the stress-strain curve.

The solution algorithm of the Quasi Runge-Kutta method is as follows:-

1. Calculate the tangential modulus $[D_t]$ corresponding to the state of stress at the start of the step (if the point is at or exceeding failure, then E_t is assigned a value close to zero):

$$\left[D_t(\{\delta_o\})\right] = \phi\left[E_t(\{\sigma_o\}), \nu_t(\{\sigma_o\})\right]$$

2. Evaluate the overall stiffness matrix

$$\left[K_t(D_t(\{\delta_o\}))\right]$$

3. Initialise the diagonal matrix $\lceil \gamma_{11} = 0.5$

4. Solve to obtain the first trial of the auxiliary vector:

$$\Delta\{\overset{*}{\delta}\} = \lceil \gamma_{1} \rfloor \left[K_t(D_t(\{\delta_o\})) \right]^{-1} \cdot \{F\}$$

5. Calculate the stresses and strains corresponding to the auxiliary displacement vector

$$\Delta\{\overset{*}{\varepsilon}\} = [B]\ \Delta\{\overset{*}{\delta}\}$$

$$\Delta\{\overset{*}{\sigma}\} = \left[D_t(\{\sigma_o\}) \right] \cdot \Delta\{\overset{*}{\varepsilon}\}$$

6. Accumulate the stresses and strains to those at the start of the step, while retaining the initial values

$$\{\overset{*}{\varepsilon}\} = \{\varepsilon_o\} + \Delta\{\overset{*}{\varepsilon}\}$$

$$\{\overset{*}{\sigma}\} = \{\sigma_o\} + \Delta\{\overset{*}{\sigma}\}$$

7. Check the position of $\{\overset{*}{\sigma}\}$ with respect to the failure criteria.
If $\{\overset{*}{\sigma}\}$ is above failure criteria, modify the local factor γ_1 until $\{\overset{*}{\sigma}\}$ is below failure surface.
This will give a new $\Delta\{\overset{*}{\delta}\}$ say $\Delta\{\overset{**}{\delta}\}$

8. Calculate the tangential stiffness matrix corresponding to a state of stress always below or equal to failure conditions

$$\left[D_t(\{\delta_o\} + \Delta\{\overset{**}{\delta}\}) \right]$$

9. Evaluate new overall stiffness matrix

$$\left[K_t(D_t(\{\delta_o\} + \Delta\{\overset{**}{\delta}\})) \right]^{-1}$$

10. Solve to obtain the displacement vector corresponding to the load vector

$$\Delta\{\delta\} = \left[K_t(\{\delta_o\} + \Delta\{\delta\}^{**})\right]^{-1} \cdot \{F\}$$

11. Calculate stresses and strains for the step

$$\Delta\{\varepsilon\} = [B] \cdot \Delta\{\delta\}$$

$$\Delta\{\sigma\} = \left[D_t(\{\delta_o\} + \Delta\{\delta\}^{**})\right] \cdot \Delta\{\varepsilon\}$$

12. Accumulate the stresses and strains of this step to that at the start of the step

$$\{\varepsilon\} = \{\varepsilon_o\} + \Delta\{\varepsilon\}$$

$$\{\sigma\} = \{\sigma_o\} + \Delta\{\sigma\}$$

The above algorithm implies two solutions for each step as compared with one solution for each step in the tangential method. From the comparison shown in figure (2.3a) it is clear that the results of one step of Quasi Runge-Kutta is better than the results of two steps of the tangential stiffness method. Figure (2.3b) shows how well the technique succeeded in following to failure the nominated stress-strain curve at one point in a problem of about 1000 degrees of freedom.

2.2.2. Iteration techniques using the residual force concept

An iterative process for the solution of a system of equations of the type mentioned above, equation (2.2),

may be defined by the statement that, if $\{\delta\}_i$, $i = 1, \cdots, n$ are approximations to the solution required, they enable another approximation $\{\delta\}_{i+1}$ to be calculated by means of some recurrence relation, called the iteration formula:

$$\{\delta\}_{i+1} = \{G_i(\{\delta\}_i \cdots \{\delta\}_{i-1} \cdots \{\delta\}_{i-n+1})\} \qquad (2.3)$$

provided that $\{\delta\}_{i+1}$ is a closer approximation to the required solution $\{\bar{\delta}\}$ than was $\{\delta_i\}$ and that $(\{\delta\}_i - \{\bar{\delta}\}) \to o$ as $i \to \infty$. That is using the trial results $\{\delta\}_i \cdots \{\delta\}_{i-n+1}$ from the previous iterations, $i, i-1, \ldots, i-n+1$ an approximation $\{\delta\}_{i+1}$ is calculated, and then replacing one of the vectors $\{\delta\}_i \cdots \{\delta\}_{i-n+1}$ by $\{\delta\}_{i+1}$, a new approximation $\{\delta\}_{i+2}$ is calculated using the remaining n vectors and so on. This expression, equation (2.3), is an example of an n-point iteration function (note that n denotes the number of previous approximations used to establish a new approximation). The iteration function G_i, will in general involve not only $\{\delta\}_i$ but also values of $f(\{\delta\})$ and some of its derivatives evaluated at one or more of the vectors $\{\delta\}_i$. This is only possible if G_i has as many continuous derivatives as required in the neighbourhood of the solution $\{\bar{\delta}\}$. The subscript i on G_i is necessary only when the iterative function itself may change from one iteration to the next. (as Nayak's method 1971); if not, the iteration function will become stationary (i.e. independant of i), thus G is used instead of G_i. If the iteration using a stationary iteration function converges to a solution $\{\bar{\delta}\}$ then the

following equation must be true:

$$\{\bar{\delta}\} = \{G(\{\bar{\delta}\} \cdots \{\bar{\delta}\})\}$$

In text books on the subject, methods for finding the solution of equation (2.2) based on equation (2.3) are called functional iteration methods. In finite element non-linear analysis, functional iteration methods could be classified here into two main approaches:

a. The Newton-Raphson methods, which iterate on the left hand side of the non-linear system (See equation 2.2a)

b. The Constant Stiffness method, which iterates on the right hand side of the non-linear system (See equation 2.2a) The so-called initial stress and initial strain methods are variations of this method.

As was said before, the physical understanding of the different parameters involved in the non-linear equation enables a valuable interpretation for the algorithm to be made. A good example is the residual force concept introduced and used as a routine technique for linear analysis accuracy assessment by the numerical analysis group at Swansea. It is an essential feature of any reasonable non-linear iterative method described in this thesis, and thus it will be described in detail. In an iteration technique an approximation to the true solution $\{\delta\}_i$ is arrived at for each iteration i, using a convenient stiffness matrix (which need not be the true one). The state of the structure during this iteration is such that the displacement

pattern is not in equilibrium with the external applied nodal forces because the stiffness matrix used is inappropriate. In matrix form this becomes

$$\{f(\{\delta\}_i)\} - \{F\} \neq 0 = \{R(\{\delta\})\}$$

Thus the residual forces $\{R\}$ are those forces which if added to the external loads would exactly balance the internal loads due to the incorrect state of stress in the structure. Any iteration process from the above two approaches will try to relax the structure by giving successive additional increments of displacement $\Delta\{\delta\}_i, i=1,..,n$ so that the residual force becomes zero or negligible, ending with a correct displacement vector:

$$\{\delta\} = \{\delta_o\} + \sum_{i=1}^{n} \Delta\{\delta\}_i$$

where n here denotes the total number of iterations.

The residual force R^k for variable k is written as:

$$R^k_{i+1} = F^k - \sum_{r=1}^{L} K_t \delta^r_i$$

where L = the number of elements contributing to the variable k, and $K_t\delta_i$ denote a non-linear function of δ and F^k is the external applied nodal force at variable k. The point here is that the computer need never encounter anything vaguely resembling K_t, if the full implications of the isoparametric elements and numerical integration are realized. The very simple and completely general process in calculating residuals is the following algorithm:

Initialize $\{R\} = 0$

Enter integrating loops over the internal regions (or boundary) of the element. At each Gauss point

a) compute the strain due to the approximate displacement vector,

b) from the strain, compute the stress using the stress-strain law,

c) by virtual work find the contribution to each nodal force due to stresses using numerical integration as described in chapter one,

d) again, by virtual work find the contribution of gravity, pressure, pore water pressure, etc. and accumulate them into $\{F\}$.

2.2.2.1. Newton-Raphson Method

The system of equations to be solved is written in the form:

$$\{R(\{\delta\})\} = R_i(\delta_r) \qquad (i,r=1,\cdots,m)$$

Suppose that the required solution is at $\delta_1+\varepsilon_1$, $\delta_2+\varepsilon_2$, $\cdots$, $\delta_m+\varepsilon_m$, then the m-variable form of Taylor's theorem gives, Booth (1966):

$$R_i(\delta_1+\varepsilon_1, \delta_2+\varepsilon_2 \cdots, \delta_m+\varepsilon_m) =$$

$$R_i(\delta_1, \delta_2 \cdots, \delta_m) + \sum_{r=1}^{m} \varepsilon_r \frac{\partial R_i}{\partial \delta r} + O(\varepsilon^2)$$

where for a second order process $\varepsilon_1, \varepsilon_2 \ldots \varepsilon_m$ is considered to be a solution of the set of linear simultaneous equations (i.e. neglecting ε^2_1, $i=1,\cdots,m$)

$$\varepsilon_1 \frac{\partial R_i}{\partial \delta_1} + \varepsilon_2 \frac{\partial R_i}{\partial \delta_2} \cdots\cdots + \varepsilon_m \frac{\partial R_i}{\partial \delta_m} = - R_i$$

and in a matrix form

$$[K]_T \{\varepsilon\} = - \{R(\{\delta\})\}$$

$$\{\varepsilon\} = - [K]_T^{-1} \{R(\{\delta\})\}$$

therefore

$$\{\delta\}_{i+1} = \{\delta_i\} - ([K]_T^{-1} \{R(\{\delta\})\})_{\delta=\delta_i} \qquad (2.4)$$

where the expansion of $[K]_T$ for two degrees of freedom as an example is

$$K_T = \begin{bmatrix} \frac{\partial R_1}{\partial \delta_1} & \frac{\partial R_1}{\partial \delta_2} \\ \frac{\partial R_2}{\partial \delta_1} & \frac{\partial R_2}{\partial \delta_2} \end{bmatrix}$$

Equation (2.4) is known as the Newton-Raphson iterative function which is a one-point stationary function. The conditions for conversion and error analysis are given by Lancaster (1966), Brown (1969) and Rall (1966). Again, it is clear that convergence is achieved if $\{R\} \to o$ i.e. by the disappearance of residual forces.

For engineering purposes the best iterative processes are in general second order , therefore a rapid convergence

for this method is expected, provided a sufficiently good initial estimate for the unknown variable $\{\delta\}$ is used (as mentioned before), however if the initial estimate is far from the final solution, the method does not succeed (Ralston 1965). The main disadvantage of this method is that in each iteration the tangential stiffness matrix for each element has to be calculated and the stiffness matrix for the whole structure ($[J] = [K]_T$ Jacobian matrix) has to be reassembled and inverted. Inverting $[J]$ requires more than $(m^3/6)$ multiplication operations based on the elimination algorithm (Crandall 1956) or $(mb^2/2)$ if the semi-bandwidth is b, Kan (1972), m = total number of degrees of freedom.

It is not uncommon for $[K]_T$ to be unsymmetrical. This may cause problems, due to the loss of many useful theorems if the $[K]_T$ matrix is unsymmetric or non-positive definite, Irons and Treharne(1971). An asymmetric $[K]_T$ matrix arises in many of the non-linear field problems Lyness (1972) and from using a non-associative flow rule in plasticity problems which gives an asymmetric $[D]$ matrix. The matrix is non-positive definite unless all the following conditions are satisfied:

$$K_{11} > 0, \quad \begin{vmatrix} K_{11} & K_{12} \\ K_{21} & K_{22} \end{vmatrix} > 0, \quad \begin{vmatrix} K_{11} & K_{12} & K_{13} \\ K_{21} & K_{22} & K_{23} \\ K_{31} & K_{32} & K_{33} \end{vmatrix} > 0,$$

This could be encountered if a material exhibiting strain-softening is modelled like brittle soils.

The Newton-Raphson method was introduced to the finite element elastic-plastic solution by Pope (1965a, 1965b). Variations of the use of this method depending on the size of the load increment in relation to the spread of the plastic zone were given by Yamada, Yoshimura and Sakurai (1968), Marcal and King (1967) and Yamada (1969). The method was attractive at that time due to the lack of other alternatives, its simple algorithm and its quadratic convergence, Traub (1964), (if it does converge). The author believes that due to high cost as well as possible numerical troubles in some cases, the $[K]_T$ method in general is to be avoided.

2.2.2.2. Constant Stiffness Method

Gallagher, Padlog and Bijlaard (1962) first used a technique which is quasi Newton-Raphson with $[K]$ instead of $[K]_T$ in all iterations of a non-linear problem and modifying the right hand side (i.e. $\{F\}$) of the equation to compensate for the error introduced by using $[K]$; their technique is now called the "initial strain method". Again the new modified right hand side physically interpreted as the residual forces needed to balance the structure. Due to the non-applicability of this method to elastic perfectly plastic material an alternative method was introduced by Zienkiewicz et al (1969), called the "initial stress method". The latter has the same distinctive feature as

the former, which is to keep the stiffness matrix of the whole structure constant in the memory of the computer, without changing it during all the iterations - hence its name. The constant stiffness method has the advantage of being easily interpreted physically as follows:

1. Apply the load vector $\{F\}$ to the nodes of the domain. Using the available stiffness matrix, find the corresponding displacement vector $\{\delta\}$. This stiffness matrix could be either the elastic or the tangential matrix at the start of the loading, and it is to be kept constant,

2. Compute the residual forces $\{R\}$ as described in Section 2.2.

3. Compute the relaxation on the residuals.

$$\{e\}_{i+1} = [K]^{-1}\{R\}_{i+1}$$

4. Then add $\{e\}_{i+1}$ to the current displacement which has been accumulated from previous iteration as a correction term giving:

$$\{\delta\}_{i+1} = \{\delta\}_i + \{e\}_{i+1} \qquad (2.4a)$$

Repeat 2, 3, and 4. If $\{e\}$ and $\{R\}$ iterate towards zero, the process converges. Any problem of non-symmetry or non-positive definitions does not appear in this procedure. It is expected to have a slower convergence than the Newton-Raphson method. See figure (2.4a) for comparison between

the two methods for one degree of freedom case. Argyris and Scharpf (1969) proved the convergence to be of first order and they concluded that the iterative initial stress method always converges as long as no physical failure occurs. The author has found that the method converges very slowly near failure and this was also reported by Nayak (1971). Due to that, an acceleration for the interation process is needed for economic reasons in order to achieve an acceptable time for the non-linear finite element solution. This will be the subject of the remainder of the chapter.

2.3 Acceleration techniques

The problem is that at iteration i of a non-linear algorithm, there is an error e_i due to the residual R_{i-1}, so in order to accelerate the iteration process, the object is to find a factor α which when multiplied by e_i gives a displacement that when used in the next iteration gives an error $e_{i+1} = o$. Figure (2.4b) shows a graphical representation of the problem for a single degree of freedom assuming that the solution between e and α is linear. In a real problem the relation is not linear and a lot of attention has been given to the evaluation of the acceleration factor.

Different over-relaxation factors were examined indetail by the author (Hamza 1972). The conclusion was that alpha constant stiffness matrix, Nayak and Zienkiewicz (1972),

was better than the others because of the following main reasons:

1. It converges more monotonically.
2. It is easy to program in its new simplified form.
3. It was the only method which succeeded in the strain softening region.

2,3,1 Alpha-Constant stiffness matrix

Nayak (1971) and Nayak and Zienkiewicz (1972) suggested the use of an over-relaxation factor $\lceil \alpha \rfloor$ to accelerate the iterative process with the use of constant $[K]$ matrix. This factor is applied in equation (2,4a) above, giving (see figure (2,4b) for one degree of freedom representation)

$$\{\delta\}_i = \{\delta\}_{i-1} + \lceil \alpha \rfloor \{e\}_i$$

They used a complicated notation for evaluating the terms of the diagonal matrix $\lceil \alpha \rfloor$. The final displacement vector at iteration i is

$$\{\delta\}_i = \{\delta_o\} + \sum_{J=1}^{J=i} \Delta\{\delta\}_J$$

The detailed formula and computational process in terms of their notation are explained in the above-mentioned papers. A different algebraic approach, using the same assumptions and arriving at the same results, which leads to a more simplified algorithm and thus easier programming, is developed to examine this method in the following two

sections. This was also represented in the author's previous work, Hamza (1972).

2.3.1.1. The structure of Alpha iterative process

The basis of Nayak's iteration is:

$$R_i^k = F^k - \sum_{r=1}^{L} K_t \delta_{i-1}^r \qquad k = 1, 2 \ldots .m$$

where L = number of elements contributing to variable k
This is to be calculated for each degree of freedom individually, using the non-linear constitutive law. The true stiffness matrix for the whole structure need not be formulated, as explained earlier.

The residual force vector $\{R\}_i$ is to be relaxed on the domain using the $[K]$ matrix as before:

$$\{e\}_i = [K]^{-1} \{R\}_i$$

where i denotes the iteration number.

Now the correction term, which is to be added to the current deflection $\{\delta\}_{i-1}$ is

$$\lceil \alpha \rfloor \{e\}_i$$

with $\lceil \alpha \rfloor$ an unknown diagonal matrix to be evaluated term by term, as shown below. The definition of $\lceil \alpha \rfloor$ is

$$\{R\}_i = [K] \{e\}_i = [K]_T \lceil \alpha \rfloor \{e\}_i$$

re-arranging

$$[K]\{e\}_i = [K]\lceil\alpha\rfloor\{e\}_i - ([K] - [K]_T)\lceil\alpha\rfloor\{e\}_i$$

As an approximation, Nayak puts $\lceil\alpha\rfloor$ in the second term the existing $\lceil\alpha\rfloor = \lceil\alpha\rfloor_{i-1}$

$$\{e\}_i = \lceil\alpha\rfloor\{e\}_i - [K]^{-1}([K] - [K]_T)\lceil\alpha\rfloor_{i-1}\{e\}_i$$

Thus he develops the recurrence formula for updating $\lceil\alpha\rfloor$:

$$\lceil\alpha\rfloor\{e\}_i = \lceil\alpha\rfloor_{i-1}\{e\}_i + [K]^{-1}([K]\{e\}_i - [K]_T\lceil\alpha\rfloor_{i-1}\{e\}_i)$$

Considering one term at a time, (i.e. equating a row from the left hand side to the same row of the result of the right hand side):-

$$\alpha^k = \alpha^k_{i-1} + \frac{\sum_{J=1}^{J=m} K^{-1^{kJ}}([K]\{e\}_i - [K]_T\lceil\alpha\rfloor_{i-1}\{e\}_i)^J}{e_i^k} \qquad (2,5)$$

when α^k = the value of α for the kth variable considered. Basu (1972) interprets the last term of equation (2,5) as follows:

$$[K]\{e\}_i - [K]_T\lceil\alpha\rfloor_{i-1}\{e\}_i = \{F\} - [K]_T\{\delta\}_{i-1} - [K]_T\lceil\alpha\rfloor\{e\}_i$$

$$= \{F\} - [K]_T(\{\delta\}_{i-1} + \lceil\alpha\rfloor\{e\}_i)$$

$$= \{F\} - [K]_T\{\delta\}_i$$

because $$\{\delta\}_i = \{\delta\}_{i-1} + \lceil\alpha\rfloor_{i-1}\{e\}_i \qquad 2,6$$

$$[K]\{e\}_i - [K]_T\lceil\alpha\rfloor\{e\}_i = \{R\}_{i+1}$$

Therefore,

$$\sum_{J=1}^{J=m} K^{-1kJ}\left([K]\{e\}_i - [K]_T\lceil\alpha\rfloor_{i-1}\{e\}_i\right)^J = \sum_{J=1}^{J=m} K^{-1kJ}\{R\}_{i+1}^J \qquad 2,7$$

Now we go to Nayak's work. He uses two re-solutions in one iteration. In order to avoid confusion of the two different notations Nayak's process will be written in words. A full process of Nayak's "iteration" may be described as follows:

* First half,

δ = δ inherited from last "iteration" +

α inherited X e of the 1st resolution

* Second half,

Update α using equation (2,5) which involves 2nd resolution, say α_{new}, then

δ = δ inherited from last iteration + α_{new} X

e of the 1st resolution

In the present work each resolve is counted as a separate iteration, i,e. Nayak's "iteration" = two separate iterations. Looking at Nayak's "iteration" through the new notation we find:

* after the 2nd resolve (i,e. iteration No. i+1)

$$\{\delta\}_{i+1} = \{\delta\}_{i=1} + \lceil\alpha\rfloor\{e\}_i \qquad 2.8$$

* after the 1st resolve of the next "iteration" (i,e, iteration No. (i+2))

$$\{\delta\}_{i+2} = \{\delta\}_{i+1} + \lceil\alpha\rfloor\{e\}_{i+2} \qquad 2.9$$

Using equation (2,5) and equation (2,7)

$$\alpha^k = \alpha^k_{i-1} + \frac{e^k_{i+1}}{e^k_i} \qquad 2.10$$

From 2,6 it would appear that α can be logically suffixed thus

$$\alpha^k_{i+1} = \alpha^k = \alpha^k_{i-1} + \frac{e^k_{i+1}}{e^k_i} \qquad 2.11$$

Substituting the value of α of equation (2,11) into equation (2.8) term by term:

$$\delta_{i+1} = \delta_{i-1} + \alpha\, e_i$$

$$= \delta_{i-1} + \left(\alpha_{i-1} + \frac{e_{i+1}}{e_i}\right) e_i = \delta_{i-1} + \alpha_{i-1}e_i + e_{i+1}$$

$$= \delta_{i-1} + \alpha_{i-1}e_i + e_{i+1}$$

$$\delta_{i+1} = \delta_i + e_{i+1} \qquad 2.12$$

giving an over relaxation factor = 1.0

This is a very interesting result. Nayak's "iteration"

has two quite dissimilar halves:

(i) as in equation (2,9) and equation (2,10). a variable α part which is dangerous

(ii) as in 2,12 a constant α part, with $\alpha = 1.0$ which is particularly safe.

It is possible now to explain tentatively why this technique has been giving good results in some cases, It may be that the second half with constant α repairs the damage done by the first part with variable α, (It has always been puzzling that the technique ever succeeds, for in the absence of any mathematical proof of convergence in a system of many degrees of freedom one expects divergence. (See discussion, section. 2.4)).

2.3.1.2. Summary of simplified algorithm comparison with Nayak's

Iteration i or 1st half of Nayak's "iteration"

1. Compute the current residual: $\{R\}_i = \{R(\{\delta\})_{i-1}\}$

2. Re-solve $\{e\}_i = [K]^{-1}\{R\}_i$

3. Update δ $\{\delta\}_i = \{\delta\}_{i-1} + [\alpha]_{prev}\{e\}_i$

Iteration (i+1) or 2nd half of Nayak's "iteration"

1. Compute the current residual: $\{R\}_{i+1} = \{R(\{\delta\})_i\}$

2. Re-solve $\{e\}_{i+1} = [K]^{-1}\{R\}_{i+1}$

3. While re-solving, store the previous e_i and update α term by term.

$$\alpha_{new} = \alpha_{previous} + \frac{e_{i+1}}{e_i}$$

and store it for the next iteration

(compared with calculation from equation (2,5) in Nayak's version)

4. Update δ $\{\delta\}_{i+1} = \{\delta\}_i + \{e\}_{i+1}$

(compared with $\{\delta\}_{i+1} = \{\delta\}_{i-1} + [\alpha]_{new}\{e\}_i$)

The differences which simplified the algorithm are

1. In calculating α
2. In applying α
3. In updating δ_{i+1}

2.3.2. Comparison between Alpha-Constant stiffness matrix and Conjugate-Newton techniques

Irons (1973) represented a method, the Conjugate-Newton method, which uses also a constant stiffness matrix with an acceleration factor. In evaluating the acceleration factor, the principle of minimizing the potential energy of

the perturbation of the residual was utilized. The details of the algorithm and its mathematical proof of convergence are given in the above-mentioned reference. Irons claimed that his method was better than the Alpha-Constant method, his argument being based on an example of a non-linear problem with five variables. The mathematics involved are difficult and a review of which is outside the scope of this work, and the program is very complex. It was the writer's intention to examine this method with bigger problems and to compare it with the Alpha-Constant method in order to use the best in a complete two-dimensional finite element program.

A simple finite element program was written to incorporate Irons' algorithm as a "black box". A force distortion relationship of the form

$$F = \frac{\delta + a\delta^3}{c + b|\delta^3|}$$

(where a,b,c are constants and F, δ are the force and corresponding distortion) is used, which could show a "strain-softening" region. The root mean square of the residual forces is used as a measure of convergence.

First, a 20 degree of freedom problem is solved under two-cases of loading, one of them producing a slight softening region (load =1, 1,05 units). Second, an 88 degree of freedom was used to justify a conclusion, also two load cases were solved, (load = 0,2, .25 units). The results are plotted in the form of iteration number against root mean

square of residuals and shown in figures (2.5, 2.6, 2.7).

In all cases, the Alpha-Constant method gave a better result. However, in all cases, except the 88 degree of freedom and load = 0.2 case, Conjugate-Newton gave either better or comparable results early in the iteration process, then stopped convergence, or even diverged (in the case of 20 degree of freedom and load = 1.0). It is worth mentioning here that if an iterative method for the solution of equation 2.2 converges mathematically, as the Conjugate-Newton proved to do, then the only limitation on the accuracy of the numerical solution is in the number of digits carried in the computation (Ralston 1965). The round-off error in a single iteration is the only inherent limitation on the accuracy. Bearing this in mind and the success of the Conjugate-Newton in the early stage of the iteration process, it can be inferred that the damage which occurred in the later iterations is due to round-off errors and not natural divergence. Thus, if this difficulty is overcome the Conjugate-Newton method might be as good as the Alpha-Constant method and it will have the support of its mathematical proof of convergence. The Alpha-Constant method has no such proof.

For the time being, the Alpha-Constant method has been adopted for non-linear work requiring iteration, due to its simplicity and ease of programming.

2.4. Discussion and Conclusions

Non-linear finite element analysis is problem dependent and a generalised algorithm for all kinds of problems is not available. Two algorithms were demonstrated here to give better answers than others. They are the Quasi-Runge-Kutta one step technique and the simplified Alpha-Constant stiffness technique. Both techniques were incorporated in a version of FESS (Finite Element System Swansea), yielding two separate programs, SAN2 for the step method and SAN3 for the iterative techniques (Soil And Non-Linearity)

For engineering problems with large degrees of freedom and the need for rapid turn-round, an iterative process is not advisable, as it has to be watched carefully and its accuracy, measured for convergence, is not always required. Thus the step technique may be sufficient. However, a strain-softening problem cannot be handled using this technique and a problem which includes unloading may cause numerical troubles because of the use of the $[K]_T$, a flexible matrix, which may predict large strains even for the unloading region. This problem faced the author in the application of this technique to Empingham main dam which includes shear unloading due to an irregular construction sequence.

The simplified Alpha-Constant stiffness matrix method is most suited for problems including strain

softening and unloading because it uses $[K]$ which is a constant matrix and does not depend on the stress level during iteration.

The best form of stress-strain law to suit the step technique as shown above is:

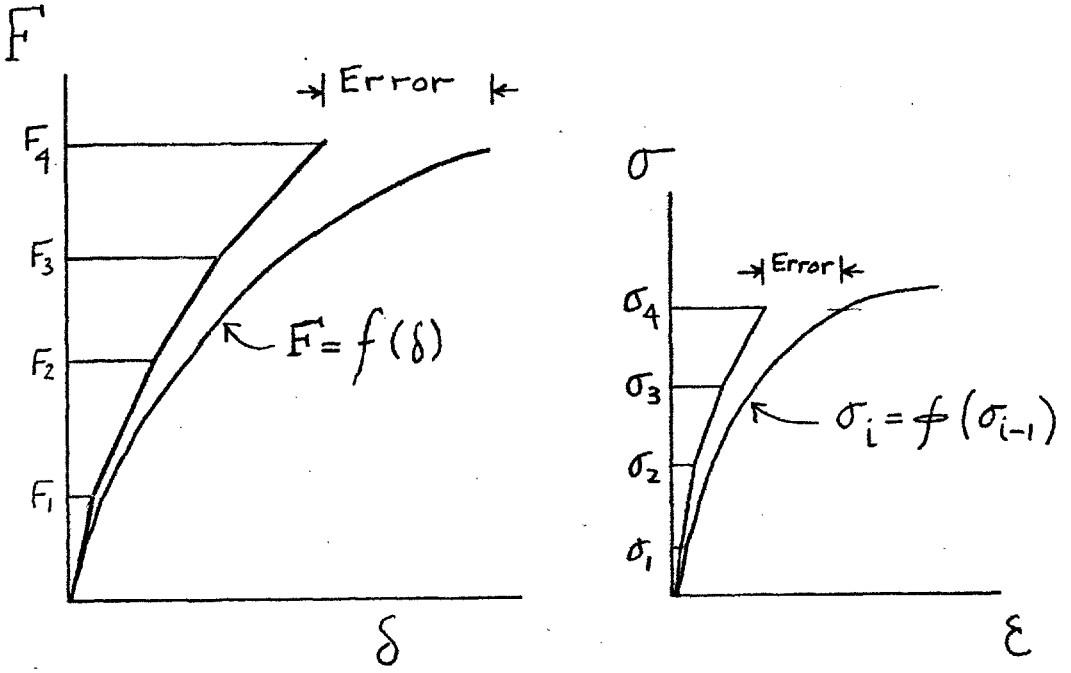
$$\Delta\{\sigma\} = [D(\{\sigma\})] \cdot \Delta\{\varepsilon\}$$

And its explicit form is given in Chapter 3.

But for the iterative technique, as used in this work, the best form for the stress-strain equation is

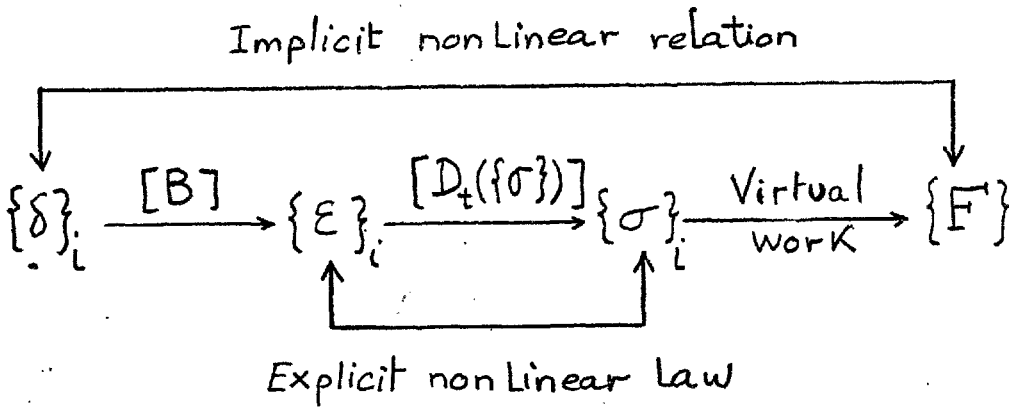
$$\Delta\{\sigma\} = [D(\{\varepsilon\})] \cdot \Delta\{\varepsilon\}$$

To avoid the use of two stress-strain equations the first one was also used in the iterative method. To achieve that, an iteration inside the Gauss-loop was implemented in SAN3 in order to evaluate the value of $\Delta\{\sigma\}$ corresponding to the strain vector $\Delta\{\varepsilon\}$.



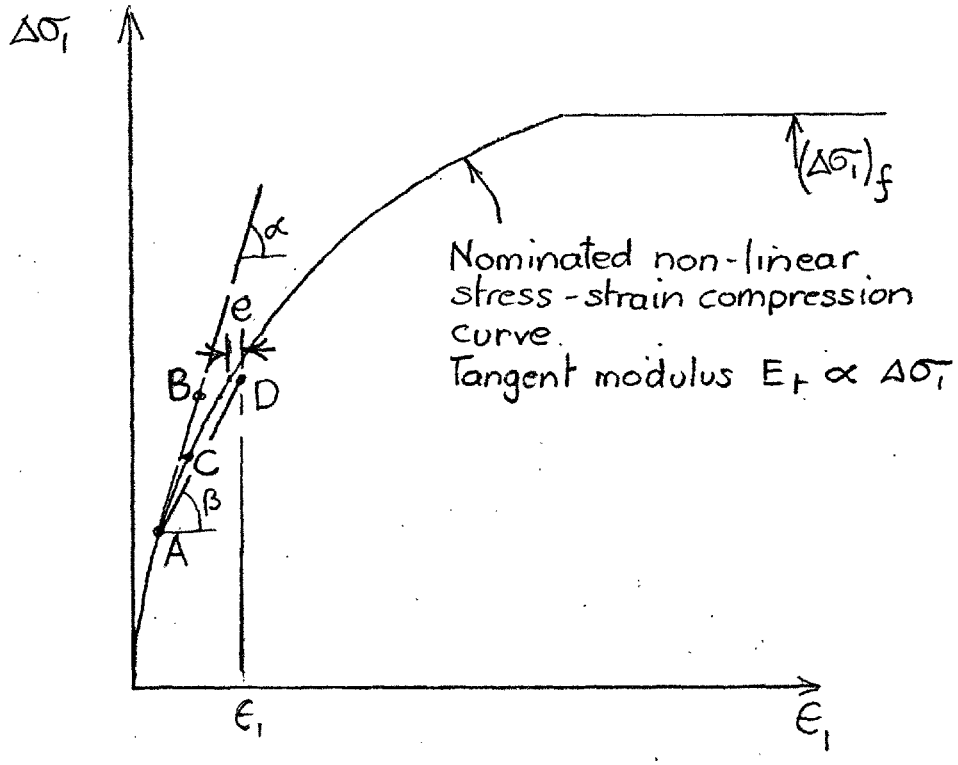
Force - displacement

Stress - strain



ONE DIMENSIONAL EXPLANATION OF THE TANGENTIAL STIFFNESS MATRIX METHOD

Fig. 2.1



After n load increments $\Delta\sigma_1 = (\Delta\sigma_1)_A$, $\epsilon_1 = (\epsilon_1)_A$

For n+1 th increment

1st solution $E = (E_t)_A = \tan\alpha$

gives $(\Delta\sigma_1)_B$ and $(\epsilon_1)_B$

2nd solution. $E = (E_t)_C = \tan\beta$

where $(\Delta\sigma_1)_C = \dfrac{(\Delta\sigma_1)_A + (\Delta\sigma_1)_B}{2}$

gives $(\Delta\sigma_1)_D$ and $(\epsilon_1)_D$, curve fitting error = e

If:- $(\Delta\sigma_1)_A > 0.95(\Delta\sigma_1)_f$, failure assumed and solution made with E very small

If:- $(\Delta\sigma_1)_C > (\Delta\sigma_1)_f$, try $(\Delta\sigma_1)'_C = (\Delta\sigma_1)_A + \dfrac{(\Delta\sigma_1)_B - (\Delta\sigma_1)_A}{4}$

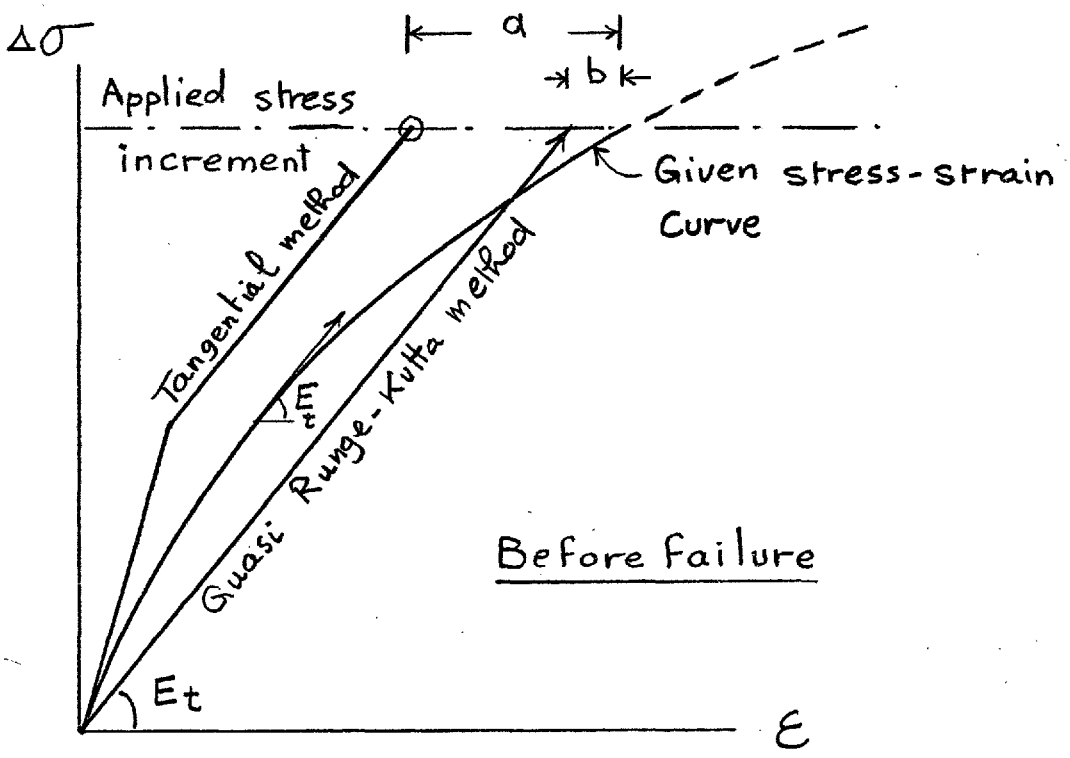
if $(\Delta\sigma_1)'_C < (\Delta\sigma_1)_f$ determine $(E_t)'_C$ & use in second solution

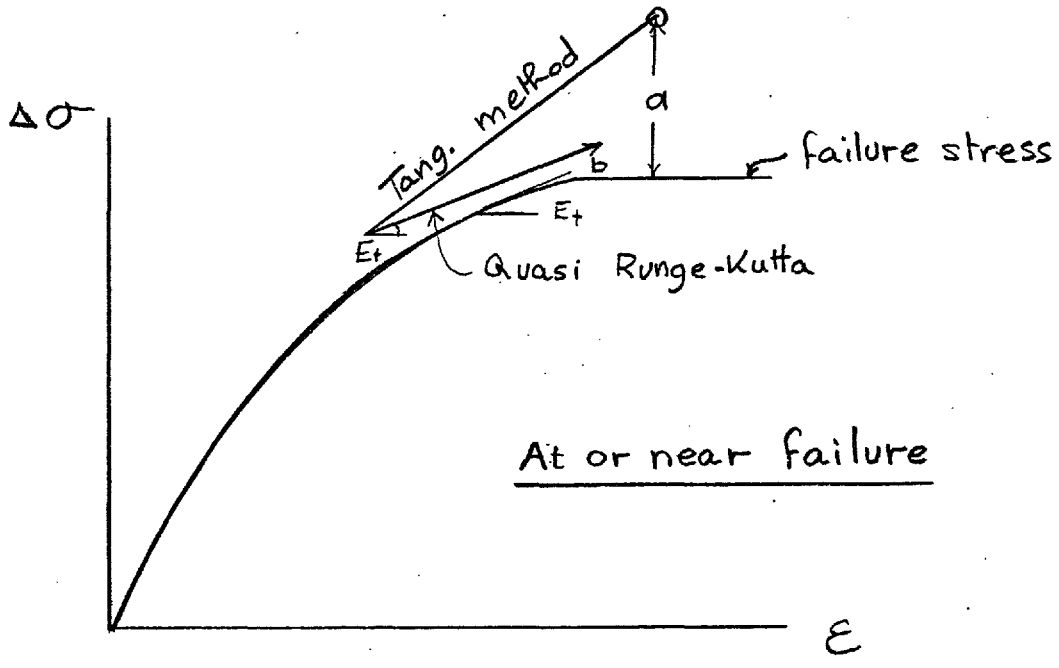
if $(\Delta\sigma_1)'_C > (\Delta\sigma_1)_f$, try $(\Delta\sigma_1)''_C = (\Delta\sigma_1)_A + \dfrac{(\Delta\sigma_1)_B - (\Delta\sigma_1)_A}{8}$

and so on.

THE RUNGE-KUTTA ALGORITHM FOR ONE VARIABLE PROBLEM

Fig. 2.2



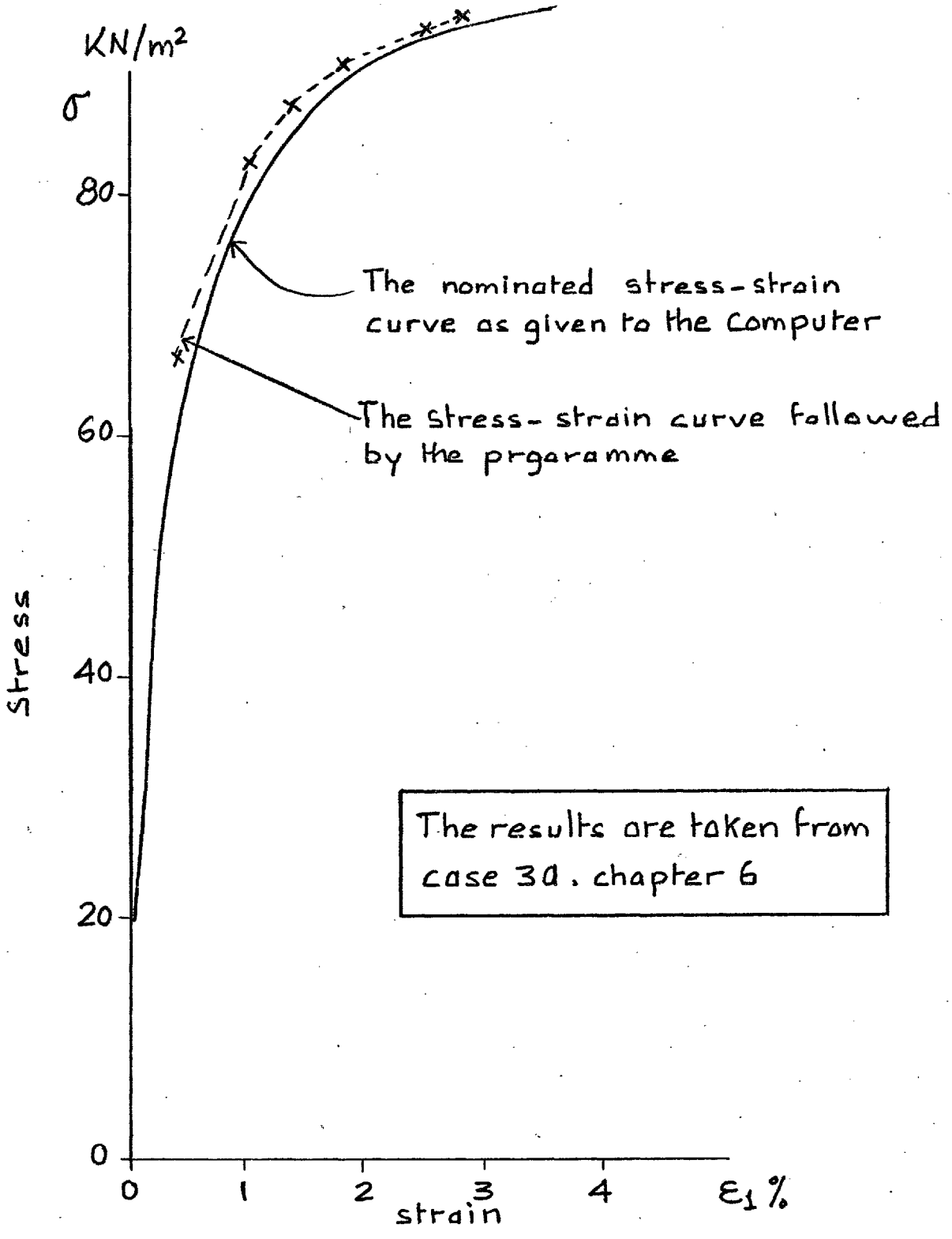


a : error in using Tangential method

b : error in using Quasi Runge-Kutta method

COMPARISON BETWEEN TANGENTIAL AND QUASI RUNGE-KUTTA METHODS FOR ONE VARIABLE

Fig. 2.3a



NOMINATED AND CALCULATED STRESS-STRAIN CURVES FOR A POINT OF A 1000-VARIABLE DOMAIN

Fig. 2.3b

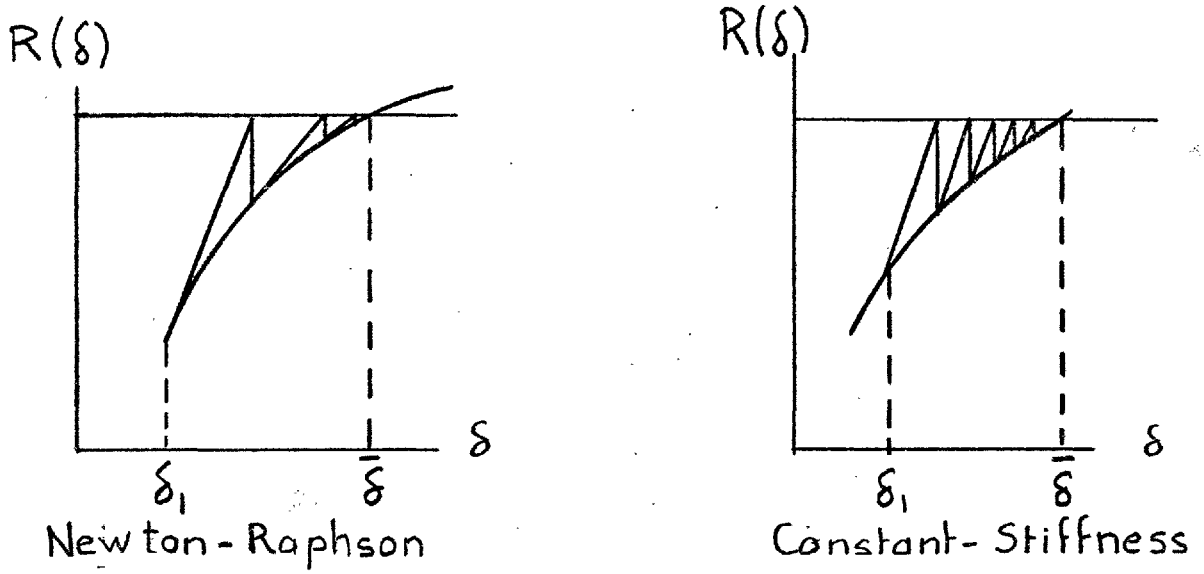


Fig. 2.4a COMPARISON BETWEEN THE TWO METHODS OF ITERATIONS

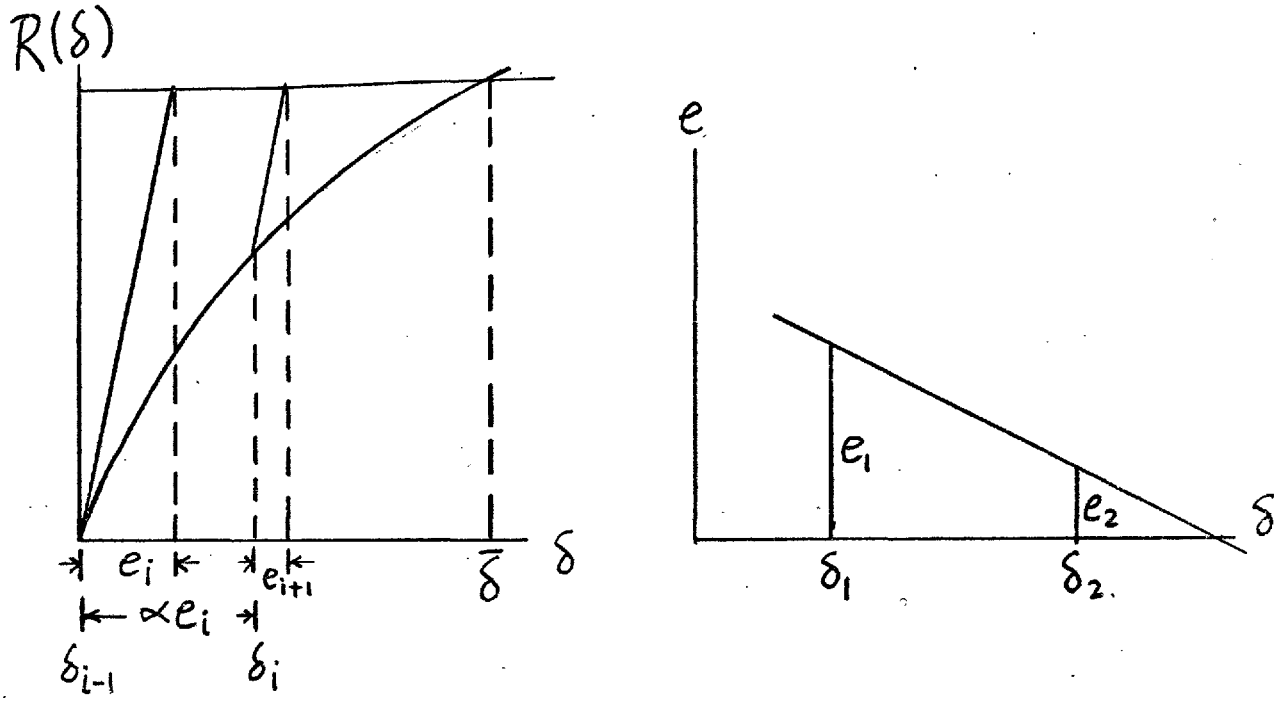


Fig 2.4b THE ALFA-CONSTANT STIFFNESS METHOD

Fig. 2.4

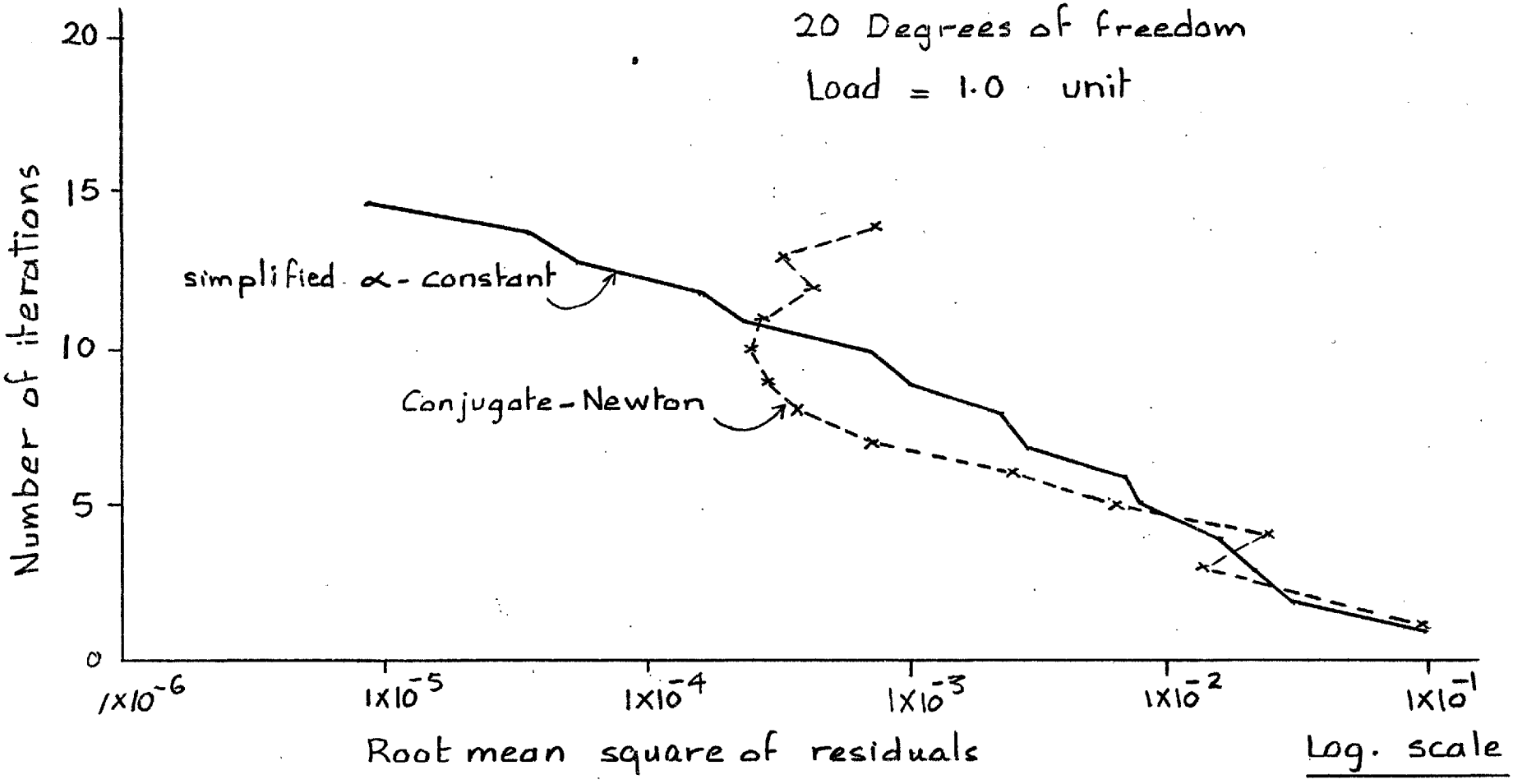


Fig. 2.5

COMPARISON BETWEEN CONJUGATE-NEWTON AND α-CONSTANT

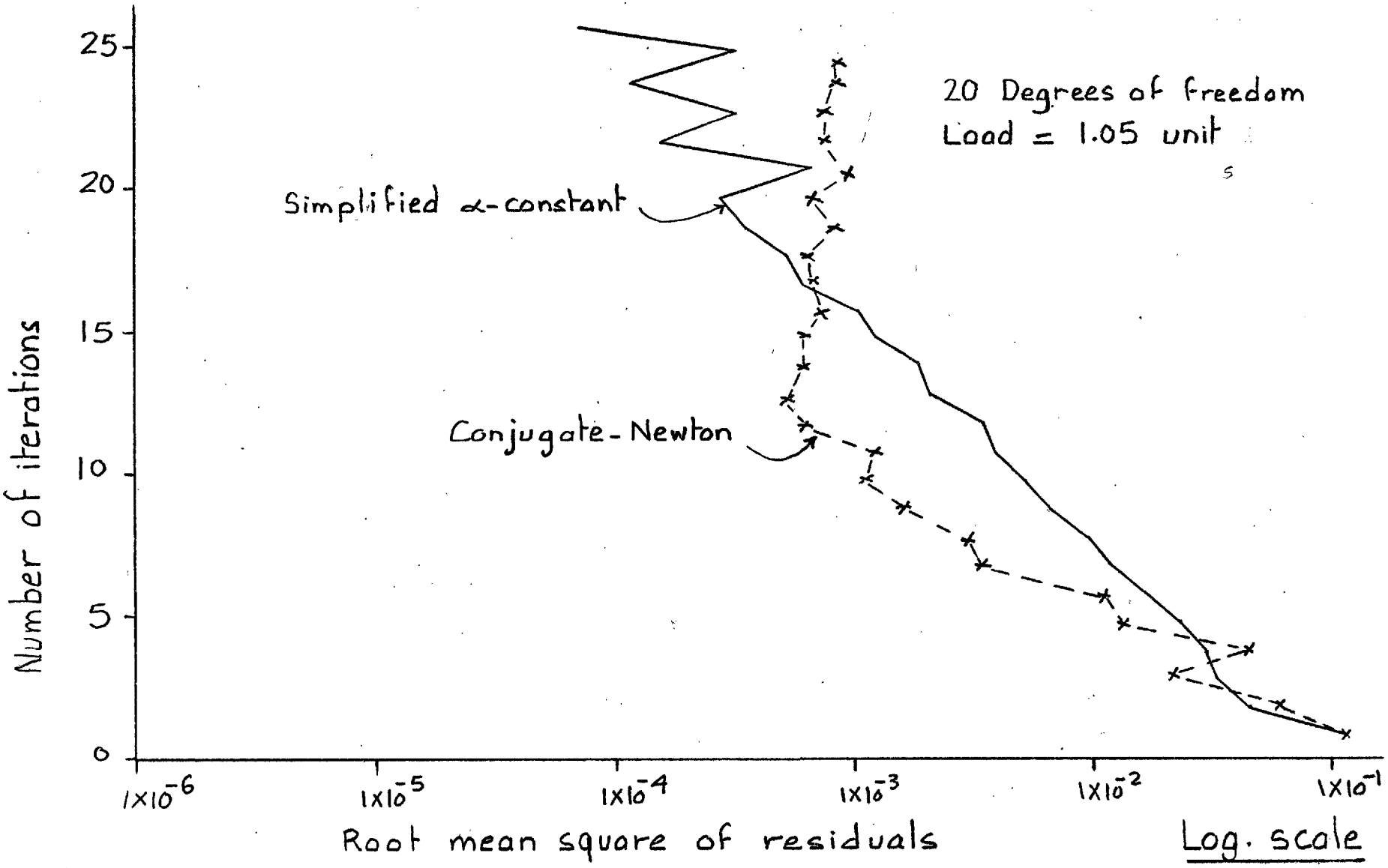

25
20
15
10
5
0
Number of iterations
20 Degrees of freedom
Load = 1.05 unit
Simplified α-constant
Conjugate-Newton
1X10⁻⁶
1X10⁻⁵
1X10⁻⁴
1X10⁻³
1X10⁻²
1X10⁻¹
Root mean square of residuals
Log. scale

Fig. 2.9

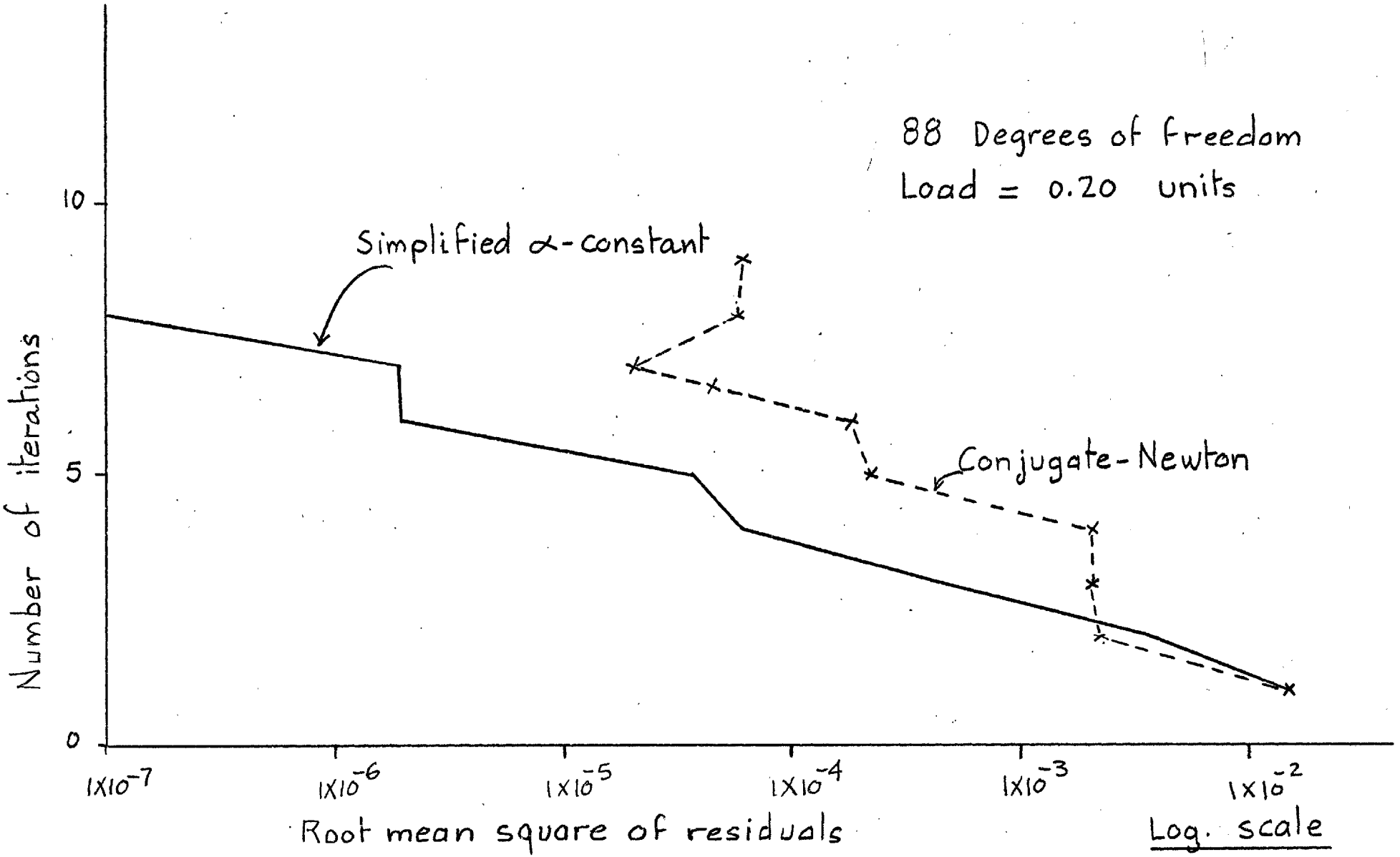

88 Degrees of freedom
Load = 0.20 units
Simplified α-constant
Conjugate-Newton
Number of iterations
10
5
0
1X10⁻⁷
1X10⁻⁶
1X10⁻⁵
1X10⁻⁴
1X10⁻³
1X10⁻²
Root mean square of residuals
Log. scale

Fig. 2.7a

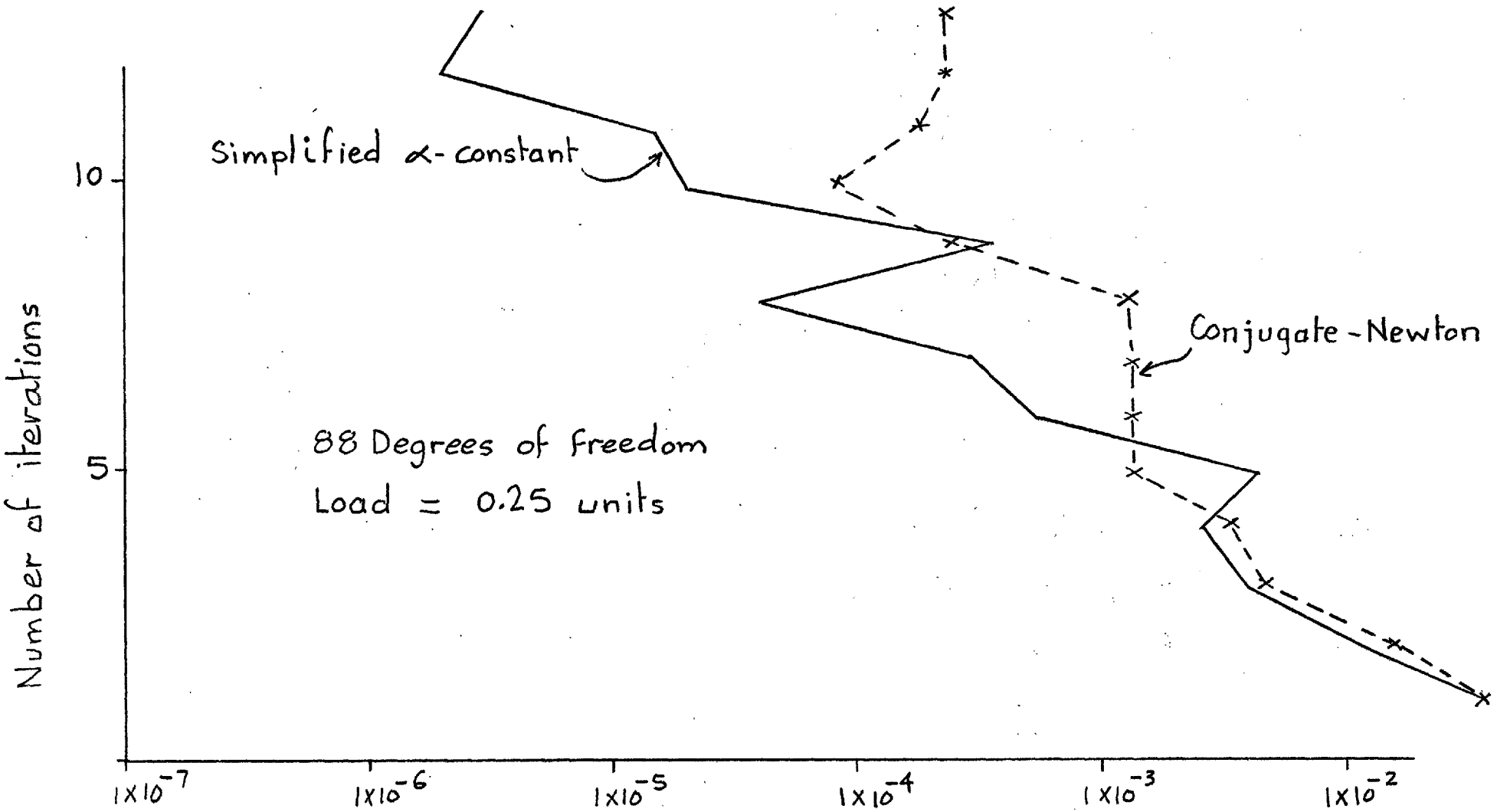

Simplified α-constant
Conjugate-Newton
88 Degrees of freedom
Load = 0.25 units
Number of iterations
10
5
1X10⁻⁷
1X10⁻⁶
1X10⁻⁵
1X10⁻⁴
1X10⁻³
1X10⁻²
Root mean square of residuals
Log. Scale

Fig. 2.7b

CHAPTER 3

THE REPRESENTATION OF SOIL PROPERTIES FOR STATIC NON-TIME-DEPENDENT STRESS-STRAIN SOLUTIONS

3.1 General

A rigorous stress-strain law should be able to describe analytically the state of stress and state of strain, including the state of failure, in all three phases, (solid particles, water and gas), of an element of soil under any case of loading having satisfied all implied boundary conditions. A stress-strain law is needed together with compatibility conditions and equilibrium equations, in order to solve a continuum problem, as shown in Chapter 1.

Soils, unlike other engineering materials, possess a mechanical behaviour highly dependent on their previous geological and stress history. If a soil element is subject to irrecoverable strain, its structure will be permanently modified; thus its future behaviour under further changes of effective stress will also be modified. Although the soil may be anisotropic due to geological deposition inducing preferred particle orientation, effective stress changes during the application of further stress may induce additional anisotropy which should be taken into account in any realistic model for soil.

Another complication is added if the element of soil is subject to principal stress and/or principal stress increment rotation, a condition which is not easy to reproduce

in the laboratory, but which very commonly occurs in reality. The effect of rotation of stresses on the behaviour of soil is reported to change the void ratio, thus causing volume change; it might cause anisotropy as well.

Some soils exhibit volume change during shearing which may be either an increase or a decrease. Finally, some classes of soil show apparent brittleness (strain softening) behaviour in varying degrees, and it may be important to model this behaviour for some engineering problems. Experimental work on these classes of soil has shown the development of a discontinuity once the peak shear stress has been achieved and after which the stress-strain curve continues as a stress-relative displacement curve, Maguire (1975). Thus a continuous solution in applying the compatibility conditions is ambiguous.

For many years the solutions of linear elasticity and limit plasticity have been utilised in solving soil mechanics and foundation engineering problems, many simplifying assumptions being made due to the lack of more sophisticated solutions. In deriving the elastic solution, the soil is assumed to be a linear elastic body which can never fail; in the plasticity solution the soil is assumed to be a rigid-plastic body usually covered by the Mohr-Coulomb failure criterion. The former predicts deformation only, the latter assesses stability only. Neither approach models the complete behaviour of a soil continuum under load.

Recent developments in numerical techniques with the ability to predict deformations in soils (e.g. FEM) using complicated stress-strain laws, have focussed attention on the need to define soil stress-strain laws, the solution techniques being limited by the availability of data on soil properties, (an example of this limitation is encountered in the use of a simple linear anisotropic soil model). Nevertheless, the literature on the subject is full of stress-strain solutions for different soil types, using mainly two categories of soil models:

(1) those utilising only the theory of elasticity, but with attempts made to account for the nonlinearity typically observed in soil stress-strain relationships including the failure stage;

(2) those utilising theories of plasticity, which are dependent on the type and variation of yield function and flow rule used; this category is more varied than the first.

In this chapter a review is made of the assumptions and basic principles of the above-mentioned models and some solutions utilising these models in finite element application are examined. The soil models used in the course of this research are also presented.

3.2 Discussion on the Isotropic Elastic Model

An ideal elastic body is characterised by its natural state in which the stress depends upon the state of deformation only and the natural state assumption requires that when the external loads are released the body assumes its natural state again, Truesdell (1966). The work done by the external forces acting on the body is stored as elastic energy (internal energy) which is available for full recovery once the loads are removed. On this basis two alternative approaches are available for defining the ideal elastic behaviour, which have the same meaning for infinitesimal strain theory:-

(1) Stress is a function of strain (Cauchy 1823, 1828, 1829)*

(2) Internal energy is a function of strain (Green, 1839, 1841)*

Based on the former definition the fundamental stress-strain equation for any elastic, but not necessarily linear or isotropic, body may therefore be written

$$\Delta\{\varepsilon\} = [C]\,\Delta\{\sigma\}$$

This equation states that:

(1) Any stress increment $\Delta\{\sigma\}$ gives rise to a set of strain increments $\Delta\{\varepsilon\}$ which are a unique function of the causative stress increment

(2) the strain increment is fully recoverable on unloading

* Referred to by Atkinson (1973)

i.e. it is path independent and the principle of superposition applies, and the system is conservative.

The matrix $[C]$ contains 21 independent parameters Love, (1927) in its general case, i.e. full anisotropy, which may not be constant over the stress increment range, it is here that non-linearity is introduced. If various conditions of symmetry are imposed the number of independent parameters in the matrix $[C]$ are reduced until in the case of an isotropic material the matrix $[C]$, contains only two independent parameters (except at "failure" as explained later) which may or may not be constant. The conventional parameters generally used are E, Young's modulus and ν, Poisson's ratio and the explicit stress-strain equations are found in Love (1927). The relationship between these parameters and conventional soil compressibility parameters m_v, c_c and k_o are found in Lambe and Whitman (1969).

It is important to note that in the case of a linear elastic isotropic body the axes of principal stress and the axes of principal strain, which are determined quite independently, coincide, Jaeger,(1956).

An important consequence of isotropic elasticity is that shear and volume stresses may be decoupled, and purely deviatoric stress increments will produce zero volume change. For the conventional triaxial test, the increments of deviatoric strain, $\Delta\gamma_d$, and volumetric strain, $\Delta\varepsilon_v$, may be

related to the corresponding stress increments $\Delta\tau_d$ and $\Delta\sigma_v$ as follows:-

$$\Delta\gamma_d = \frac{1}{G}(\Delta\sigma_1 - \Delta\sigma_3) = \frac{1}{G}\Delta\tau_d$$

$$\Delta\varepsilon_v = \frac{1}{K}\frac{\Delta\sigma_1 + 2\Delta\sigma_3}{3} = \frac{1}{K}\Delta\sigma_m$$

where G and K are the shear and bulk moduli respectively and they are related to E + ν by the following equations Jaeger, (1956)

$$G = \frac{E}{2(1+\nu)}$$

$$K = \frac{E}{3(1-2\nu)}$$

So far, no reference has been made to whether E and ν are drained or undrained parameters. In soil mechanics engineering problems, the solution required may be for one or more of the following cases:-

1) Undrained loading where no drainage is assumed.

2) Undrained loading followed by drainage (either consolidation or swelling)

3) Drained loading

4) Partly drained loading, as in the case of sand drain zones.

For the first class, the author believes that undrained deformation parameters are sufficient to carry out

the analysis. Although the deformation is always a function of effective stress:-

$$\delta = f(\bar{\sigma}) = f(\sigma - u)$$

the pore water pressure u is a function of the total stress:-

$$u = f_1(\sigma)$$

thus the deformation is a function of total stress

$$\delta = f_2(\sigma - f_1(\sigma))$$

and hence there is no need to use the effective stress parameters E', ν' which need more elaborate tests and more time for their measurement. The undrained Poisson's ratio ν for fully saturated soils is theoretically only slightly less than 0,5. Due to the compressibility of soil grains and that of the water, Bishop (1966a) showed that $\nu \neq 0.5$ but is very close to it and thus the numerical problem of using $\nu = 0,5$ for the analysis of such a case is removed by using $\nu = 0,499$ say, which with the use of isoparametric elements (see Chapter 1) and the reduced integration rule proves to give acceptable answers Naylor, (1974) provided that the mesh is fine enough (this was found during the course of the author's research) and the stresses are only considered at the Gauss points, not at the nodes. The undrained Young's modulus E_u may be obtained from the conventional undrained triaxial test where $\Delta\sigma_3 = 0$.

Naylor (1974) has proposed a method by which the excess pore-water pressure under undrained conditions can

be evaluated using the effective stress parameters E', ν' and an apparent bulk modulus of compressibility K_a of the pore fluid which is expressed in the form

$$\frac{1}{K_a} = \frac{n}{K_f} + \frac{1-n}{K_s}$$

where K_s is the bulk modulus of the solid part of the material skeleton (i.e. soil particles), K_f, the actual bulk modulus of compressibility of the pore fluid and n is the porosity.

Naylor's approach requires the use of the effective stress parameters E', ν' which, can only be determined by slow tests. An alternative way is to carry out the analysis in undrained terms and to use the pore water pressure parameters A and B (Skempton, 1954, and Bishop, 1954) to evaluate the excess pore-water pressure as follows:-

$$u = B\left[\Delta\sigma_1 + A(\Delta\sigma_1 - \Delta\sigma_3)\right]$$

A could be a function of the stress level. Generally, if loading is at usual engineering rates, the pore-water pressure is relatively easy to measure Vaughan,(1972a)and a sophisticated method for its determination may be unnecessary.

For the third class, where the loading is such that no excess pore-water pressure is set up, the drained parameters E', ν' should be used and they could be most easily determined from a triaxial test keeping $\Delta\sigma_3' = 0$ and measuring either the minor principal strain El-Ruwayih (1975)

as well as the major or by measuring the volume change and using the relation :-

$$\nu' = \frac{1}{2} + \frac{\Delta V/V}{\Delta \varepsilon_1}$$

which assumes that the volume change is isotropic, Poisson's ratio is found to vary greatly with stress level. In dilatant soil a value of $\nu' > 0,5$ might be obtained which is meaningless in terms of an elastic analysis due to energy considerations ; Sokolnikoff, (1956). Reasonable values are obtained only during the early stages of the test when the specimen decreases in volume.

The ratio between the 'elastic modulus' for drained and undrained conditions for real soils might vary within very wide limits, especially for fine grained soils ; Maksimovic, (1971). But assuming elastic behaviour and that the water in the soil voids does not transfer shear stresses (either the viscosity of water is neglected or the rate of undrained loading is very slow), a relationship can be easily obtained (from $G_u = G'$)of the form

$$E_u = \frac{1.5}{1+\nu'} E' \quad \text{(isotropic)}$$

Since ν' is typically about 0,3 at low stress levels, then the approximate relationship between E_u and E' for an elastic soil can be taken as

$$E_u = 1,15E'$$

Wroth (1971), using an equation given by Henkel (1971), has shown that for London clay E_u/E' = 1.34 assuming isotropy and E_u/E' in the vertical direction was equal to 1.616 for transverse anisotropy.

The second class of undrained loading followed by dissipation whether swelling or consolidation, is of particular interest and difficulty. A rigorous solution must consider the complete problem of pore-water pressure dissipation and the stress dependency of the compressibility of the soil skeleton (and the compressibility of the pore fluid if the soil is partly saturated). The formulation of the problem assuming a linear elastic soil skeleton and an incompressible pore fluid was given by Biot (1941) and incorporated in a finite element solution by Christian and Boehmer (1970) and Hwang, et al (1971). A solution with the non-linear compressibility of the soil and/or compressible pore fluid is not yet available (1975).

An approximate alternative approach, suggested here, is to decouple the problem by carrying out firstly and independently the undrained stress analysis case of loading and then either to evaluate the pore-water pressure set up by one of the two approaches mentioned above (Naylor's method or Skempton's A and B method) or to use field measurements of Δu at selected points and then to establish a reasonable distribution from experience; with either approach the initial values of the unknown Δu are evaluated.

A separate analysis should then be carried out to evaluate the pore-water pressure distribution after a certain time interval, the span of which needs to be considered carefully, using a standard consolidation program. This presents the second approximation as the total stresses are assumed to remain constant during the consolidation analysis, which is not the case in reality due to changes in ν'. The time interval should be small enough to account for that and also for the non-linearity of the soil skeleton if it is considered. If the soil skeleton is assumed to be linear elastic and the results are only required at the end of consolidation, only the final pore-water pressure distribution at the steady state is needed, Naylor (1974).

The effect of dissipating an increment of pore-water pressure, whether it is after an interval of time or after the steady state is achieved, on the state of stress of the soil skeleton is obtained by carrying out a finite element stress analysis for the soil skeleton using the pore-water pressure increment as the case of loading as follows. If the general equations of equilibrium of an element of soil are considered, then these take the form for the x direction:-

$$\frac{\partial \sigma_x}{\partial x} + \frac{\partial \tau_{xy}}{\partial y} + \frac{\partial \tau_{xz}}{\partial z} + X = 0$$

with two other equations of similar form in the direction of y and z. In this case X represents the total body force/

unit gross volume of the material. But:

$$\sigma_x = \sigma'_x + u$$

Thus

$$-\frac{\partial \sigma_x'}{\partial x} + \frac{\partial \tau_{xy}}{\partial y} + \frac{\partial \tau_{xz}}{\partial z} + (X - \frac{\partial u}{\partial x}) = 0$$

This equation is of identical form to the above one of page 61, but the body force terms have now been changed by the amount.

$$-\frac{\partial u}{\partial x}, \quad -\frac{\partial u}{\partial y} \quad \text{and} \quad -\frac{\partial u}{\partial z}$$

in the appropriate directions and the analysis is carried out after converting the gradient of the pore-water pressure into an equivalent body force, which is technically achieved without problems once the values of Δu are input at the nodes in an isoparametric finite element program.

The soil parameters used during this stage of the analysis are the effective stress parameters E', ν' and they may be nonlinear in which case E' and ν' are related to $\Delta\sigma_3'$ and $\Delta\sigma_1 - \Delta\sigma_3$ by a family of curves. If the pore-water pressure is known only at the steady state and the soil skeleton is nonlinear, the analysis cannot be carried out because the principle of superposition can no longer be applied, due to the expected irregularity of the dissipation sequence and the soil skeleton's response to it. Only by knowing the pore-water pressure distribution at close time

intervals during which

(1) the dissipation could be considered regular

(2) the total stress could be considered constant during consolidation.

could the method be applied, Thus the span of the time interval represents the third approximation.

It is worth mentioning here that whether the dissipation is consolidation or swelling, the procedure described above is valid. In case of condolidation, the soil skeleton will exhibit a decrease of volume due to an increase in the compressive effective stress, and in case of swelling, the soil skeleton will increase in volume due to the decrease in the compressive effective stress,thus the volume change and the causative stresses have the same sign, hence the analysis for swelling does not imply $\nu' > 0.5$. But it must be pointed out that the swelling process is an unloading one in terms of volumetric stresses so unloading parameters should be used in the analysis.

The fourth loading case, that where partial consolidation occurs during loading can be handled in three ways. Firstly, a fully coupled solution can be used. The only solutions known to the Author involve the assumption of linear elastic soil deformation parameters together with the Biot consolidation equations. Secondly, soil deformation parameters in terms of effective stress may be used, as in

the second class of loading previously described, with the pore pressure changes estimated independently from undrained loading behaviour and uncoupled consolidation theory, and applied to the soil skeleton as nodal drag forces. Thirdly, as a crude approximation that has been used in modelling the behaviour of the sand drain zone at Empingham Dam (Chapter 7), the pore pressure changes can be estimated independently, volume changes can be deduced from the pore pressure changes and the total stress deformation parameters can be modified to account for the volumetric strains. The method of doing this is set out in Chapter 7. It may be noted that the effect of consolidation or swelling could be simulated using the strain method of loading mentioned in Chapter 4.

One of the main obstacles to using the isotropic elastic model for soils is the volume change exhibited by some soils during shear loading, which can be either contraction or expansion. To illustrate this behaviour, the results of tests on field compacted Lias clay (Sodah, (1974)) are plotted in the form of volume change versus allround total pressure during consolidation and shear stages, see figure (3.1). In the application of shear a sudden change in the value of bulk modulus K is observed. Using extrapolation, the volume change due to shear V_s could be appreciated. Thus the use of the bulk modulus K from an isotropic consolidation test for the stress analysis of a continuum which may have an arbitrary stress path is not

representative for the actual behaviour of soil. The use of Poisson's ratio obtained from the conventional triaxial test takes account of both volume change due to shear as well as that due to allround pressure up to a limit of $\nu' = 0,5$.

At the failure stage, modelled using the incremental tangential $E = 0$, the two parameters E, ν are no longer independent. Writing Poisson's ratio in terms of bulk modulus K and Young's modulus E :-

$$\nu = \frac{3K - E}{6K}$$

shows that at $E = 0$, ν takes a value of 0,5 for all values of K. This dependency is of importance for partly saturated clays used as fill material and for granular soils. The physical explanation is that at failure, where $E = 0$, the maximum principal strain is very large and if $\nu \neq 0.5$, the soil will exhibit a very large volume change which is not the case in reality. The author believes that an analysis which uses an isotropic elastic model at failure should account for this dependency otherwise the model is inconsistent.

3.3 Review of the Models Using "Isotropic Elasticity"

A review of selected examples is given here to cover the different approximate models used for soil stress-strain behaviour assuming "nonlinear elasticity".

Since the early application of nonlinear finite element analysis to soil mechanics a bilinear approximation of the stress-strain curve has been used in several solutions.

Dunlop and Duncan (1970), D'Appolonia and Lambe (1970), Wong (1971), and Lu and Scott (1972), studied stress conditions in excavated slopes, immediate settlements of footing on clay, earth pressure on sheet piles and stability of cuts respectively. In such a model the stress-strain parameters defining the soil model are Young's modulus before and after failure, the failure stress and Poisson's ratio.

Variations in the initial Young's modulus may be assigned in accordance with the confining pressure or depth. The elements in which the stress exceeds the failure stress* are ofter assigned a low value of modulus about 0.001 or 0,0001 times its initial value. For best results it was found that Poisson's ratio is also modified after yield so that the volumetric compressibility remains constant during failure, as explained in Section 3.2. Dunlop and Duncan (1970) used a value of Poisson's ratio equal to 0,475 before failure and a value of 0.49999 after failure, while D'Appolonia and Lamb (1970) used 0,499 before failure and 0,4999995 after failure. In all cases five parameters were needed for the analyses.

D'Appolonia and Lambe (1970) checked the validity of the model by comparing the experimental stress-strain curves obtained in plane strain extension and compression tests with the analytical predictions. Dunlop and Duncan (1970) showed that their finite element analysis gave reasonable behaviour in a qualitative comparison with the field

* Generally, overshooting is expected.

observation of slope failure in over consolidation clay excavation for Seatle Freeway reported by Bjerrum (1967).

Another approximation of the stress-strain curve was the use of a multi-linear elastic model, Ellison (1968), and Ellison et al (1971), to represent the behaviour of Chattahoochee River sand in a study of a single pile foundation. Ellison (1968) compared the finite element prediction with the experimental results of Vesic (1967) determined from embedded and driven piles in Chattahoochee sand. Good agreement was claimed. In this model the initial Young's modulus was assumed to vary as:-

$$E_i = (A + B\ \sigma_3)$$

in which A and B were experimentally determined parameters. The coefficient A is assumed to be constant for all densities while B varies with relative density. The modulus was subsequently decreased to $0.5E_i$, $0.16E_i$, $0.042E_i$, and a very small value at 25%, 72.5%, 93% and 100% of deviatoric stress at failure. The model was tested by comparing the triaxial stress-strain curve with the multi-linear approximation and utilising the model in finite element analysis of the pile test. For the pressure range considered, the dense Chattahoochee sand is nearly incompressible for small strains ($\nu = 0.5$) and would tend to expand as failure is approached with a pseudo-Poisson's ratio increasing to about 0.6 or 0.7. For medium dense and loose sands, the appropriate Poisson's ratio lies between 0.25 and 0.4. No provision for Poisson's

ratio variation was made in the computer analysis used by Ellison (1968) and constant values of 0,45, 0,35 and 0,32 were assigned to dense, medium dense and loose sand respectively. A total of ten parameters, to define the five different slopes of the hypothetical stress-strain curves, and a Poisson's ratio value are necessary for the solution.

A more realistic approximation of the stress-strain behaviour is the use of a curve representation. Generally two approaches are possible to feed the test data into the computer for the evaluation of the parameters. In one approach the test data is supplied in digital form and in the other it is supplied in functional form. In the digital form, a number of closely spaced points on a stress-strain curve are given as input. Hence the modulus is calculated by considering two adjacent points (by chord slope) approximate to the tangent modulus. Because of their dependence on stress level, the relationships between stress and strain must be supplied at a number of closely spaced values of stress levels. From the set of data supplied in digital form the moduli are calculated at the required stress level, Gopalakrishnayya, (1973).

In the second approach, the stress-strain relationships are supplied in functional form assuming either hyperbolic stress-strain relationships Kulhawy et al,(1969) and Duncan and Chang, (1970) or using mathematical spline

functions Desai,(1971). The hyperbolic representation, involving the use of a small number of parameters with identifiable physical significance, has the advantage that it is easier to compare the properties of different soils and to develop experience and judgement in terms of parameters and it is of particular advantage while carrying out a sensitivity study. However, in general, it involves more approximation to the measured stress-strain behaviour than those obtained by spline function or digital form.

Duncan and Chang (1970) adopted the procedure of representing nonlinear stress dependent soil stress-strain behaviour by fitting the loading stress-strain curve with a hyperbola. The procedure attempts to account for inelastic soil behaviour by using a different relationship for shear unloading-reloading cycles. For loading the hyperbolic stress-strain relationship proposed by Kondner and his co-workers (1963) is used, defining the tangent modulus as

$$E_t = \left[1 - \frac{R_f(1 - \sin \phi)\ (\sigma_1 - \sigma_3)}{2C\cos \phi + 2\sigma_3 \sin \phi}\right]^2 \cdot E_i$$

in which E_i is the initial tangent modulus, C and ϕ are the Mohr-Coulomb shear strength parameters and R_f is the failure ratio defined as

$$R_f = \frac{(\sigma_1 - \sigma_3)_f}{(\sigma_1 - \sigma_3)_{ult}} = \frac{\text{compressive strength}}{\text{asymptotic value of the hyperbolic curve used to approximate the true stress-strain curve.}}$$

The initial tangent modulus was defined using Janbu's (1963) equation as follows:-

$$E_i = KP_a \left(\frac{\sigma_3}{P_a}\right)^n$$

in which K and n are experimentally determined parameters and P_a is the atmospheric pressure. The values of the five parameters C, ϕ, R_f, K and n may be determined conveniently from the results of a series of triaxial or plane strain compression tests, the drainage conditions corresponding to the conditions to be analysed.

The unloading and reloading behaviour of a soil is represented by a single modulus independent of the percentages of strength mobilised and of the directions of the shear unloading. The unloading-modulus is defined by:-

$$E_{ur} = K_{ur} P_a \left(\frac{\sigma_3}{P_a}\right)^n$$

with n the same as in first loading and K_{ur} determined from results of tests involving one or more cycles of unloading. The determining factor in deciding whether to calculate an unloading-reloading or first loading modulus was the maximum previous value of $(\sigma_1 - \sigma_3)$ only. If this value increased, a first loading modulus was calculated, but if this value decreased an unloading-reloading modulus value was calculated which is a poor way of modelling shear unloading. A better way is to store both the last and the

maximum previous $(\sigma_1 - \sigma_3)$ and also the principal stress rotation, as discussed in Chapter 8.

The stress-strain curves defined by this model were compared to the experimental ones obtained from laboratory tests, but no attempt was made to compare predicted and observed volumetric changes. The model was also used in analyses of excavation behaviour, Chang and Duncan (1970), and of footing tests, Mitchell and Gardner (1971). In each case good agreement with observed field behaviour was claimed.

The same model was modified by Kulhawy and Duncan (1970) to include an empirical relationship for tangent Poisson's ratio which reflects the nonlinearity and stress dependency of volume changes observed in soils during first loading. Comparison of published data of volume change for contractive soils with this empirical relationship showed that it can predict the observed behaviour over some range of the curve well enough.

The empirical relationship used for the tangent Poisson's ratio, ν_t, was very closely related to that for the tangent modulus, the variation of axial strain with radial strain being assumed hyperbolic. The nonlinear stress dependent tangent Poisson's ratio relationship derived was:-

$$\nu_t = \frac{\nu_i - F \log (\sigma_3/P_a)}{(1 - d\varepsilon_a)^2}$$

σ_3 and P_a in same units,

ν_i = initial tangent Poisson's ratio at one atmosphere,

F = constant expressing the rate of change of ν_i with σ_3

d = constant to be determined during the triaxial test

$$\varepsilon_a = \frac{\sigma_1 - \sigma_3}{KP_a\left(\frac{\sigma_3}{P_a}\right)^n \left[1 - \frac{R_f(\sigma_1 - \sigma_3)(1 - \sin\phi)}{2(C\cos\phi' + \sigma_3 \sin\phi')}\right]}$$

No relationship was developed for the variation of Poisson's ratio on unloading. The five parameters C, ϕ, R_f, K and n are the same as in the tangent modulus relationship and the three last parameters, d, ν_i, and F are determined from volume change measurements during triaxial tests. With the nonlinear Poisson's ratio effect incorporated into the Duncan and Chang model, a total of nine parameters is needed. These parameters are assumed to be determined from simple triaxial compression tests.

Desai (1971) used a cubic spline to approximate the stress-strain curves of a cohesive soil mass and compared finite element predictions of footing settlements to the experimental load-deformation behaviour of a model circular footing.

A spline function approximates a given curve by a number of polynomials of a given degree spanning a number of nodes or data points. The polynomials are fitted in such a way that representation over the nodes of successive

polynomials is as smooth as it can be made without resorting to a single polynomial over the complete range.

It is therefore only necessary to supply the finite element program with limited chosen stress-strain data points for different confining pressures and by using the routine for solution of simultaneous equations, always included in a finite element program, the spline and its first derivatives are completely defined. The spline itself gives the relationship between stresses and strains and its first derivatives allow one to obtain the variations of the tangent modulus for different confining pressures and at different strain or stress levels, whether the spline has been defined as a function of strains or stresses. Its main disadvantage is the use of more computer time, especially if this procedure has to be repeated for each Gauss point in each element for each increment of load.

No unloading-reloading behaviour was considered by Desai (1971) and only undrained behaviour of clays was analysed, thus, Poisson's ratio was assumed to be a constant equivalent to 0,48. To define the stress-strain curves no parameter is required but a fixed number of points should be selected, the number of points depending on the order of accuracy required. In addition a value of the Poisson's ratio has to be chosen.

The use of bulk modulus and shear modulus as alternatives to the conventional Young's modulus and

Poisson's ratio was first introduced by Clough and Woodward (1967). They derived the elastic constitutive matrix (C) for plane strain conditions with separate components as follows:-

$$\begin{Bmatrix} \sigma_1 \\ \sigma_3 \\ \tau_{max} \end{Bmatrix} = \begin{bmatrix} (M_b + M_d) & (M_b - M_d) & 0 \\ (M_b - M_d) & (M_b + M_d) & 0 \\ 0 & 0 & M_d \end{bmatrix} \begin{Bmatrix} \varepsilon_1 \\ \varepsilon_3 \\ \gamma_{max} \end{Bmatrix}$$

in which σ_1, σ_3 τ_{max} denote the major, minor principal stresses and maximum shear stress respectively and ε_1, ε_3, γ_{max} the corresponding strains.

The bulk modulus M_b was assumed to remain constant during loading and all the nonlinearity was accounted for by modifying the shear modulus M_d. Such analysis requires six parameters to describe the stress-strain behaviour of soil. This model was employed in analysis of construction of the Otter Brook dam. Little data is available to confirm this model's behaviour, but reasonable agreement was found with the available observed data for Otter Brook dam.

Domaschuk and Wade (1969) derived a nonlinear stress dependent model from an extensive series of tests on Chattahoochee River sand which enabled separate values for bulk and shear moduli to be calculated. Two types of tests

were conducted: isotropic compression and constant mean normal stress tests. The isotropic compression tests were employed to determine the relationships for the bulk modulus, while the constant mean normal stress tests were used to determine the relationships for the shear modulus.

The bulk modulus was related to the mean normal stress, σ_m, using a bilinear relationship of the form:

$$\varepsilon_v = \frac{1}{m_1} \ln (K_{i1} + m_1 \sigma_m) + C_1 \qquad (0 < \sigma_m < \sigma^*)$$

and

$$\varepsilon_v = \frac{1}{m_2} \ln (K_{i2} + m_2 \sigma_m) + C_2 \qquad (\sigma^* < \sigma_m < 100 \text{ psi})$$

in which the constants m_1, m_2 and K_{i1}, K_{i2} were obtained from an analysis of the test data, C_1 and C_2 were evaluated at σ^* which represented the stress at which there was change in slopes m_1 and m_2, and ε_v denotes the volumetric strain.

From the experimental results obtained in the drained triaxial constant mean normal stress tests, the stress-strain relation was characterised by hyperbolic parameters similar to those used by Kondner et al (1963), resulting in the equation relating the deviatoric stress S_d, to the deviatoric strain ε_d as follows:

$$S_d = \frac{\varepsilon_d M_{di}}{1 + b \varepsilon_d M_{di}}$$

in which M_{di} is the initial tangent shear modulus and b is

the reciprocal of the ultimate value of S_d. Values of M_{di} were obtained by taking a tangent to the deviatoric stress-strain curve at the origin plotted on an enlarged scale. This has the disadvantage of relying on the part of the curve which is less accurate due to bedding errors. An average value of b for given values of the initial density and mean normal stress was obtained by selecting several points at random on the deviatoric stress-strain curves and substituting the coordinates in the previous hyperbolic equation for S_d. Still this model did not take account of the value of strain at failure as an independent variable.

In the finalised equations the bulk modulus was related to σ_m by the following equation:

$$M_b = M_{bi} + m\ \sigma_m$$

in which M_{bi} is the initial slope of the volumetric strain-isotropic stress relationship. Values of the shear modulus were established from the instantaneous slope of the deviatoric stress-strain relationship:-

$$M_d = M_{di}\ (1 - b\ S_d)^2$$

The validity and performance of the model was checked by comparing experimental and predicted variations of volumetric strain with mean normal stress in the isotropic compression tests and by comparing experimental and predicted variations of resultant deviatoric stress with resultant

deviatoric strain as obtained from drained triaxial constant mean normal stress tests. Good agreement between predicted and observed results was found, but the model was not tested against a different stress path, i.e. one which coupled shear and mean stress. A total of nine parameters is necessary to define this model. Both isotropic compression and constant mean normal stress tests must be conducted to determine the required parameters. Because the bulk modulus is formulated in terms of σ_m it is necessary to know the value of the intermediate principal stress σ_2 as well as σ_1 and σ_3.

A third bulk and deviatoric moduli model was developed by Clough and Duncan (1969) which represented a hybrid between a strict bulk and deviatoric model and the Duncan and Chang model (1970). The first loading tangent modulus value E_t, the initial modulus value E_i, and the unloading-reloading modulus value E_{ur}, were calculated as prescribed by the Duncan-Chang model. However, these values were employed as follows to determine the bulk and deviatoric modulus values.

From the theory of elasticity, the deviatoric modulus was calculated as:-

$$M_d = \frac{1}{2} \quad \frac{E}{1+\nu}$$

in which E was E_t on primary loading and E_{ur} on unloading-reloading. And the bulk modulus in plane strain conditions

was determined by:-

$$M_b = \frac{1}{2} \quad \frac{E}{(1+\nu)(1-2\nu)}$$

in which E was E_i on primary loading and E_{ur} on unloading-reloading.

Thus, the deviatoric modulus varied with confining pressure and shear stress on primary loading and with confining pressure on unloading-reloading while the bulk modulus varied only with confining pressure in either case. By following this procedure, the bulk modulus increases with increasing confinement as shown by Domaschuk and Wade (1969) and a reasonable bulk compressibility is guaranteed even when the deviatoric modulus is reduced at failure. Only triaxial tests need to be conducted to determine the six input parameters required for the model.

The accuracy of the model was tested against observed soil behaviour in triaxial tests where it was found to closely fit observed stress-strain curves. It was also utilised in finite element analyses of two instrumented navigation locks and the observed and predicted behaviour showed reasonable agreement.

In a non-linear elastic analysis in which the tangent modulus is reduced as failure is approched, there is a danger that the bulk compressibility of the soil will be seriously underestimated unless the Poisson's ratio of the soil is increased towards failure, as mentioned in Section 3.2. Thus

the case of M_d and M_b is a useful model in this aspect because it guaranteed a reasonable value of the bulk compressibility at failure. But, as mentioned in Section 3.2, evaluating its value from a stress path which does not include shear and then applying the same values for a stress path which couples shear and normal stresses may lead to an error.

3.4 Concepts in Plasticity

In this section the main assumptions of plasticity theory are reviewed briefly. One of the most important assumptions is the time independence in stress-strain relationships; the deformations are assumed to occur instantaneously. The second main assumption is that deformation has two components: an elastic one which is recoverable during unloading and a plastic one which is permanent. These two components are independent of each other and the total strains are given by

$$\{\varepsilon\}_T = \{\varepsilon\}_e + \{\varepsilon\}_p$$

where the elastic strains obey the equations in section 3.2.

The material is generally assumed to be isotropic, and it remains isotropic during the loading process. But some of the following concepts are also valid for anisotropic materials. The principal axes of the stress vector $\{\sigma\}$ and elastic and plastic strain vectors $\{\varepsilon\}_e$ and $\{\varepsilon\}_p$ coincide

as long as the material is isotropic. Bauschinger noticed that if a sample is loaded in extension to a yield stress YE, then unloaded and reloaded in compression, the yield stress in compression YC, is less than YE; this is called the Bauschinger effect.

Plasticity theory is based on the existence of a yield function, i.e. there exists a function of the stresses, $f(\{\sigma\}) = K^2$, fulfilling the following conditions: the material behaves elastically if $(f\{\sigma\}) < K^2$ and yields for $f(\{\sigma\}) = K^2$, if the material is a perfectly elastic plastic one.

A work-hardening material is a material in which plastic and elastic deformations occur at the same time during yielding. For such a material, yielding occurs if $f(\{\sigma\}) > K^2$, and a new yield function going through the new stress point is developed. The domain in the stress space, where the material behaves elastically, is extended. Because of the assumptions of the isotropy and no Bauschinger effect, all the yield surfaces developed during the work-hardening are geometrically similar.

Another assumption based on experimental evidence for metals, is that yielding is unaffected by hydrostatic pressure because no permanent volume changes are recorded.

Drucker (1950, 1951, 1953) has shown that for materials that are stable at yield, the normality principle must apply. Simply, this implies that the strain rate vector for a stress increment applied to a yielding material

must be normal to the yield surface. This principle has extremely important implications in soil mechanics in that the limit analyses, which have been employed for many years in design of footings and retaining walls, have only been proven for materials in which the normality principle is valid, Davis (1968). However, a number of investigations have presented evidence that normality does not necessarily hold for soils, (Hansen (1953), De Josselin de Jong (1964), Poorooshasb, Holubec and Sherbourne (1966), (1967), El-Ruwayih (1975)). This has resulted in a number of attempts to develop modifications to conventional plasticity theory to correct the discrepancies created through use of the normality principle. These attempts have taken two forms:

1. development of alternative yield criteria for which an associative flow rule (normality) is valid or

2. development of non-associated flow rules.

One of the results of the application of the normality principle to a material which yields upon reaching a stress state defined by the Mohr-Coulomb criterion is that the material must expand or increase in volume upon yielding. This type of behaviour does occur in dense sand, for instance, but not in loose sands nor in most clayey soils which actually contract on yielding. Drucker, Henkel and Gibson (1958) suggested a solution to this problem by proposing that the yield surface looked like the Mohr-Coulomb surface

with its open end capped by a dome which would expand and contract as the volume of the soil changed. The application of the normality principle with this surface produces a material which would contract on advancement of the yield surface cap. They obtained remarkable qualitative agreement with the behaviour of clay in triaxial test under a single stress path. Experimental results by Henkel (1958) however, proved that this theory was too simple for soils since, among other discrepancies, it predicted strain rates which did not agree with the data from laboratory triaxial shear tests.

Roscoe and his co-workers (1958, 1963) made several modifications to this basic capped yield surface showing that a bullet shaped yield was more appropriate. From more recent work by Roscoe and Burland (1968) for normally consolidated clays, the bullet shape was changed to an ellipse. One of the principal axes of the ellipse coincides with the stress isotropic line.

As mentioned above, several workers have suggested that the normality rule may not hold for some soils. Hagmann (1971), and Zienkiewicz (1971) have therefore proposed models where the normality principle was not retained. These models are reviewed in a subsequent section. Unfortunately no experimental studies or field results were used to check the validity of these models.

3.5. Review of the development of plasticity models as applied to soil mechanics solutions

The plasticity models used in soil mechanics solutions could be classified into five classes according to the choice of the yield surface and flow rule used:

Class 1 Elastic plastic model with uncapped yield surface and associative flow rule (allowing volume change during yielding)

Class 11 Elastic plastic model with uncapped yield surface and non-associative flow rule (no volume change during yielding is allowed)

Class 111 Strain-hardening model with uncapped yield surface and associative flow rule

Class 1V Strain-hardening models with capped yield surface and associative flow rule

Class V Hybrid model with one or more yield surfaces and associative or non-associative flow rule

In the following paragraphs a brief review is given of some of the soil problems solved using the above models; no details of the techniques are provided as they are already described in the original references quoted here.

Class 1

This represents the earliest and simplest plasticity model which might be utilised in solving some soil problems. The theory and assumptions of this model were given by Drucker

and Prager (1952) and Drucker (1953). Taking the effects of the intermediate principal stress on the behaviour of frictional soil into account, they established a generalisation of the Mohr-Coulomb failure criterion. The yield surface derived is conical in the principal stress space. The generalised yield function is given as follows

$$\alpha\, I_1 + I_2^{\frac{1}{2}} = K$$

where α and K are physical positive constants at each point of the material; I_1 is the sum of the principal stresses:

$$I_1 = \sigma_x + \sigma_y + \sigma_z$$

I_2 is the second invariant of the stress deviation:

$$I_2 = \frac{1}{6}\ (\sigma_x - \sigma_y)^2 + (\sigma_y - \sigma_z)^2 + (\sigma_z - \sigma_x)^2$$

$$+\ \tau_{xy}^2 + \tau_{yz}^2 + \tau_{xz}^2$$

Thus the yield function for elastic perfectly plastic material is given as:

$$f(\{\sigma\}) = 0$$

In this case, if normality holds the plastic strain increment $\Delta\{\varepsilon\}$ is proportional to the gradient of the yield function, or, in other words:

$$\Delta \{\varepsilon\} = \lambda \frac{\partial f(\{\sigma\})}{\partial \{\sigma\}}$$

where λ is a positive factor of proportionality which is characteristic of the flow rule adopted. This equation implies that plastic strains during drained plastic shearing are positive (expansive).

Christian (1966) used the Drucker-Prager model in a finite difference study of the behaviour of a flexible footing on frictional material, and presented the resulting constitutive equations in incremental form. The footing analysis showed that the plastic zone in the soil under the footing had a greater lateral extent than truly occurs for non-frictional materials. Displacements increased almost linearly with loads until failure. The surface displacements were similar to those of the general shear. No comparisons were made with actual behaviour, so no exact test was possible of the predicted behaviour.

Hagmann (1971) performed a finite element analysis of the settlement of a strip footing using a dilatant Mohr-Coulomb material, but the effect of the intermediate principal stress was not considered. The shape of the load deformation curve was also found to be similar to that of a soil failing in general shear failure, but its slope never actually became vertical. The failure load was about three times as large as the corresponding failure load given by the Terzaghi (1943) bearing capacity analysis which has been shown in laboratory experiments to yield a reasonably good estimate of bearing load. The increase in volume of

the dilatant material during plastic shear produced unrealistically large surface heave.

Class 11

In order to reduce the unrealistically large surface heaves noted in the previous model, Hagmann (1971) derived the constitutive relations for an elastic-plastic frictional material having no volume change on yielding: this type of flow rule is non-associative for the material whose yield surface develops from the stress isotropic line. This non-dilatant Mohr-Coulomb model was used in a finite element study of a strip footing. The calculated failure loads were still more than twice those predicted by Terzaghi (1943) solution. This improved model however gave more realistic values of the displacements at the surface. The predicted settlements were about twice as large as the settlements predicted by the material which dilates during plastic shear. The load deformation curve was again similar to that of a general shear failure.

Class 111

Dibaj and Penzien (1969) studied non-linear seismic response of earth structures employing an elastic-plastic strain hardening model using the Mohr-Coulomb yield criterion extended according to Drucker and Prager (1952). The normality condition was assumed to hold giving a dilatant associative flow rule. The study analysed hypothetical earth dams subjected to dynamic loading but no comparison

with experimental or field data was presented. The writers reported that their findings looked reasonable.

Class IV

Christian (1966) derived the incremental plasticity equations for an elastic plastic strain hardening material having an ellipsoidal cap. For the flow rule the volumetric plastic strains were assumed directly proportional to the volumetric stresses even though it is recognised that plastic volume changes vary logarithmically with stresses. Failure was defined by the Drucker-Prager yield surface but strain rates were not normal to its surface. Normality was only applied for the ellipsoidal cap. It was assumed that the ratio of the major and minor axes of the ellipse is a constant. Because the model contracts during plastic shear it was not intended to represent dilatant materials such as dense sands.

This model was used in the analysis of a flexible footing acting on the strain hardening material. Christian (1966) reported vertical displacements at the surface almost ten times greater than those obtained in previous runs using a Drucker-Prager material. The initial portion of the loading curve was largely due to plastic volumetric compression. Lateral and normal stresses were also much larger than in previous runs on Drucker-Prager materials. The load-deformation curve was similar to that of local shear failure.

Tang and Hoeg (1968) also performed footing analysis using this model and found that the predicted settlements increased with increasing friction angle or increasing cohesion a predicted behaviour which is in disagreement with reality.

Hagmann (1971) modified Christian's elliptical yield surface model by adopting the Mohr-Coulomb failure criterion and assuming a flow rule in which the volumetric strain varies logarithmically with volumetric stress. Using this model, Hagmann analysed the case of a lubricated end plane strain sample and a strip footing.

The plane strain sample was represented by one finite element. The finite element analysis indicated that the ideal plane strain sample failed without experiencing the large shear strains occuring in the triaxial samples. This behaviour is in agreement with plane strain data reported by several workers Bishop (1966b).

The model was also applied to a strip footing problem. The shape of the deformation curve obtained was similar to that of a soil failing in local shear. The entire surface experienced settlement, which is unrealistic even in the case of very loose soil. This was a consequence of the contracting behaviour of the model as it strain-hardened.

Roscoe, Schofield and Wroth (1958) and Roscoe and Burland (1968) have presented a number of strain hardening

models for the drained behaviour of normally consolidated clays and granular materials such as loose sands. One important concept of this model is the "critical state surface". It is assumed that after uniform shearing a soil reaches a critical state surface and no further changes in volume occur under shear. The model in effect assumes that the bulk modulus of a soil varies approximately linearly with volumetric stress. But this relation might be expected to vary with different powers for different soil types. The soil was also assumed to be stable in the sense defined by Drucker (1959) and therefore the normality principle was incorporated into the model (the strain rate vector expressed in terms of only the plastic components of strain $\Delta\gamma_p$ and $\Delta\varepsilon_{vp}$ must be normal to the yield locus). The complete equations defining the material behaviour of "Cam-Clay", modified "Cam-Clay" and revised modified "Cam-Clay" are found in the above-mentioned reference, a review of which is outside the scope of this work.

In an independent study Zienkiewicz and Naylor (1971) utilised the modified "Cam-Clay" theory in a finite element study of a triaxial sample of a hypothetical clay. They found reasonable qualitative behaviour although no experimental data were compared to give any quantitative evaluation of the model performance. Naylor and Zienkiewicz (1971) used the same model to analyse a footing on a lightly overconsolidated clay. They found good agreement between

the early part of the load-settlement curve predicted by the model and the curve predicted by conventional methods. There was no experimental data for the clay used and comparison was only hypothetical.

Smith and Kay (1971) analysed hollow cylinder specimens of "wet" clay using both the "Cam-Clay" with a non-associative flow rule and the modified "Cam-Clay" models. They concluded that the "Cam-Clay" (with non-associative flow rule) predictions were in closer agreement with observed data than those of the modified "Cam-Clay" model.

Class V

In all of the "Cam-Clay" models a discontinuity arises in the yield surface where the yield cap intersects the critical state surface. For deviatoric effective stress states less than the critical state, yielding is stable in the sense defined by Drucker (1959) and a reduction in the plastic component of volumetric strain occurs. For deviatoric stress state beyond the critical, the yield cap diverges from the space diagonal. Yielding is then unstable and the associative normality rule no longer applies. This state is designated super-critical whereas the former is designated sub-critical, Zienkiewicz and Naylor (1971).

Roscoe et al (1958)recognised the form of the yield surface for the super-critical region but did not attempt to associate a flow rule with it. All the "Cam-Clay" models only attempted to define behaviour of a clay in the

sub-critical region. It was postulated that stiff and overconsolidated clays had behaviour associated with the super-critical region.

Zienkiewicz and Naylor (1971) attempted to develop a model which includes the behaviour associated with the super-critical region. First they reformulated the "Cam-Clay" model in terms of conventional invariants of stress. The parameters p and q of Roscoe and Burland (1968) were expressed as

$$p = \frac{1}{3} \; I_1$$

$$q = \sqrt{3 \; I_2}$$

where I_1 and I_2 are as defined previously. A third parameter θ was adopted, following Nayak (1971) and defined as follows:

$$\sin 3\theta = \frac{27 \; I_3}{2q^3}$$

where I_3 the third stress invariant is expressed as:

$$I_3 = \sigma_1 \, \sigma_2 \, \sigma_3$$

The complete family of yield surfaces was written in the form:

$$F(p, q, \theta, h) = 0$$

h is a strain hardening parameter. This new formulation allows extension of the yield surfaces to a three-dimensional

stress space. For Roscoe and Burland (1968) model, F is discontinuous at the critical state, and separate forms were defined for the sub-critical and super-critical stress states. Schofield and Wroth (1968) and Roscoe and Burland (1968) had proposed forms for the sub-critical state but these were not generalised for three dimensional applications, therefore Zienkiewicz and Naylor (1971) recommended the use of a sub-critical yield surface defined by

$$H\ (p,\ q,\ \theta,\ h) = 0$$

the form of H being selected to suit experimental or theoretical considerations.

For the super-critical stress region, the yield surface F should demonstrate the three following characteristics:

1) strain softening
2) yield according to the Mohr-Coulomb criterion
3) dilation on yielding.

Criteria 1 and 3 are in contrast to the sub-critical yielding which is both strain hardening and non-dilatant. It should be noted that the proposed yield surface differs from the conical surface of revolution about the space diagonal used by Drucker and Prager (1952) in that it is an hexangular pyramid.

A further important refinement made by Zienkiewicz and Naylor (1971) was to make the cohesion a variable, depending on the strain hardening parameter h. This

corresponds to the fact that strain softening is associated with a decrease of the cohesion while strain hardening increases the cohesion for the proposed model.

Since soil is found to be dilatant in the super-critical region, a flow rule producing some dilation, but not as much as would be given by an associate flow rule specifying normality to the yield surface, is necessary. Zienkiewicz and Naylor (1971) introduced a plastic potential similar in shape to the yield surface but with a modification to allow the dilatancy to vary with distance (in stress space) from the critical state. Finally they assumed a linear elastic isotropic behaviour within the yield surface to be applicable. No experimental proof or observational evidence of the applicability and performance of their model was presented.

3.6 The stress-strain model used in this work

In the preceding sections of this chapter, it has been demonstrated that a wide diversity exists in the models proposed to describe the stress-strain behaviour of soil. There appears to be more fundamental differences between the various plasticity models than between the elasticity models. For example, all of the isotropic elasticity models must predict contractive behaviour as long as Poisson's ratio is kept less that 0.5, and non-linearity in the soil behaviour is accounted for by reducing the Young's modulus or the shear

modulus value. On the other hand, volume changes in the plasticity models may vary from strongly expansive to strongly contractive, and non-linearity may be simulated by strain-hardening based on the conventional failure envelope or on a capped yield surface. One fact is clear: more fundamental testing is needed to determine the most suitable model for soil behaviour.

However, the proof of the adequacy of most of the non-linear elastic approaches has come from the successful use of these models in analyses of observed field behaviour. On the other hand no proof has been presented for the accuracy of most of the plasticity models. Only the Roscoe and Burland (1968) plasticity model has been demonstrated to adequately simulate certain classes of soil behaviour observed in laboratory tests.

Still there are uncertainties about the basic assumptions of the theory of plasticity if it is to be applied to soils. These could be summarised in the following points:

1) Does a yield function $f(\{\sigma\}) = K^2$ exist such that if $f(\{\sigma\}) < K^2$, the material behaves elastically, and if $f(\{\sigma\}) > K^2$ it behaves plastically with two independent components of elastic and plastic strains ?

2) Is the soil a stable material as it was described by Drucker (1959)?

3) Is the ratio of plastic stress increment determined by the existing state of stresses ?

4) If so, is the plastic strain increment vector normal to the yield surface ?

Due to these uncertainties in the plasticity assumptions and the successful use of non-linear elasticity models in embankment dam analysis, the non-linear elasticity model has been utilised for the work in this thesis. It is important to note that although the model may be adequate for design purposes, it still does not fully represent the soil behaviour, but there is not sufficient experimental data for using other models at this stage for the soils considered in this thesis.

It is interesting to note that most of the plasticity and elasticity models employ some form of empirical curve fitting procedure in their formulation. The flow rule for most plasticity models is determined by a curve fitting technique. Curve fitting is also employed in the non-linear elasticity models to simulate the stress-strain curves so that a tangent or secant modulus may be found at any stress level.

The widely used equation in the finite element analysis of soil structures to fit the stress-strain curves is the hyperbolic equation, as shown earlier. This curve was first tried for the Empingham trial bank analysis, but

the approach adopted for this example was that of parametric study, which requires a study of the effect of a small change in one at a time of the several variables on the overall stress and displacement fields. The hyperbolic equation is believed not to qualify for this approach, if each parameter which controls the stress-strain curve is tested (i.e. strain at failure, curvature and initial tangent modulus). It was noticed that the initial tangential modulus E_i and the strain at failure as determined by curve fitting using this equation are controlled only by the ratio of the fictional ultimate strength to the actual shear strength (R_f in Kulhawy et al, 1969). Thus full control of a small variation in the strain at failure, which may be crucial for high stress level problems or of small variations in initial modulus, could not be achieved.

The second disadvantage of the hyperbolic fitting relates to the pattern of the family of curves as σ_3 varies. Writing the hyperbolic equation in the form

$$\varepsilon_f\ (\sigma_3) = \left(\frac{1}{1 - R_f}\right) \quad \frac{2\ \tau_{max}\ (\sigma_3)}{E_1\ (\sigma_3)}$$

where ε_f (the strain at failure) is the only constant in the equation, it could be seen that variation of ε_f with σ_3 is dependent on the variation of $\frac{2\tau max}{E_1}$ with σ_3. In other words, if $\frac{2\tau_m}{E_1}$ is kept constant, then ε_f is

also constant as σ_3 varies, which might not be true for real soils.

The second curve fitting used in the application of non-linear elasticity is the exponential equation Janbu (1963) relating the initial tangential modulus E_1 to the minimum principal stress σ_3, using two constants. This equation has been used in finite element work for a wide range of soils under drained and undrained conditions. This equation predicts a value of E_1 equal to zero if $\sigma_3 = 0.0$. This is not the case for undrained clay materials, which hold a value of effective stress (σ_3') while the total $\sigma_3 = 0.0$. Thus this equation is only to be used for drained conditions or undrained conditions of clays which have a high percentage of granular material.

During the course of this research a logarithmic equation is used to represent the stress-strain curve as shown on figure 3.2. Having tried some other functions, the proposed equations provide flexibility and control over the various variables defining the stress-strain behaviour. The explicit form of the equation for axial strain is

$$\varepsilon_r = - \frac{1 + b}{ab^2} \log (1 - ab\, \sigma_r) + \frac{1}{b} \sigma_r$$

where ε_r denotes the strain ratio $= \frac{\varepsilon}{\varepsilon_e}$

ε_e denotes the linear strain $= \frac{(\sigma_1 - \sigma_3)_f}{E_i}$

σ_r denotes the max. shear stress mobilised = $\frac{(\sigma_1-\sigma_3)}{(\sigma_1-\sigma_3)_f}$

a,b denote constants to be determined from the test data.

The equation is written in a dimensionless form, thus enabling a family of curves to be normalised to a single curve from which the two constants a and b can be determined. Normalisation is achieved first by normalising against the shear strength, and then against the linear strain ($\varepsilon_e = \frac{(\sigma_1 - \sigma_3)_f}{E_i}$)

The strain at failure could be written in the form:

$$\varepsilon_f = - \left(\frac{1 + b}{ab^2} \log (1 - ab) + \frac{1}{b} \right) . \frac{2\tau_{max}}{E_i}$$

This value (ε_f) may vary with the variation of σ_3 independently of $\frac{2\tau_{max}}{E_i}$ by linking the constant a with the profile of strain at failure vs σ_3. In this case the constant a will be constant for single curve behaviour, but will vary for the family of curves.

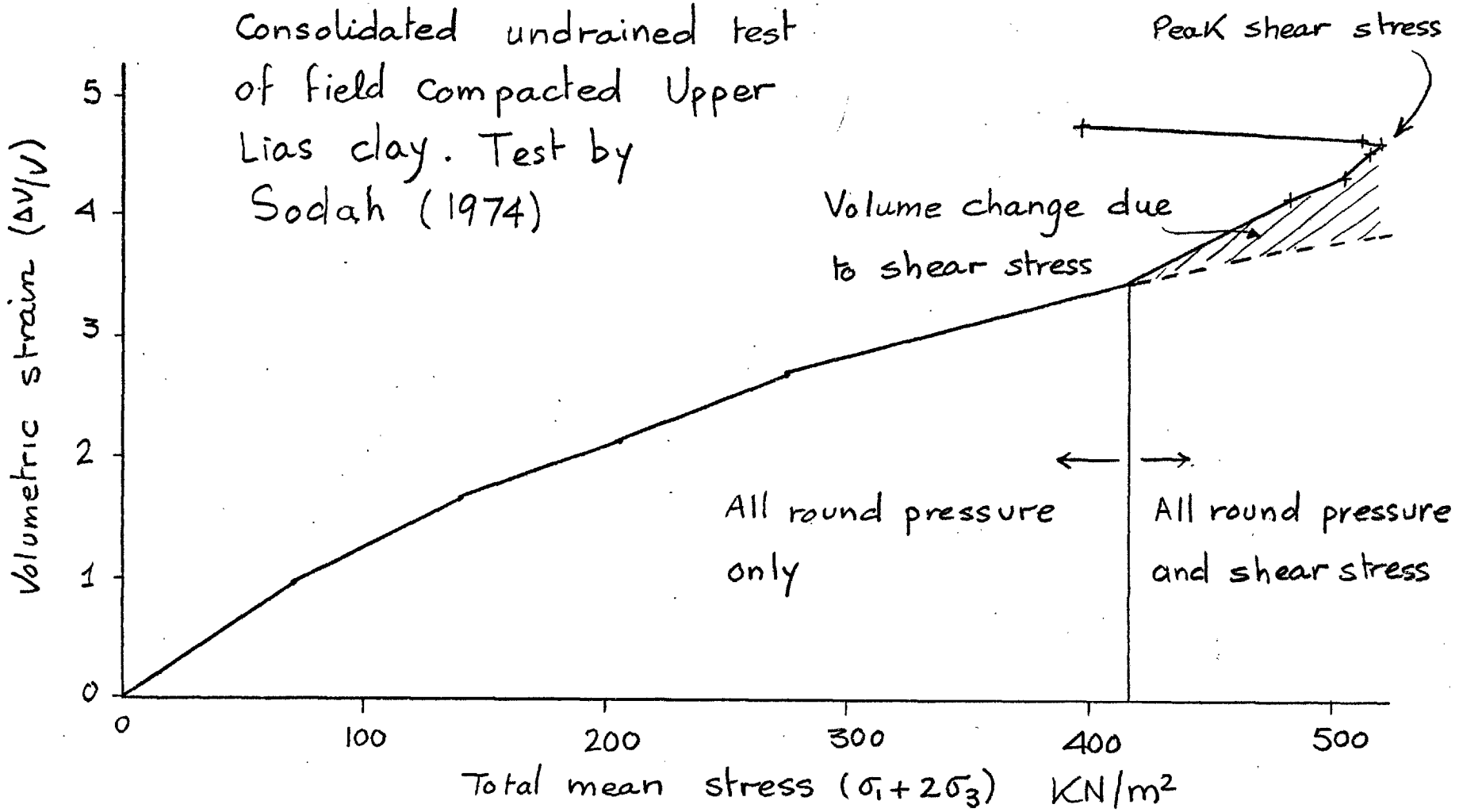
A small program is written to evaluate the constants a and b, in case ε_f does not vary independently with σ_3. If ε_f varies independently, the program will evaluate the values of the constant a at various σ_3 values. In the main program, SAN2, the value of the constant a is evaluated from the given data at the certain stress state using Lagrangian interpolation.

The above equation is fed into the computer in the following form:

$$E_t = E_i \frac{1 - ab\,\sigma_r}{1 + a\sigma_r}$$

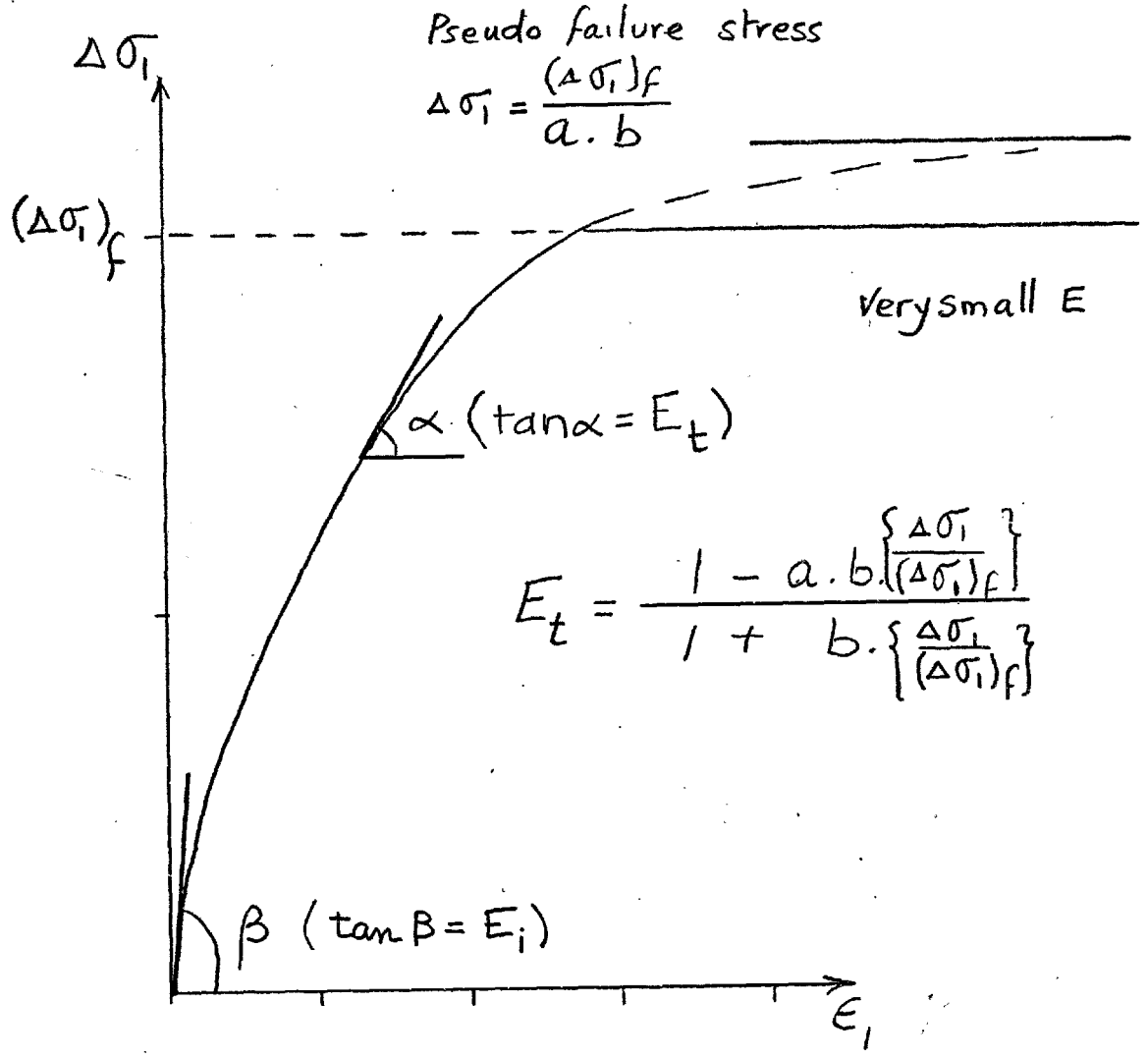
which can be obtained by differentiating the original form. The latter form is more suitable for the non-linear algorithm adopted in SAN2, and for any tangential stiffness method.

The equation relating E_i and τ_{max} with the state of stress and with depth (in the case of foundations) is described in Chapter 4. The constants required to completely define the soil properties are summarised in Chapter 4. Poisson's ratio ν has generally been kept constant in the work described in this thesis as a value close to 0.5 is required to simulate undrained shear. A variation of the programme with ν increasing to 0.5 as failure is approached is described in Chapter 4.



VOLUME CHANGES DURING ALL-ROUND AND SHEAR STRESS STAGES

Fig. 3.1



THE STRESS STRAIN EQUATION

Fig. 3.2

CHAPTER 4

PROGRAMMES

4.1 General

In this chapter is given a description of the programmes developed and used during the course of this research. The main finite element programmes SAN2 and SAN3 are based on a modified version of FESS, which was under development by Naylor in Swansea 1971-72. Input of geometry, boundary conditions, initial stresses, material properties and applied loads are described. Input instructions are the same for SAN2 and SAN3 to facilitate the convenient use of the programmes, although the non-linear techniques and the flow charts are essentially different. The main difference between them is that SAN2 employs a step method and SAN3 an iterative method to follow a non-linear stress-strain curve.

The embankment problems for which the programmes were intended involve large meshes with irregular displays and with distortions of elements to fit complexities of problem geometry. Manual checking of the geometry data input is tedious, yet an undiscovered error wastes computing time and causes delays. To avoid these problems a simple programme (called CHECK) was developed, using the Calcomp facility in the Imperial College Computer Centre. This programme checks co-ordinates and element topography before a finite element computation is made.

To handle and display the vast amount of stress and displacement data produced by each stage of an analysis, a technique to display results graphically was considered essential. The aim of this display was to represent the pattern of general behaviour, rather than to show the variation of some particular function at specific points. Two graphics programmes were written; EASY, which utilises the microfilm hardware machine in the University of London Computer Centre, and HANDY, which utilises the kingmatic machine at the Imperial College Computer Centre.

Finally, a small programme was written to examine the non-linear properties of the stress-strain equations, given the test data, as described in Chapter 3, section 6.

4.2 Programmes SAN2 and SAN3

4.2.1 General descriptions

SAN2 and SAN3 are two-dimensional (plane strain, plane stress or axisymmetric) stress-strain and displacement analysis programmes. The element used is the isoparametic 8-noded element, Irons and Zienkiewicz (1968). The capacity is up to 250 elements and 900 nodes (1800 degrees of freedom). The reduced Gaussian integration rule is used, which is a 2 x 2 integrating point formula. The main solution routine (SOLVE), which is the same as that in FESS, uses the direct Gaussian elimination method, which is the best for solving a system of simultaneous linear equations. The

element stiffness matrix subroutine (ELSTIF), which is almost the same as that in SPAN*, was written for the elastic constitutive law using Lame's parameters, Some error diagnoses were injected in (SOLVE) and (ELSTIF) in order either to warn the user in case of ill-conditioned numbers, or to stop the calculation. Also, (ELSTIF) was modified to deal with the type of stress-strain non-linearity and the techniques introduced in Chapters 3 and 2.

Displacements of nodes at boundaries can be restricted to fixed values, which may be zero. The fixed values may be varied incrementally. The maximum total number of restricted degrees of freedom is 250. Restrictions are only possible in the horizontal and vertical directions. Restrictions in an inclined direction are not available in the programme, but they could be implemented easily.

External loads can be applied as nodal forces, as body forces (force per unit volume) suface normal stresses and surface tangential stresses. These loads may be applied automatically in increments, once the number of increments is specified. The printed output is given in any combination of the following forms for some or all the elements of the problem:-

1) Basic values of accumulated stress and strain
2) Maximum and minimum accumulated principal stresses and strains and their angles and the maximum shear

* SPAN was the name given to Naylor's modified version of FESS.

stress.

3) The first and second stress and strain invariants.
4) The incremental values of the displacements at the nodes.
5) The strength and deformation parameters used during the increment.
6) The maximum shear stress mobilized and maximum to minimum principal stress ratio.

The stresses and strains can be obtained at the Gauss points, at the nodes and/or at selected points within some or all the elements. The values of stress at Gauss points have been shown to be better conditioned than those elsewhere, Naylor (1974), and most attention has been given to these stresses.

The accumulated stresses and strains at the Gauss points and the increments of displacements at the nodes can be stored on magnetic tape or discfile for subsequent graphic plotting and/or for future reference, or to be used as input data for subsequent Loading Conditions. The forces calculated at the nodes, equivalent to the final state of stress are compared to the load vector representing the applied loads in order to check the equilibrium. The results of this comparison are also given in the printed output for each increment of load.

4.2.2 Input of Geometry.

The domain is divided into four-sided elements. The ratio of length to width is kept to a minimum, particularly for areas of concentrated stress variations. A four sided element can be distorted to a triangular element with 5 nodes in one of its sides. A test was carried out using such elements and the results compared with the closed form solution for a hollow cylinder. The stresses at the Gauss points showed acceptable agreement, as did displacements at the nodes. Stresses at nodes showed very poor agreement.

During the preliminary analyses of Empingham main dam it was found that elements which had a large length to width ratio* and which were also severely distorted from the rectangular did not transmit their own weight in a uniform way during simulation of construction in layers. It is recommended that particular care should be taken in proportioning elements which will act as applied loads, particularly if ν close to 0,5 is used. (A badly conditioned element can be tolerated for stress calculation, since it has no effect on the overall solution and the error it produces is only local. However, a badly conditioned element which is used to apply load will apply an incorrect load and therefore effect the overall solution).

The geometric input data is presented as the coordinates of the corner and/or mid-side nodes and as the element topography, i.e. a list of the nodes around each

* A maximum ratio of 1:5 was usually adopted in the work presented, based on previous experience. When stress variation along the long axis of the elements was small, ratios up to 25 were used without any apparent instability resulting.

element. If the coordinates of a mid-side node are given and they do not lie in a straight line with the two corner nodes, the computer will assume a parabolic curve for the element side. If the mid-side node is not given, the programme will assume that the node lies on a straight line between the corner nodes and midway between them.

4.2.3 Input of material properties.

Up to 15 different materials can be modelled in one analysis. The number of parameters available to describe each material property is 32. Only 16 have been used in the work so far, the remainder being available for the future development of more sophisticated soil models, The soil model so far programmed is that described in Chapter 3, plus some recent developments described subsequently.

The initial tangent modules, E_i, is programmed as the general equation, which can be used as it stands or to define certain special cases.

$$E_i = \text{PROP1} \quad \left(P\left(\frac{\sigma_3}{p}\right)^{\text{PROP7}} + \text{PROP6}.\ z + \text{PROP14}.\sigma_3\right) \qquad 4.1$$

where:

PROP1, PROP7, PROP6, PROP14 are constants

σ_3 = min. principal stress (compressive)

z = depth of point below ground surface

p = atmospheric pressure.

This equation facilitates the use of an initial tangent modulus which may be varied either:

a) linearly with depth z (PROP1 and PROP6)

b) Exponentially with σ_3 (Janbu,1963) (PROP1, PROP7)

or c) linearly with σ_3 (PROP1, PROP14)

In each case the unwanted constants may be set to zero.

The following are illustrative examples.

a) E_i varies with depth z only.

PROP14 = PROP7 = 0

It is programmed that if PROP7 = 0, then p = 1,0 and the general equation becomes

$$E_i = PROP1\ (1 + PROP6.z)$$

b) If E_i varies with σ_3 only (linear)

PROP6 = PROP7 = 0

and the general equation becomes

$$E_i = PROP1\ (1 + PROP14.\ \sigma_3)$$

c) If E_i varies exponentially with σ_3

PROP14 = PROP6 = 0

and the general equation becomes

$$E_i = PROP1.p\ \left(\frac{\sigma_3}{p}\right)^{PROP7}$$

The shear strength programmed is that defined by the Mohr-Coulomb or Tresca failure criteria in the form

$$\tau_f = PROP9\ (1 + PROP10.z + PROP11.\sigma_3) \qquad 4.2$$

where PROP9, 10, 11 are constants. Giving appropriate values the general equation (2) can take the following terms

$$\tau_f = \text{PROP9}$$

$$\tau_f = \text{PROP9}\ (1 + \text{PROP10}.z)$$

$$\tau_f = \text{PROP9}\ (1 + \text{PROP11}.\sigma_3)$$

These equations can deal with drained shear with constant pore pressure, undrained shear of saturated and partly-saturated soil and the variation of undrained shear strength with depth.

The tangent modulus, E_t, for a given $(\sigma_1 - \sigma_3) < \tau_f$ is programmed as follows (See Chapter 3, Section 6)

$$E_t = E_i \frac{1 - \text{PROP12} \times \text{PROP13}\ (\frac{\sigma_1 - \sigma_3}{2\ \tau_f})}{1 + \text{PROP13}\ (\frac{\sigma_1 - \sigma_3}{2\ \tau_f})} \qquad 4.3$$

where PROP12, 13 are constants from test data

E_i & τ_f are calculated from equation 4.1 & 4.2.

The programme in which PROP12 and PROP13 are determined from test date is written in FORTRAN and BASIC. A very small value is assigned to E_t when $(\sigma_1 - \sigma_3)$ is equal to (or greater than) τ_f.

The value of Poisson's ratio ν is assigned the constant PROP2. The variation of ν with state of stress, as discussed subsequently, has not been used in the work

presented in this thesis.

Uniform linear material properties is a special case, obtained as follows:

a) PROP12 = PROP13 = 0, Equation 4.3 becomes $E_t = E_i$

b) PROP7 = PROP14 = PROP6 = 0, Equation 4.1 becomes E_i = PROP1.

c) PROP9 = PROP10 = PROP11 = 0, Then it is programmed that PROP9 takes a very large value.

4.2.4 Input of initial stresses.

The initial stresses in the soil at the start of loading must be known so that moduli may be selected for the first loading increment which are equivalent to the point on the stress-strain curve which matches the initial stresses. For real soil with negligible ground slopes

$$\sigma_z = \Sigma \gamma \delta_z$$

where σ_z = vertical stress

z = depth below ground surface

The horizontal stress is given by the coefficient of earth pressure at rest, K_o, where

$$\sigma_x' = K_o . \sigma_z'$$

K_o may vary with depth, Skempton (1961) K_o may be different on the x and y planes, and it is convenient to programme in

terms of total stress. Hence the initial stresses are programmed according to the following equations.

$$\sigma_z = C.z$$

$$\sigma_x = K_{ox}^* . \sigma_z , \quad K_{ox}^* = C_1 + C_2 . z$$

$$\sigma_y = K_{oy}^* . \sigma_z , \quad K_{oy}^* = C_3 + C_4 . z$$

where

C = bulk unit weight of the soil

C_1, C_2 = the constants linking K_{ox}^* with z

C_3, C_4 = the constants linking K_{oy}^* with z

Values of the above constants are specified for each element and the initial stresses are calculated automatically for each node for which a value z is specified. The initial stresses at the Gauss points are then computed using the shape functions and the values at the nodes, for those elements which share nodes at which the initial stresses were specified. Nodes may be shared by more than two elements, and, where construction in layers is simulated, initial stresses may not be required in all the elements. The programme contains a facility for restricting the assumption of initial stresses to specified elements in this situation. It is also possible to specify initial stresses (σ_x, σ_y, σ_z, τ_{xz}) directly at the nodes, as well as calculating them by the above method.

4.2.5 Dealing with the construction sequence

Simulating the construction of an embankment dam may involve excavation and/or building in layers. Excavation may be simulated by eliminating tractions at the post-excavation surface. This is easily programmed by adding a system of nodal forces equal in magnitude and opposite in directions to the forces acting, at the excavation surface due to the state of stress before excavation. This process is performed automatically by specifying the code numbers of the appropriate nodes in the appropriate input queue. The elements to be 'excavated' are assigned a stiffness close to zero, which gives an upper bound to the displacement field.

Construction in layers is simulated by using the dense liquid technique, King (1964), for the new layers. The elements representing the new layers are initially assigned a very small Young's Modulus and a Poisson's ratio close to 0.5. There are two ways of applying the load due to placing a new layer to the underlying soil. Firstly, the elements in the new layer may be given weight. The stresses obtained within the elements are correct for fluid properties assumed in the elements. The stiffness of the layer is increased subsequently and the increased stiffness operates during subsequent loading, see figure (4.1) for description of the method. Secondly, placing the new layer may be simulated by applying a pressure normal to surface between

the new layer and the rest of the soil, equivalent to the height of fill. The stresses within the new layer are specified as initial stresses for subsequent calculations.

The first approach predicts horizontal stresses initially nearly equal to vertical stresses. In the second approach horizontal stresses initially greater than vertical stresses can be specified, which may correspond more nearly to over-consolidation by compaction. The effect of different initial stresses will appear when values of E are selected for subsequent loading steps.

The disadvantages of the dense liquid technique are, firstly, that the wrong stiffness is used for the layer, resulting in an underestimated overall stiffness matrix, secondly that no shear stresses are transmitted by the new layer during the application of its own load, and, thirdly, that the strains in the new layer are very large. A subroutine (CORSTN) has been written to correct the values of strain for the new layer using the correct stresses and the true stress-strain properties (in secant modulus form). The algorithm is as follows:-

Enter Gauss point loop

1. Look up stress values
2. Calculate shear strength (τ_f)
3. Calculate max shear stress ($\sigma_1 - \sigma_3$)
4. Calculate secant modulus corresponding to the stress level
5. From 1 & 4, Calculate the strain vector.

The subroutine is used for only these elements which represent the new layers. These elements are identified by the computer as they are assigned a very small value for PROP1 and the true values of PROP1 to PROP16.

4.2.6 Non-linear Programme - SAN2

This programme is based on the quasi Runge-Kutta one step technique, described in principle in Chapter 2. A flow chart is given in Appendix.

As described previously, the load vector is applied in one step. However, the non-linear algorithm includes the evaluation of each element stiffness matrix, assembling them to form the overall stiffness matrix, solving, and repeating the complete process for a second time. During the first solution, the properties of the soil are set according to the pre-existing stresses, and may include failure ($E \neq 0$). The stresses derived from the first solutions are calculated to correspond to some proportions of the displacement vector obtained from the first solution (Subroutine SELECT), as explained in the subsequent algorithm . These stresses are stored in a local disc and are not added to the initial stresses at the start of the increment, because they do not contribute to the final stress results; they are only used as a pilot estimate of the magnitute and direction of the new stress increment.

In the second solution, the stiffness matrix for each element is calculated according to the following algorithm (Subroutine NLELAST)

Enter Gauss point loop

set $\gamma_1 = 1.0$ (γ_1 is defined in Chapter 2)

1. Retrieve the stress vector corresponding to half the displacement increment obtained in the first solution. Multiply it by γ_1. The output is, say, $\Delta\sigma^*$

2. Add $\Delta\sigma^*$ to the initial stresses at the start of the increment.

3. Calculate principal stresses and shear strength from the stresses resulting from (2).

4(i) If the max. shear stress from (2) is less than 95%* of the shear strength from (3), then the modulus is calculated from equation (4.3) and stored in a local disc. (RETURN).

(ii) If the max. shear stress is more than 95% of the shear strength but less than it, half the value from equation 4.3 is taken and stored (RETURN).

(iii) If the max. shear stress from (2) is more than the strength from (3), then γ_1 is set to $0.5\gamma_1$. (GO TO STEP 1).

4(iii) is the start of an iterative process which is performed for each Gauss point. Following this algorithm

* This was tried empirically and found satisfactory for the problems tried herein.

(1 - 4(i)) ensures that deformation properties equivalent to the average stresses for the increment are adopted, Steps 4(ii) and 4(iii) ensure that this does not imply significant overshooting if the stresses are near failure, which would otherwise occur in a one step, non-iterative method.

Subroutine NLELAST selects material properties for the second solution. The stress and strain increments from this second solution are then added to the stresses existing before the load increment to give the final result.

4.2.7 Non linear Programme - SAN3

This programme is based on the Alpha-Constant stiffness matrix technique Nayak, (1971). This technique has been simplified in SAN3, as described in Chapter 2. It was the first non-linear technique developed, but was replaced by SAN2 for the embankment analyses presented in this thesis for the following reasons.

(i) SAN3, if terminated at an arbitrary residual error, will result in a situation where the stresses are in agreement with the stress-strain curve but the finite element structure is not in equilibrium with the applied loads. In this situation the engineering significance of the errors is difficult to evaluate.

(ii) SAN2, should always produce a solution in equilibrium which allows a result to be checked manually. The errors occur due to the failure to follow the stress-strain curves exactly, they can be readily examined by comparing the

nominated and actual stress-strain curves (see Chapter 2) and they can be controlled by reducing the size of the loading increment.

(iii) SAN2, is naturally suited to a problem such as a simulation of embankment construction in layers, where results after a number of small loading increments are required, and, for this type of problem it appeared to be more efficient.

SAN3 may prove a useful tool for single load increment problems and it may allow strain-softening problems to be examined.

In SAN3 the root mean square of the residual is used as a measure of convergence which should decrease and become very small as the iteration proceeds. The iteration is terminated when the root mean square reaches a pre-set value, or when a pre-set number of iterations have been performed. The acceptance standard is arbitrary, and is based on experience, especially in the case of non-monotonic convergence.

The principal factors concerning the acceleration vector alpha are:-

a) The alpha vector which is equal in size to the number of degrees of freedom used should be stored in the computer core, increasing the space required.

b) The alpha vector is only updated every second iteration. This is the main simplification to this method which was developed by Nayak (1971).

c) Nayak's limits on the calculated value for the components of the vector are used. These are, firstly, if alpha is updated to a value greater than 8, it is set to 4, and, secondly, if alpha is updated to a value less than zero, it is set to 1.

SAN3 is an iterative method which requires careful examination during the solution. Its use is potentially dangerous for large problems with high non-linearity unless the user is fully familiar with the programme.

4.2.8 Shear unloading.

SAN2 has been modified to accommodate shear unloading. In the first solution of the non-linear technique it is established whether the shear stress will increase or decrease, and the Gauss points at which a decrease will occur are identified. For these points a linear modulus is adopted during the second solution. If shear stresses increase again after unloading the first loading stress-strain curve is followed.

4.2.9 Poisson's ratio ν varying with stress.

This programme development has not been used in the analyses presented in this thesis but has been used to simulate drained shear. Two variation equations are used. Following Kulhawy et al (1969) the initial value, ν_i is

varied as

$$\nu_i = M - N \ln \frac{\sigma_3}{pa}$$

where M and N are constants

pa = atmospheric pressure,

During shear, the following equation is used:

$$\nu = \nu_i (1-R) + R/2$$

where $$R = \frac{\sigma_1 - \sigma_3}{(\sigma_1 - \sigma_3)_f}$$

thus $\nu = \nu_i$ under isotropic stress and $\nu = 0,5$ at failure,

In the computation ν is selected and modified in the subroutine NLEAST for each loading increment in the same way as is described for E in section 4,2,6,

4.2.10 Strain loading.

In Chapter one it was shown, using the virtual work principle, that, the subjection of an element e to a strain vector $\{\varepsilon\}$ over its region Ω, maybe represented by a nodal force vector $\{F\}^e$ of the form:

$$\{F\}^e = - \int [B]^T [D] \{\varepsilon\} \, d\Omega$$

at its boundary, where $[B]$ and $[D]$ are the geometrical and material properties matrices of that element respectively.

This strain loading is programmed in SAN2 taking account of the fact that non-linearity exists not only on the

left hand side but also on the right hand side of the overall stiffness matrix equation because the load vector $\{F\}^e$ is dependent on the modulus matrix $[D]$.

The strain loading facility may have a wide range of applications in the soil mechanics field, for example:

1. It could be used to simulate a volume change during shear and/or a volume change corresponding to $\nu > 0,5$.
2. It is a technique for solving the problems associated with a sudden change in the volume of materials such as loess or rock fill shoulders under impounding.
3. It could be used to simulate the mechanical effect of freezing a soil foundation.
4. It could be used as a means of simulating the partly-drained loading case.

4.3 The graphics programmes EASY and HANDY

The microfilm programme EASY is written to process the output from either SAN2 or SAN3, previously stored on magnetic tape, and to display it in graphic form. The input is in two parts:-

a) The stresses and strains for each Gauss point of each element. This is read, element by element, in the form of the element code number first, then the number of Gauss points in the element, then the values for the Gauss points in present order.

b) The geometric input data is as for SAN2 and SAN3. The

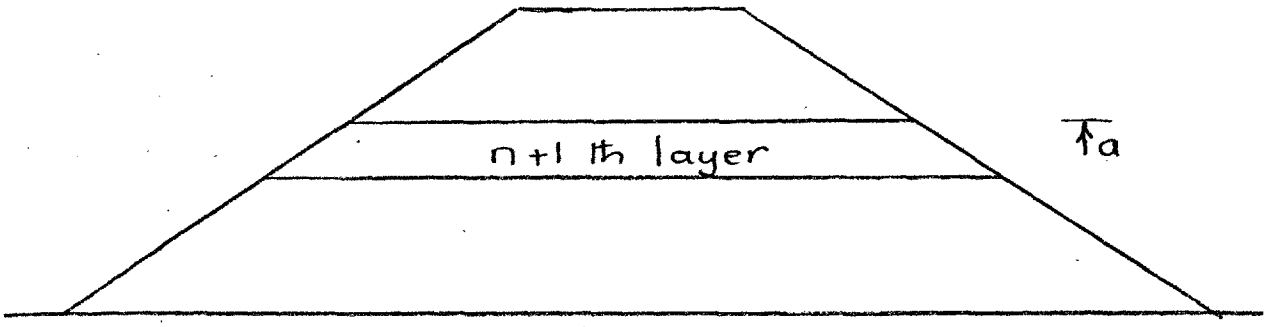
geometry is fed in afresh, rather than stored on magnetic tape with the stresses and strains, as this method was found to be quicker and cheaper.

Functions which can be printed as numbers at some or all of the Gauss points are:-

Horizontal, vertical and shear stresses and strains.
Maximum and minimum principal stresses and strains
Maximum shear stress and strain
The ratio between maximum shear stress and the shear strength.
The stress ratio σ_1/σ_3.

Functions which can be printed graphically are:-
Principal stresses and their rotation with respect to the horizontal, shown as crosses drawn to scale.
Displacements represented in vector form by arrows, which can be a sequence of straight lines representing displacements for each successive load increment.
Displacement vectors can be requested for all corner and mid-side nodes, for Corner nodes only, for part of the domain only or for any selected nodes.

The Kingmatic programme HANDY was written to display horzontal strains and displacements as a continuous function along any horizontal surface at any stage of incremental loading. An outline of the structure is automatically drawn. Data is input in the same way as for EASY.



Solution for n+1 th layer

Layers 1→n have stiffnesses determined from stresses developed during placing of n+1 th layer.

Layer n+1 + subsequent layers have very low stiffness.
Layer n+2 + " " have zero weight.

Solution is obtained, with surface of n+1 th layer kept at elevation a.
Loading on n th layer equivalent to that of a heavy fluid.
Stresses in n+1 th layer are isotropic.
Strains in n+1 th layer are discarded.
n+1 th layer given stiffness from computed stresses.
Strains and displacements in n+1 th layer computed from these stiffnesses and from computed stresses.

Process repeated for layer n+2

Since layer n+1 has negligeable stiffness as its weight is applied, displacements in layers 1→n are overestimated.

N.B. If n+1 th layer were made stiff before its weight was added, displacements in underlying layers would be underestimated.

In prototype construction, both weight and stiffness would be added together as each load of fill was placed + compacted.

Errors will be a function of the layer Thickness used in the computer model.

SIMULATION OF CONSTRUCTION IN LAYERS

Fig. 4.1

CHAPTER 5

STABILITY OF NON-LINEAR SOLUTION TECHNIQUES

Two questions must be posed when judging the validity of a finite element solution to a soil continuum problem,

(i) How well does the mathematical stress-strain model represent that part of the soil behaviour which is relevant to the problem ?

(ii) How well does the numerical solution technique obey the nominated mathematical stress-strain model ?

The first question was considered in Chapter 3. In this Chapter the second question is discussed in engineering terms drawing only on examples encountered by the author.

A numerical solution technique should ideally produce stresses, strains and displacements satisfying both equilibrium, locally and overall, and the stress-strain relationship. In practice the solution technique may result in one or more of the following numerical 'crimes' being commited; the effect of each crime on the acceptability of the solution will vary:-

(i) The nominated stress-strain curve is not followed precisely. The extent to which the nominated stress-strain curve is followed by the SAN2 programme is shown in figure (2.3b) of Chapter 2, which indicates that the solution technique, although satisfying equilibrium, does not satisfy the stress-strain relationship but follows

a slightly stiffer one.

(ii) The nominated strength of the soil is exceeded (i.e. over-shooting) leading to a state of stress beyond the soil capability, a situation which over-estimates the safety of the structure, especially for problems involving low factors of safety.

(iii) Numerically badly-behaved regions of the domain may lead to a complete failure of the solution.

In extreme cases, failure of the numerical solution technique to obey the nominated mathematical stress-strain model may result in numerical instability. This instability may occur when the technique has to deal with one of the following:-

a) nearly incompressible materials.
b) two adjacent materials with very different moduli (e.g. concrete adjacent to soft rock),
c) the introduction of a shear strength cut-off in the stress-strain relationship.

The first point was investigated by Naylor (1974) and is examined further in Chapter 6 of this thesis. Using linear material properties and a Poisson's ratio of 0.499, Naylor showed that, provided the reduced Gauss integration rule is used with the 8-noded isoparametric element, the stress results based on the average of the 4 Gauss points are smoothly distributed without oscillation. This finding is

also demonstrated to be true for both the non-linear cases presented in Chapter 6 and subsequently in this Chapter.

The author has not had to deal with the second point during the course of the work presented here, but it can be speculated that a large ratio of moduli, depending on the computer used, may cause numerical instability.

The third and the most important point is that of the shear strength cut-off. At low factors of safety, a large part of the soil domain will be in 'local failure', i.e. the soil elements can not sustain any increase in shear stress, which is normally associated with increase in strains. A sound non-linear solution technique should reproduce this state with acceptable over or under-shooting. A point with a shear stress higher than its shear strength is an indication of an inadequate solution algorithm. While inability to follow the lower part of the stress-strain curve may lead to an error in the strain and displacement field, inability to follow the strength cut-off leads to an error in stresses which is the most important factor in the assessment of a structure's stability, especially if the behaviour of the soil forming the structure is controlled by the strength parameters. With increasing applied load, the local failure zone is bound to increase until the whole structure fails. Again, a sound non-linear technique should allow the structure to "fail" before any numerical troubles are encountered, i.e. the stresses, strains and displacements

are still satisfying equilibrium and the stress-strain relationship.

Predicting failure, in the way it is described above, is a valuable facility for some classes of soil problems, although assessing stability of the structure under working loads is another matter. The numerical behaviour of the solution at failure load has to be checked if the programme is to be used for stability studies. Such a check has been made by Davachi (1976). Using the programme SAN2, he has solved the strip footing problem and compared the failure load predicted by the finite element solution with the exact solution of Prandtl (1920).

Figure (5,1) shows the stress-strain curve and the geometry of the problem solved. Figure (5,2) shows the settlement-load curve, in which the shape shows general shear failure, and a very close prediction of the collapse load is obtained. Figures (5,3, 5,4, 5,5, 5,6) show the values of some stresses, at the failure load, which are stable and local over shooting did not exceed 12% .

Thus it is demonstrated that the solution is stable and accurate for failure with simulated undrained saturated soil properties.

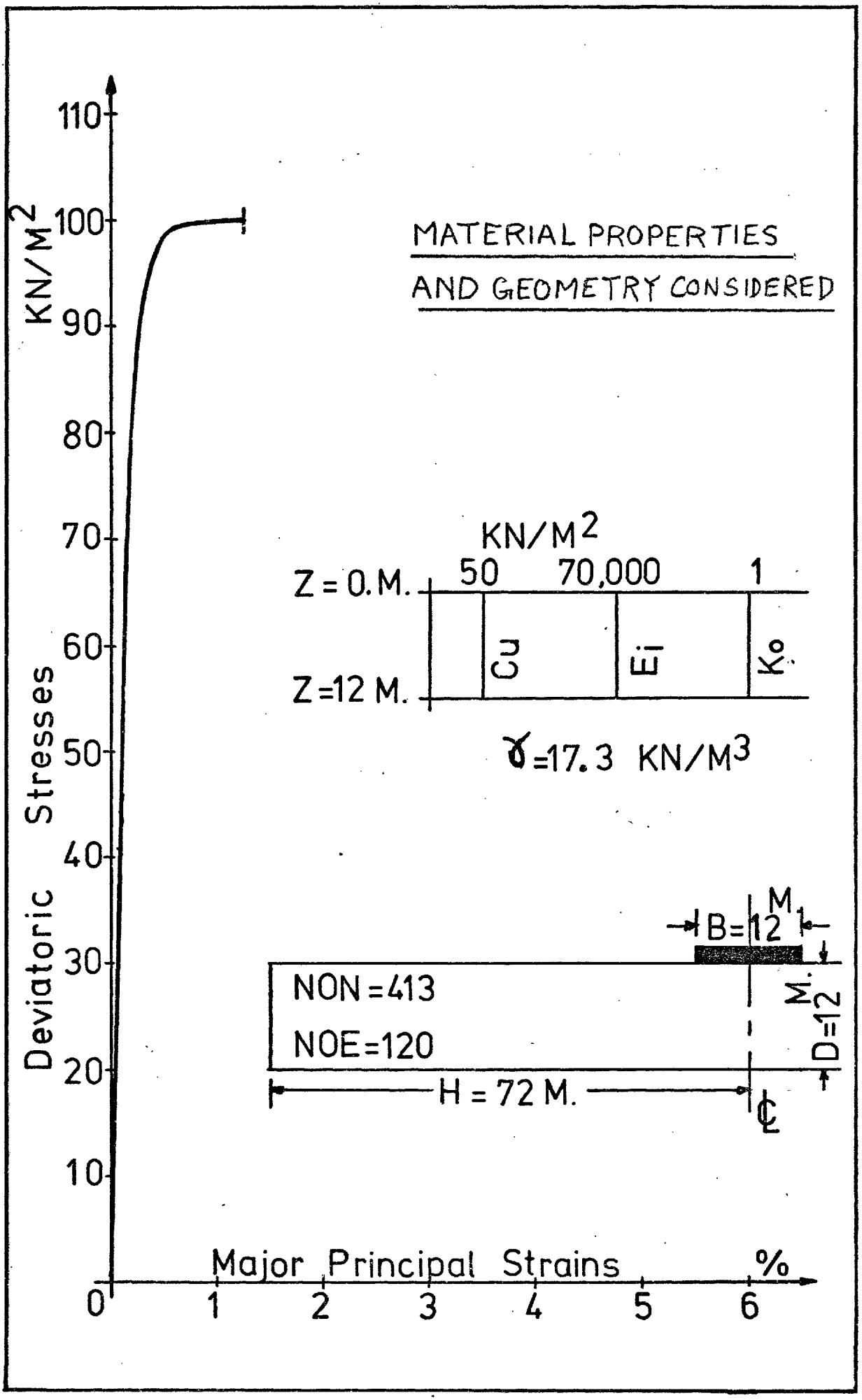
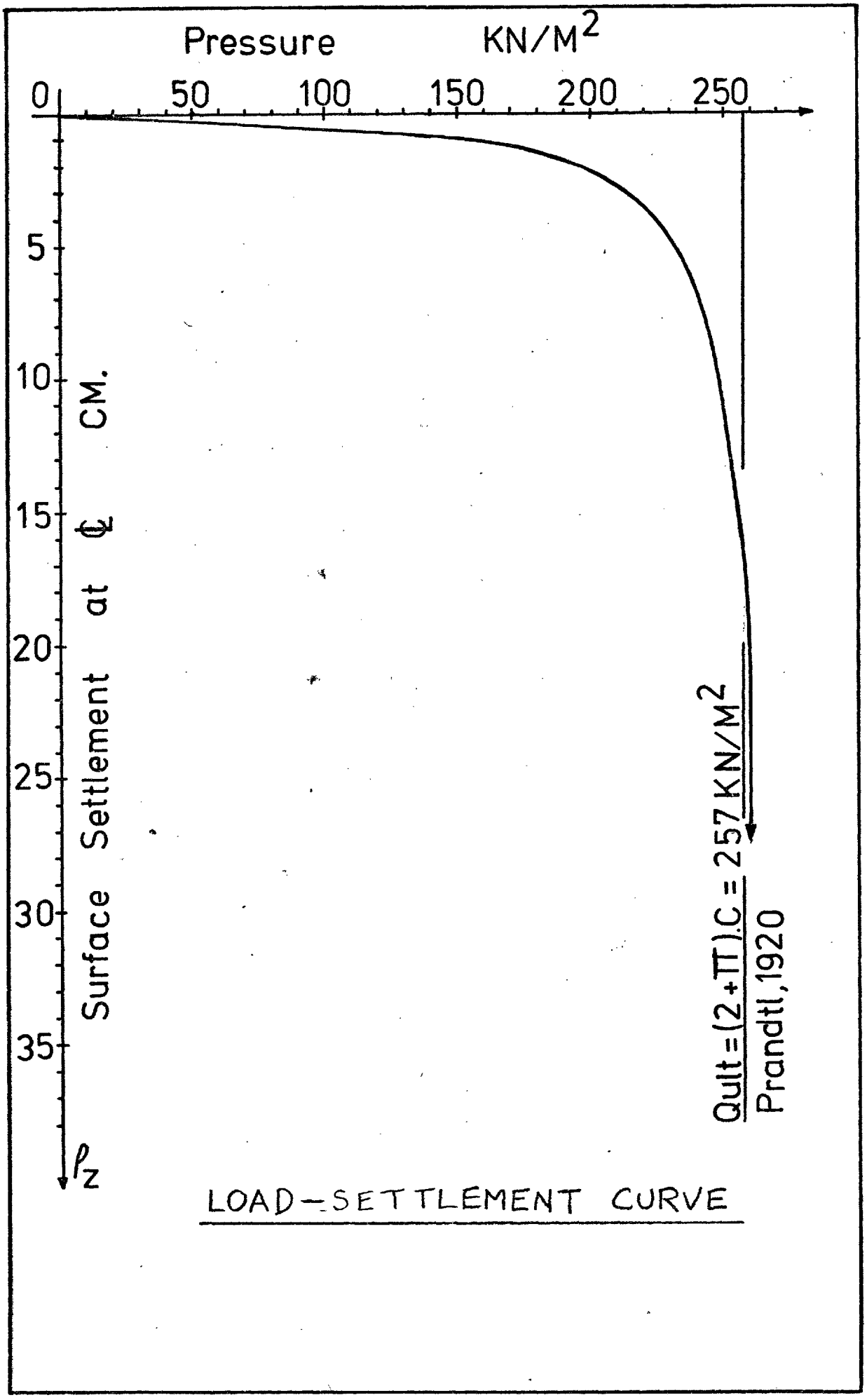
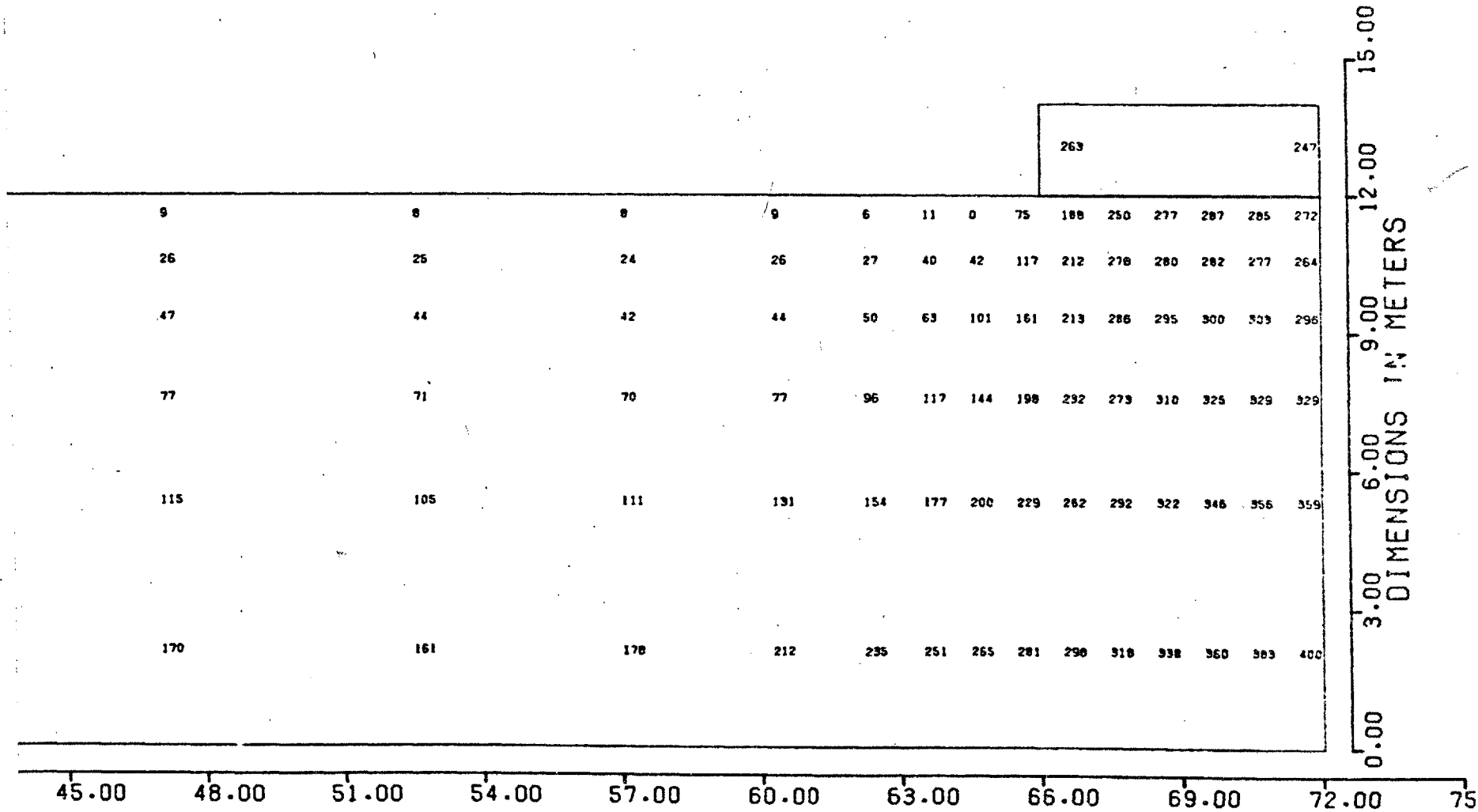

MATERIAL PROPERTIES
AND GEOMETRY CONSIDERED
KN/M2
Deviatoric Stresses
110
100
90
80
70
60
50
40
30
20
10
0
1
2
3
4
5
6
Major Principal Strains
%
KN/M2
50
70,000
1
Z = 0.M.
Z =12 M.
Cu
Ei
Ko
γ =17.3 KN/M3
M1
B=12
NON =413
NOE=120
M.
D=12
H = 72 M.
℄

Fig. 5.1



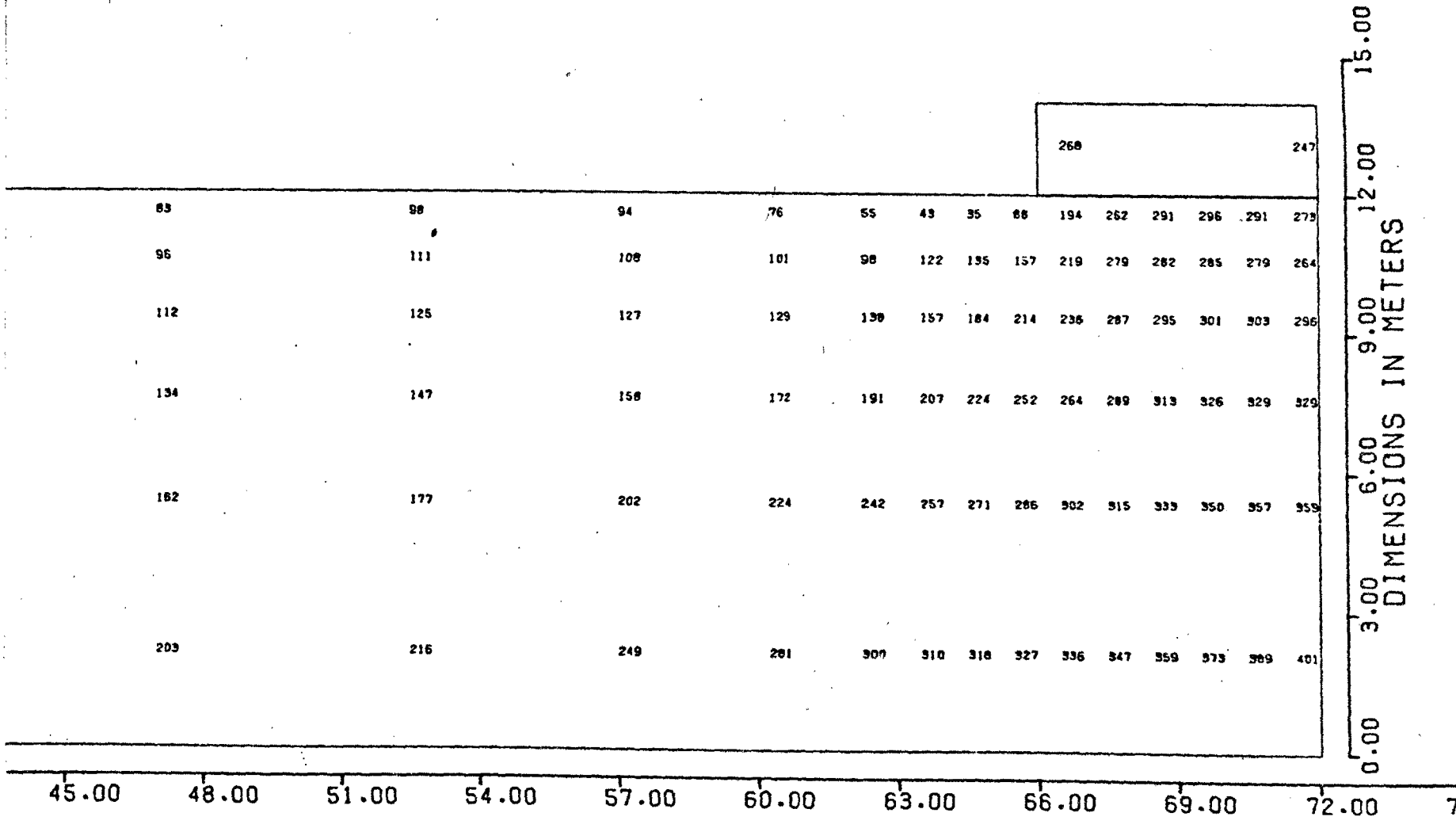
LOAD-SETTLEMENT CURVE

Fig. 5.2



VERTICAL STRESSES AT FAILURE

Fig. 5.3



MAX. PRINCIPLE STRESSES AT FAILURE

Fig. 5.4

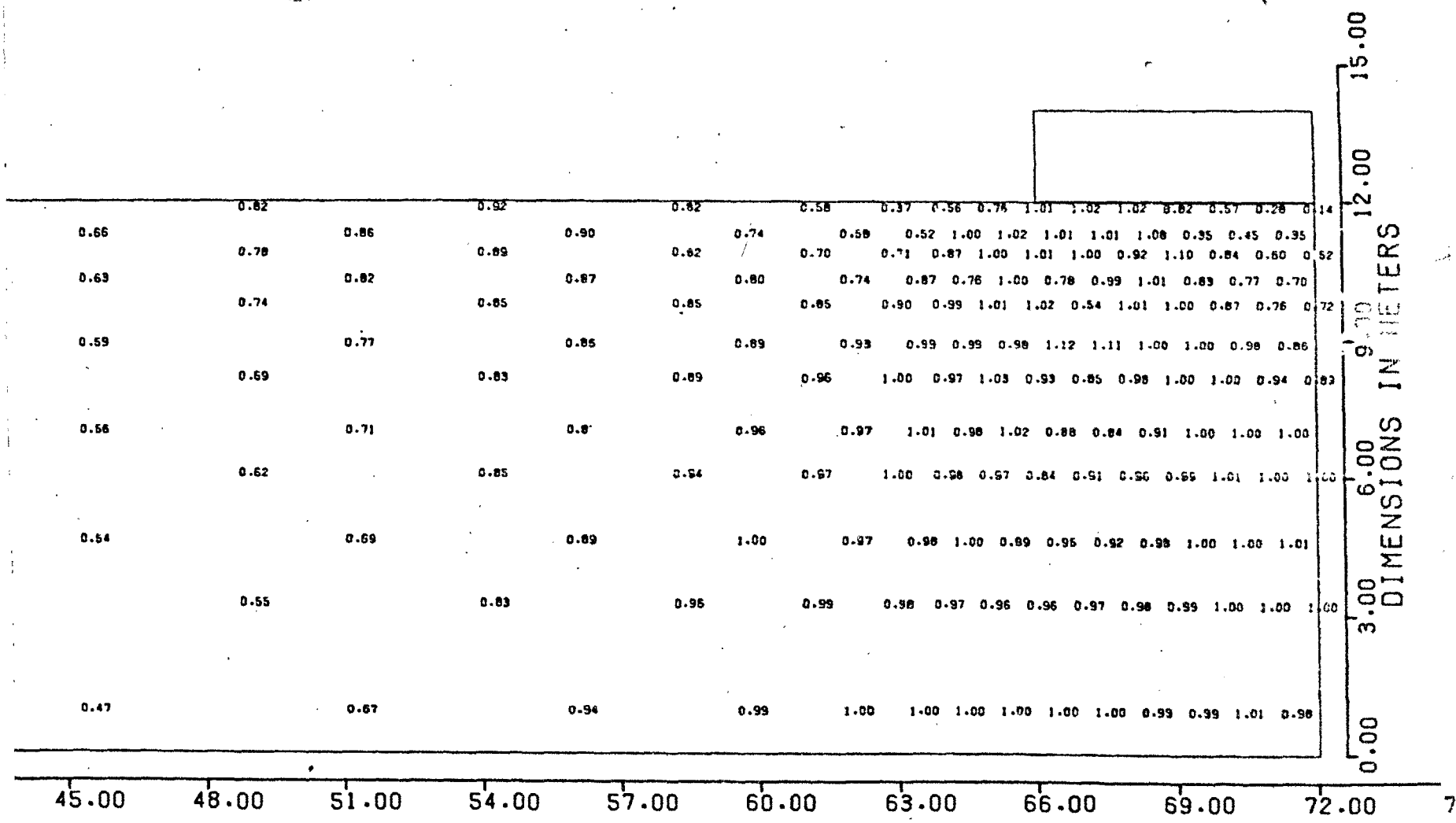
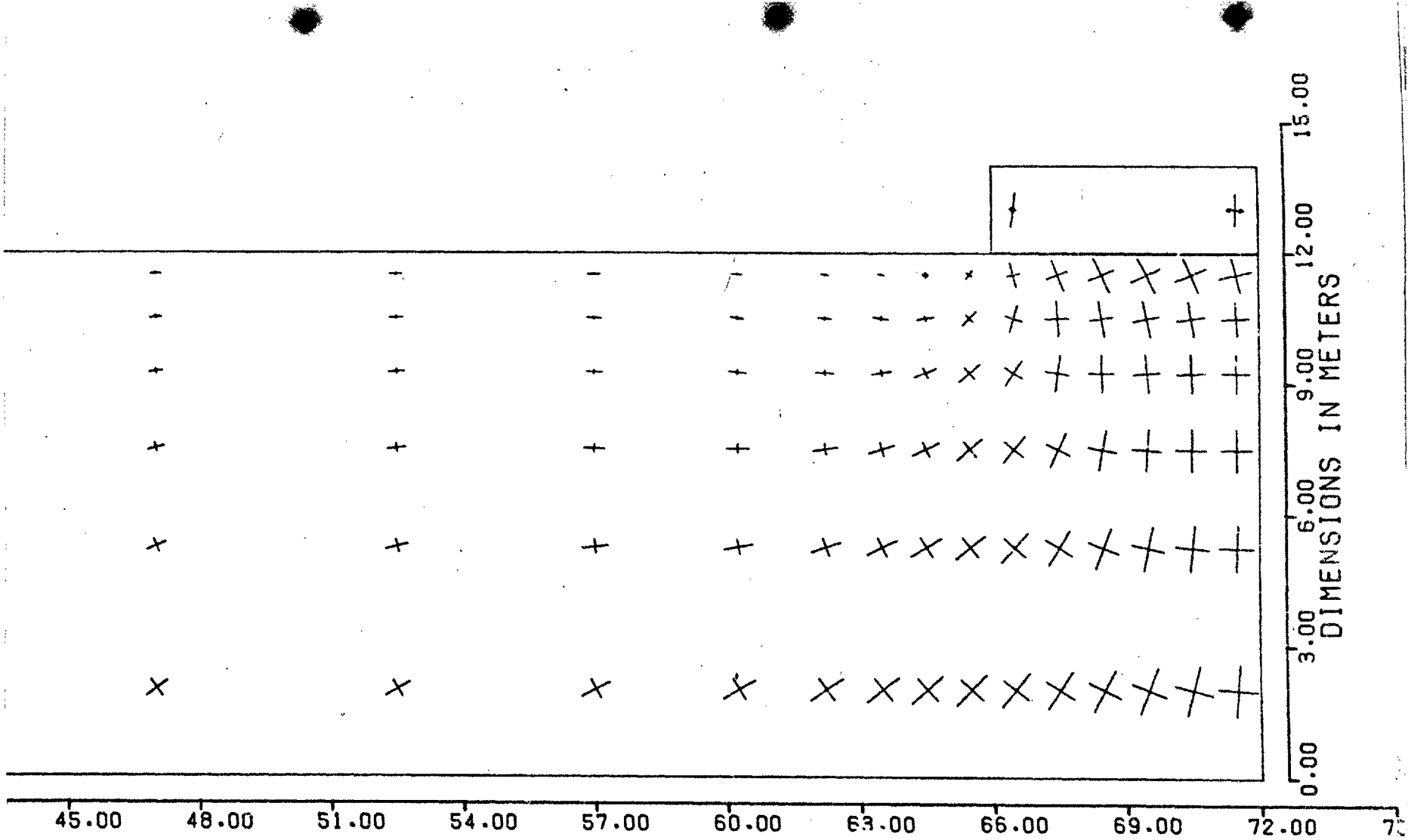


Fig. 5.5

MOBILIZATION OF SHEAR STRENGTH



DIRECTIONS OF PRINCIPLE STRESSES

Fig. 5.6

CHAPTER 6

ANALYSIS OF EMPINGHAM TRIAL BANK

6.1 Introduction

Empingham dam was constructed during the period 1970-1974 for the Welland and Nene River Authority as part of a pumped storage scheme for water supply. The Consultant engineers were T & C Hawksley. Professor A.W. Bishop, Dr.P.R. Vaughan and Mr.J.M. McKenna acted as geotechnical advisors.

General descriptions of the site geology and of the dam are given by Werneck (1974) and Maguire (1975) and will not be repeated here. A brief description of the problems which lead to the construction of the trial bank are given in section 6.2. The purposes of the finite element analysis are discussed in section 6.3. The remaining part of the chapter deals with analysis, results and conclusions.

6.2 Purpose and brief description of the trial bank

The dam is 40m high, of compacted Upper Lias Clay fill, on a foundation of over-consolidated brecciated Upper Lias Clay which was severely sheared and distorted by valley bulging and peri-glacial frost action. Figure (6.1) shows a section of the valley at the dam. A typical cross-section of the main dam is shown diagrammatically in figure (6.2). The properties of the clay foundation, both undrained and partly drained where sand-drains are used, controlled the

stability. Operational shear strengths of over-consolidated clays are difficult to predict by laboratory testing, as they involve sample size problems, test rate effects, anisotropy, progressive failure, variation of strength with depth, etc, These problems are discussed in detail by Maguire (1975).

The operational shear strength determination was the major problem in making design assumptions. There was limited information on the properties of the Upper Clay from previous engineering works. There was scarce and somewhat conflicting information on the undrained and drained strength of the foundation.

The general site investigation utilized conventional tests on standard-sized soil samples and the results were all subject to sample size effects. 260mm diameter plate tests were performed to examine the undrained strength and these gave results similar to the 100mm diameter triaxial tests. The application of this result to the design without further confirmation was not considered prudent. Further in-situ tests were considered, but time was short and only the bulk undrained strength could have been examined for a relatively small volume of the clay, thus a reliable bulk design strength including the full effect of foundation shears could not be determined. A conservative final design could have been prepared but it would have relied largely on judgement, unconfirmed by quantitative information,

Also, it has been shown by Sodah (1974) that

properties of compacted clay fills cannot be predicted from tests on laboratory compacted specimens but can be predicted from tests on samples taken from field compacted material.

As a consequence of these difficulties the decision was taken to construct a large instrumented trial bank, which is discussed in detail by Werneck (1974). The trial embankment was constructed as part of the main contract, which was let on a provisional cross-section, and was later incorporated in the main embankment. The construction sequence was arranged to allow the trial bank to be built within the upstream berm early during construction. Figure (6,3) illustrates its relative position. Provision was made in the contract for modification of the final dam cross-section after completion of the trial bank, thus a method of designing as construction proceeded was adopted. The main provisonal element was the extention of the berms which was to be decided four months after completion of the trial bank.

With a steep slope, the shear stress on the trial bank foundation would be greater than that imposed by the final higher but much flatter embankment. Thus the undrained strength could be checked and with measurement of pore pressure it was hoped that the strength in terms of effective stress could be deduced. Preliminary studies using linear finite element analysis, Hamza (1972), showed that the design strength of the foundation would be exceeded.

The properties of the fill as placed could be

established and the delay would enable the rate of consolidation of the foundation, examined intially by laboratory and in-situ tests, to be checked by pore pressure measurements during the initial construction. The trial embankment would also allow the deformation behaviour of the fill and foundation to be studied and it was hoped that, by back analysis, the stress strain relationship could be deduced. This understanding of the deformation behaviour might provide a check on the method of analysis. While it was hoped that complete failure of the embankment could be avoided, only an acceptably small part of the main dam foundation would be weakened if failure occurred.

The final arrangement of the trial bank is shown in figure (6.4). The bank was placed to one side of the valley centre line, to avoid the main valley bulge, which contained a typical material, Vaughan et al.(1973). A trench was cut into the side of the valley to give a sufficient length at the same height. While the section of the bank was not constant, it was hoped that this would give behaviour sufficiently close to two-dimensional plane strain conditions for two dimensional methods of analysis to be valid. Instrumentation was placed on three cross-sections, chainages 487, 514 and 537. Subsequent deformation observations showed that plane strain behaviour was effectively achieved, Wernek (1974).

Before the embankment was completed, several slips

occured in temporary borrow pit slopes. Back analysis of these slips, showing an average undrained strength of 50KN/m^2 (half the average of 100mm diameter triaxial tests) over the upper 15m of the clay, gave partial confirmation of the undrained strength assumed in the design and lessened the need to test the trial bank to failure. In the event this did not fail, construction being terminated when large deformations had occured. This enabled four months of creep measurements to be made, but it also prevented the direct determination of the shear strength by limit equilibrium methods, as discussed subsequently. Thus the use of finite element analyses became necessary.

6.3 Aims of the finite element analysis

This instrumented trial bank provides a very good opportunity for one development of a greater understanding of the behaviour of embankment dams on weak foundations during and immediately after construction. A stress-strain analysis provides a mathematical model, through which a rational framework of interpretation of observed behaviour may be constructed, and thus the analysis may be of great importance. The main aims of the finite element analysis of this particular exercise can be summarized as follows:

i) To back analyse the trial bank to deduce the foundation deformation parameters and strength using observed deformation and non-linear stress-strain solutions.

(ii) From the number of analyses carried out for the purpose of bank analysis and others, where only one variable changed at a time, a sensitivity study could be made to determine the importance of the different variables at different stages of construction.

(iii) To provide a framework through which the instrumentatio results could be interpreted.

(iv) To study the range of the stress paths followed by the different points of the domain.

(v) To check the extent of the foundation in which the undrained shear strength was mobilized, thus testing the design shear strength assumption.

(vi) To provide a firm base for predicting the behaviour mechanism of the main dam during and immediately after construction.

(vii) To predict the total stresses which, together with the measured pore-water pressures, would enable the drained shear strength parameters $\bar{c}$, ϕ' to be evaluated.

(viii) At the same time that these analyses were carried out, a laboratory testing programme was conducted to give more information about the foundation stress-strain behaviour; thus a comparison between the laboratory and predicted stress-strain curves could be made.

(ix) Last and by no means least, this exercise is used as a means for developing the non-linear techniques and for solving other associated problems; thus a complete package was ready for the main dam analysis,

It is worth mentioning here that limit equilibrium analysis could not have replaced the finite element one for the following reasons:-

i) Limit equilibrium does not predict the mechanism of behaviour*, a requirement which is of importance in this case, especially because of the speculation about the effect of progressive failure.

ii) There was a major difference in strength between the fill and the foundation, The interpretation of the bank behaviour prior to failure depends entirely on the relative mobilisation of the strength of the fill and foundation which could not be assessed in a limit equilibrium analysis.

iii) A limit equilibrium analysis gives no information on deformation and pre-failure stress distribution, and thus is of no use as far as the interpretation of field measurements of deformation is concerned,

iv) The limit equilibrium method necessitates the assumption of a stress distribution within the sliding mass, which could be severely in error due to the difference

* although it can evaluate different assumptions

between the properties of fill and foundation,

v) The limit equilibrium method yields only a number to assess stability, the Safety factor, The definition and limited use of this number is discussed by Vaughan (1975).

It is also important to mention here that three-dimensional analysis would have been very complicated, costly and time-consuming, especially for non-linear material properties.

6.4 Schedule and results of the analysis

As explained before there were three instrumented cross-sections of the trial bank Chainage 487 was adopted, rather than Chainage 514 or 537 as the main section for finite element analysis for the following reasons:-

i) More foundation material was involved in the section because of the trench.

ii) It is remote from the valley bulge, thus it includes more typical material.

The programme for analysing the trial bank attempting to achieve the above mentioned aims (Section 6.3.) can be divided into the following three stages:-

Stage 1: Analyses before completion of the trial bank construction Hamza,(1972),

Stage 2: Preliminary analyses after the construction of the trial bank.

Stage 3: Final Non-linear analyses.

For both stages 1 and 2 the stress-strain relationship for fill and foundation was assumed to be linear, but the variation of E with depth was modelled in the upper 15 metres of the foundation and the dependence of E on the mean stress was modelled for the fill. In stage 3, complete non-linearty of the stress-strain relationship was incorporated for both the fill and foundation soils. In all analyses made (except 2 runs for stage 1) the construction sequence was modelled i.e. a layered analysis was performed. The results of stresses, strains and incremental displacements were stored on a magnetic tape, or disc, after each layer was applied, and used for the following layer as initial data. To simplify operations, the finite element mesh and numbering were kept the same for all construction stages.

6.4.1 Stage 1: Primary analyses before completion of the trial bank construction.

These analyses were carried out before the construction of the trial bank was completed. They are all linear analysis but with E varying with $(\sigma_1 + \sigma_3)$ in the fill and with variation of modulus with depth in the foundation. The results of this stage were reported in detail by Hamza (1972) but no interpretation of the results was then given.

The main purpose of this stage of analysis was to confirm that the shear stresses in the foundation would be

greater than those under the main dam. A limit equilibrium analysis was of limited value because of the wide difference between the strength of fill and foundation.

The material properties used for the fill and the foundation were taken from a report by Vaughan (1972b) based on the site investigation information. Four sets of soil properties were considered to cover the uncertainties of this information, these were (all in kN/M^2) :-

a) Foundation: $E = 11,600 + 767\ d$ (Low)
Fill : $\nu = 0.35$

b) Foundation: as set (a)
Fill : $\nu = 0.45$

c) Foundation: $E = 38,890 + 2537\ d$ (High)
Fill : $\nu = 0.35$

d) Foundation: as set (c)
Fill : $\nu = 0,45$

In all analyses Poisson's ratio for the foundation was given a constant value of 0,48, and the fill modulus was given by:

$$E_{fill} = 4,700 + 8\ p$$

where: d = depth below ground surface
p = the mean stress

It is worth mentioning that the shear strengths were not introduced in the analysis, although the choice of E was based on a factor multiplied by the shear strength. The

ratio between the fill and foundation moduli is likely to be critical for stress prediction. Variation in this ratio was covered by the varying values of E of the foundation as shown above.

The findings of this stage could be summarized as follows :-

i) The ratio between the foundation and the fill moduli is an important factor in the foundation deformation behaviour. Figure (6,5) illustrates the effect on the vertical and horizontal displacements of the foundation.

ii) The use of Possion's ratio ν_{fill} of 0,45 or 0,35 for the fill did not affect the foundation deformations of the foundation significantly, as shown in figure (6,5). However the use of ν_{fill} = 0,45 gave higher shear stresses in the foundations. Figure (6,6) shows that the use of ν_{fill} = 0.45 gave higher shear stress mobilizations for the three depths considered, for both values of foundation stiffness.

iii) From comparison of displacements of selected points in the trial bank measured early in construction with the analysis predictions, it was found that the high values of foundation moduli gave better agreement,

iv) Examining the change of horizontal displacement of the foundation with bank height for both foundations showed a nearly linear relationship. The ratio between horizontal deformations in the two cases was directly

proportional to the ratio between the foundation moduli. The linear relationship shows that, while a global modulus in a linear analysis may give coincidence with any one measured displacement pattern, a fit with field observations can only be expected at low stress levels when there is no local failure. Non-linear assumptions must be used if local failure occurs.

v) From the comparison of single lift and layered analyses it was found, for this particular case of linear properties and a regular construction sequence, that the maximum shear stresses in the foundation differed slightly, figure (6,7),

This part of the work lead to the following conclusions -

i) Further analysis should take into account the non-linearity of the material properties in order to predict a realistic pattern of deformation.

ii) The case of $\nu_{fill} = 0,45$ and high foundation moduli should be the starting point for the back analysis.

iii) Layered analyses should be employed as they gave higher shear-stresses in the foundation.

iv) The mobilized shear-stresses exceeded the "design" shear strength over the full width of the foundation to a depth of up to 12 metres by up to 50%, figure (6,8). This confirmed that the shear stresses imposed by the trial bank, were higher than those which imposed by the main dam.

6.4.2 Stage 2: Analysis after the Construction of the trial bank

During construction, the slope design was changed by introducing a berm, because large deformations and a slight discontinuity were observed near the toe. Thus a new geometry had to be modelled. The new analyses also included the actual construction sequence and the actual stripped ground levels.

6.4.2.1 The Meshes: Two meshes were designed, figure (6,9) and figure (6,10):-

1) Without filling of the main dam on the down stream side of the trial bank,
2) With filling of the main dam to model the horizontal thrust imposed on the bank by the main dam.

The principles for designing those meshes were:-

i) Modelling the construction sequence in 7 stages, including the excavation of the trench. The first layer was made thicker than subsequent ones because the stress difference introduced by it is low. This is not true of the increase of stress ratio in drained behaviour, and similar treatment of a drained case would lead to some numerical instability. The layers at the top were made thinner in order to help the non-linear technique in following the stress-strain curve near failure. Table (6,1) shows the fill levels corresponding to the idealized layers.

ii) The nodes were designed to coincide with the location of the inclinometers and horizontal deformation gauges.

iii) The site investigation indicated that the depth of the soft brecciated upper clay was about 15 metres. Below this the clay was stronger and nearer in properties to a soft mud-stone. The foundation was divided into 3 layers of elements of about 5 metres thick each, underlain by a buffer zone 10.0 metres thick to act as a transition zone.

iv) Smaller elements were used where higher shear stresses were anticipated.

6.4.2.2 <u>The initial stresses</u> There were no field measurements at the start of the analysis to indicate a value for K_o, thus some assumptions were required to assign a reasonable value.

The vertical stresses were taken to be equal to the over-burden pressure. The pore water pressure was observed to be approximately equivalent to a standpipe level at ground level. The foundation is nominally heavily over-consolidated and thus the initial horizontal stresses should correspond to a value of K_o greater than 1. However, the Upper Lias Clay at Empingham is subjected to three effects, all acting to reduce K_o; these are:-

i) Extensive periglacial frost shattering, which may have released the horizontal stresses.

ii) The embankment was built on the lower part of the slope (near the valley bulge) a condition which reduces the maximum value which the horizontal stress σ_y can have downslope, Figure (6,11)

iii) The plane of the trial bank cross-section zx, is parallel to the strike of the valley slope. The horizontal stress σ_x will therefore be closer to σ_z than it is to σ_y.

Figure (6,11) shows a qualitative illustration in three dimensions of the last two factors. Thus it was decided that a value of $K_o = 1$ would be a reasonable starting point for the analyses of stage 2. Maguire (1975) found subsequently that $K_o = 1$ was consistent with the suctions in samples of the Upper Lias Clay.

6.4.2.3 Summary and aims of stage 2 analyses

This stage was carried out, as mentioned before, using linear material properties to investigate the effects of various relevant factors before starting the non-linear analysis. The main aims of this intermediate stage were:

i) To check that the foundation, with the berm in the upstream slope of the bank, is stressed more highly than the undrained strength assumed for design purposes.

ii) To check on the development of a realistic active pressure in the fill and to check if shear unloading occured within the fill in the upstream slope, a condition which would require the introduction of a shear unloading model in the programme.

iii) To investigate the effect of upstream main dam filling and whether it caused shear unloading in the downstream slope and foundation of the bank.

iv) To investigate the effect of using a Poisson's ratio in the foundation very close to 0,5, namely from 0.48 to 0.49999, on the numerical stability of the solution and as a parameter influencing the results.

v) To investigate the effect of the different side boundary conditions employed in the analysis (rigid smooth and controlled stress) on the behaviour of the bank.

Table (6.2) contains a summary of the finite element analyses performed in this stage together with their purposes and conclusions.

6,4.2.4 Material properties for Stage 2

For the foundation: i) the undrained modulus was assumed to be independent of the state of stress, but to vary linearly with depth, as case (d) of Stage 1, up to 15,0 meters below a horizontal line passing through the toe, ii) Poisson's ratio was kept constant for each analysis, but varied for different analyses as shown in Table (6,2).

The fill was assigned a modulus which varied with the mean total stress, and a Poisson's ratio of 0.45, as case (d) of Stage 1.

Figure (6.12) shows details of the material properties used in Stage 2.

6.4.2.5 Findings of Stage 2 Analyses

Run 1: Figure (6.13) shows the development of horizontal and vertical stresses at the bank centre line. The values of the stresses illustrate that the fill model worked reasonably.

Figure (6.14) shows the values of maximum shear stresses in the fill at different vertical sections starting from the centre line through the upstream slope. The maximum shear stresses are increasing monotonically as the construction proceeds at all locations, thus it was believed that there is no shear unloading and hence the modelling of unloading behaviour was not needed. Figure (6.15) shows development of maximum shear stresses at three different levels in the foundation. Design strength is exceeded over full foundation width. The absence of down-stream filling simulation gave significant shear stresses under the centre and down stream side of the bank.

Run 2: This run is the same as run 1 except that down-stream filling was modeled, ie. the mesh in figure (6.10) was used.

Figure (6.16) shows fill stresses at the bank centre-line. Horizontal stresses have increased slightly due to the extra thrust imposed by the down-stream filling. Figure (6.17) shows the development of maximum shear stresses after each layer at three different levels in the foundation. The following were observed as an effect of simulating the down-

stream filling in the analysis:-

i) shear stresses under the upstream slope increased slightly,

ii) shear stresses under the centre line decreased due to the support given by the fill,

iii) Shear unloading and reloading occurs in the foundation due to the irregular construction sequence of the bank and the downstream filling as shown in table (6.1). This behaviour affected only the part downstream of the centre-line,

Runs 3,6,7 and 8: These runs were mainly to investigate the effect of the use of a foundation Poisson's ratio very close to 0.5, namely varying from 0,48 to 0.49999. The points examined were:-

i) What is the effect of a small variation of Poisson's ratio on the maximum shear stress distribution?

ii) What is the safest (numerically) and the value closest to 0,5 to be used in the further, non-linear, analyses?

Figure (6,18) shows the influence on the maximum shear stress at the end of construction, The increase in Poisson's ratio,has only a small effect which was not regarded as significant, Only the averages of the stress at the 4 Gauss points of each element were used and in no case considered was numerical instability encountered. Nevertheless, the value of 0,499 was chosen for further work because;

i) it was doubtful whether a higher value was needed,

ii) the difference in results between 0.499 and 0.49999 was negligible in terms of stresses, and iii) the further work was non-linear, which might have caused additional numerical instability.

Runs 4 and 5: Those runs were carried out to investigate the extent of the side boundary effects on the solutions, and whether a displacement boundary or a "stress boundary" was more suitable. Poisson's ratio was kept at a constant value of 0.495. In run 4, a horizontal stress at the side boundary was applied using the value of foundation Poisson's ratio and assuming a one dimensional elastic model to be valid at this 'sliced boundary'. The values of the horizontal stress applied were varied during the construction depending on the external applied loads. Figure (6.19) shows the assumptions and the way the stresses were calculated.

In run 5, the side boundary was considered rigid and smooth.

The results are shown in figure (6.18) which shows that the side boundary effect does not spread towards the area of interest, ie. under the upstream slope. Rigid smooth side boundaries were adopted in all further solutions rather than 'stress boundaries' because of convenience in input data, as the 'boundary stress' will necessitate a new calculation, depending on ν of the foundation, for every layer added, as described in figure (6.19).

To investigate the sensitivity of the solution to the variation in Poisson's ratio, the vertical and horizontal stresses and displacements for the end of construction stage are plotted in figure (6.20). The vertical stresses for both cases are virtually identical. The vertical settlement has increased by 50% due to the decrease of ν from 0.48 to 0.49999, while the horizontal stresses and displacement only changed by about 8% of maximum value.

6.4.3 Stage 3: Final non-linear Analyses

The aim was to back analyse the trial bank in order to obtain the non-linear stress-strain properties of the foundation (strength being of particular importance) which could reasonably fit the real performance and hence be used in predicting the behaviour of the main dam during completion (Chapter 7). The factors which needed to be considered in the back analyses were:

i) Non-linearity of the foundation deformation properties
ii) Horizontal variation of the foundation strength
iii) Increase and decrease of the design strength profile
iv) Non-linearity of the fill properties
v) Variation in K_o of the foundation.
vi) Drainage of the soil adjacent to the drainage blanket between the fill and foundation, which would cause softening of the surface layer of the foundation near the toe.

The work was limited by the following short-comings:
a) final estimates of the actual prototype deformations were not available immediatly because at that time they were being examined and corrected by Wernek (1974) concurently with the finite element calculations, and only preliminary plots of field data were available for the early stages of the back analysis, b) final soil test data from laboratory not immediately available for comparison, Maguire, (1975).

The philosophy of the analyses was based on the following 3 points:-

(1) The local failure zone should be reproduced in the analysis as it was believed to control the over-all pattern of behaviour.

(11) Foundation behaviour would not be sensitive to the fill properties assumed.

(111) As shown in section 6.4.25 and figure (6.20) the vertical deformation could be more affected by a small variation of the foundation's Poisson's ratio than would horizontal deformations. Also the measured vertical deformation included the consolidation of the base of the Upper Lias clay which is not reproduced in the analysis. Hence, the horizontal displacements are more critical for comparison with prediction of prototype performance.

Table (6.3) lists all the analyses of this stage; and their assumptions, purposes and conclusions.

6.4.3,1 Field Performance

Locations of the instruments of the cross-section of the trial bank analysed are shown in figure (6.21). Measured horizontal movements, adjusted for consistency of location and fill level between field and finite elements results, are summarized in figures (6,22, 6.23, 6.24, & 6.25). It must be noted that not all the information in those figures were present at the start of the work.

6.4.3.2 Preliminary non-linear solutions:-
Cases 2a, 2c, 2d,

Three diffrent stress-strain curves were assumed for the foundation properties and three finite element analyses were carried out to see what type of behaviour resulted. The foundation non-linear deformation and strength properties are summarized in figure (6.26). The foundation strength was assumed to vary with depth from the inclined stripped ground level according to the design profile given by Vaughan (1972). The fill properties were kept the same as previously (ie stage 2)

Based on field measurements available in April 1973, a comparison with the predicted horizontal movements are shown in figures (6.27, 6.28, 6.29, 6.30, 6.31, & 6.32). Inspection of those figures showed that case 2c (ie. that of a steep stress-strain curve) gave the best fit to the field measurements. It is worth mentioning here that, although case 2a (ie. that of a bi-linear stress-strain curve) gave a better fit at end

of construction, the development of displacements with fill height and the profile with depth at inclinometers IB3 and IB4 were not well represented. However, the results of the best fit (case 2c) gave an over-prediction everywhere and during all construction stages. The difference between predicted and measured values was least at the toe and increased regularly towards the middle of the bank. Thus, changed assumptions which would counteract these trends were thought of. The aim at that stage was to get a better fit with the field pattern of behaviour rather than a fit with the absolute values of the field measurements.

6.4.3.3 Effect of strength: Cases 3a, 3b.

Case 3a:- Inspection of the preliminary solutions suggested that an increase of the shear strength varying from a minimum at the toe to a maximum at inclinometer IB4 would produce the required effect. This was readily achieved by starting the design shear-strength profile from a horizontal line and not from the inclined stripped ground surface as assumed in case 2c.

The normalised stress-strain curve and the fill properties are kept the same as case 2c. The summary of the foundation properties of this case is given in figure (6.33).

Figures (6.34, 6.35, 6.36, 6.37, 6.38, & 6.39) shows the horizontal displacements as compared to case 2c (last best fit) and to the measured values, which indicate an overall better fit due to the new strength assumption. At the toe,

the predictionswere very close but as the distance increases from the toe the finite element over-predicted until reference point H3A beyond which the over-prediction is relatively consistent.

Case 3b:- Due to the consistency of the over-prediction over part of the foundation, a uniform increase in shear strength was introduced and case 3b was carried out. Also, this case was thought important as it would show the sensitivity of the solution to the shear strength. It was hoped that this change would not affect significantly the good fit observed at the toe for case 3a.

The profile of shear strength with depth assumed for this case, which is 10% higher than case 3a over all the foundation depth and the corresponding stress-strain curve are shown in figure (6.40). Again the fill properties and the foundation normalized stress-strain curve were kept the same as before.

The horizontal displacements at the six reference points for this case and case 3a as compared to the field measurements are shown in figures (6.41, 6.42, 6.43, 6.44, 6.45, & 6.46). Reduction in displacements is observed everywhere of a magnitude of about 30% near the toe and about 20% at reference point I4, This yielded an apparent better fit at the inner 3 points (ie. H3B, H3C and I4) and a much worse fit at the other points. However, figure (6.47) shows, for the selected 4 reference points, that, having eliminated

the initial part of the displacement Vs. fill height curve, (ie, that part which is controlled by the initial part of the stress-strain curve) and comparing the remaining parts of the displacements Vs. fill height curve (which are most likely to be governed by the shear strength). The results of case 3a are closer to the measured horizontal displacements than are those of case 3b. Thus case 3b was not considered an improvement, and case 3a still gave the best fit.

6.4.3.4 Effect of fill non-linearity: Case 3c,

At this stage the non-linear fill deformation and strength properties were derived from field compacted triaxial samples and field pore water pressure measurements. The final stress-strain curve and strength, varying with σ_3, are represented in figure (6,48).

The comparison of this case with case 3a and the measured horizontal displacements are shown in figures (6.49, 6.50, 6.51, 6.52, 6.53, 6.54). Apart from at the toe (point HX3), case 3c gave a better fit everywhere. The reduction in the displacements due to the non-linear assumption is an apparent paradox, arising from the fact that the stress level in the fill is low, thus a modulus close to the initial modulus was selected, by the programme algorithm, while in the previous cases with linear fill properties a lower value corresponding to 50% stress level secant modulus was used. Hereafter case 3c is considered the best fit, however, it is

worth noticing that there is under-prediction at the toe and over-prediction at the inner inclinometer (ie the error in the prediction is not consistent).

6.4.3.5 Effect of K_o: Cases 3d, 3e.

The next step was to find a realistic assumption which could produce the required effect (ie. predicts more displacement at the toe and less towards the centre). Thus it was hoped that $K_o>1$ would produce this effect. Near the toe, the local failure is mainly due to an increase of the horizontal stresses and hence failure is reached quicker with $K_o>1$, while in the centre of the dam, local failure will be mainly due to an increase of vertical stresses, hence, failure is reached less quick with $K_o>1$.

Values of K_o = 1,25 and 1.1 were chosen and cases 3d and 3e were run. Comparison for case 3d of K_o = 1.25 with case 3c (last best fit) and the measured displacements at foundation level and at inclinometers IB3 and IB4 are shown in figures (6.55, 6.56, 6.57, 6.58, 6.59, 6.60, 6.61, & 6,62). The comparison demonstrates that the use of K_o = 1,25 predicts more displacements for all locations considered (the use of K_o = 1.1 gave an intermediate results). Also, at the two inclinometers the profile of deformation was essentially different from the measured deformations, giving a bulge starting at a depth of 8 meters, where the measured displacements were very small.

It is worth noticing that the predicted displacements at foundation level for cases 3c and 3d are nearly parallel with the exception of a slight increase of displacements for case 3d due to placing of the last layer. However the aim of this run was not achieved (ie. the prediction of more displacement at the toe and less at inclinometer IB4). Also, the pattern of displacement with depth for $K_o > 1$ was worse than with $K_o = 1$, figures (6,61, 6.62), hence the value of $K_o = 1$ was used in subsequent analyses.

6,4.3,6 Effect of the swelling of the toe: Case 3f.

Full mobilisation of undrained shear strength of the foundation near the toe requires the maintenance of a negative pore water pressure. However, the presence of the horizontal drainage blanket would allow swelling to occur, thus the drained shear strength would be operating. Under low confining pressure, the drained strength is lower than the undrained strength. Due to the drop of shear strength near the toe, it was speculated that a better fit would be obtained if the swelling is modelled.

Assuming that $\phi' = 23^{o}$ and c' = o.o Maguire, (1975) a simple calculation was carried out to determine the undrained shear strength equivalent to swelling at the toe, and the length over which the reduced strength would operate. Although the spread with depth of this weaker zone is limited to only one metre or so, a linear distribution was assumed, within

the element concerned, between the lower strength at the top to the strength previously assumed (case 3c) at the bottom.

The results were compared with measured displacements and results from case 3c. The modelling of the swelling effect at the toe slightly improved the over-all fit, but not enough to explain the inconsistency between measured and predicted displacements. Therefore the effect of a drained toe is insignificant and the back analysis was with case 3c still considered the best fit.

6.4.3.7 Interim Conclusions

Case 3c gave the best fit. At this stage the stress-strain curve and strength profile were considered adequate for main dam analysis and this was proceeded with, as discussed in Chapter 7.

The horizontal displacements at foundation level, berm level and the inclinometers, IB3 and IB4 for the six construction stages for cases 3a, 3b, 3c and 3d are shown in figures (6.63, 6.64, 6.65, & 6.66).

6.4.4 Systematic back analysis.

Using the "trial and error" method of back analysis, previously described it was considered that, with the large number of parameters which could be varied independently and comparing the results only with field displacement measurements at selected points, further improvement of fit

would be a matter of chance and uniqueness of results could not be demonstrated. For instance, it was found that cases 2c and 3d gave similar results at the reference points although they assumed different strengths and values of K_o. This emphasised the need to develop a more direct and systematic method for back analysis.

Displacements result from the integration of strains over the stressed domain. The same displacement at a particular point may arise from an infinite number of strain fields, and thus it is not possible to demonstrate uniqueness by comparisons of computed and measured displacements. As the number of points at which comparisons can be made increases, the probability of a unique solution being available increases, but progressive modification of the input data can only be made on the basis of semi-intuitive qualitative judgement.

Ideally, a stress-strain curve can be measured directly in the field, if complete stresses and strains are measured at a point. In general, the extreme difficulty in measuring stresses makes such an approach impractical. However, the values of stress predicted by finite element analyses are relatively insensitive to the input soil properties, whereas the strains and displacements are directly dependent on them. Field strains may be measured more easily and accurately than stresses. Thus if stresses are predicted from an analysis with approximate input stress-strain data and then combined with measured field strains to give a

revised stress-strain curve, this should be nearer to the correct one. This revised curve may be used to predict revised stresses, which can be recombined with the measured strains to give a further stress-strain curve, and so on. Hopefully, the process would iterate towards a unique curve.

The power of such a technique could only be examined by a detailed programme of investigations, involving, perhaps, the back analysis of actual finite element solutions. Problems could arise in determining K_o, in dealing with large principal stress rotations, in determining strength in zones of local failure, and in dealing with drained problems in which shear and volumetric strains occur simultaneously and in which volumetric strain results in increasing strength and stiffness in shear. It is doubtful if uniqueness can be proved in other than simple cases. It must be mentioned that, although the method might be in principle a valid one, it might not give good results for real problems in which the simple non-linear elastic model used in the analysis does not represent the real soil.

A method of back analysis for undrained shear with $K_o = 1$ based on the above approach would be as follows:-

a) Assume a linear stress-strain relationship and carry out a finite element analysis.

b) Couple the measured strains, at different loading stages, with the corresponding stresses obtained in step a. This produces a 'deduced curve' at the point considered. This

coupling should be made for a number of points in the domain, the number depending on the variation of stress-strain properties with depth. From the 'deduced curves' at the several points considered, a stress-strain relationship for the domain can be derived.

c) Using the stress-strain relationship derived in step b, carry out a finite element analysis.

d) The stresses resulting from step c and the field measured strains will yield a new stress-strain relationship, as described in step b.

Repeat steps c and d until the stress-strain relationship assumed and deduced are near enough for practical purposes. Unfortunately, the instrumentation of the Empingham trial bank was not designed to determine local strains, but strains can be approximately determined for two points near the foundation surface where horizontal and vertical instrument systems cross, Werneck (1974). As a preliminary investigation of the method steps (a) and (b) were carried out using the deduced field strains. The deduced curve from one interation is compared with the curve for case 3c in figure (6.67). The fit is encouragingly good.

6.4.4.1 <u>The use of systematic back analysis for the trial bank - Case 4A.</u>

A complete systematic back analysis was not possible because:

(a) There were not enough strain measurements to

enable the variation of properties with depth to be examined.

(b) The strain measurements were not precisely made.

(c) They were not available until a late stage of the work.

(d) The technique was not developed until a late stage of the work.

Nevertheless, an attempt has been made to improve on the prediction made in case 3c, using strain versus fill elevation plots prepared by Werneck(1974) for the two points near the stripped foundation level at the two inclinometers.

Figures (6.68, 6,69) show the stress-strain curves constructed from stresses from case 3c and the measured strains. The constructed curves are stiffer but show a lower strength than the original case 3c curves. It was speculated from the previous analyses that a general decrease in strength would produce mush larger deformations (this was confirmed in a subsequent analysis, described in Chapter 8) It seemed probable that the change in strength with depth was probably different from the linear distribution assumed, a conclusion supported by the differences between the shapes of the measured and predicted profiles of deformation with depth.

Thus case 4a was run using the back analysed stress-strain curves to 80% of failure but retaining the strength distribution as in case 3c, as shown on figure (6.68). The fill properties were kept as before.

A comparison between case 4a, case 3c and the measured displacements is shown in figures (6.70, 6.71, 6.72, 6.73, 6.74, 6.75, 6.76, 6,77, & 6.78). Case 4a underpredicts near the toe, but gives a better prediction than case 3c towards the centre of the bank. At depth, and early in the construction sequence,case 4a gave better results than case 3c. The other cases involving changing the rate of increase of shear strength and stiffness with depth were tried but they gave no improvement, and it was thought that the absence of adequate strain measurements at depth, which would have enabled a systematic back analysis to be performed, made further work unrewarding. However, the limited use of the technique which was possible using the trial bank data suggests that it is worthy of further examination and it is discussed further in Chapter 8, Its use will require revised methods of field instrumentation designed to measure local strains.

6,4,5 Modelling of shear unloading: Case 4au.

An overall good fit had not yet been obtained, Case 3c and 4a gave the best fit, Although predictions in both cases showed compression near the toe, this was not measured in the field.

The presence of the berm would induce shear unloading due to the filling of the middle of the bank (see Chapter 8 for more discussion). Shear unloading will increase the

stiffness of the berm and it was thought that reproducing this might decrease the compression at the toe. Inspection of the development of the shear stress in the berm showed some shear unloading, figure (6,79). The magnitude of unloading is small and also the shear stress level is low.

Shear unloading was modelled in the Programme as described in Chapter 4, and case 4au was carried out, keeping all the other variables unchanged. The results are shown in figures (6,70, 6,71, 6,72, 6,73, 6,75, 6,77, & 6,78), and compared with case 4a and the measured displacement. The results show no significant improvement of fit.

To investigate the differences between cases 4a and 4au further the horizontal shear strains at foundation level and the vertical settlement at the berm level were compared in figures (6,80 and 6,81) which shows a slight difference in the settlements and a large difference in the horizontal shear strains which arises mainly due to a difference in principle stress rotation.

6.4.6 Shear strength parameters in terms of effective stress

As previously described, one of the aims of the finite element analysis was to examine if the predictions of total stress could be combined with measured pore pressures to give an indication of the effective stress shear strength parameters c' and ϕ'. The predicted stresses at the piezometers are shown on figure (6,82) for the end of construction

when the total stress analysis showed that most of the foundation was at or near local failure. The measured pore pressures have been used to give the effective stresses, which, ideally should define the failure envelope in terms of effective stress. The points show considerable scatter although on average they define failure within about 15% of the values $c' = 3\ kN/m^2$, $\phi' = 23^o$, found by Maguire (1975) for large laboratory samples. It is clear that this method is ill conditioned as the effective stresses are a small difference between large predicted total stresses and large measured pore pressures and a small proportionate error in either would produce a large error in the average effective stress. If the errors lie in the total stress predictions they could be due to three-dimensional effects in the trial bank which could increase the average total stress (and hence the pore pressures) without affecting the stress-strain behaviour in terms of total stress. It is of interest that the errors appear to increase away from the toe of the bank, as three-dimensional effects might be expected to increase. Errors in the bulk unit weights assumed and in the layer simulation techniques used seem less likely causes of error.

6.4.7 Inspection of stresses

The maximum shear stresses for a range of the cases considered are represented in figures (6.83, 6.84, 6.85, 6.86, 6.87, 6.88, 6.89, & 6.90). In all the cases a concentration

of shear stress under the slope was observed, Figure (6,91) shows that the shear stresses are insensitive to the soil parameters assumed,

The over-stressed zone predicted in a linear analysis (case 1H) and that predicted by a non-linear analysis (case 3a) are compared in figures (6,92) and (6,93). The local failure zone of case 3d is larger than the over-stress zone of case 1H and the shear stresses adjacent to it are higher, as should be expected,

It is of interest to note that a calculation of the average factor of safety along the potential slip surfaces indicated by the two analyses gives the same answer; and the indicated critical surfaces are the same,

Stress paths for 3 points in the foundation and 2 points in the fill are represented in figures (6,94, 6,95, 6,96, & 6,97), for the purpose of inspecting principal stress rotation and shear unloading. The principal stress rotation in the foundation is small. It acheives a value very early in the construction and then the principal stress increment rotation is negligible. Shear unloading was observed in the fill under the berm coupled with larger rotation of principal stresses.

6,4,8 Vertical Settlements of fill and foundation

It was explained earlier that comparisons with field measurement were made only with horizontal displacements,

Nevertheless, it was of interest to inspect the vertical settlements for educational reasons and sensitivity studies.

Vertical settlements at foundation level for cases 3a, 3b, 3c and 3d after construction stages 3 and 5 are shown in figure (6.98). The figure shows that for all cases considered the vertical settlements lay within a small band. It is of interest to note that the range of variation of vertical settlement due to the use of different stress-strain relationships compared, with a constant Poisson's ratio of 0.499 is less than that due to a variation in Poisson's ratio from 0.48 to 0.49999 with a linear stress-strain relationship as shown previously in figure (6.20)

The vertical settlements at berm level after construction stages 3, 4 and 5 for cases 3a, 3b, 3c and 3d are shown in figure (6.99). The range of vertical settlements variation for the cases plotted is only 17% of the maximum predicted. To check on the performance of the fill behaviour, the vertical settlements of case 3c at a point in the middle of the fill was compared with the field settlements for construction stages 3, 4 and 5 in figure (6.100) which shows excellent agreement.

6.4.9 Comparison of the deduced stress-strain curves with those from laboratory triaxial tests

Maguire (1975) has reported the average stress-strain curve obtained from undrained slow triaxial tests on 260mm diameter specimens of the Empingham foundations clay from a particular

depth at which the 'design' strength was 50kN/m^2. This curve is compared with the back analysed curves for the same effective depth as used in cases 3c and 4a. Strengths agree closely, as do strains at failure. The initial stiffness of the laboratory curve is less than that of the back analysed curves. The underestimate of initial modulus by triaxial tests starting from an initial isotropic stress is common in soil mechanics.

6.5 Conclusion

A reasonable fit between the measurements of horizontal displacement and the finite element predictions was obtained by a back analysis process and a good knowledge of the operating stress-strain and shear strength parameters was obtained. However, prediction gave too much displacement at depth and not enough at shallow depth. Inspection of field measurements indicated 'failure' occurring at a relatively shallow zone, 4-5 metres below stripped ground surface, while this was not reproduced by the analysis.

The reasonable fit obtained and the comparison with laboratory stress-strain and strength measurements suggests that the coupled use of non-linear stress-strain analysis and a good instrumented trial bank could bypass the need for an intensive laboratory testing programme.

The semi-intuitive approach of back analysis by successive investigation of variables has shown the following

conclusions:-

1. The results are sensitive to the undrained shear strength and K_o assumptions, especially at the surface. Hence the back analysed strength and K_o are apparantly quite reliable for use in the final dam design.

2. The results are relatively sensitive to the curvature of the stress-strain curve and especially the strain at failure.

3. The results are least sensitive to the fill properties.

4. Cases 3c and 4a gave a better fit than other cases.

5. Any further improvement on the fit obtained based on trial and error would have been a matter of chance.

The systematic back analysis method proved to be a promising technique, its development needs further research and more field strain measurements.

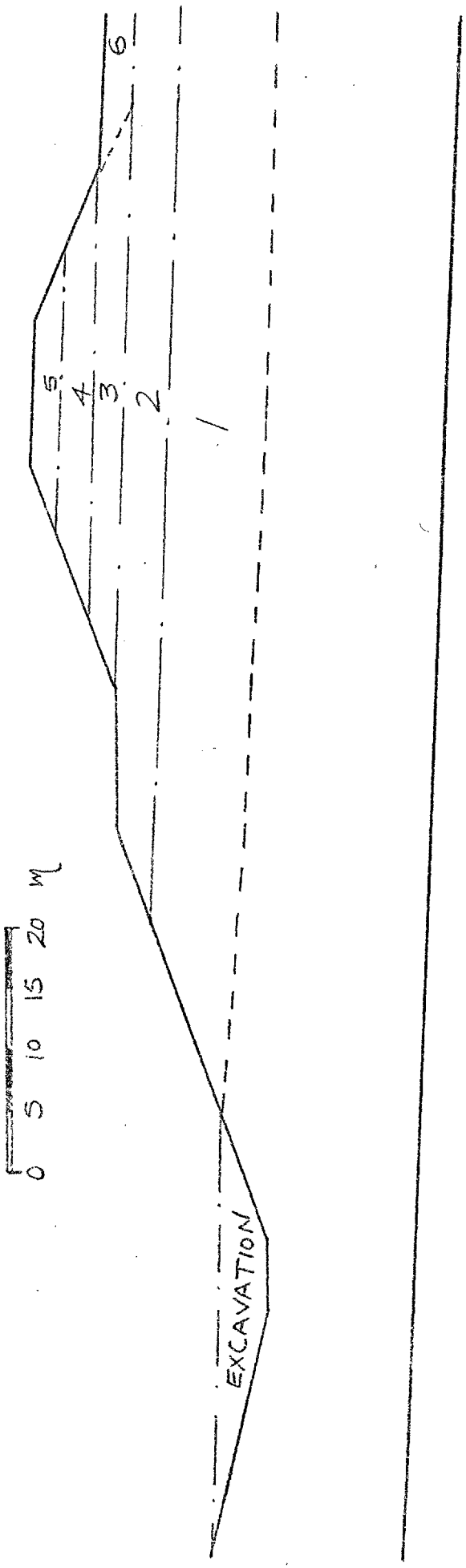


TABLE 6.1

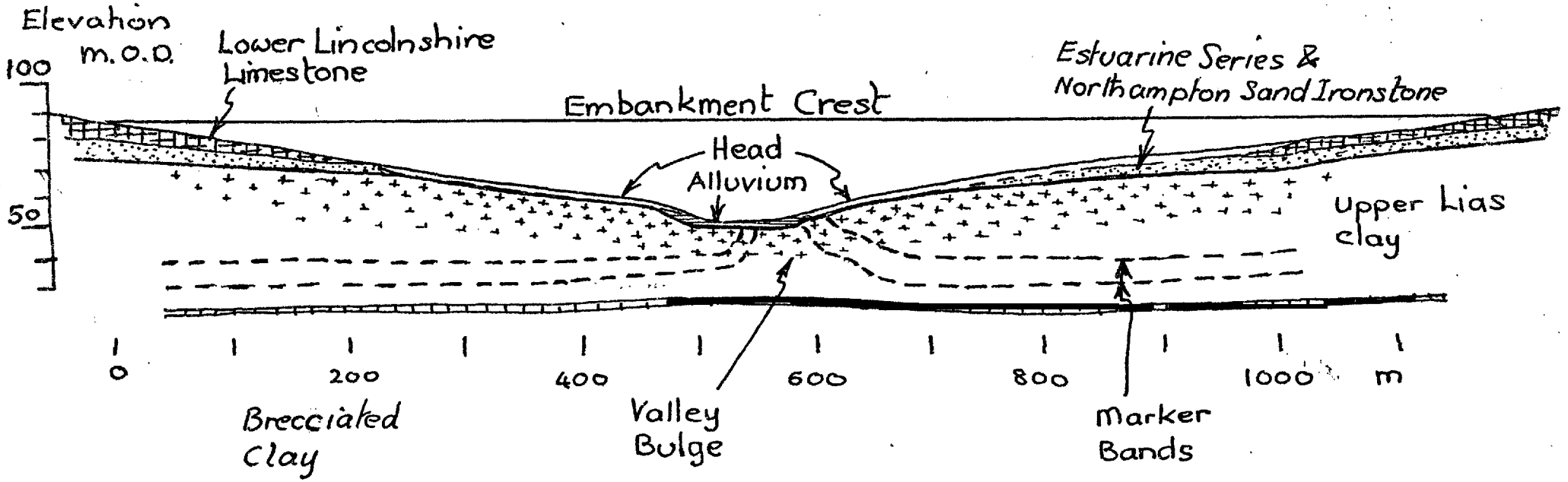
Layer No.	Level of fill (m AOD)
1	59.0
2	62.7
3	65.0
4	67.7
5	70.2
6	Downstream filling to level 3

TABLE 6.2 : SUMMARY OF STAGE 2

RUN	CASE	GEOMETRY	BOUNDARY		SOIL PROPERTY		K_o	PURPOSE AND COMMENTS
			BASE	SIDES	FOUND	FILL		
1	Case 1a	Actual geometry for the upstream side – No downstream Filling Fig. 6.9	Rigid – rough	Free, only initial stress	$\nu = 0.48$ Fig. 6.12	$\nu = 0.45$	1	Trial solution for the new geometry – Over stress ratio – τ max. of fill – Development of σ_H and σ_v with respect to over-burden pressure
2	1b	Actual geometry for the upstream with downstream filling Fig. 6.10	As Case 1a	As Case 1a	As Case 1a	As Case 1a	1	Effect of downstream filling on stress in the highly stressed zone τmax. and σ_H/σ_v is increased – Shear Loading + unloading cycles and τmax drop under D/S slope
3	1C	Same	Same	Same	$\nu = 0.495$	Same	1	Effect of $\nu = 0.495$ is small
4	1d	Same	Same	Stress B. Fig. 6.19	Same	Same	1	Local small effect
5	1e	Same	Same	Rigid – smooth	Same	Same	1	Local small effect Easier than Case 1d
6	1f	Same	Same	Same	$\nu = 0.4999$	Same	1	Refer Fig. 6.18 $\nu = 0.499$ is Chosen for the subsequent analyses
7	1g	Same	same	same	$\nu = 0.49999$	Same	1	
8	1h	Same	Same	Same	$\nu = 0.499$	Same	1	

TABLE 6.3: SUMMARY OF STAGE 3

RUN	CASE	GEOMETRY	BOUNDARY		SOIL PROPERTY		K_o	PURPOSE AND COMMENTS
			BASE	SIDES	FOUND.	FILL		
9	2a	As Case 1h	AS 1h	AS 1h	Bilinear Fig. 6.26	As 1h	1	Introducing the design shear strength
11	2c	Same	Same	Same	Steep Curve Fig. 6.26	Same	1	Keeping shear strength constant and varying the curvature (i.e. strain at failure). Case 2d gave very large displacements
12	2d	Same	Same	Same	Flat Curve Fig. 6.26	Same	1	
13	3a	Same	Same	Same	As 2C but Cu, Ei start from Hℓ. Fig 6.33	Same	1	Try to improve on fit obtained in 2C by increasing the Cu horizontally by starting from Horizontal
14	3b	Same	Same	Same	10% higher Cu Fig. 6.40	Same	1	Higher shear strength did not improve fit
15	3c	Same	Same	Same	As 3a	Nonlinear properties Fig. 6.48	1	Introducing fill nonlinear properties. Slight improvement
16	3d	Same	Same	Same	Same	Same	1.25	Effect of $K_o > 1$ Worse predictions especially pattern
17	3e	Same	Same	Same	Same	Same	1.1	
18	3f	Same	Same	Same	Soft toe	Same	1	Not important effect.
19	4a	Same	Same	Same	Stiffer	Same	1	Slight improvement
20	4au	Same	Same	Same	Same + Unload	Same	1	No improvements



REPRESENTATION OF THE GEOLOGY OF EMPINGHAM DAM SITE

Fig. 6.1

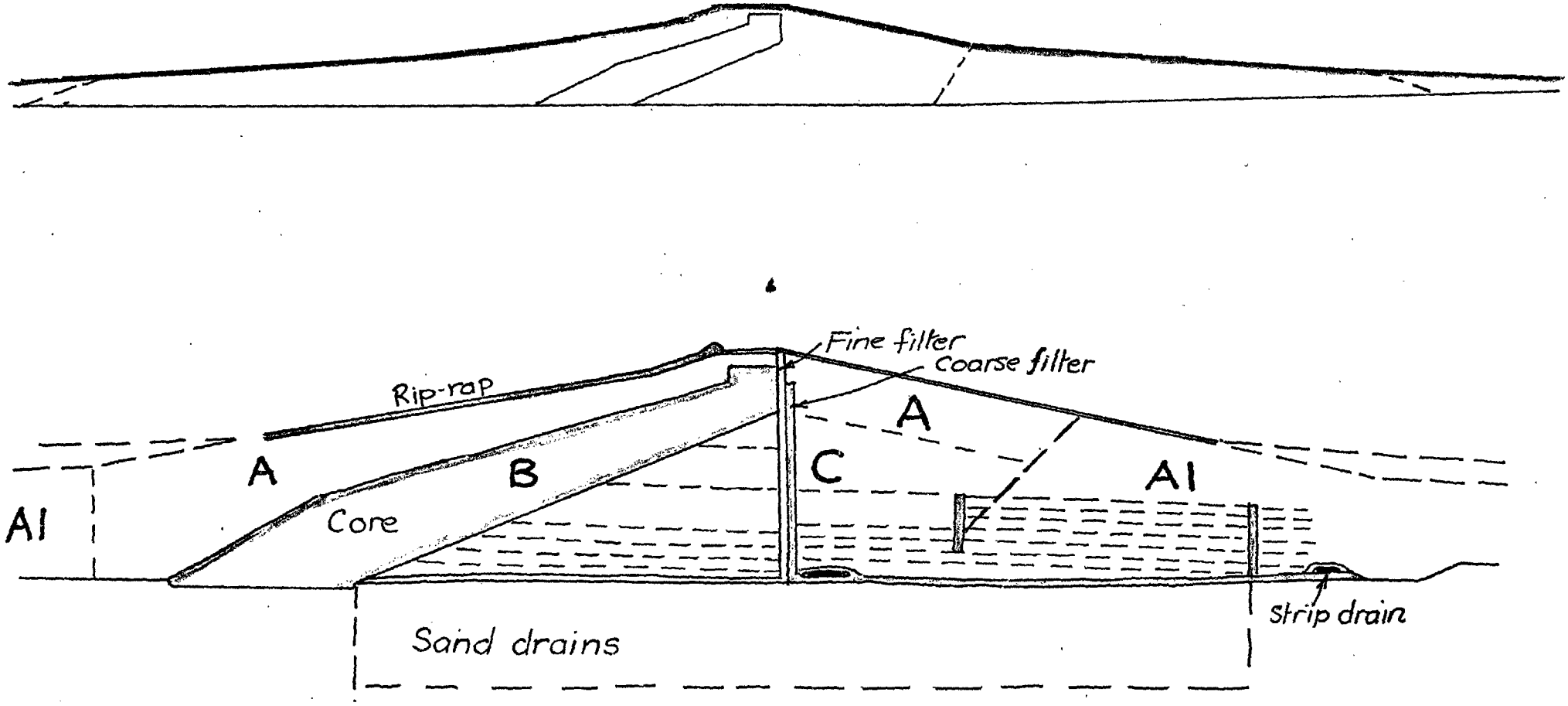
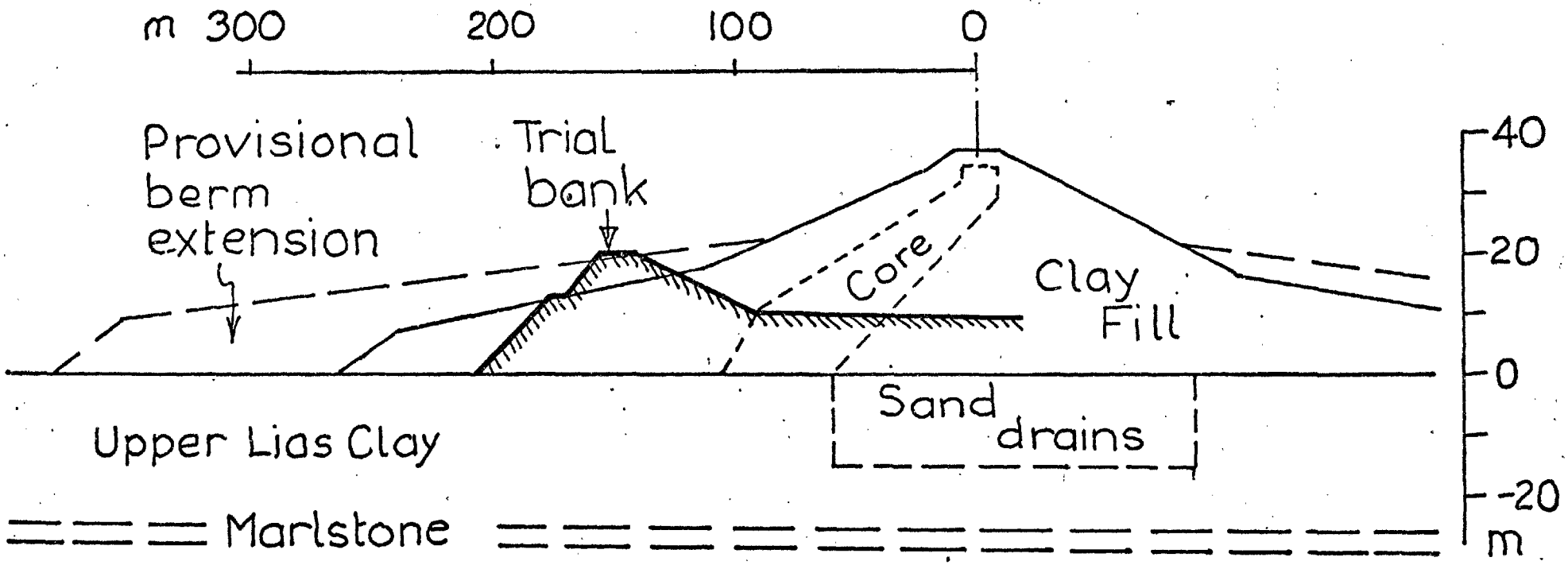


Fig. 6.2

DIAGRAMMATIC REPRESENTATION OF A TYPICAL CROSS-SECTION OF EMPINGHAM MAIN DAM



THE POSITION OF THE TRIAL BANK WITHIN THE MAIN SECTION

Fig. 6.3

FINAL GEOMETRY AND INSTRUMENTATION ARRANGEMENT FOR THE TRIAL BANK

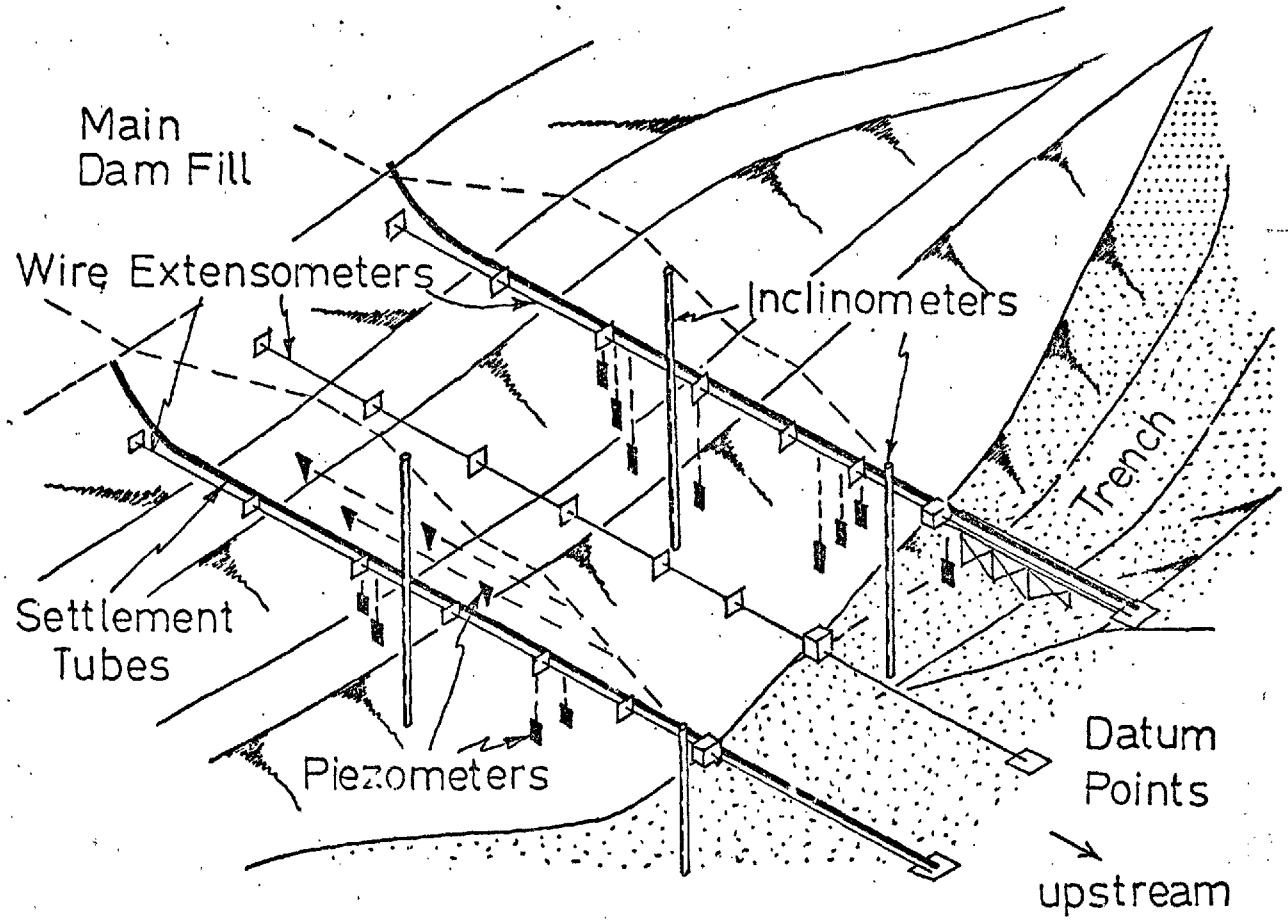
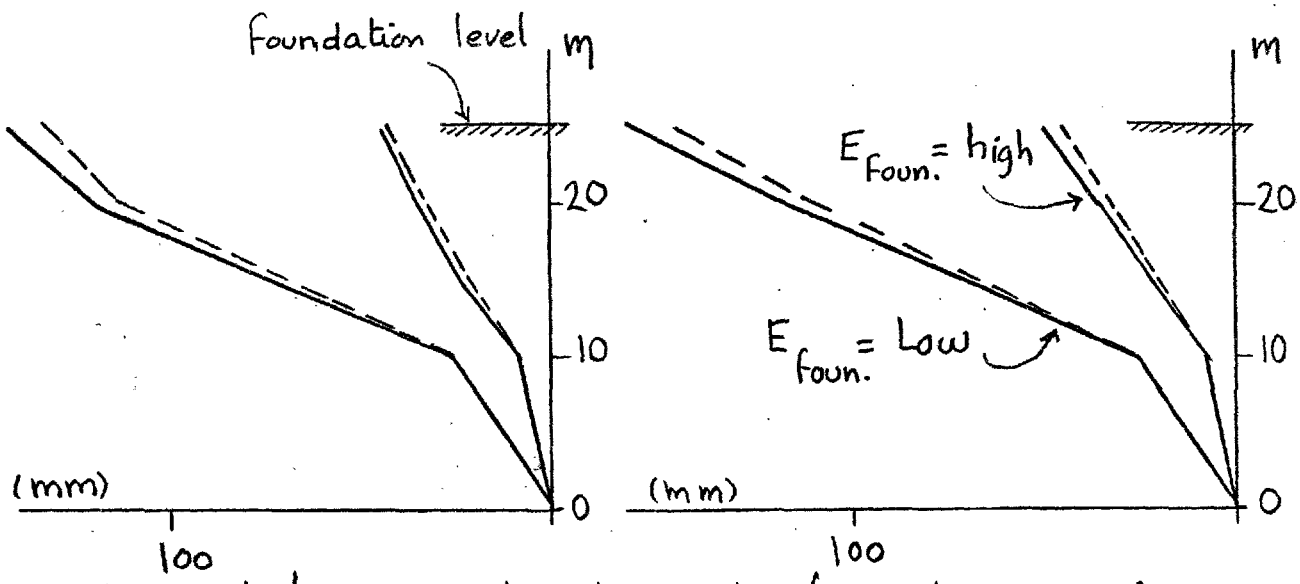
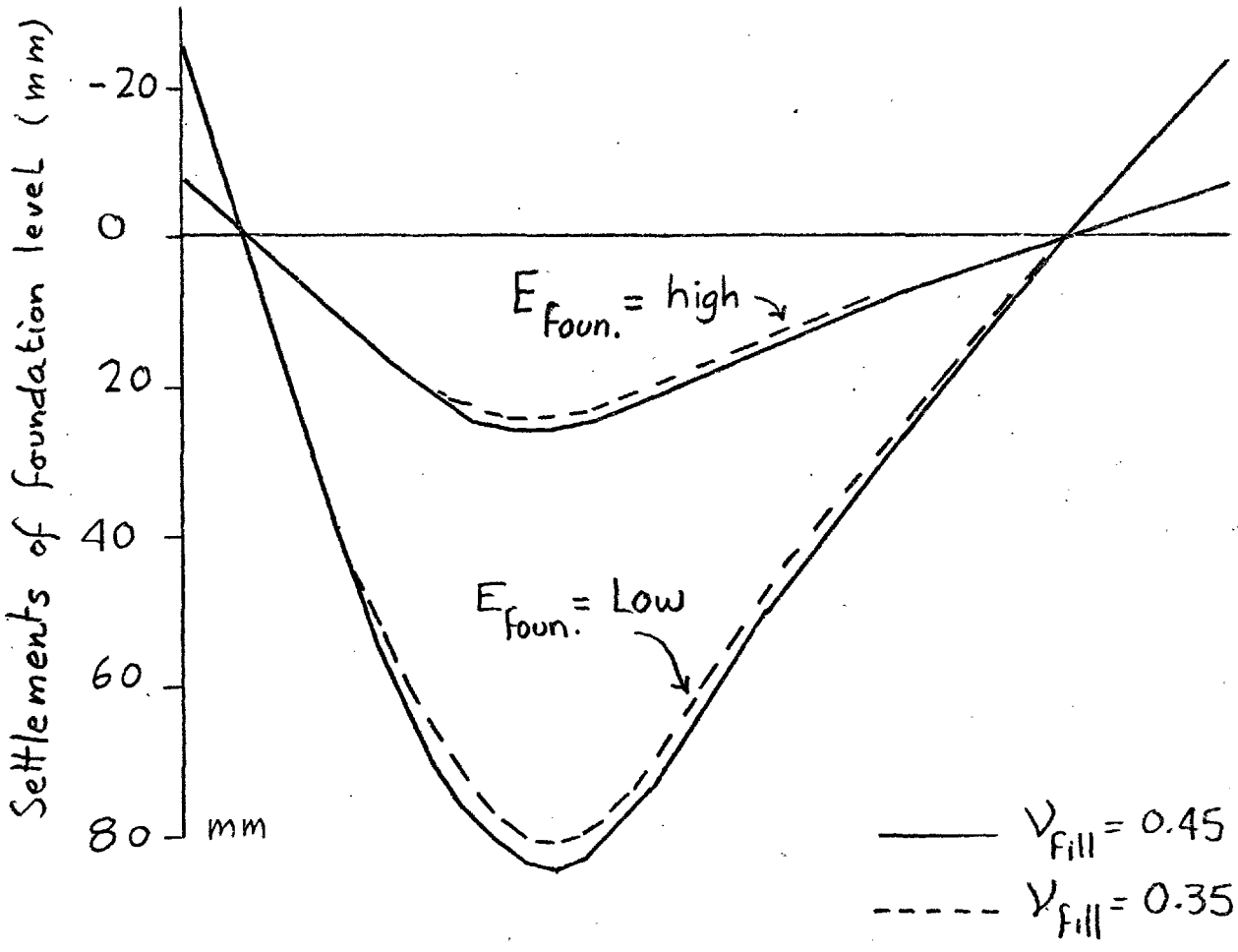


Fig. 6.4

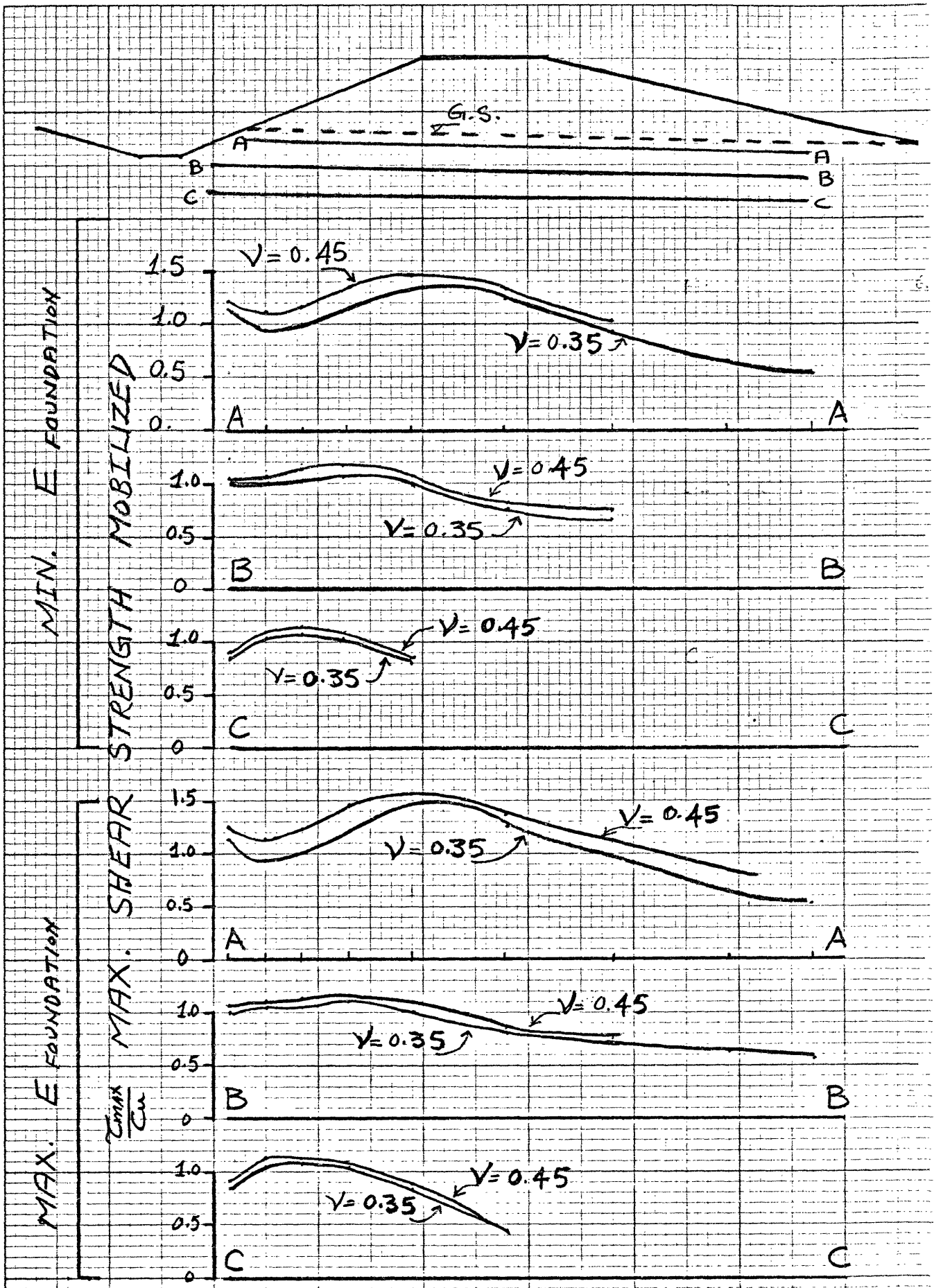


Horizontal movements at 2 vetical sections in the foundation under the upstream slope. (mm)



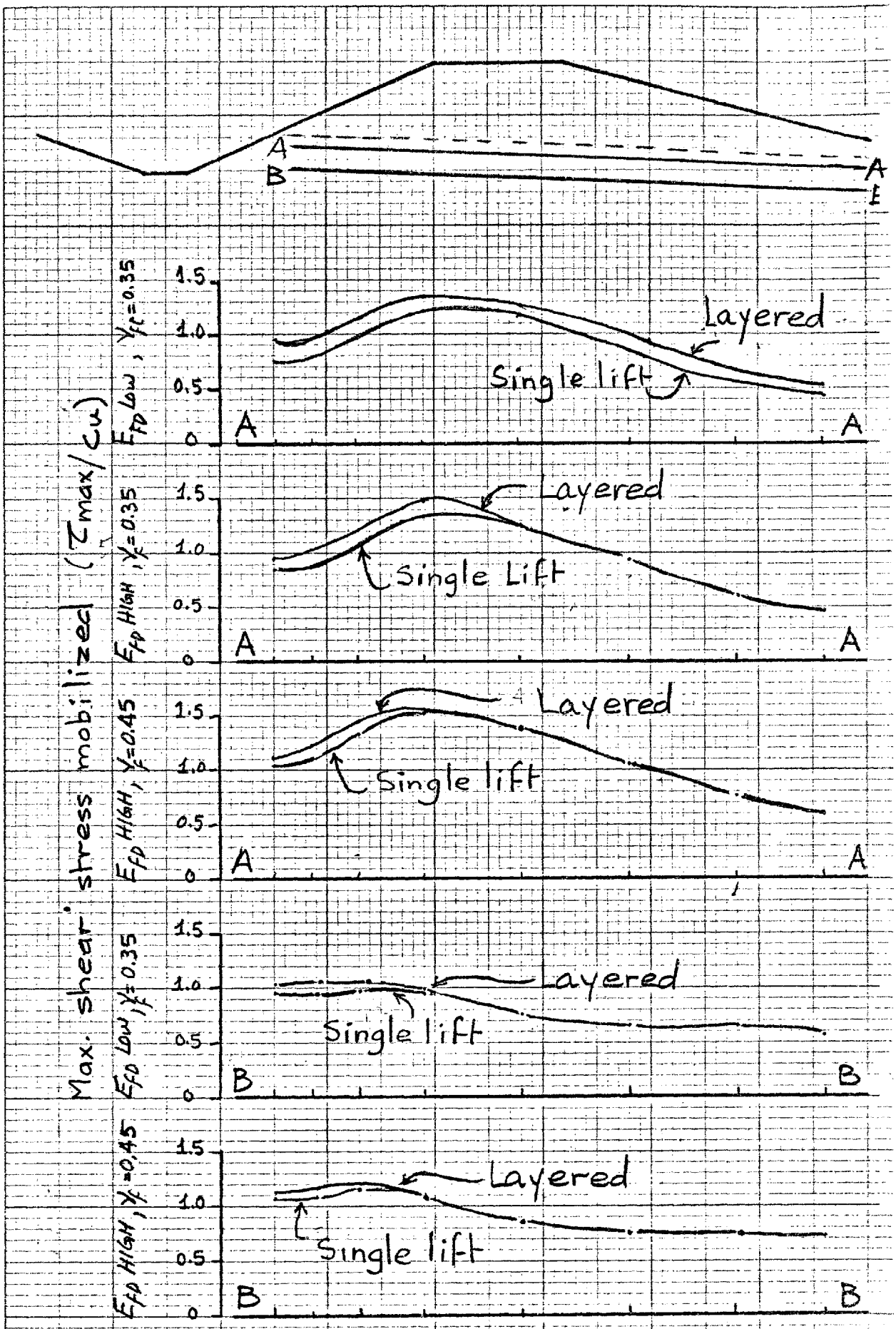
EFFECT OF FOUNDATION MODULUS AND FILL POISSON'S RATIO ON THE FOUNDATION MOVEMENTS

Fig. 6.5



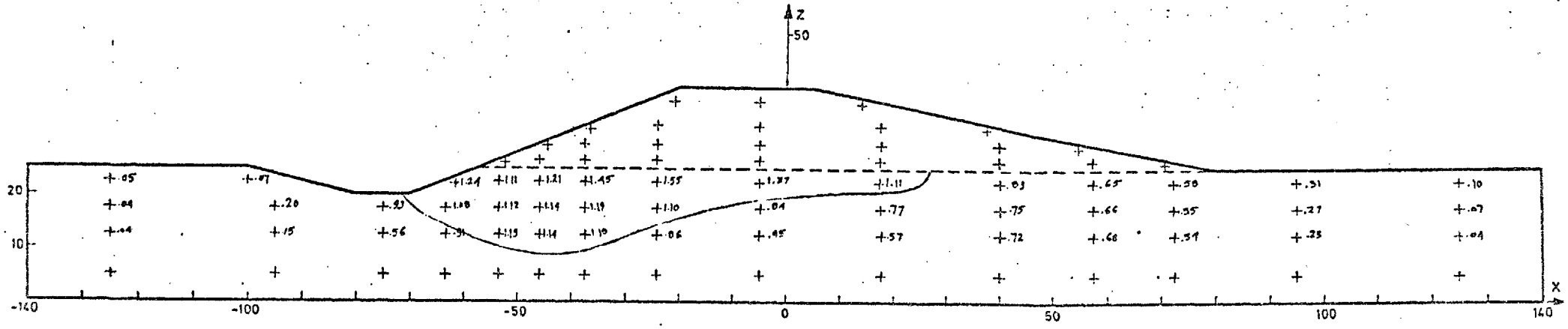
EFFECT OF FILL'S POISSON'S RATIO ON THE MAX. SHEAR STRESSES OF FOUNDATION

Fig. 6.6



THE EFFECT OF LAYERED ANALYSIS AS COMPARED TO SINGLE LIFT ANALYSIS

Fig. 6.7

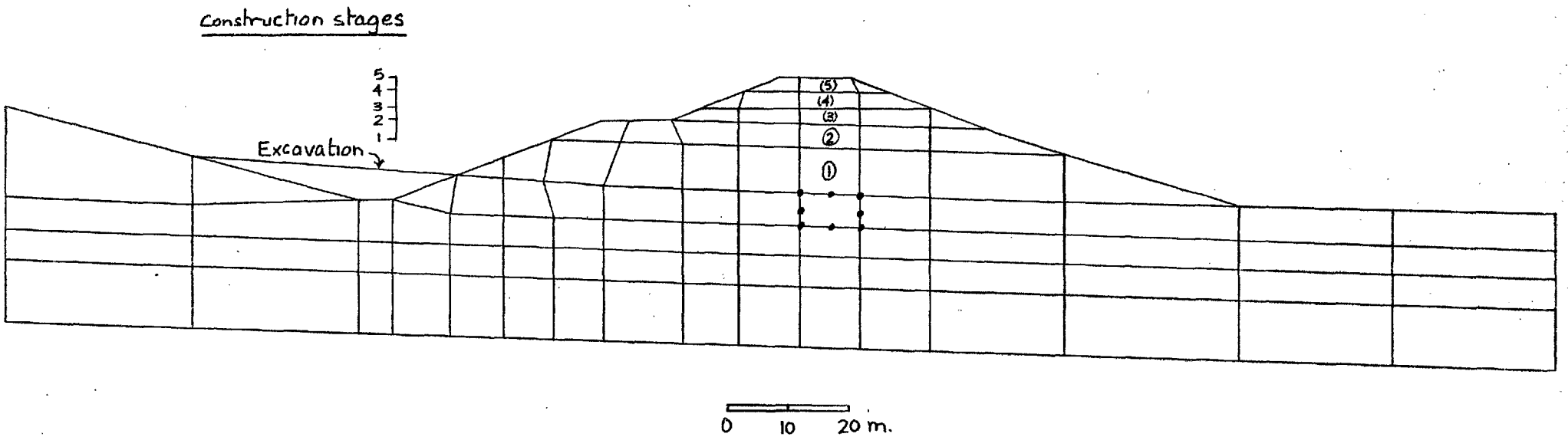


Dimensions are in metres

OVER STRESS RATIO $[(\sigma_1 - \sigma_3)/2c_u]$ _ ANALYSIS BEFORE END OF ACTUAL CONSTRUCTION _ FOUNDATION MODULUS : HIGH.

FILL'S POSSION'S RATIO : 0.45

Fig. 6.8

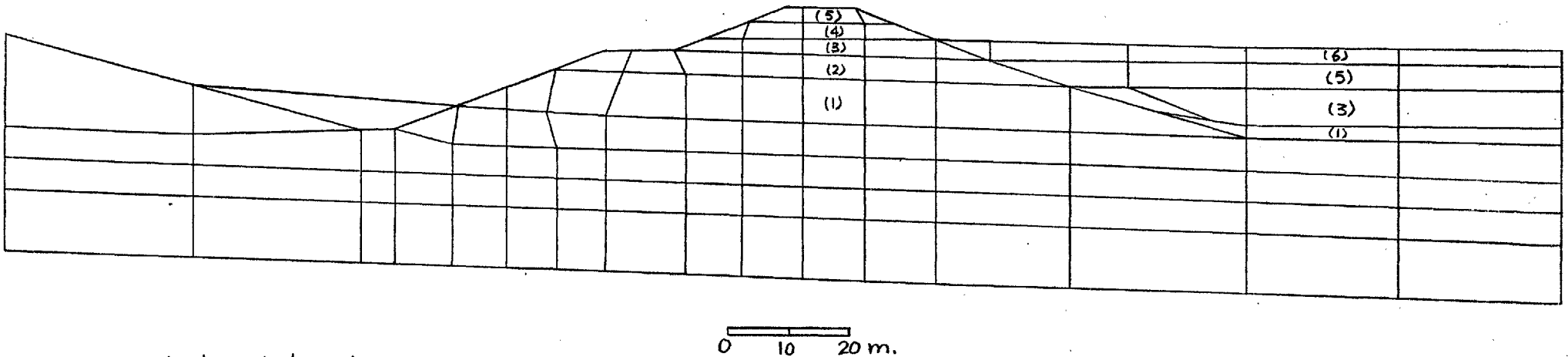


Number of elements = 92

Number of nodes = 329

FINITE ELEMENT MESH _ TRIAL BANK _ NO DOWN-STREAM FILLING

Fig. 6.9



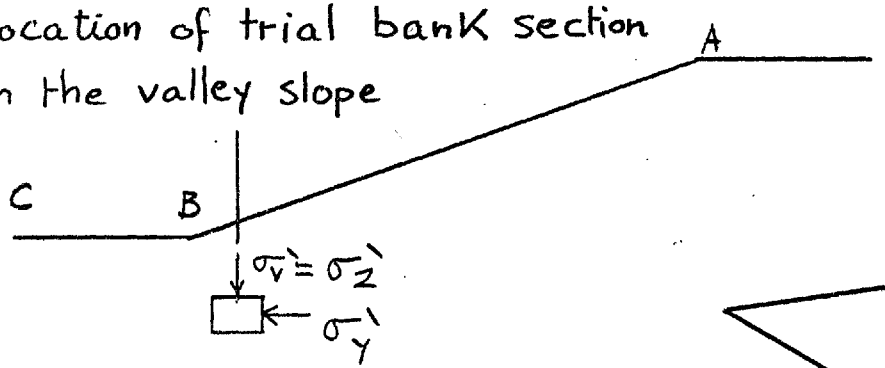
Number of elements = 108

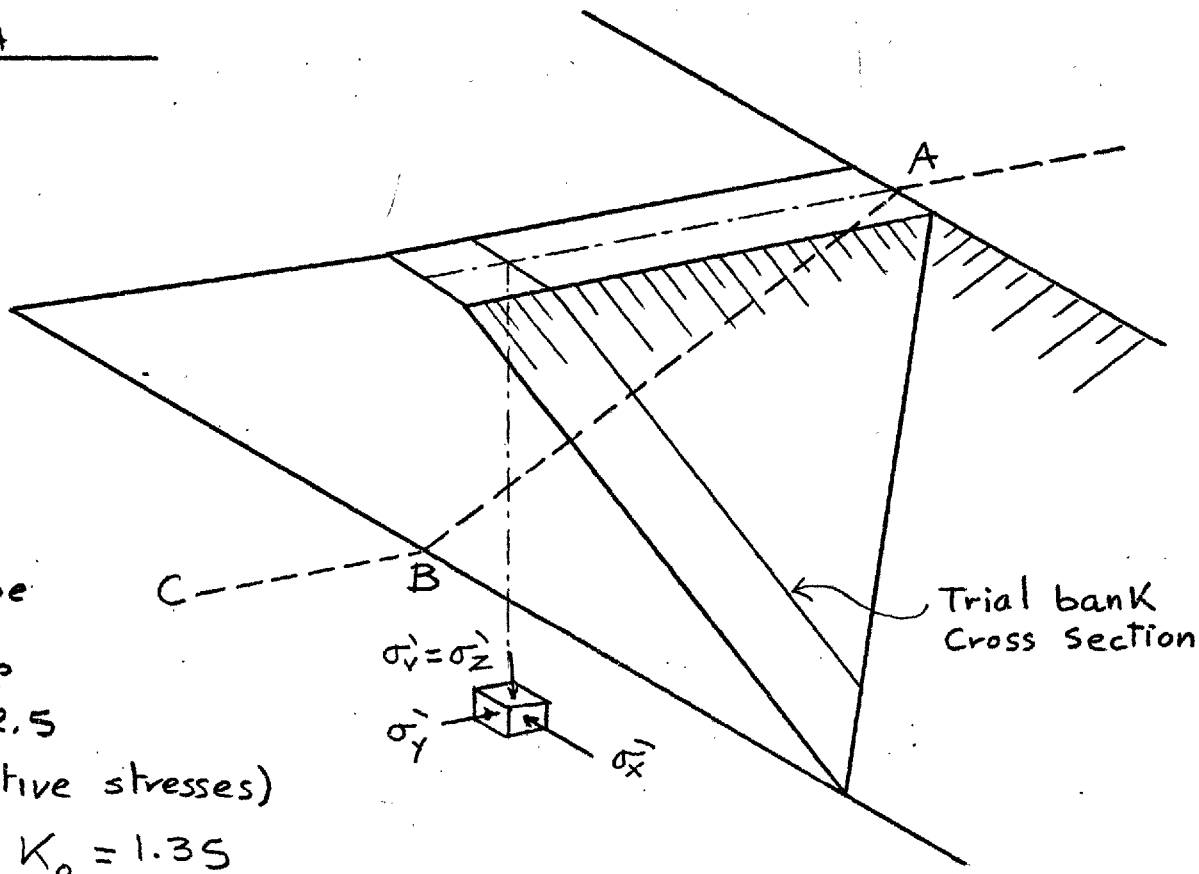
Number of nodes = 379

FINITE ELEMENT MESH _ TRIAL BANK _ WITH DOWN-STREAM FILLING

Fig. 6.10

Location of trial bank section in the valley slope





In ZY plane

1. T.B. is in passive zone,
   Thus $\bar{K}_o \doteq \bar{K}_p$
2. Due to the valley slope of 1:4 $\bar{K}_o = 2/3 \cdot \bar{K}_p$
3. IF $\bar{K}_p$ was equal to 2.5 the $\bar{K}_o = 1.7$ (effective stresses)
4. In total stresses $K_o = 1.35$
   (ground and water table at same level)

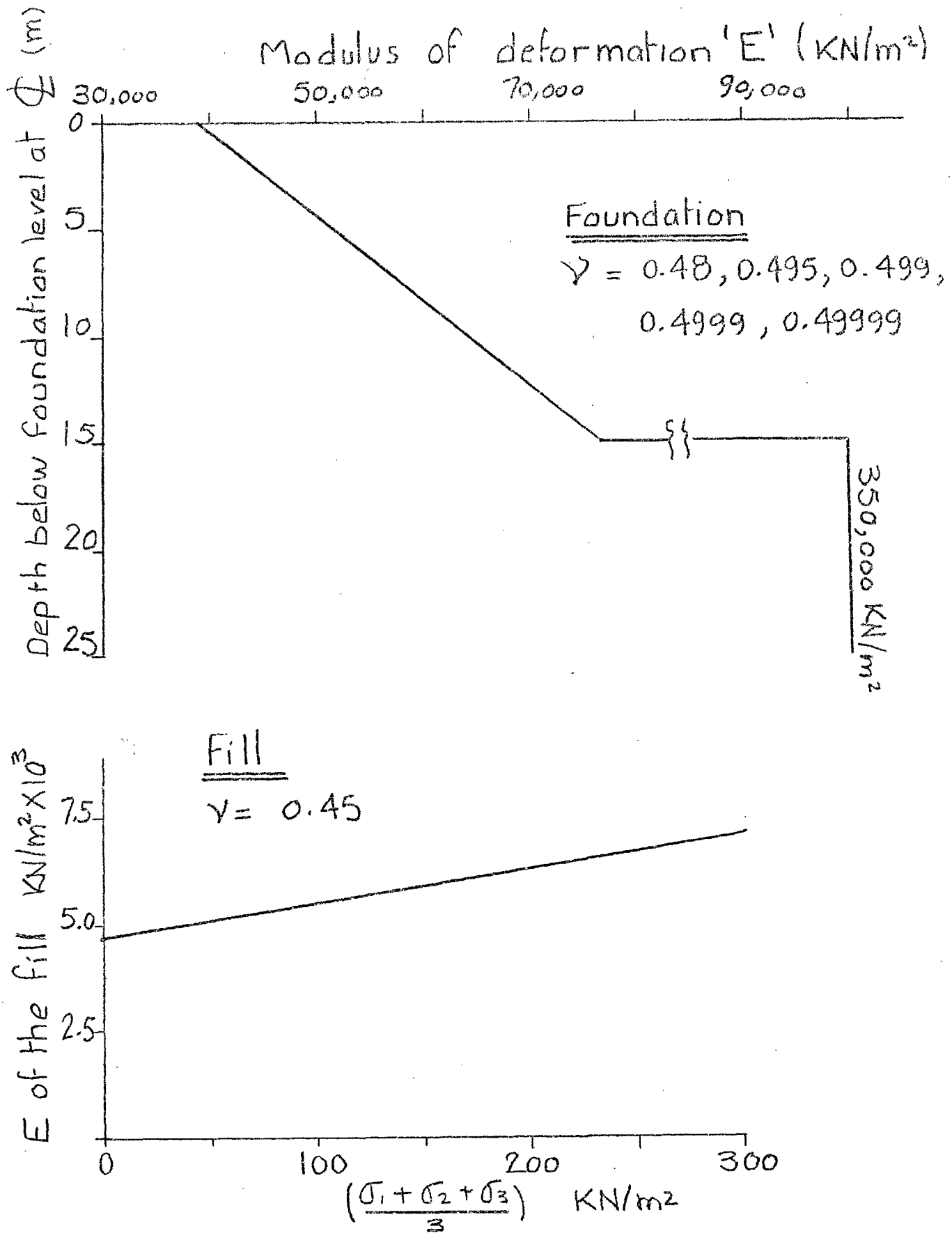
In Zx plane

$$\bar{\sigma_x} = \bar{\nu} (\sigma_z' + \sigma_y') \doteq 0.8\ \sigma_z'$$

Thus a further reduction to give $K_o = 0.9$

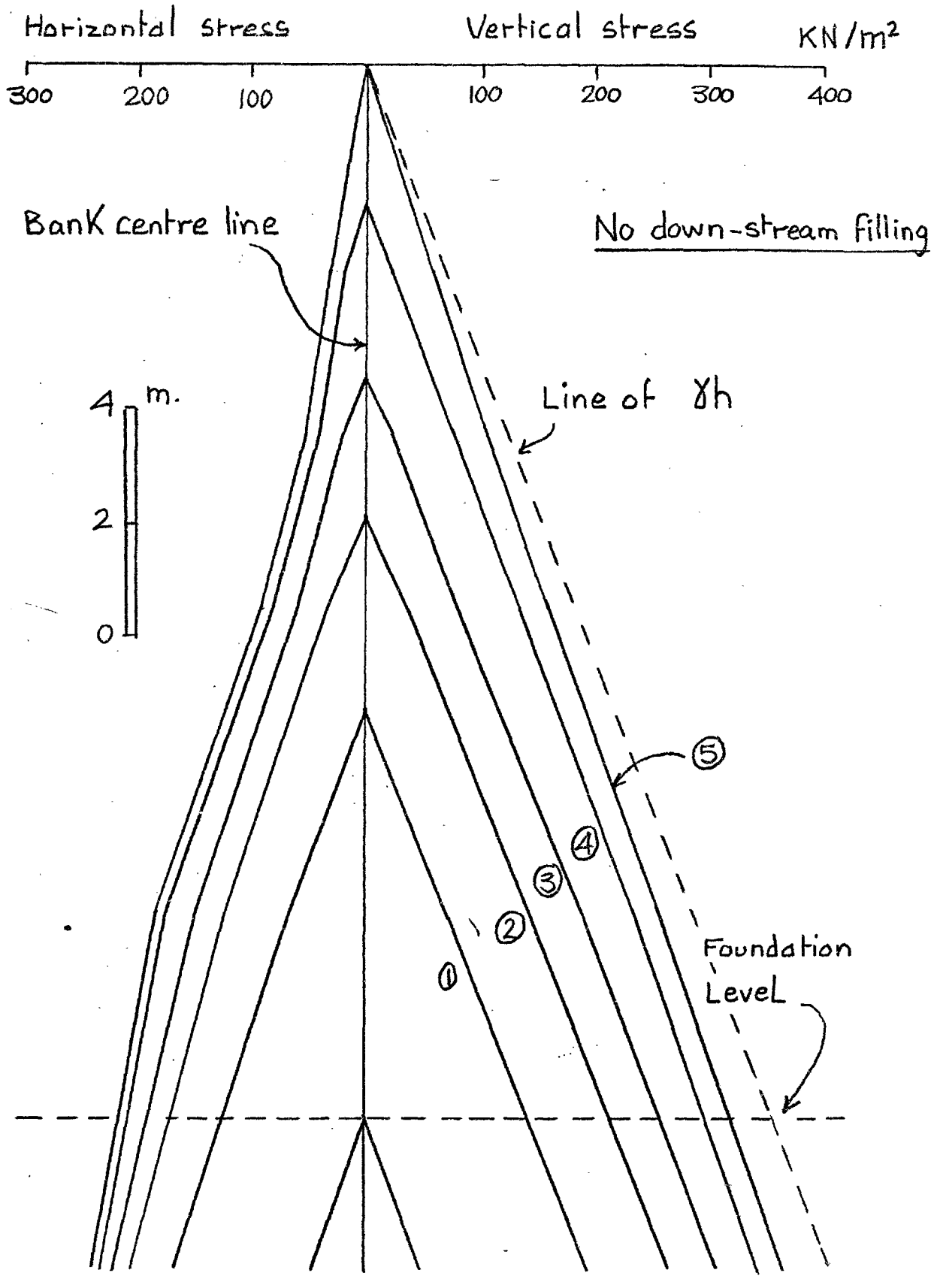
A diagrammatic representation of the reduction in horizontal stresses

Fig. 6.11



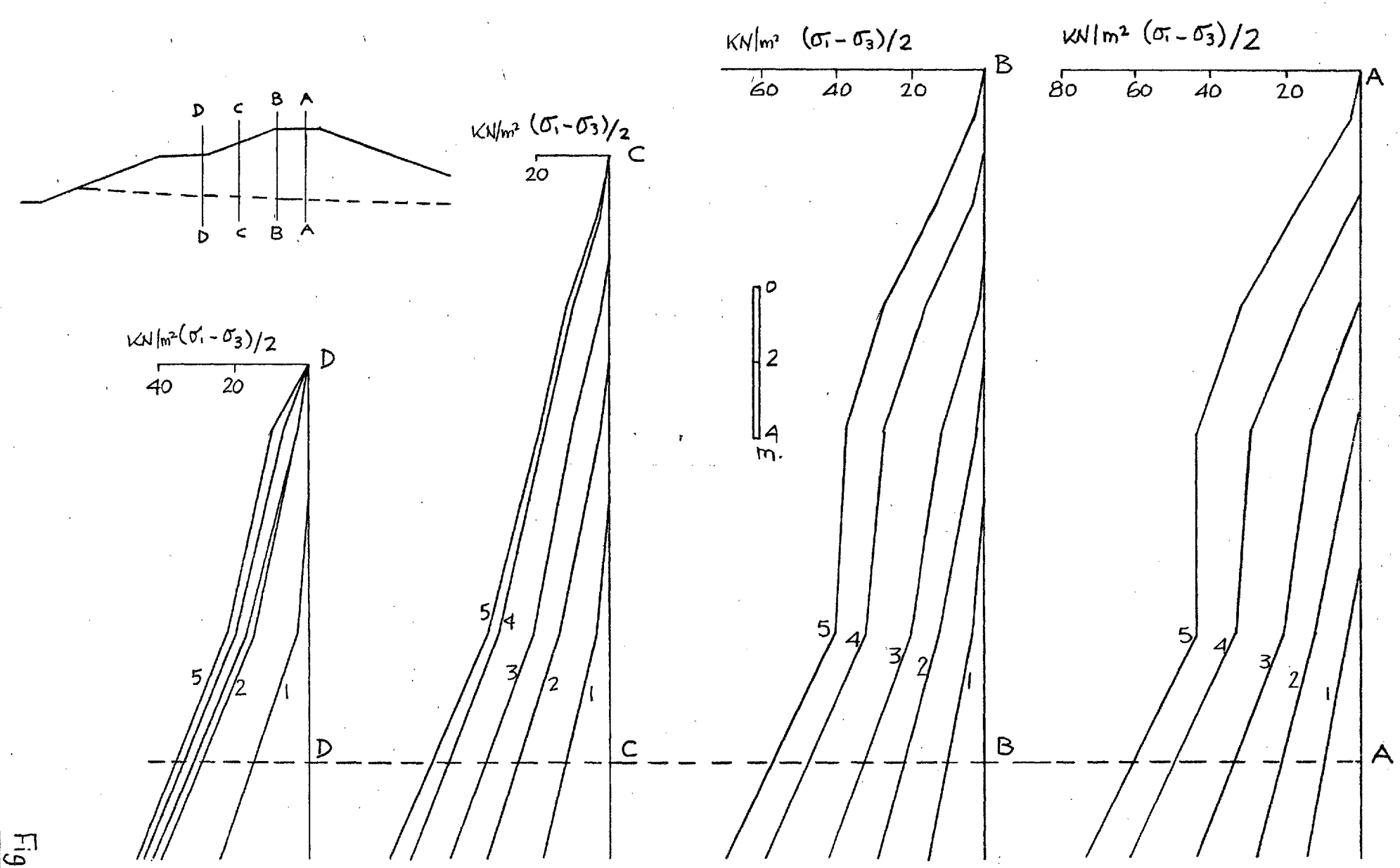
SUMMARY OF MATERIAL PROPERTIES FOR STAGE 2

Fig. 6.12



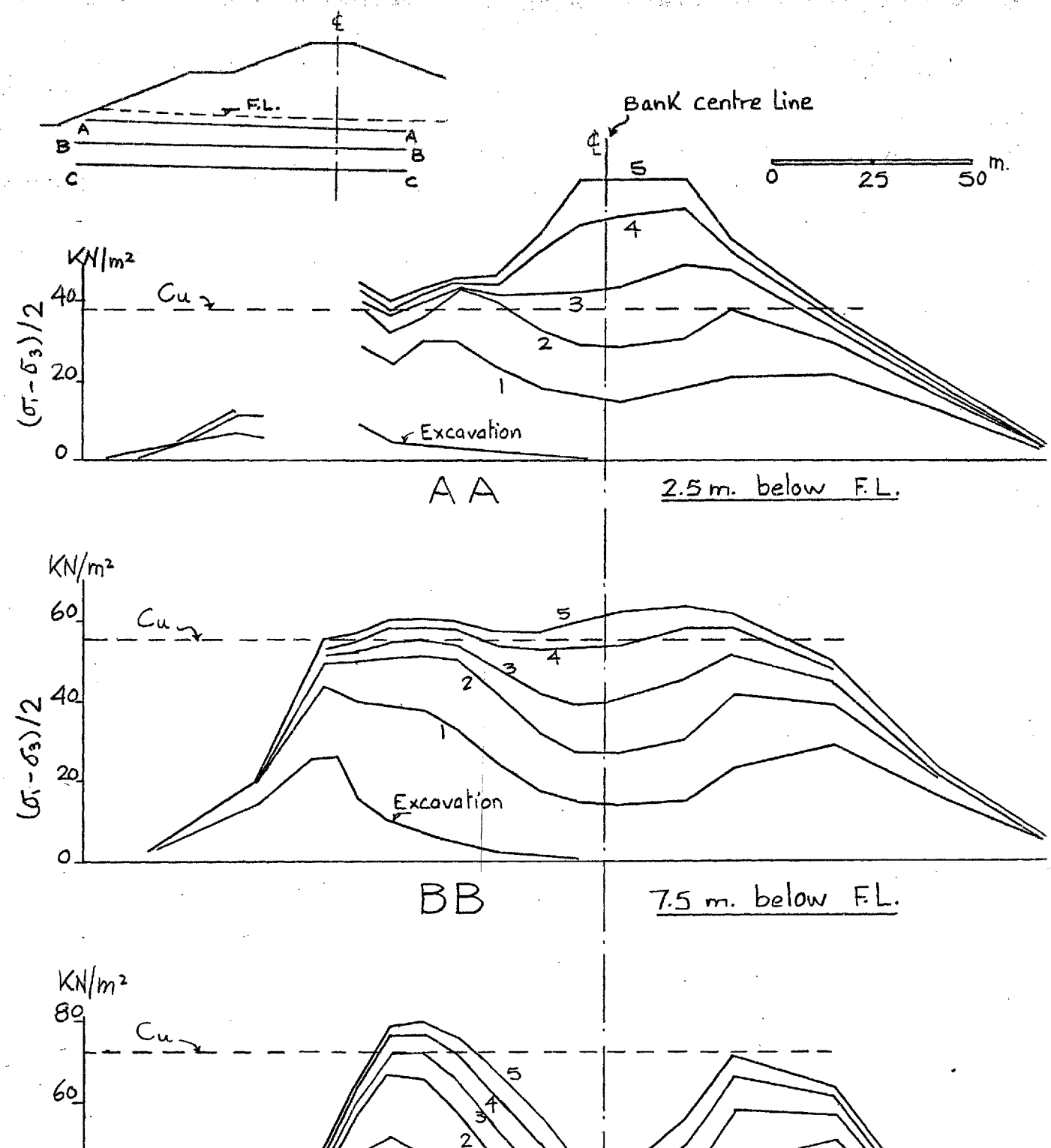
DEVELOPMENT OF VERTICAL AND HORIZONTAL STRESSES AT BANK'S CENTRE LINE_ RUN1

Fig. 6.13



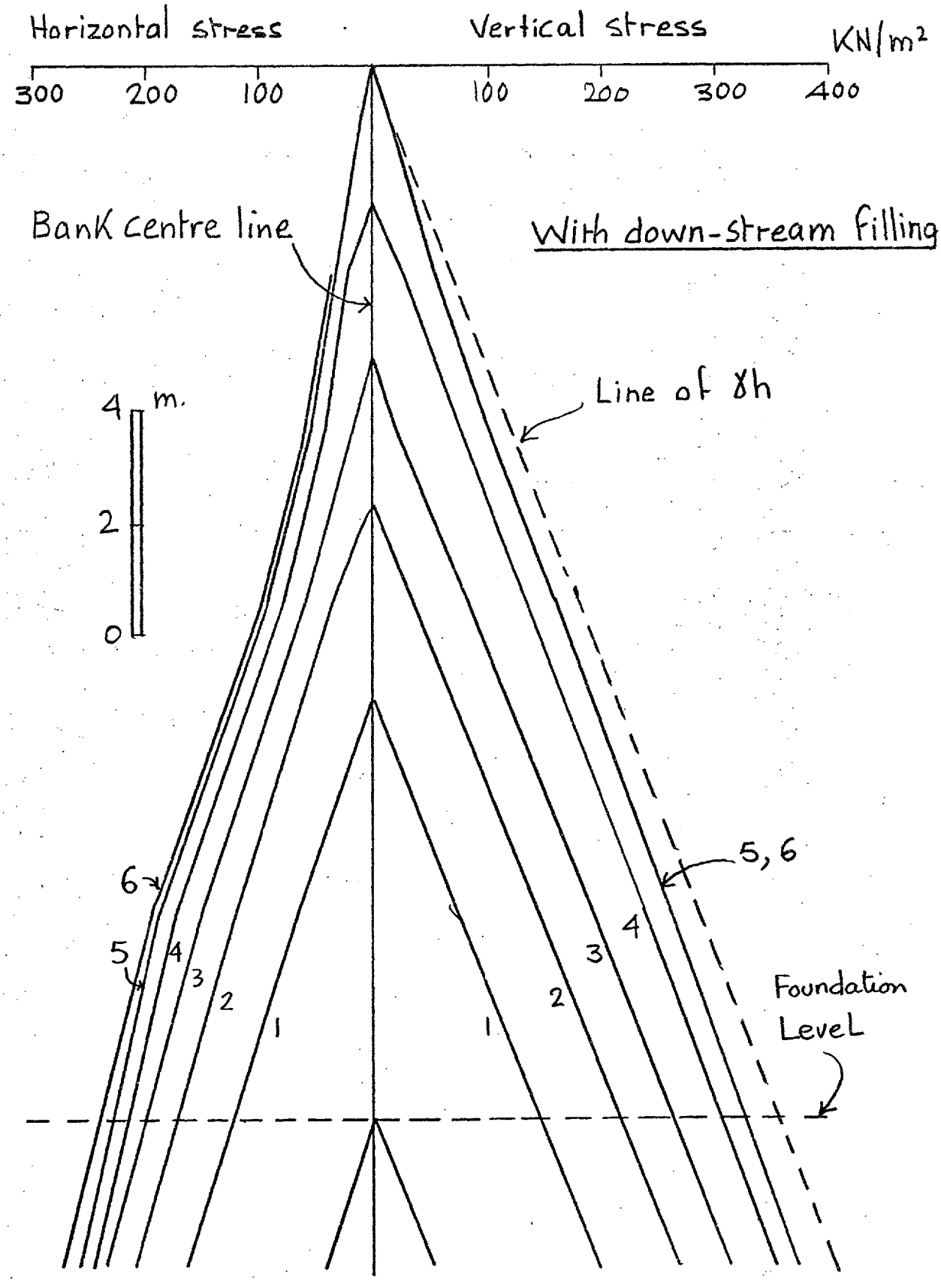
MAX. SHEAR STRESSES AT VERTICAL SECTIONS IN THE FILL_ RUN 1

Fig. 6.14



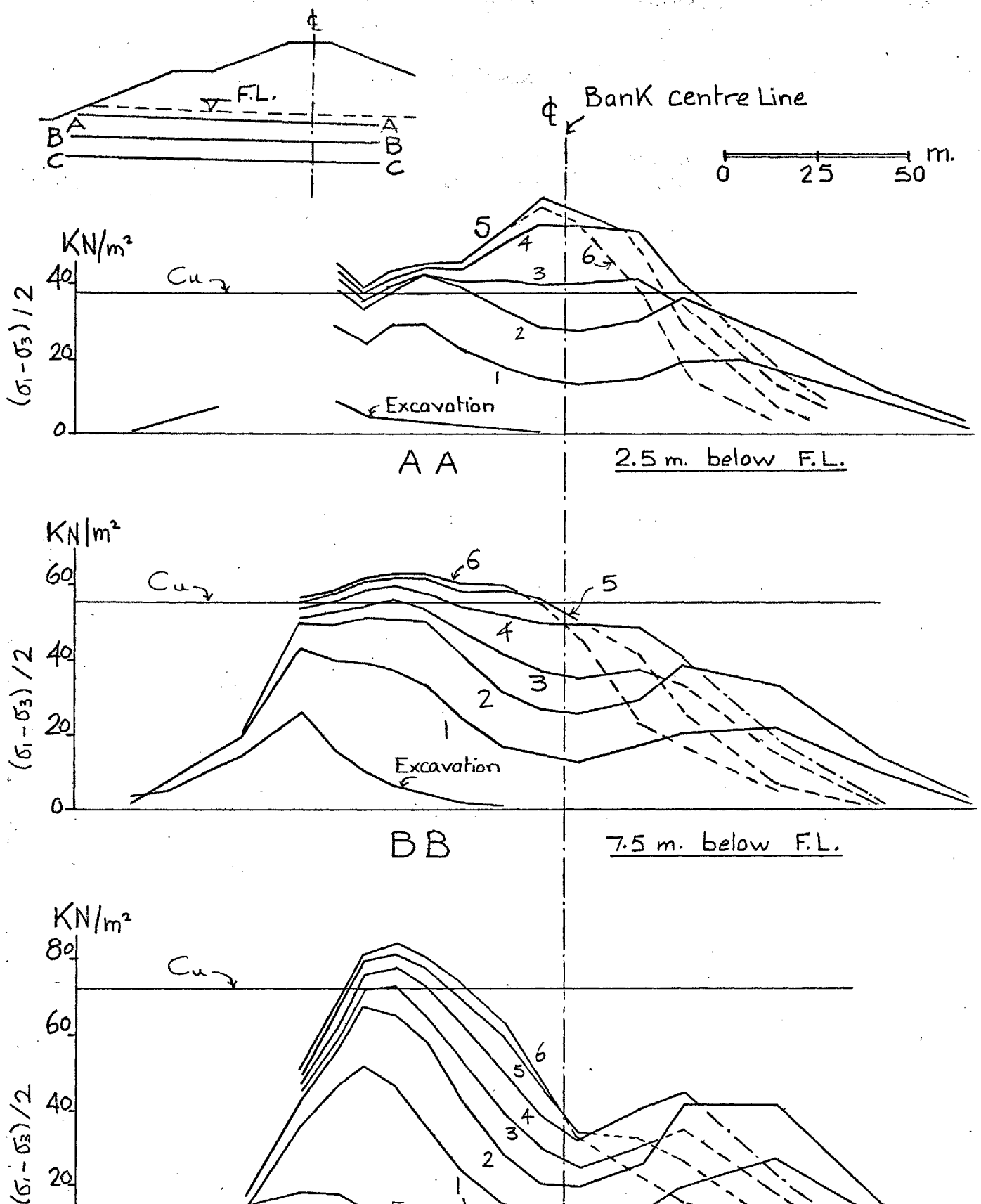
DEVELOPMENT OF MAX. SHEAR STRESSES IN THE BANK'S FOUNDATION - RUN 1

Fig. 6.15



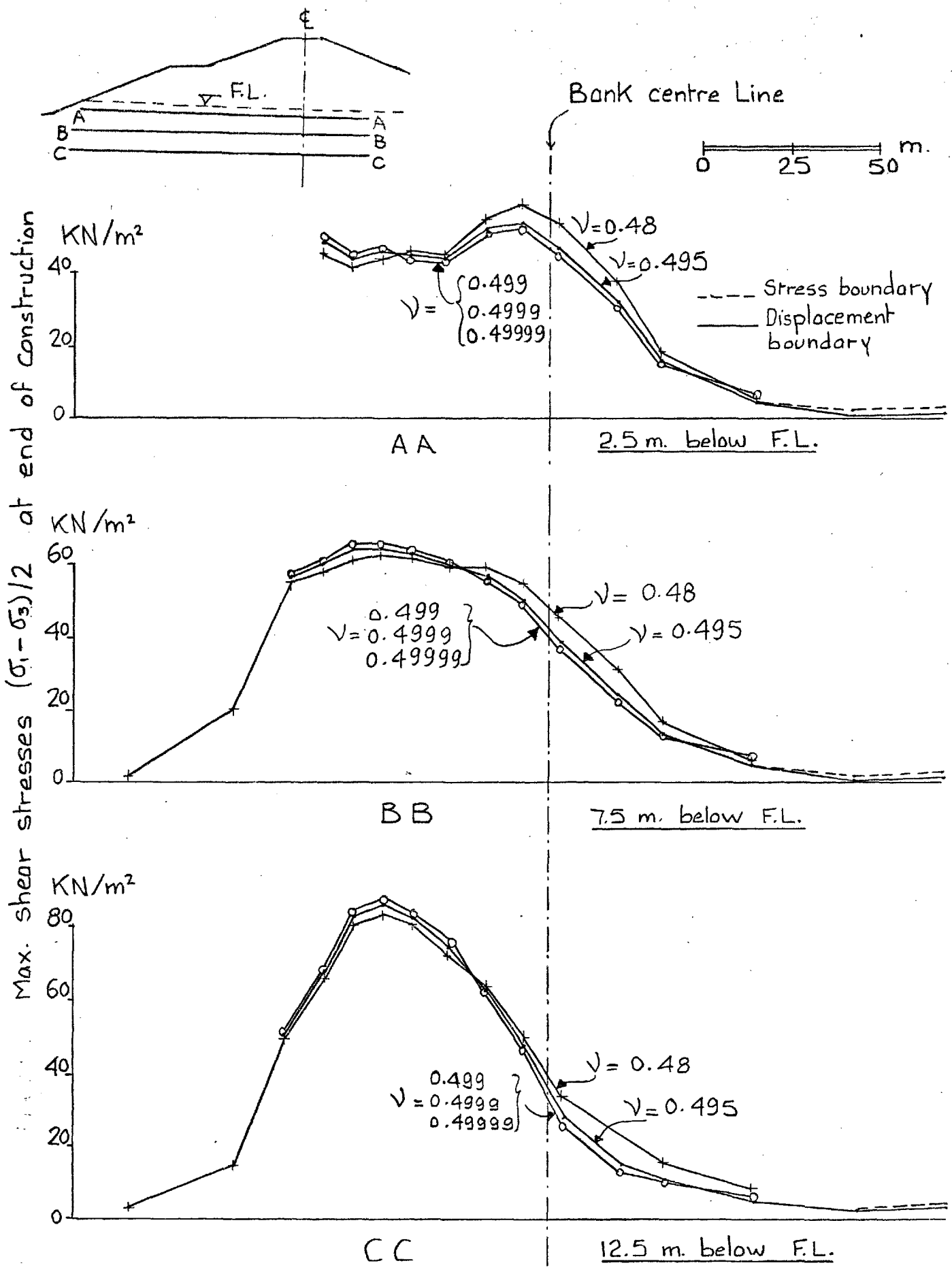
DEVELOPMENT OF VERTICAL AND HORIZONTAL STRESSES AT BANK'S CENTER LINE_RUN 2.

Fig. 6.16



DEVELOPMENT OF MAX. SHEAR STRESSES IN THE BANK'S FOUNDATION _ RUN 2

Fig. 6.17

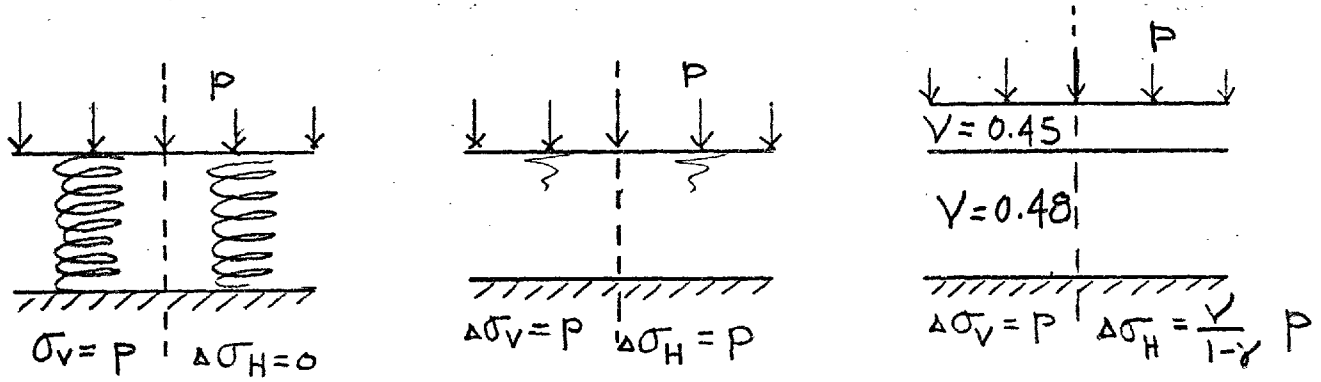


EFFECT OF USING POISSON'S RATIO CLOSE TO 0.5 AND DIFFERENT SIDE BOUNDARY ON THE MAX. SHEAR STRESS AT END OF CONSTRUCTION

Fig. 6.18

Boundary stress - Sliced boundary

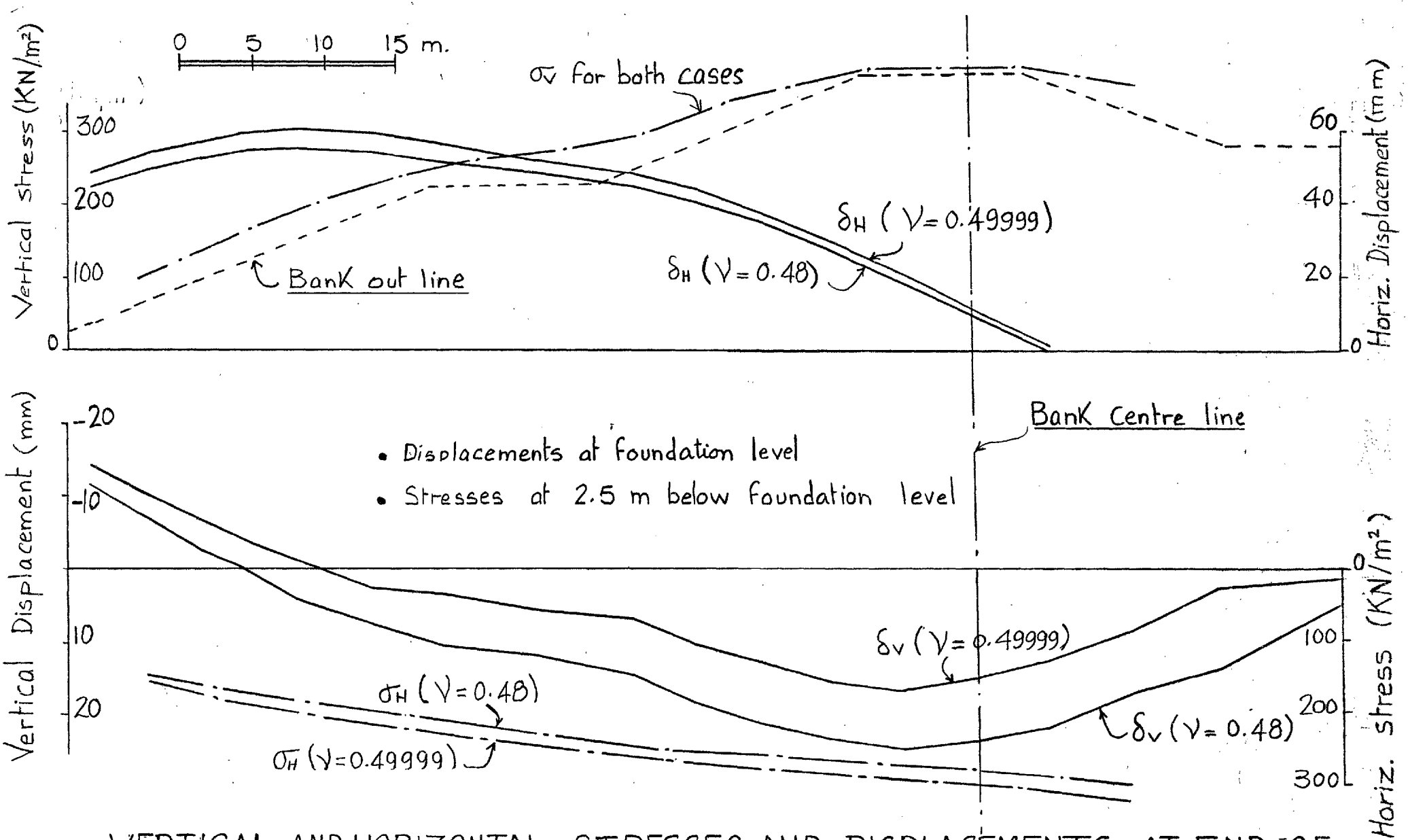
1. In principle a prescribed stress boundary is not possible in the displacement approach of the finite element formulation.
2. If the side boundary is not far enough, the rigid displacement boundary will present an incorrect stress.
3. It was believed that allowing the side boundary to move but imposing on it the stresses resulting from slicing the domain at the boundary will give a better stress near the boundary.
4. Step 3 implies predicting the stresses at the sliced face. A one dimensional elasticity assumption is employed as follows:-



Strain $\varepsilon_H = \frac{1}{E}\left(\Delta\sigma_H - \nu(\sigma_H + \Delta\sigma_V)\right) = 0$

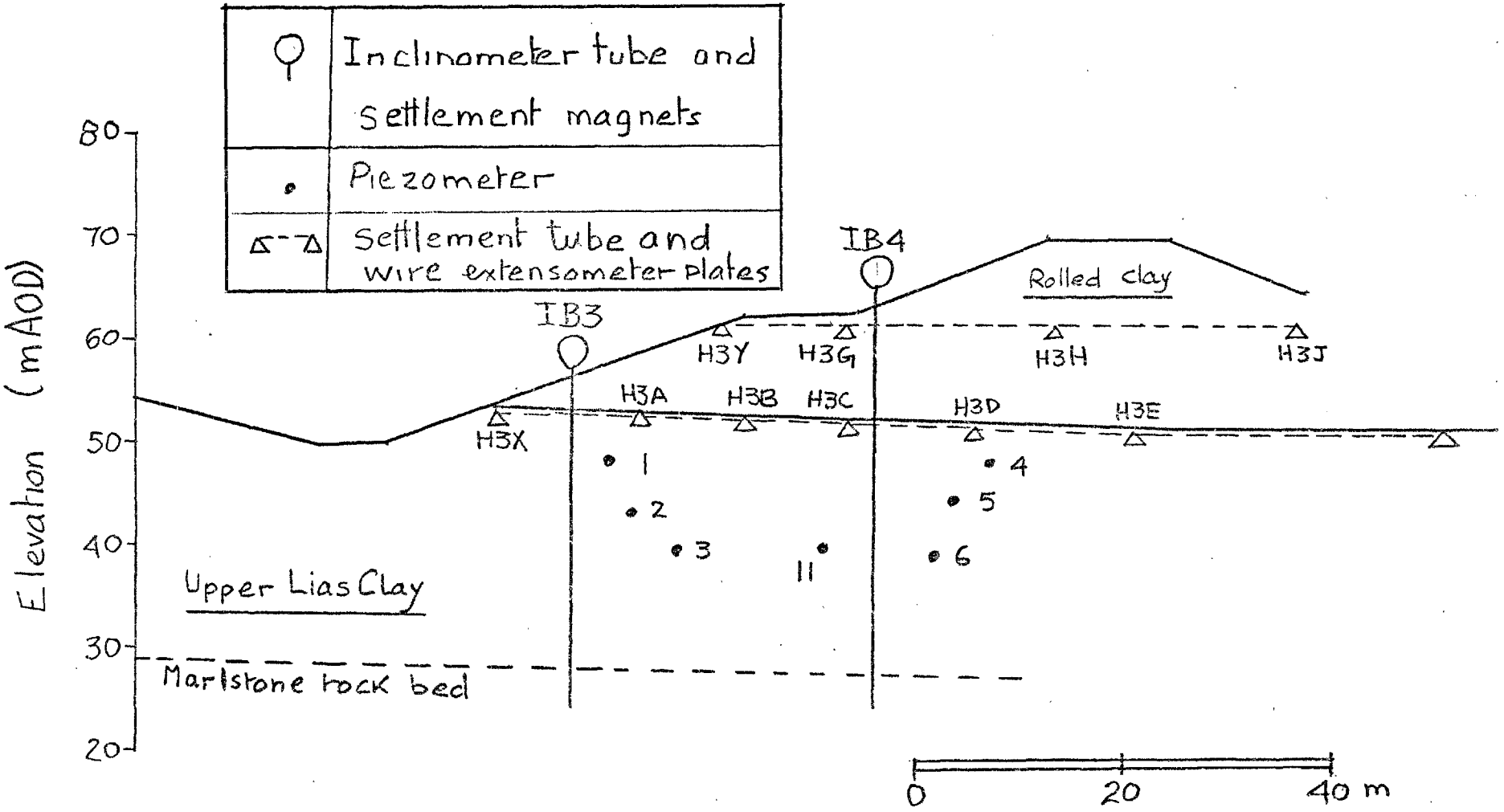
$$\Delta\sigma_H = \frac{\nu}{1-\nu}\,\Delta\sigma_V$$

Fig. 6.19



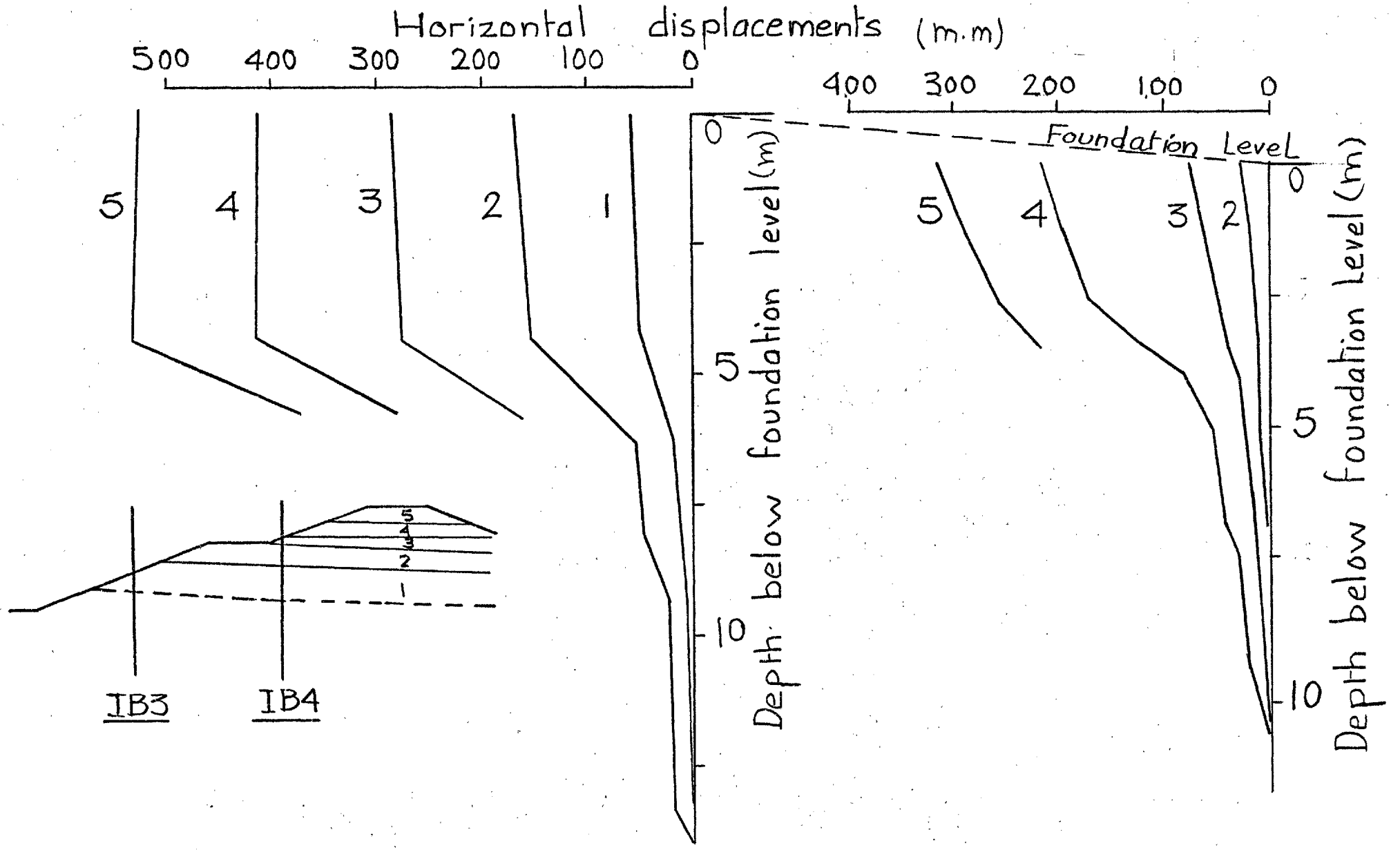
VERTICAL AND HORIZONTAL STRESSES AND DISPLACEMENTS AT END OF CONSTRUCTION FOR FOUNDATION'S POISSON'S RATIO OF 0.48 + 0.49999.

Fig 6.20



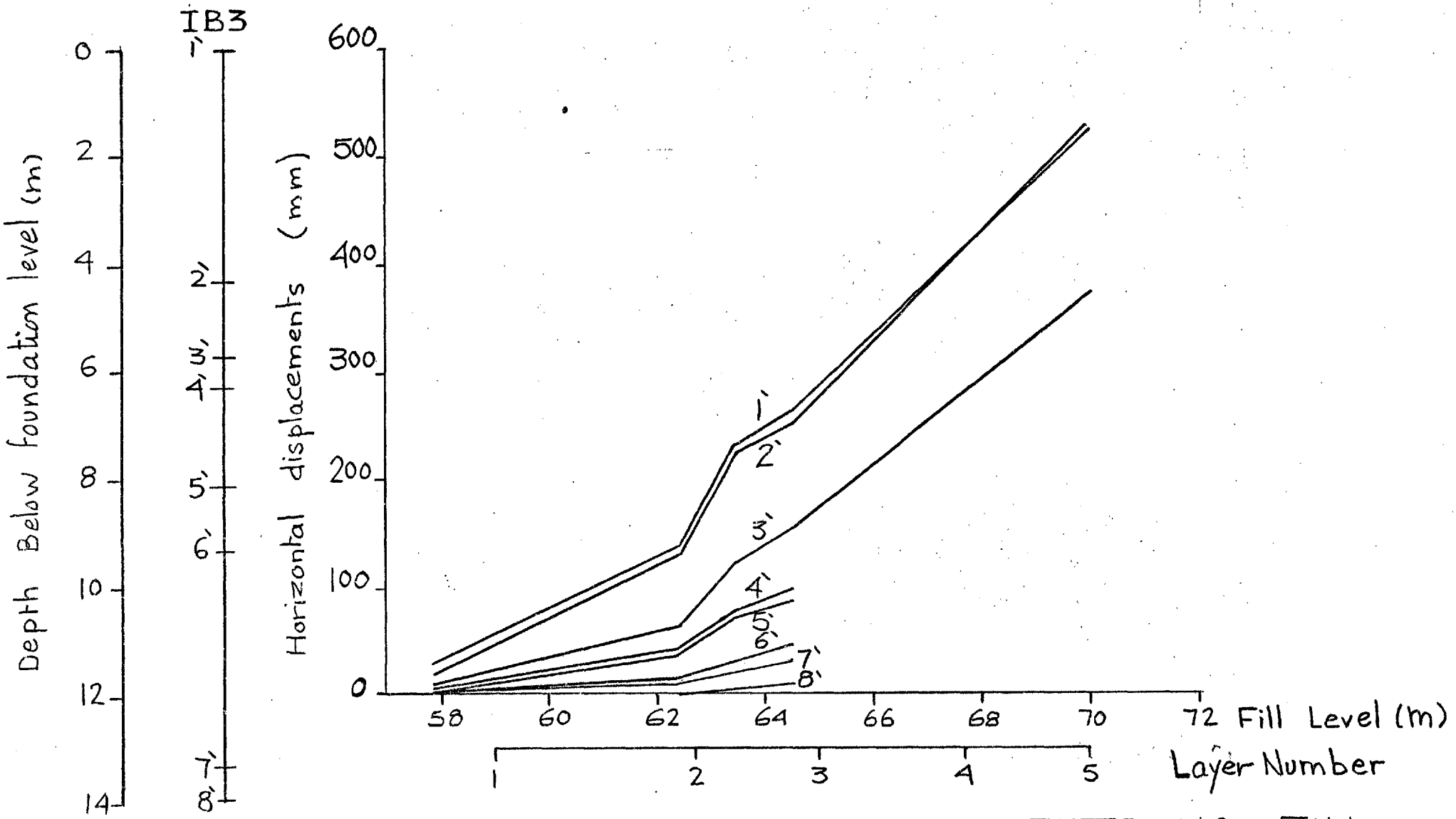
LOCATIONS OF THE INSTRUMENTS IN THE ANALYSED CROSS-SECTION

Fig. 6.21



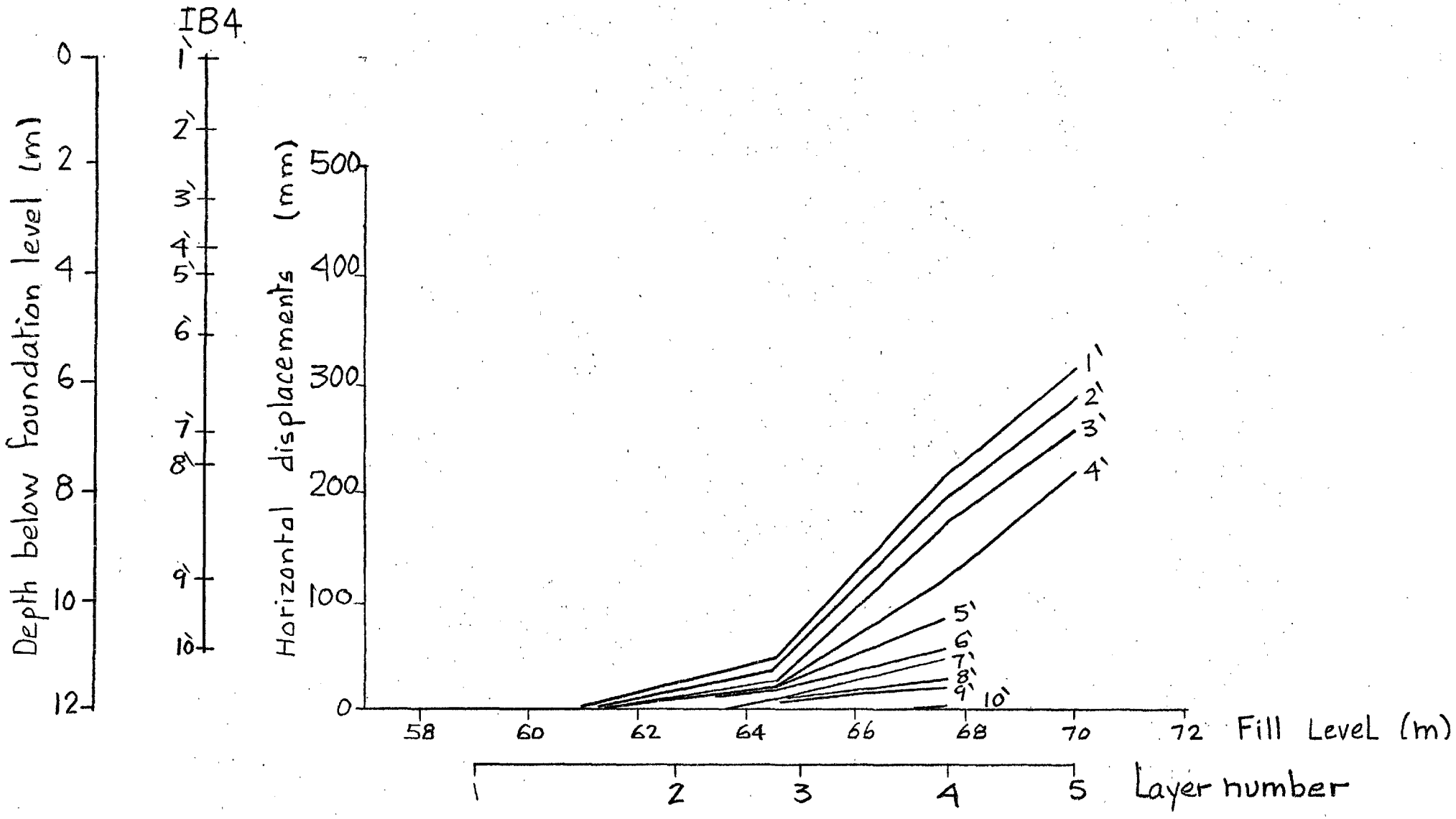
FIELD MEASUREMENTS OF HORIZONTAL MOVEMENTS - IB3, IB4

Fig. 6.22



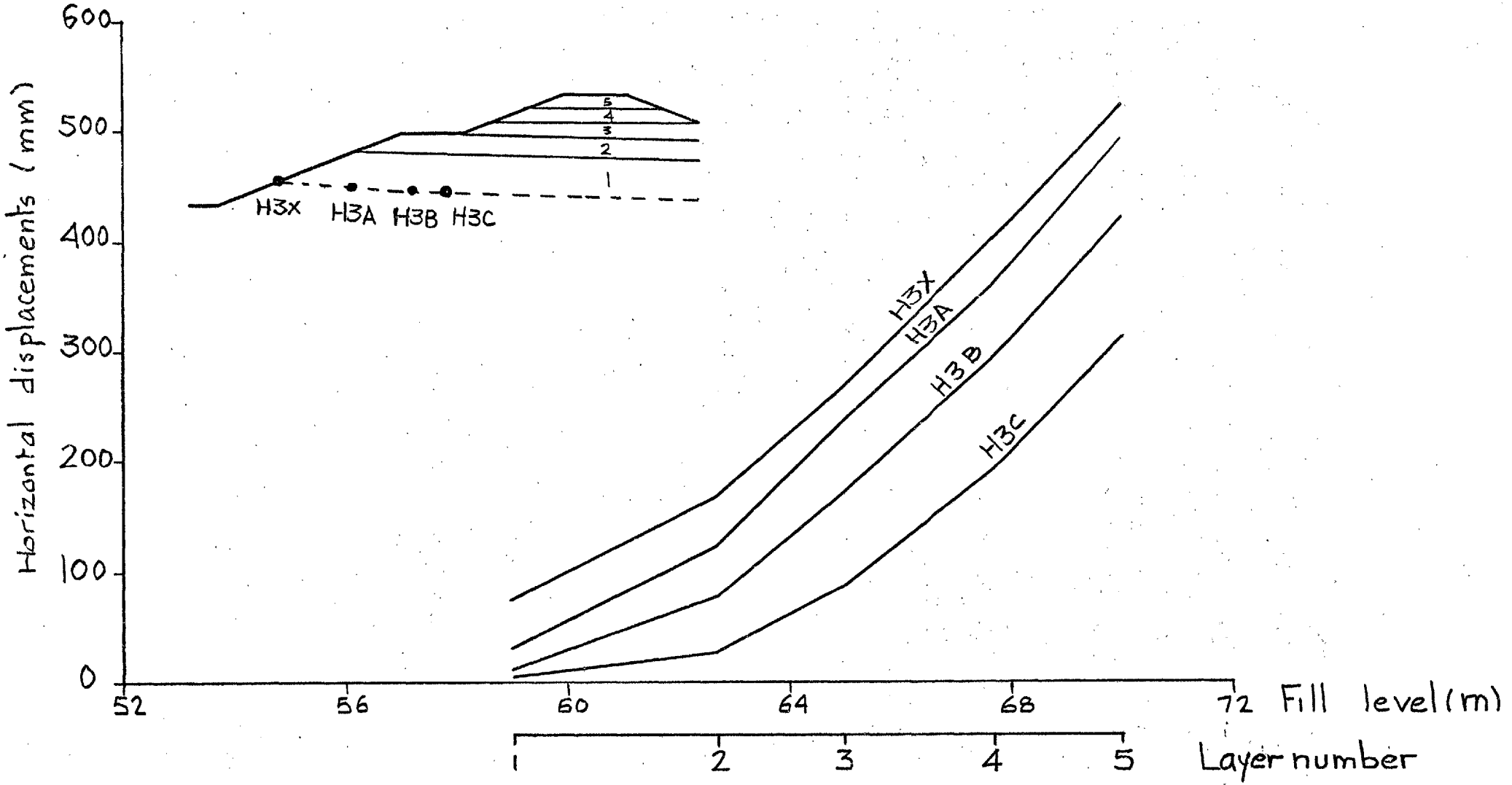
FIELD MEASURMENTS - HORIZONTAL DISPLACEMENTS VS. FILL HEIGHT AT SOME POINTS ON INCLINOMETER IB3.

Fig. 6.23



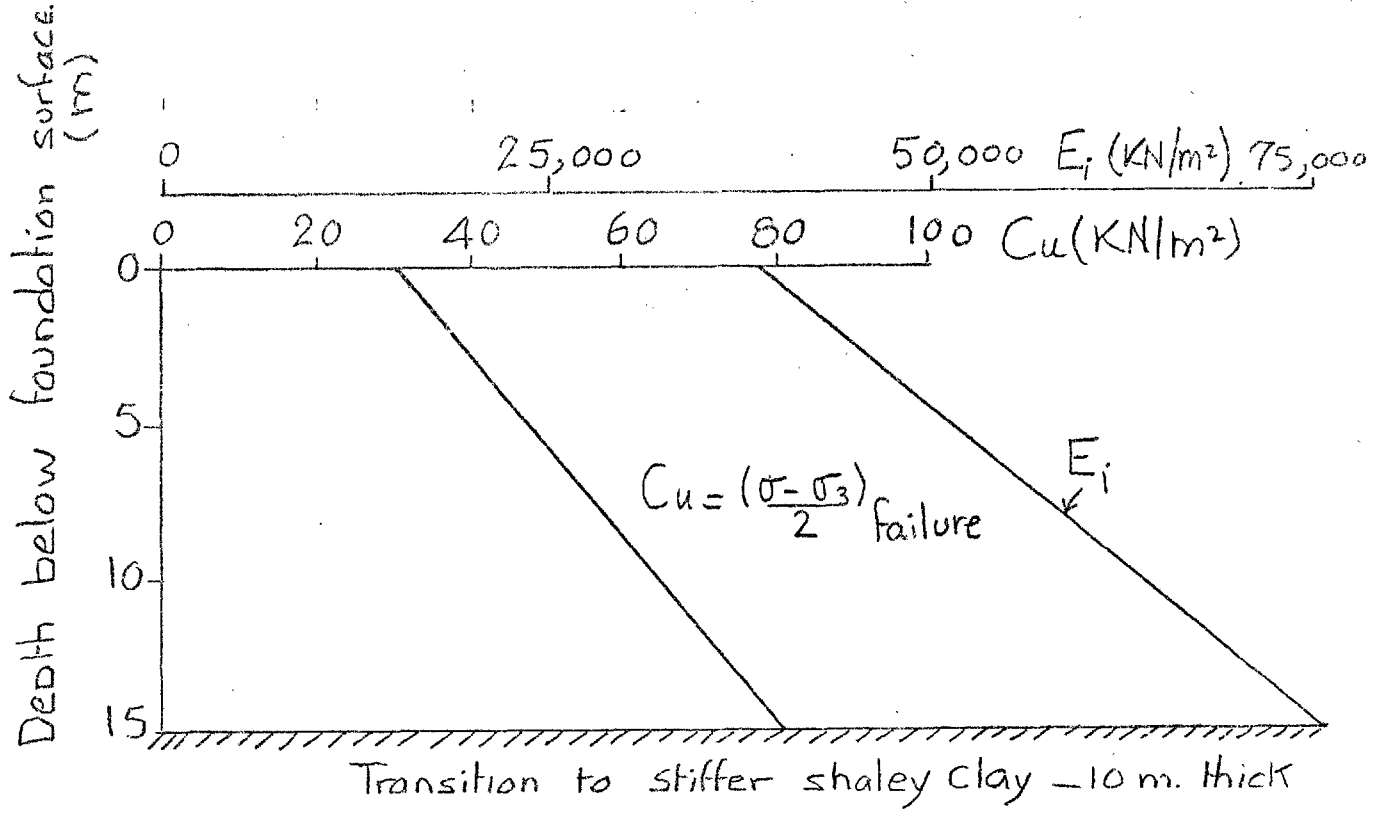
FIELD MEASURMENTS _ HORIZONTAL DISPLACEMENTS VS. FILL HEIGHT AT SOME POINTS ON INCLINOMETER IB4.

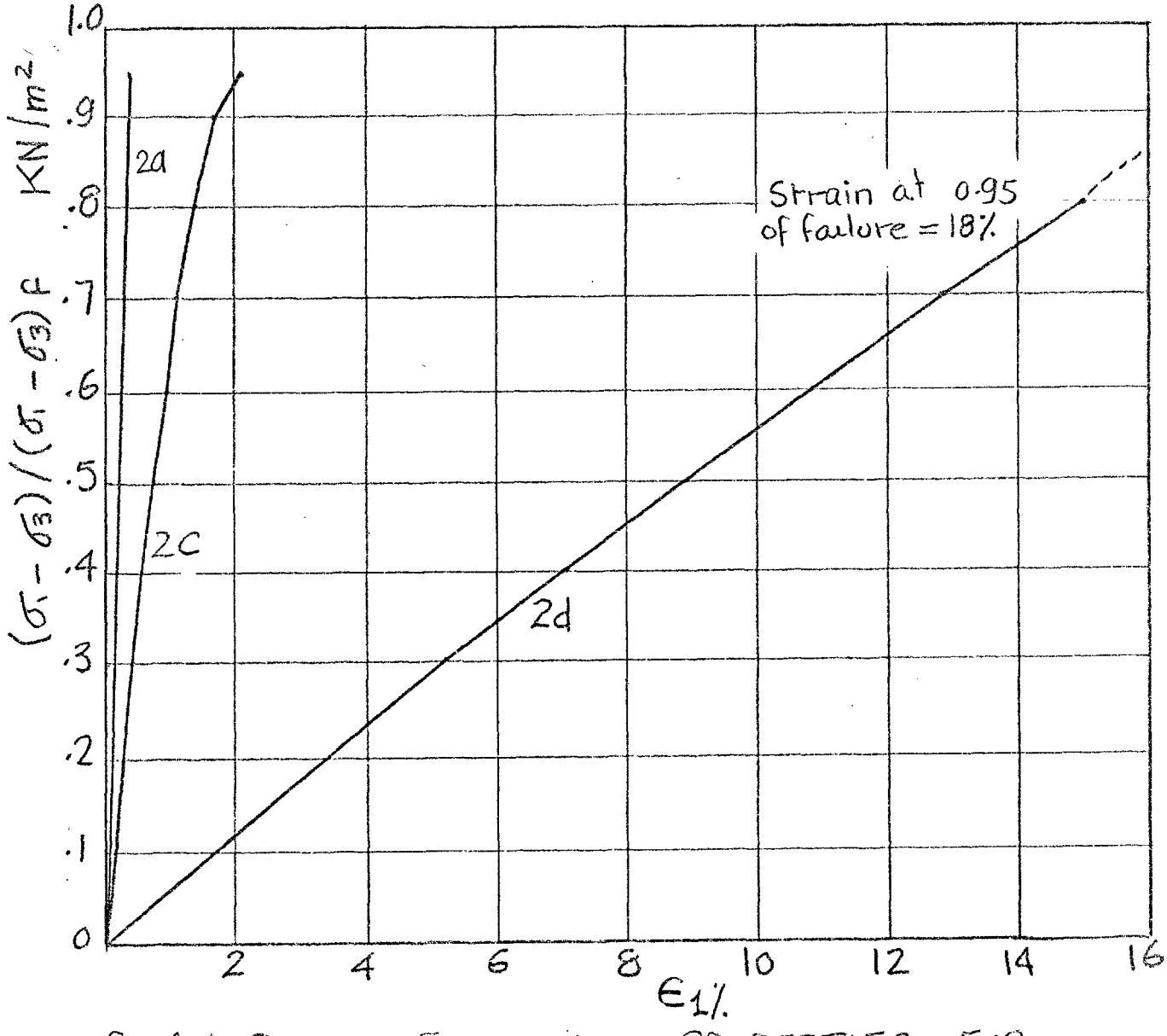
Fig 6.24



FIELD MEASURMENTS _ HORIZONTAL DISPLACEMENTS VS. FILL HEIGHT AT SOME POINT ON THE FOUNDATION SURFACE.

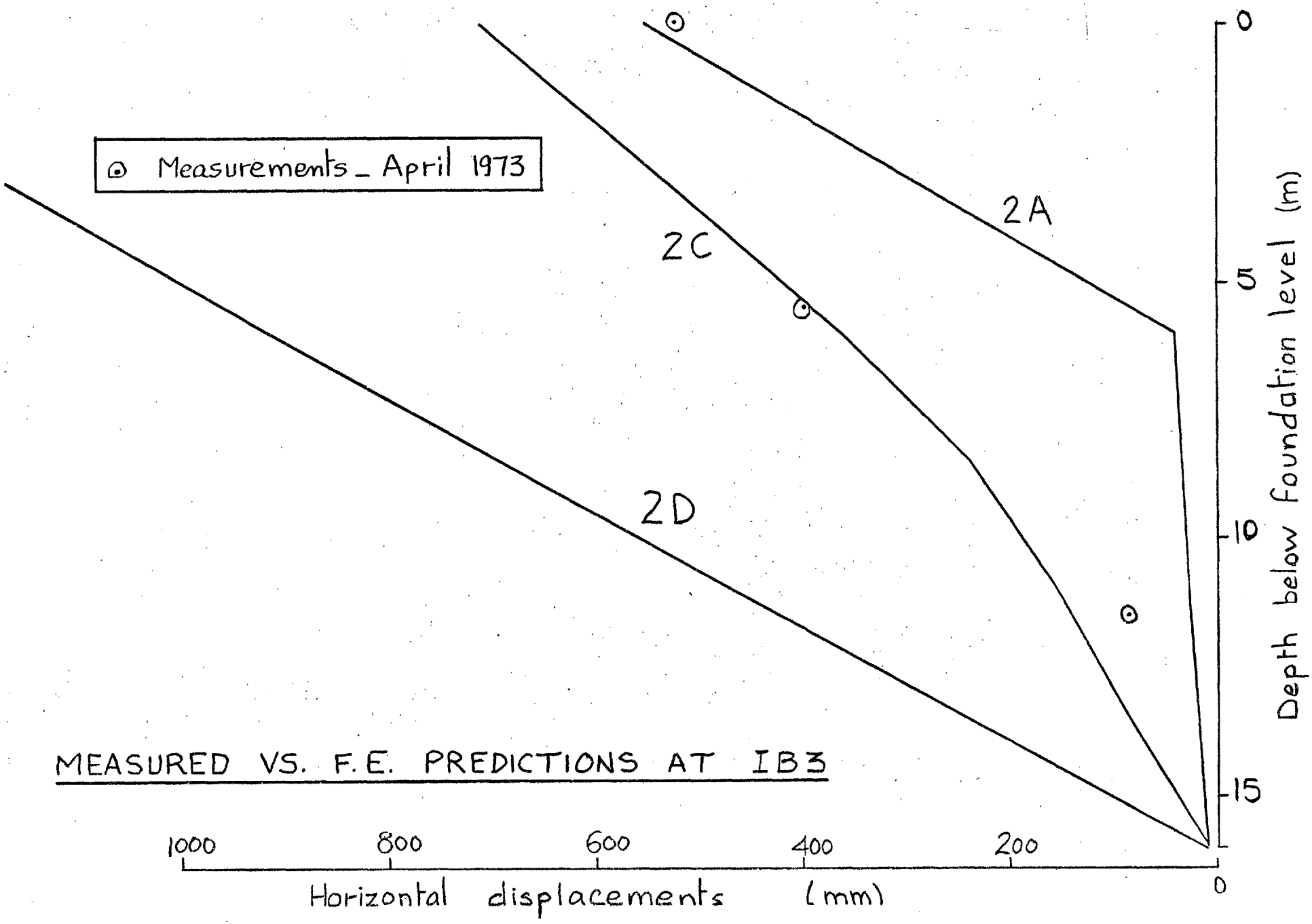
Fig. 6.25





SUMMARY OF FOUNDATION PROPERTIES FOR STAGE 3 : CASES 2a , 2c , 2d

Fig. 6.26



MEASURED VS. F.E. PREDICTIONS AT IB3

Fig. 6.27

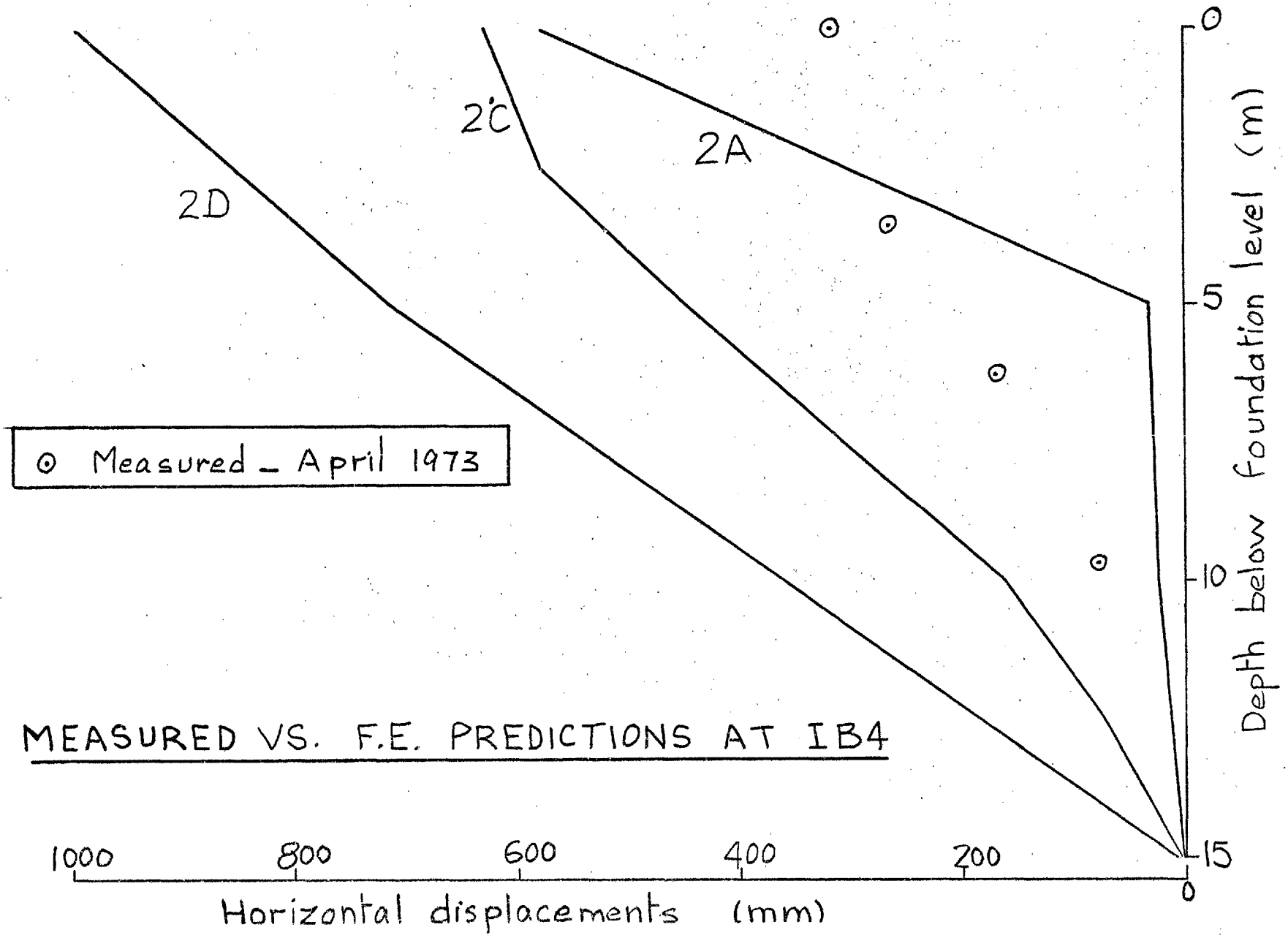

2D
2C
2A
⊙ Measured – April 1973
MEASURED VS. F.E. PREDICTIONS AT IB4
1000
800
600
400
200
0
Horizontal displacements (mm)
0
5
10
15
Depth below foundation level (m)

Fig. 6.28

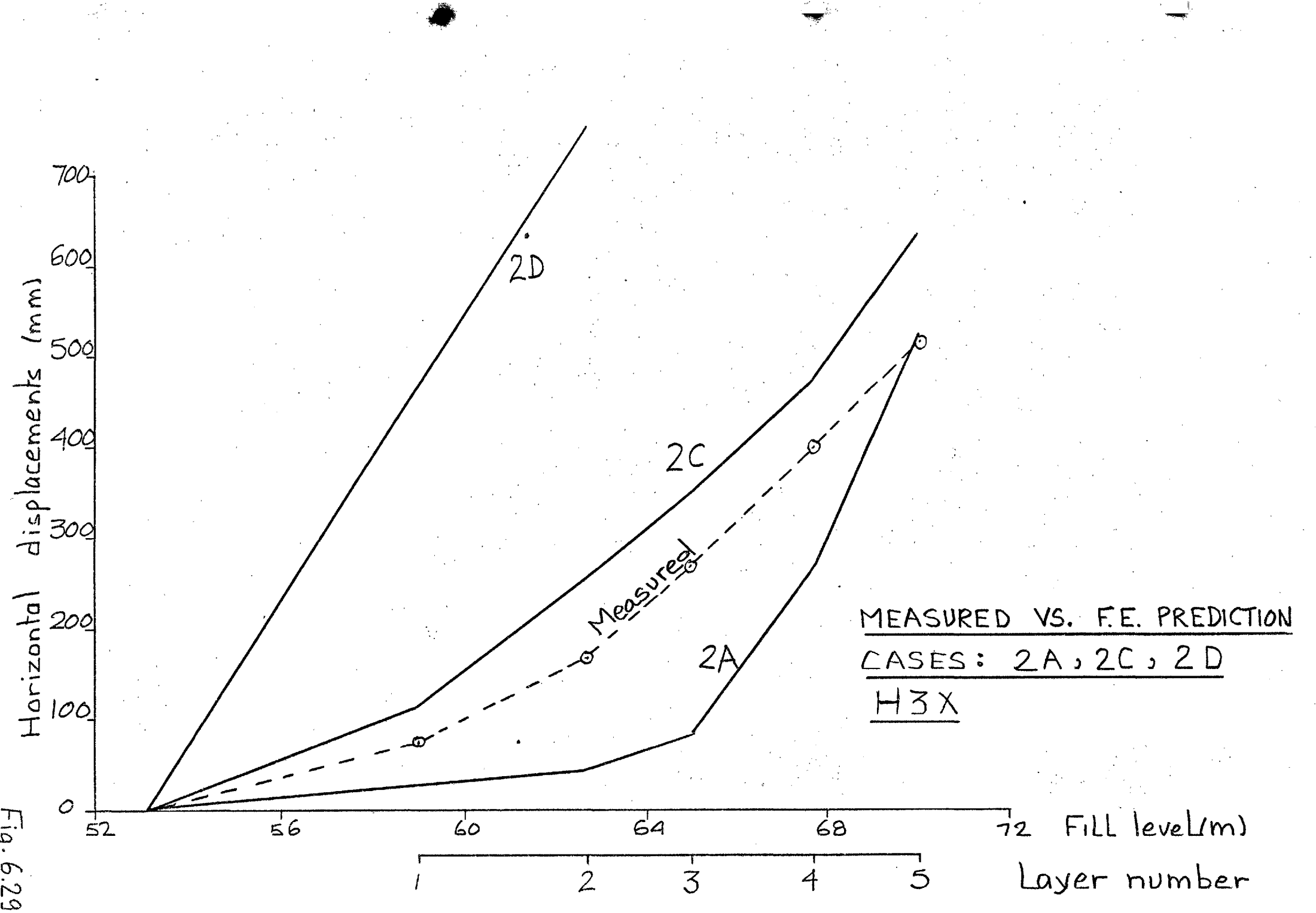

Horizontal displacements (mm)
700
600
500
400
300
200
100
0
2D
2C
Measured
2A
52
56
60
64
68
72
FILL level(m)
1
2
3
4
5
Layer number
MEASURED VS. F.E. PREDICTION
CASES: 2A, 2C, 2D
H3X

Fig. 6.29

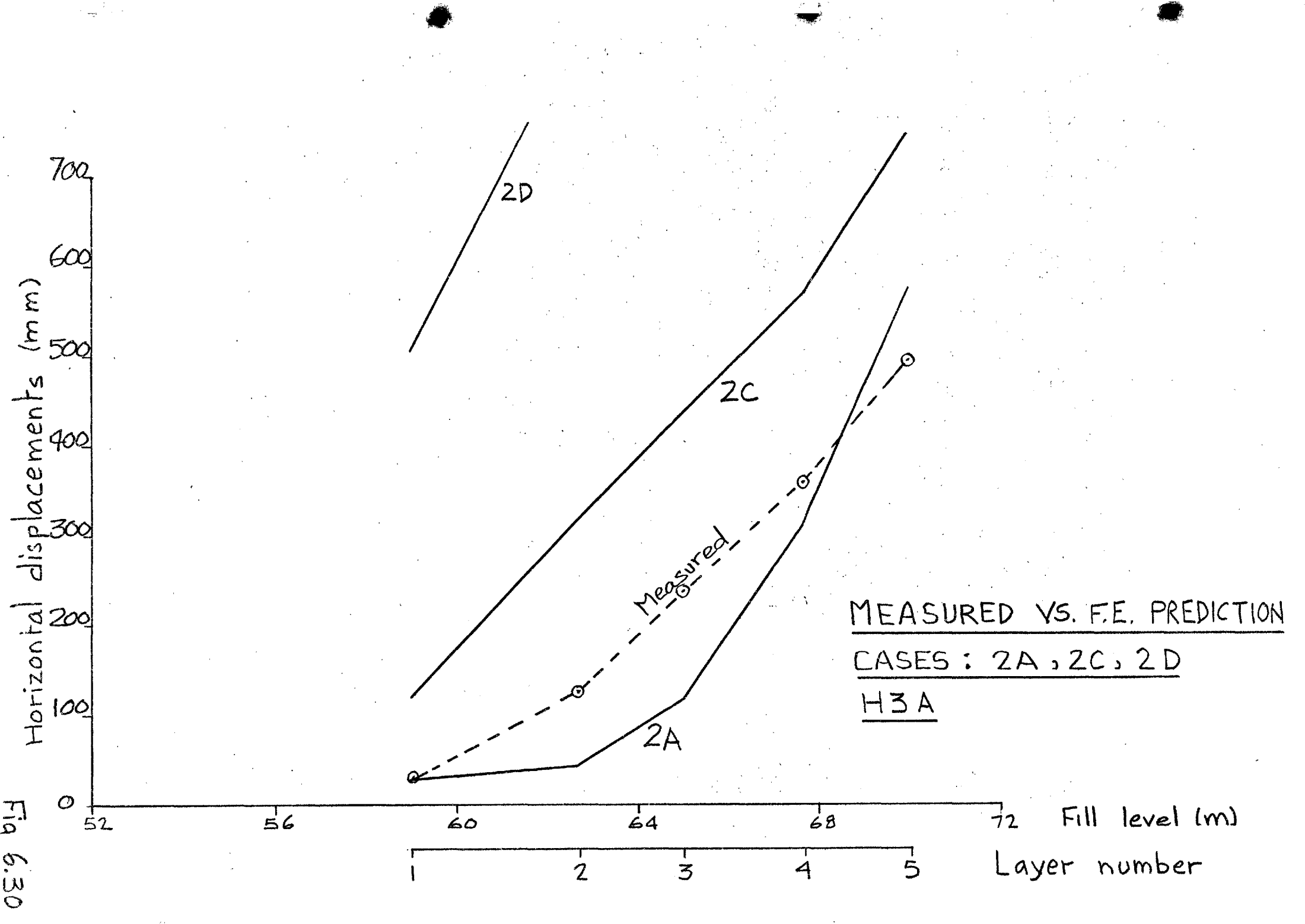

700
600
500
400
300
200
100
0
Horizontal displacements (mm)
2D
2C
Measured
2A
MEASURED VS. F.E. PREDICTION
CASES : 2A , 2C , 2D
H3A
52
56
60
64
68
72
Fill level (m)
1
2
3
4
5
Layer number

Fig 6.30

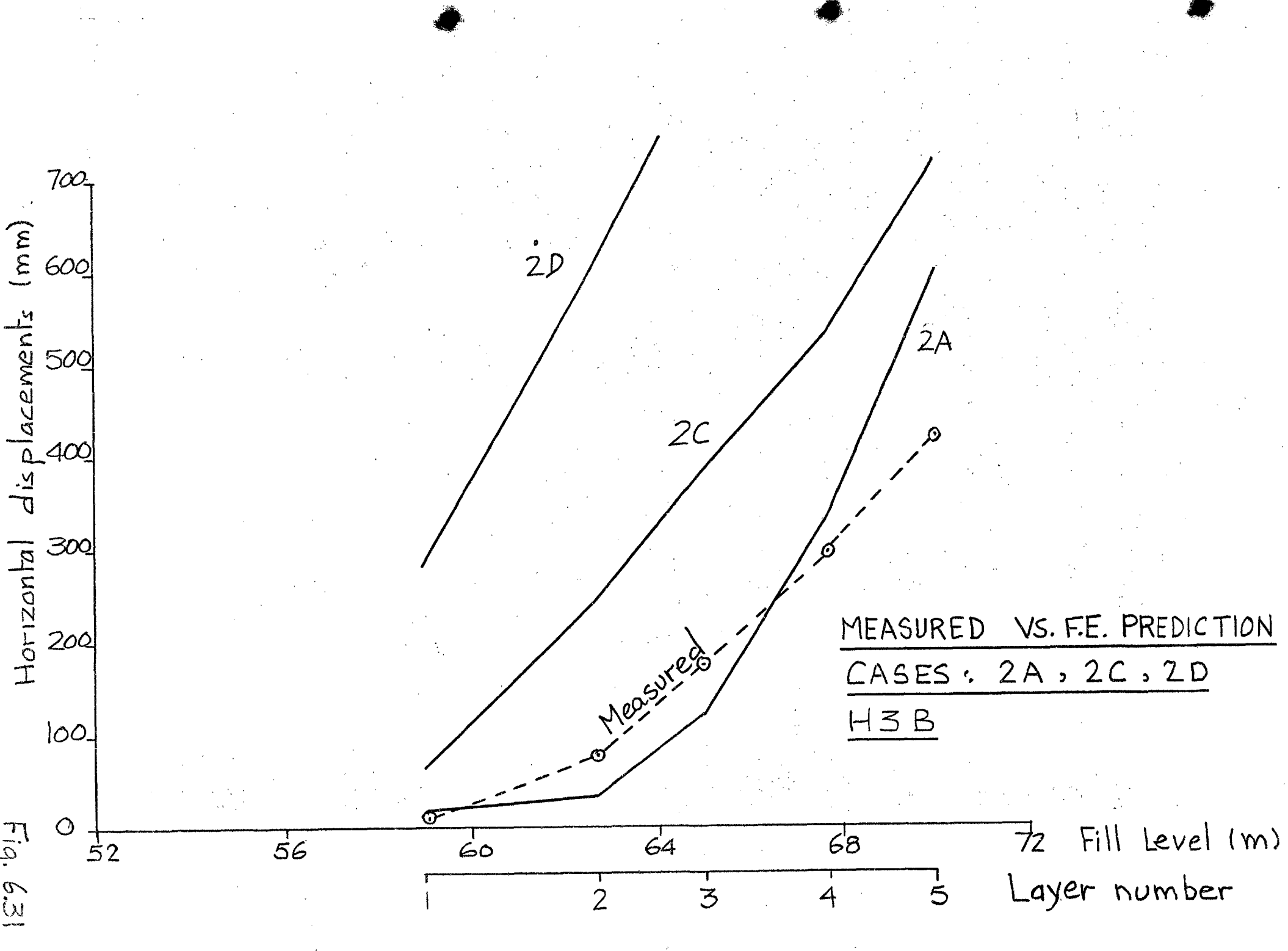
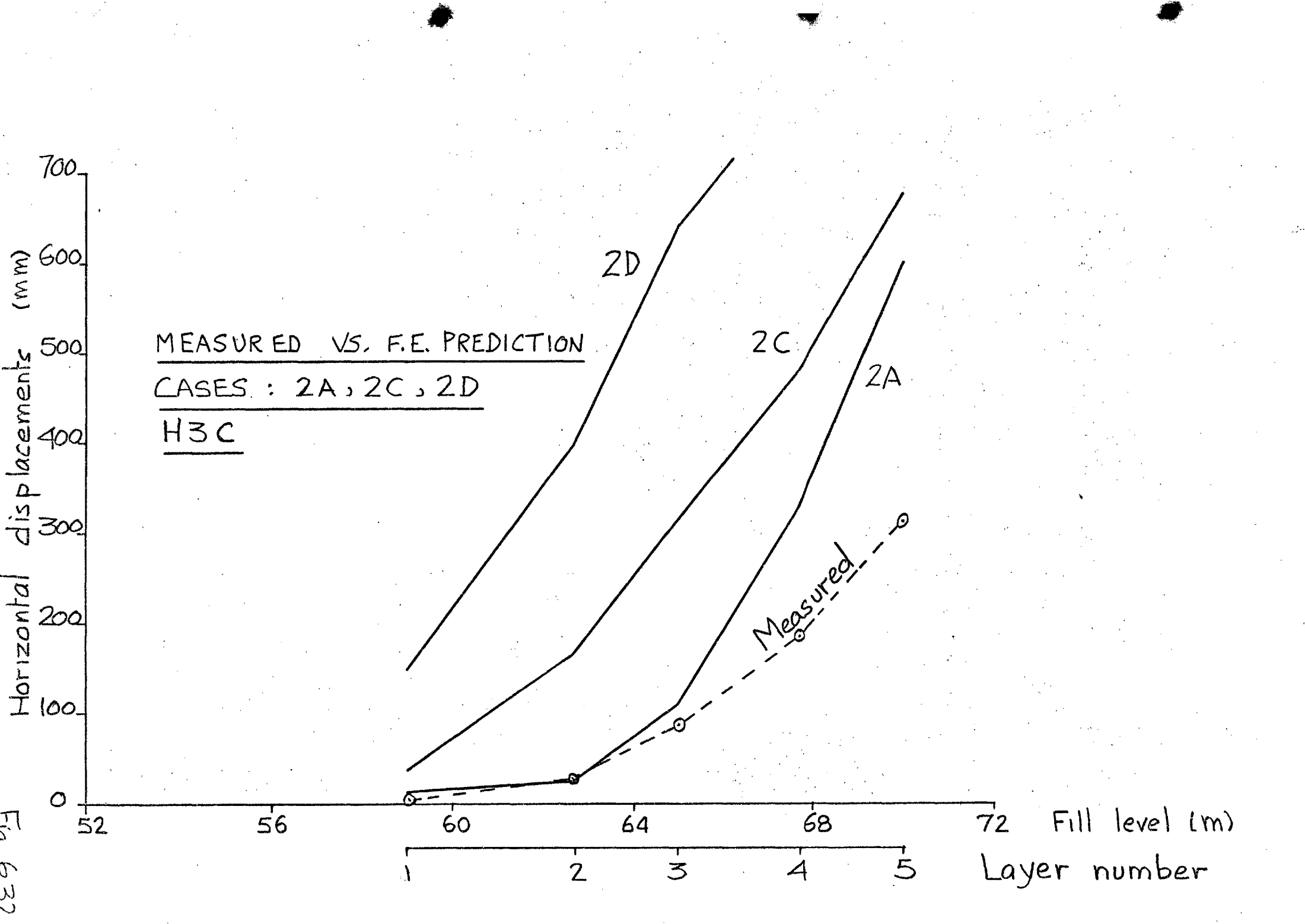
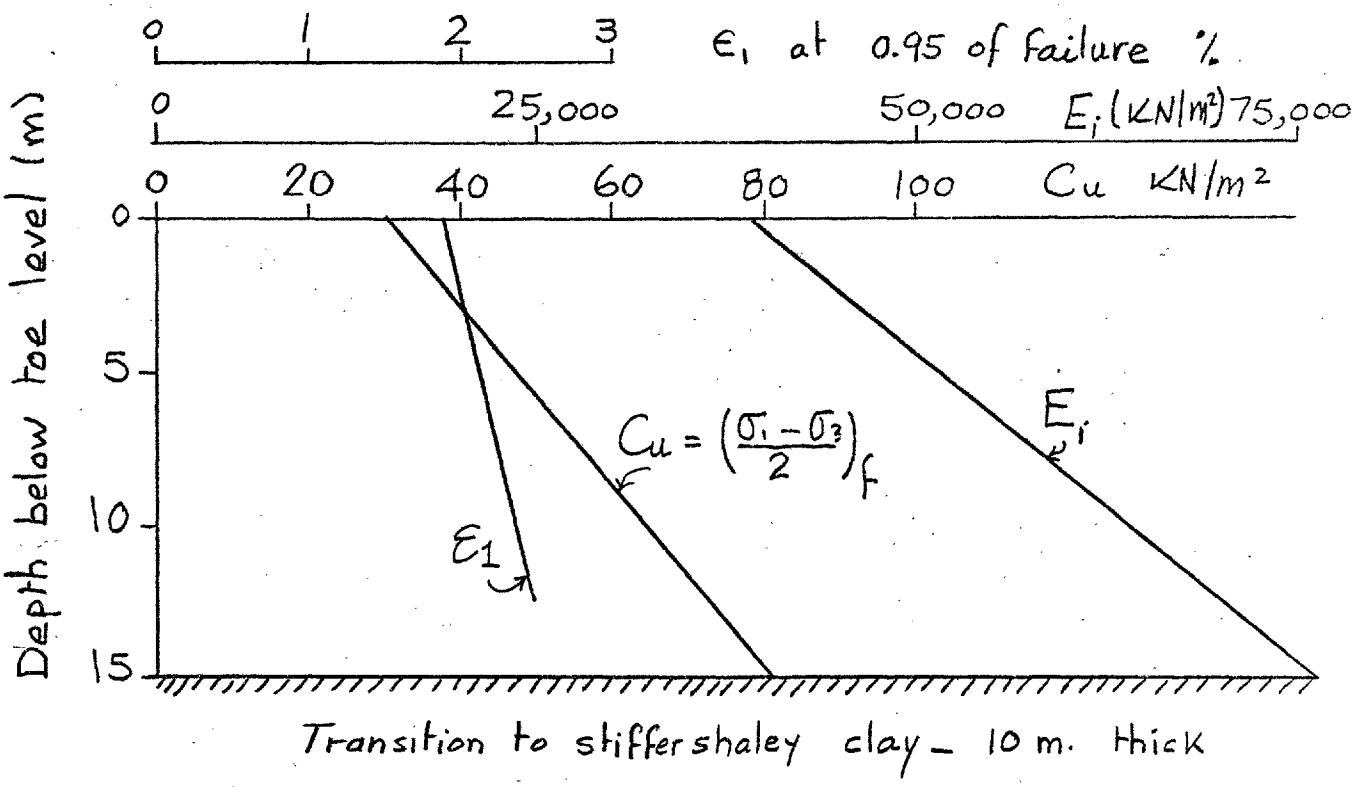
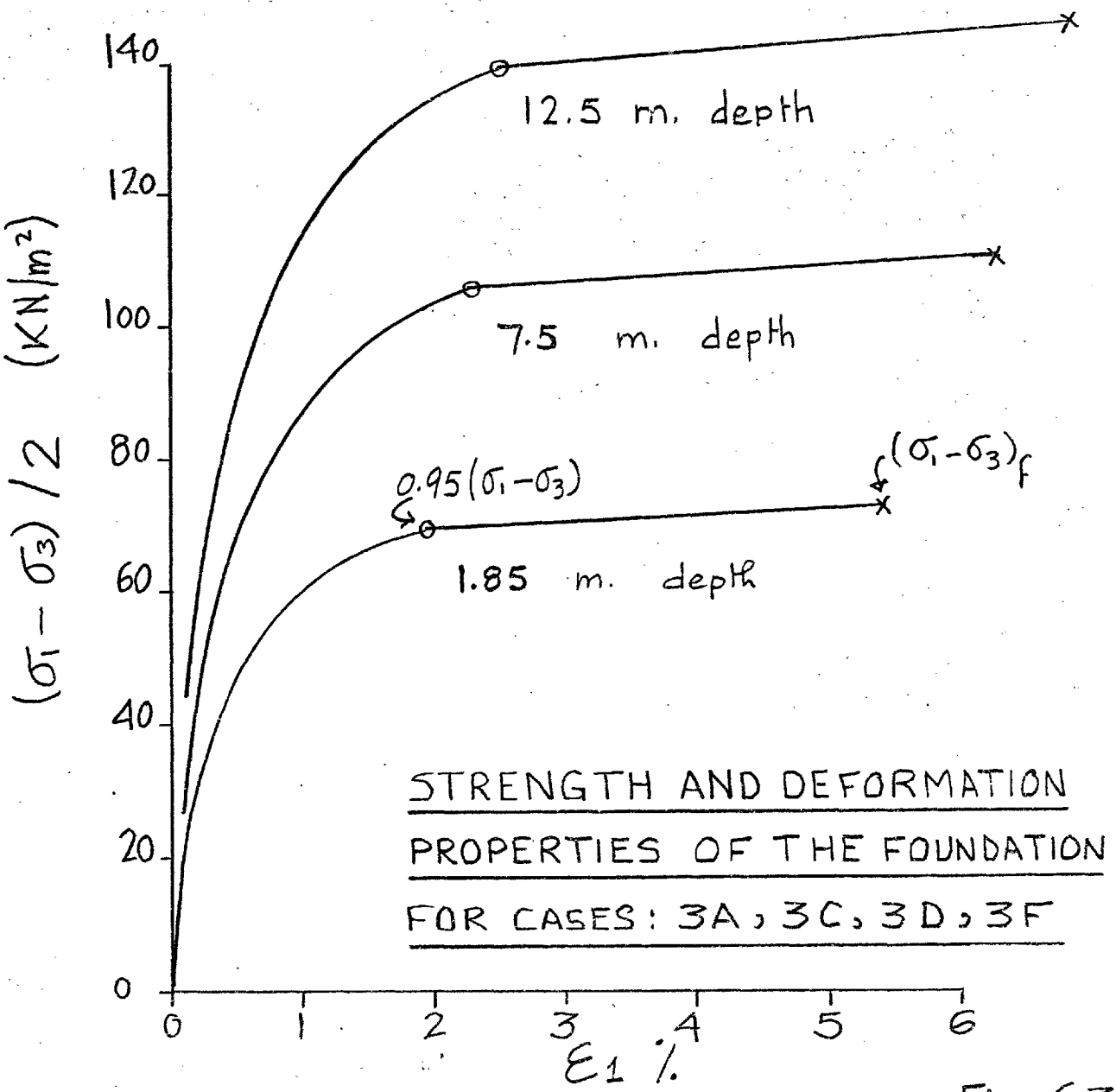

Horizontal displacements (mm)
700
600
500
400
300
200
100
0
2D
2C
2A
Measured
MEASURED VS. F.E. PREDICTION
CASES : 2A , 2C , 2D
H3B
52
56
60
64
68
72
Fill Level (m)
1
2
3
4
5
Layer number

Fig. 6.31

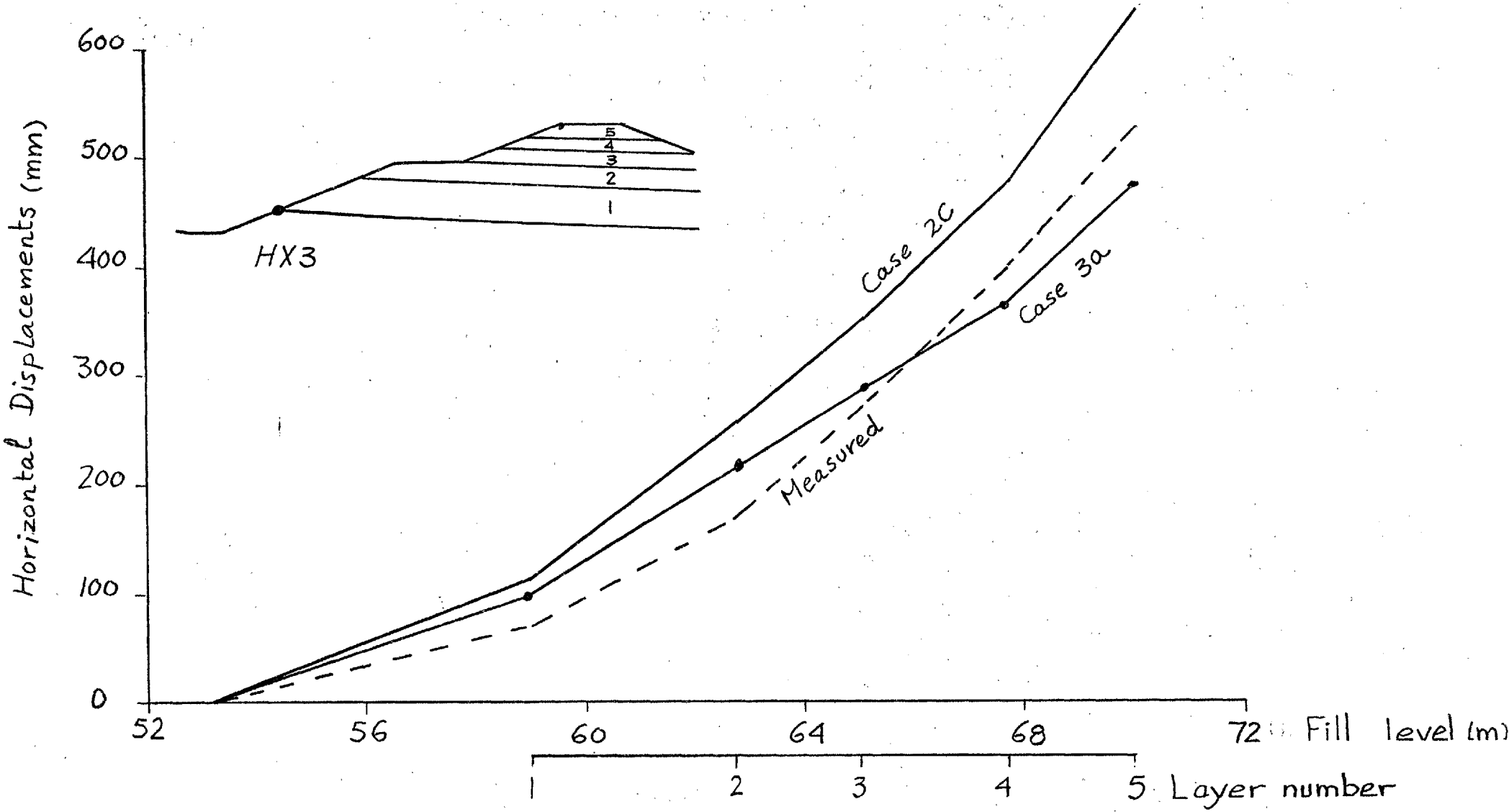

MEASURED VS. F.E. PREDICTION
CASES : 2A, 2C, 2D
H3C
2D
2C
2A
Measured
Horizontal displacements (mm)
700
600
500
400
300
200
100
0
52
56
60
64
68
72
Fill level (m)
1
2
3
4
5
Layer number





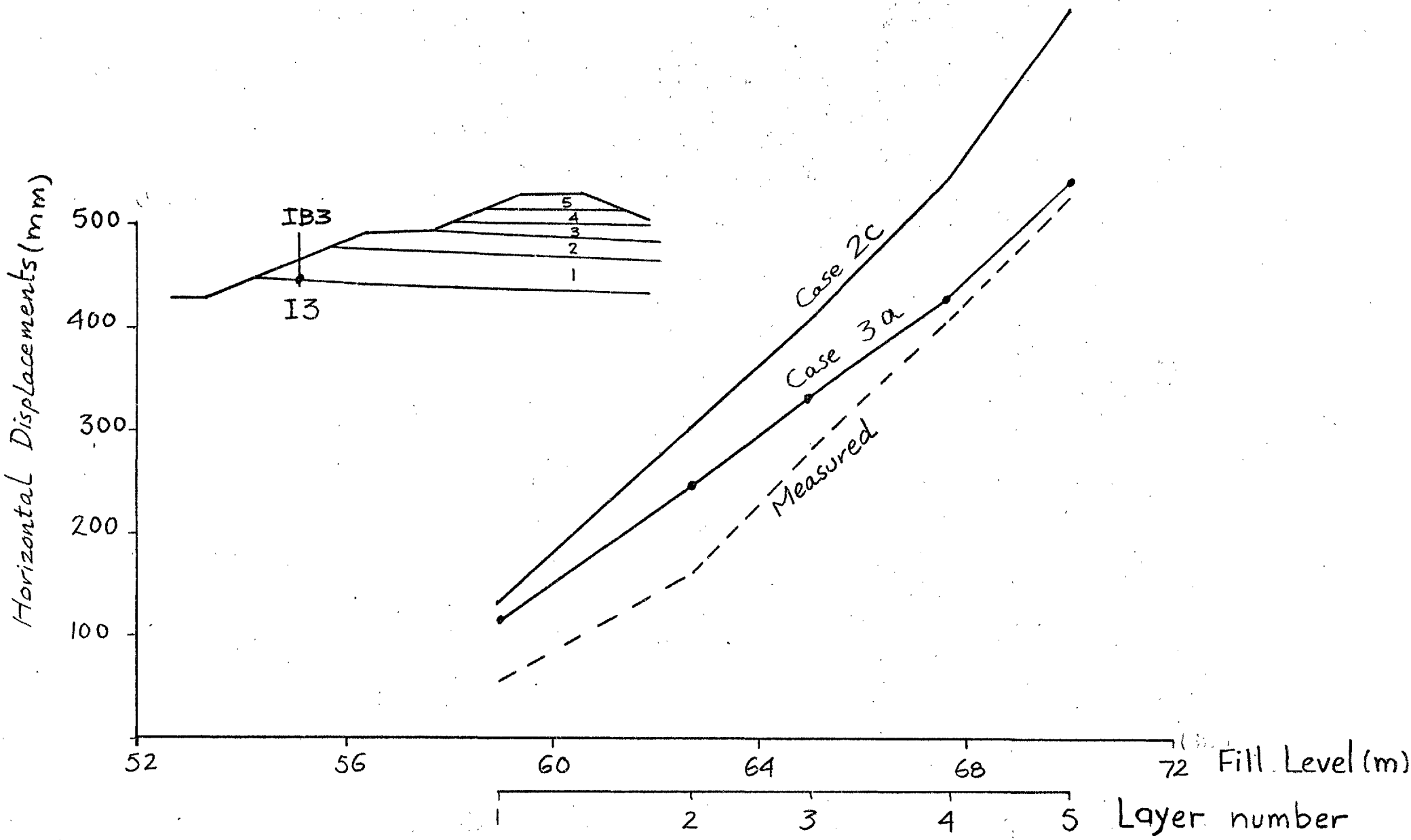
STRENGTH AND DEFORMATION PROPERTIES OF THE FOUNDATION FOR CASES: 3A, 3C, 3D, 3F

Fig. 6.33



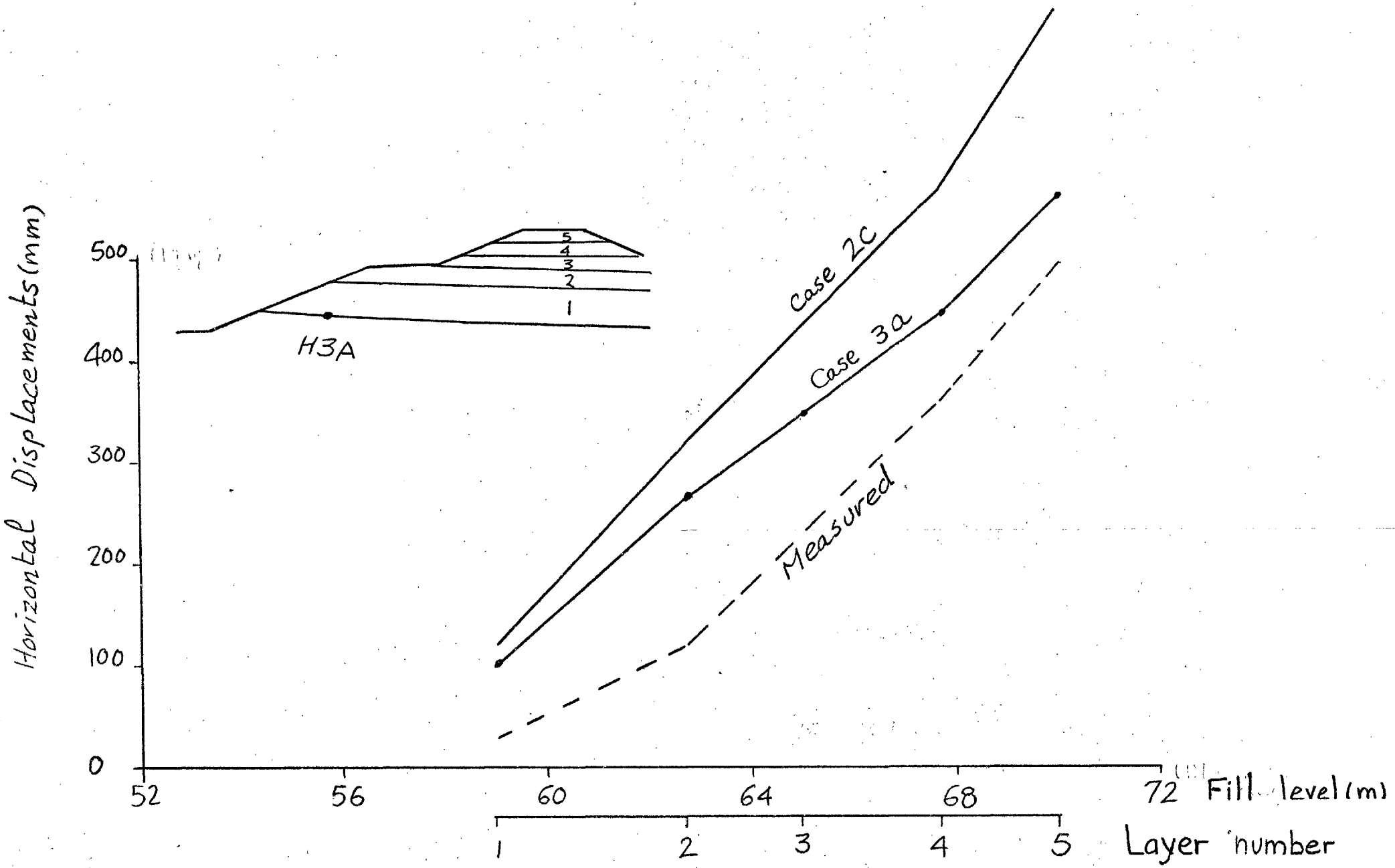
MEASURED VS. F.E. PREDICTION _ CASES 2C & 3a _ HX3

Fig. 6.34



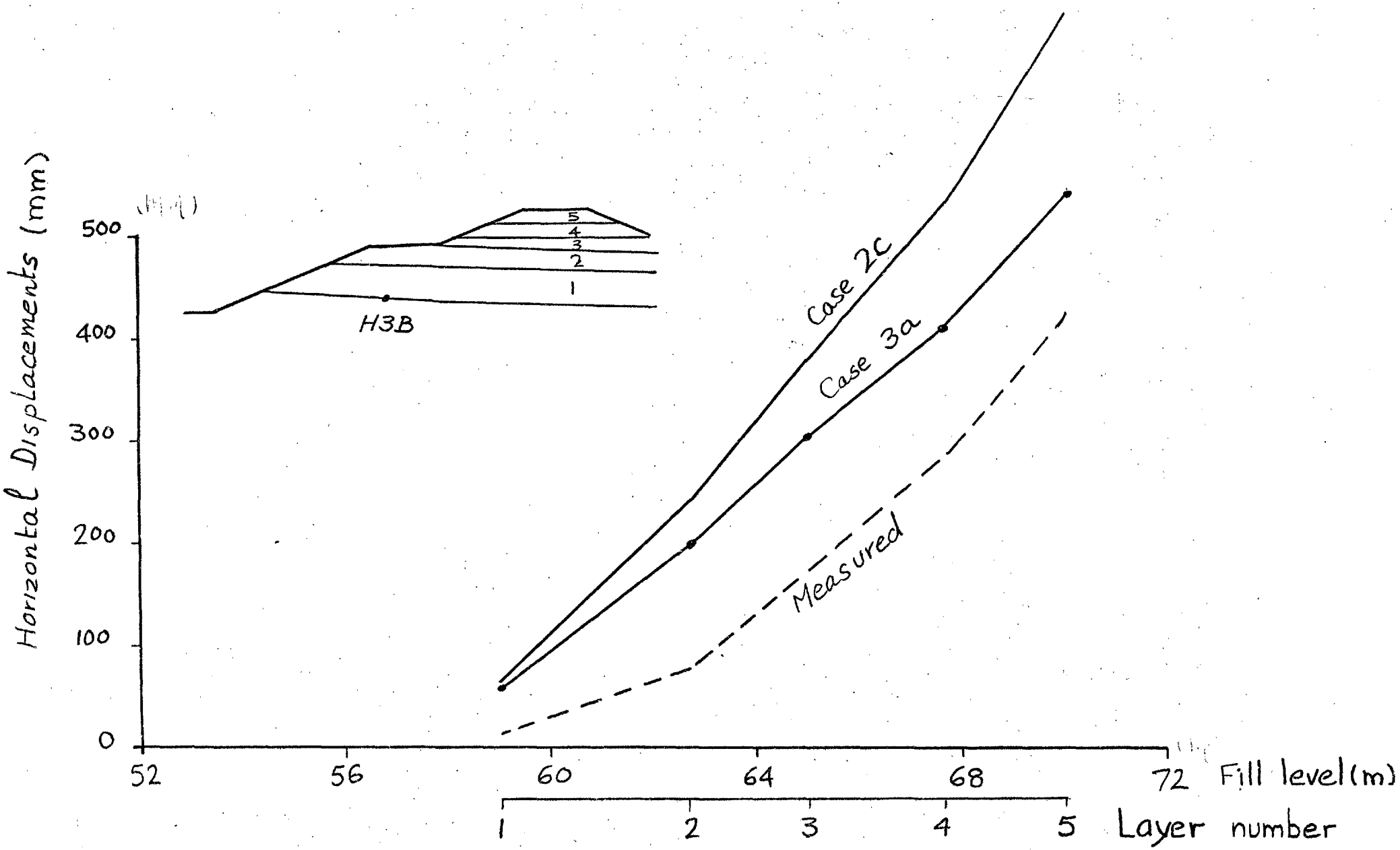
MEASURED VS. F.E. PREDICTION _ CASES 2C ; 3a _ POINT I3

Fig. 6.35



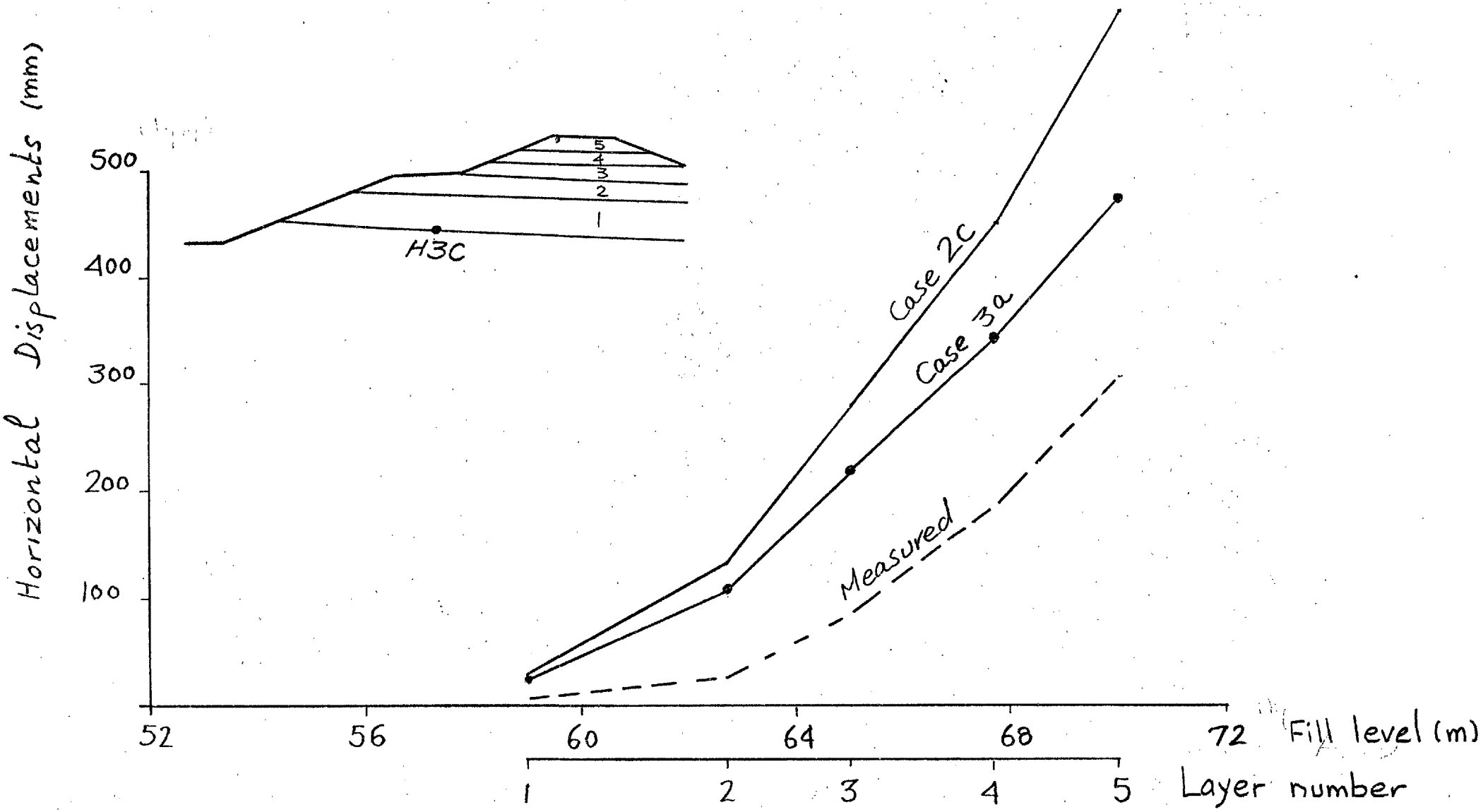
MEASURED Vs. F.E. PREDICTION _ CASES : 2C, 3a _ H3A

Fig. 6.36



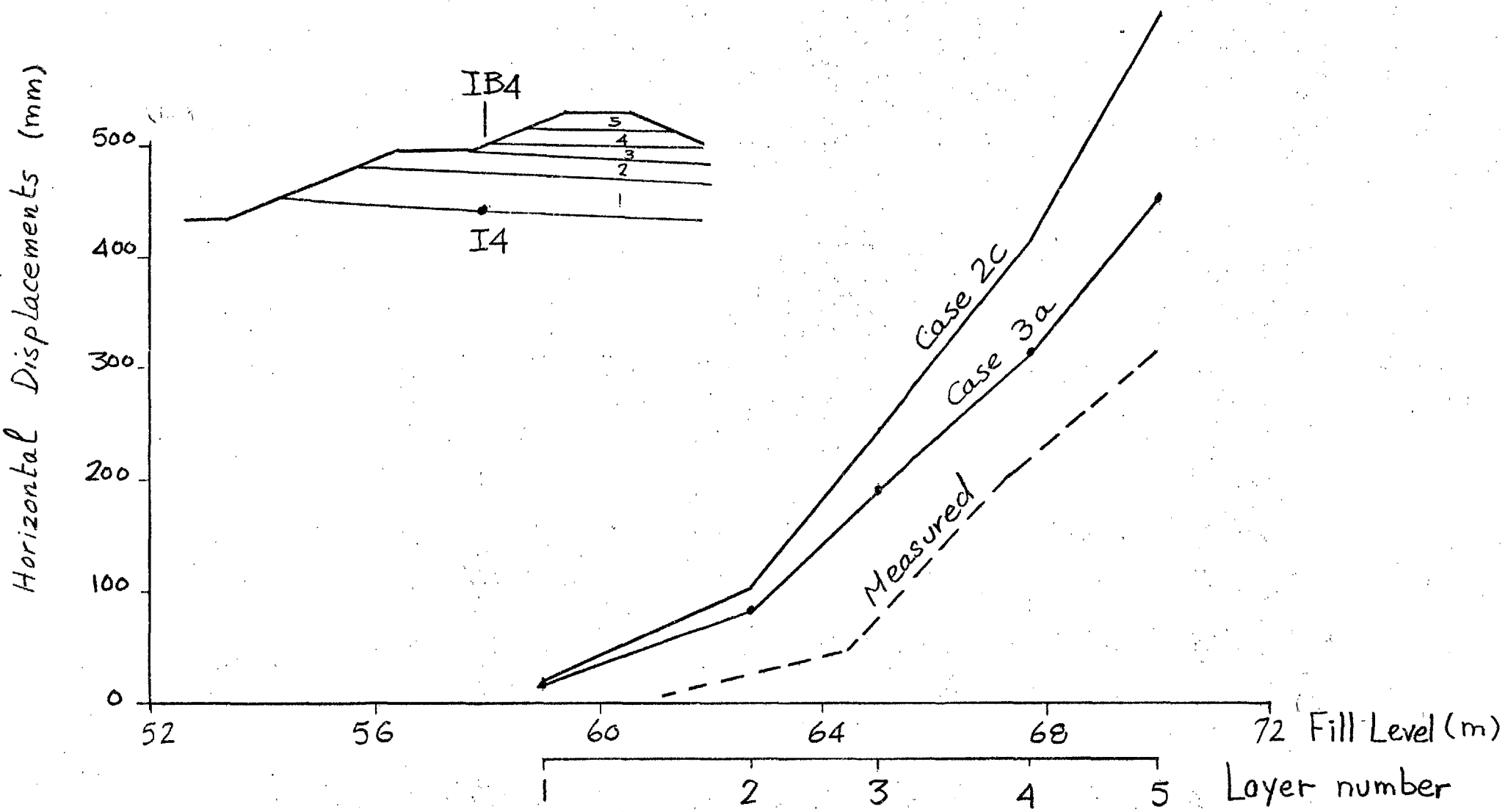
MEASURED VS. F.E. PREDICTION _ CASES 2C, 3a _ H13B

Fig. 6.37



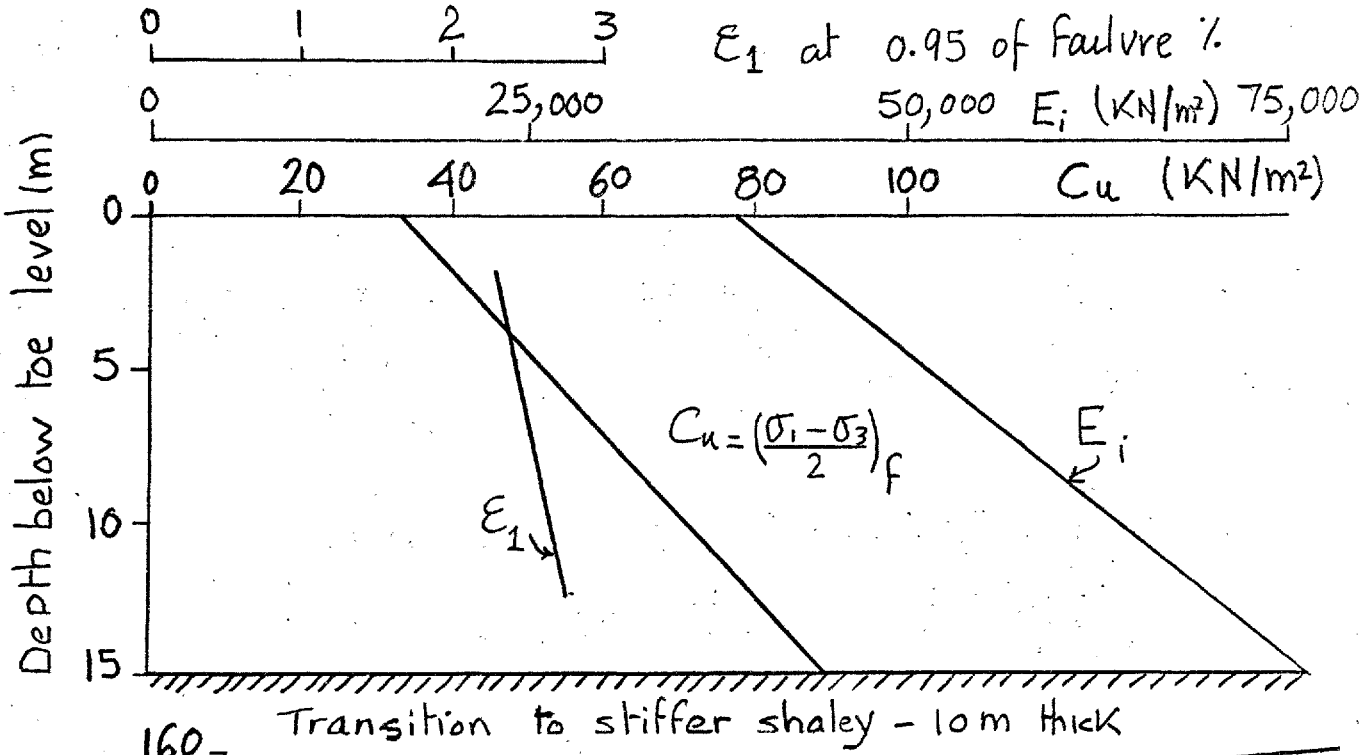
MEASURED VS. F.E. PREDICTION _ CASES 2C, 3a _ H3C

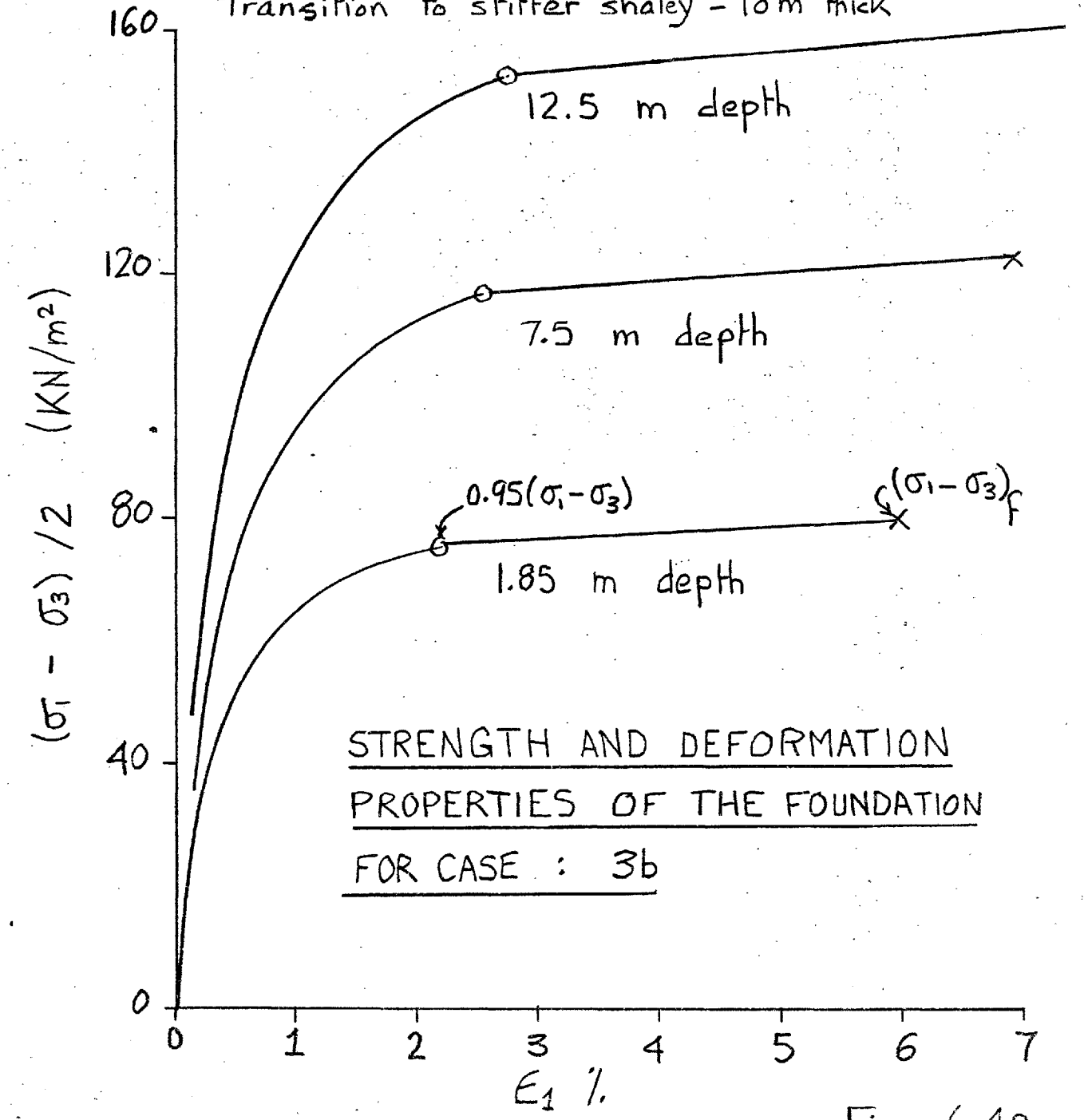
Fig. 6.38



MEASURED VS. F.E. PREDICTION _ CASES: 2C, 3a _ POINT I4

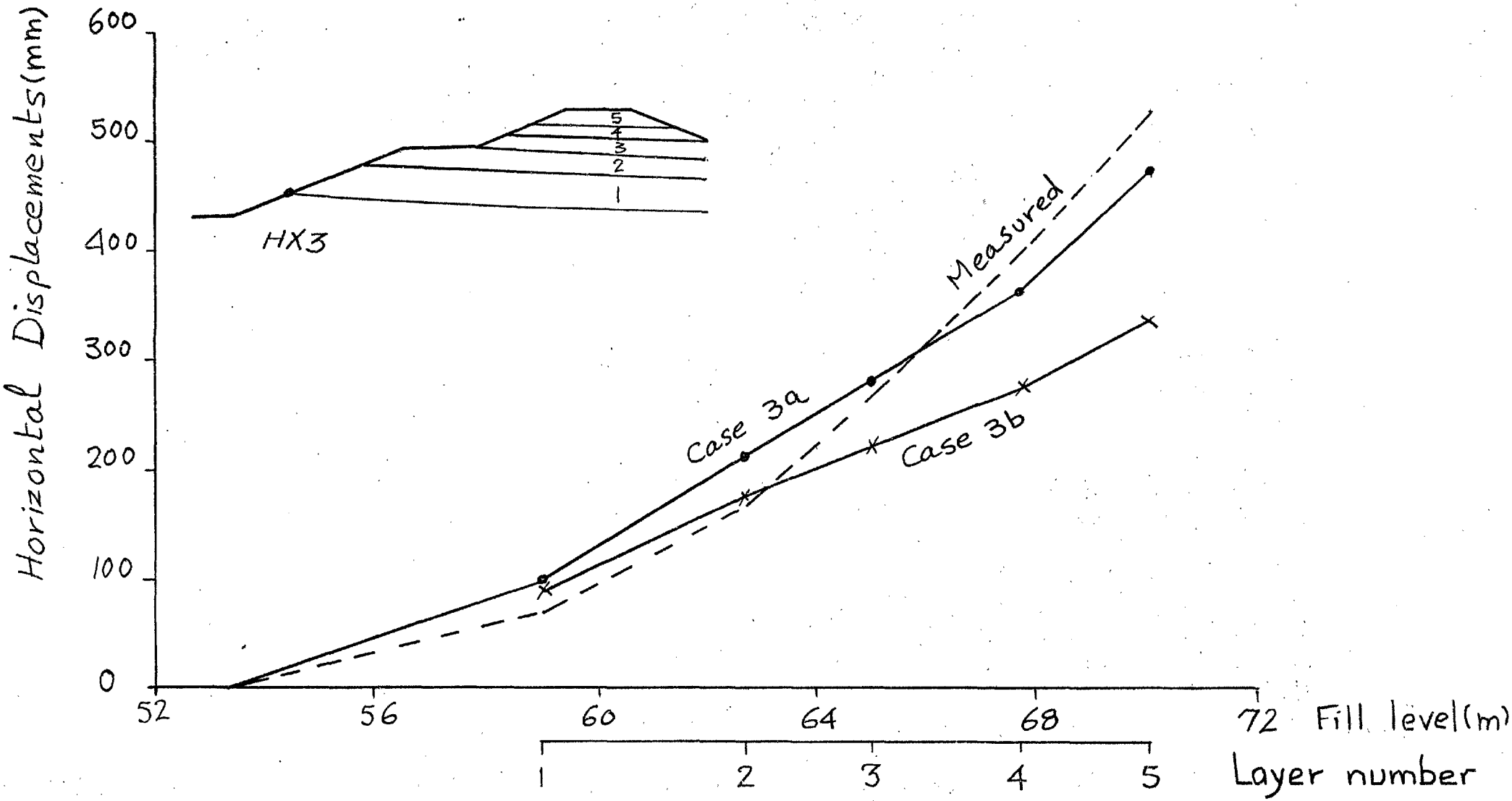
Fig. 6.39





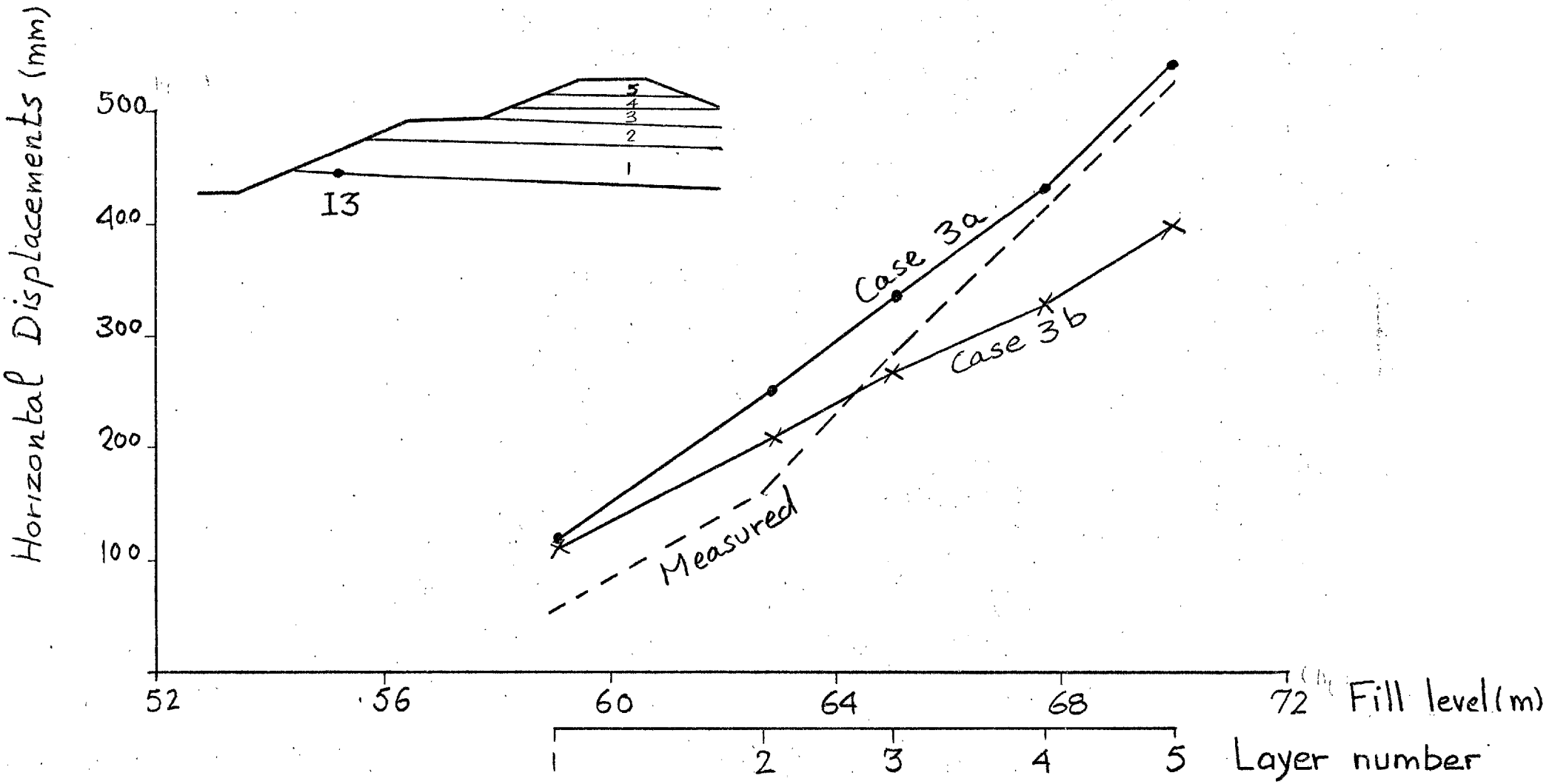
STRENGTH AND DEFORMATION PROPERTIES OF THE FOUNDATION FOR CASE : 3b

Fig. 6.40



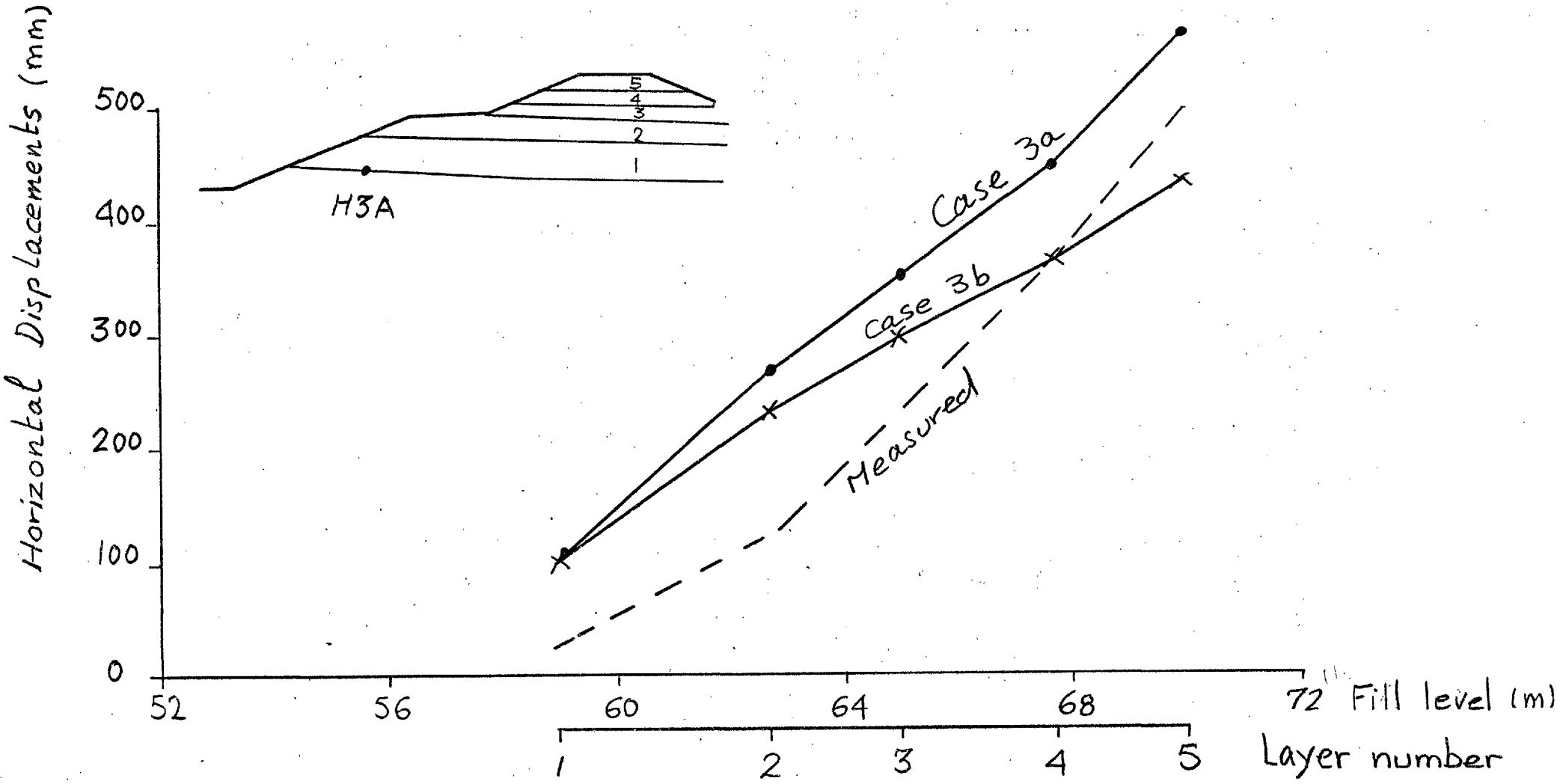
MEASURED VS. PREDICTION _ CASES : 3a , 3b _ POINT HX3

Fig. 6.41



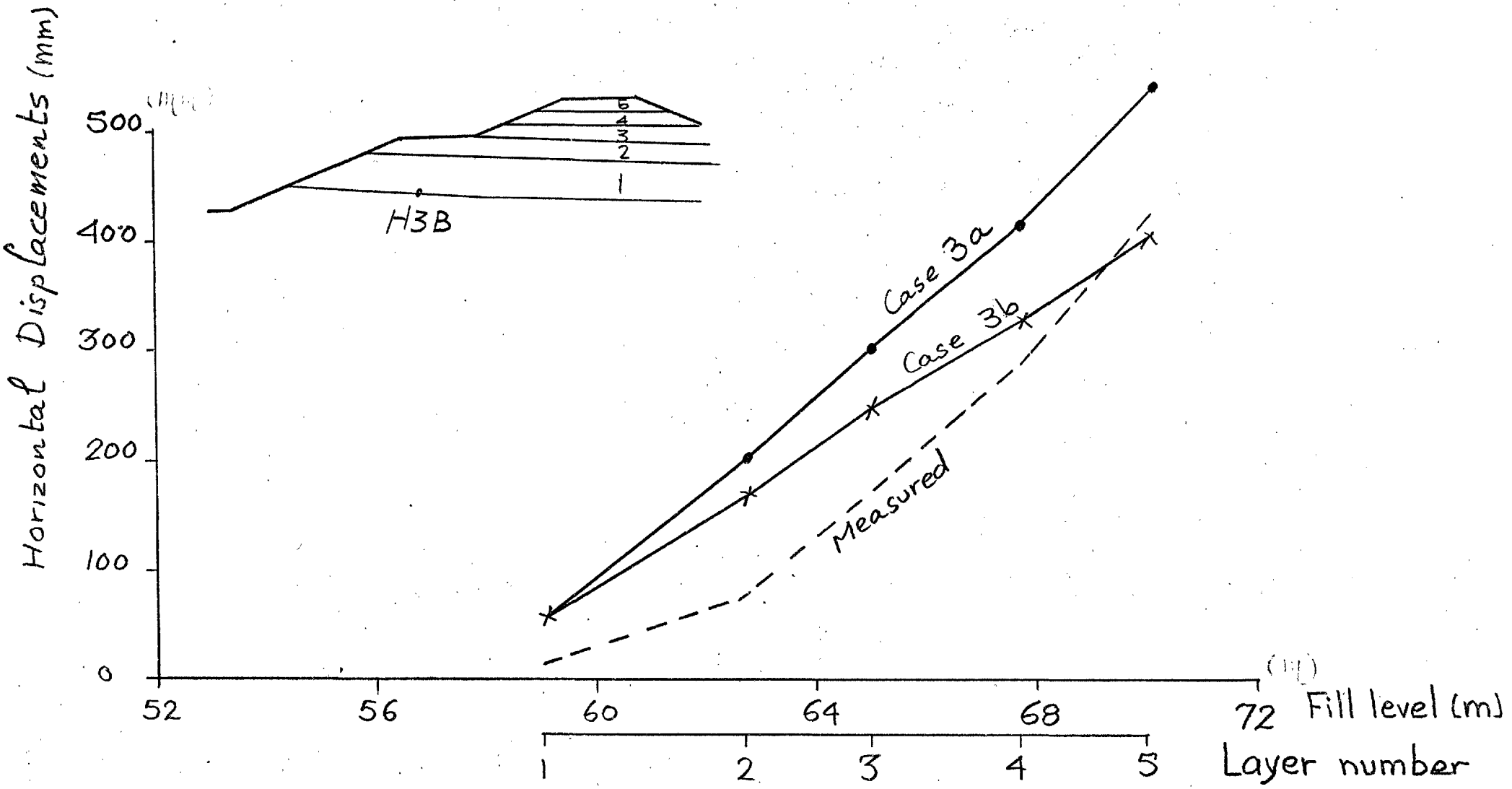
MEASURED VS. F.E. PREDICTION _ CASES : 3a , 3b _ POINT I3

Fig 6.42



MEASURED VS. F.E. PREDICTION — CASES: 3a, 3b — PIONT; H3A

Fig. 6.43



MEASURED VS. F.E. PREDICTION_ CASES : 3a ;3b_ POINT; H3B

Fig 6.44

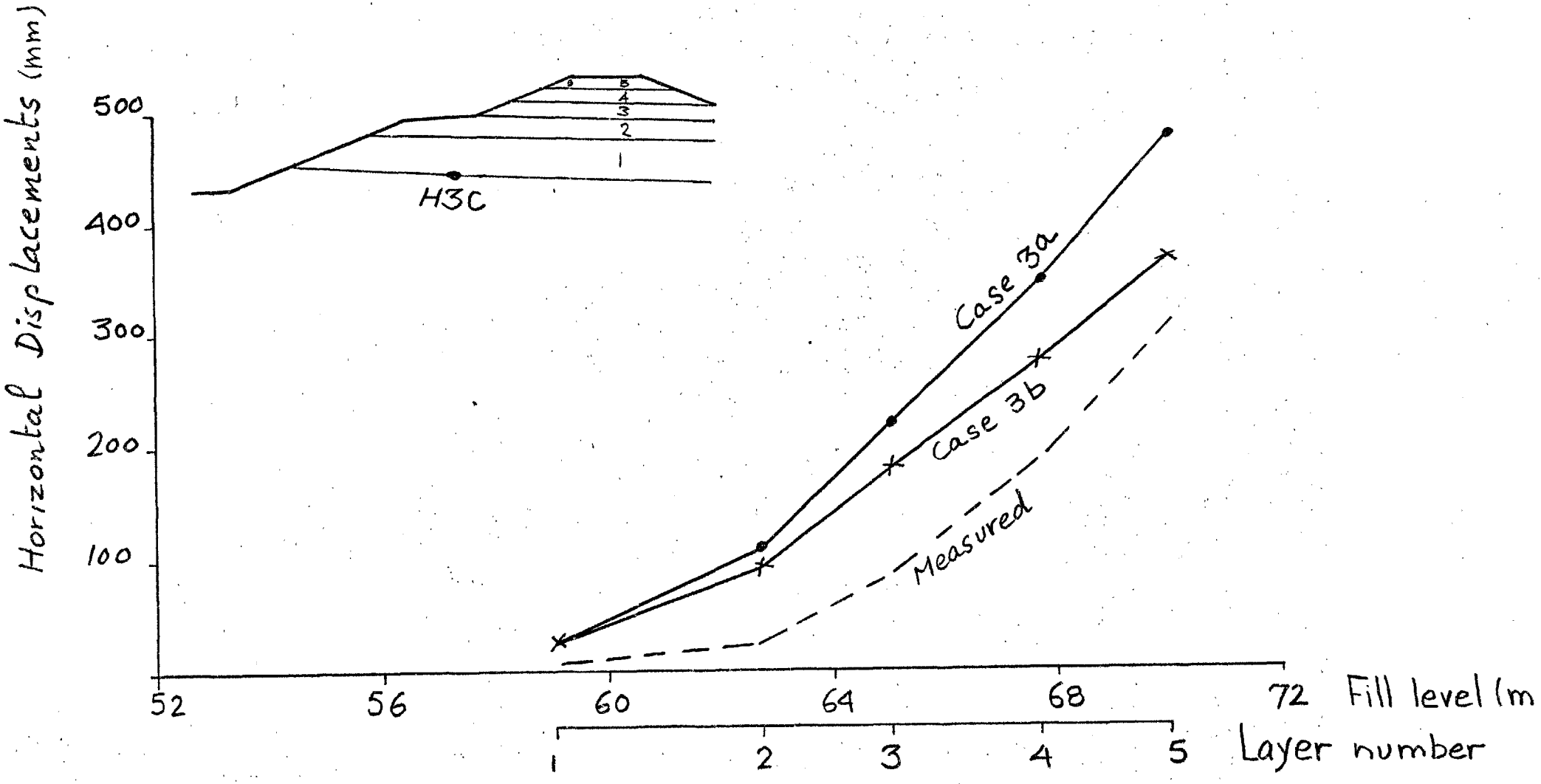
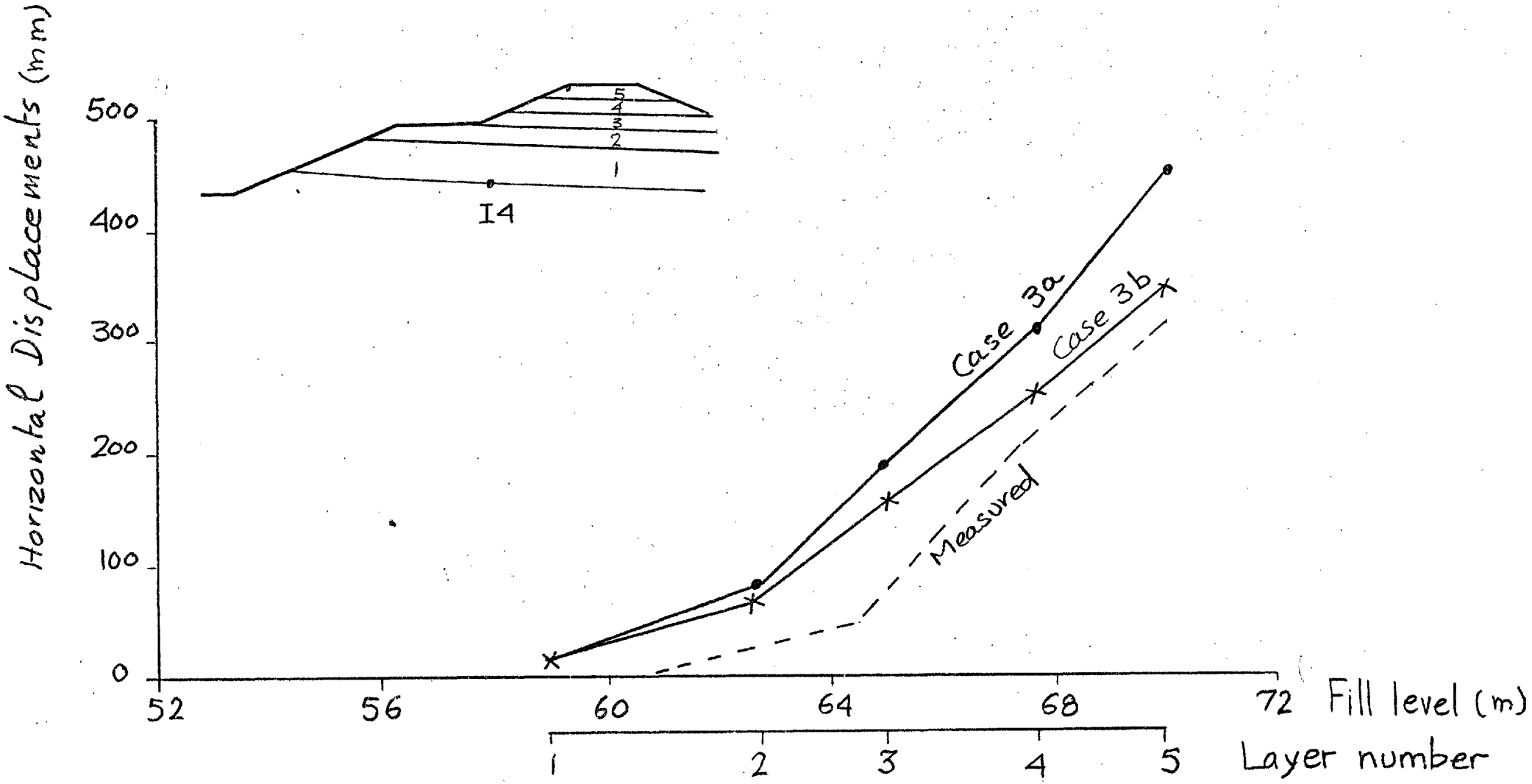
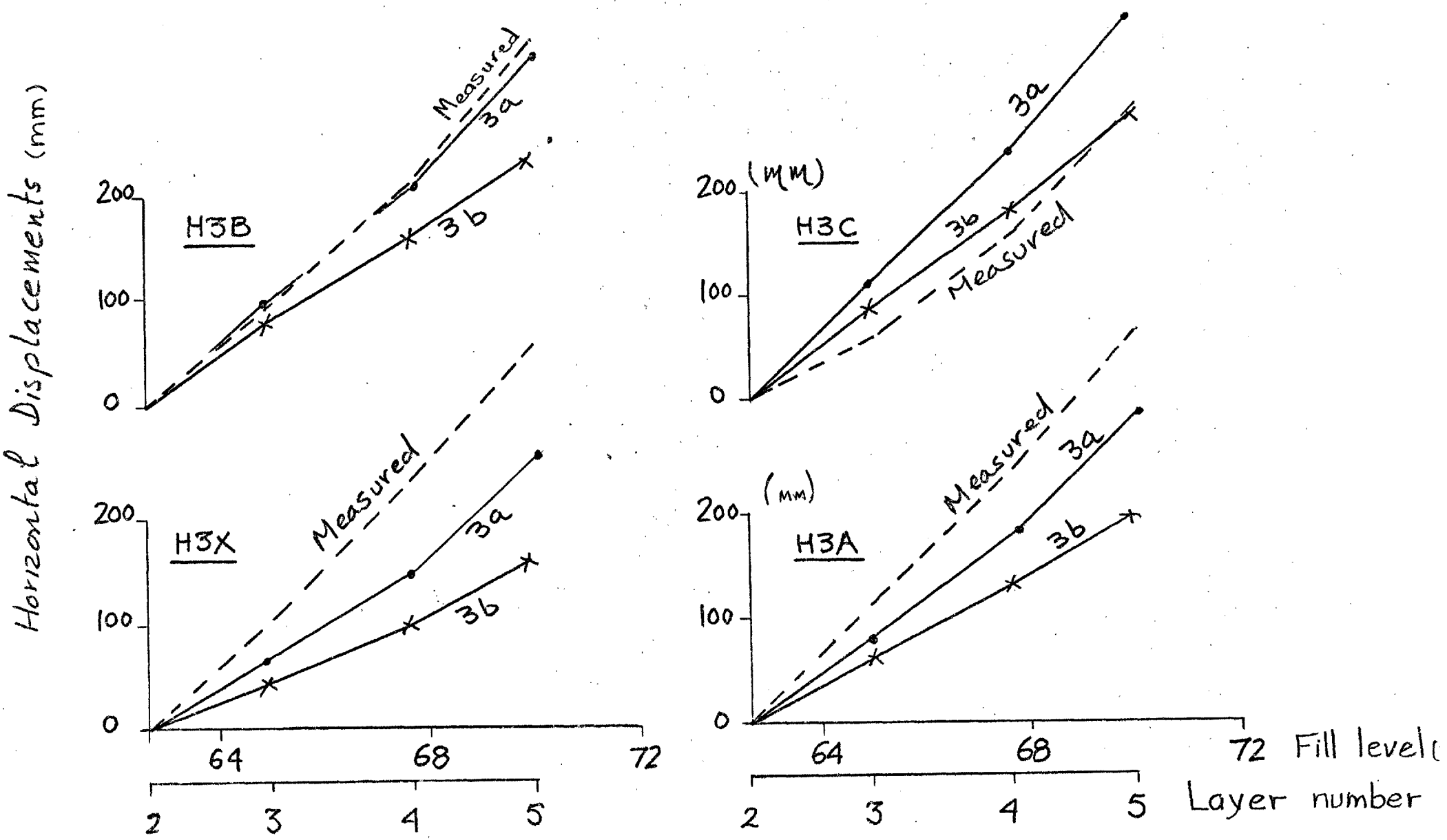


Fig. 6.45 MEASURED VS. F.E. PREDICTION_CASES: 3a . 3b _ POINT: H3C



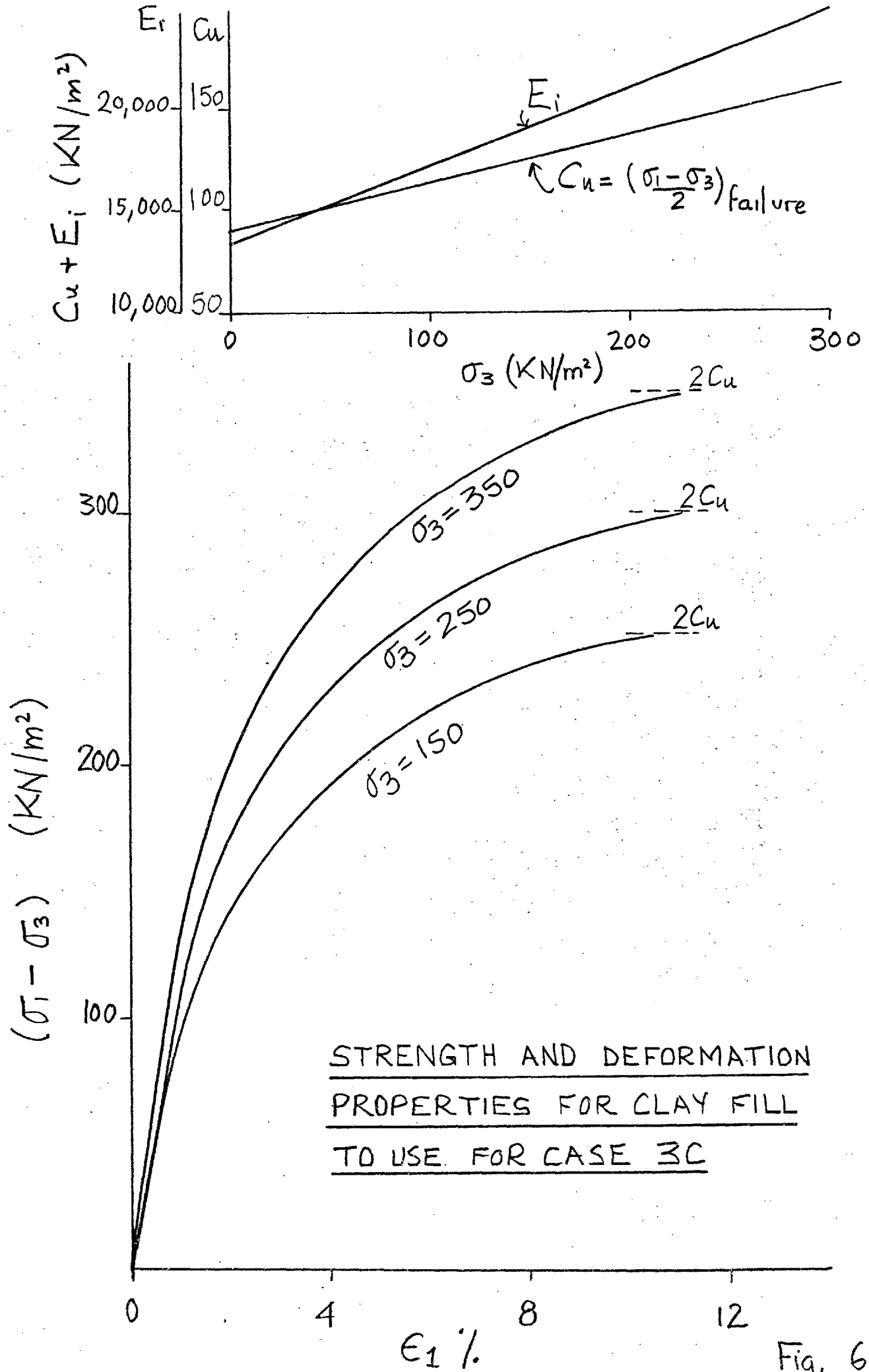
MEASURED VS. F.E. PREDICTION _ CASES: 3a ; 3b _ POINT: I4

Fig. 6.46



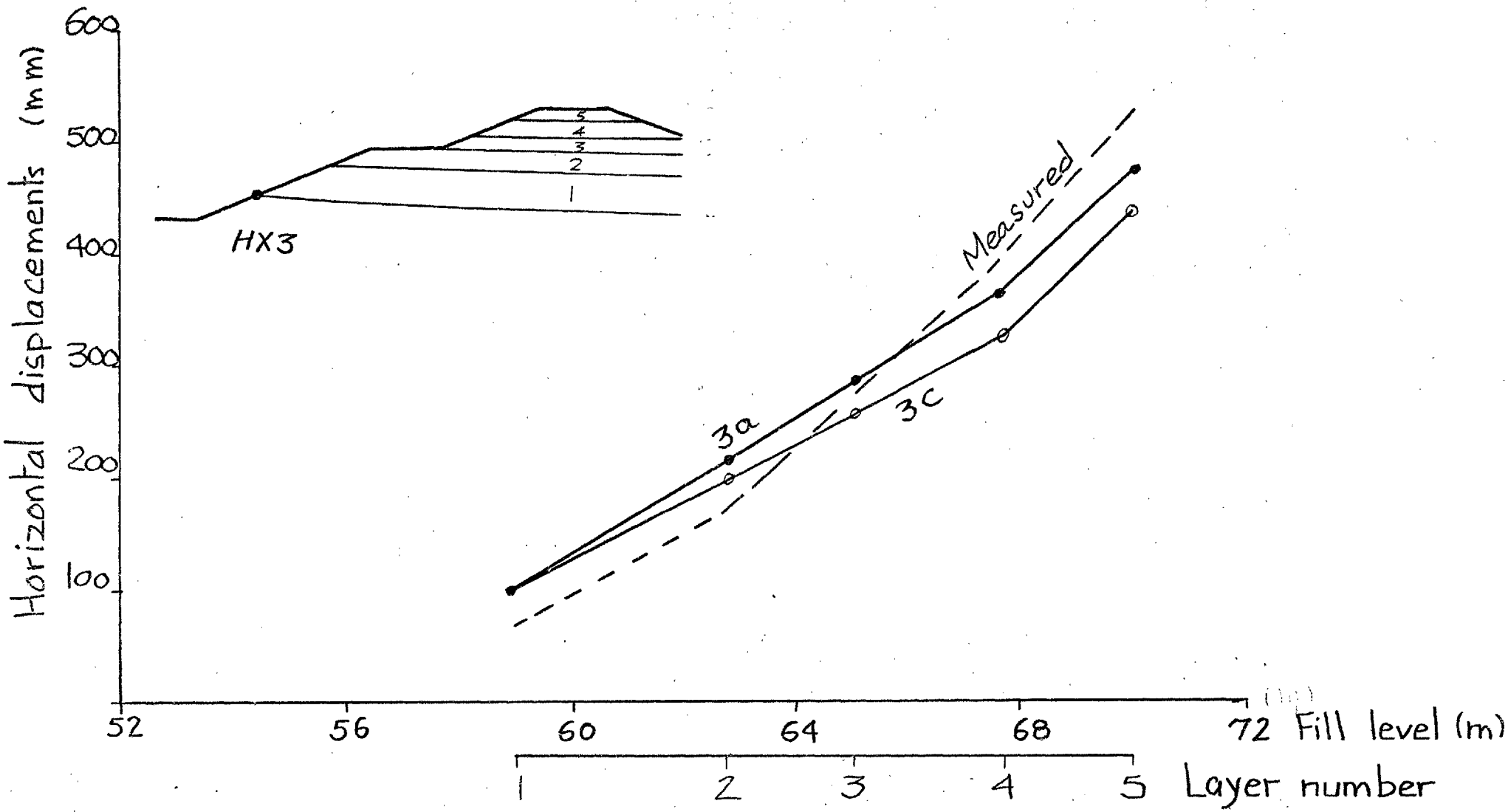
MEASURED VS. F.E. PREDICTION_ CASES 3a, 3b _ FROM LAYER 2

Fig. 6.47



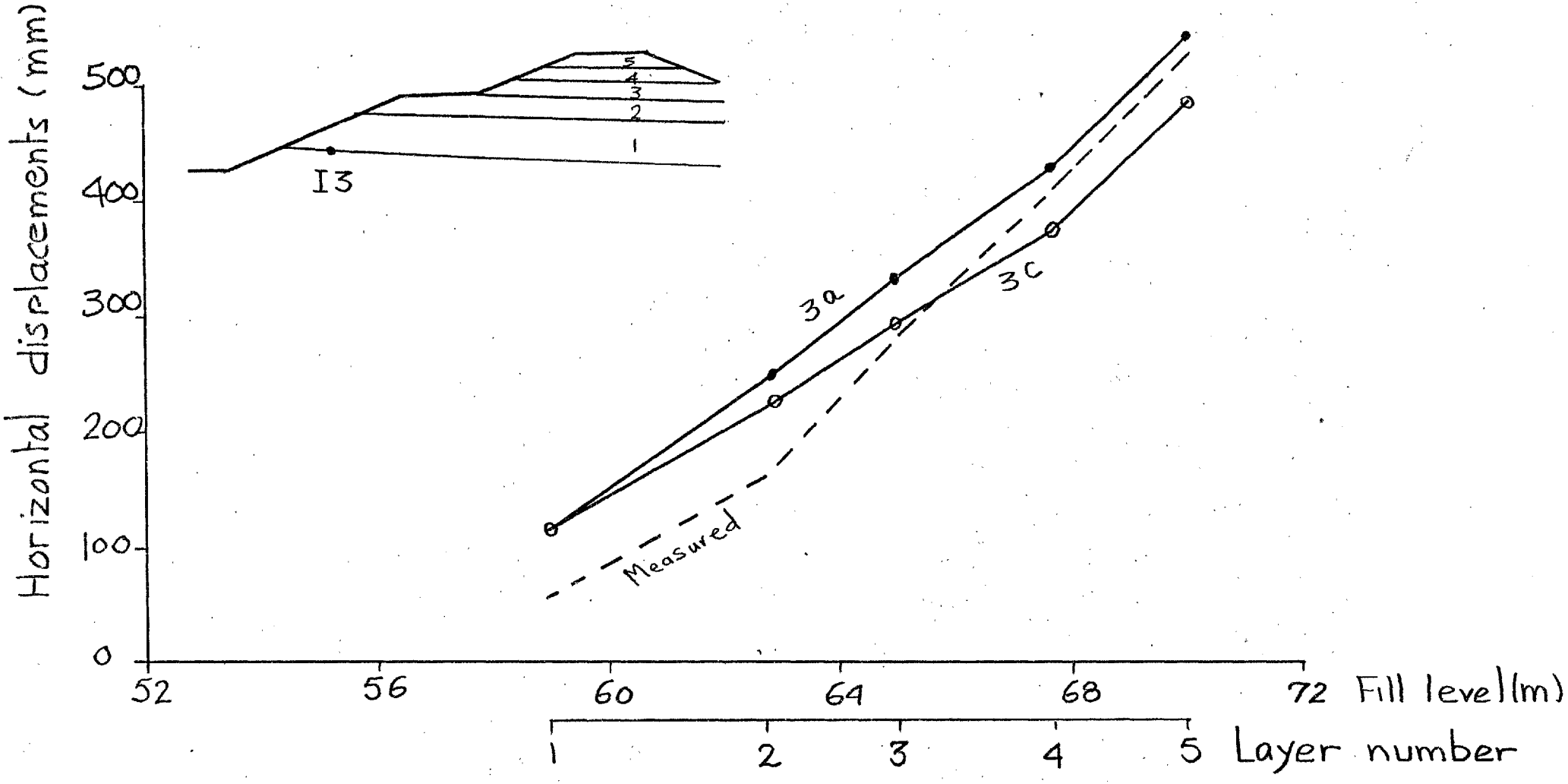
STRENGTH AND DEFORMATION PROPERTIES FOR CLAY FILL TO USE FOR CASE 3C

Fig. 6.48



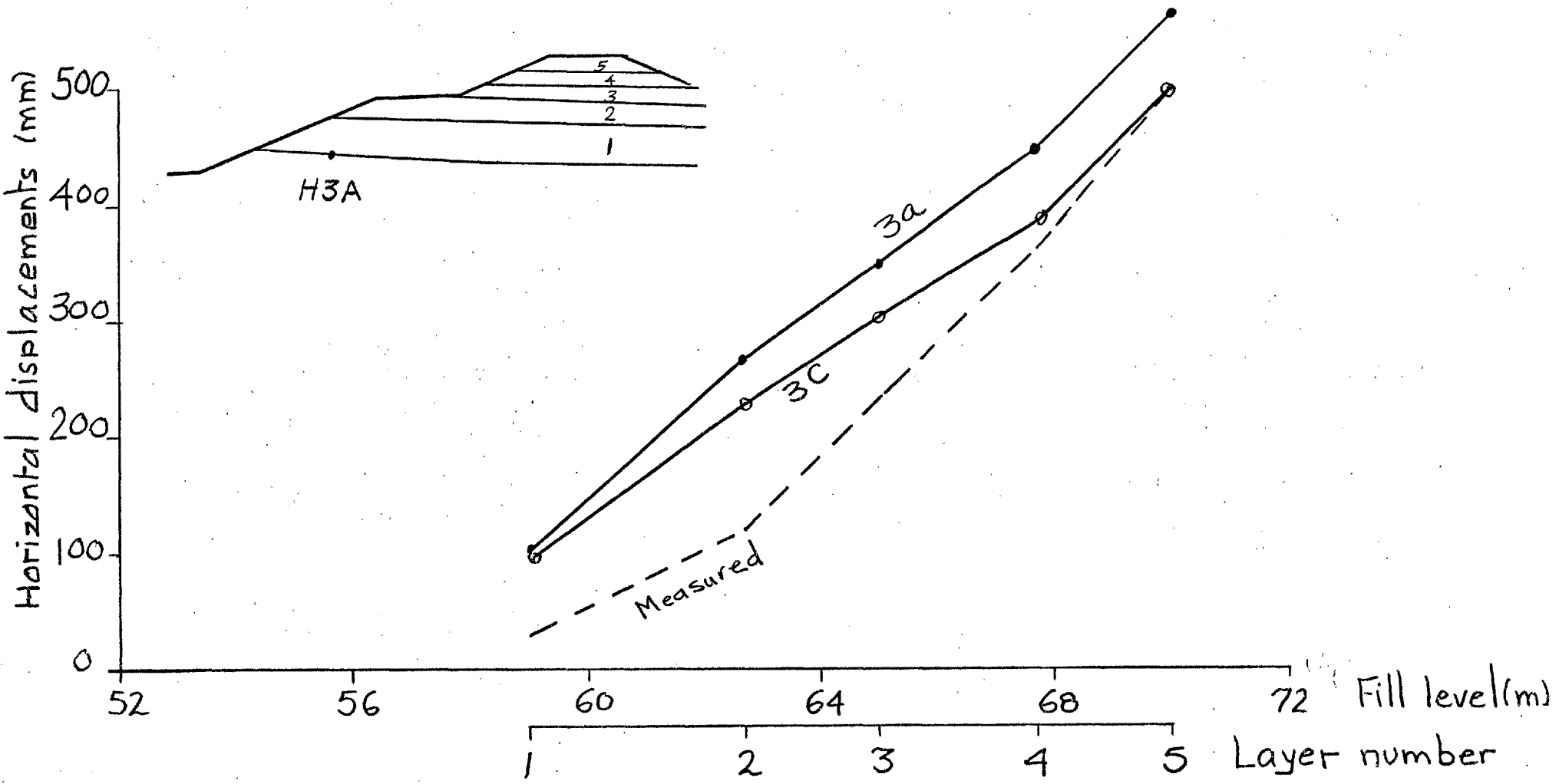
MEASURED VS. PREDICTED (F.E.) _ CASES: 3a, 3c _ POINT HX3

Fig 6.49



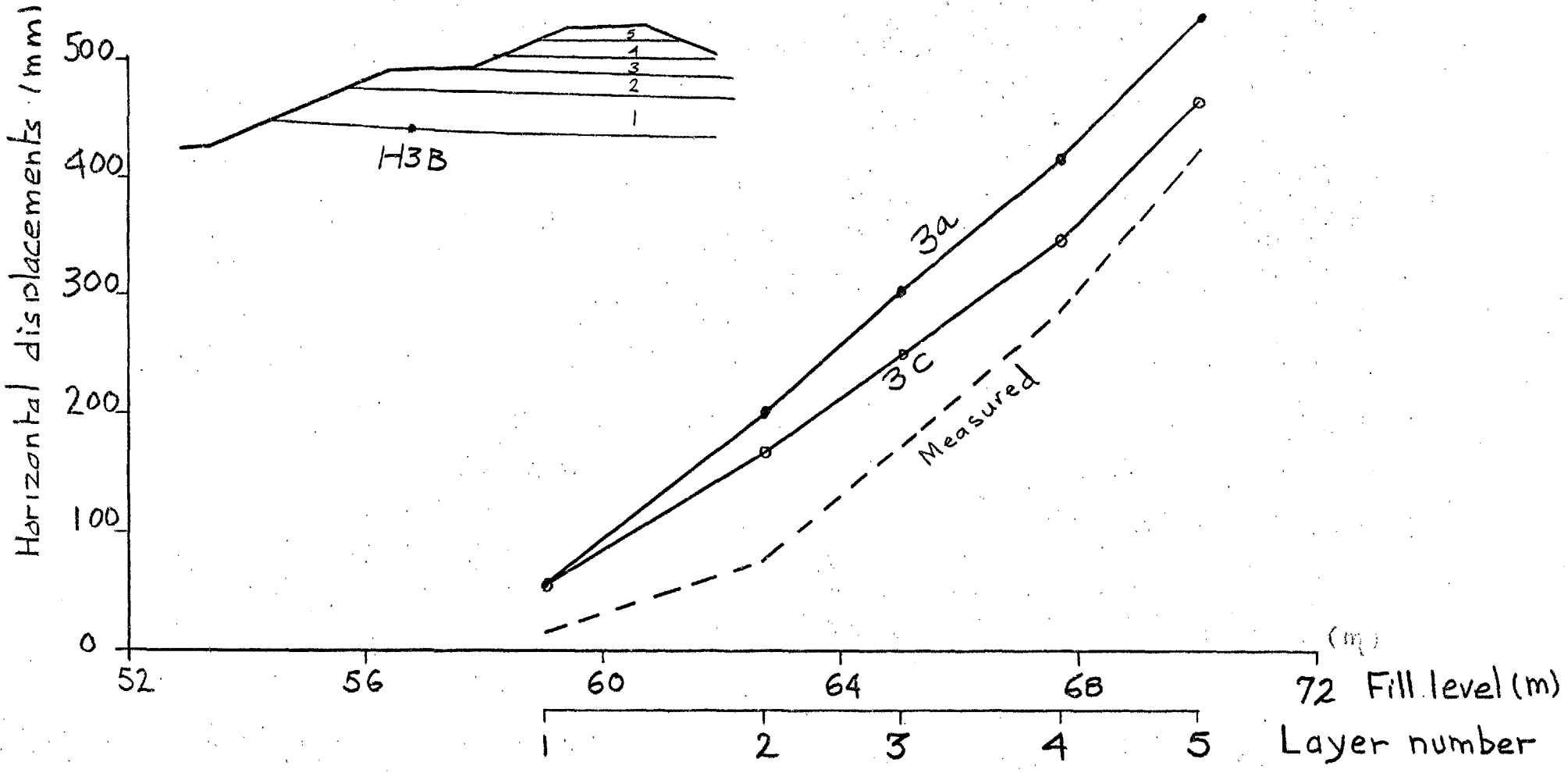
MEASURED VS. F.E. PREDICTION _ CASES : 3a , 3C _ POINT I3

Fig. 6.50



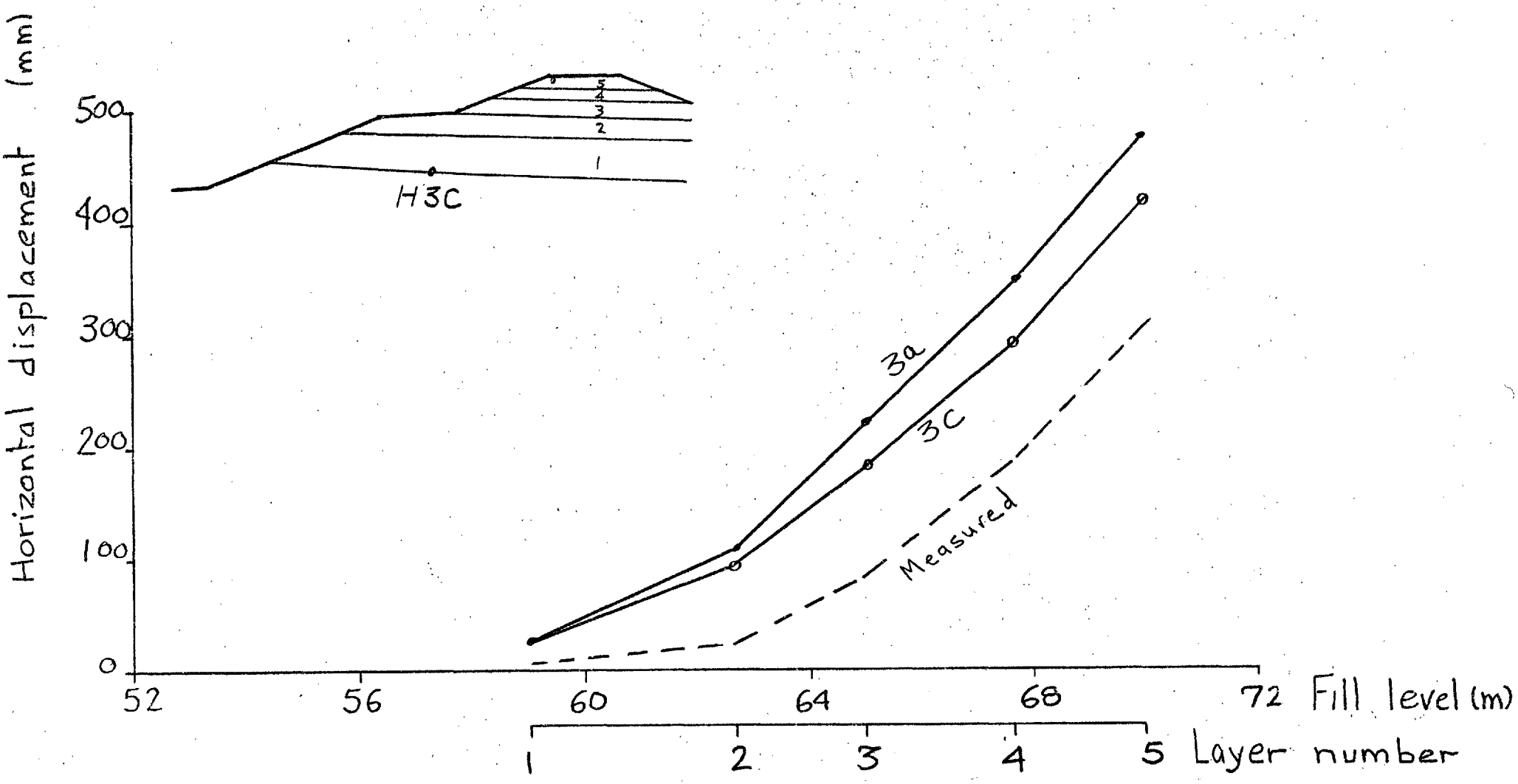
MEASURED VS. F.E. PREDICTION _ CASES: 3a, 3C _ POINT H3A

Fig. 6.51



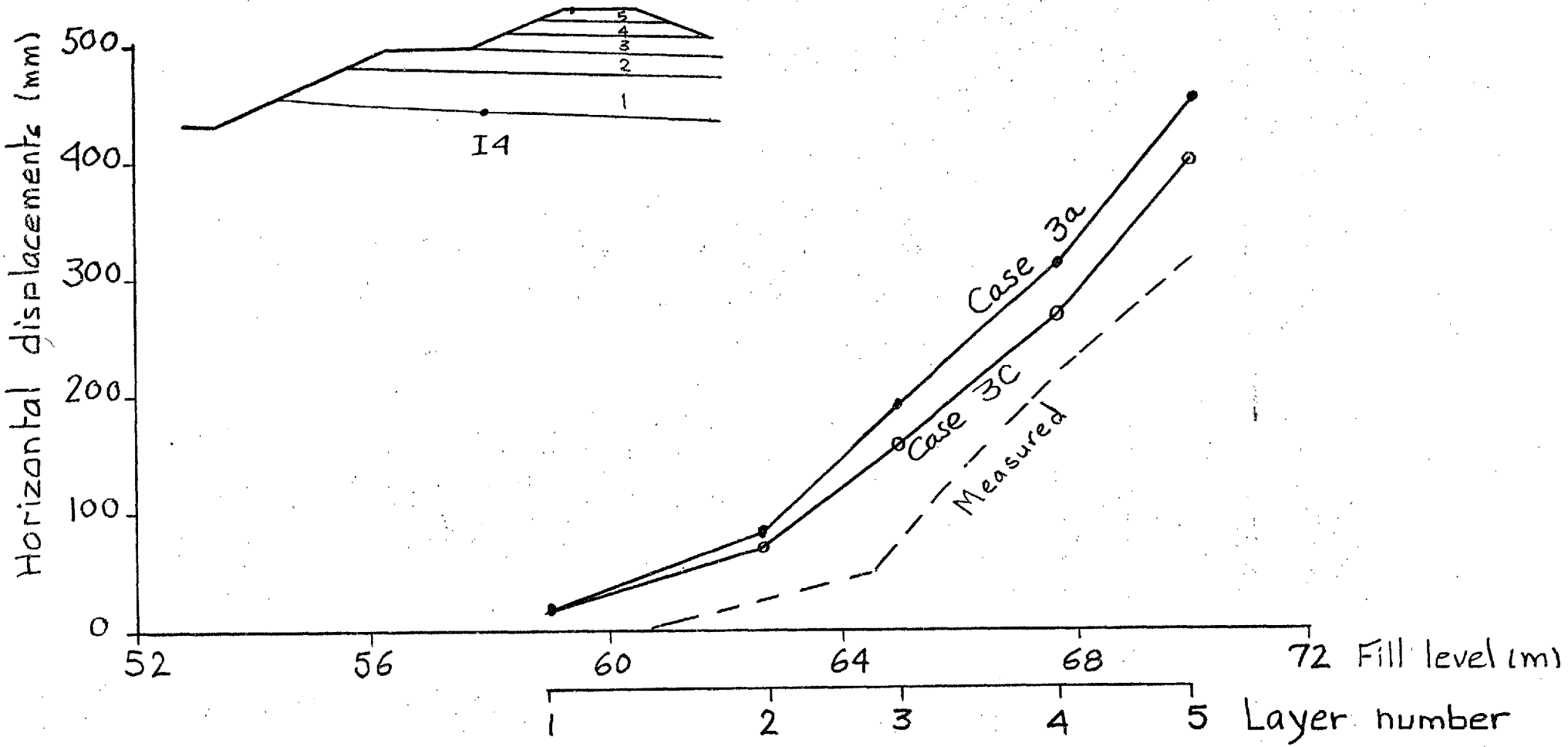
MEASURED VS. F.E. PREDICTION _ CASES : 3a, 3c _ POINT H3B

Fig. 6.52



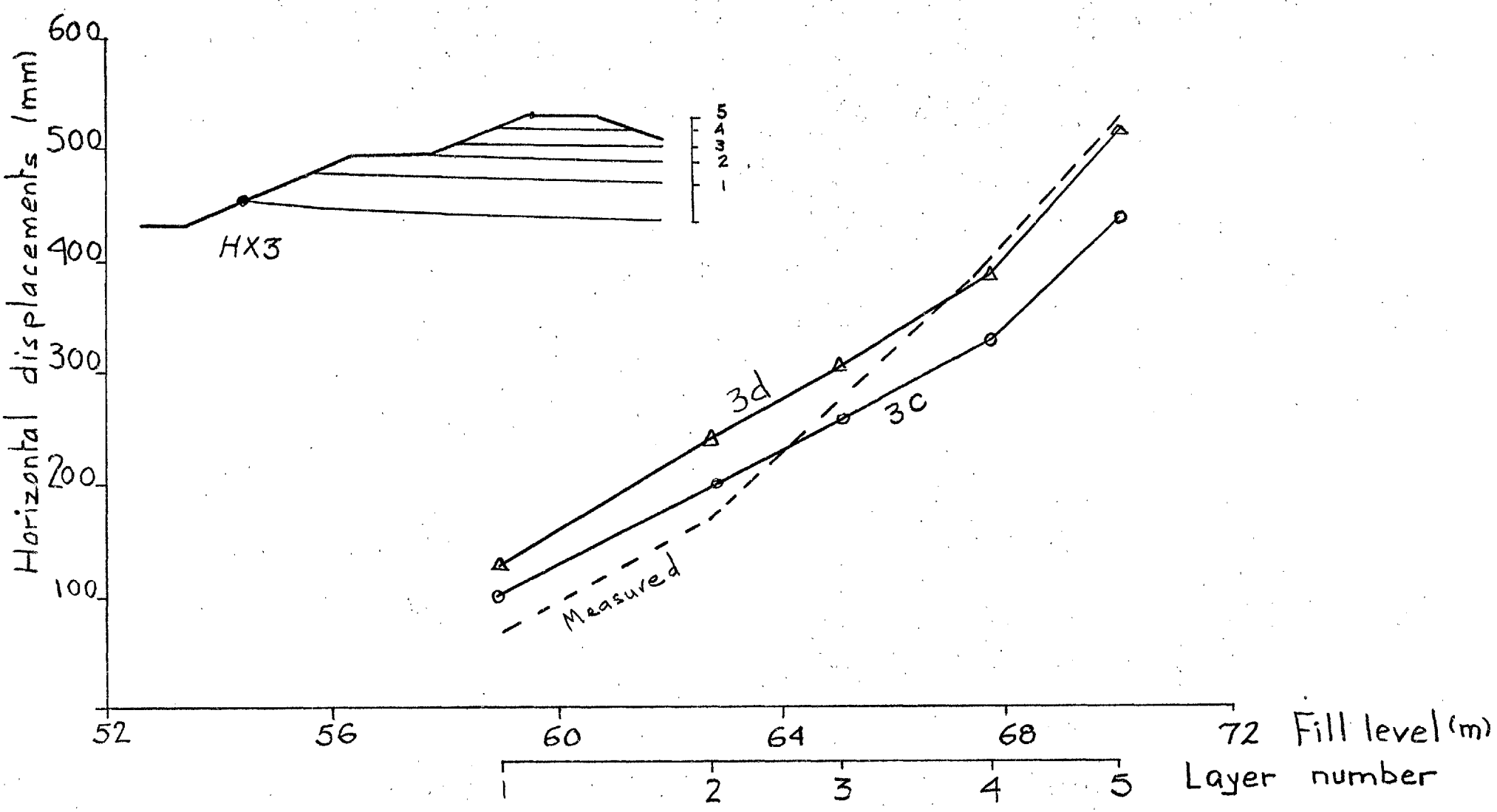
MEASURED VS. F.E. PREDICTION _ CASES : 3a , 3C _ POINT H3C

Fig. 6.53



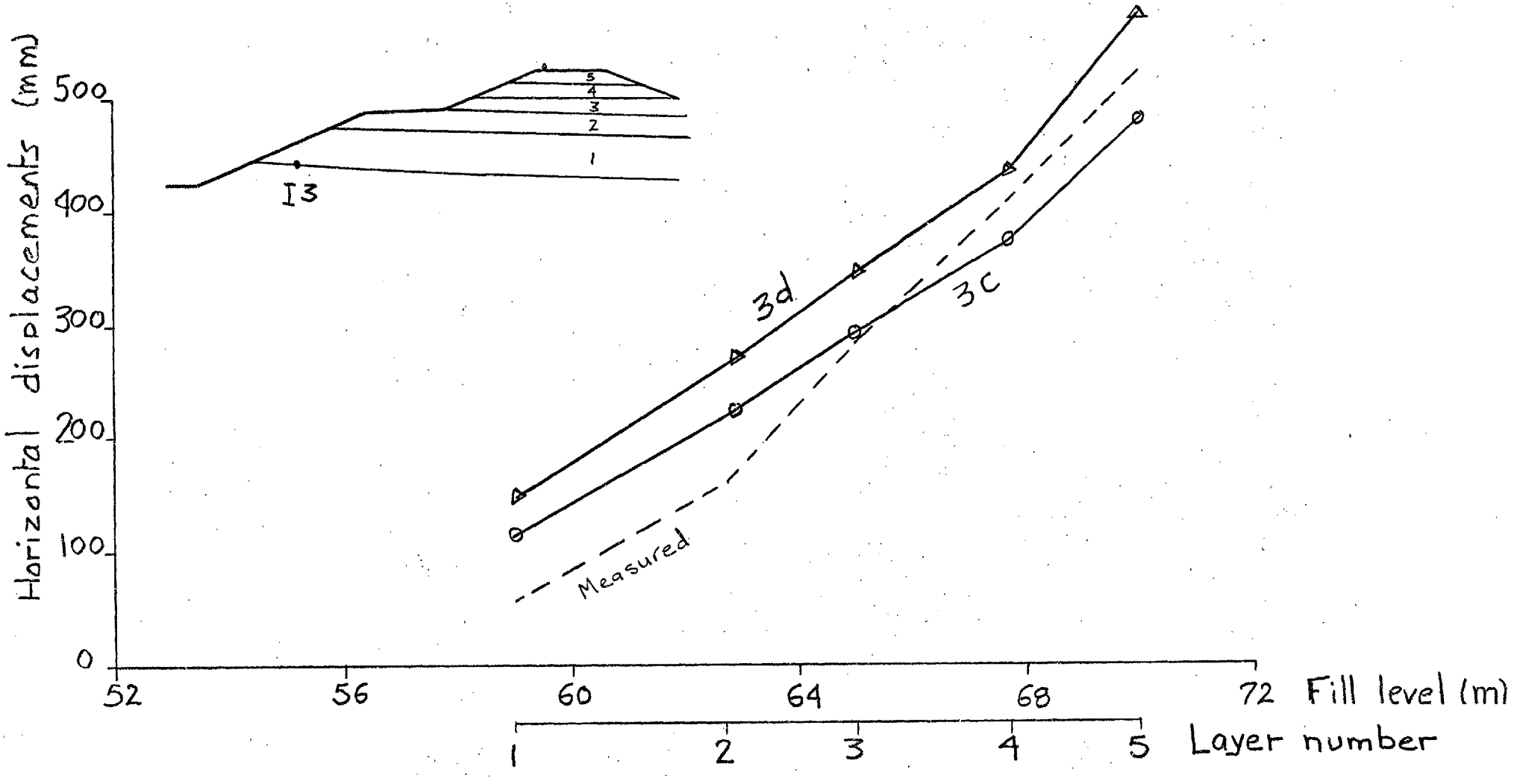
MEASURED VS. F.E. PREDICTION _ CASES : 3a , 3C _ POINT I4

Fig. 6.54



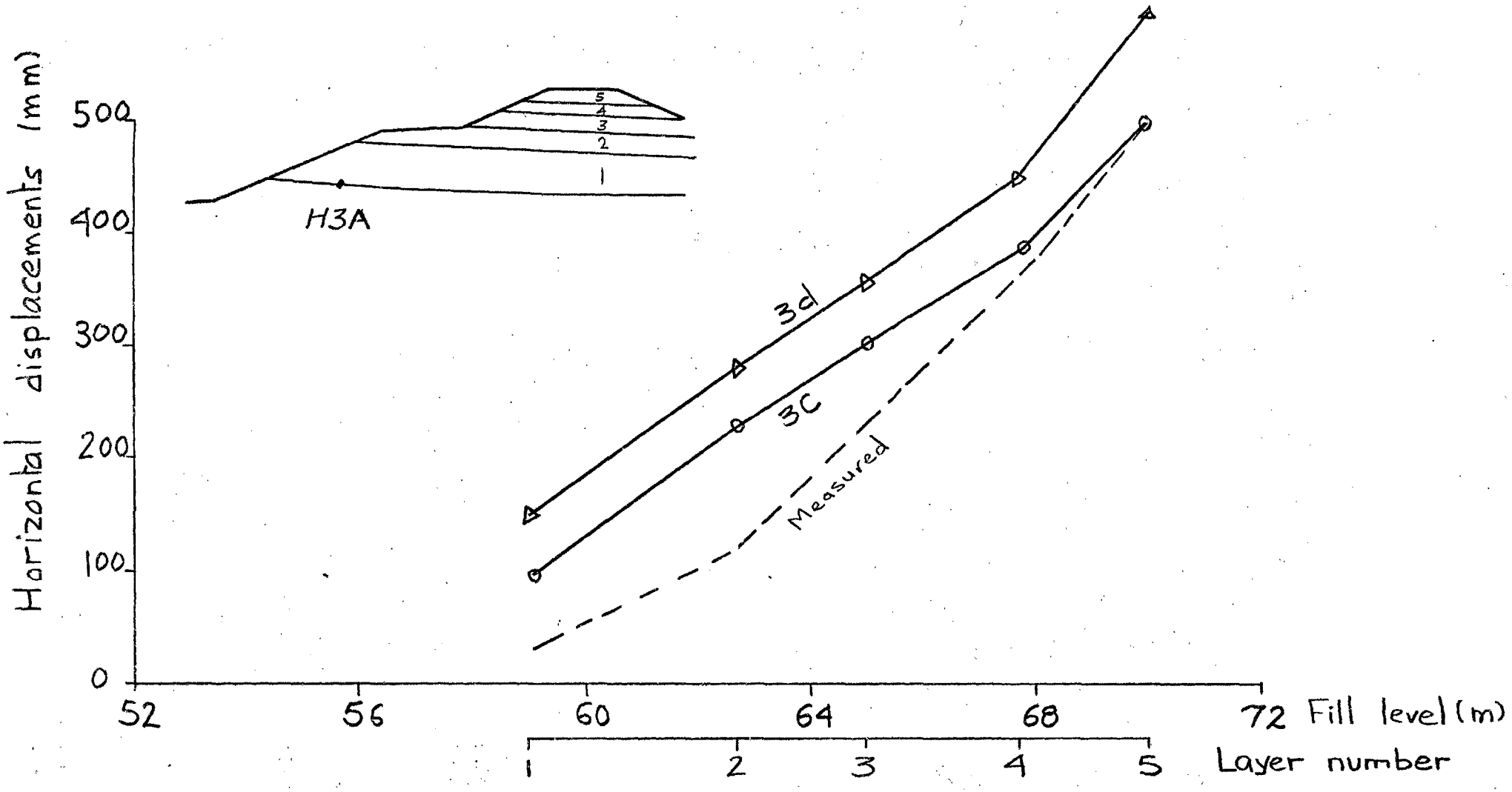
MEASURED VS. F.E. PREDICTION _ CASES : 3d , 3c _ POINT HX3

Fig. 6.55



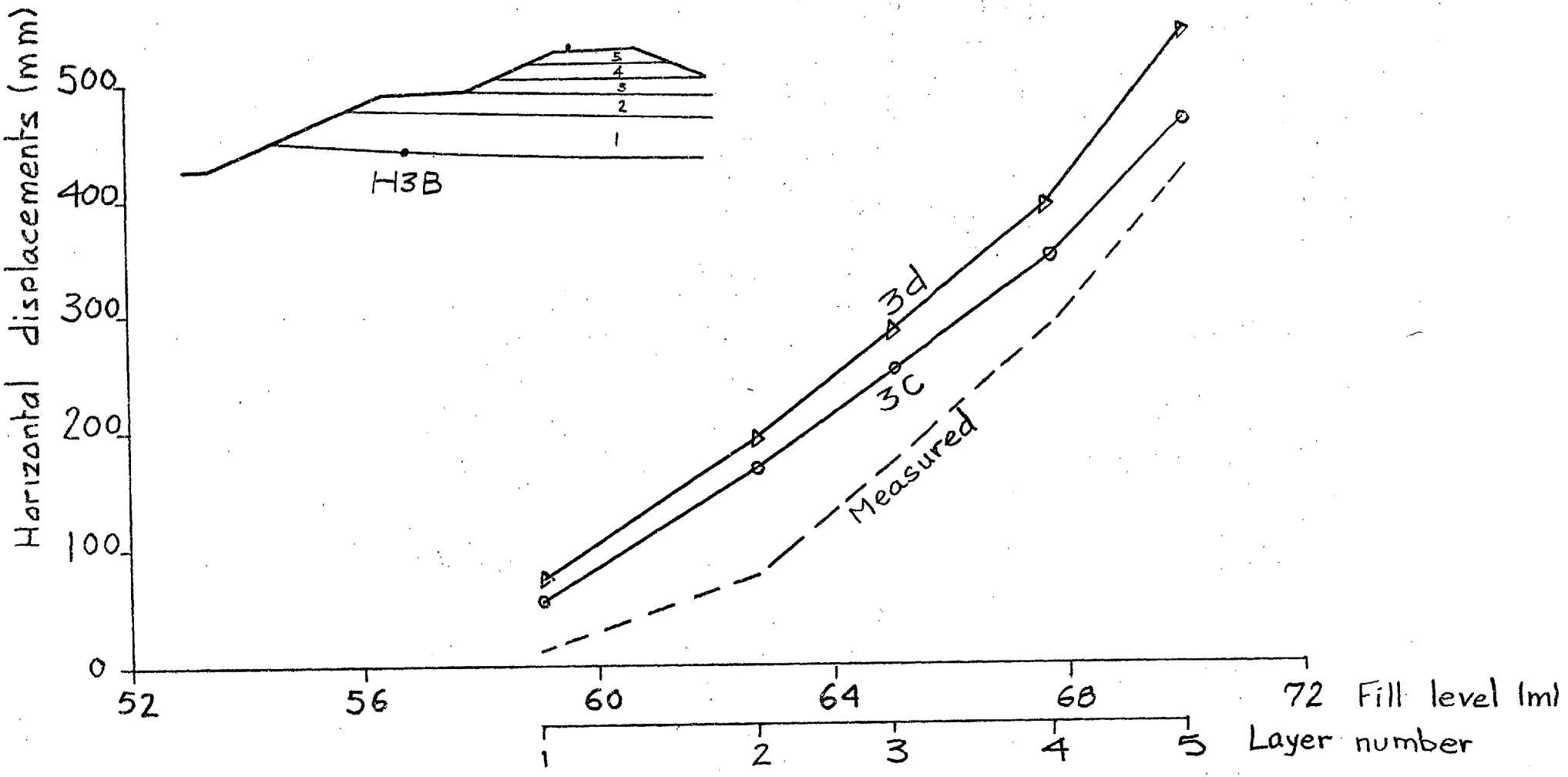
MEASURED VS. F.E. PREDICTION _ CASES: 3d ; 3C _ POINT I3

Fig. 6.55



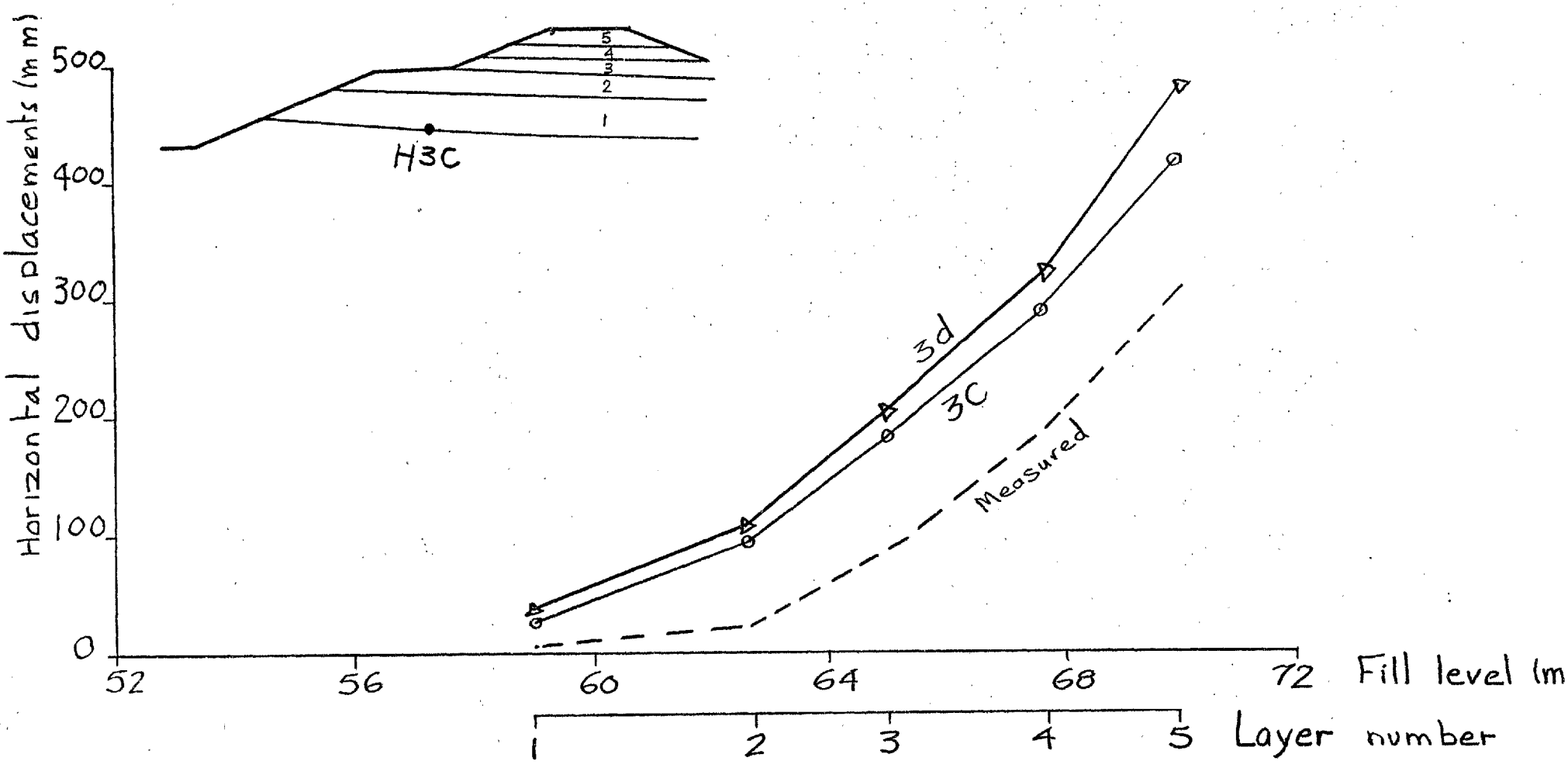
MEASURED VS. F.E. PREDICTION _ CASES : 3d , 3C _ POINT H3A

Fig. 6.57



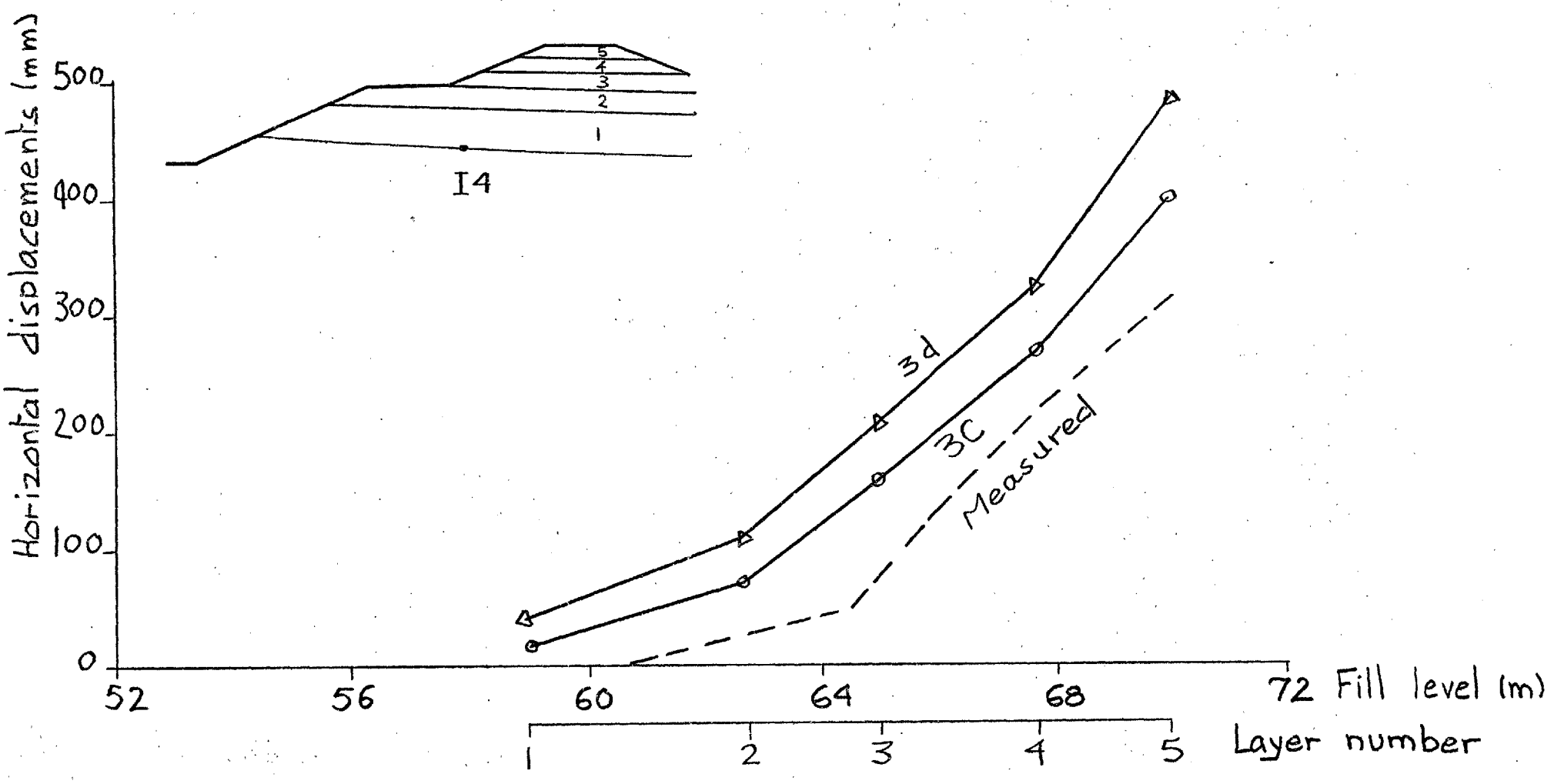
MEASURED VS. F.E. PREDICTION _ CASES : 3d , 3c _ POINT H3B

Fig 5.58



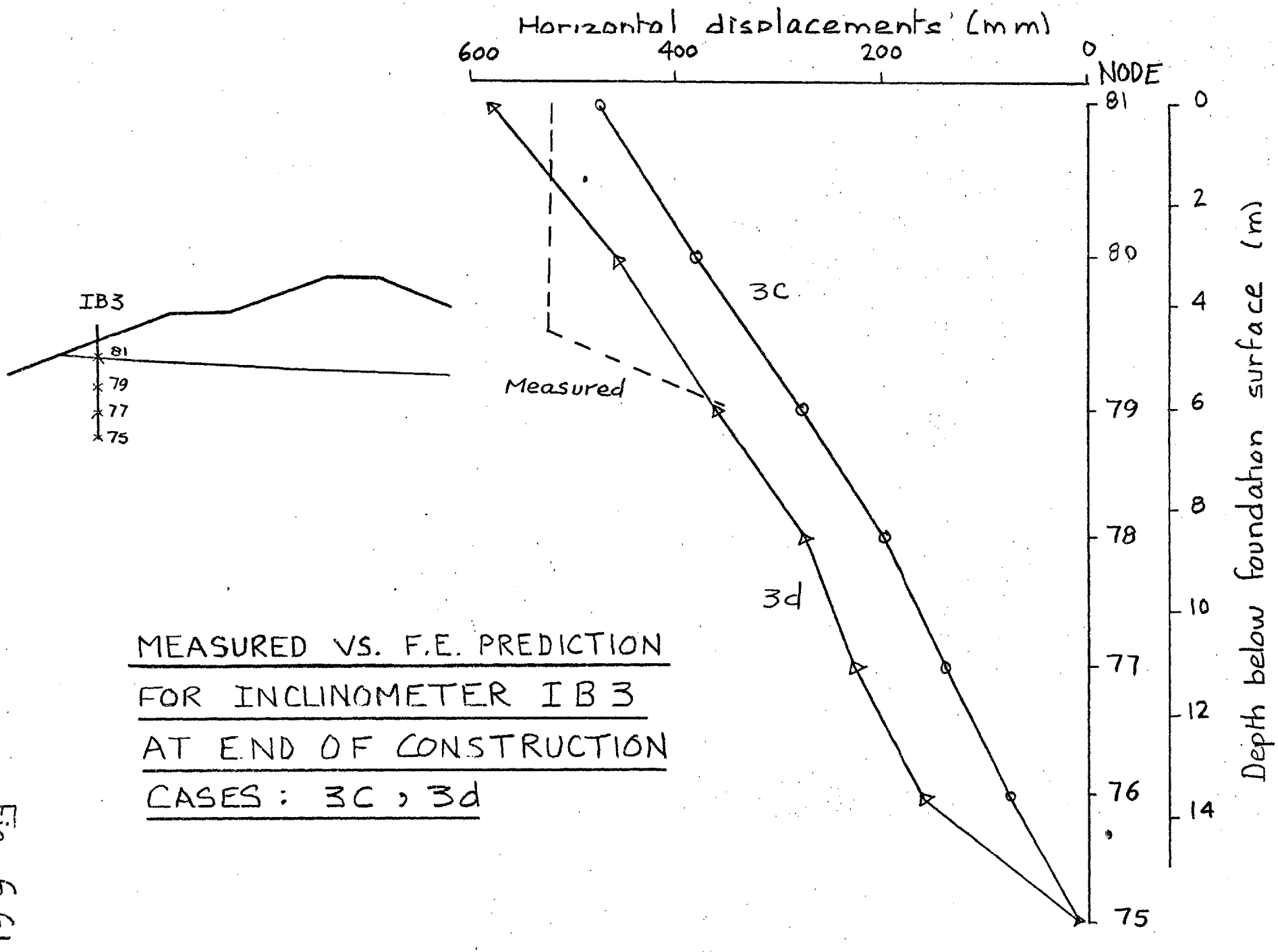
MEASURED VS. F.E. PREDICTION _ CASES : 3d , 3c _ POINT H3C

Fig. 6.59



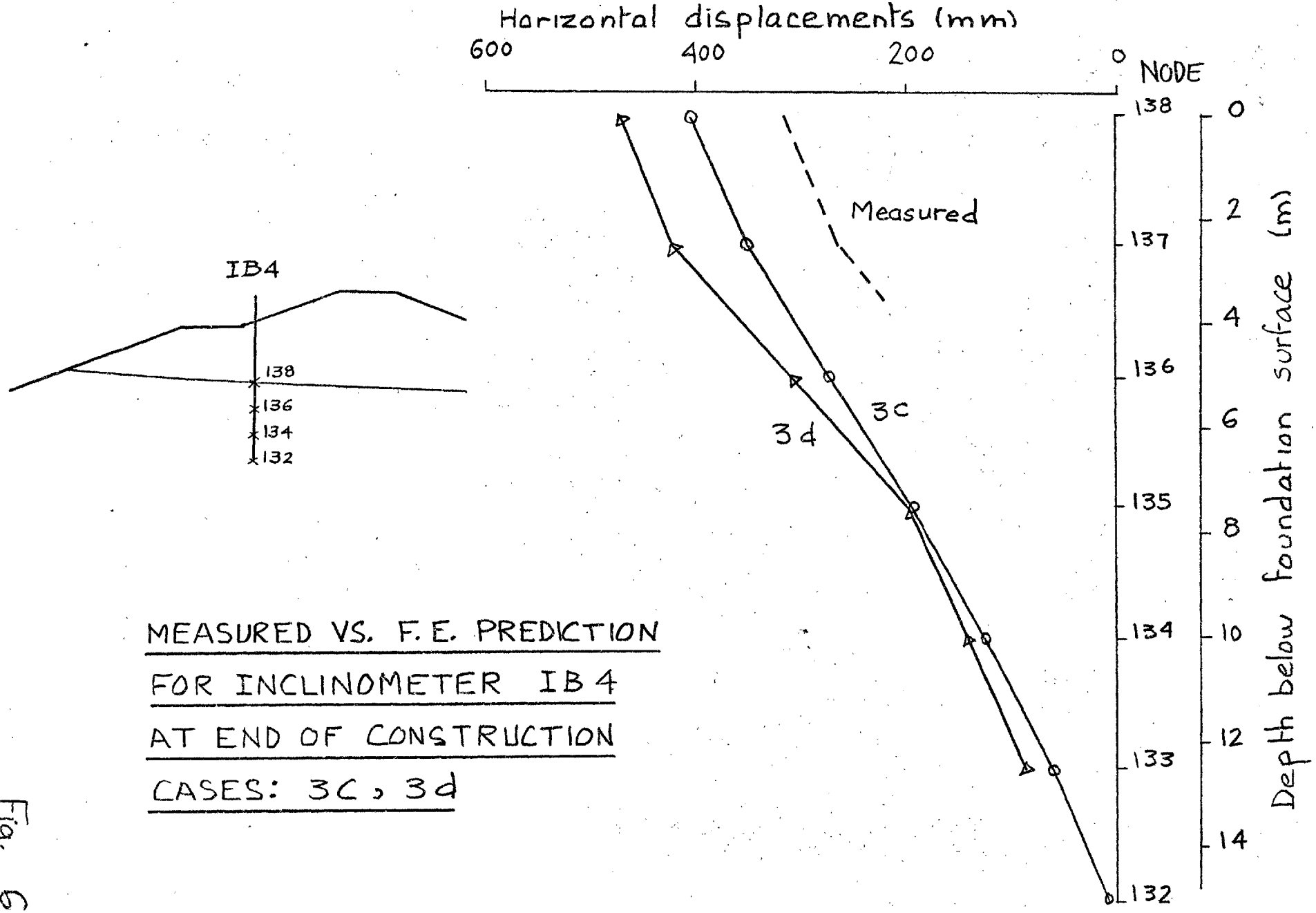
MEASURED VS. F.E. PREDICTION _ CASES 3d , 3c _ POINT I4

Fig. 6.60



MEASURED VS. F.E. PREDICTION
FOR INCLINOMETER IB3
AT END OF CONSTRUCTION
CASES : 3C , 3d

Fig. 6.61



MEASURED VS. F.E. PREDICTION FOR INCLINOMETER IB 4 AT END OF CONSTRUCTION CASES: 3C, 3d

Fig. 6.62

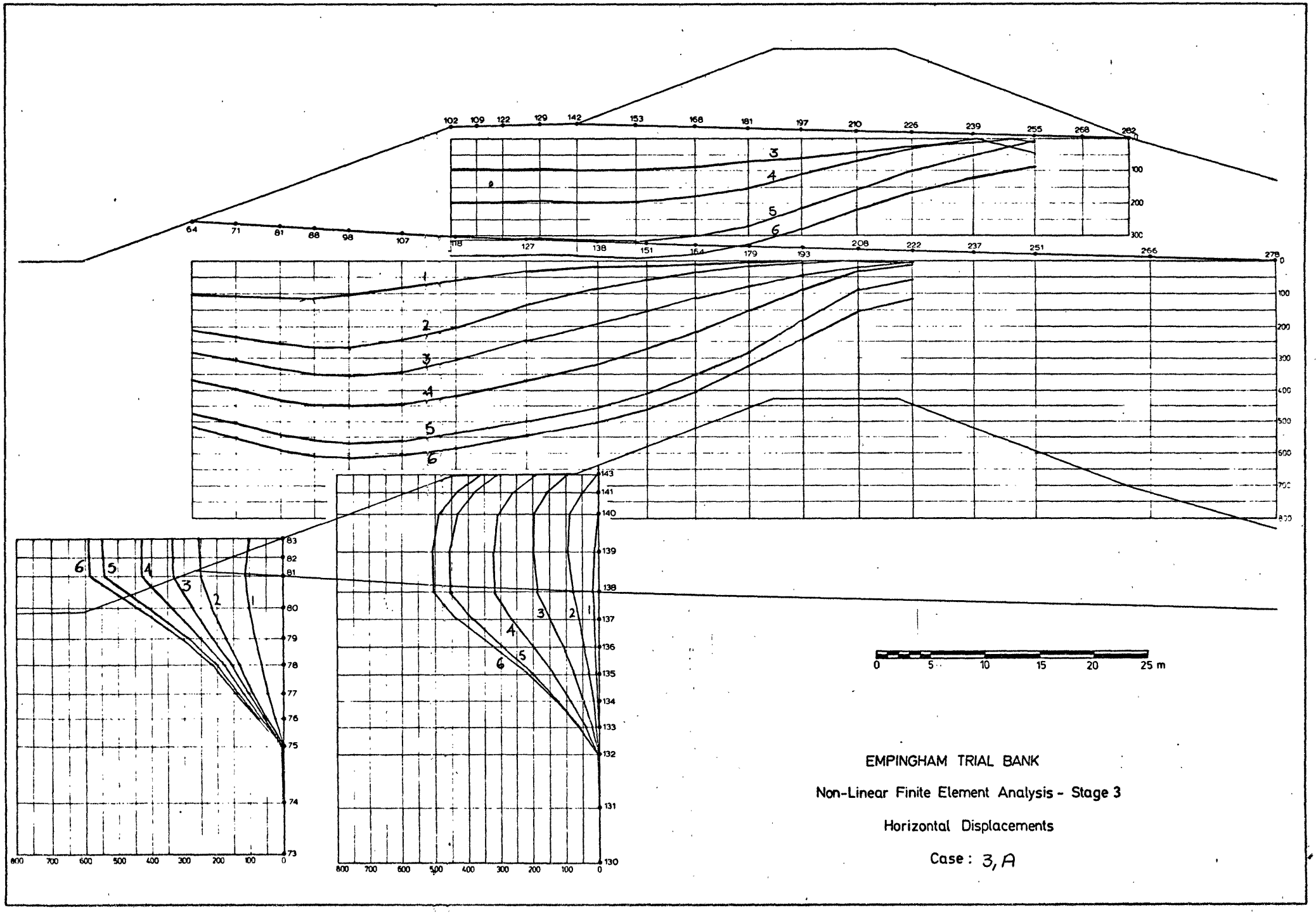
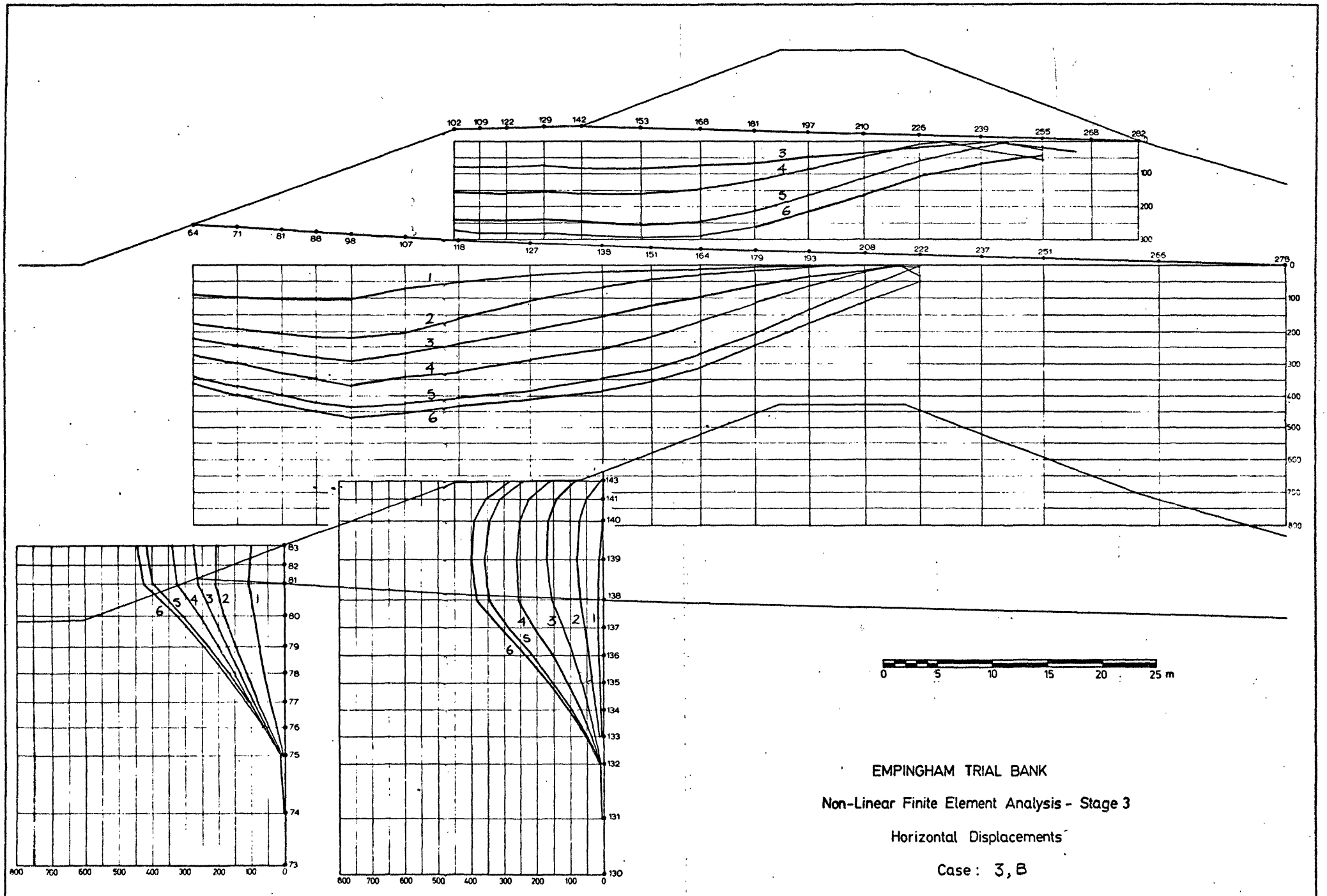

102 109 122 129 142 153 168 181 197 210 226 239 255 268 282
64 71 81 88 98 107 118 127 138 151 164 179 193 208 222 237 251 266 278
3
4
5
6
1
2
3
4
5
6
0 5 10 15 20 25 m
EMPINGHAM TRIAL BANK
Non-Linear Finite Element Analysis - Stage 3
Horizontal Displacements
Case : 3, A

Fig. 6.63



EMPINGHAM TRIAL BANK

Non-Linear Finite Element Analysis - Stage 3

Horizontal Displacements

Case: 3, B

Fig. 6.64

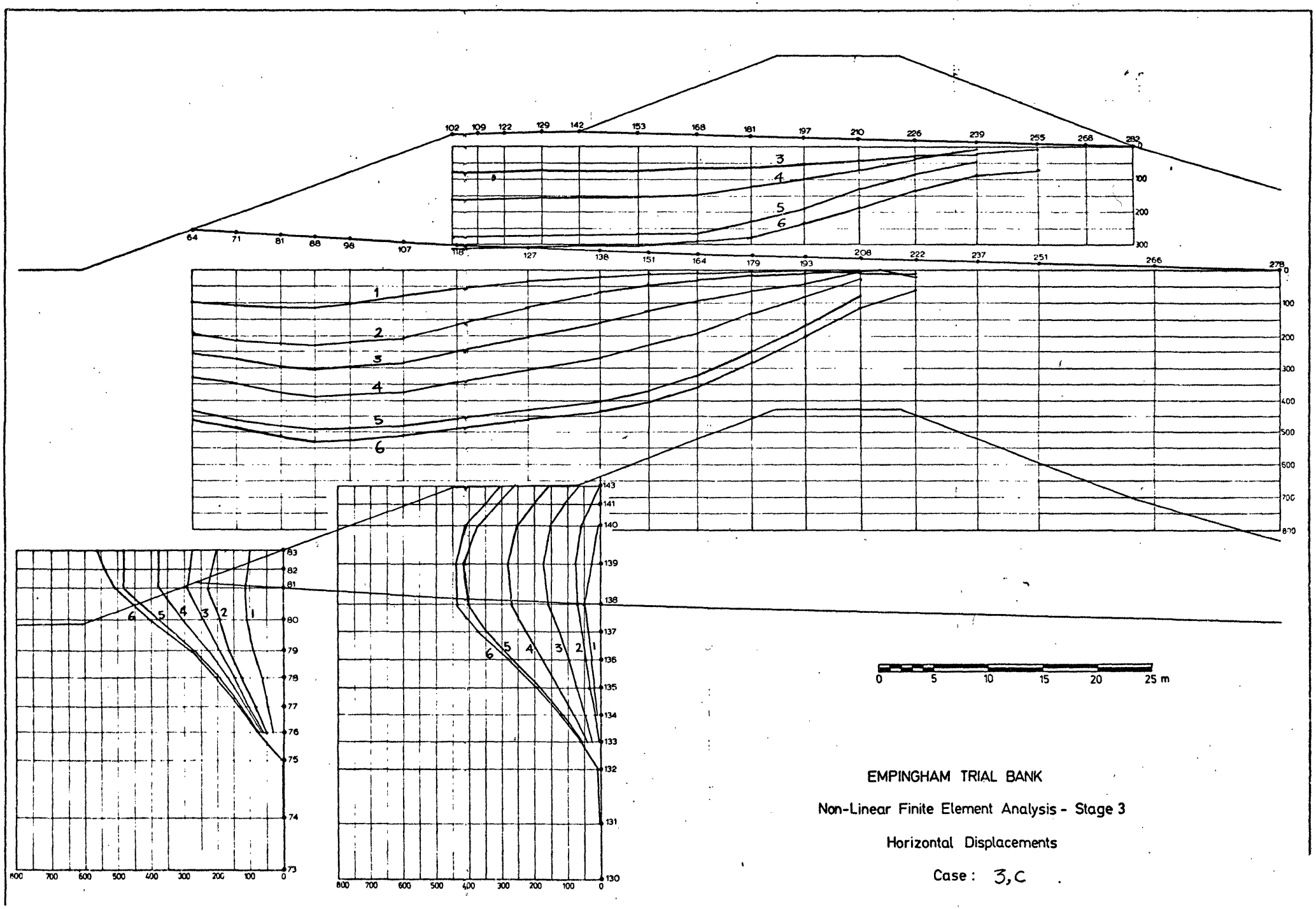

102 109 122 129 142 153 168 181 197 210 226 239 255 268 283
64 71 81 88 98 107 118 127 138 151 164 179 193 208 222 237 251 266 278
1
2
3
4
5
6
0 5 10 15 20 25 m
EMPINGHAM TRIAL BANK
Non-Linear Finite Element Analysis - Stage 3
Horizontal Displacements
Case: 3,C

Fig. 6.65

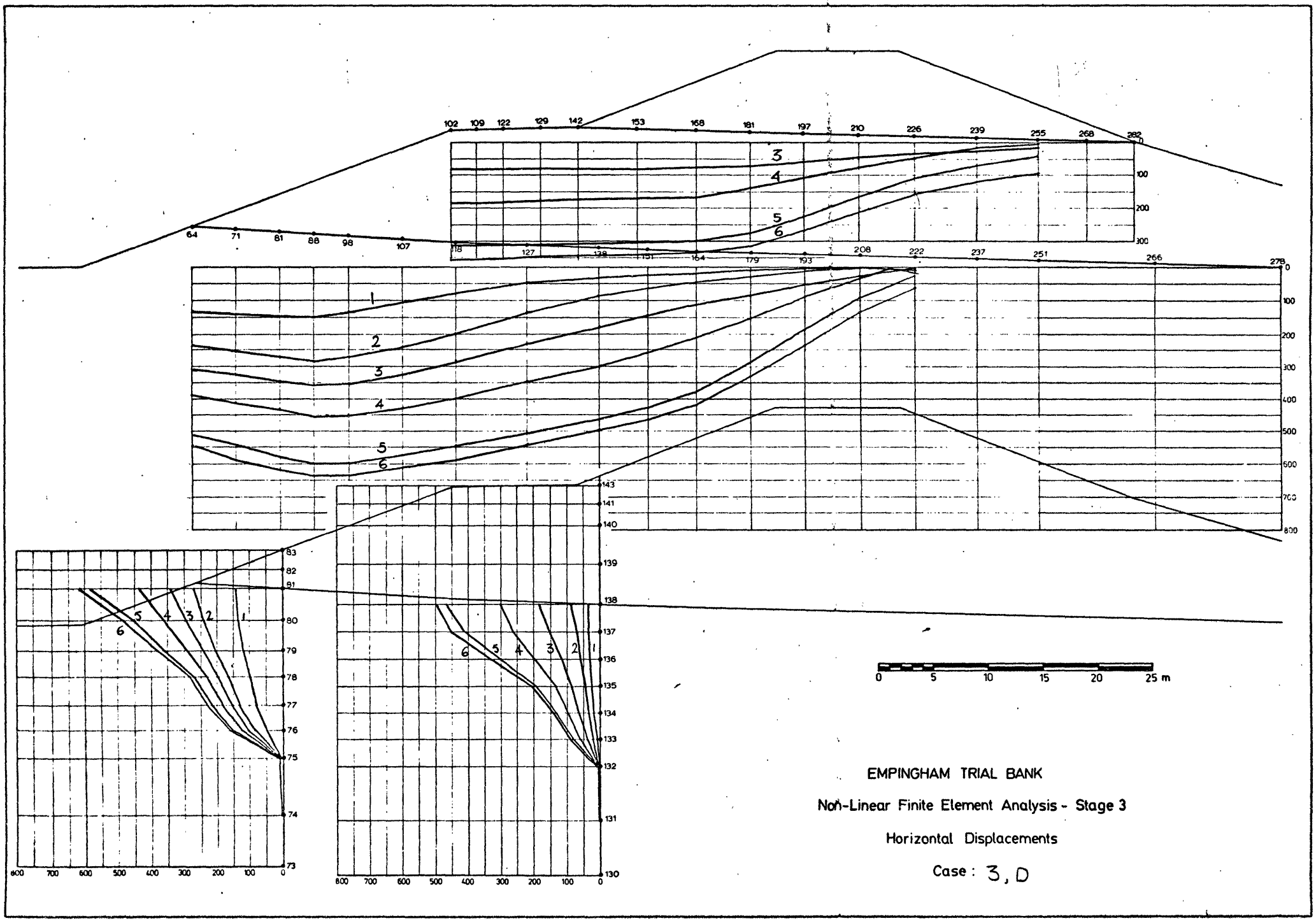

102 109 122 129 142 153 168 181 197 210 226 239 255 268 282
64 71 81 88 98 107
118 127 139 151 164 179 193 208 222 237 251 266 278
1
2
3
4
5
6
0 5 10 15 20 25 m
EMPINGHAM TRIAL BANK
Non-Linear Finite Element Analysis - Stage 3
Horizontal Displacements
Case : 3, D

Fig. 6.66

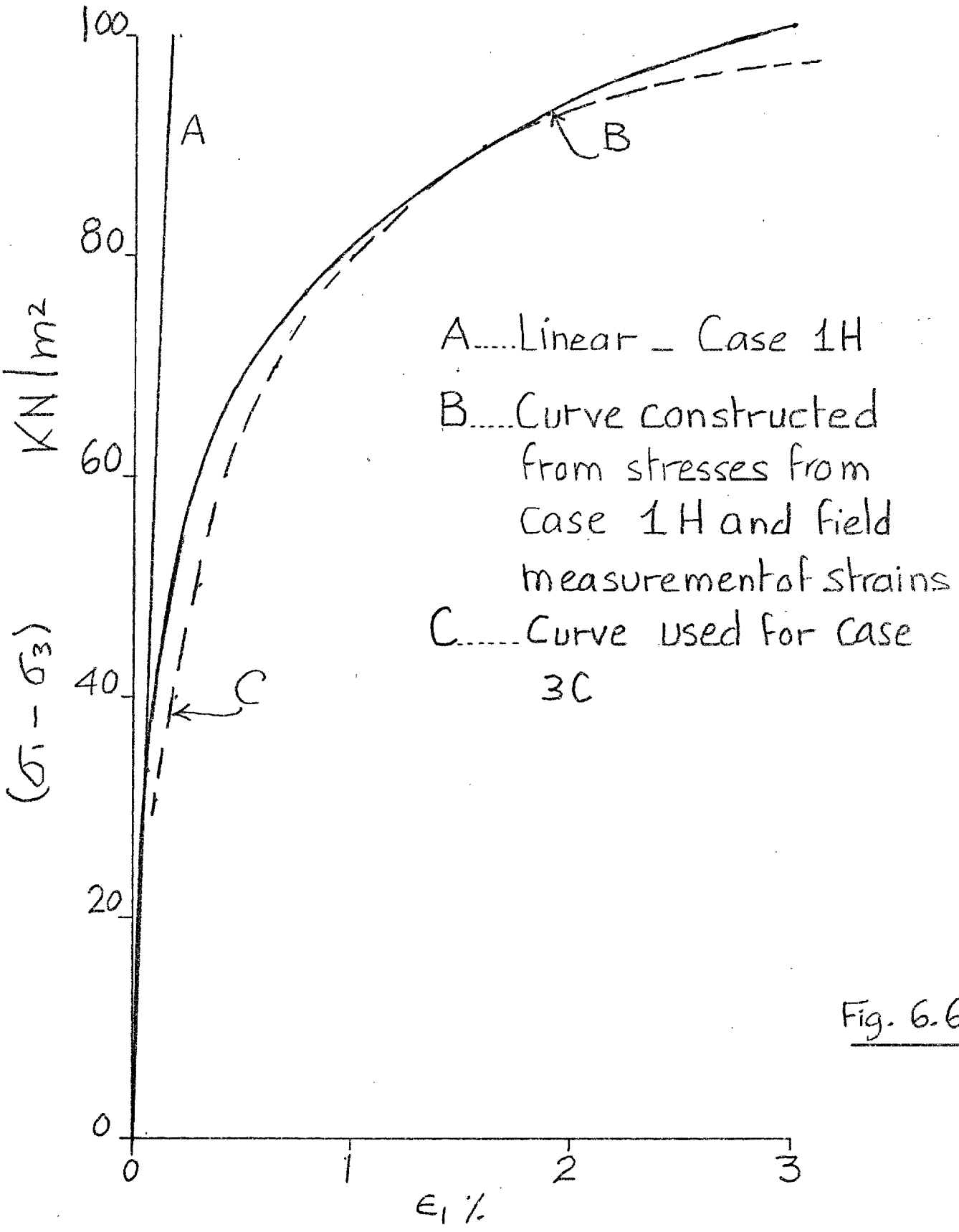
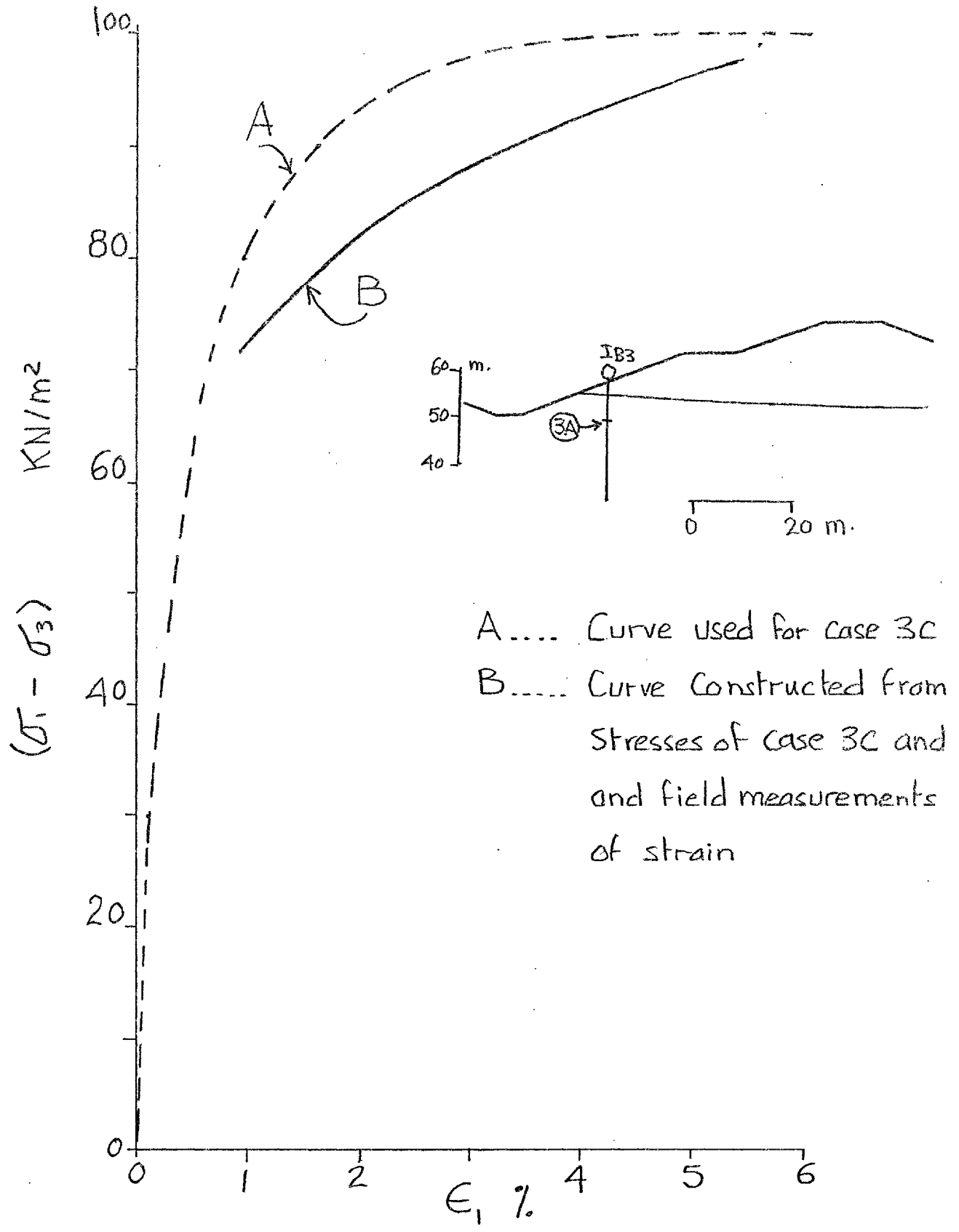


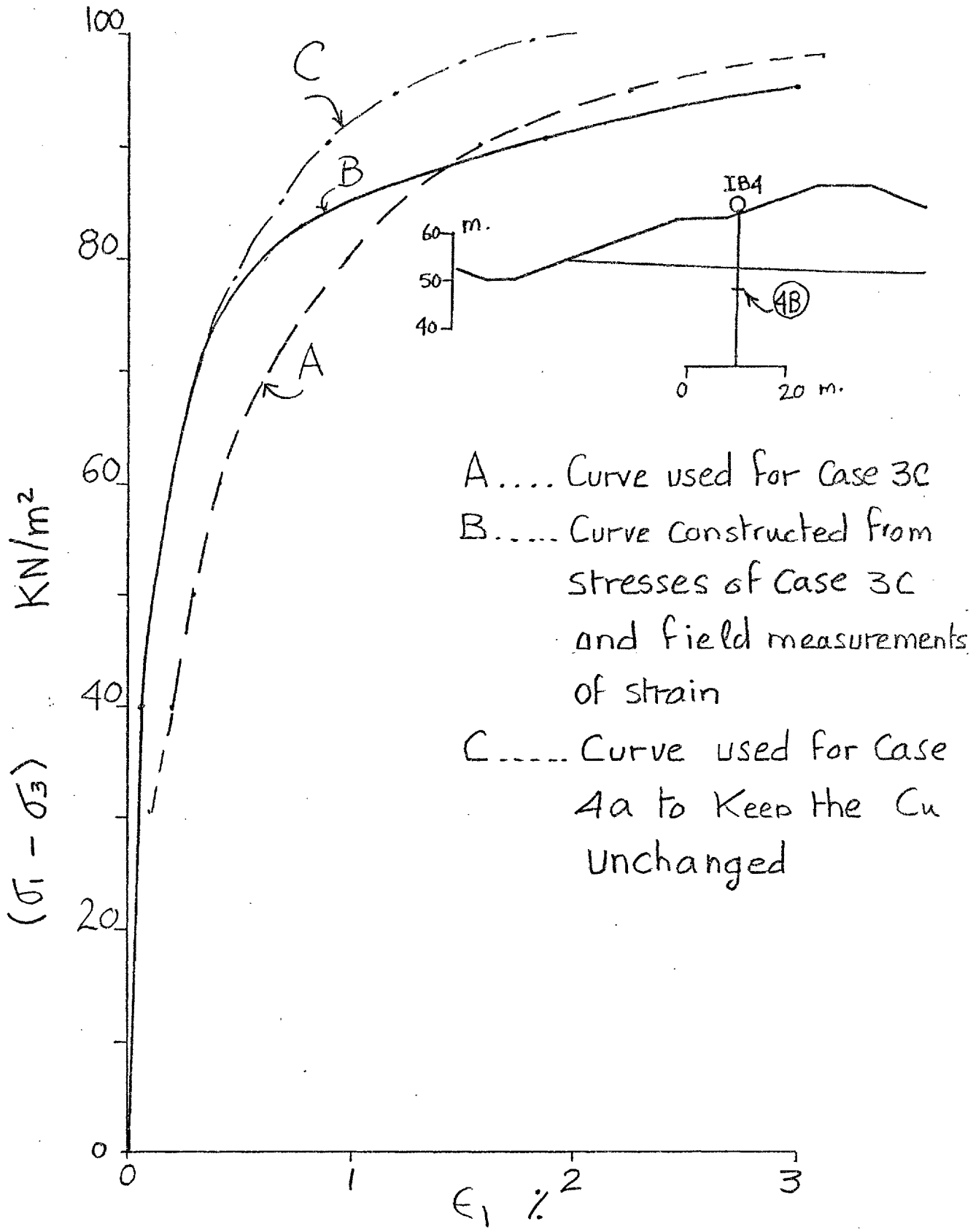
Fig. 6.67

THE DEDUCED STRESS-STRAIN CURVE USING THE SYSTEMATIC BACK ANALYSIS METHOD. (ONLY ONE ITERATION STARTING FROM LINEAR)



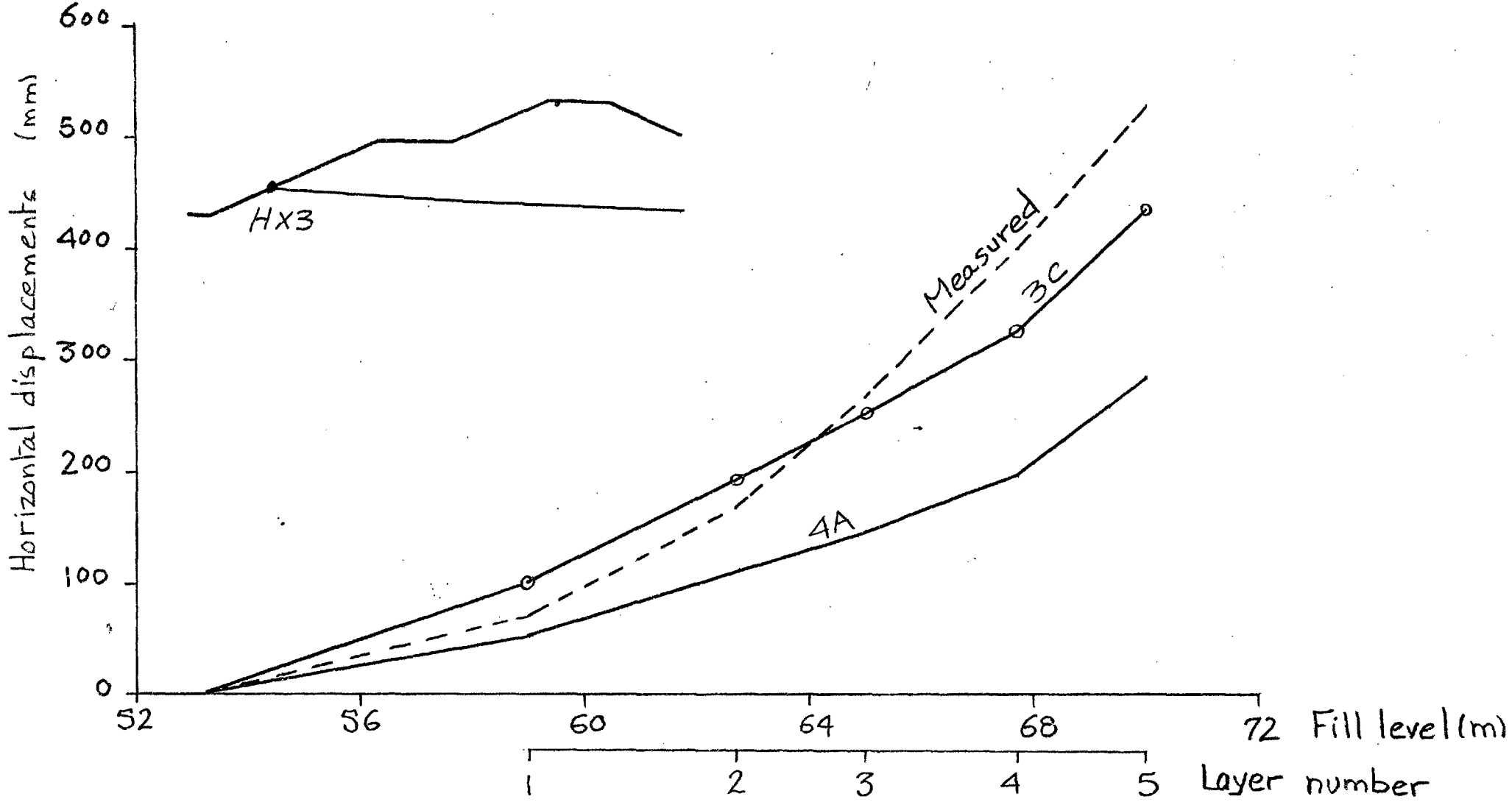
DEDUCED STRESS-STRAIN CURVE AT POINT 3A FROM CASE 3C'S STRESSES AND MEASUREMENTS OF STRAIN

Fig 6.68



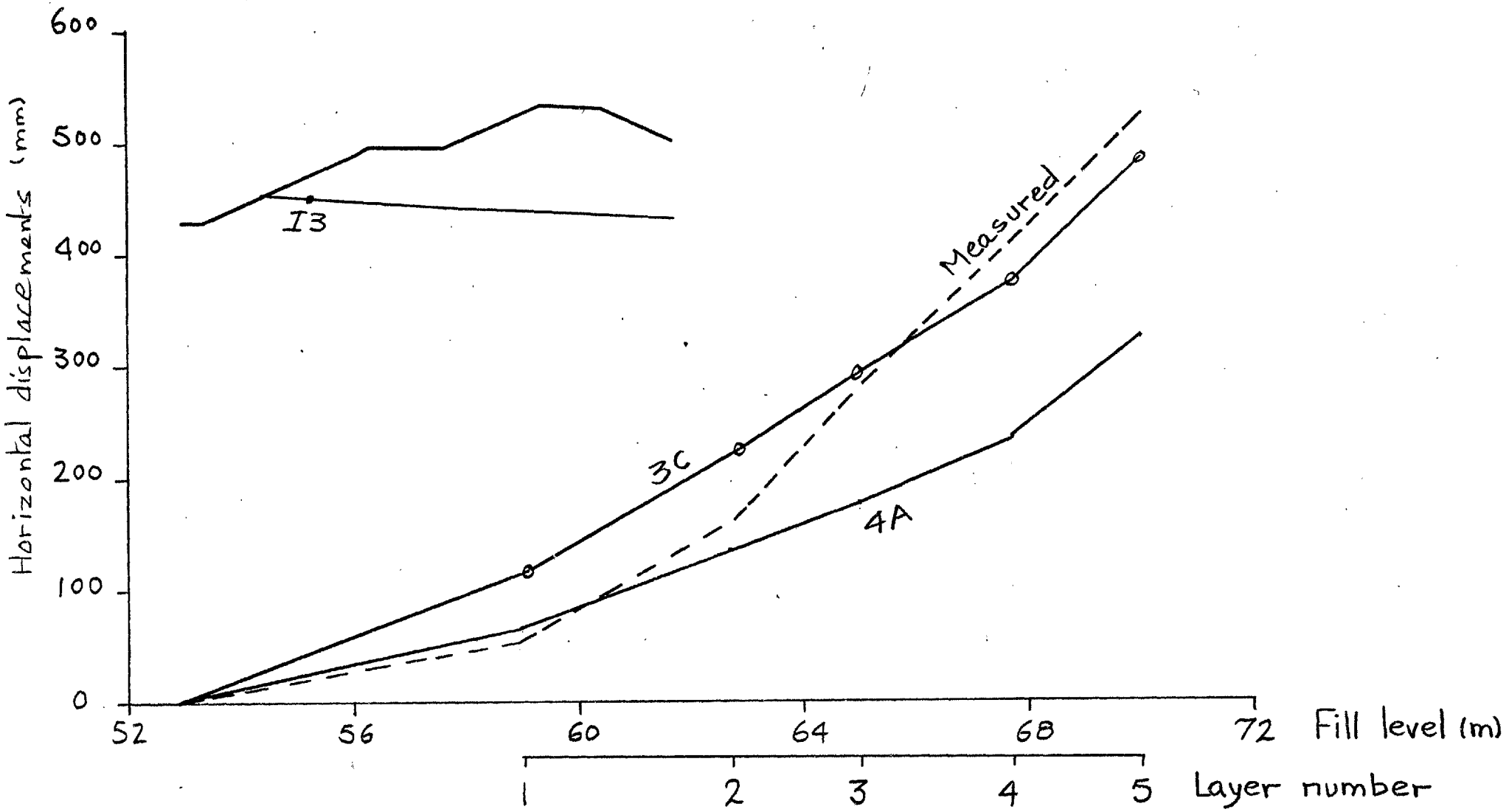
DEDUCED STRESS-STRAIN CURVE AT POINT 4B FROM CASE 3C'S STRESSES AND MEASUREMENTS OF STRAIN

Fig. 6.69



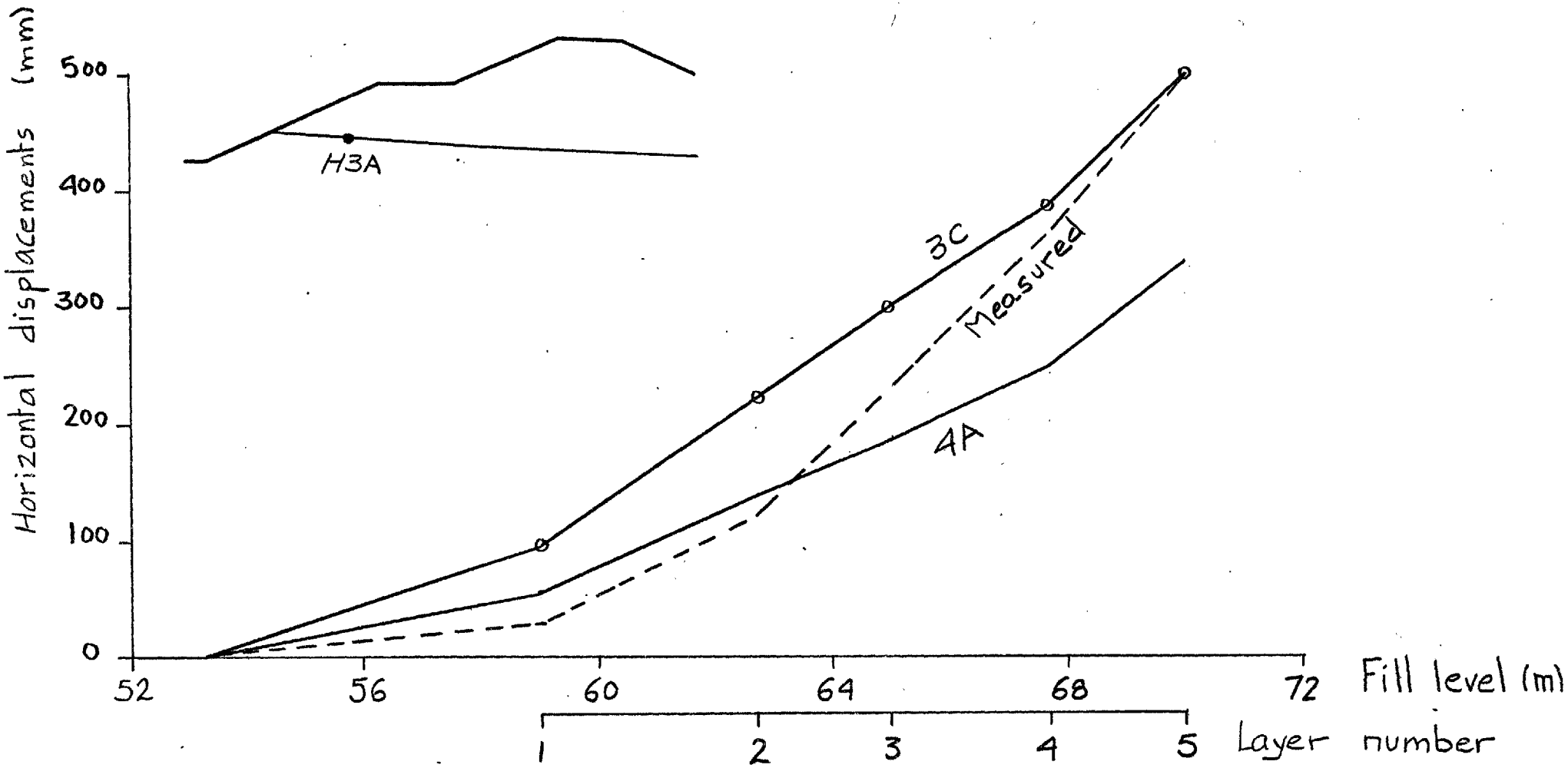
MEASURED VS. F.E. PREDICTIONS_ CASES: 3C, 4A _ POINT HX3

Fig. 6.70



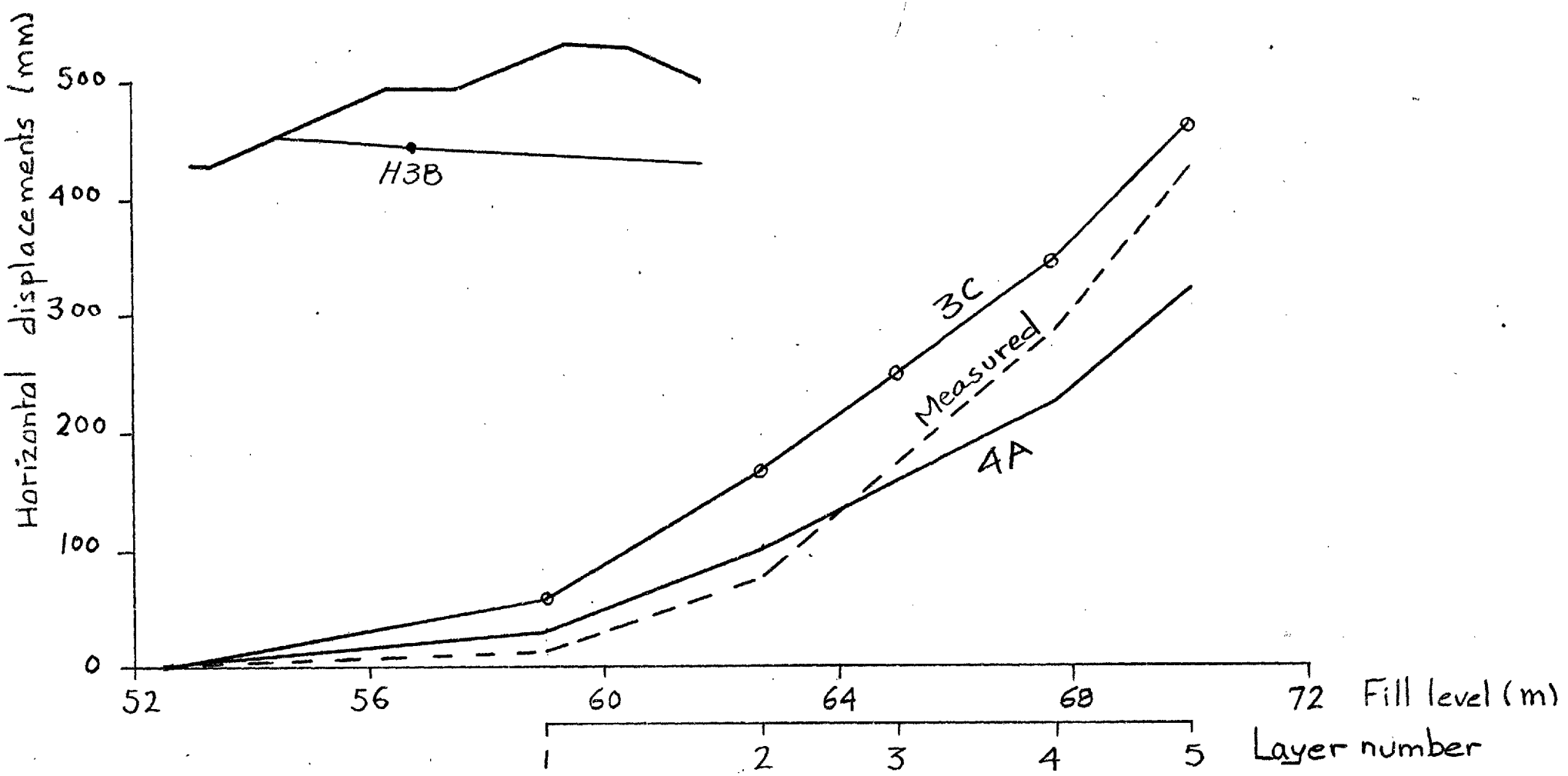
MEASURED VS. F.E. PREDICTIONS _ CASES : 3C , 4A _ POINT I3

Fig. 6.71



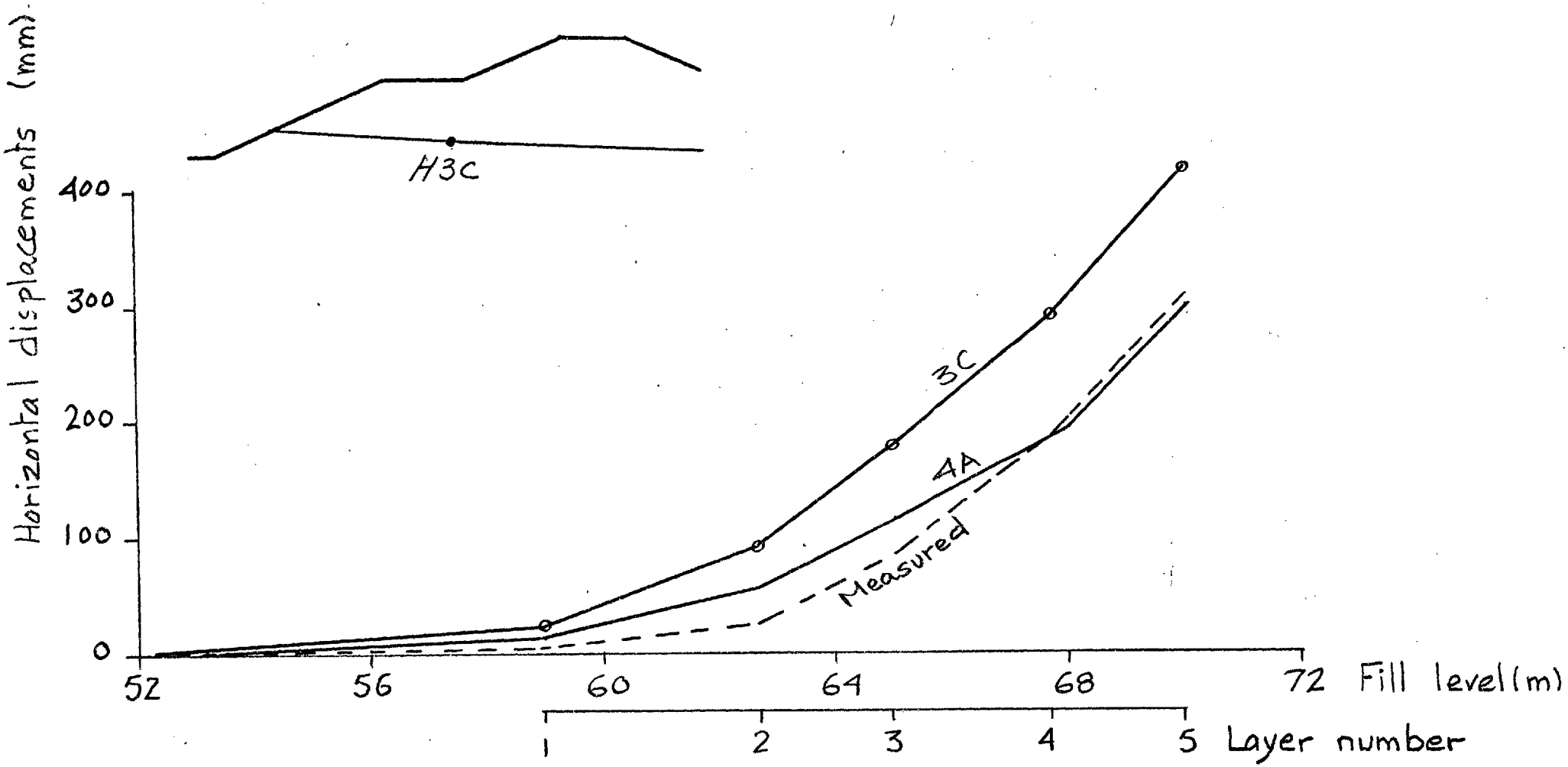
MEASURED VS. F. E. PREDICTIONS _ CASES : 3C , 4A _ POINT H3A

Fig. 6.72



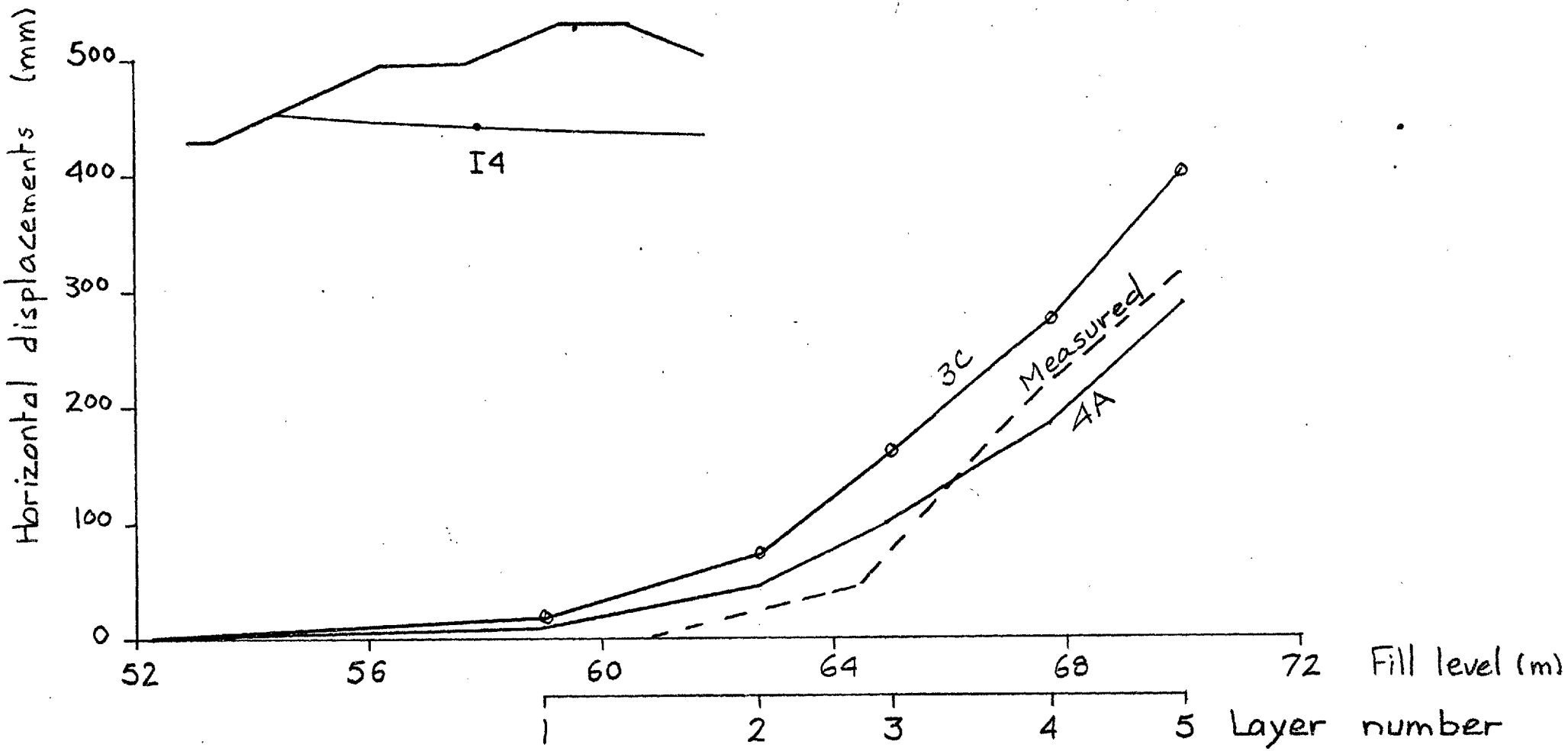
MEASURED VS. F.E. PREDICTIONS _ CASES : 3C , 4A _ POINT H3B

Fig. 6.73



MEASURED VS. F.E. PREDICTIONS _ CASES : 3C, 4A _ POINT H3C

Fig. 6.74



MEASURED VS. F.E. PREDICTIONS _ CASES: 3C, 4A _ POINT I4

Fig. 6.75

MEASURED VS. F.E. PREDICTIONS _ CASES: 3C, 4A _ INCLINOMETER IB3

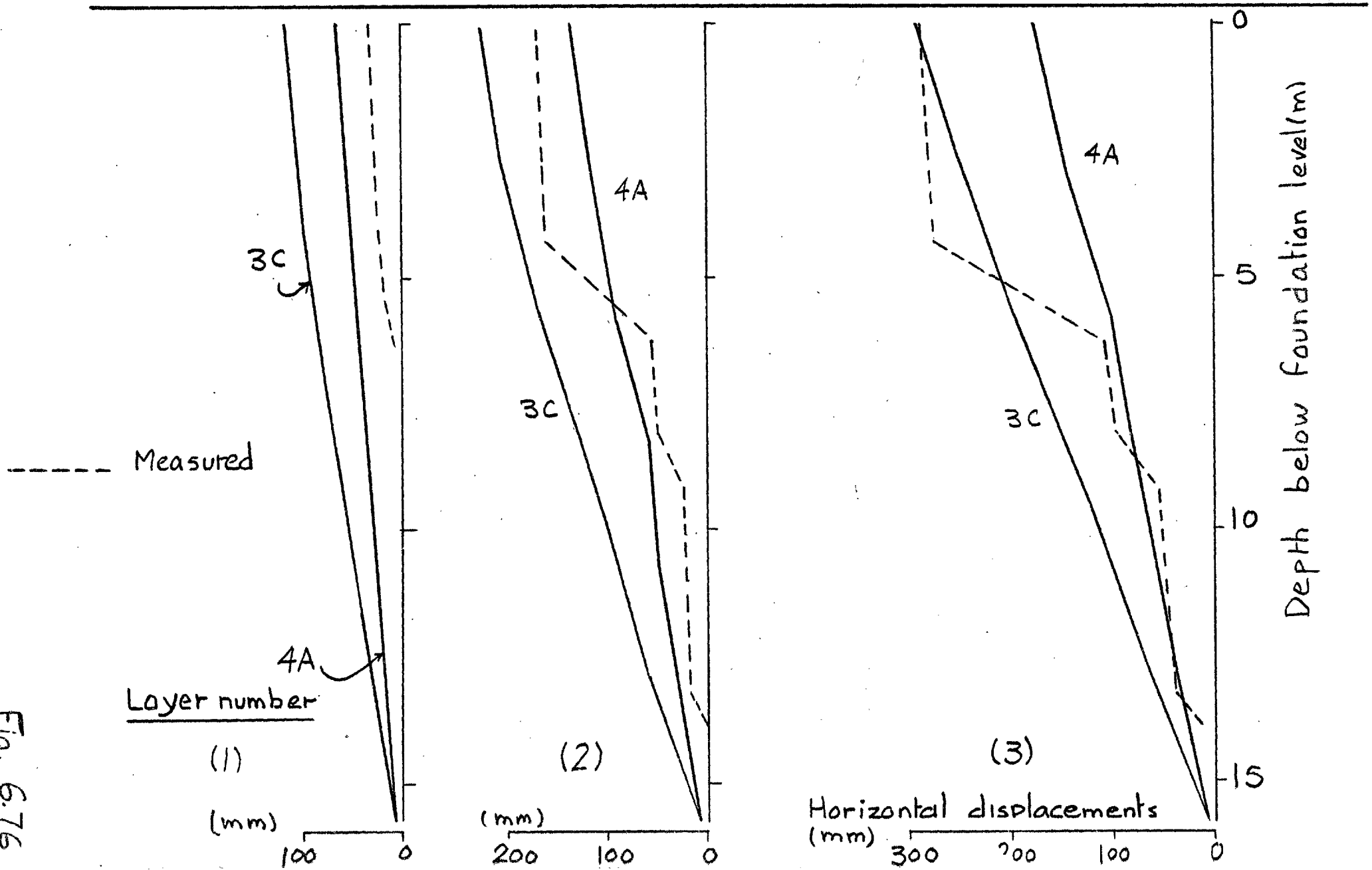


Fig. 6.76

MEASURED VS. F.E. PREDICTIONS – CASES : 3C, 4A – INCLINOMETER IB3

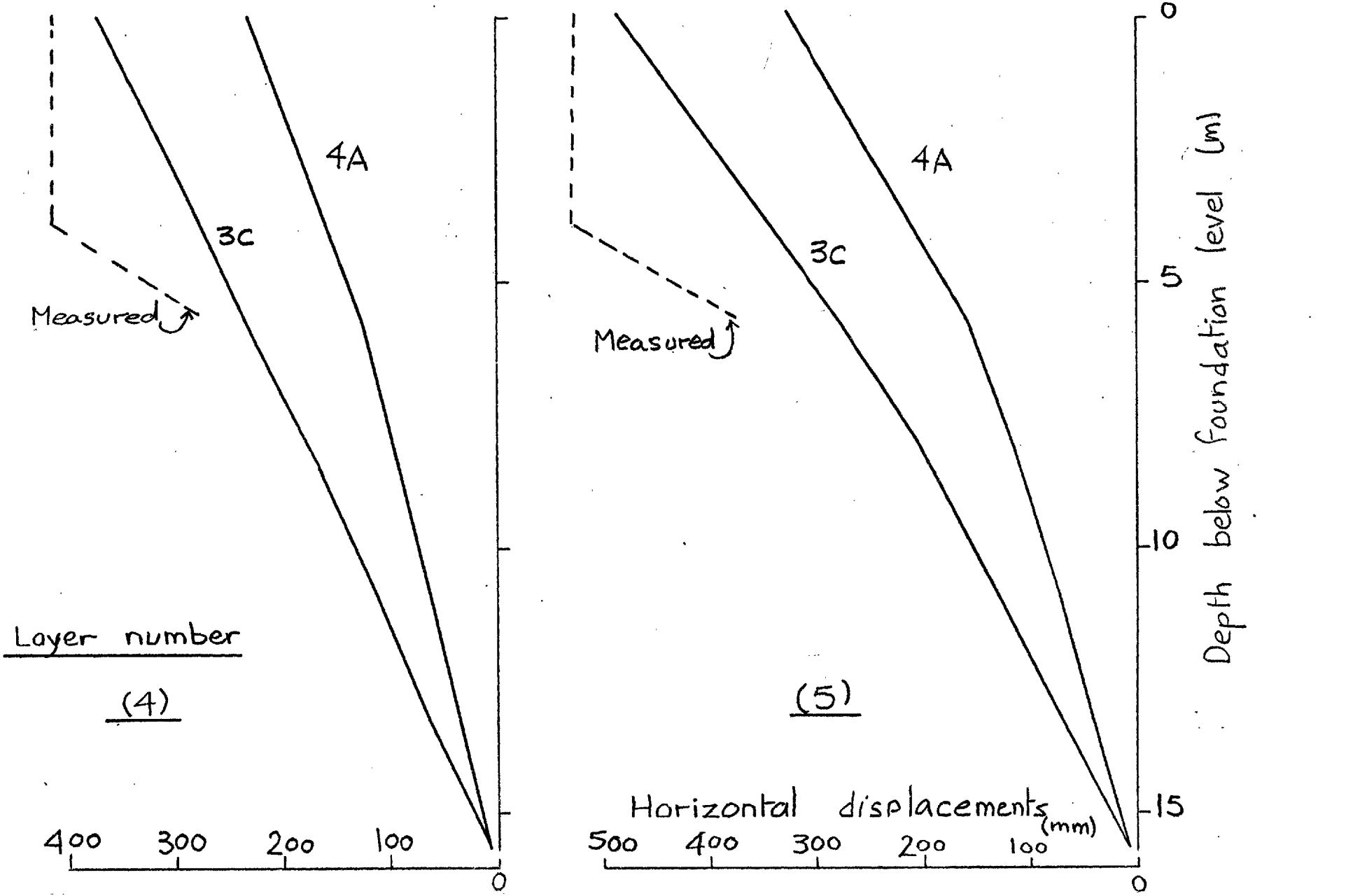


Fig. 6.77

MEASURED VS. F.E. PREDICTIONS _ CASES: 3C , 4A _ INCLINOMETER IB4

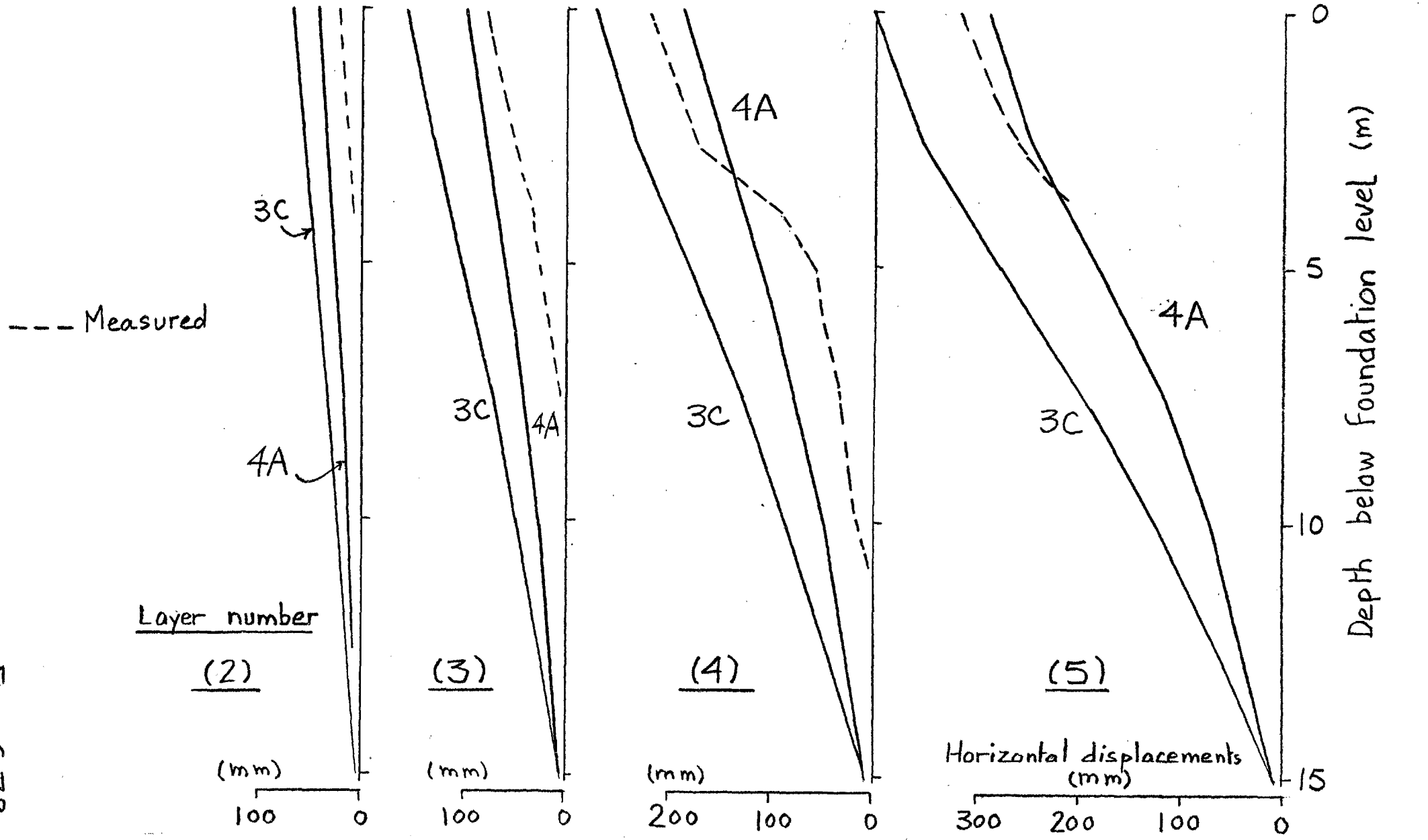
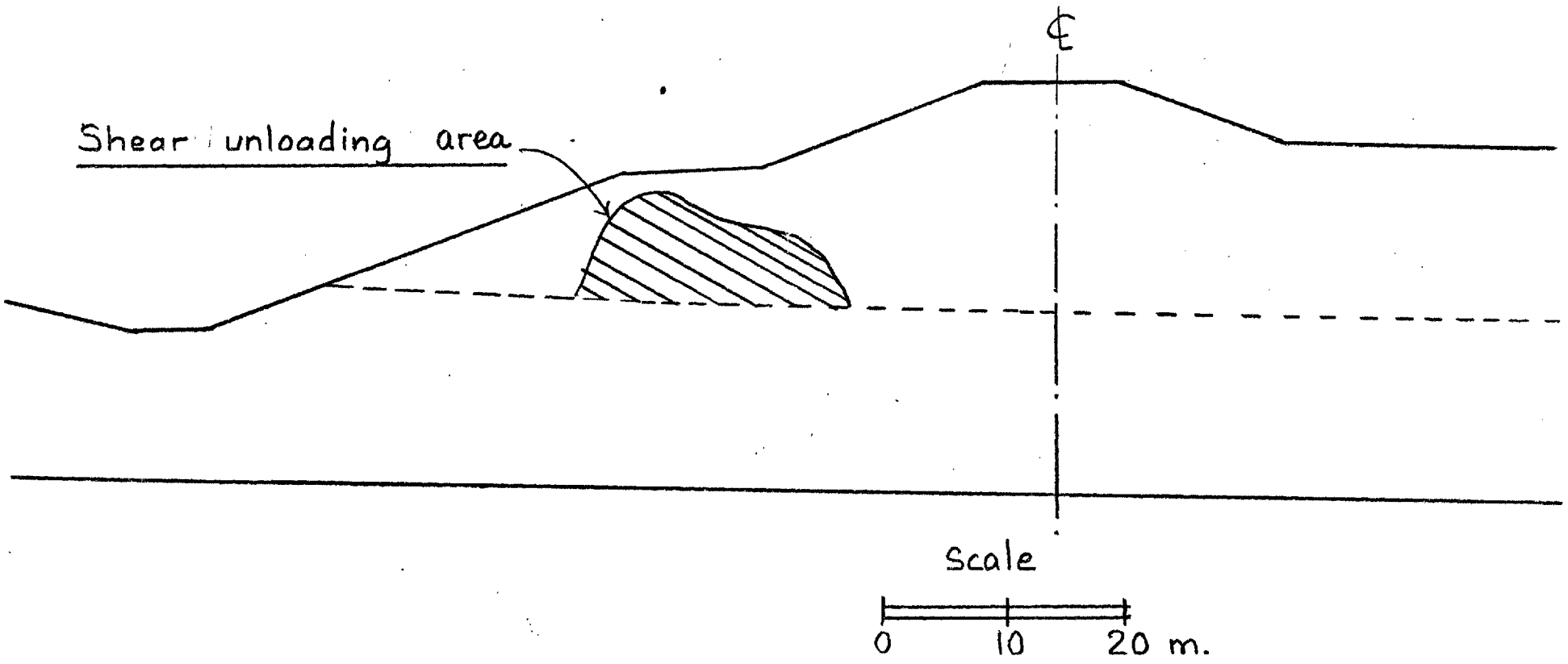


Fig. 6.78



AREA OF SHEAR UNLOADING_ CASE 4A

Fig. 6.79

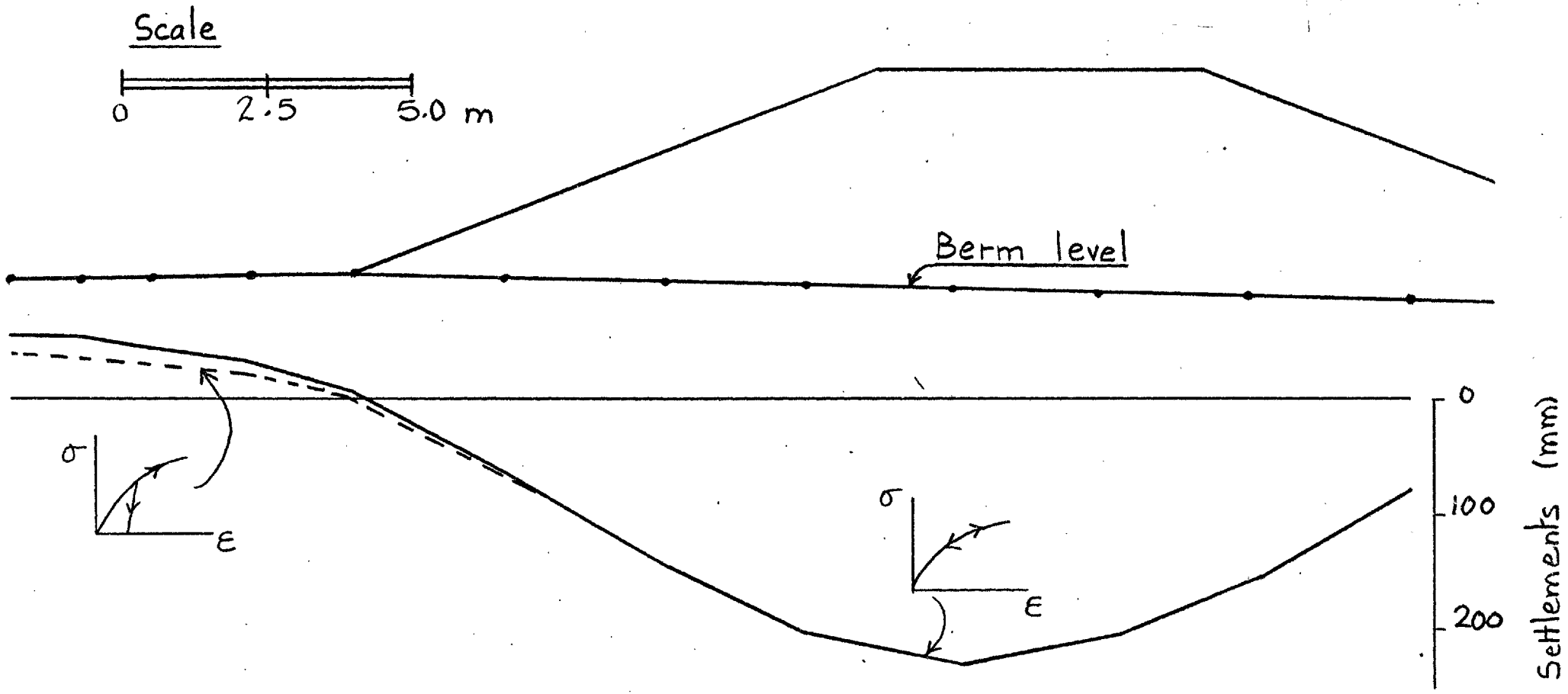


Fig. 6.80

SETTLEMENTS AT BERM LEVEL FOR CASE 4A (WITHOUT MODELLING OF SHEAR UNLOADING) AND CASE 4AU WHICH CONSIDERS SHEAR UNLOADING

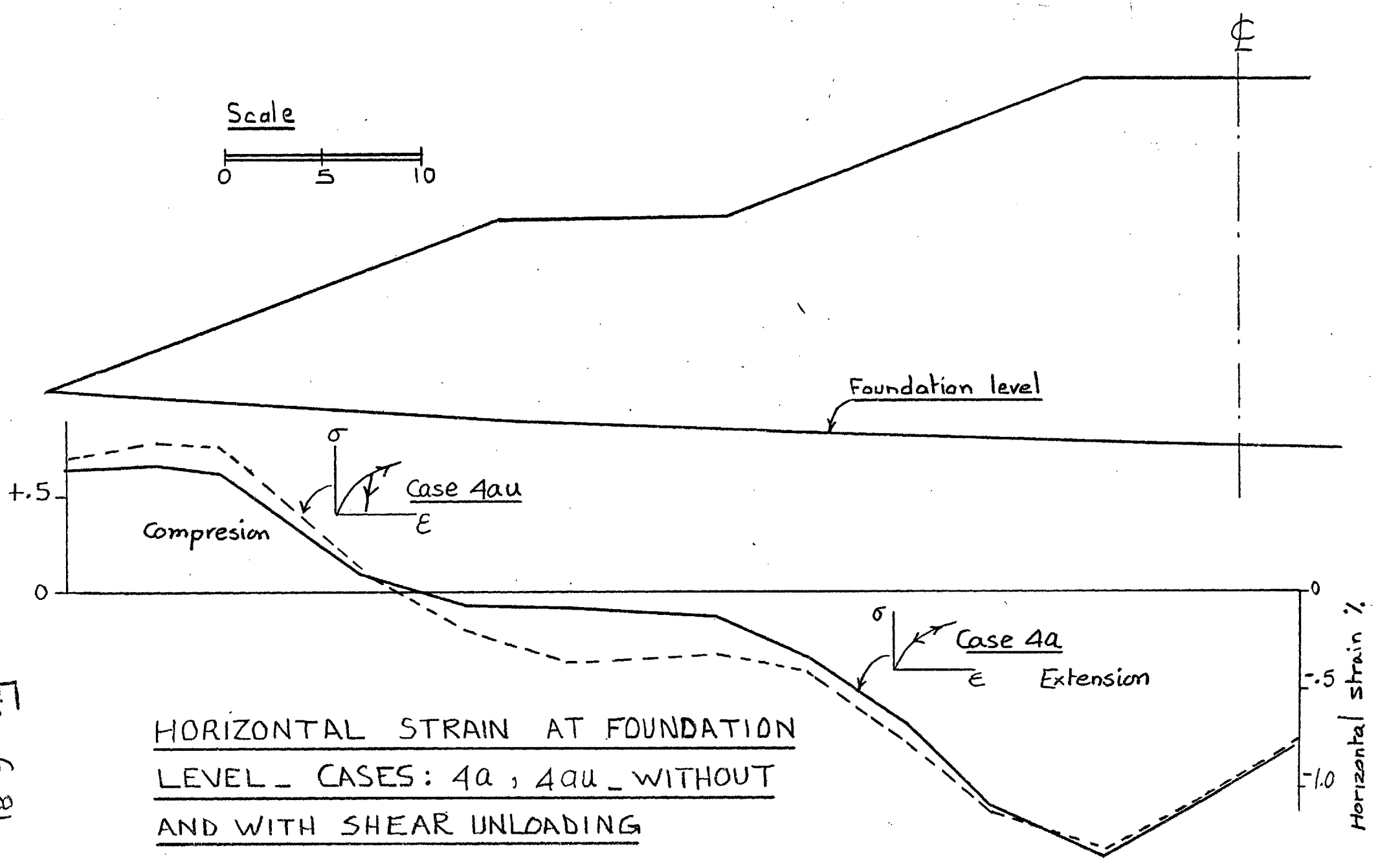


Fig. 6.81

HORIZONTAL STRAIN AT FOUNDATION LEVEL _ CASES: 4a , 4au _ WITHOUT AND WITH SHEAR UNLOADING

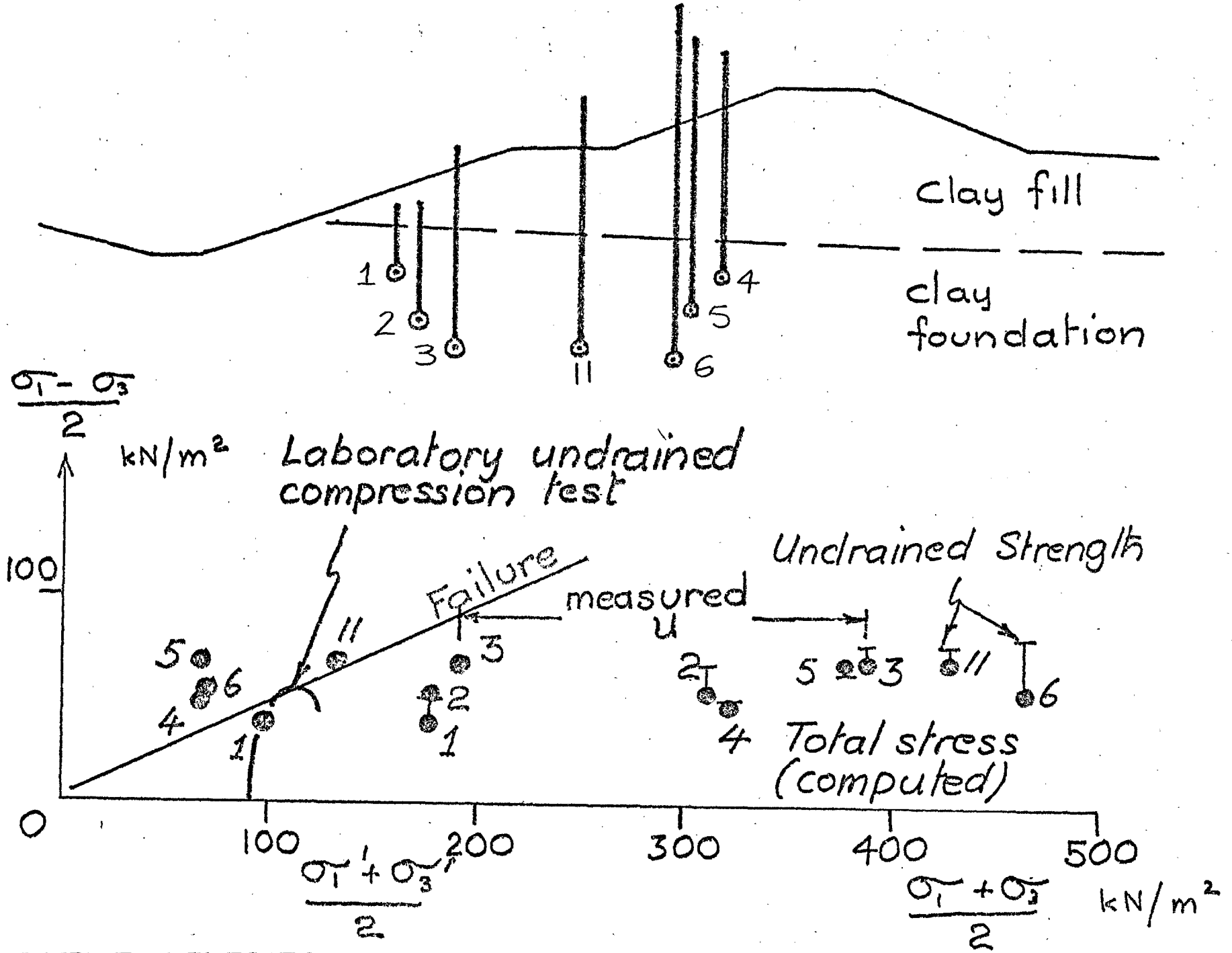
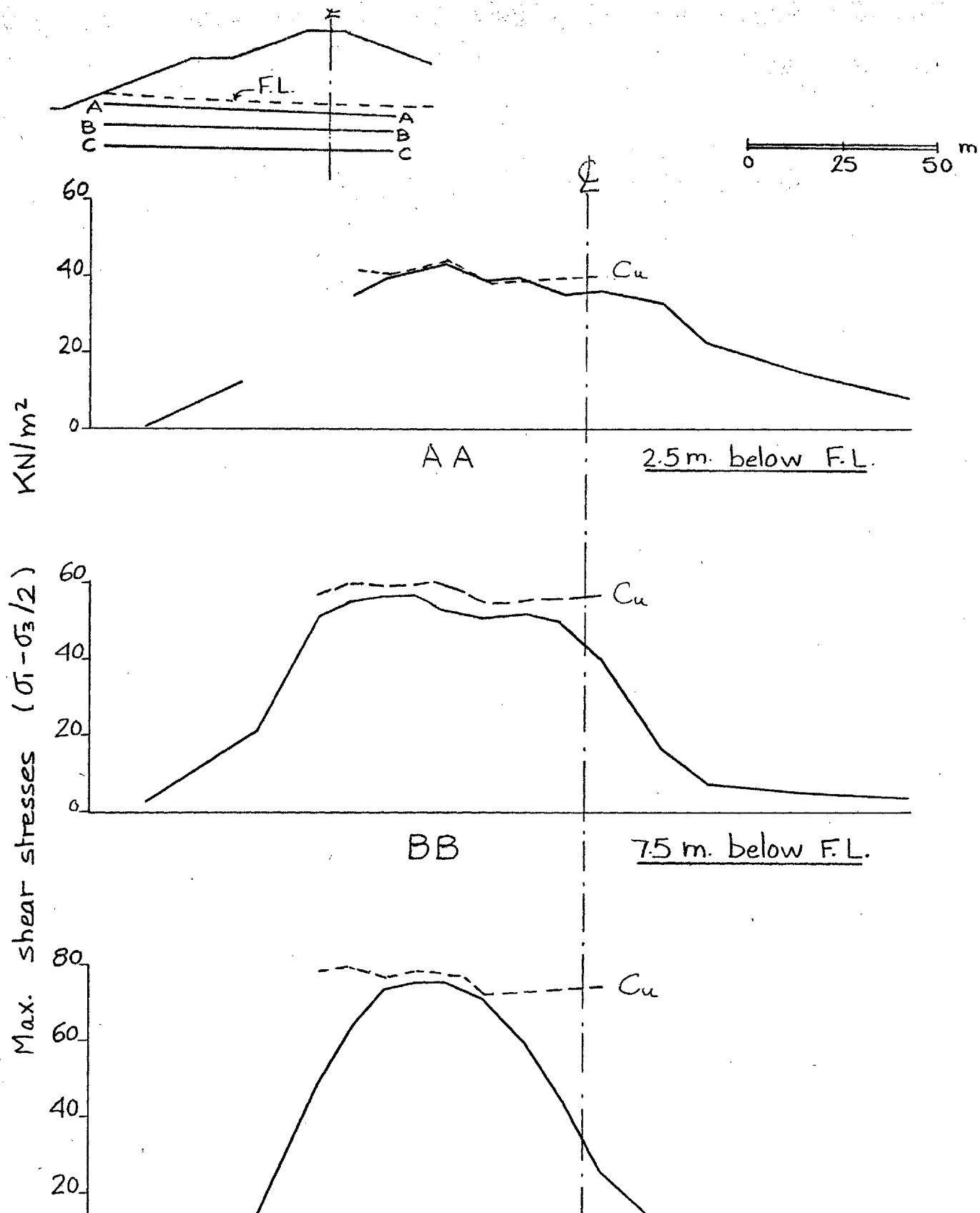


Fig. 6.82

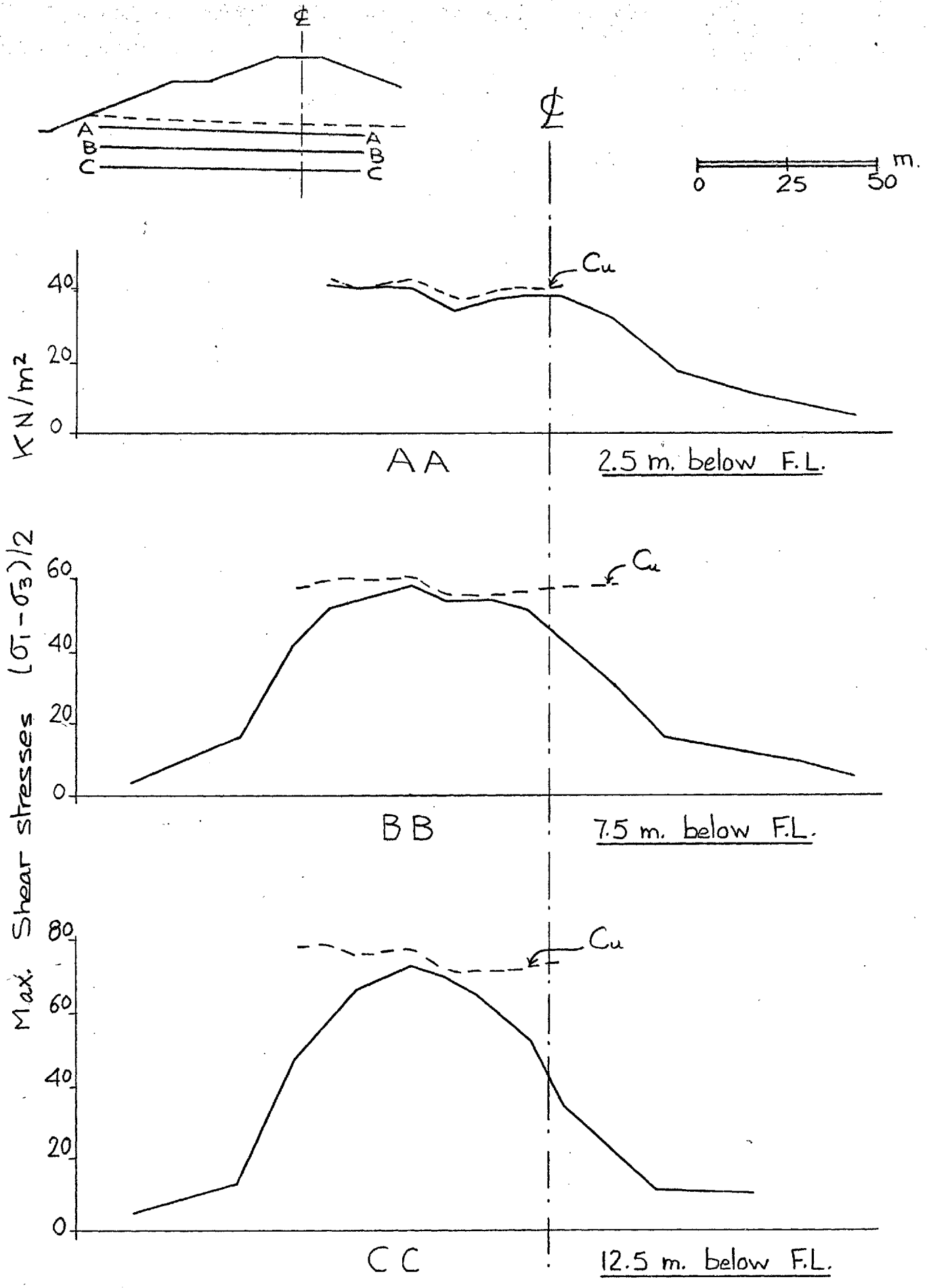
EFFECTIVE STRESSES FROM MEASURED PORE WATER PRESURE AND TOTAL STRESSES FROM FINITE ELEMENT ANALYSIS



MAX. SHEAR STRESSES AT END OF CONSTRUCTION

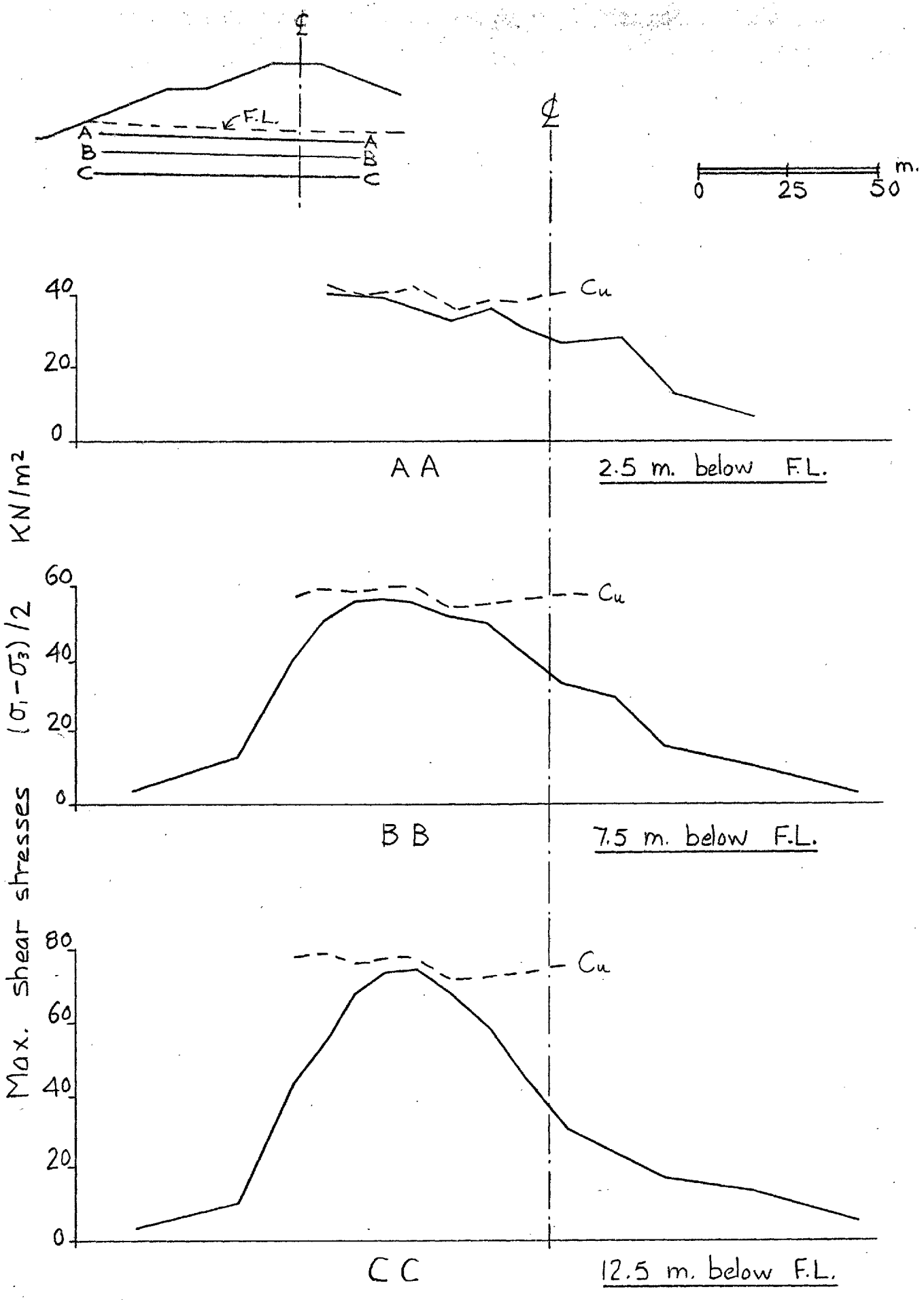
CASE 2a

Fig. 6.83



MAX. SHEAR STRESSES AT END OF CONSTRUCTION
CASE 2C

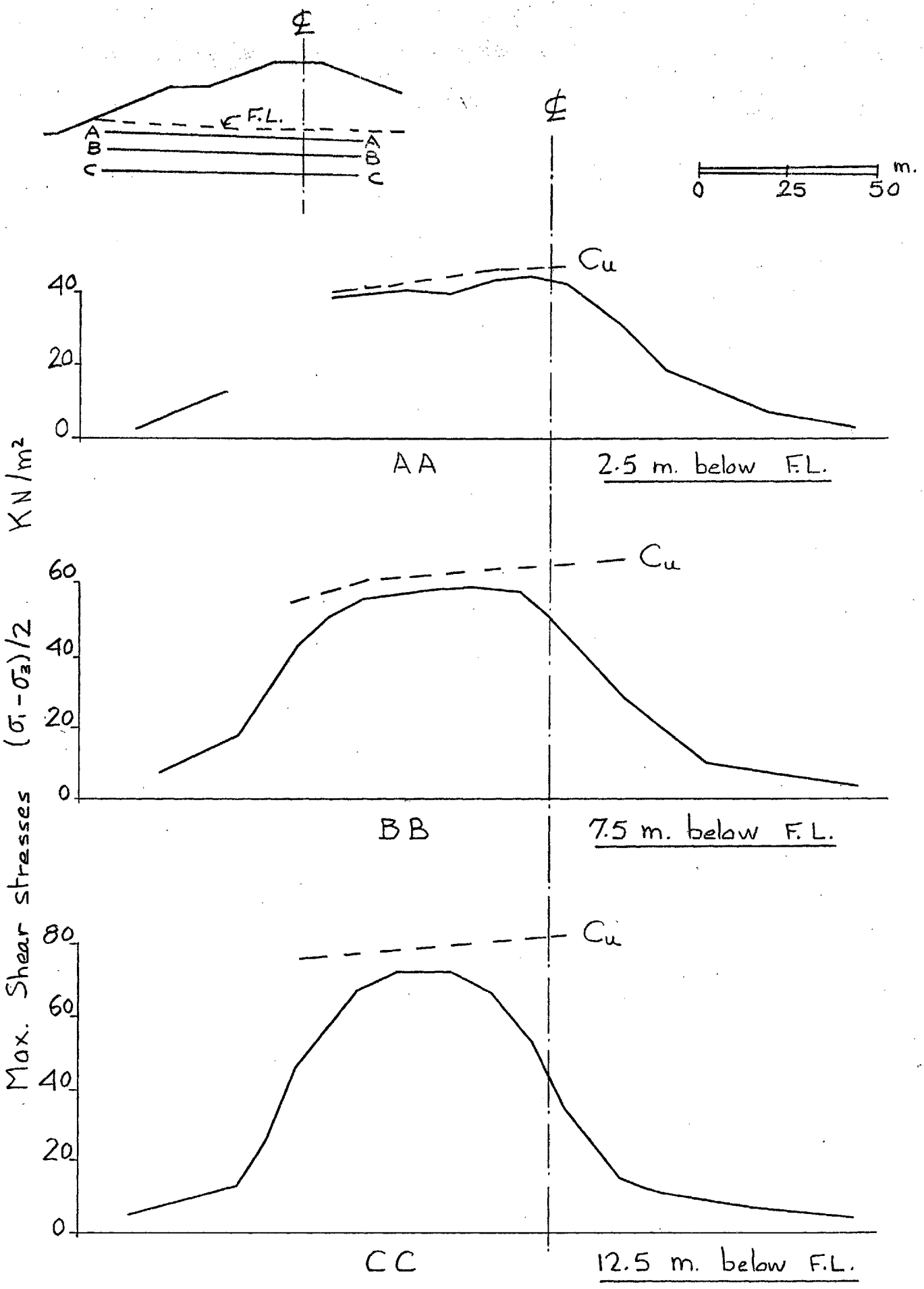
Fig. 6.84



MAX. SHEAR STRESSES AT END OF CONSTRUCTION

CASE 2d

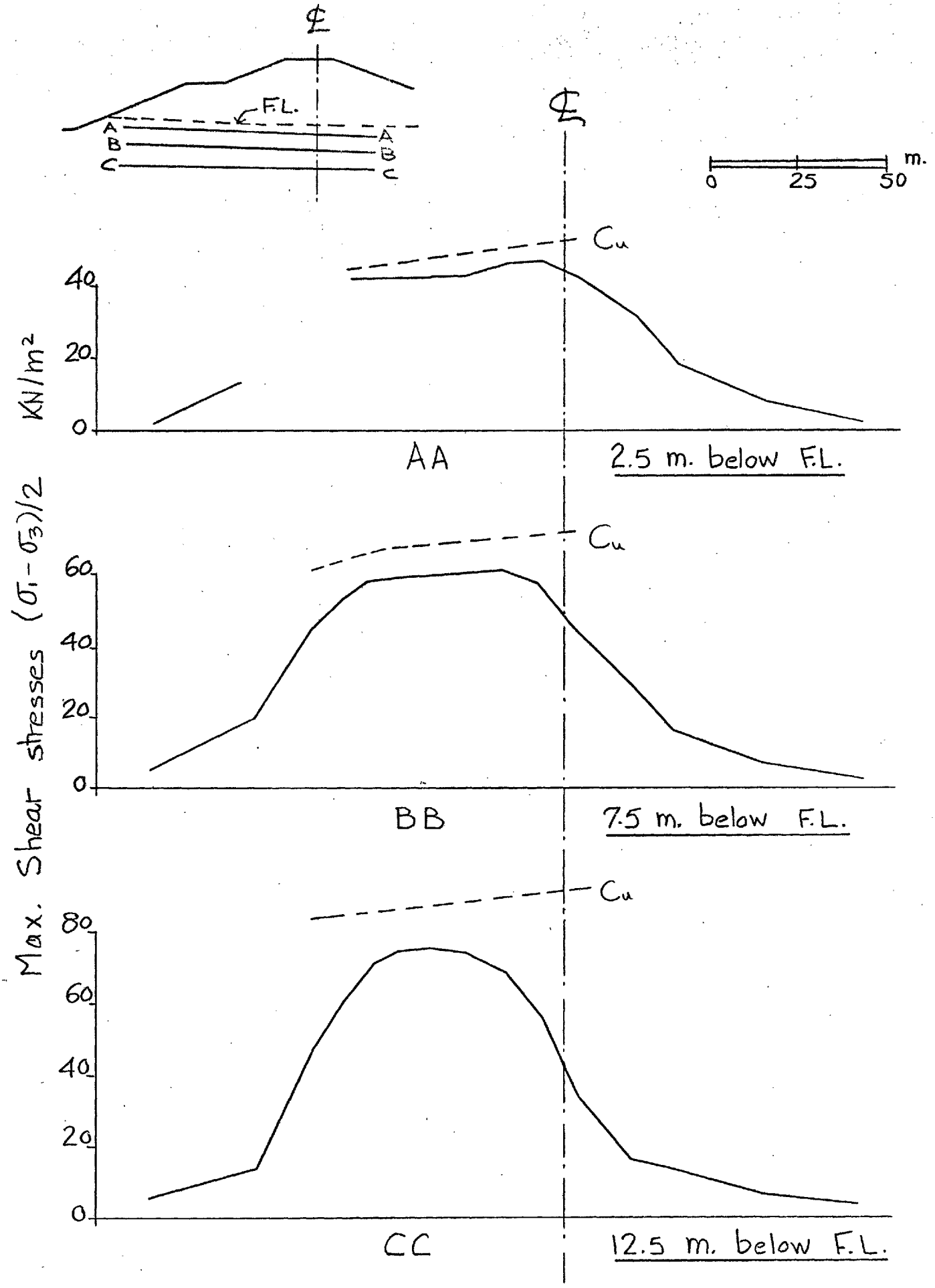
Fig. 6.85



MAX. SHEAR STRESSES AT END OF CONSTRUCTION

CASE 3a

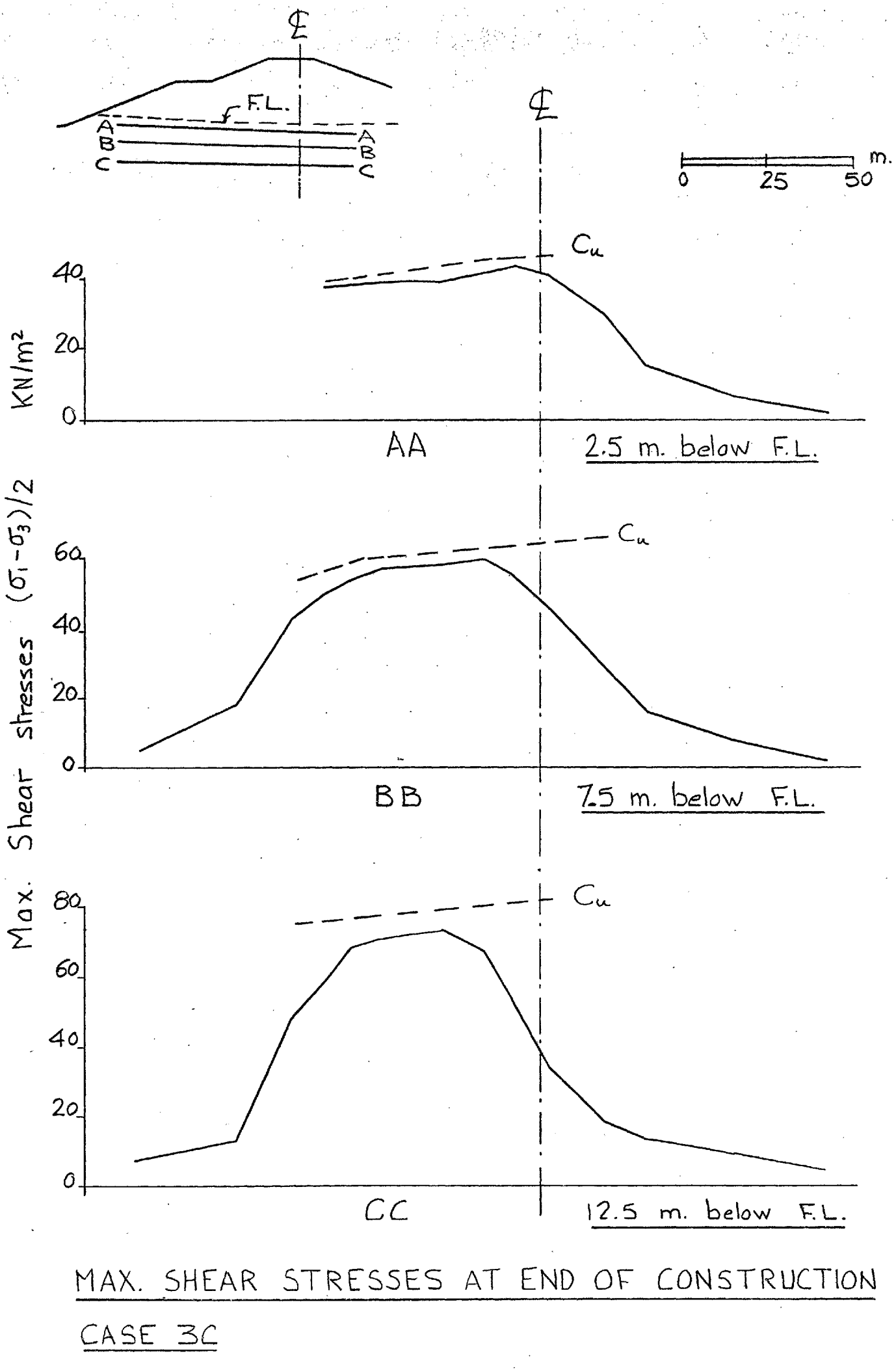
Fig. 6.86



MAX. SHEAR STRESSES AT END OF CONSTRUCTION

CASE 3b

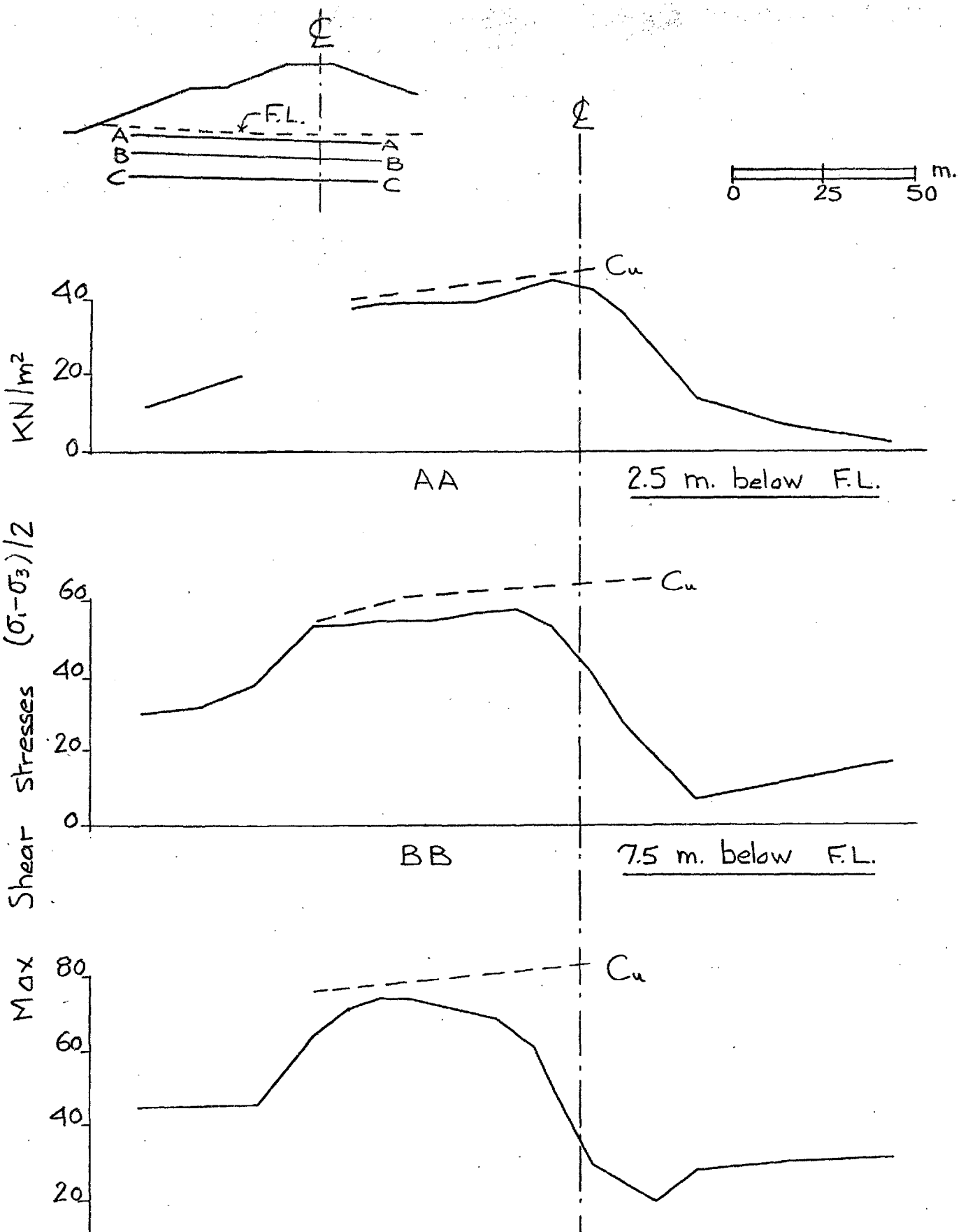
Fig. 6.87



MAX. SHEAR STRESSES AT END OF CONSTRUCTION

CASE 3C

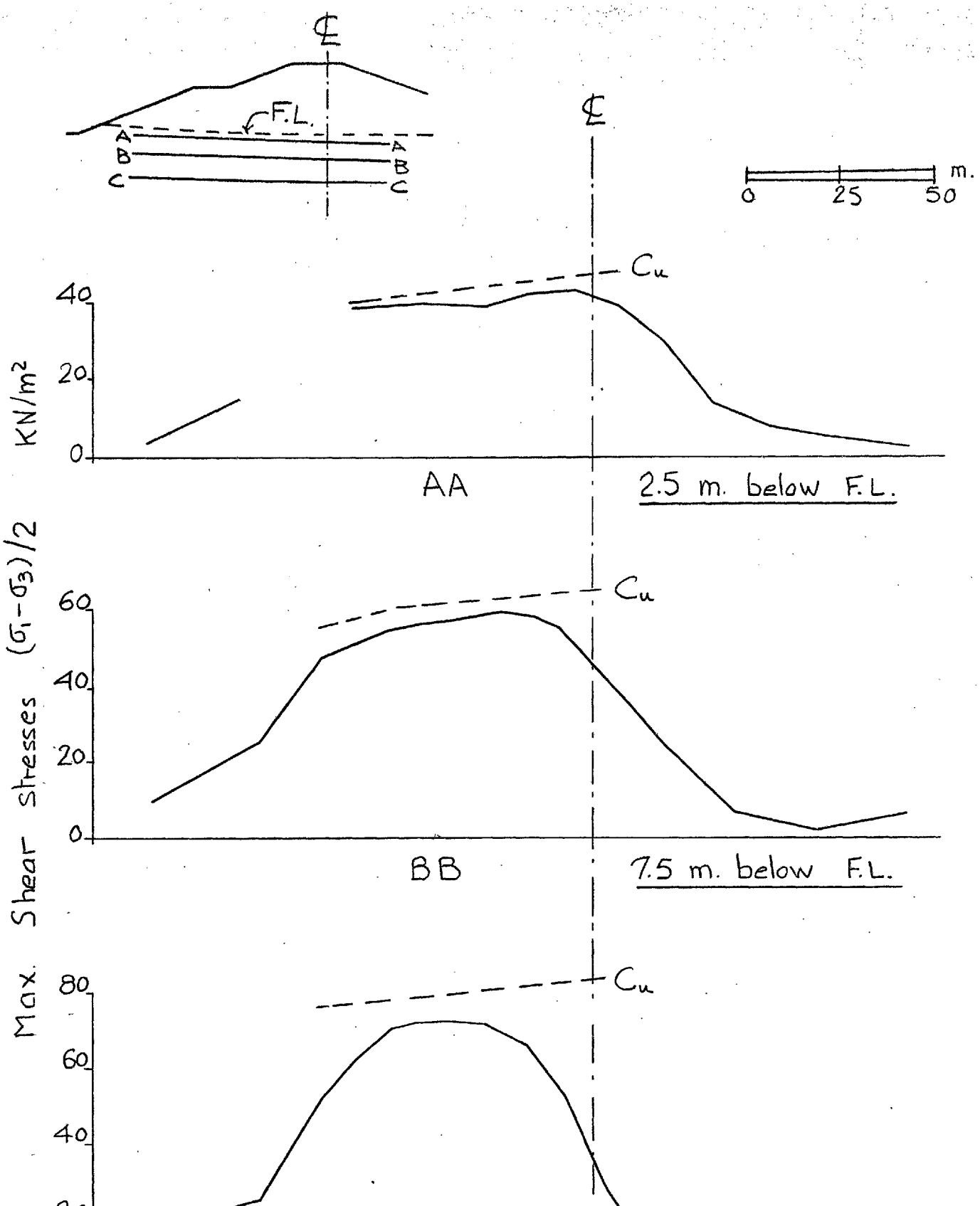
Fig. 6.88



MAX. SHEAR STRESSES AT END OF CONSTRUCTION

CASE 3d

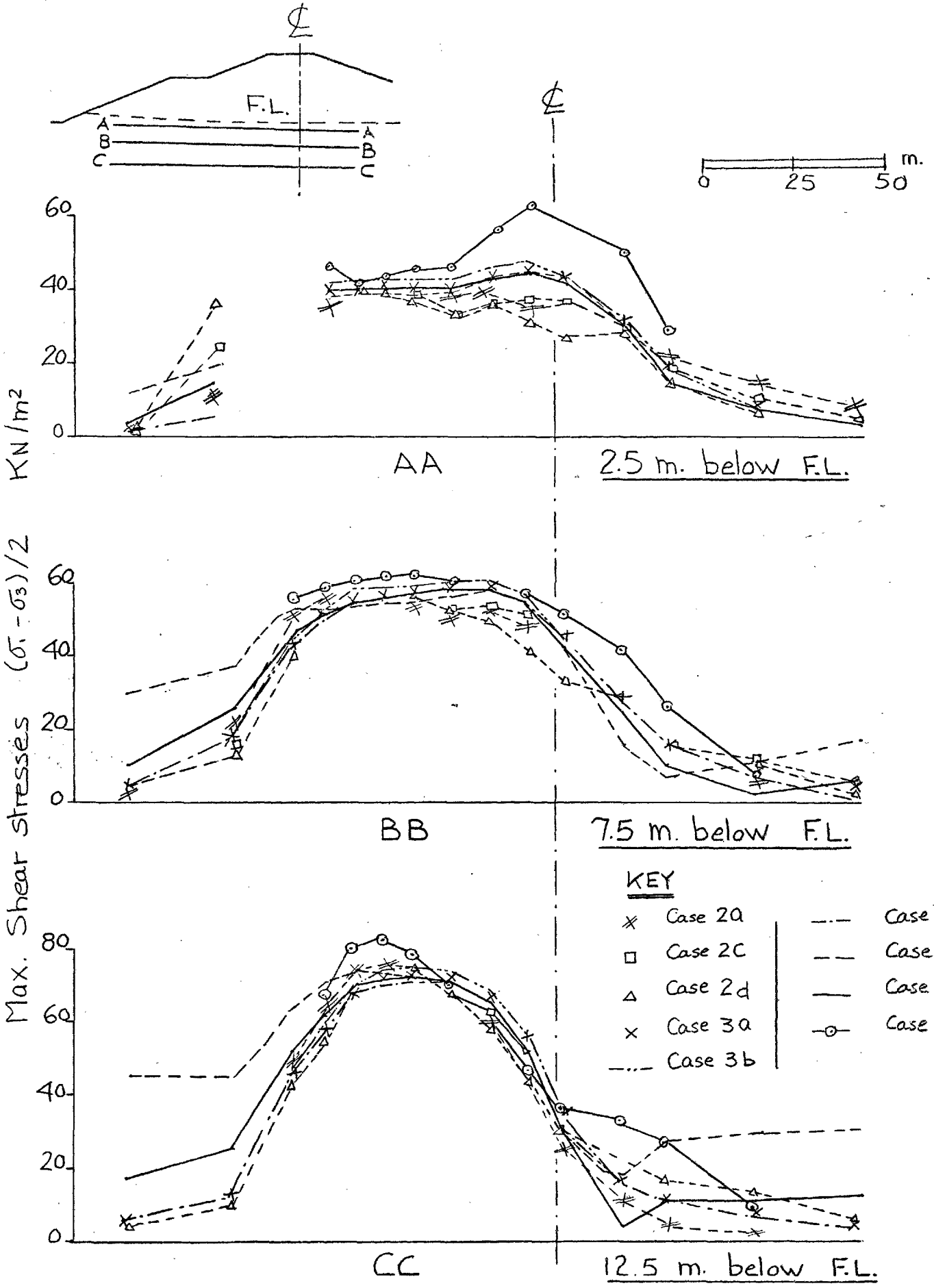
Fig. 6.89



MAX. SHEAR STRESSES AT END OF CONSTRUCTION

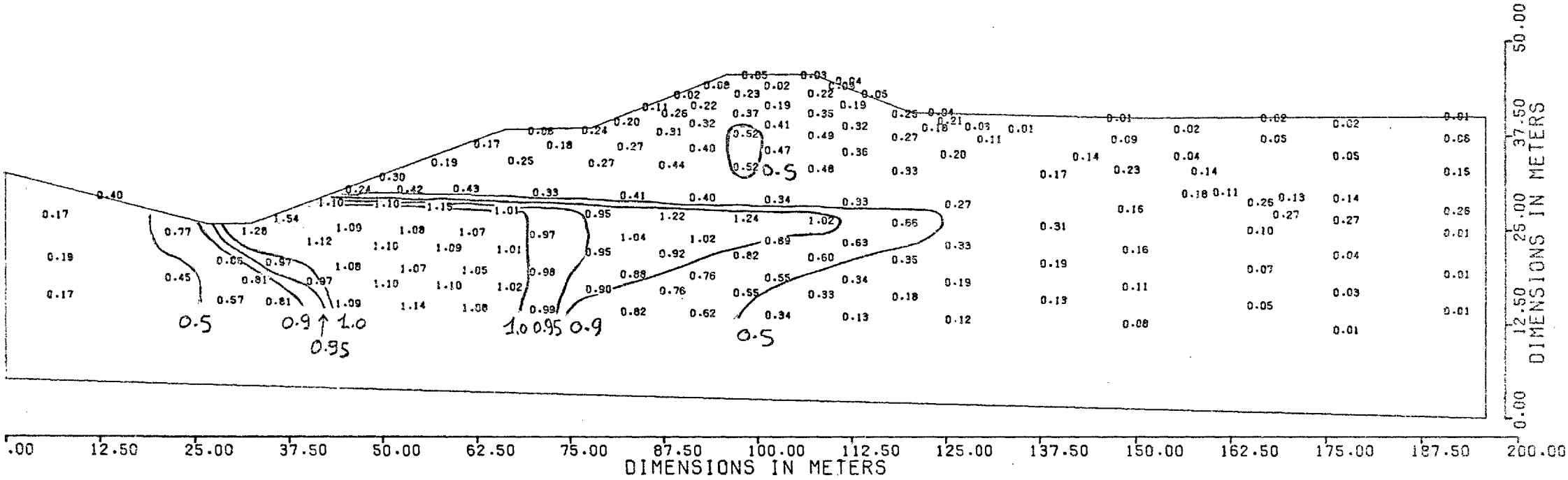
CASE 3e

Fig. 6.90



MAX SHEAR STRESSES AT END OF CONSTRUCTION FOR ALL NONLINEAR CASES AND CASE 1H (LINEAR)

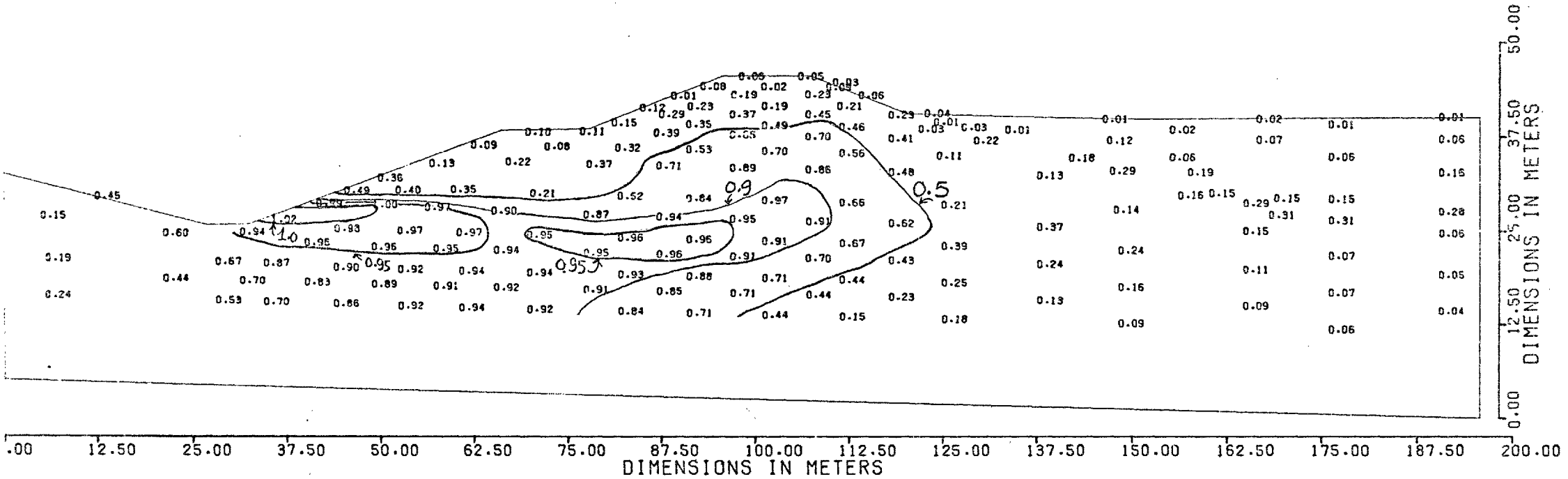
Fig. 6.91



MAX. SHEAR STRESS MOBILISED AFTER DOWNSTREAM FILLING . CASE 1H (Shear stress expressed as % of c_u)

Over stress zone

Fig. 6.92



MAX. SHEAR STRESS MOBILISED AFTER DOWNSTREAM FILLING . CASE 3A (Shear stress expressed as % of c_u)

Local Failure zone

Fig. 6.93

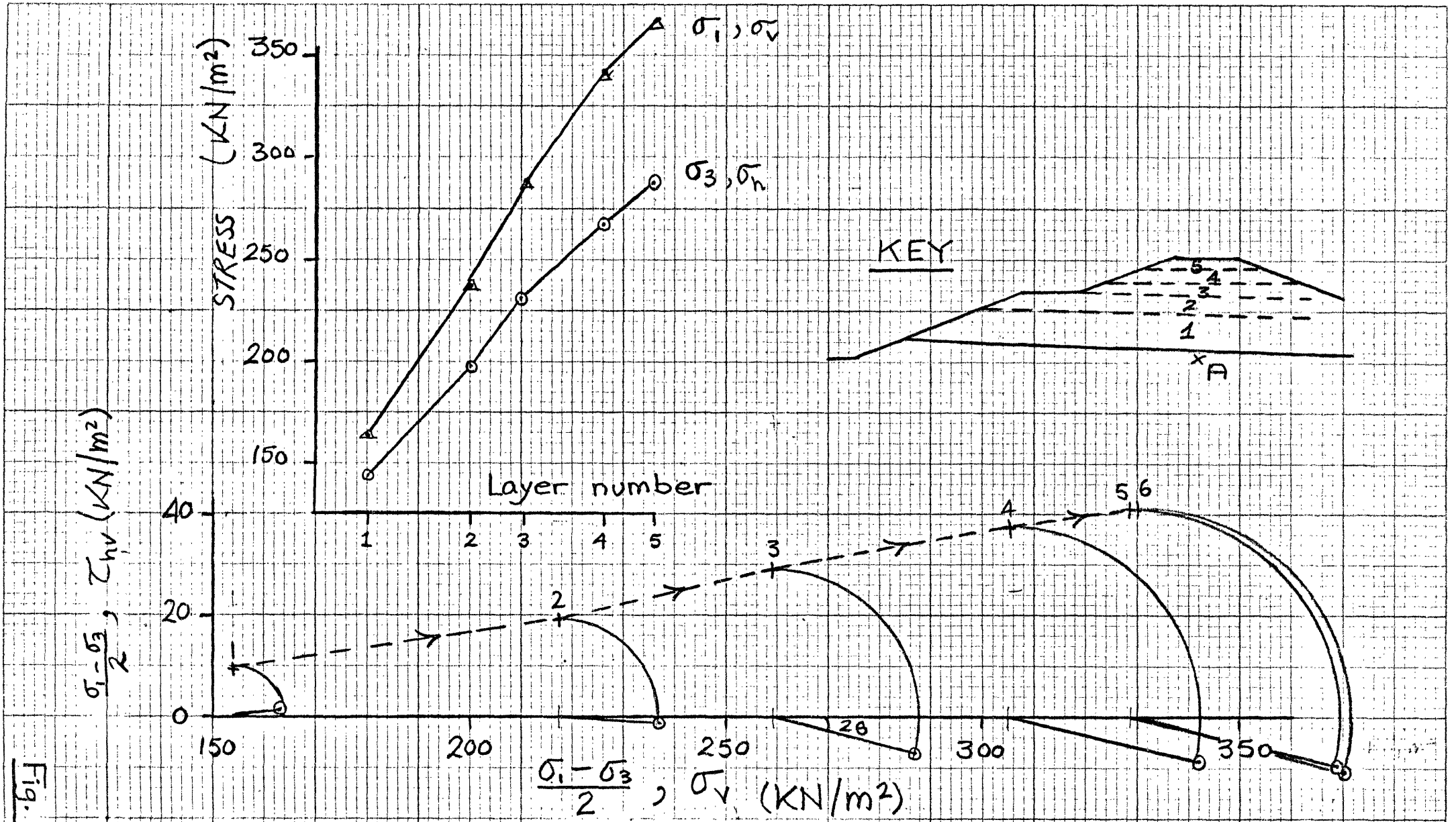


Fig. 6.94

STRESS PATH OF POINT (A) DURING CONSTRUCTION

CASE 3C

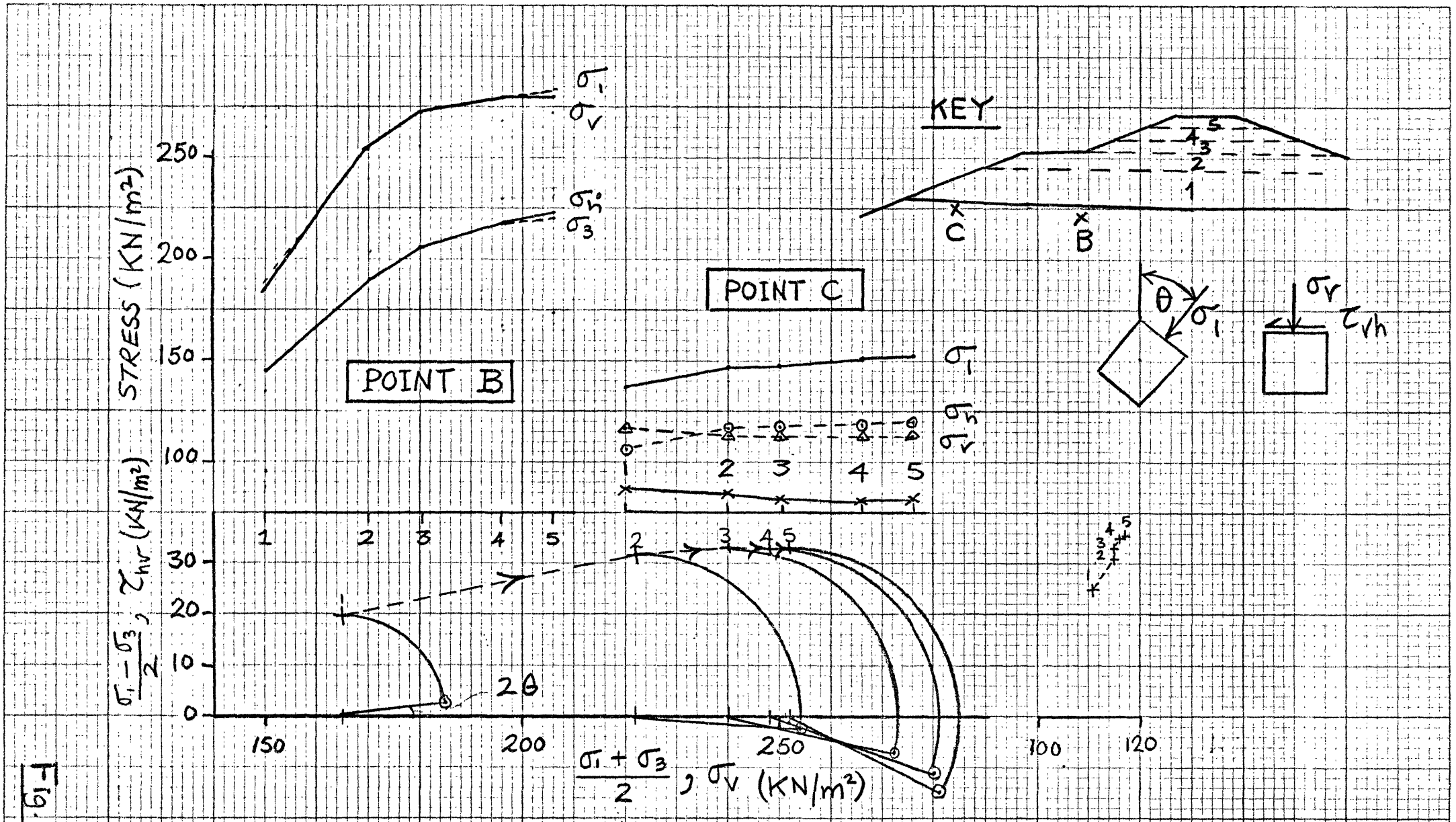


Fig. 6.95

STRESS PATH OF POINT (B) & (C) DURING CONSTRUCTION

CASE 3C

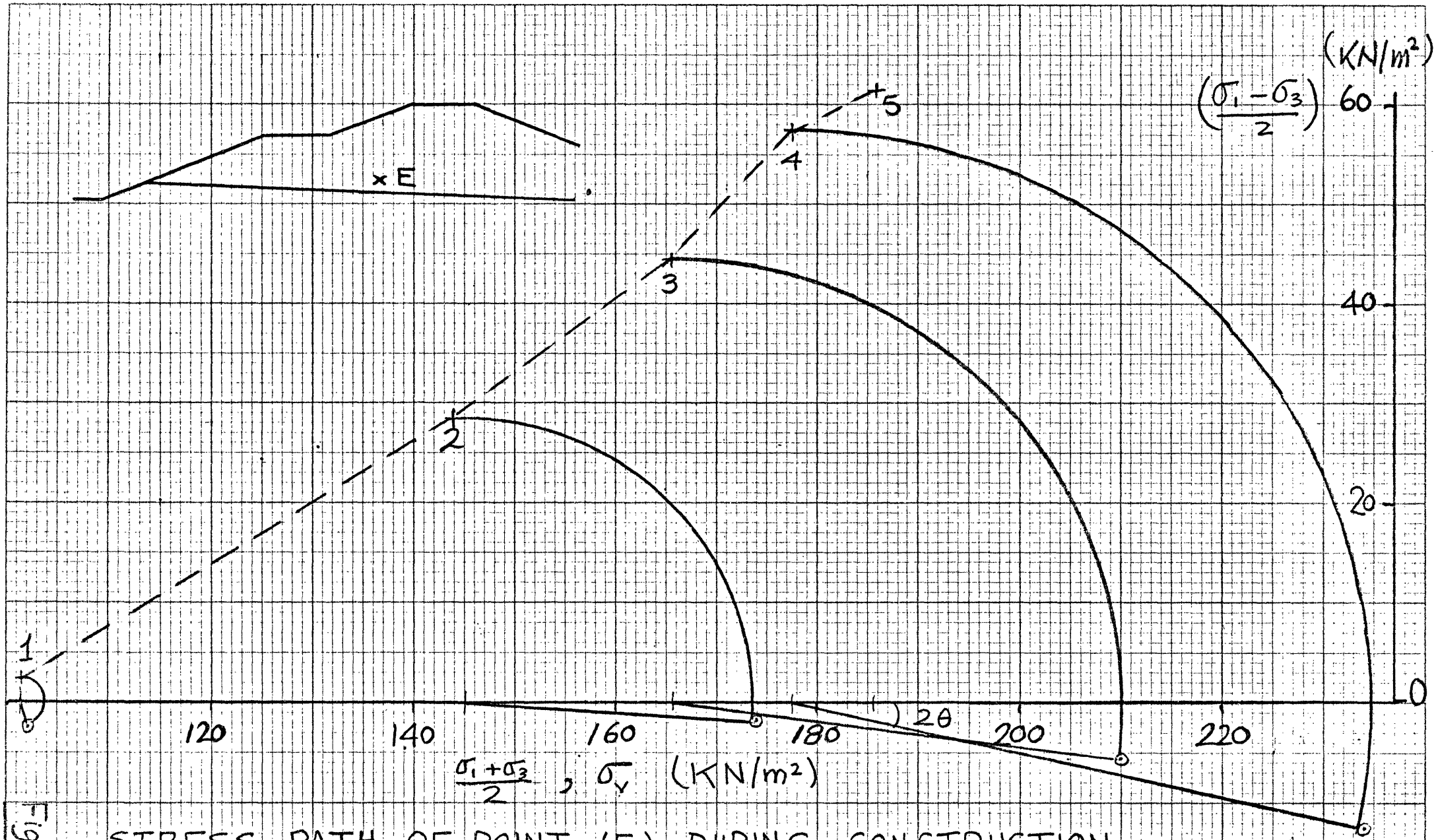
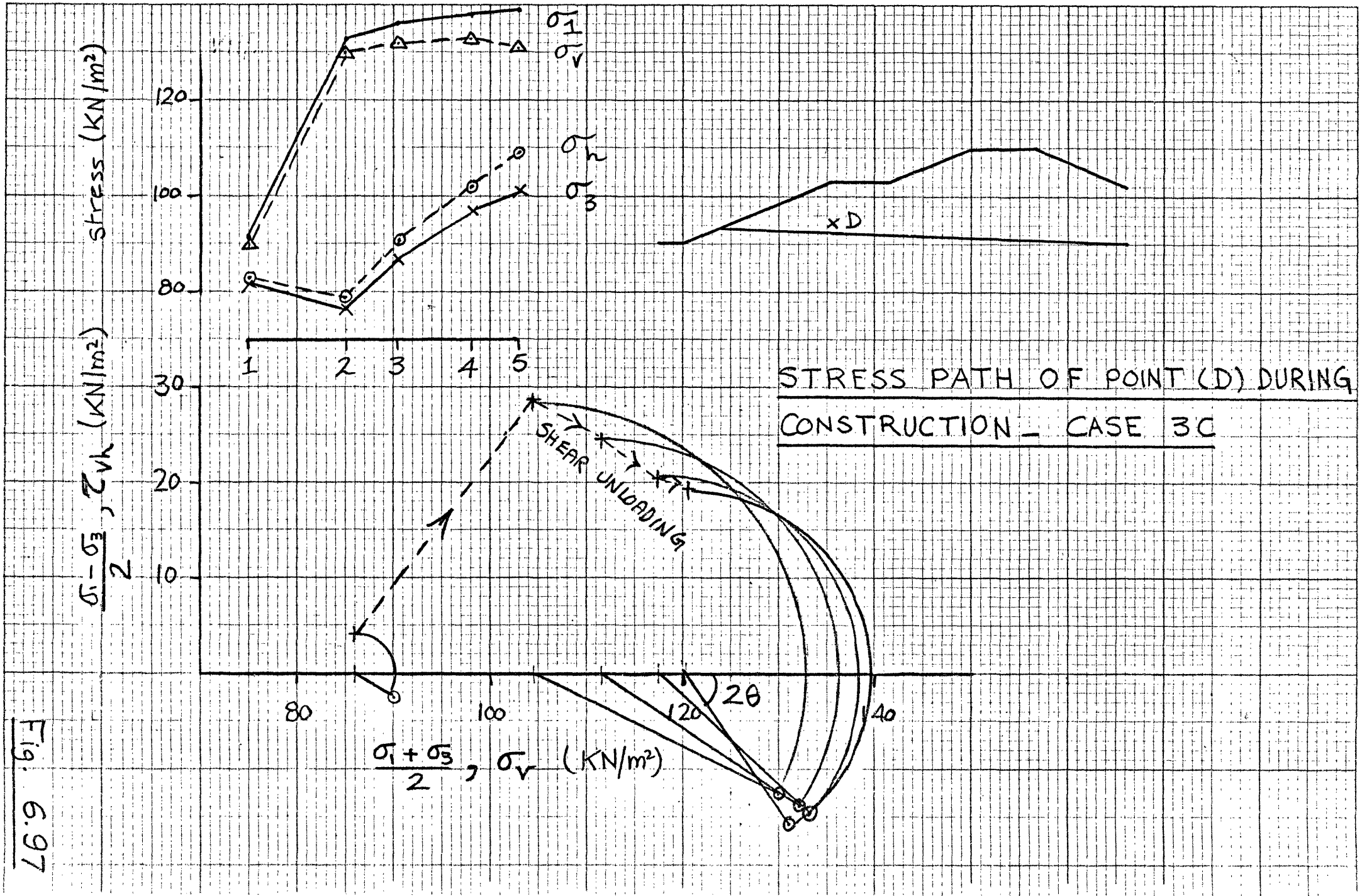


Fig. 6.96

STRESS PATH OF POINT (E) DURING CONSTRUCTION

CASE 3C



STRESS PATH OF POINT (D) DURING CONSTRUCTION – CASE 3C

Fig. 6.97

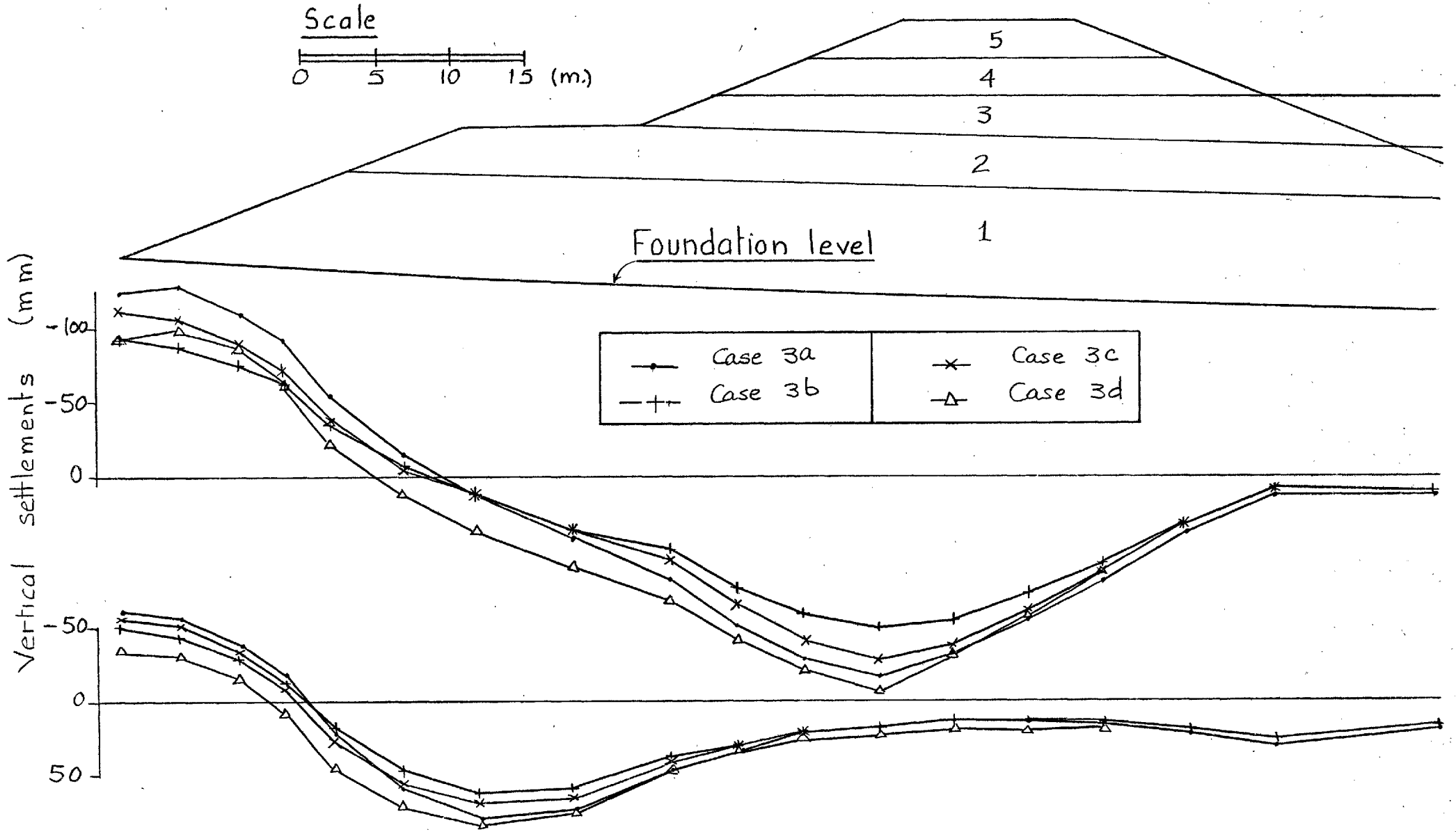
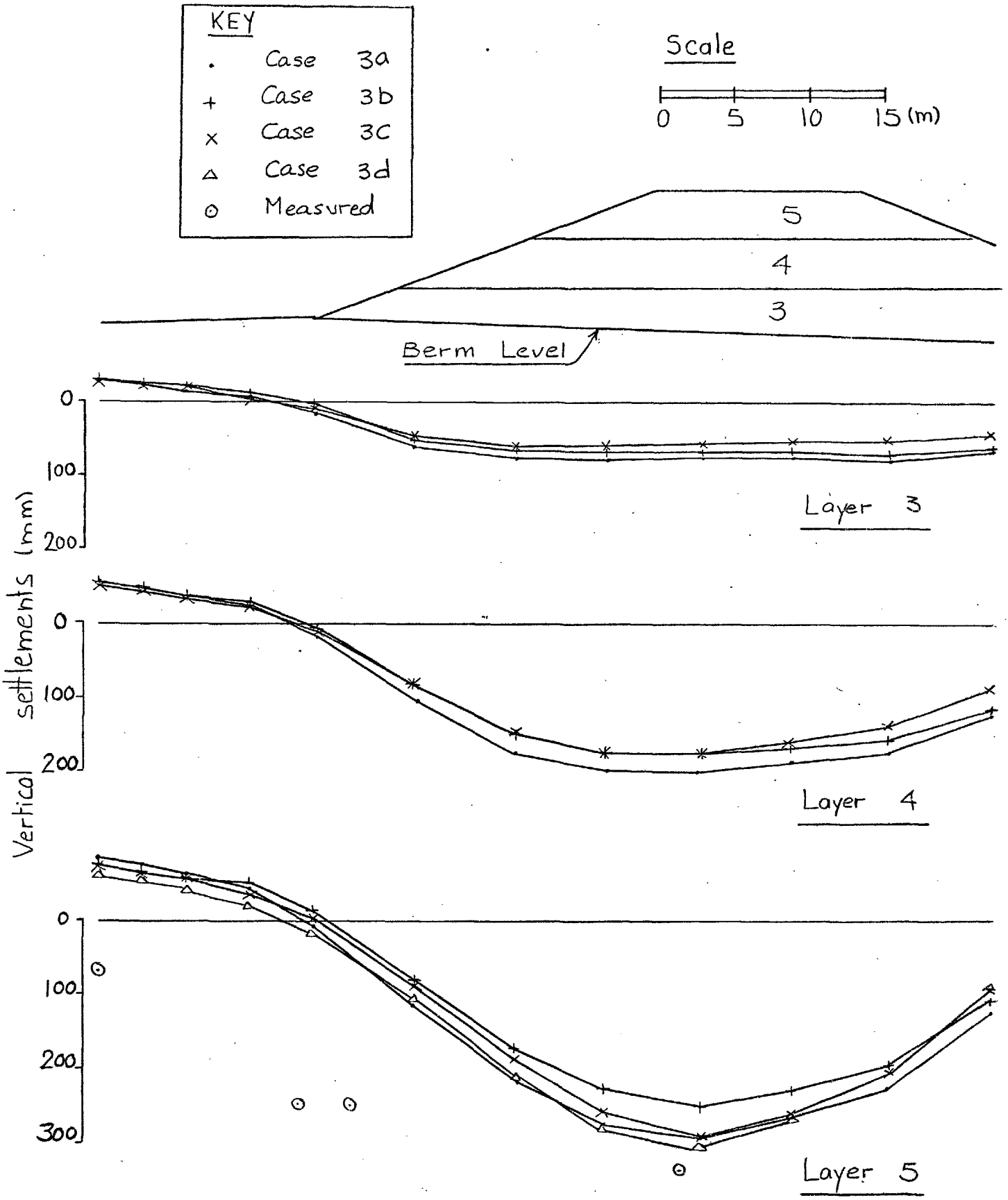


Fig. 6.98

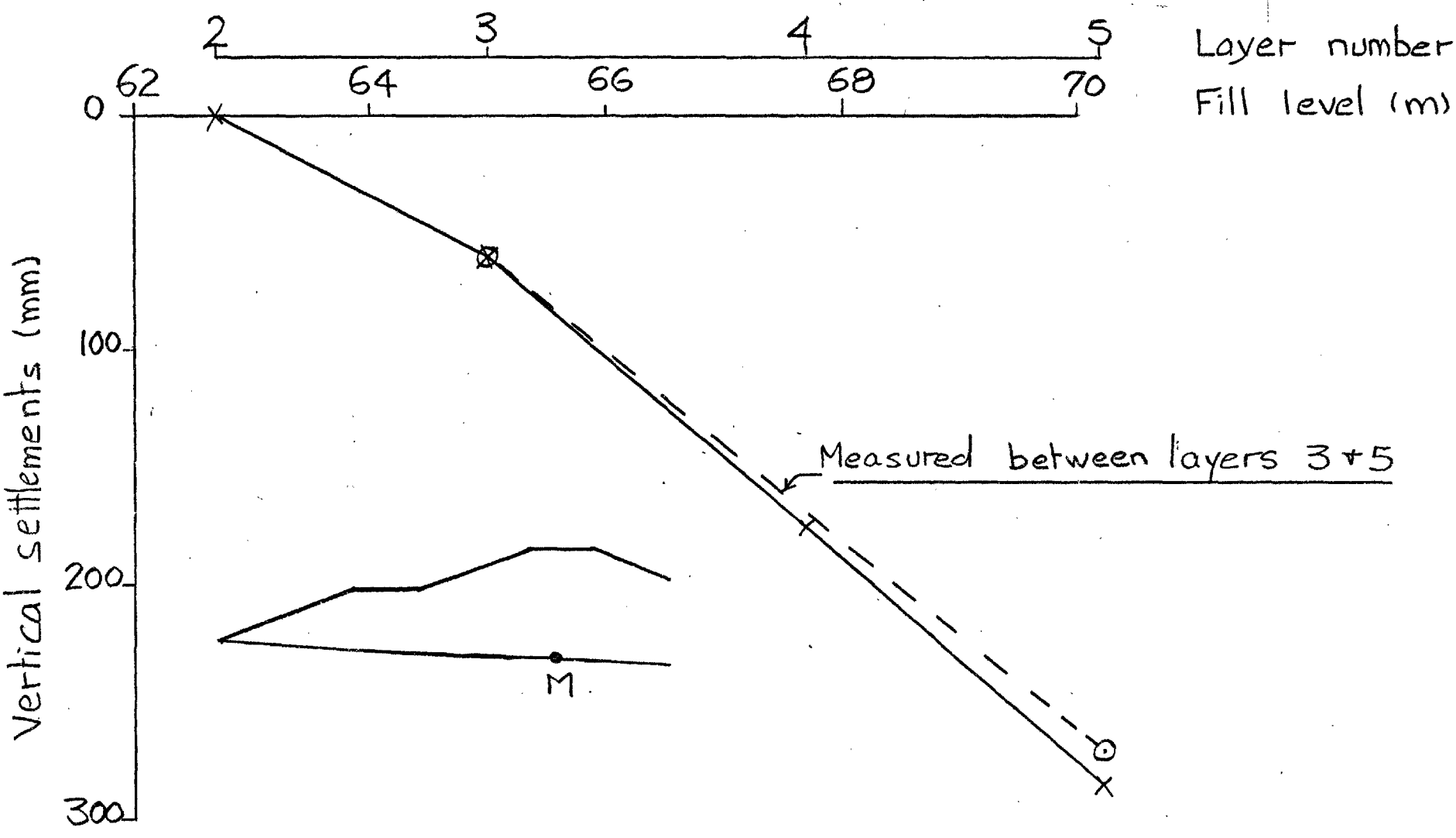
VERTICAL SETTLEMENTS AT FOUNDATION LEVEL AFTER LAYERS 2, 5

CASES: 3a, 3b, 3c, 3d



VERTICAL SETTLEMENTS AT BERM LEVEL AFTER LAYERS 3, 4, 5 _ CASES: 3a, 3b, 3c, 3d

Fig. 6.99



PREDICTED AND MEASURED VERTICAL SETTLMENTS AT POINT (M) BTWEEN LAYERS 3 AND 5. CASE 3C

Fig. 6.100

CHAPTER 7

ANALYSIS AND PREDICTION OF EMPINGHAM MAIN DAM BEHAVIOUR

7.1 Introduction

The main Empingham dam section was analysed immediately after the analyses of the trial bank reached the stage represented by Case 3c (Chapter 6). At this stage it was considered that the existence of an undrained strength equal to or in excess of the design strength profile had been proved to exist beneath the trial bank, and there was insufficient time to refine the analyses further. The purpose of the analyses was to examine likely stresses and deformations which might arise during completion of the main dam, to aid the interpretation of the field observations, and the analyses were completed about 3 months before completion of construction. Thus they represent a Class A prediction, Lambe (1973), and they are presented in Section 7.2 as the original report in which they were presented, from which only sections describing the technique of analysis have been deleted. The analyses cover a typical section 34m high with sand drains in the foundation, which was analysed undrained and with partial drainage simulated in the sand drain zone. They also cover the North Section which represents the highest and most critical section with a completely undrained foundation. Since the sand drains produced a degree of consolidation in excess of the design assumption, it was expected that the North Section would

represent the most critical stability case. Although they had not apparently played a significant part in the performance of the foundation of the trial bank, the presence of major shear zones within the foundation was still feared, and the North Section was analysed with two such shear zones simulated within the foundation.

The predictions made before the completion of construction are compared with the observed field behaviour in Section (7.3), and it is found that the observed deformations were considerably smaller then those predicted. Further post construction analyses of the main embankment sections, matching the further analyses of the trial bank reported in Section 6.4. of Chapter 6, have been performed to see to what extent a better match with the field observations can be obtained. The main modifications consist of using the stiffer stress strain curve resulting from the systematic back analysis of the trial bank , inreproducing shear unloading in the embankment fill and foundation, and of using a strength profile representing the average 'best fit' strength deduced beneath the trial bank, rather than the design profile strength, which was a proven lower bound. The additional analyses and the extent to which the fit between predicted and observed deformations was improved are presented in Section 7.4.3.

7.2 Analyses before completion of construction, taken from the original report.

7.2.1. Soil and structural model

The soils are assumed to have isotropic properties, and the non-linear stress strain properties are assumed to be elastic, i.e. the soil is assumed to follow the same curve during unloading and reloading. This assumption is generally untrue for real soils, which are much stiffer during unloading and reloading than in first loading. The assumption will lead to error in as far as unloading and reloading occurs in the solutions. Unloading may be defined as a reduction in principal stress difference. Two areas in the solutions can be identified where this may occur. Firstly, shear unloading will occur in parts of the foundation if $K_o \neq 1$. Fortunately, at Empingham, the available evidence sugests that $K_o = 1$. Shear unloading and reloading of the foundation will also occur at an early stage of construction beneath the reverse slopes formed at the inside of the berms when these were higher than the central fill. These reverse slopes have not been modelled in the solutions as the number of elements required would have exceeded the capacity of the programme (the total height of the dam is modelled in 7 layers). It is not thought that this omission will significantly influence the predictions for the later stages of construction, which are of main interest as they can be compared with the field observations. Shear unloading may also occur in the fill near the inside of

the berms. As the bank reaches berm height, horizontal stresses will be less than vertical stresses. As the central part of the dam is raised the thrust generated will increase the horizontal stresses in the berm fill, while the vertical stresses remain substantially constant. Thus there is a probability of shear unloading. Since in the solutions of this stage shear unloading is not reproduced, the stiffness of the berm fill during construction of the dam centre is likely to have been underestimated. This would lead to an overestimate of deformation, as discussed in more detail subsequently.

7.2.2. Soil properties used in the solutions.

7.2.2.1. Undrained saturated clays in the foundation.

The stress-strain behaviour depends only on the principal stress difference. In the solution, $\Delta\sigma_1$ on the nominated stress-strain curve is taken to be equal to $\sigma_1 - \sigma_3$ figure (3.2). The value of $\Delta\sigma_{1f}$ is taken to be equal to $2.C_u$ and C_u is assumed to vary with depth according to the design profile. The values of the curvature parameters a and b defining the shape of the stress strain curve are those which gave a reasonable fit to the behaviour of the trial bank. Typical stress-strain curves used are shown on figure (7.1). At 15m depth a transition to much stiffer shaley clay was assumed. This assumption is consistent with the performance of the foundation of the trial bank.

For incompressible, undrained, saturated clay Poisson's ratio $\nu = \frac{1}{2}$. This value cannot be used in finite element solutions, and a value of 0.49 has generally been used. 0.48 was used for one run to check the importance of this parameter.

In the weak layers assumed in the one solution of the north actual section the undrained strength was assumed to be reduced by a factor of 0.6. The stress-strain curves assumed are shown on figure (7.2).

7.2.2.2. Undrained, unsaturated clays as fill.

All fill materials have been assumed to be partly saturated but undrained during construction. For such materials the strength and stress strain properties are a function of the minor principal stress operating on them. This process is modelled by assuming a family of stress-strain compression curves dependent on σ_3. The ultimate strength for these curves is assumed to vary as determined in the previous design tests. Their shape is based on compression tests performed on these materials. Typical assumptions are shown in figures (7.3, 7.4 and 7.5).

The method of using these curves is a modification of that illustrated on figure (2.2). At any stage in the solution, values of the minor principal stress and the principal stress difference are known for all points in the fill. When the next load increment is applied, a first solution is made using a curve selected according to the

initial value of σ_3, and a tangent modulus E_t from this curve equivalent to the initial value of $\sigma_1 - \sigma_3$. As before, an average value of $\sigma_1 - \sigma_3$ is determined, and also an average value of σ_3 for the increment. A new curve appropriate to this value of σ_3 is selected, and a new value of E_t is found equivalent to the average value of $\sigma_1 - \sigma_3$. A second solution is obtained using this value. The families of curves are defined by (1) a constant failure strain, (2) a linear variation of strength with σ_3, and (3) a linear variation of E_i with σ_3.

Partly saturated fill is compressible and thus a value of Poisson's ratio less than a half and consistent with the compressibility of the fill must be used. A value of 0.45 has been adopted, based on the results of laboratory tests performed during the previous design work.

The stress-strain properties assumed are consistent with the results obtained from the control tests performed on the samples of compacted fill as construction has proceeded. The Al fill is very heterogeneous and an adjustment has been made to allow for the fact that the control tests will have been weighted towards the more clayey and softer parts of the fill.

7.2.2.3. Partly drained, saturated clays in the sand drain zone.

Modelling of the stress-strain behaviour of the clay in the sand drain zone presents considerable problems. The influence of an independently varying pore pressure cannot

be reproduced directly and the solution must be performed in terms of total stresses. There is nonuniformity of pore pressure around the sand drains, yet the material properties must be given average properties. The construction occurs in three placing seasons, with shut-down seasons between them. Deformations cannot be predicted during the shut-down seasons, and the first two construction and shut-down seasons must be considered as two stages in the construction sequence, rather than four.

This problem is overcome by giving the soil 'elastic' properties which it is estimated will give the same deformations and stresses after a one step solution as would have occurred in the prototype after the construction and shut-down season. As performed, the analyses assume an estimated compression modulus and Poisson's ratio.

The material assumptions and the method of solution interrelate and are summarised on figure (7.6). The solution involves the selection of equivalent 'partly drained' elastic parameters for the first two years combined placing and shutdown behaviour. The clay is assumed to be undrained during the last placing season. The actual material properties assumed are summarised on figures (7.7, 7.8, and 7.9).

It may be noted that drainage has two effects. Firstly, drainage allows volumetric strains, which increase the predicted deformations. Secondly, drainage and

consolidation make the clay stronger and stiffer in as far as shear strains are concerned, this effect reducing the predicted deformations. While an allowance for partial drainage will increase the overall factor of safety against shear failure, the predicted deformations, when compared to a completely undrained case, may decrease or increase, depending on the relative importance of volumetric strains, which increase, and shear strains, which decrease. The difference between the undrained and partly drained cases may be illustrated in terms of the influence of stress changes on strains and subsequent material deformation properties. In the undrained case, strains and material properties are wholly dependant on the principal stress difference $\sigma_1 - \sigma_3$. In the partly drained case, both the strains and the material properties depend on the value of the minor principal stress σ_3 as well as on the principal stress difference. The effect is illustrated in figure. (7.9), where the actual maximum axial strains obtained from the solution are compared with the composite compression curve in terms of the compression moduli used by the computer during the various load increments. The curves differ most where drainage has been simulated. During the undrained stage the curves still differ, due to (1) the transformation from radial stress to plane strain made in the solution, (2) the fact that Poisson's ratio is 0,49 and not 0,50, and (3) errors due to the failure of the solution to follow the specified curve exactly.

7.2.3. Solutions obtained

Main Section — Half way between centre of valley and end of sand drain zone. Typical section, height 34m. Finite element mesh shown in figure (7.10).

Solution A — No sand drains. Poisson's ratio of undrained found. = 0.48

Solution B — No sand drains. Poisson's ratio of undrained found. = 0.49

Solution C — With sand drains, Poisson's ratio of undrained found. = 0.49

North Section — The actual section at Ch.722, just beyond the end of the sand drain zone. Height 25m. Finite element mesh shown in figure (7.11) and figure (7.12).

Solution D — Undrained foundation with strength as design profile, Poisson's ratio = 0.49.

Solution E — Undrained foundation with two weak layers, Poisson's ratio = 0.49.

The deformations and strains predicted are summarised on figures (7.13, 7.14, 7.15, 7.16 and 7.17). Deformations are shown for the surface of the berms, where they may be compared with field survey information; for a horizontal surface across the centre of the dam, comparable to the location on which rod gauge readings will be available and along the surface of the foundation. Sample stresses have been examined and some are plotted subsequently.

7.2.4. Discussion of the results.

The function of these solutions is considered to be twofold. Firstly, the solutions provide insight into the behaviour of what is a rather unusual embankment section and indicate general mechanisms of behaviour from which the limit analysis design calculations, which involve assumed mechanisms of behaviour, can be checked. Secondly, the prediction of deformation and deformation patterns provide a guide to the likely magnitude of the deformations of the real embankment and a framework within which field deformation observations can be related to stability.

It may be noted that horizontal deformations only are presented and discussed. Vertical deformations may be in substantial error, due primarily to the use of a Poisson's ratio less than 0.5, which will allow volume changes and spurious vertical settlements, as discussed in Chapter 6 in detail.

7.2.4.1. Main Section

The two solutions A and B allow the effect of the necessary assumption of a Poisson's ratio less than 0.5 for the saturated, undrained clay foundation to be assessed. The deformations predicted from solution B are typically 10% less than those of solution A and it can be concluded that a Poisson's ratio of 0.5 would give a further reduction in predicted deformation of the order of 10%. It may be noted that the effect of a small error in Poisson's ratio is

greatest when σ_3 is large and $\sigma_1 - \sigma_3$ is relatively small, as is the case with a flat embankment section such as Empingham. Solution B, figure (7.14), Drawing 2, shows that the embankment would have been stable without sand drains. However, the plot of shear stress along the top of the foundation figure (7.18) shows that there would have been yield under the whole of the centre of the dam and the factor of safety would have been relatively low. This solution shows that the sand drains have been installed in exactly the right zone, where they occupy the zone of yield.

The deformations predicted with the presence of sand drains (solution C) are shown on figure (7.15) Drawing 3. The deformations are less than those predicted without sand drains. Those on the upstream side are reduced by 25% whereas those on the downstream side are reduced by 50%. This is consistent with the finding of the limit analyses, which showed that with the final revised design assumptions, the thrust on the upstream berm, which controls the deformations of it, is controlled by the thrust of the sloping core rather than by the centre of the dam. The thrust of the core is not influenced by the presence of the sand drains. The deformation pattern is one of 'contained' plasticity, with measurable deformations spreading out to about 120m from the dam centre line.

The shear stresses along the top of the foundation are shown on figure (7.18). Comparison with the stresses

from solution B shows an interesting and consistent effect. Solution B shows a value of τ_{max} near yield right across the dam centre. The value of the horizontal shear stress τ_{xz} decreases to zero at the dam centre, as it must where the horizontal displacements are zero. Solution C shows a much higher value of τ_{max} in the sand drain zone, even before the dam centre has been raised above berm level. This arises from the simulated effect of consolidation. With Poisson's ratio less than 0.5, vertical loading produces a stress difference, e.g.

$$\tau_{max} = \left(1 - \frac{\nu}{1-\nu} \right) \sigma_v/2$$

The plot of τ_{xz} shows that the horizontal shear stress on the foundation is consistent with the displacements. Solution C shows slightly lower values beneath the berms and rather larger values beneath the dam centre, giving a total mobilised horizontal force rather greater than solution B. This is consistent with the smaller strains predicted in the dam centre for solution C, which imply a larger active pressure exerted on the dam shoulders and a higher factor of safety.

7.2.4.2. North Section

This section has been given more detailed consideration, as preliminary limit analyses have indicated that it is the more critical stability case. The displacements predicted from solution D, which has a foundation with

an undrained shear strength equivalent to the standard design assumption, are shown on figure (7.16) (Drawing 4). The displacement is again one of 'contained' yield. Measurable displacements (of the order of 50mm) extend about 110m on both sides of the centre line. The downstream displacements are greater than the upstream ones.

Shear stresses on horizontal planes 1.06 and 9.6m below the surface of the foundation clay are shown on figure (7.19). The foundation is close to yield near the surface (where local consolidation may make the design assumptions conservative). The proportion of the strength mobilised decreases with depth, which confirms the previous findings from the limit analyses. These stress distributions show the embankment section to be well proportioned, with no zones of complete yield in the foundation. They also indicate that there is an adequate factor of safety in the foundation. Stresses in the embankment fill have not yet been examined.

Since the foundation is undrained, it is possible to predict pore pressures at the piezometers in this section from the predicted stress changes, and thus to compare these with the measured pore pressures. These predictions are shown on figures (7.20, 7.21, 7.22, 7.23, & 7.24) for piezometers N,F,2, 5, 8, 11, & 14. Stresses are taken for the nearest Gauss points and the measured piezometric elevation is assumed to apply to these points. The pore

pressures are predicted using a value of the Pore Pressure Coefficient B=1, and A=0 & ½.

Solution E is for the north section with two weak layers introduced into the foundation. The layers are 0,5m thick and their strength has been reduced by a factor of 0,6. It should be noted that the strength within these layers is isotropic, and they are not the equivalent of shear planes, which would have a reduced strength only with a horizontal component of shear stress. However, it is considered that their overall effect on the deformation and stress pattern would be similar to that of shear planes. The purpose of this analysis is to indicate what effect such planes might have and how best their presence could be detected from the field observations.

The predicted deformations are shown on figure (7.17) (Drawing 5). It can be noted first that their influence is to increase deformations by only about 30%, which is less than the overall accuracy of the solutions. Thus general deformations are an inadequate guide to the presence of such zones. The shear stresses developed in this solution are summarised on figures (7,25 & 7.26). Shear stresses near the foundation surface are similar to those found in solution D, figure (7.19). The stress distributions at depth show that yield has occured in both layers. Yield in the upper layer is extensive and symmetric about the centre line. Yield in the lower layer

is less on the upstream side. Stresses in the dam fill have not been checked in detail, but an adequate factor of safety against complete failure seems to exist, even with the weak layers in the foundation.

The reason for the similarity in the displacements predicted by solutions D and E may be deduced. Figure (7.27) shows stresses and displacements on a typical vertical section through the foundation. The stresses from solution E are slightly lower. The shear stresses in solution E are restricted by the yield stresses in the weak layers. While there are large relative displacements along the weak layers in solution E, the restriction of the shear stress means that strains in the clay on either side of the weak layers are less than those from solution D. Thus solution E shows increased displacements due to large strains in the weak layers but reduced strains and displacements in the remainder of the foundation. Overall displacements are not increased by the total relative displacements along the weak layers. The numerical values from figure (7.27) are:-

	Solution D	Solution E
Cumulative displacement in clay on either side of weak layers.	225 mm	181 mm
Cumulative displacement in weak layers.	10 mm	117 mm
Total surface displacement.	235 mm	298 mm

The increase in overall surface displacement is about 60% of the increase in displacement in the weak layers. Thus an

increase in overall displacement is ill-conditioned as a means of detecting the presence of weak layers.

Figure (7.26) shows shear stresses and relative displacements along the upper weak layer. As might be expected, relative displacements are a function of horizontal shear stress, not maximum shear stress. Relative displacements would be readily measurable by an inclinometer tube over a length slightly less than that over which yield has been reached. From figure (7.26), this would be out to a distance of approximately 80m from the centre line. Once significant relative displacement has occured at a point, it increases rapidly with increasing fill height. Thus it may be concluded that the presence of critical continuous weak layers could be detected most readily by rapidly increasing 'kinks' in inclinometer tubes located within about 80m from the dam centre line. It is probable that relative displacements could propagate further than this before instability ensued.

7.2.4.3. General pattern of movements

It is convenient to consider the rate at which movements develope with increasing height of the dam. Deformations for typical points are plotted on figures (7.28, 7.29, 7.30, & 7.31). They show that for solutions A-D the rate of increase of deformation with increasing fill height reduces slightly during the final stages of construction.

Solution E, which is for the foundation containing weak layers, shows a slight increase in deformation rate with increasing fill height during the final construction stages. It may be concluded tentatively that field results which show an increase in deformation with fill height during the final construction stages show either a safety factor less than those consistent with the design assumptions and/or the presence of weak layers. Such observations would not necessarily be immediately crucial as the embankment sections have relatively high factors of safety if the design assumptions are correct.

7.2.4.4. Possible errors in the solutions.

Errors may arise due to incorrect assumptions of material properties and due to approximations and over simplifications in the method of solution. Many of the soil stress-strain properties assumed are based on limited evidence, and the conversion of compression test results to predict plane strain behaviour via the equations of isotropic elasticity used in the programme presents a further uncertainty. While the properties were selected to give a best estimate of deformations, it is thought that there is some element of conservatism in these assumptions.

As discussed previously, the programme requirement for a Poisson's ratio marginally less than a half may have caused an overestimate of the deformations of the undrained saturated clay of the order of 10%.

The modelling of the stress-strain behaviour of the partly drained clay in the sand drain zone of solution C is subject to major uncertainties which are likely to be reflected in the accuracy of the deformation predictions.

The most probable source of major error in the formulation and solution techniques is thought to be due to the absence of modelling unloading in the berm fill. The final design prepared in 1973 included a thickening of the berm fill at the inside of the berms to take advantage of shear unloading and to make the berms behave more like rigid plates. The more rigid their behaviour during the final stages of construction, the more uniformly the foundation beneath the berms will be stressed and the greater the passive resistance which can be mobilised for a given displacement at the toe of the upper slope will become.

The effect of shear unloading is illustrated on figure (7.32), which shows the stresses predicted by solution D at a Gauss point within the upstream berm fill. During the later stages of construction, there is a reduction in maximum shear stress, and σ_3 increases more than σ_1. The effect is more marked if horizontal and vertical stresses are considered. The horizontal normal stress increases until it is only slightly less than the vertical. It may be noted that the final limit analyses were adjusted to give a final horizontal stress which should have exceeded the vertical stress by $20kN/m^2$, on average.

The inclusion of a shear unloading model in the solutions requires a further development of the programme. The magnitude of its effect on the deformations predicted cannot be assessed, but the effect can be deduced on a qualitative basis.

The shear stresses in the berm fill are a long way from failure and thus the berm fill is operating on the stiffest part of its first loading stress-strain curve. However, the deformations show that the berm is far from operating as a 'stiff plate'. An unloading characteristic equivalent to an infinite compression modulus would give 'stiff plate' behaviour, with uniform displacement along the base of the berm. The effect of stiffer berm fill can be assessed as follows:-

The berms will behave more like rigid plates, and displacements along the berm will be more uniform. The more stiff the fill, the larger the passive resistance which can be mobilised for the same displacement at the inside of the berm. Thus the displacements at the inside of the berm will be reduced. This reduction will imply lower strains in the centre of the dam, and a larger active thrust generated. This in turn will require a higher passive berm resistance and larger berm displacements, and it will partly compensate for the increase in berm stiffness.

The effect of berm stiffness is likely to become apparent from the field survey measurements. If the decay

of displacement with distance from the centre line is less than that predicted it can be inferred that this is due to berm stiffness. If this effect is significant, the results can be reassessed. It is possible to make a preliminary reassessment by inspection. The results show that deformation of the foundation surface is generally a function of the horizontal shear stress operating on the foundation, and that the deformation is also a function of the proportion of the foundation strength which has been mobilised. Thus, for each of the sections analysed we can identify a section through the foundation where a maximum of $\frac{2}{3}$ of the foundation strength has been mobilised. The deformation of the foundation at the top of the section can therefore be identified with a factor of safety of 1.5 in the clay beneath. If, as a limiting case, the berm behaves as an infinitely stiff plate, the displacements along its base would be uniform. If these displacements are the same as the value for the surface where F= 1.5, then the overall factor of safety against failure beneath the berm would be 1.5. Thus the values of foundation surface deformation identified above are lower bound values for the permissible deformations for a factor of safety of 1.5 beneath the berms if the berms behave as rigid plates. These values are:-

Main section with sand drains	70mm
North section without weak layers	80mm

If the field measurements show rigid berm behaviour, these

values may be used immediately to assess whether the deformations are acceptable.

7.2.4.5. Summary

1) The analyses confirm that both sections have an ample stability reserve assuming soil properties previously used in the limit analyses.

2) The North section remains quite stable even if weak zones are introduced into the foundation with strengths reduced by a factor of 0.6.

3) Deformations equivalent to those which are being measured are predicted, for completion of the dam centre. They are probably overestimates.

4) The analyses indicate that the increase in horizontal displacement fill height reduces towards the end of construction unless weak layers are present. An acceleration of deformation with increasing fill height may therefore be used as an indicator of potentially dangerous behaviour.

5) The presence of weak layers may not lead to a detectable increase in overall deformations. The presence of critical weak layers should be detected by inclinometers within the distances specified, and will be indicated by discontinuities which rapidly increase with increasing fill height. Discontinuities which develop and then stop may indicate a local discontinuity rather than a general failure plane.

5) The most probable error in the analyses is due to the absence of a shear unloading model in the berm fill. The berms may behave in a more rigid manner than has been predicted, This should be detectable from the survey measurements. Lower bound values for acceptable deformations for rigid berm behaviour are suggested. The significance of this shortcoming in the analyses, and the implications concerning stability, can be assessed from the continuing field observations.

7.3 Comparison with field observation

The field measurements available for comparison with predictions are:-

a. Horizontal movements

North Section: Observations from a three point wire extensometer (shown in figure (7,16)) are available. The absolute movements of the extensometer datum are not currently available.

Main Section: Horizontal movements are available from two inclinometers in the berms (shown in figure (7.15)). Wire extensometers at these locations showed very small deformations and have not been used for comparison. The displacements indicated by the inclinometers at foundation level and at the surface of the dam have used.

b. Pore water pressure

North section: Piezometer records are available from 15

piezometers in the undrained foundation. Five of these, located as shown in figure (7.16), have been used for comparison of measured pore water pressures with those predicted from total stresses.

c. Comparison with measured displacements

The comparison between predicted and measured displacements for the North section is shown in figures (7.33 + 7.34) in the form of relative displacements between the points 1-2, 2-3 and 3-4 of the extensometer versus fill height. The prediction was taken from solution D, i.e. that without the assumption of weak layers. The pattern of movements for the 3 points were similar, but the magnitude of prediction were 3 times that measured for interval 1-3 and 3 times for the interval 3-4. The error was nearly constant over the development of the fill height and no increase in the rate of movement was predicted when end of construction was approached which confirms the stress predictions of figure (7.19)and which indicate that no zone of local failure occured. Improvement of this fit might be obtained by the over-all stiffening of the stress-strain curve and there is no reason to suggest that the shear strength should be modified from that of the design profile.

The comparisons for the main section are shown in figures (7.35 + 7.36) in the form of absolute displacements versus fill height. The patterns for predictions and measurements are essentially different, although the final predicted and measured values are very close for the 4 points considered. The measured horizontal displacements for the

4 points showed a low rate of increase of displacements in the early stages of construction followed by a distinct increase in the rate of movements at about construction stage number 9. However, the predictions showed opposite patterns of behaviour having a large rate of increase at the early stages of construction followed, smoothly, by a small rate of movement at the end of construction. Thus, the two patterns indicate different mechanisms; predictions give a decaying mechanism while field measurements give an accelerating one.

The undrained factor of safety, based on the design strength profile, for end of construction case, and the stress predictions shown in figure (7.18) do not suggest that the accelerating mechanism was due to imminent shear failure, and the difference between the two mechanisms indicates a basic error in the predictions:

a) If predicted movements for solutions D & E of the North section (i.e. with and without weak layers) are compared, figure (7.37), it is seen that the weak layers produce an accelerating mechanism of the same type as that displayed by the field measurements. This is an interesting and important observation. It may be inferred that the existence of a strength discontinuity localizes the strain and causes the bulk accelerating behaviour. Modelling this mechanism implies dealing with a discontinuity in strength leading to geometrical discontinuity. Since most natural soil will contain slightly weak zones this mechanism may control

deformation once local failure has occured, and failure to model it may prevent accurate deformation predictions from being made. This point requires further research.

b) Creep movement was observed after the end of construction and movements nearly doubled after completion of loading. It can be assumed that some part of the displacement recorded for the last stages of construction is due to creep movement.

Improvements to the fit of the main section might be obtained as follows:-

i) Using a stiffer stress-strain curve to overcome the high rate of movement predicted at the start of construction.

ii) To eliminate the creep movement or to incorporate a creep model.

iii) To model a strength discontinuity in the foundation soil.

c) Comparison of predicted and measured pore pressures.

As mentioned in section 7.24.2, the predicted pore water pressure are compared with measured values in figures (7.20, 7.21, 7.22, 7.23 & 7.24) and a plot of total and effective stress at failure is shown in figure (7.38). A value of mobilized friction angle was calculated from the total pressures and pore water pressure. The results are reasonable and indicate stability. However, these plots should only be considered as a check on the consistency of the field observations of pore pressure with the solution, as:-

Values of τ_{max}, C_u, A, $\phi'_{mob.}$ and ϕ'_f are not necessarily consistent. Pore pressures predicted are very sensitive to values of σ_3.

$\phi'_{mob.}$ is very sensitive to σ_3 and pore pressure.

The plots indicate that only piezometers NF8 & 11 showed significant further rises during completion of the dam, but that creep was accompanied by increases in pore pressure. It should be noted that plots of this type were an unsatisfactory method of explaining the pore pressure observations beneath the trial bank. It is thought that this may have been due to three-dimensional effects, which may have caused discrepancies between the true and predicted average stresses, which control the pore pressures, while the true and predicted shear stresses, which control the horizontal displacements, may have been equivalent.

The results confirm that the north section had an ample reserve of stability if the foundation strength is equivalent to the design assumption, which reinforces the view that the accelerating behaviour of the North section was not due to under-estimation of the bulk shear strength but due to a shear strength discontinuity.

7.4 Analyses after the completion of the trial bank back analysis.

7.4.1 Solutions obtained

Following the improvement in the fit obtained in the

trial bank due to the use of the systematic back analysis (cases 4a and 4au), further predictions of the main embankment behaviour have been made, incorporating the stiffer stress-strain curves from analysis 4a and shear unloading. The predictions, were:-

North section: Cases analysed are

F1 stress-strain curve and strength as case 4au (modelling of shear unloading with $E_i = E_{unloading}$)

F2 As case F1 but no modelling of shear unloading.

F3 As case F1 but with $E_{unloading} = 5\ E_i$.

F4 As case F3 but $Cu_{F4} = Cu_{F3} + 5\ KN/M^2$

Main section: Cases analysed are

F5 As case F4.

The displacements and strains from these solutions are shown on figures (7.39, 7.40, 7.41, 7.42 & 7.43).

7.4.2. Comparison with field observation:-

a) N. Section

The introduction of a stiffer stress-strain curve and shear unloading reduces the deformations generally, and produces a better fit to the measured relative displacements. However, the 'spread' of points 1-2 is still overestimated and it is predicted to occur at a lower fill height.

b) Main Section.

The introduction of a stiffer first loading curve and shear unloading substantially decreases the predicted

displacements (by about ½) and the predicted values at the end of construction are substantially less than those measured. The shape of the predicted displacement/fill height curves remains the same and shows the same major difference from the shape of the measured displacement curve. It may be noted that the rod gauges in the main sections showed movements much smaller than the inclinometers and less than those predicted by the 'improved' analysis.

7.5 General Conclusion

Both the initial analyses and the 'improved' analysis give a poor prediction of the measured field deformations. While the accuracy of these measurements is difficult to assess, the poor prediction must be considered mainly a failure of the predictive approach. Possible reasons have been summarised in section 7.3. The main causes may be creep, the development of discontinuities during failure, and failure strain.

(a) Creep appears unlikely to be a main cause of the discrepancy, as the stress-strain data used, which was derived from the trial bank, was obtained for similar loading times.

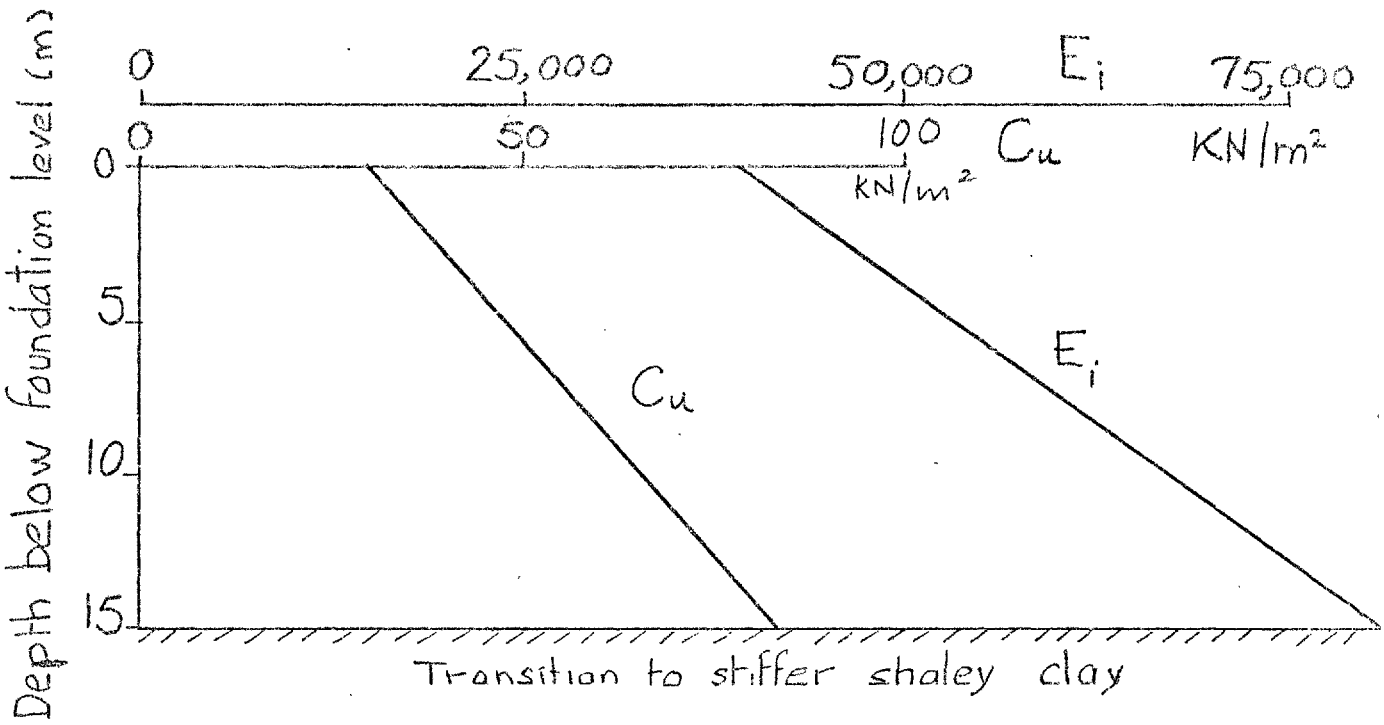
(b) Shear discontinuities. The solutions of the North Sections with simulated weak layers, along which discontinuities developed, showed a very substantial difference in deformation pattern from the solutions with a strength varying smoothly

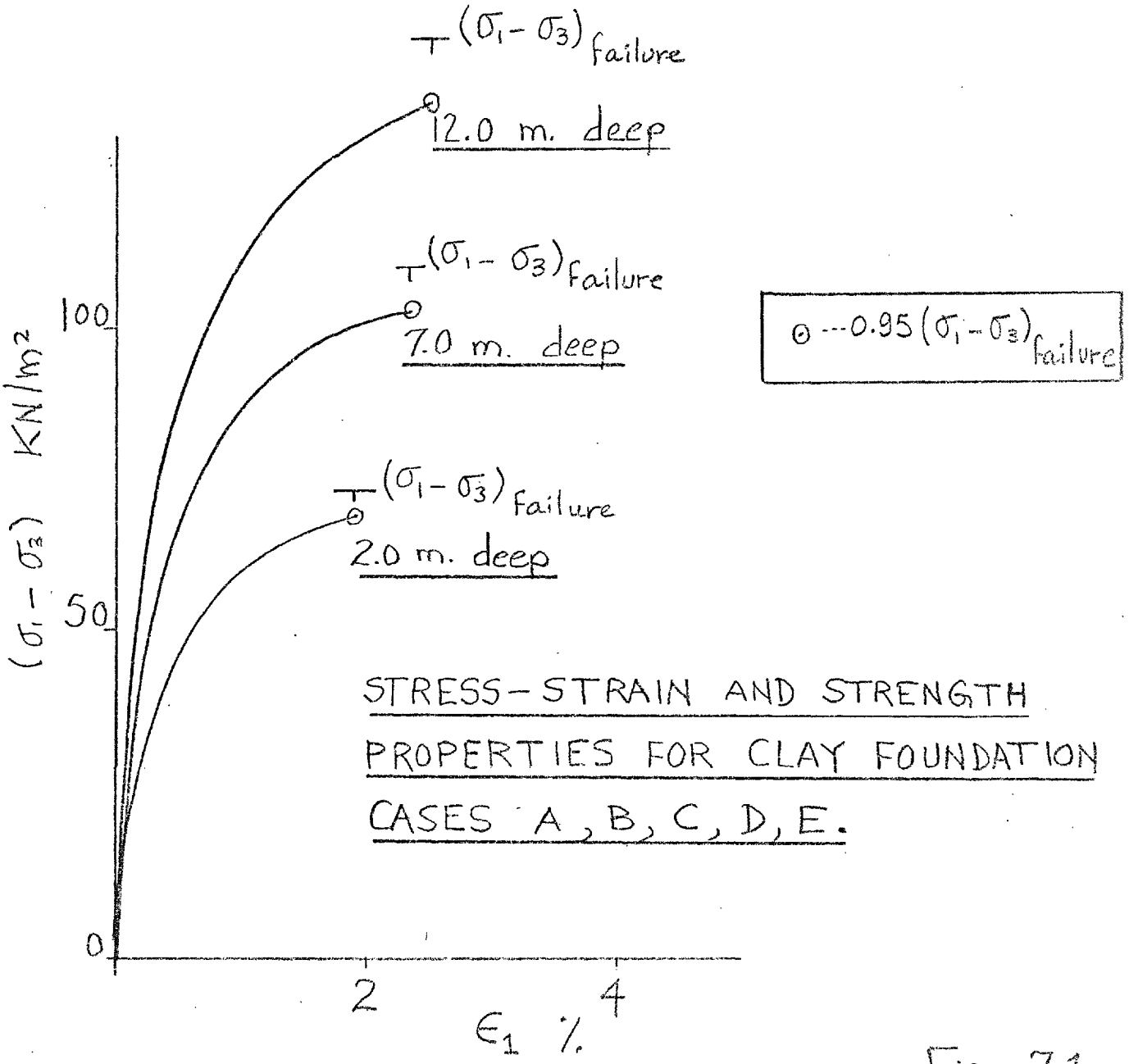
with depth. The inclinometers (both in the trial bank and the main dam) tended to show the development of shear in relatively narrow zones, whereas the solutions show more uniform strain. It seems possible that the failure of the analyses to reproduce the deformation pattern is due primarily to the failure to model the formation of local shear discontinuities. However, the predicted stresses show that local failure should not have occured, and thus this argument is not consistent.

(c) Failure strain. Reexamination of the trial bank analyses shows that the bi-linear solution (case 2a) exhibited a displacement - height characteristic more like the observed behaviour of the main dam. A smaller strain at failure, associated with the formation of shear discontinuities at shear stresses a little less than the average value, might more nearly represent the mechanism of local failure, and might change the stress pattern predicted for the main dam. This mechanism clearly requires further examination. However, it is difficult to see how it can be modelled by a continuum technique of analysis. If this mechanism can be demonstrated it may imply a limitation to the use of finite elements to predict deformation patterns in clays exhibiting it, at stresses greater than those causing local contained failure.

The analyses gave a valuable insight into the mechanisms of failure of the embankment, particularly when

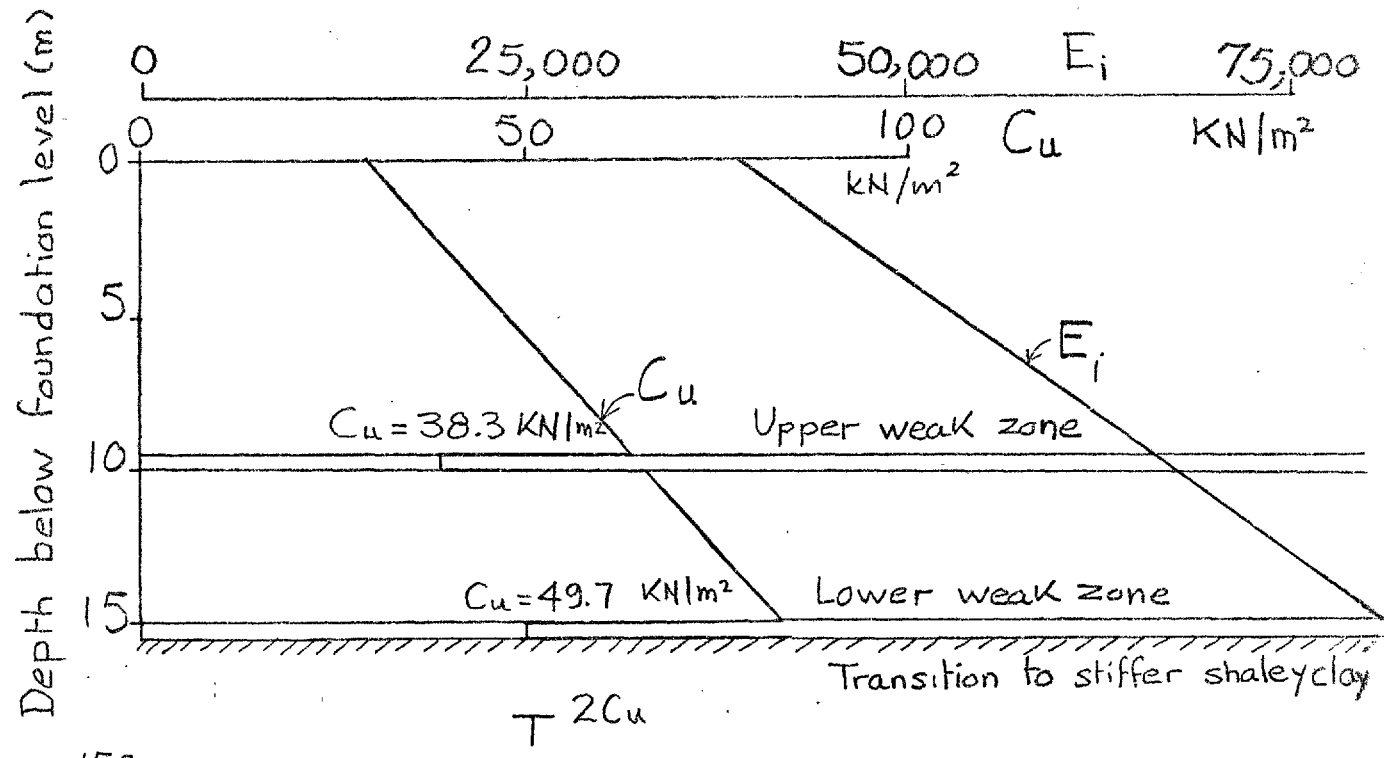
the stresses and stress changes were studied and they are of great value in planning the location of instrumentations. The relative failure of the predictions of displacement and displacement pattern, particularly of the main dam, to agree with those observed shows that the overall approach was of much more limited value as a method of assisting in the interpretation of field observations of displacements and in particular, of relating deformation to stability. Thus the main (and very important) practical contribution of the analyses lay in the proving of the existence of the design strength beneath the trial bank without the need for failing it.

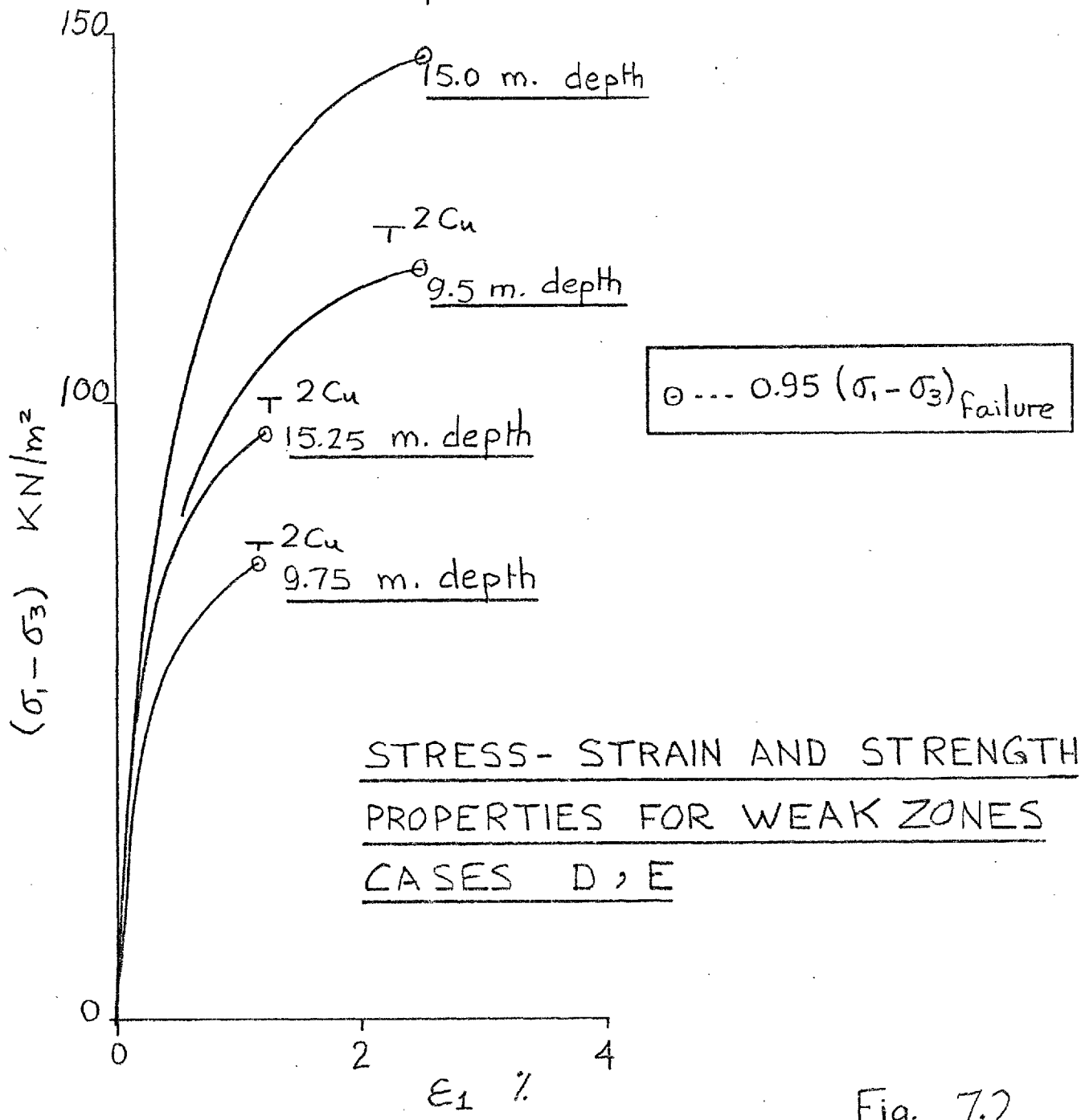




STRESS-STRAIN AND STRENGTH PROPERTIES FOR CLAY FOUNDATION CASES A, B, C, D, E.

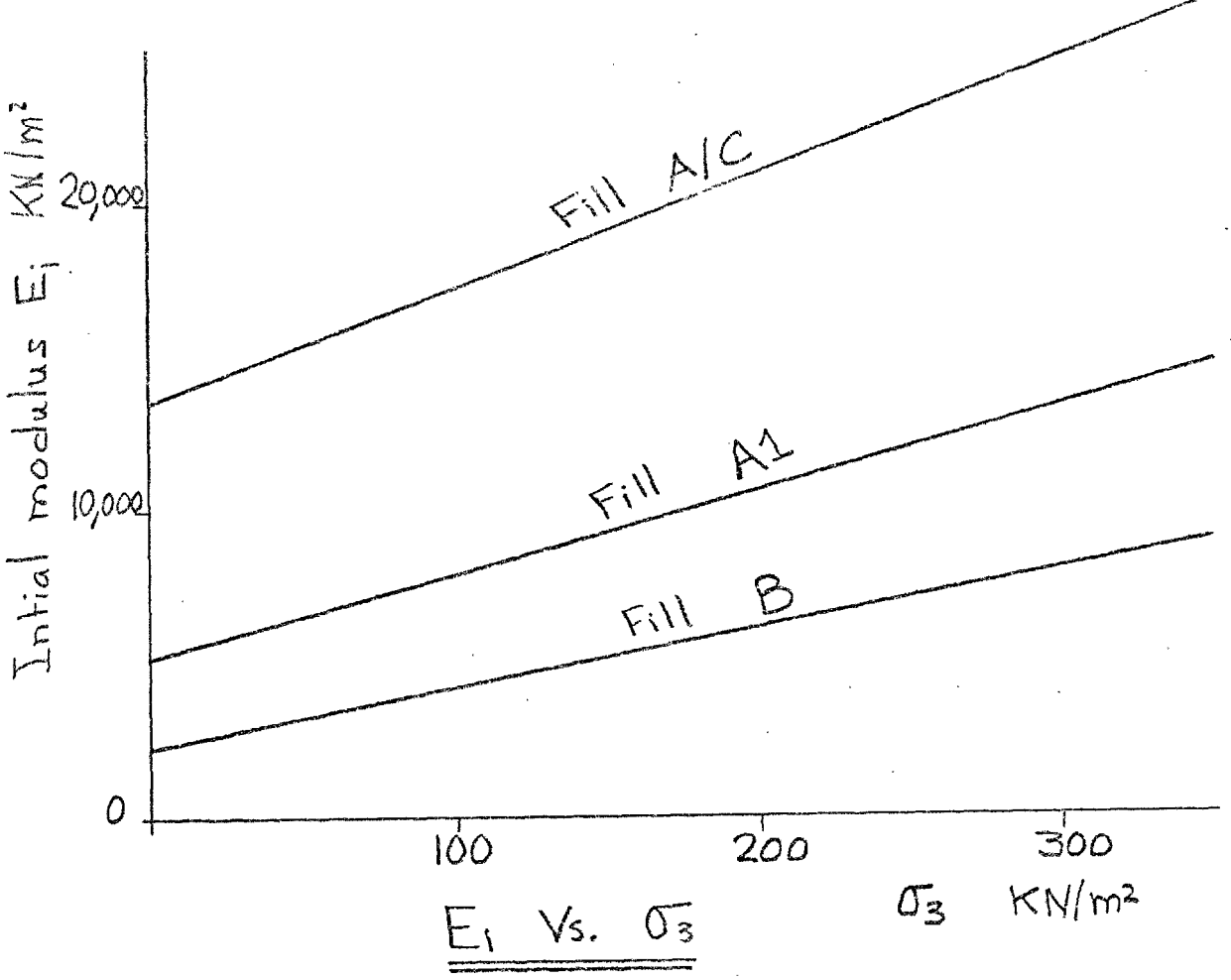
Fig. 7.1



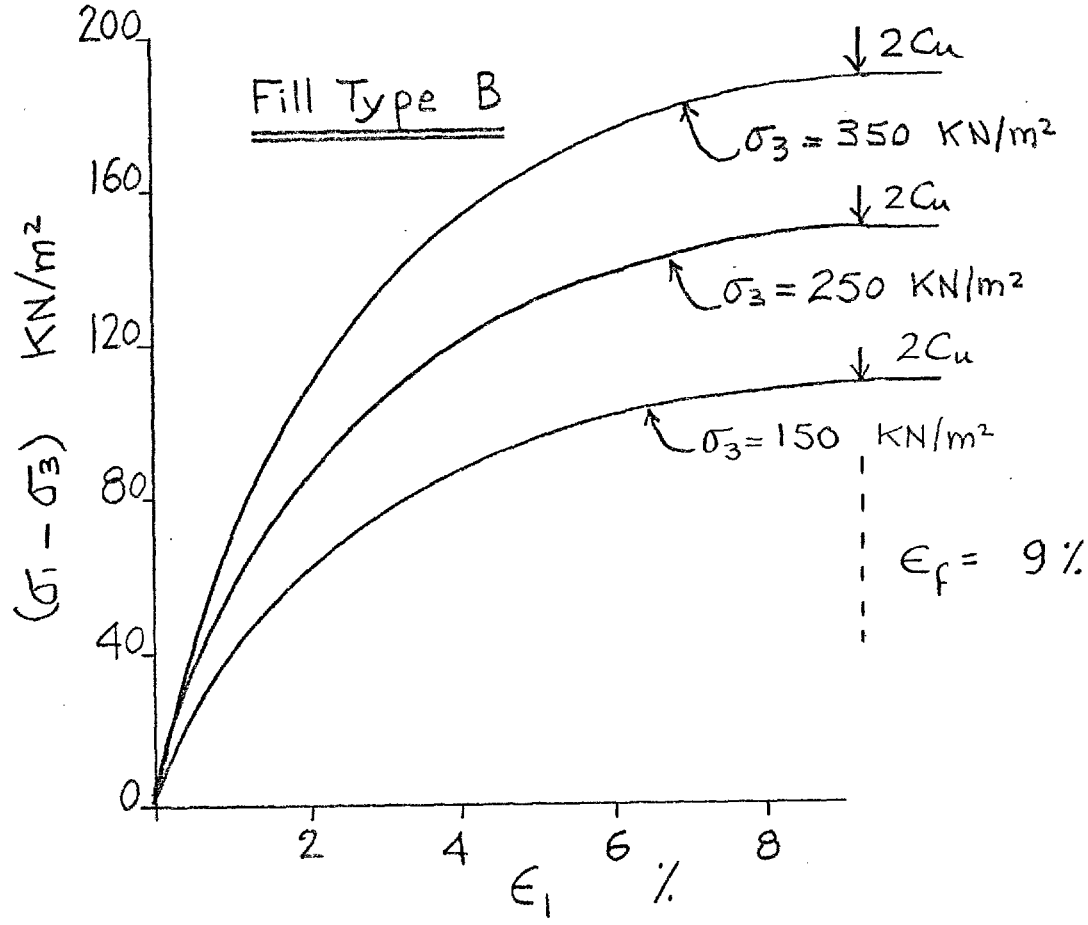


STRESS- STRAIN AND STRENGTH PROPERTIES FOR WEAK ZONES CASES D, E

Fig. 7.2

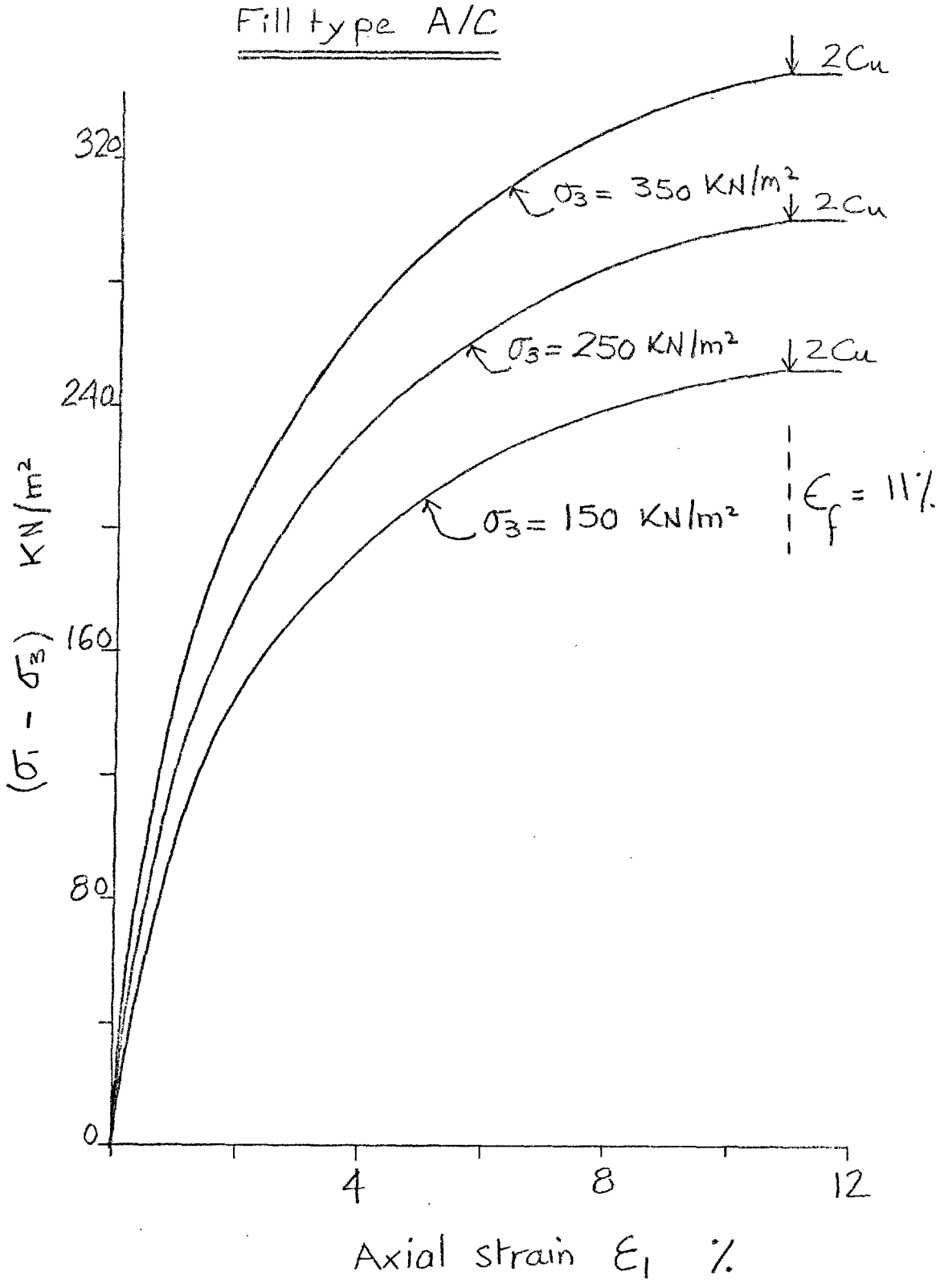


E_i Vs. σ_3



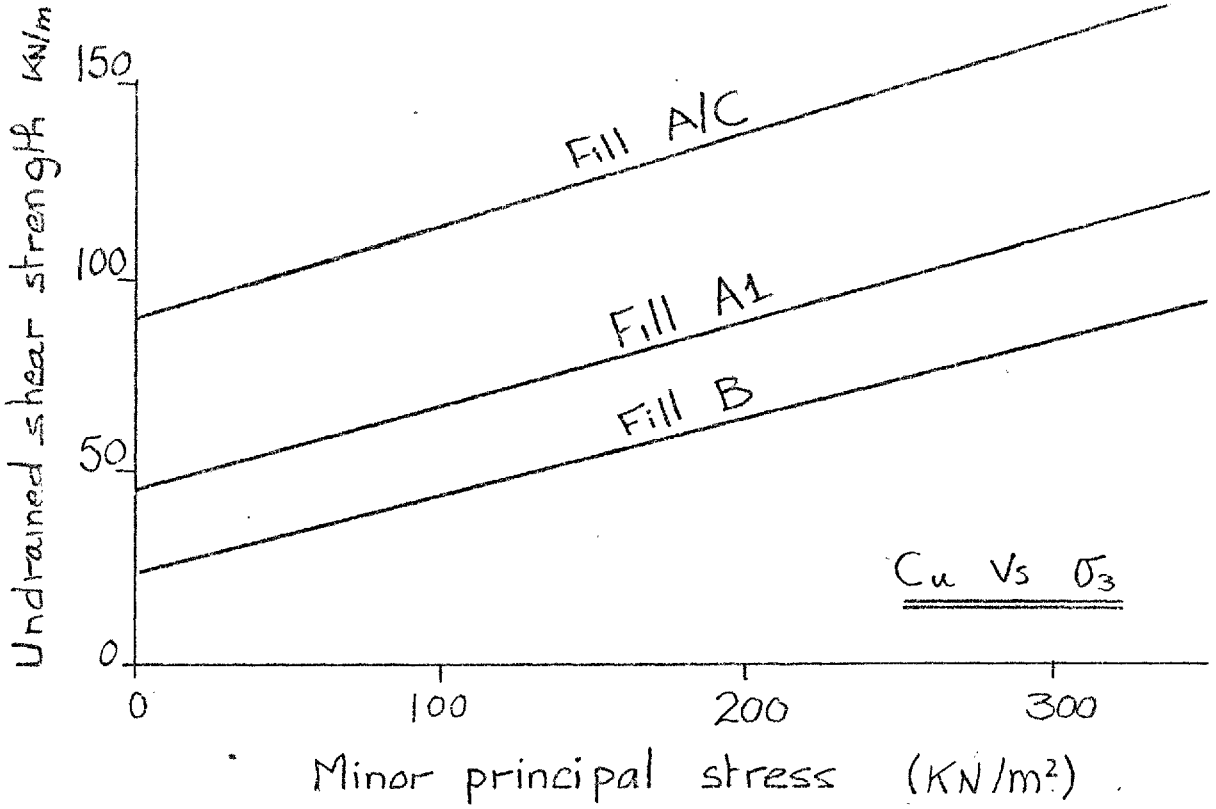
FILL PROPERTIES_ TYPICAL CURVES

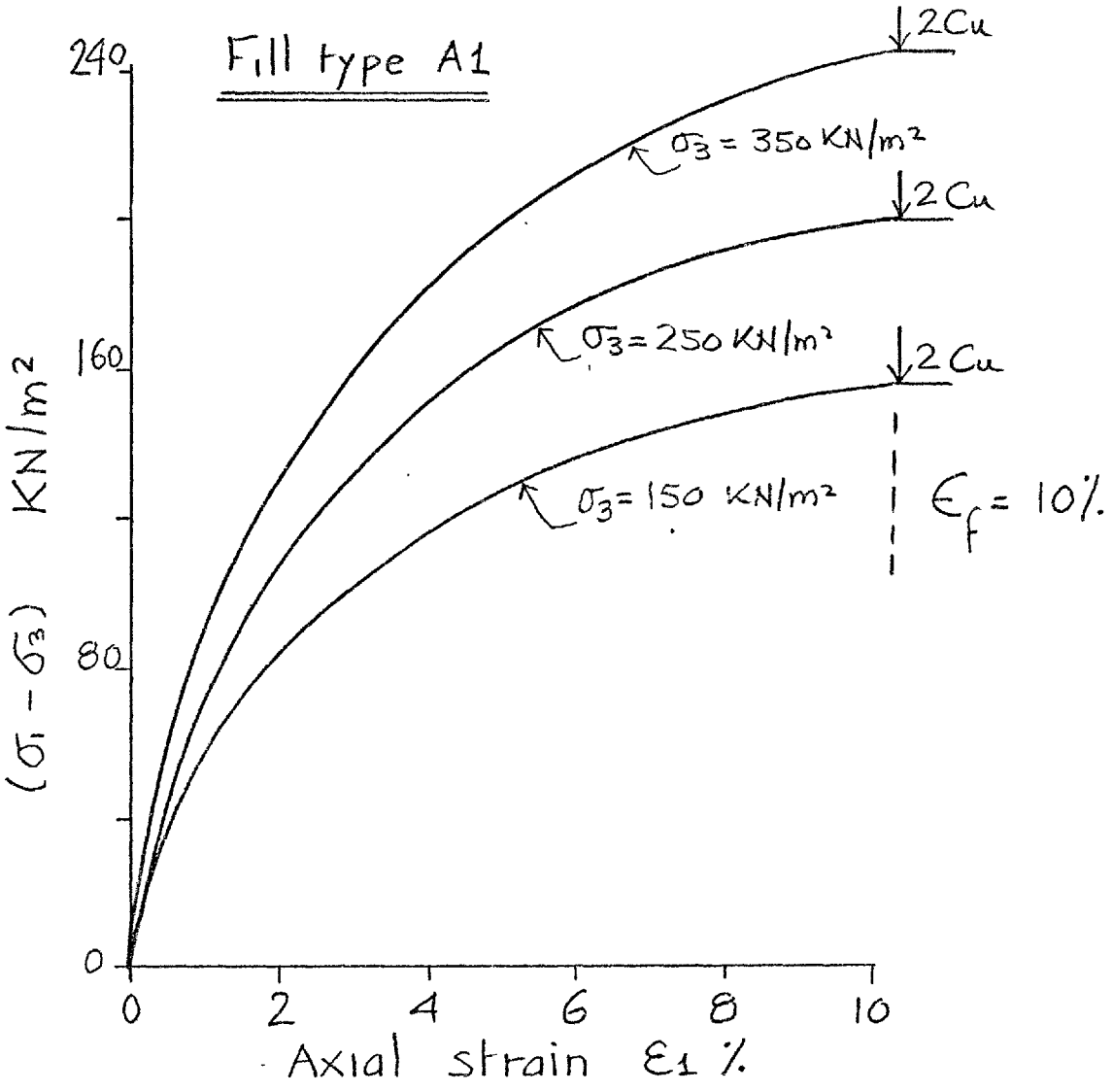
Fig. 7.3



FILL PROPERTIES _ TYPICAL CURVES

Fig. 7.4



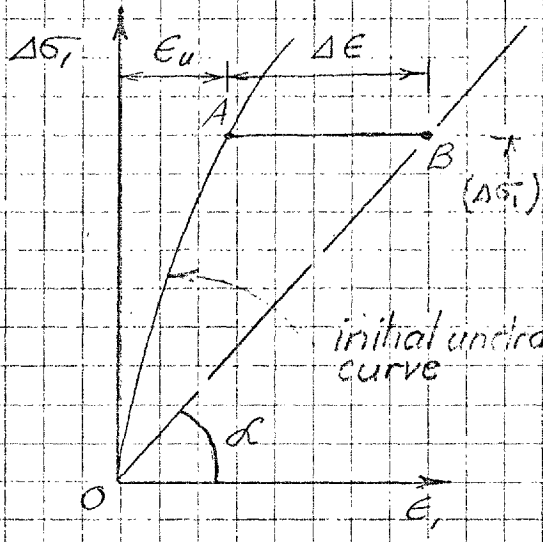


FILL PROPERTIES _ TYPICAL CURVES

Fig. 7.5

Sand drain zone - Modelling of soil properties

1st Season



A 2 step solution would be OA, AB

ε_u = undrained strain.
$\Delta\varepsilon$ = strain due to drainage.

We need to deduce $E_{pd} = \tan\alpha$ giving a linear relationship for O-B.

We also require ν_{pd}.

Assumptions

1) Assume isotropy $\therefore \Delta\varepsilon = (\Delta V/V)/3$

Thus $E_{pd} = \dfrac{(\Delta\sigma_1)_1 / \varepsilon_u}{1 + (\Delta V/V)/3\varepsilon_u}$

2) $\Delta V/V$ calculated as follows.
m_v given by assumed vertical stress e.g.

σ_v'	=	50	100	230	400 kN/m²
m_v	=	0·3	0·2	0·1	0·05 m²/MN

$\sigma_v' = \gamma H_1 - (H_1 - \Delta H_1)\gamma_w$ $0.4.\Delta H_1.\gamma_w$ ($\bar{B}=1$, 60% consolidation)

$\Delta V/V = m_v.\Delta u$ where $\Delta u = 0.4.\Delta H_1.\gamma_w$

H_1 = height of fill above point, ΔH_1 = thickness of fill placed.

3) ν_{pd} deduced as follows:-

$$\nu_{pd} = 0.5 - \frac{0.5.\Delta V/V.E_{pd}}{(\Delta\sigma_1 - \Delta\sigma_3) + 3.\Delta\sigma_3}$$

Fig. T.6a

WELLS... A4 210 x 297 mm

Method of solution

a) (2) → $\Delta V/V$

b) Undrained solution with initial undrained curve → $(\sigma')_b$

c) $(\sigma')_b$, (a) → $(E_{pd})_c$, $(\sigma')_b$, (a) → $(\nu_{pd})_c$ $[(\nu_{pd})_c = 0.32]$

d) Partly drained solution with $(E_{pd})_c$, $(\nu_{pd})_c$ → $(\sigma')_d$

e) $(\sigma')_d$, (3) → $(\nu_{pd})_e$ $[(\nu_{pd})_e = 0.40]$

f) Final solution using $(E_{pd})_c$, $(\nu_{pd})_e$

2nd Season

Assumptions

(1) $(\sigma_1' - \sigma_3')$, σ_3' from solution for 1st season

(2) $\Delta\sigma_v'$ → increase in undrained strength and, with constant failure strain and constant E_i/C_u a new undrained curve is obtained (a & b remain constant)

(3) new volume change from σ_v', m_v, $\Delta\sigma_v'$

Method of solution

a) Undrained solution with curve from (2) → $(\sigma')_a$

b) $(E_{pd})_b$ from $(\sigma')_a$, (3); $(\nu_{pd})_b$ from $(\sigma')_a$, (3) $[(\nu_{pd})_b = 0.42]$

c) Assume $\sigma_v' = \gamma.h = \sigma_1'$, $\sigma_h' = K_o.\gamma.h = \sigma_3'$, $K_o = \nu_{pd}/1-\nu_{pd}$.

d) Iterate to give final ν_{pd} e.g. $(\nu_{pd})_b \rightarrow K_o \rightarrow \sigma_1', \sigma_3' \rightarrow \nu_{pd} \rightarrow K_o \rightarrow \sigma_1', \sigma_3' \rightarrow \nu_{pd}$
[final value, $(\nu_{pd})_d = 0.463$]

e) Final solution with $(E_{pd})_b$, $(\nu_{pd})_d$.

3rd Season

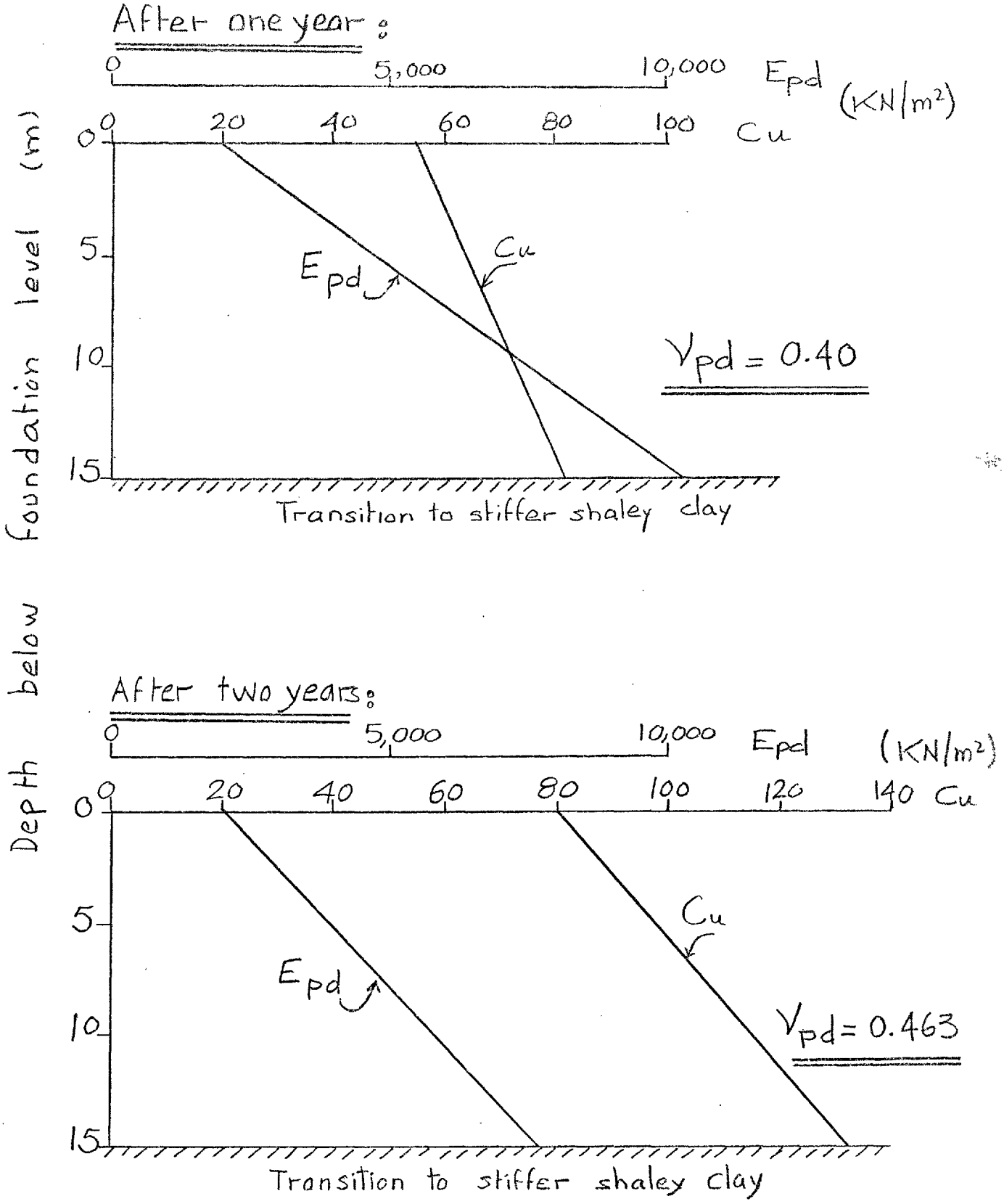
(1) New gain in strength calc. - with E_i/C_u constant → new undrained curve.

(2) Solution performed with this curve & $\nu = 0.49$

SAND DRAIN ZONE - MODELLING OF SOIL PROPERTIES

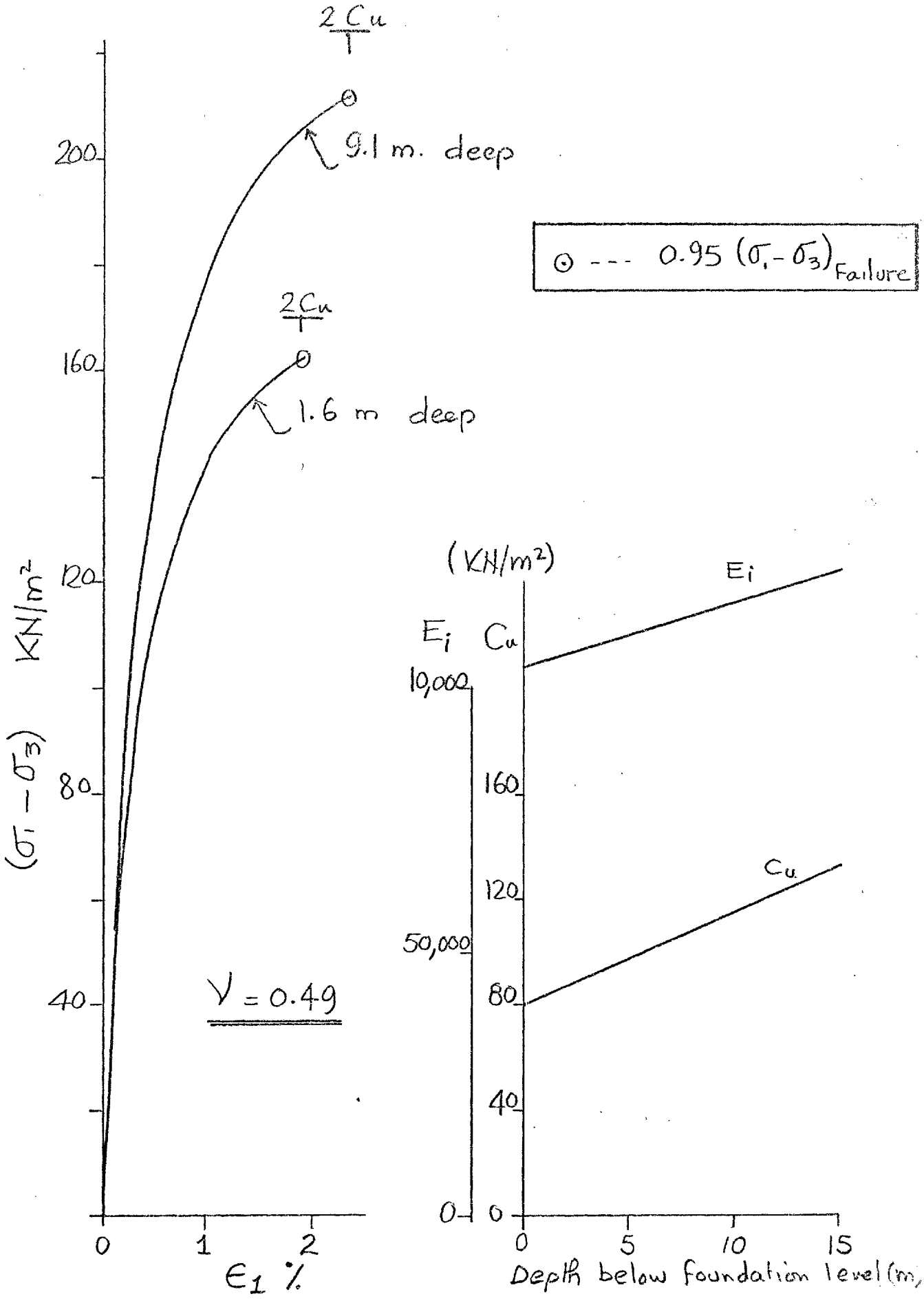
Fig. 7.6b

WELL... A4 210 x 297 mm



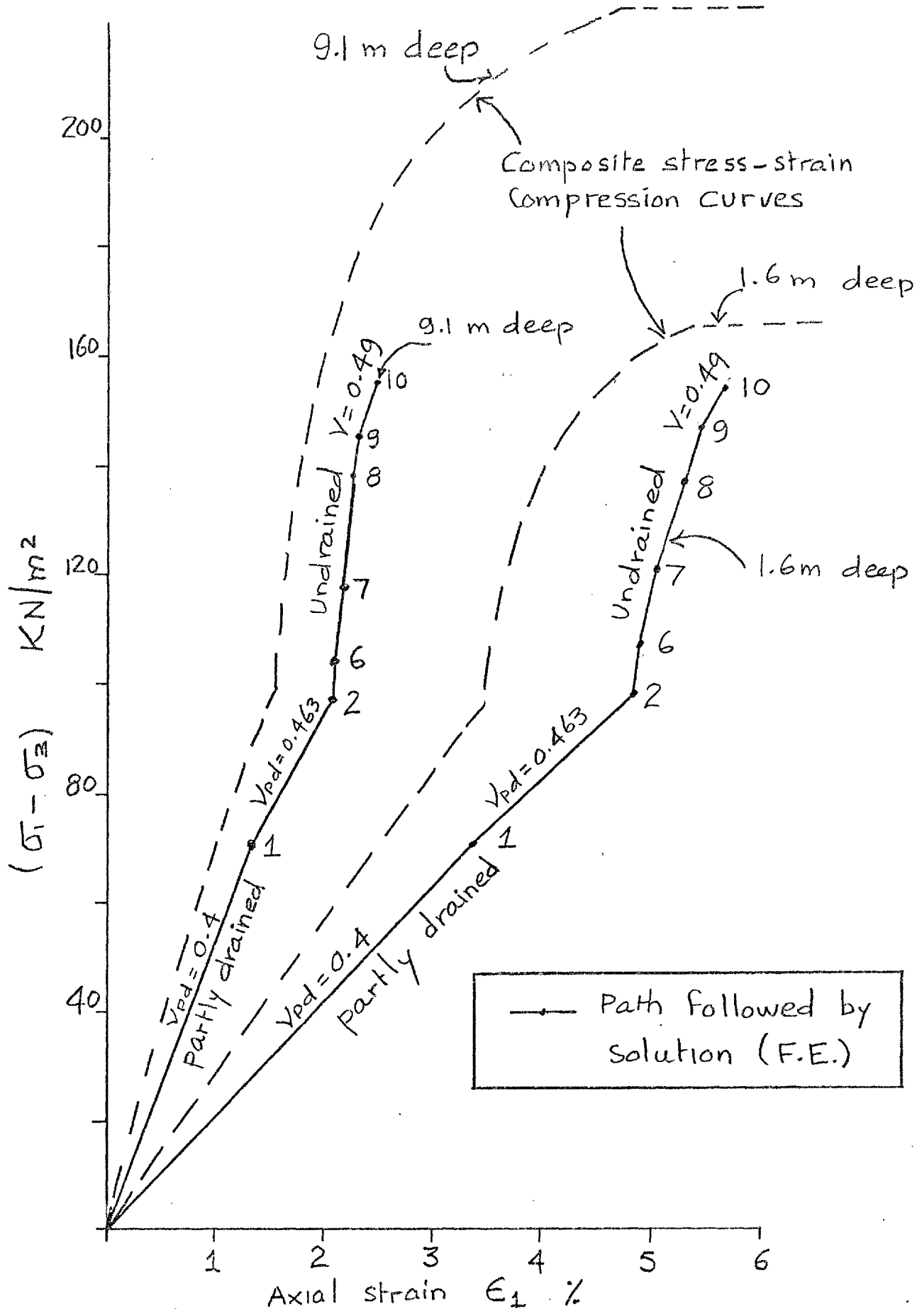
DEFORMATION AND STRENGTH PROPERTIES FOR SAND DRAIN ZONE_ FIRST AND SECOND YEARS

Fig. 7.7



DEFORMATION AND STRENGTH PROPERTIES FOR SAND DRAIN ZONE _ BEGINNING OF THE THIRD YEAR

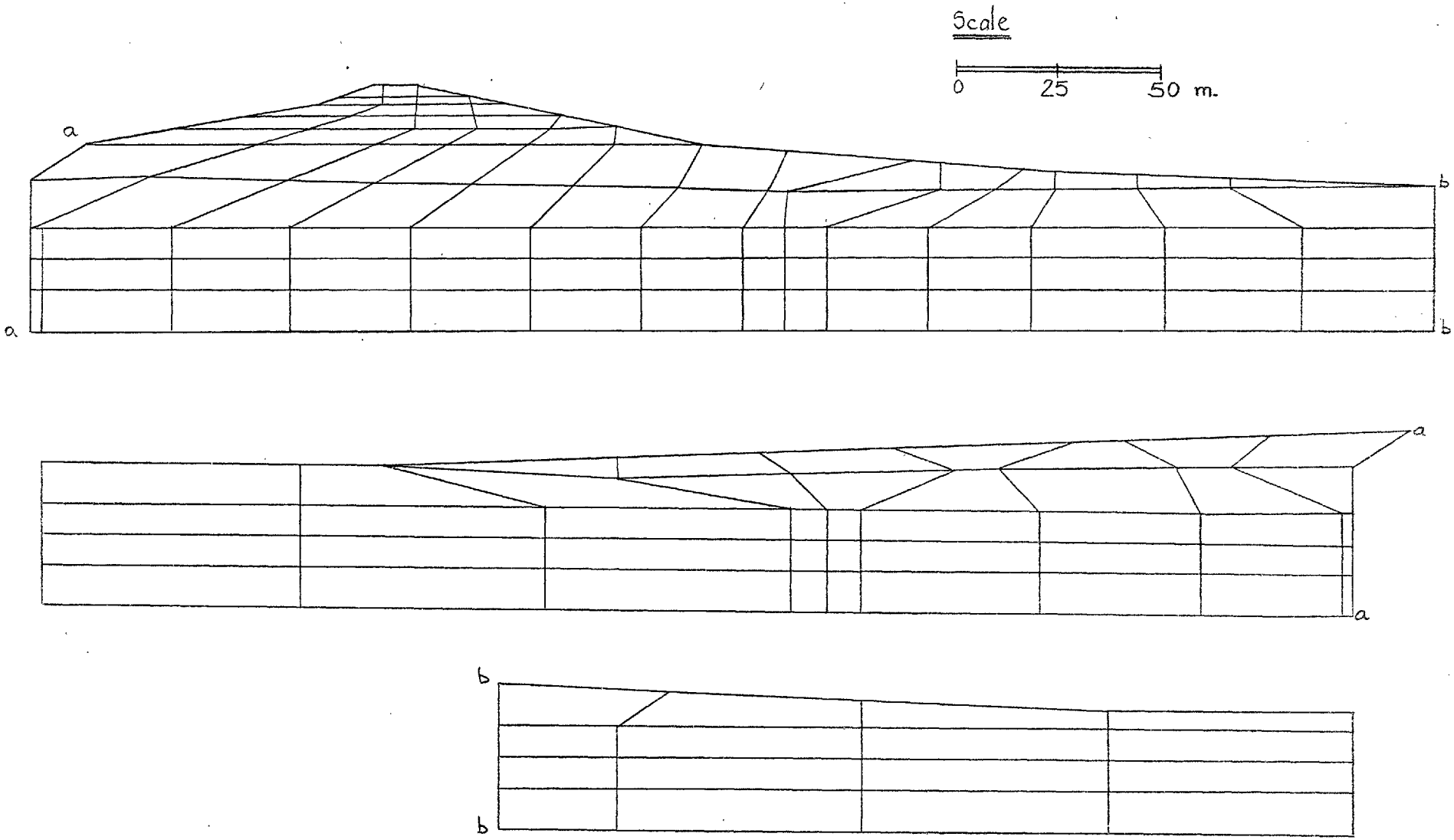
Fig. 7.8



COMPOSITE STRESS-STRAIN BEHAVIOUR

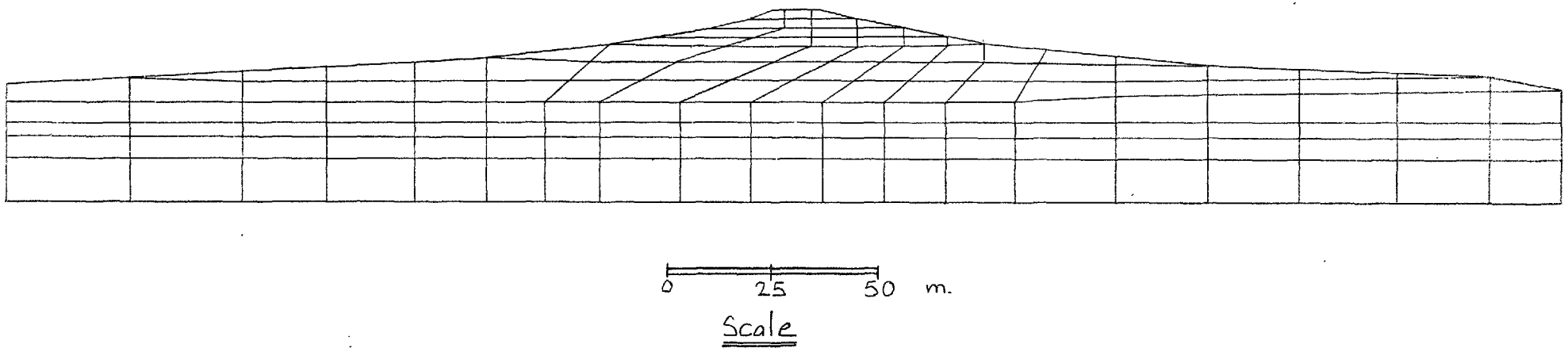
SAND DRAIN ZONE

Fig. 7.9



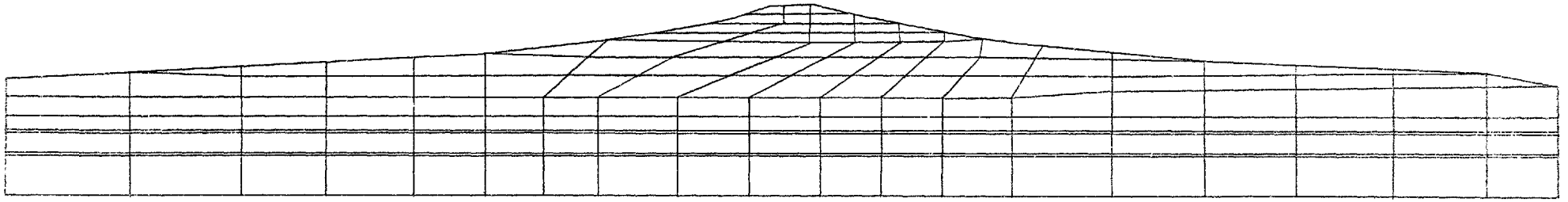
FINITE ELEMENT MESH _ MAIN DAM_ TYPICAL SECTION

Fig. 7.10



FINITE ELEMENT MESH _MAIN DAM_ NORTH SECTION_ NO WEAK LAYERS

Fig. 7.11

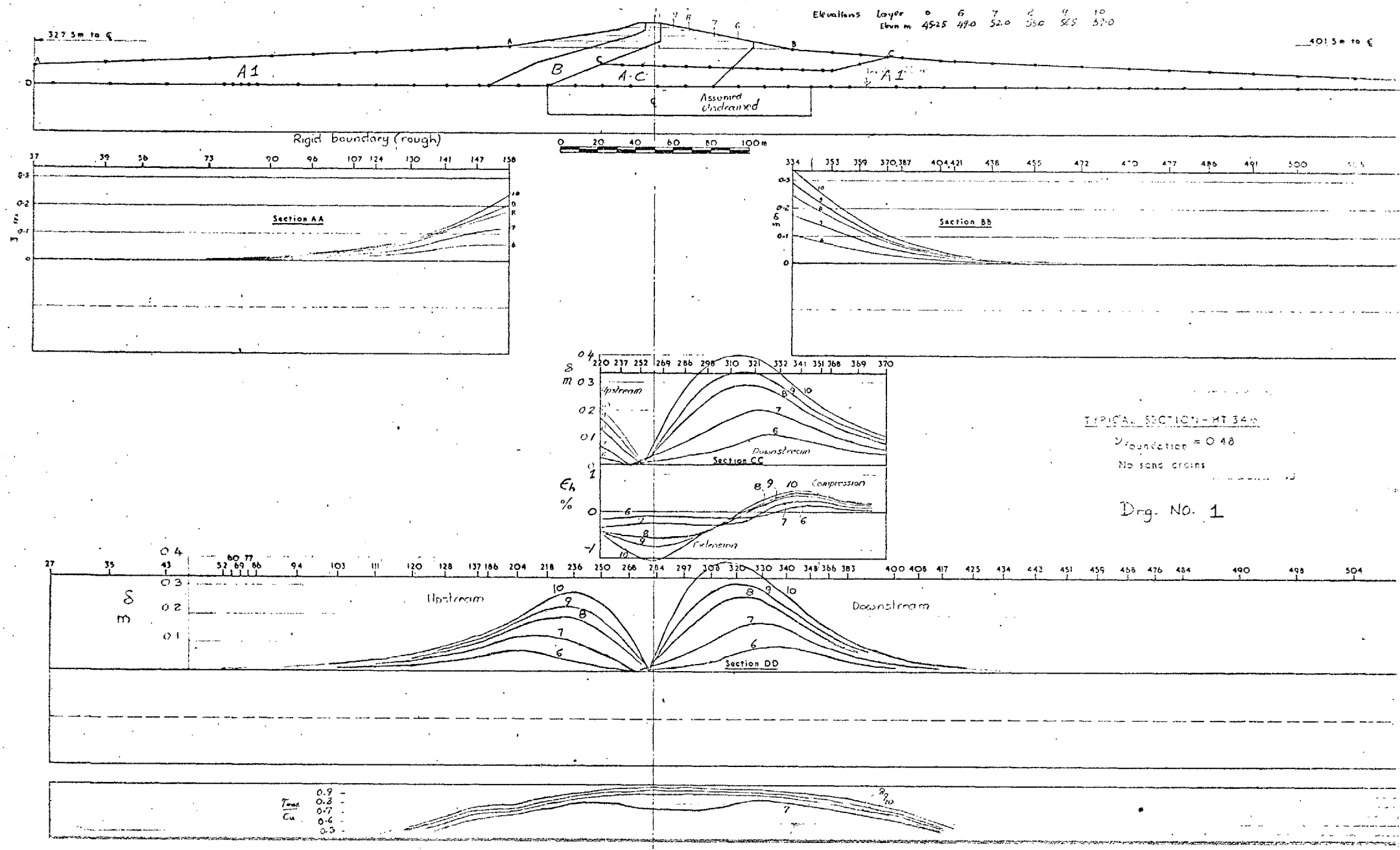


0 25 50 m.

Scale

FINITE ELEMENT MESH _ MAIN DAM _ NORTH SECTION _ WITH WEAK ZONES

Fig. 7.12



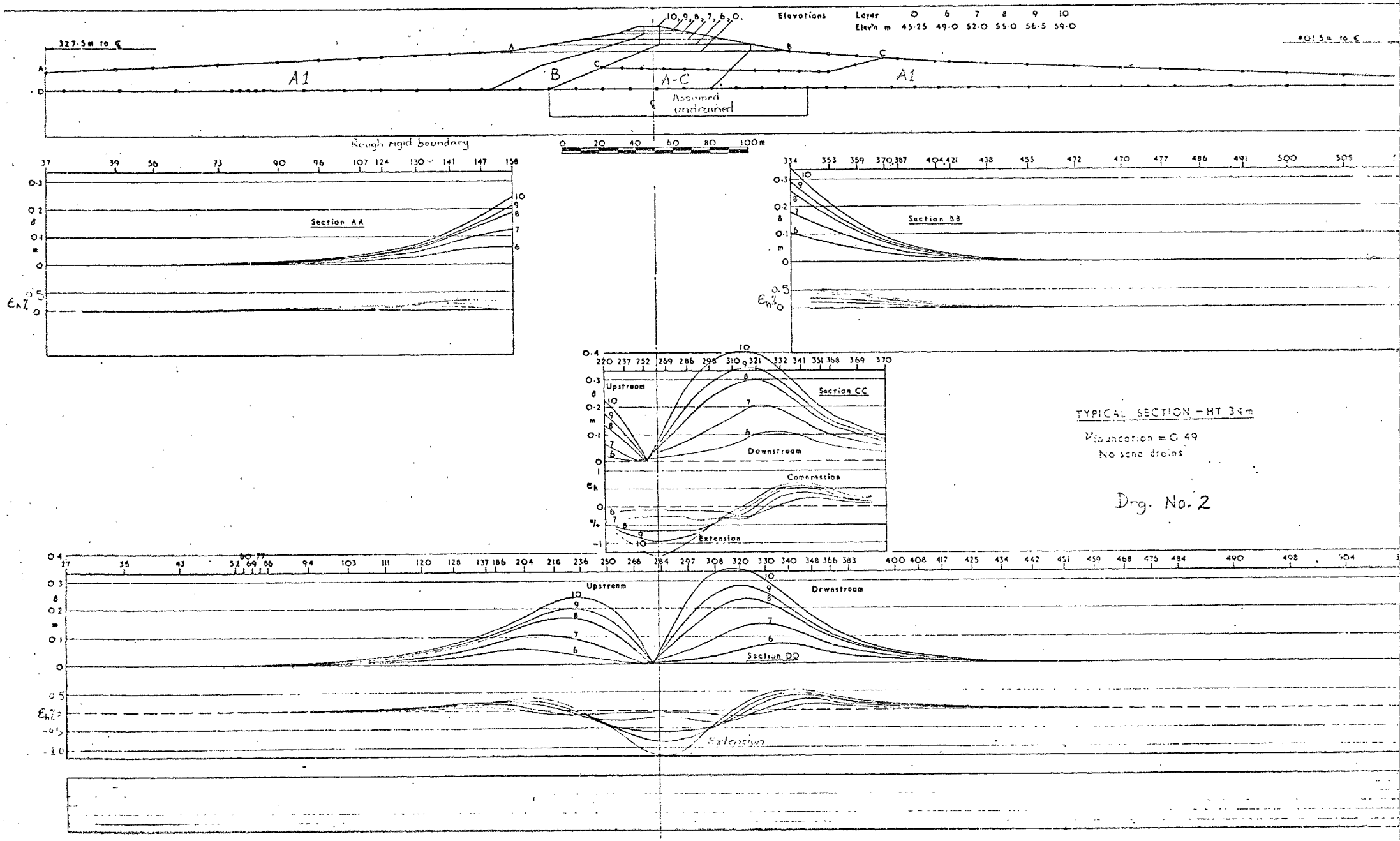
TYPICAL SECTION - HT 340

$\gamma_{foundation} = 0.48$

No sand drains

Drg. No. 1

Fig. 7.13


10, 9, 8, 7, 6, 0.
Elevations
Layer 0 6 7 8 9 10
Elev'n m 45·25 49·0 52·0 55·0 56·5 59·0
327·5m to ℄
401·5m to ℄
A1
B
A-C
A1
Assumed undrained
Rough rigid boundary
0 20 40 60 80 100m
Section AA
Section BB
Section CC
Upstream
Downstream
Compression
Extension
Section DD
TYPICAL SECTION – HT 34m
Mu junction = 0·49
No sand drains
Drg. No. 2
Fig. 7.14

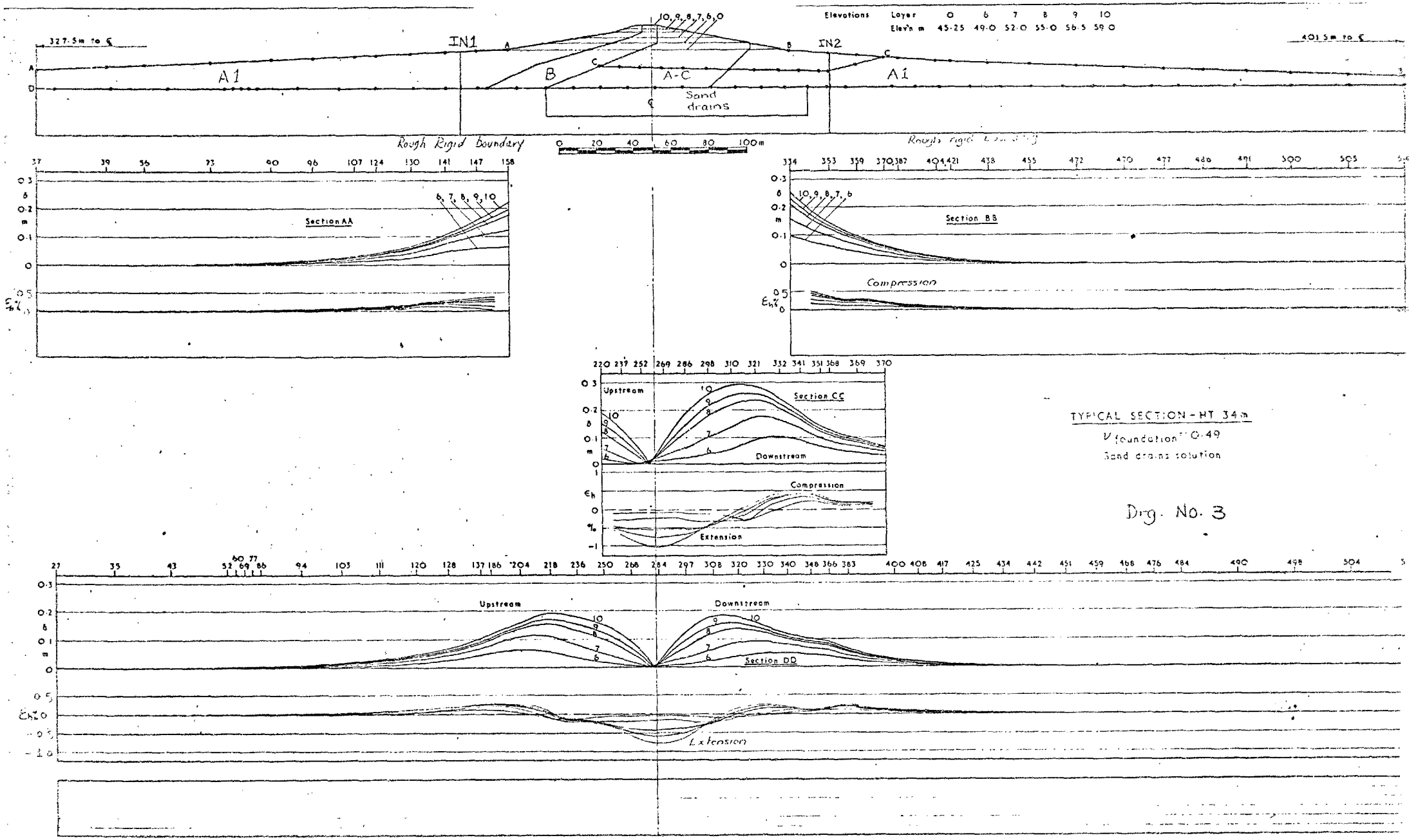

Elevations Layer 0 6 7 8 9 10
Elev'n m 45·25 49·0 52·0 55·0 56·5 59·0
327·5m to ℄
401·5m to ℄
IN1
IN2
A1
B
A-C
A1
Sand drains
Rough Rigid Boundary
0 20 40 60 80 100m
Section AA
Section BB
Compression
Extension
Upstream
Downstream
Section CC
Section DD
TYPICAL SECTION - HT 34 m
ν foundation = 0·49
Sand drains solution
Drg. No. 3

Fig. 715

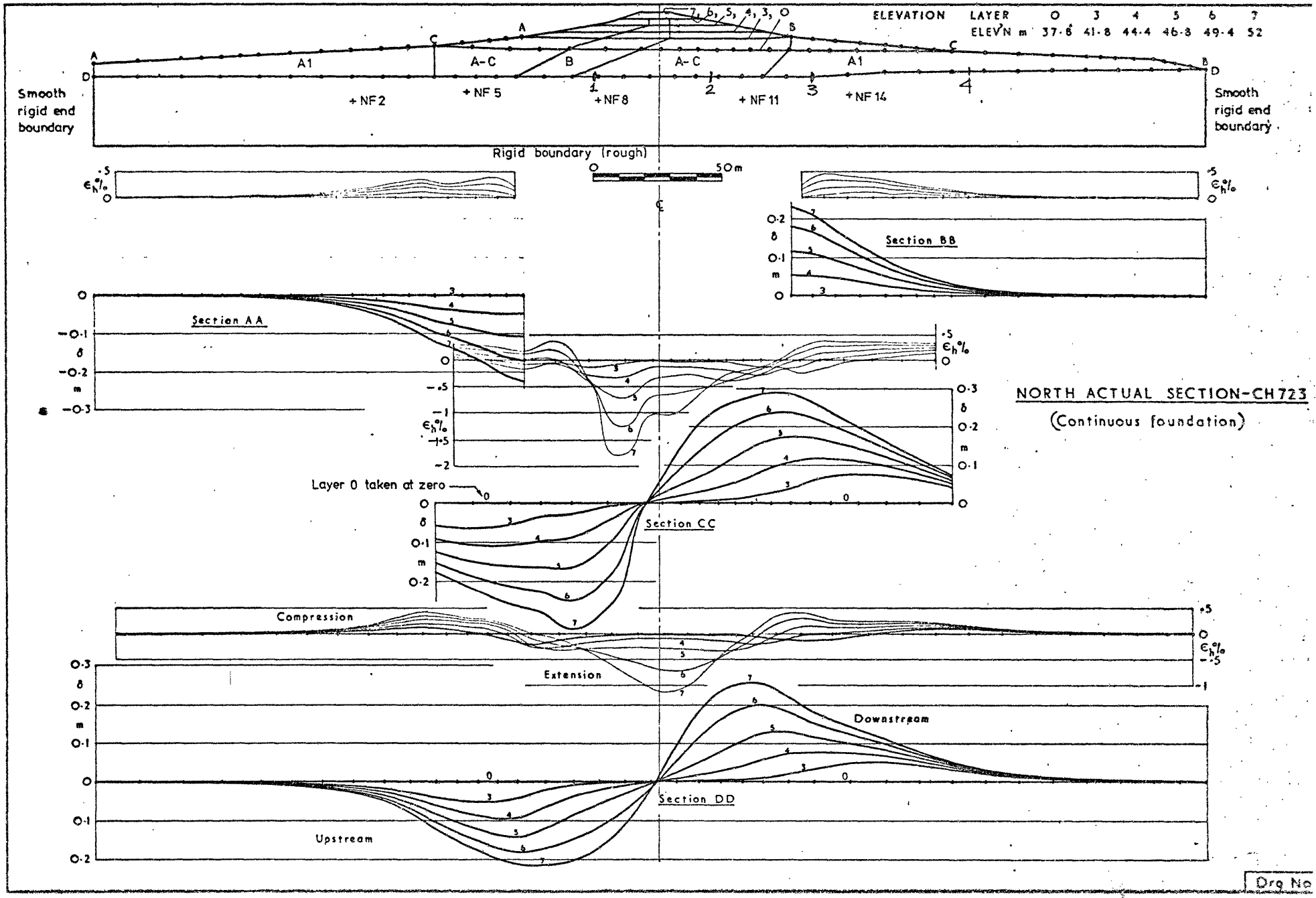
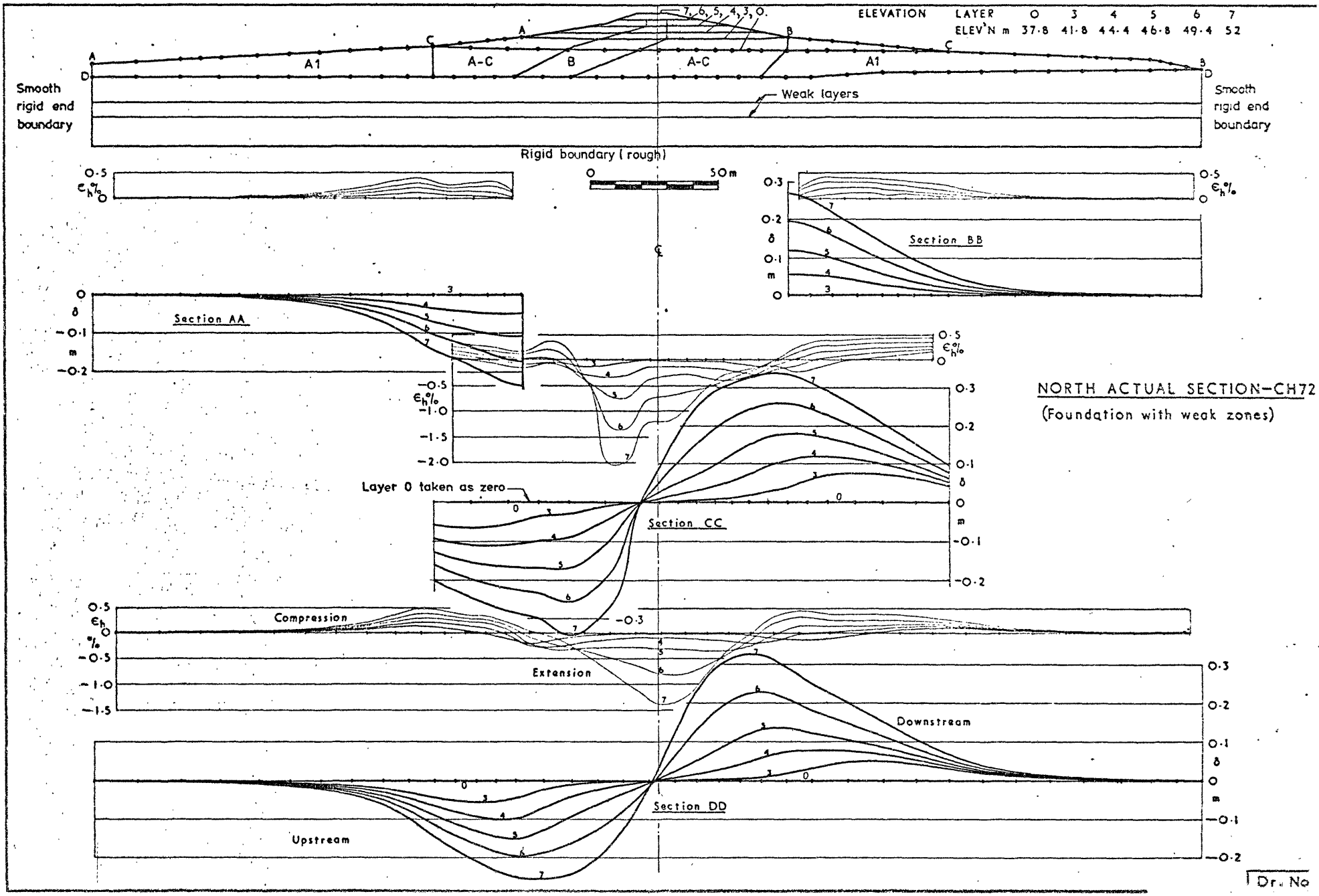

ELEVATION
LAYER 0 3 4 5 6 7
ELEVN m 37·6 41·8 44·4 46·8 49·4 52
A1
A-C
B
A-C
A1
+NF 2
+NF 5
+NF 8
+NF 11
+NF 14
Smooth rigid end boundary
Smooth rigid end boundary
Rigid boundary (rough)
50m
Section BB
Section AA
Layer 0 taken at zero
Section CC
Compression
Extension
Downstream
Upstream
Section DD
NORTH ACTUAL SECTION-CH723
(Continuous foundation)
Drg No

Fig. 7.16



NORTH ACTUAL SECTION–CH72

(Foundation with weak zones)

Fig. 7.17

Dr. No

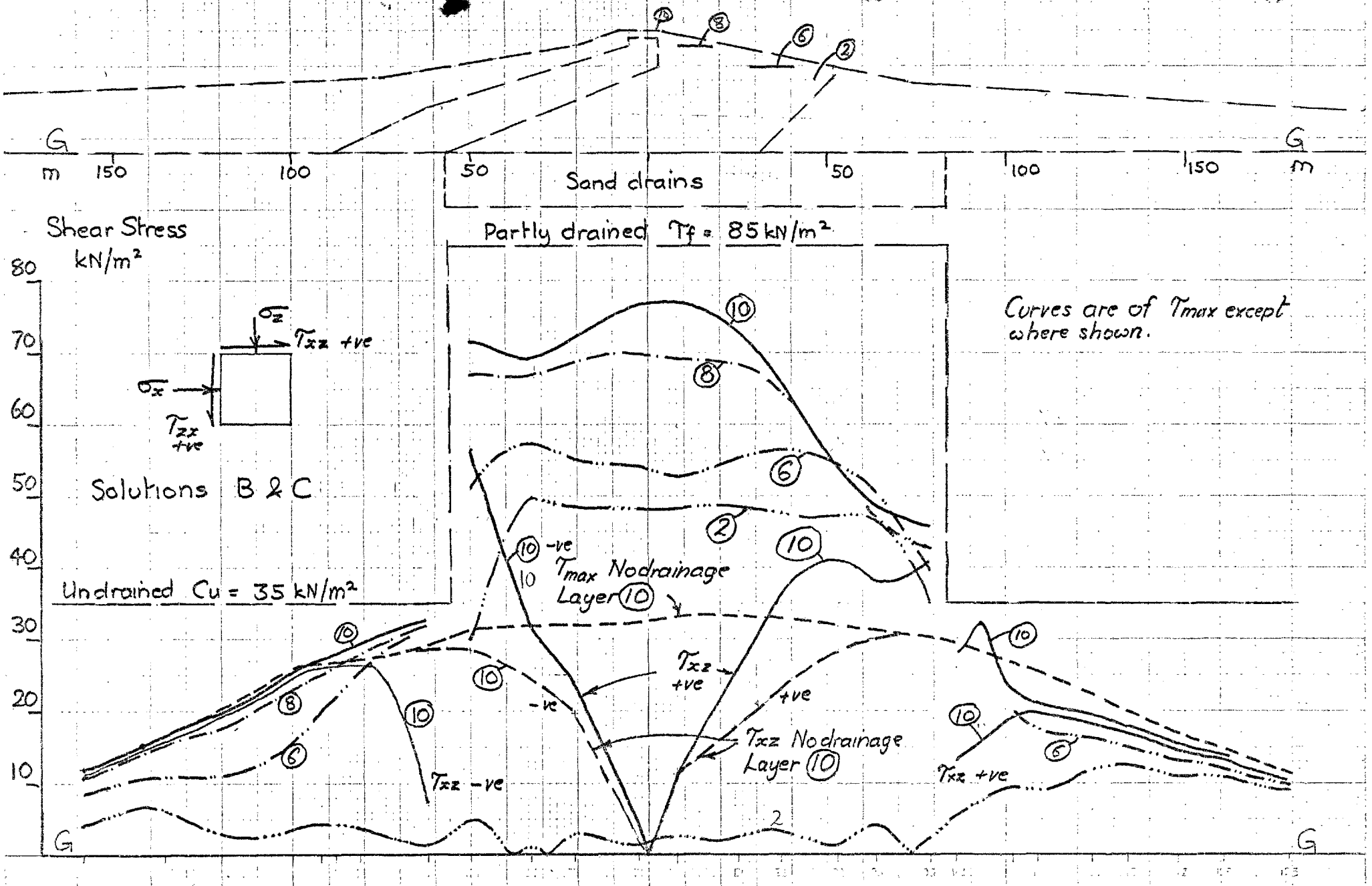
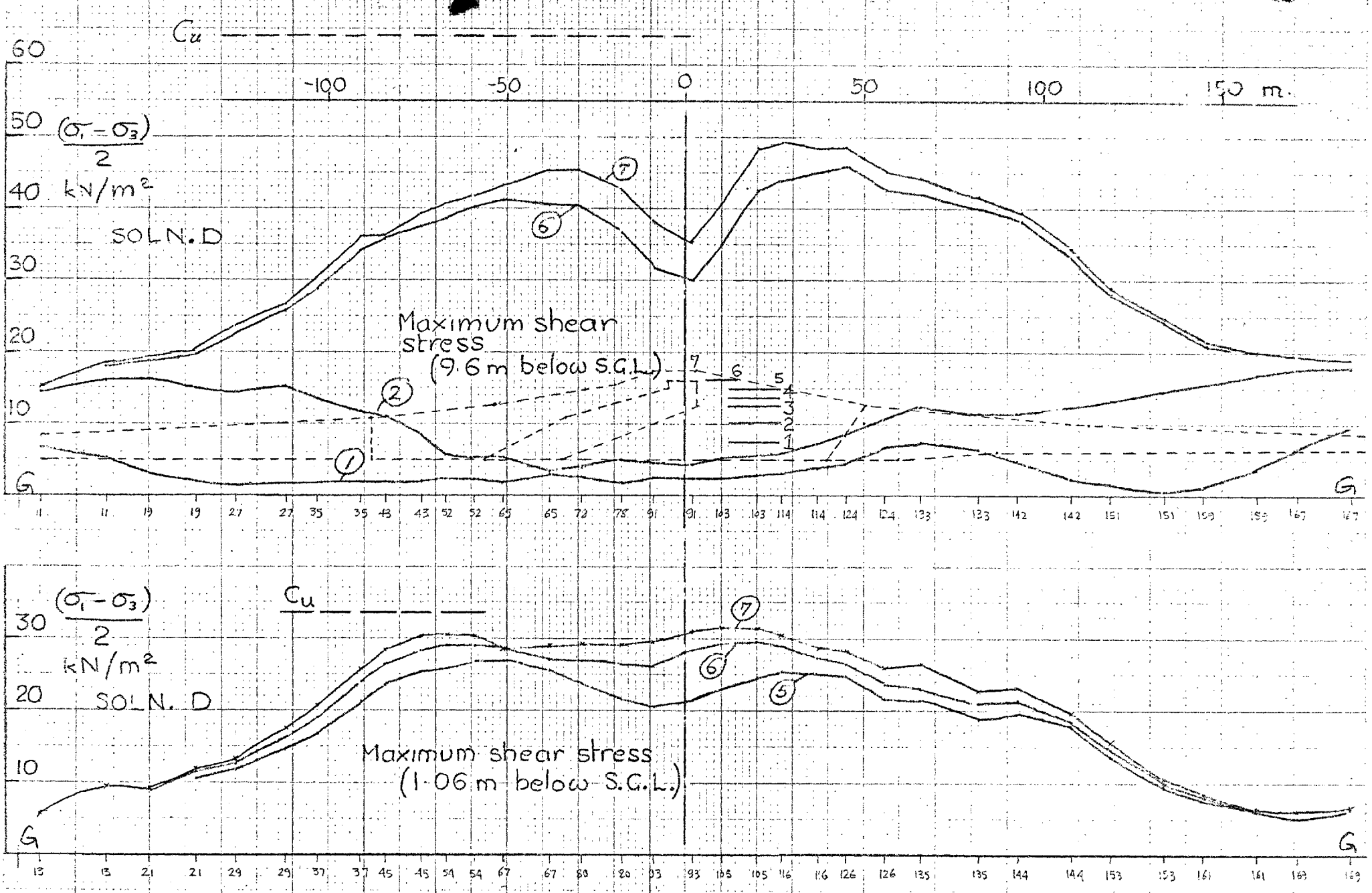


Fig. 7.18

SHEAR STRESS DEVELOPED TYPICAL SECTION STRESSES 1·6 m BELOW GROUND LEVEL



SHEAR STRESS DEVELOPED - NORTH SECTION - WITHOUT WEAK LAYERS

Fig. 7.19

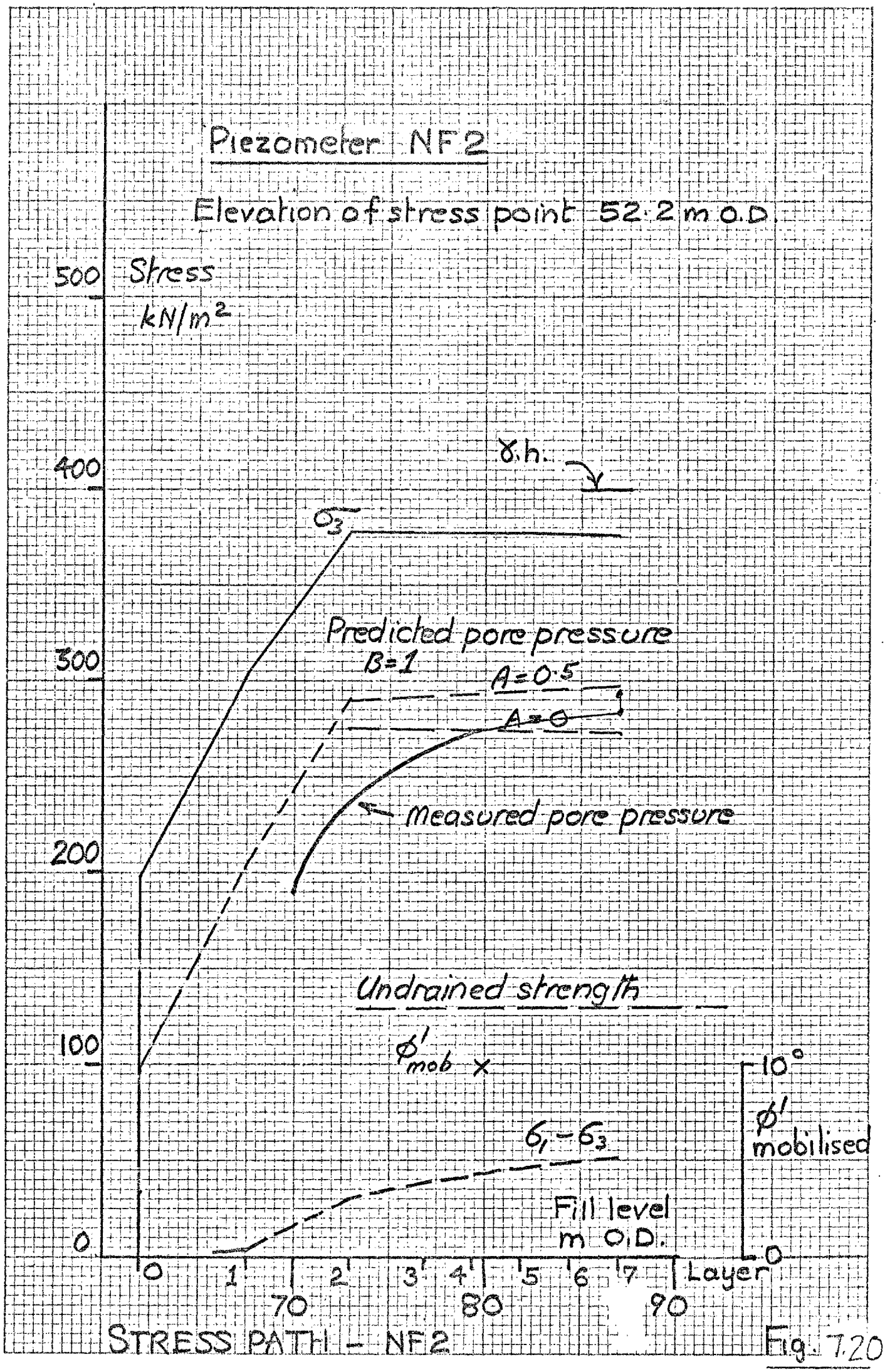
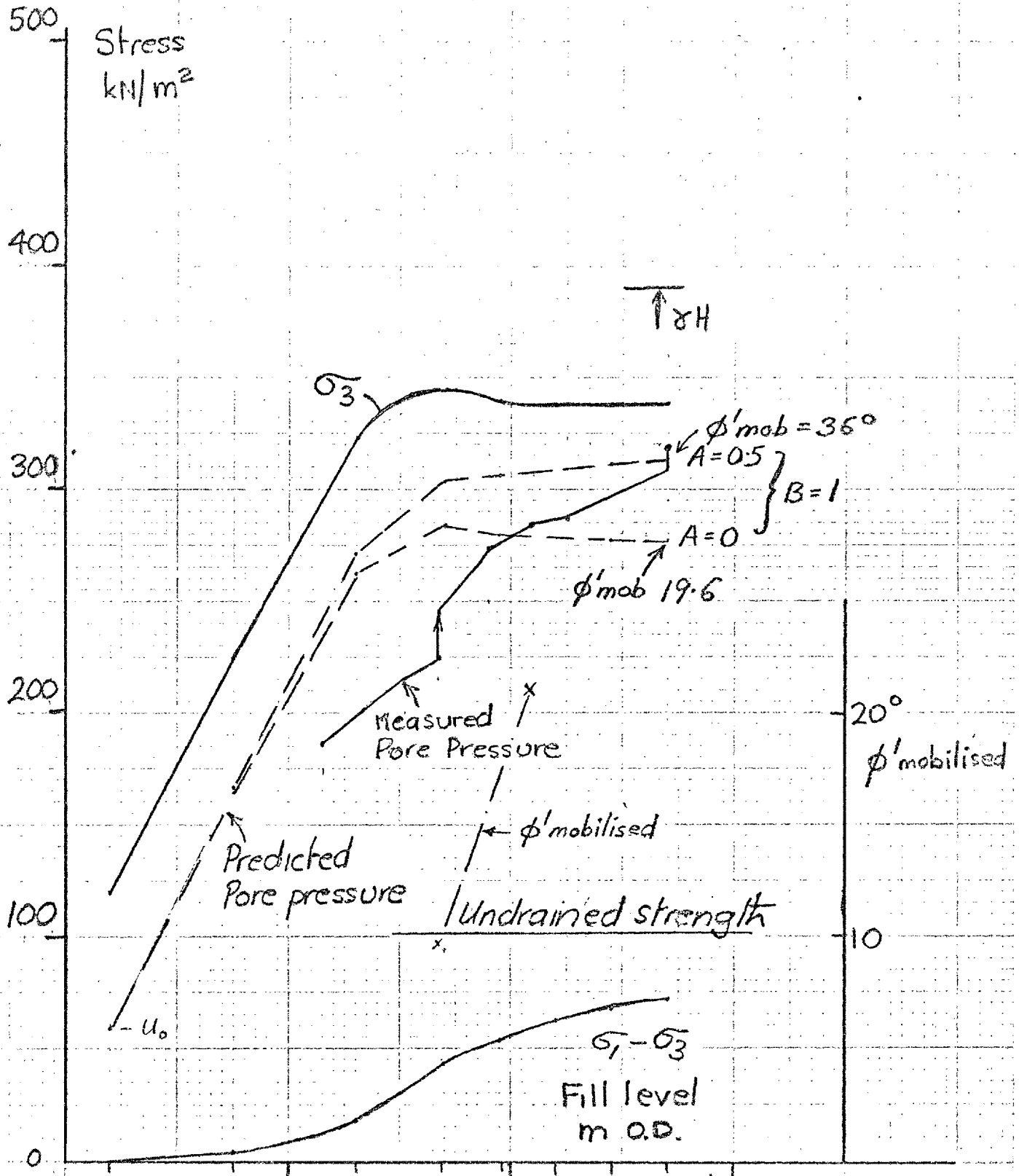

Piezometer NF2
Elevation of stress point 52·2 m O.D.
500
Stress
kN/m²
400
γ.h.
σ3
Predicted pore pressure
B=1
A=0·5
A=0
300
Measured pore pressure
200
Undrained strength
100
φ'mob
10°
φ'
mobilised
σ1−σ3
Fill level
m O.D.
0
0
1
2
3
4
5
6
7
Layer
0
70
80
90
STRESS PATH – NF2

Fig. 7.20

PIEZOMETER NF 5

Elevation of stress point 56·0 m o.d, 74·5 m u/s.



STRESS PATH - NF5

Fig. 7.21

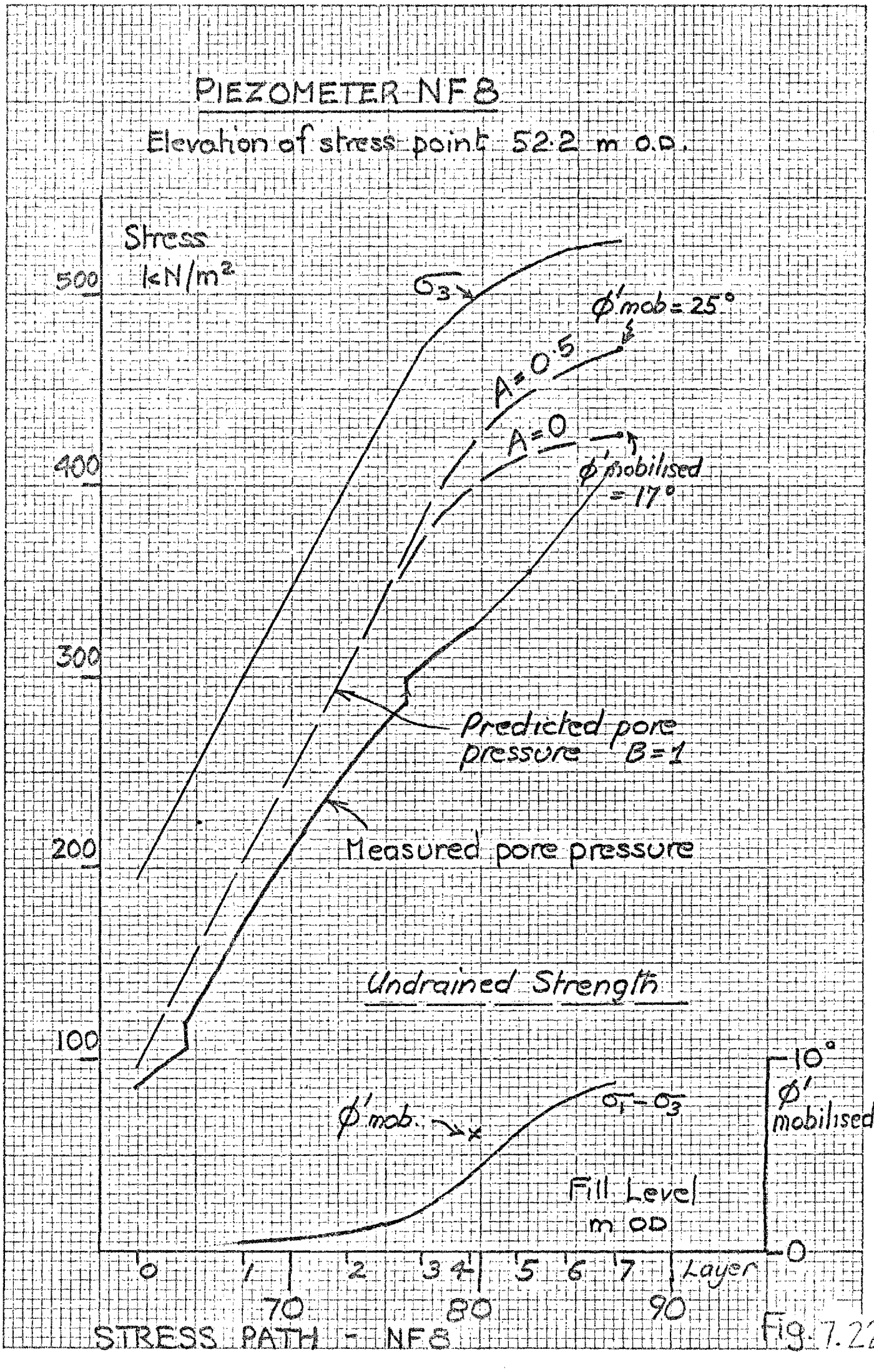
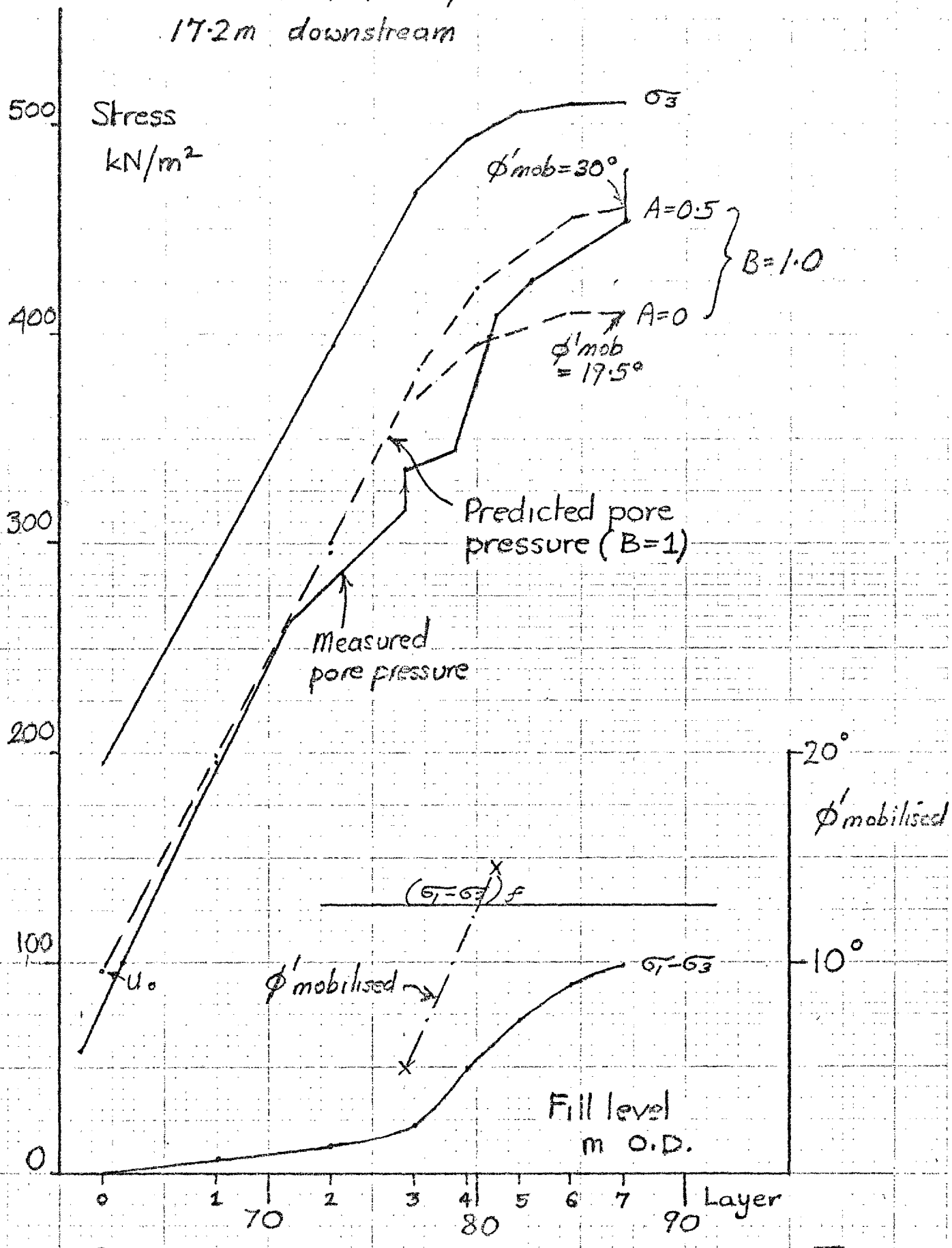

PIEZOMETER NF8
Elevation of stress point 52.2 m O.D.
Stress kN/m²
500
400
300
200
100
σ3
φ'mob = 25°
A=0.5
A=0
φ' mobilised = 17°
Predicted pore pressure B=1
Measured pore pressure
Undrained Strength
φ'mob.
σ1 − σ3
10°
φ' mobilised
0
Fill Level m OD
0
1
2
3
4
5
6
7
Layer
70
80
90
STRESS PATH - NF8

Fig. 7.22

PIEZOMETER NF 11

Elevation of stress point 52·2 m O.D.
17·2 m downstream

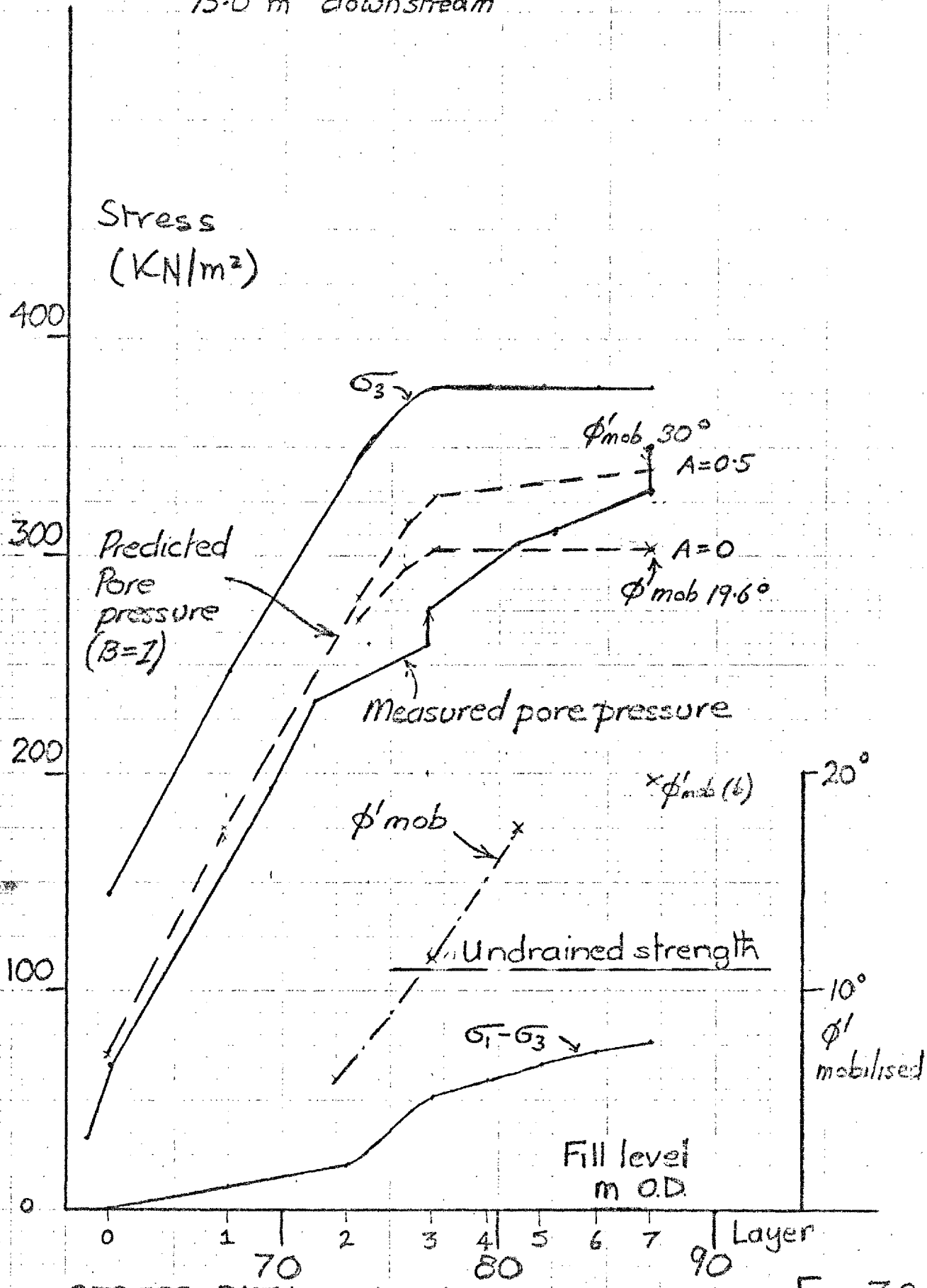


STRESS PATH - NF11

Fig. 7.23

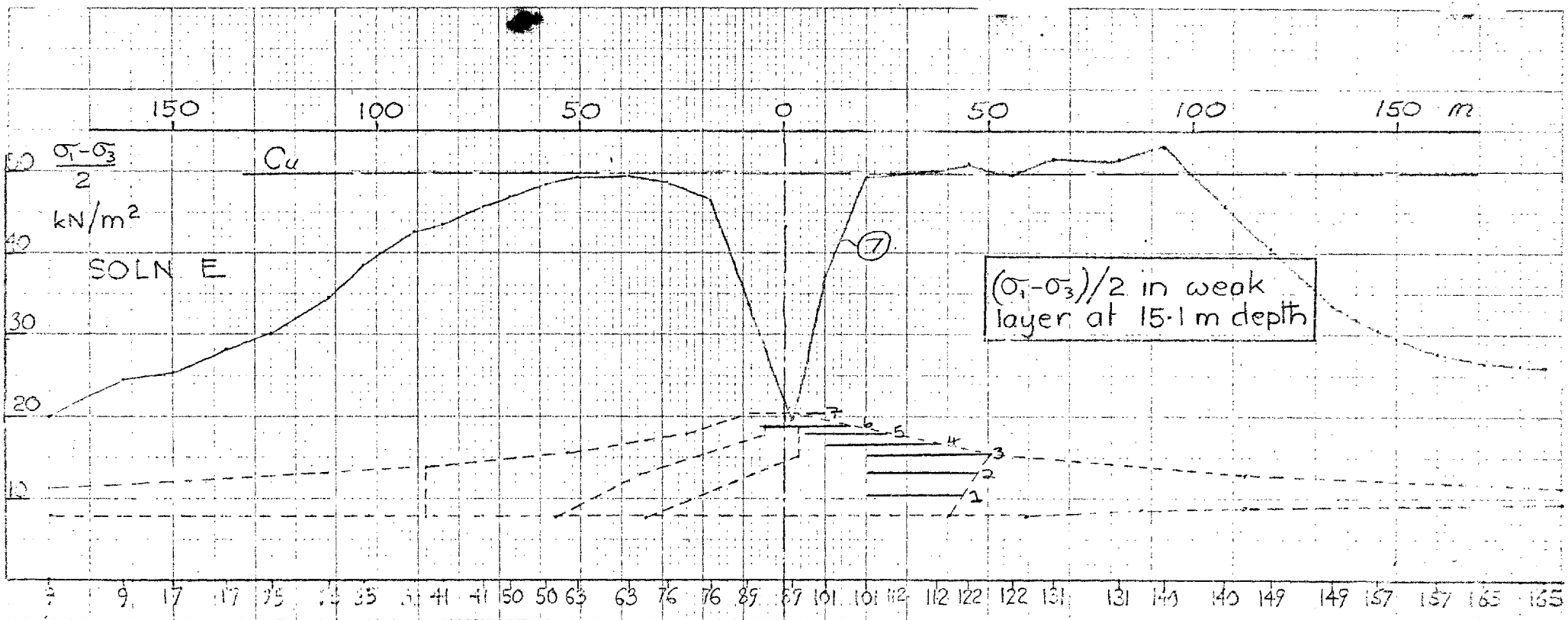
PIEZOMETER NF 14

Elevation of stress point 54.75 m OD
75.0 m downstream



STRESS PATH - NF 14

Fig. 7.24



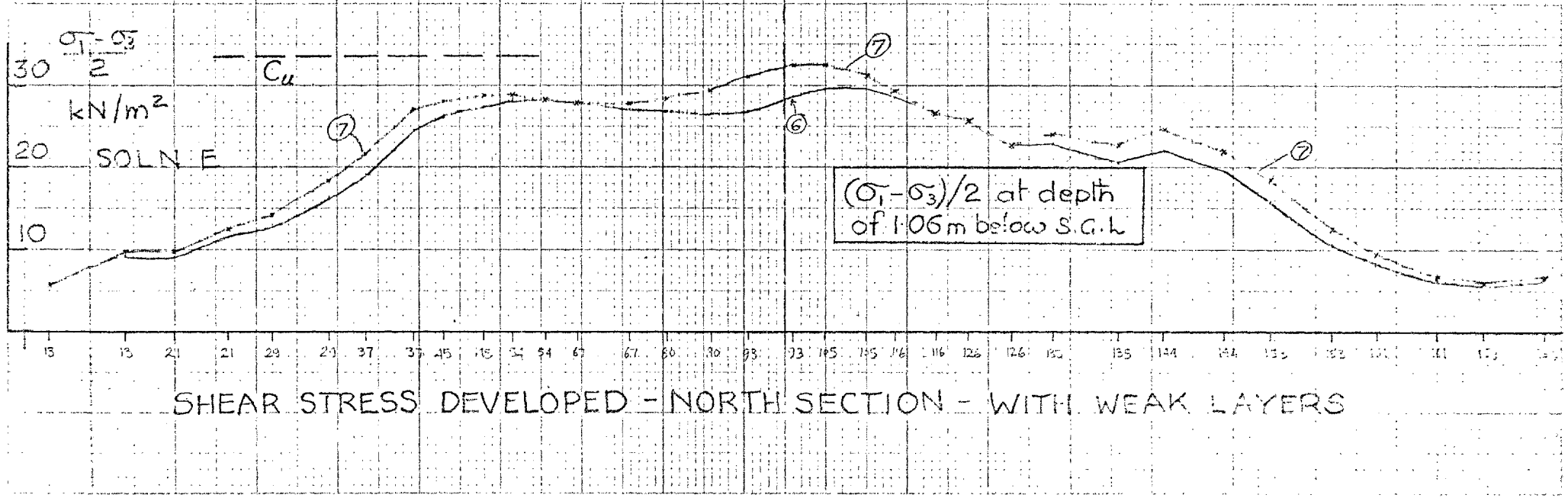


Fig. 7.25

SHEAR STRESS DEVELOPED - NORTH SECTION - WITH WEAK LAYERS

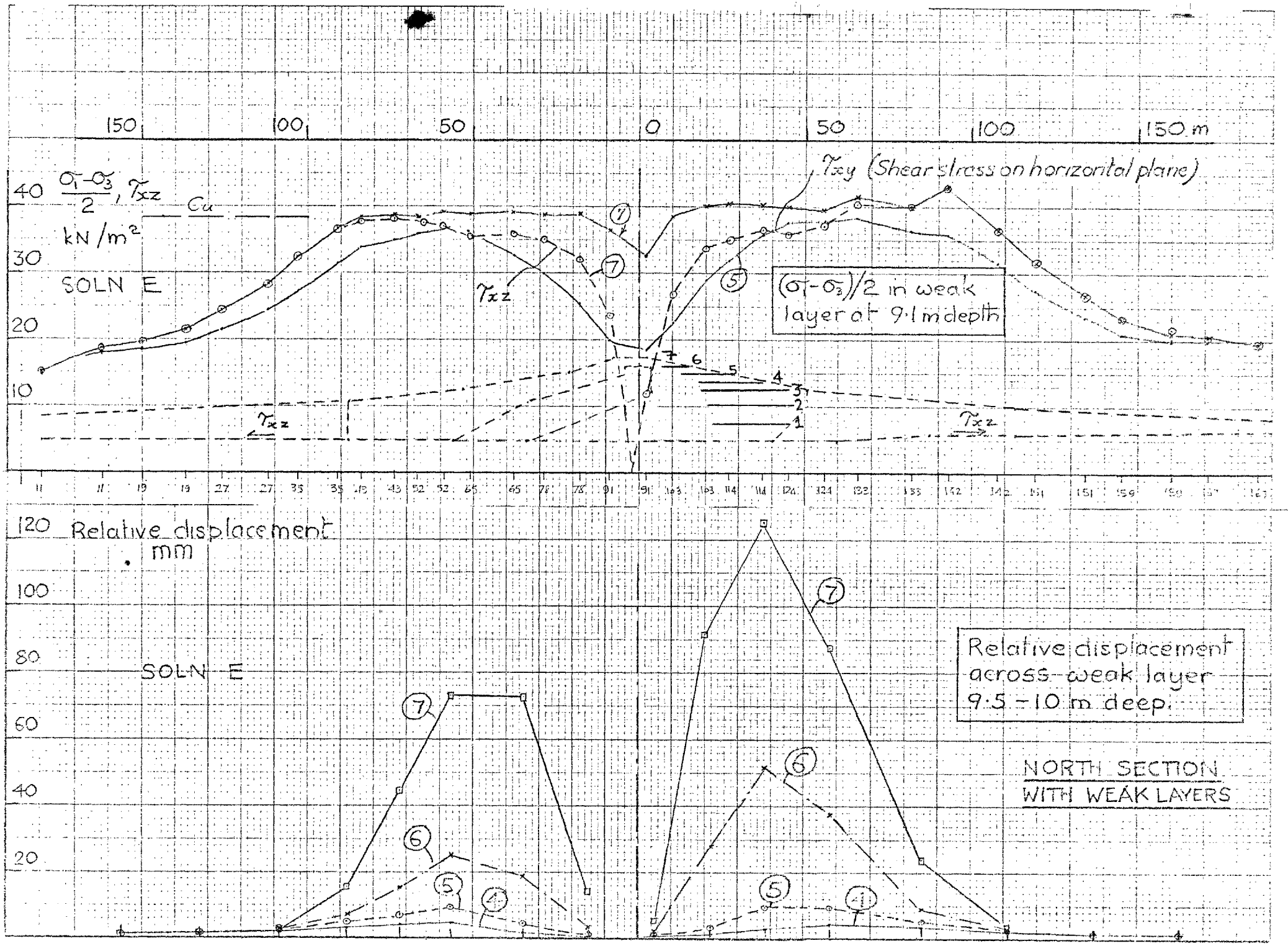

150
100
50
0
50
100
150 m
40
30
20
10
$\frac{\sigma_1-\sigma_3}{2}, \tau_{xz}$
Cu
kN/m²
SOLN E
τ_{xy} (Shear stress on horizontal plane)
τ_{xz}
$(\sigma_1-\sigma_3)/2$ in weak layer at 9.1 m depth
7
6
5
4
3
2
1
τ_{xz}
τ_{xz}
120
Relative displacement
mm
100
80
60
40
20
SOLN E
Relative displacement across weak layer 9.5 - 10 m deep.
NORTH SECTION
WITH WEAK LAYERS

Fig 7.26

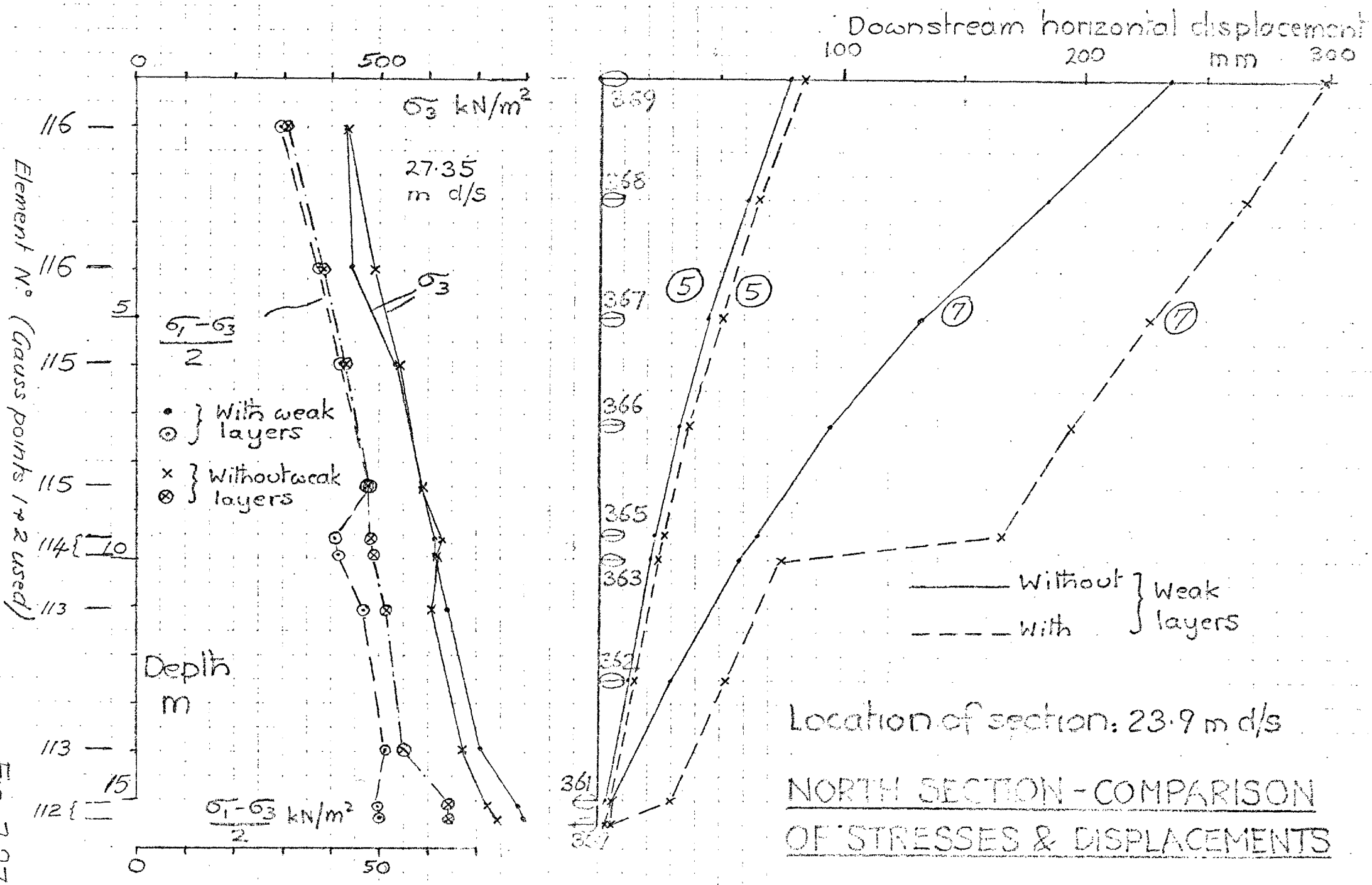
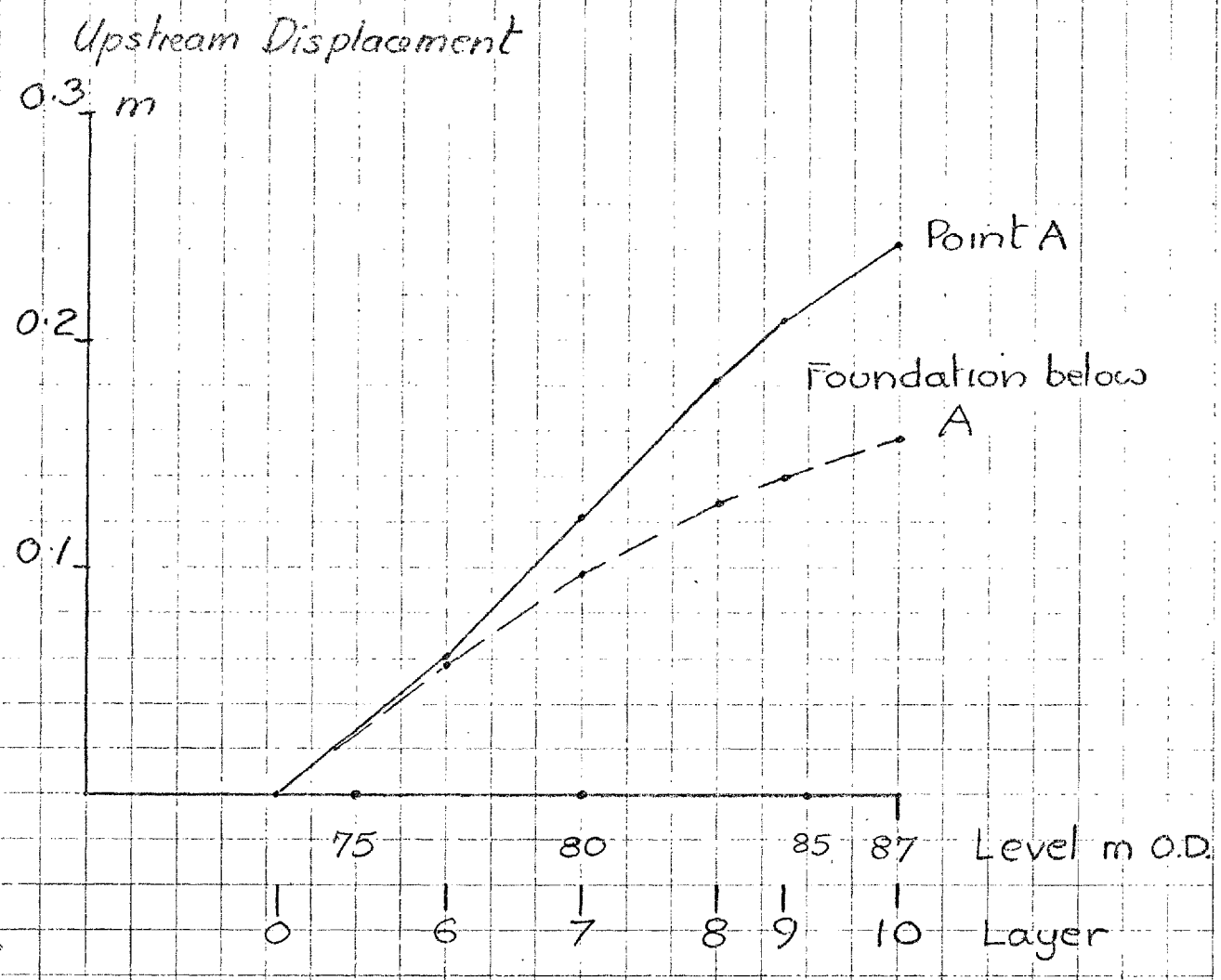
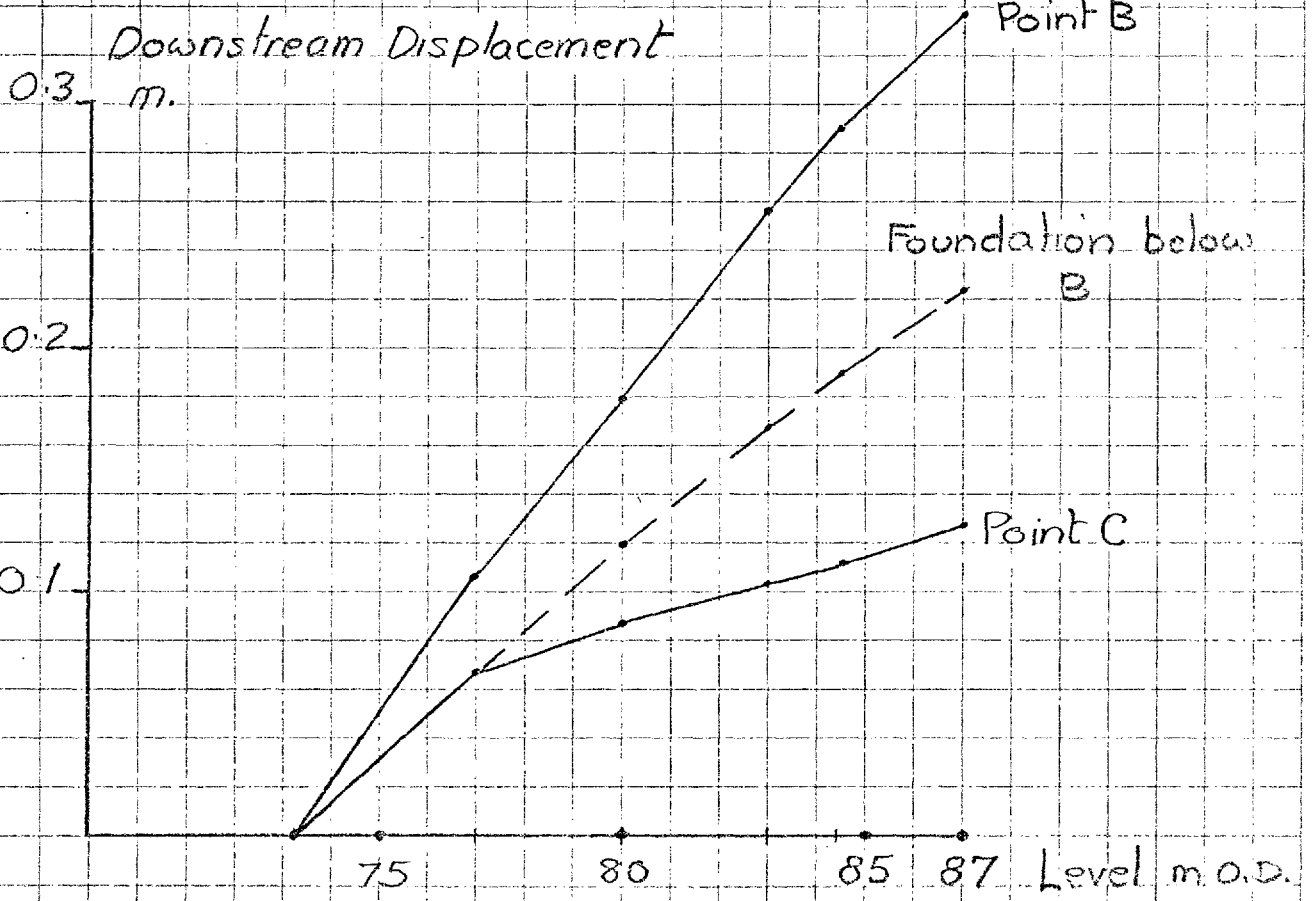

Downstream horizontal displacement
100
200
mm
300
0
500
$\bar{\sigma_3}$ kN/m²
27·35
m d/s
σ_3
$\frac{\sigma_1-\sigma_3}{2}$
With weak layers
Without weak layers
Element N° (Gauss points 1 & 2 used)
116
116
115
115
114
113
113
112
5
10
15
Depth
m
$\frac{\sigma_1-\sigma_3}{2}$ kN/m²
0
50
359
358
357
366
365
363
362
361
360
5
5
7
7
Without
With
Weak layers
Location of section: 23·9 m d/s
NORTH SECTION - COMPARISON OF STRESSES & DISPLACEMENTS

Fig. 7.27

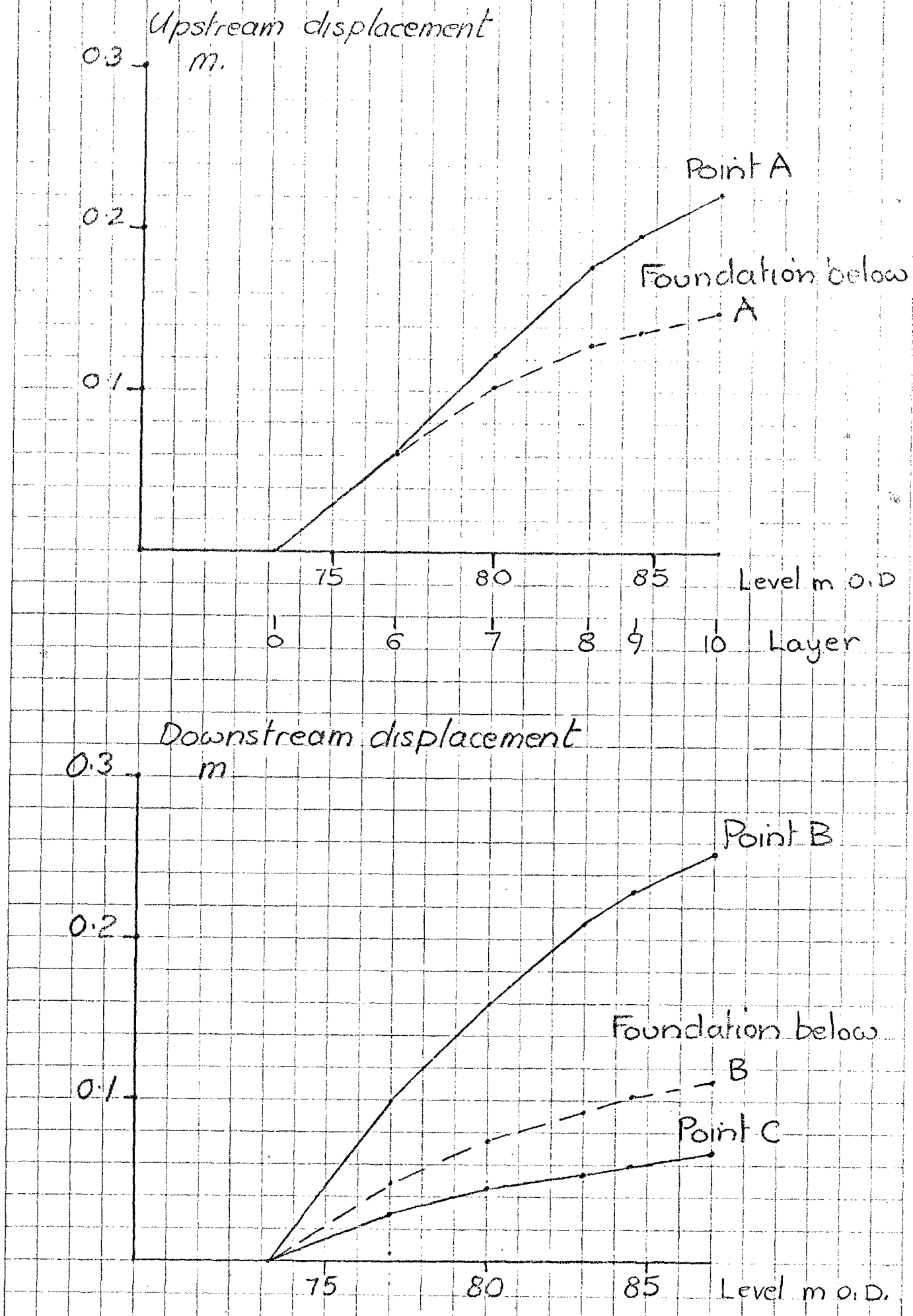




MAIN SECTION (B) - $\nu = 0.49$ - NO SAND DRAINS

Fig. 7.28

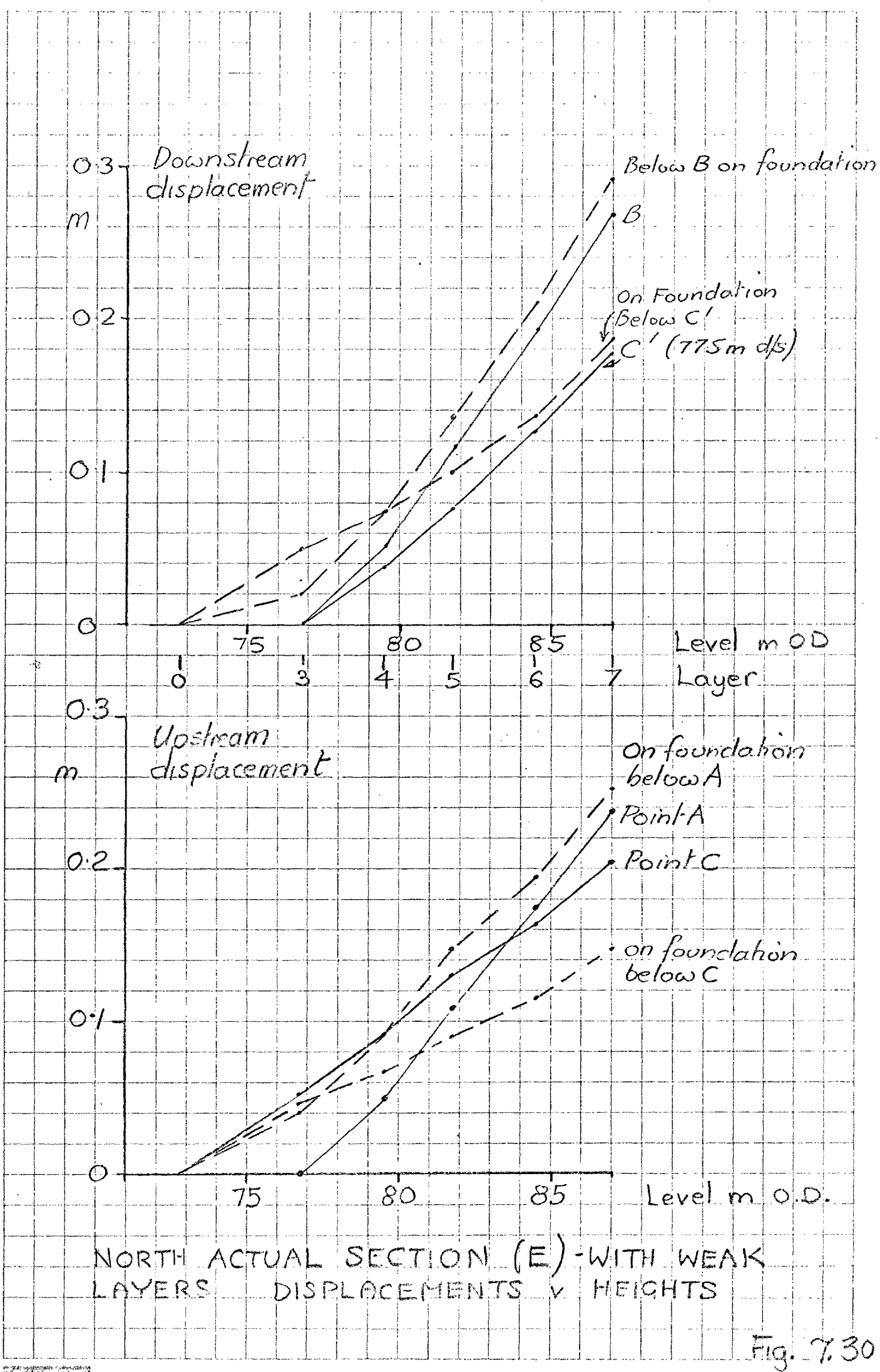
A4 210 x 297 mm



MAIN SECTION (C) - $\nu = 0.49$ - WITH SAND DRAINS

Fig 7.29

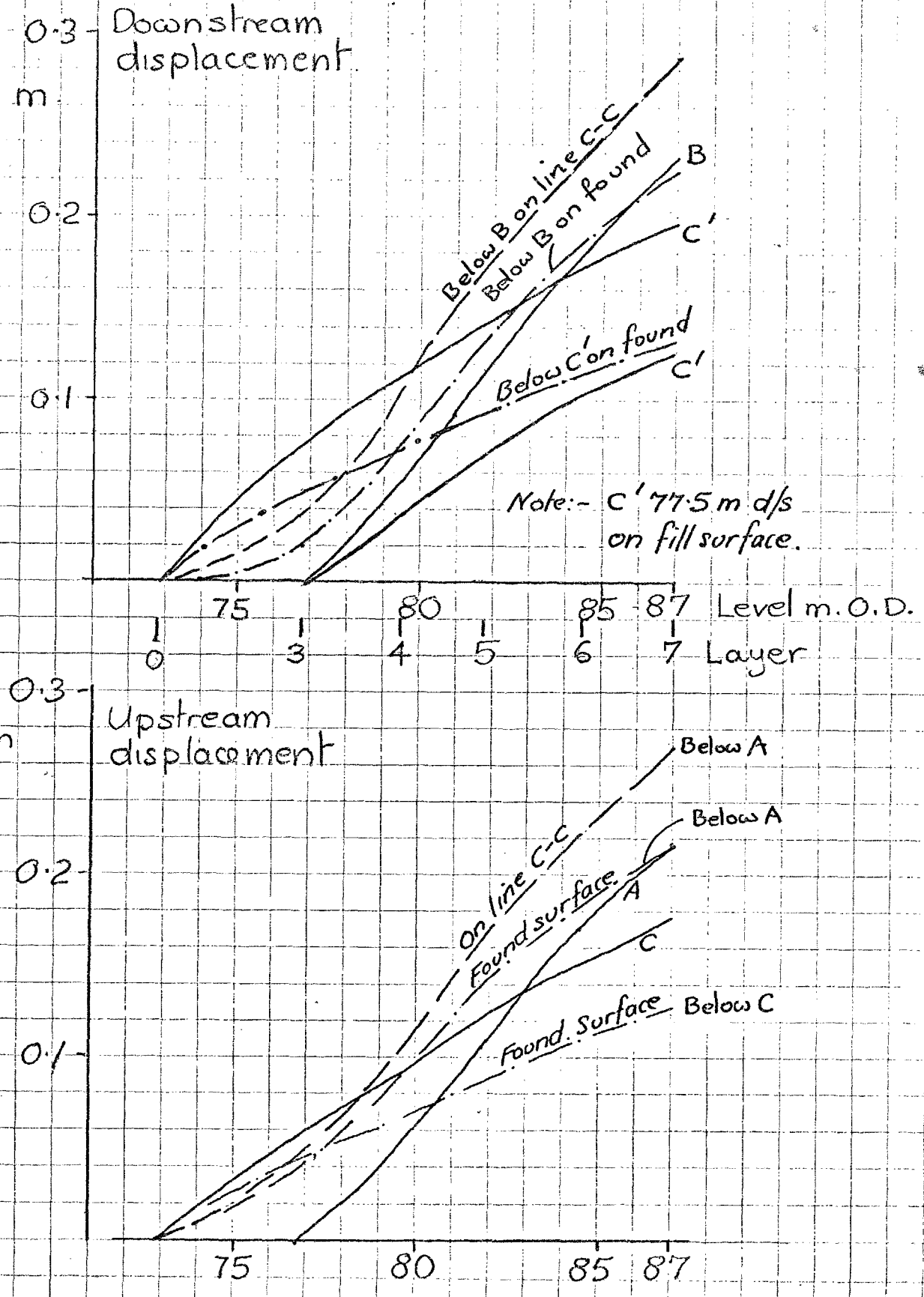
A4 210 x 297 mm



NORTH ACTUAL SECTION (E) - WITH WEAK LAYERS DISPLACEMENTS v HEIGHTS

Fig. 7.30

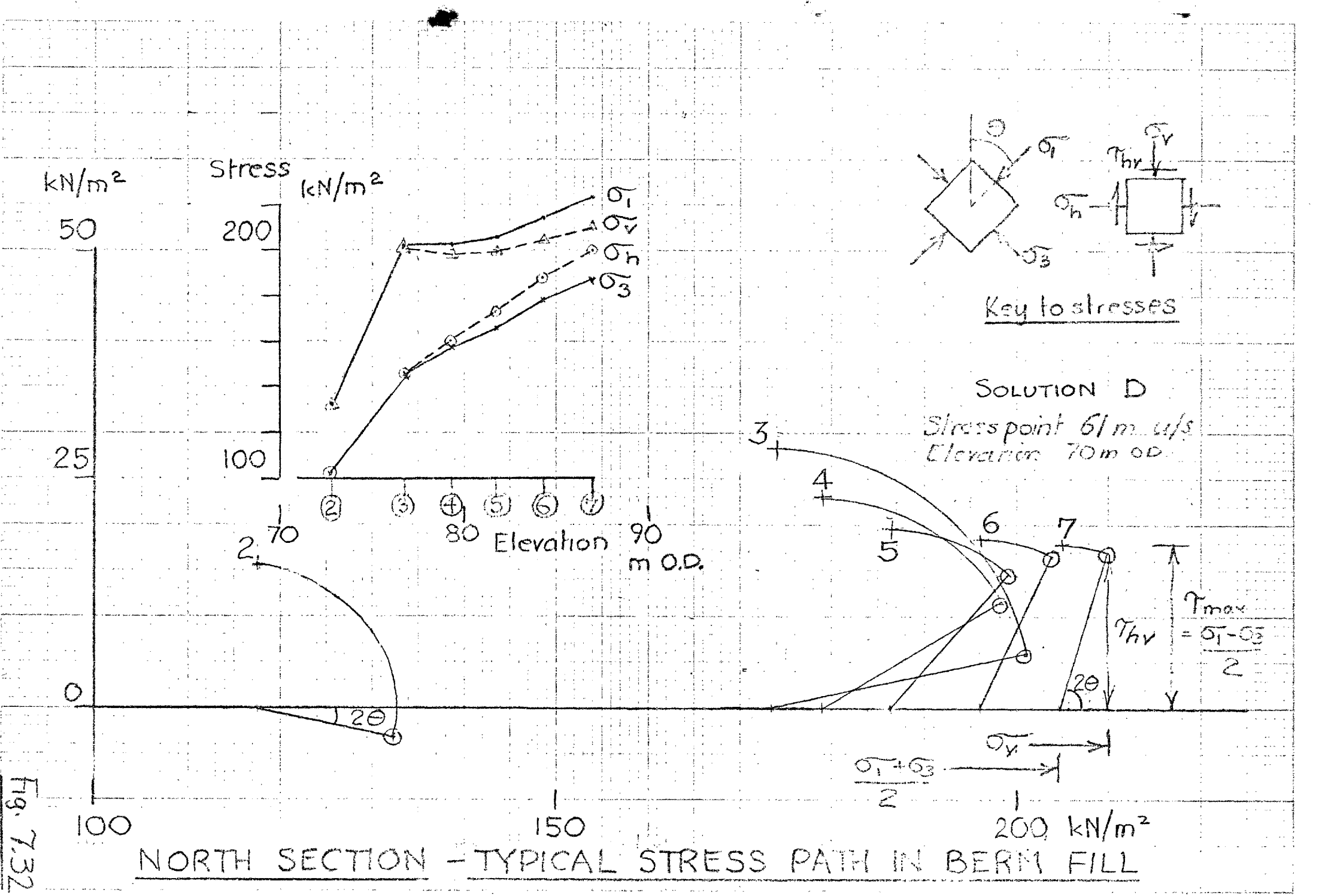
WELL A4 210 x 297 mm



NORTH ACTUAL SECTION (D) (NO WEAK LAYERS)
DISPLACEMENTS v FILL HEIGHTS

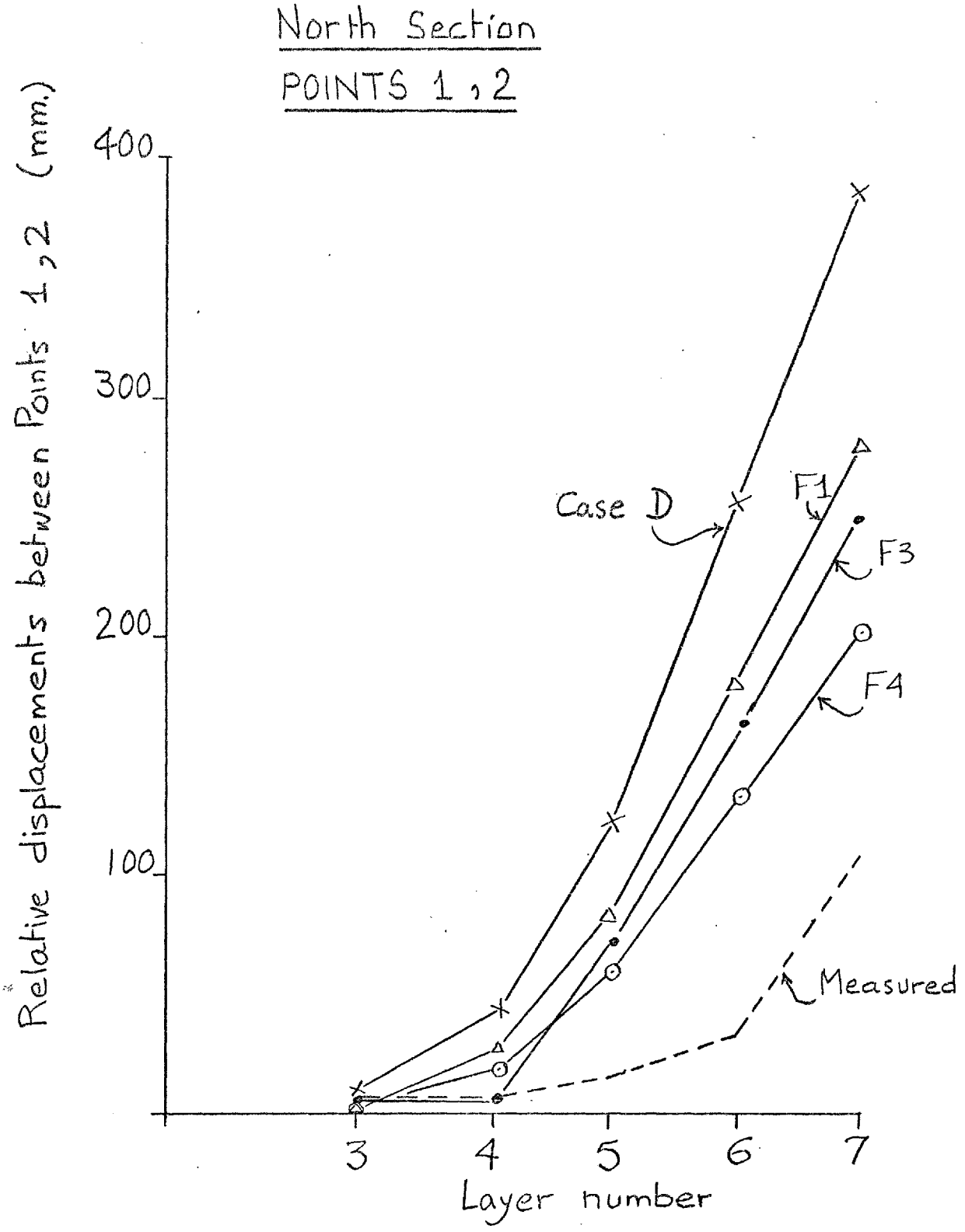
Fig. 7.31

W.R.L. A4 210 x 297 mm



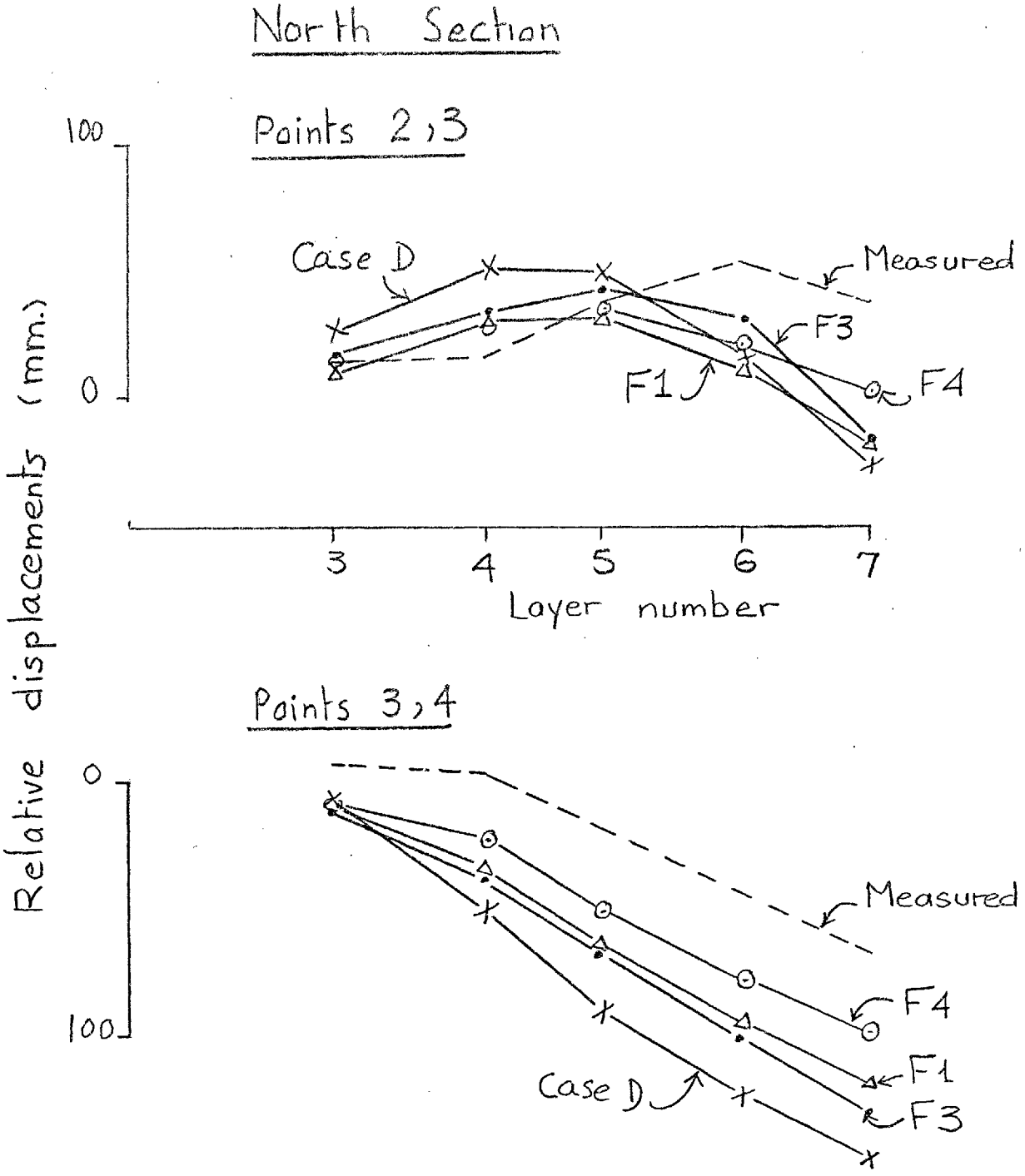
NORTH SECTION - TYPICAL STRESS PATH IN BERM FILL

Fig. 7.32



PREDICTED AND MEASURED HORIZONTAL MOVEMENTS_ CASES : D , F1 , F3 , F4

Fig. 7.33



PREDICTED AND MEASURED HORIZONTAL MOVEMENTS _ CASES : D , F1 , F3, F4

Fig 7.34

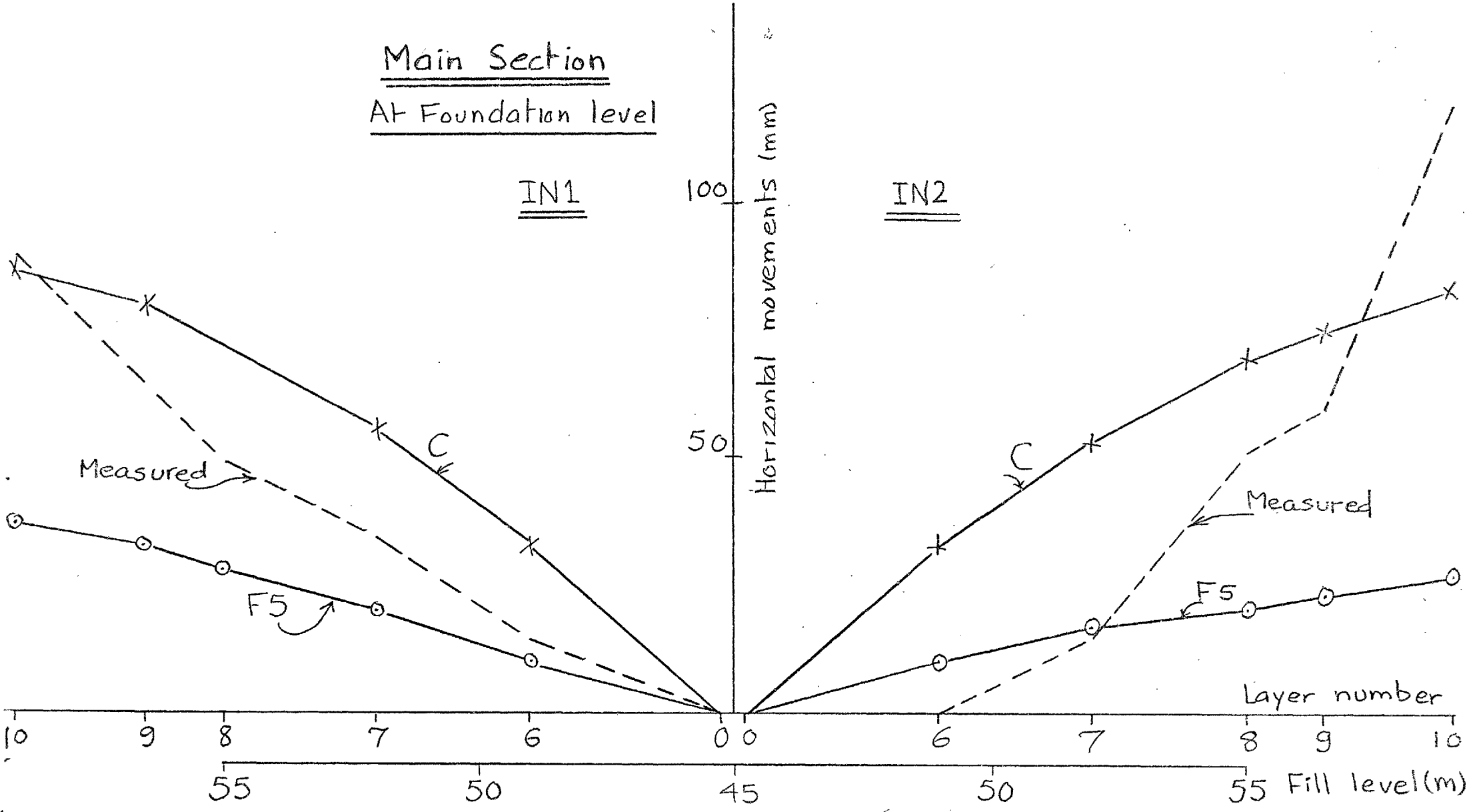


Fig. 7.35

PREDICTED AND MEASURED HORIZONTAL MOVEMENTS _ CASES C, F5 _ FOUNDATION

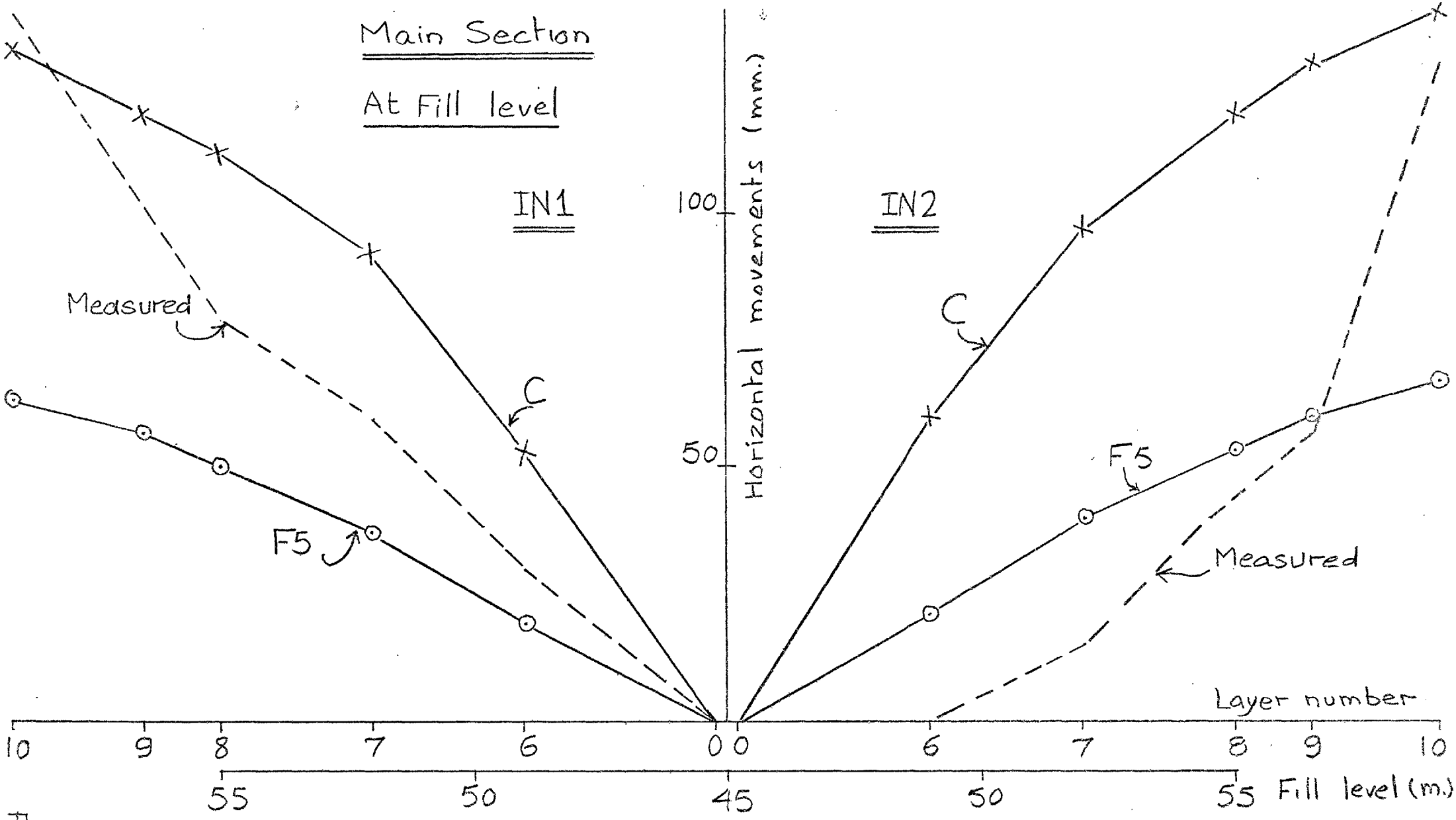


Fig. 7.35

PREDICTED AND MEASURED HORIZONTAL MOVEMENTS_ CASES C , F5 _ FILL

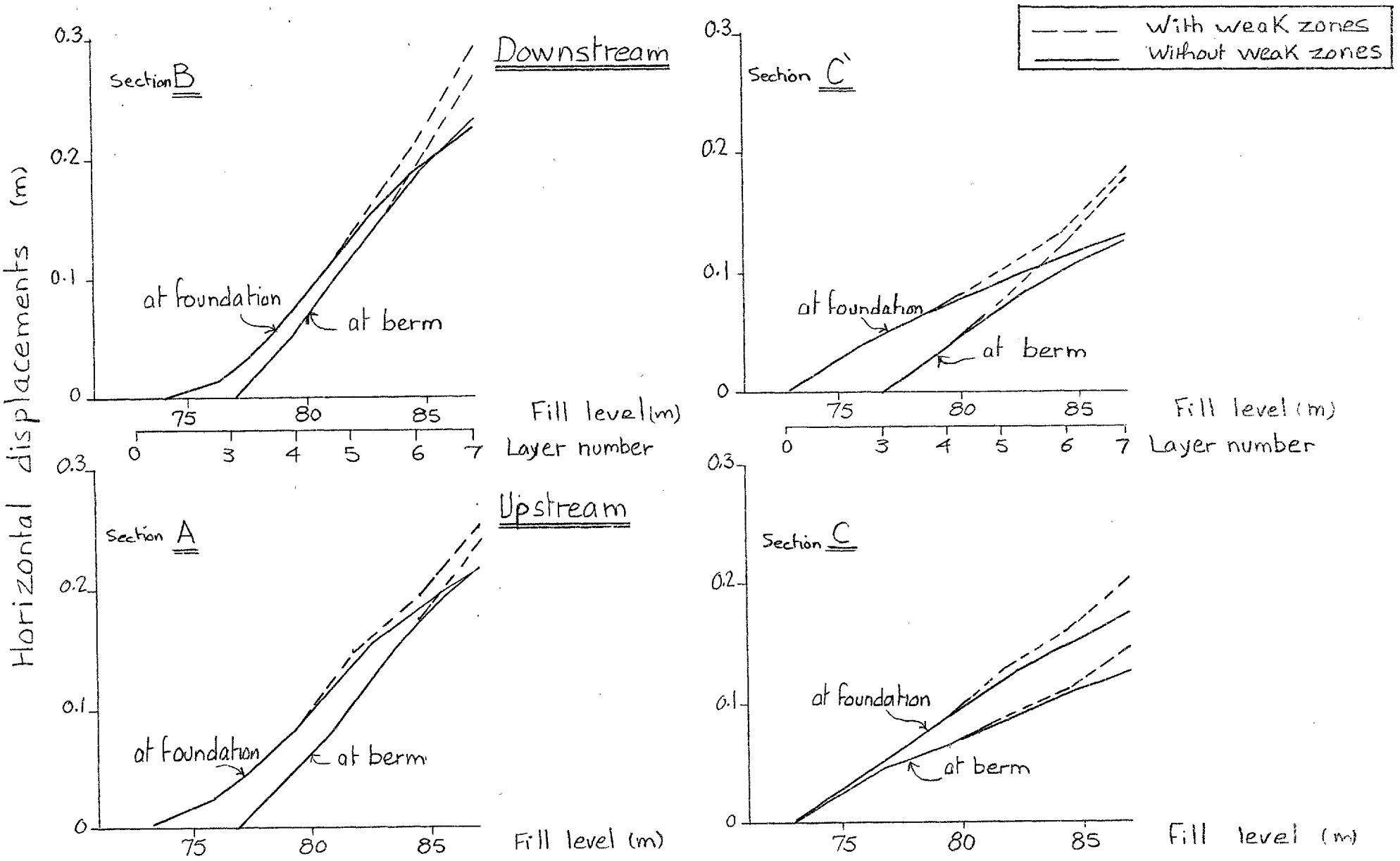


Fig. 7.37

COMPARISON BETWEEN SOLUTIONS WITH AND WITHOUT WEAK ZONES

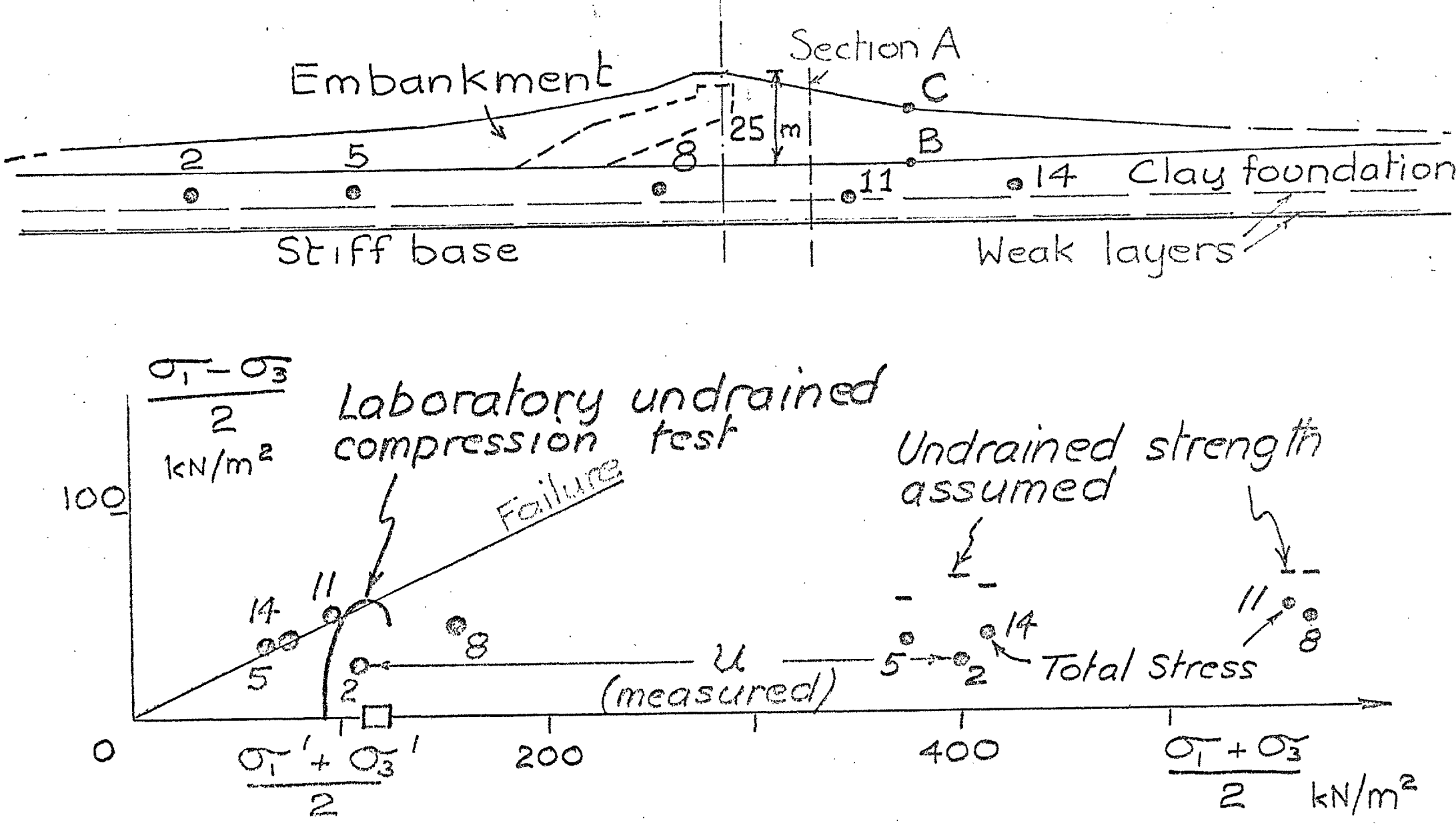
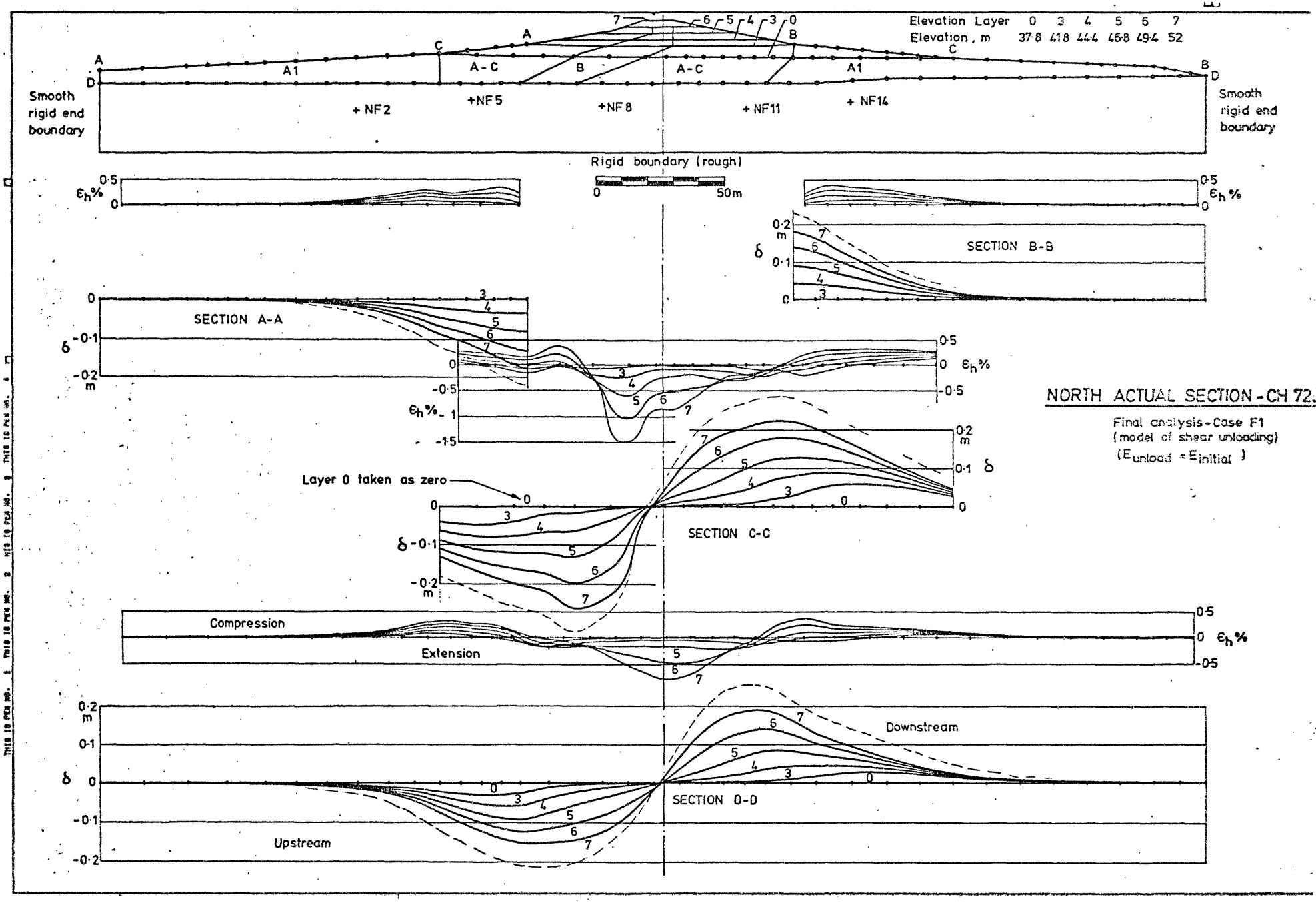


Fig. 7.38

EFFECTIVE STRESSES USING F.E. PREDICTION OF TOTAL STRESSES AND MEASURED PORE WATER PRESSURE



NORTH ACTUAL SECTION - CH 72.

Final analysis - Case F1
(model of shear unloading)
($E_{unload} = E_{initial}$)

Fig. 7.39

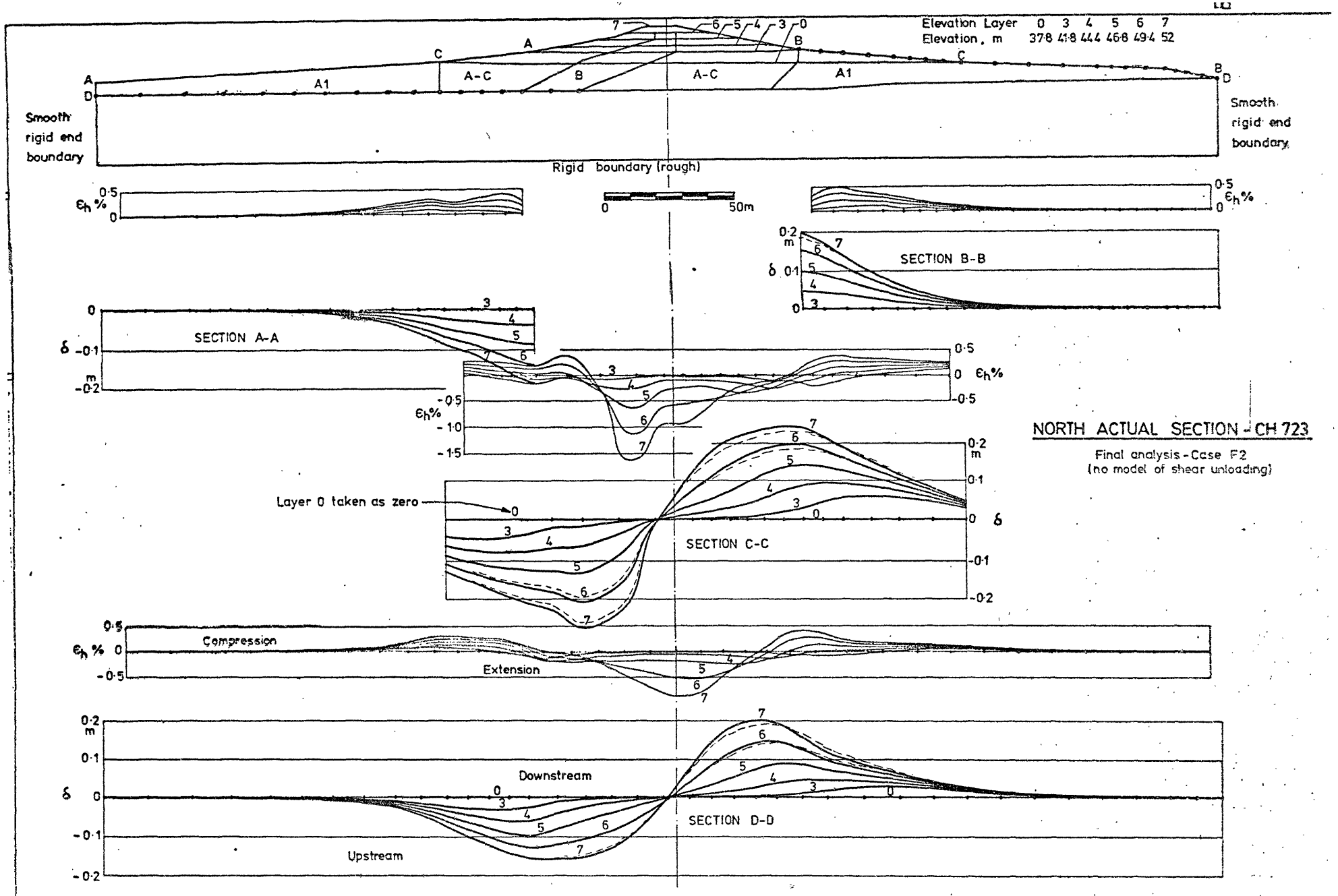
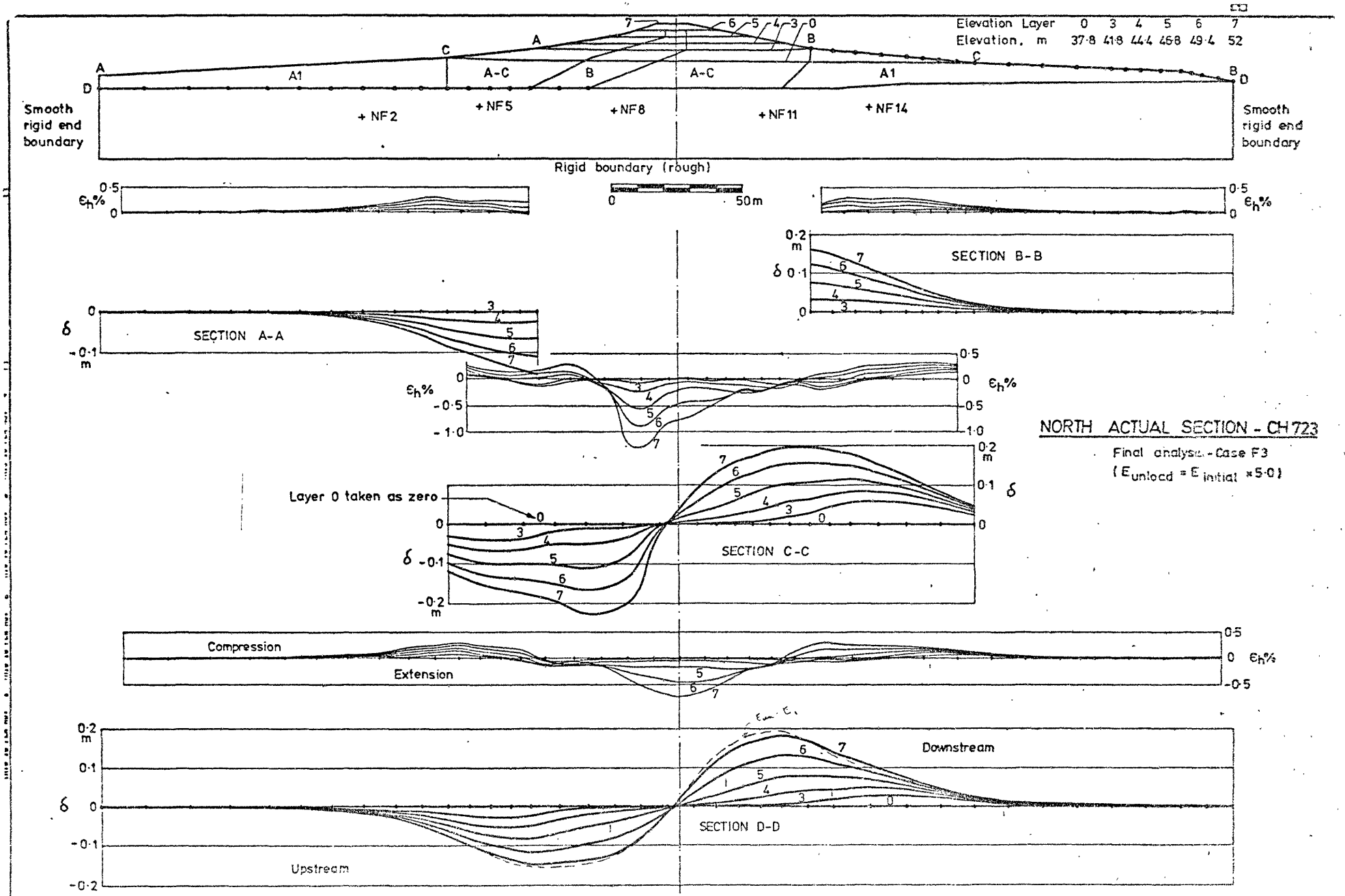

Elevation Layer 0 3 4 5 6 7
Elevation, m 37·8 41·8 44·4 46·8 49·4 52
A1
A-C
B
A-C
A1
Smooth rigid end boundary
Smooth rigid end boundary
Rigid boundary (rough)
0 50m
SECTION B-B
SECTION A-A
SECTION C-C
SECTION D-D
Layer 0 taken as zero
Compression
Extension
Downstream
Upstream
NORTH ACTUAL SECTION - CH 723
Final analysis - Case F2
(no model of shear unloading)

Fig. 7.40



NORTH ACTUAL SECTION - CH 723

Final analysis - Case F3
($E_{unload} = E_{initial} \times 5{\cdot}0$)

Fig. 7.41

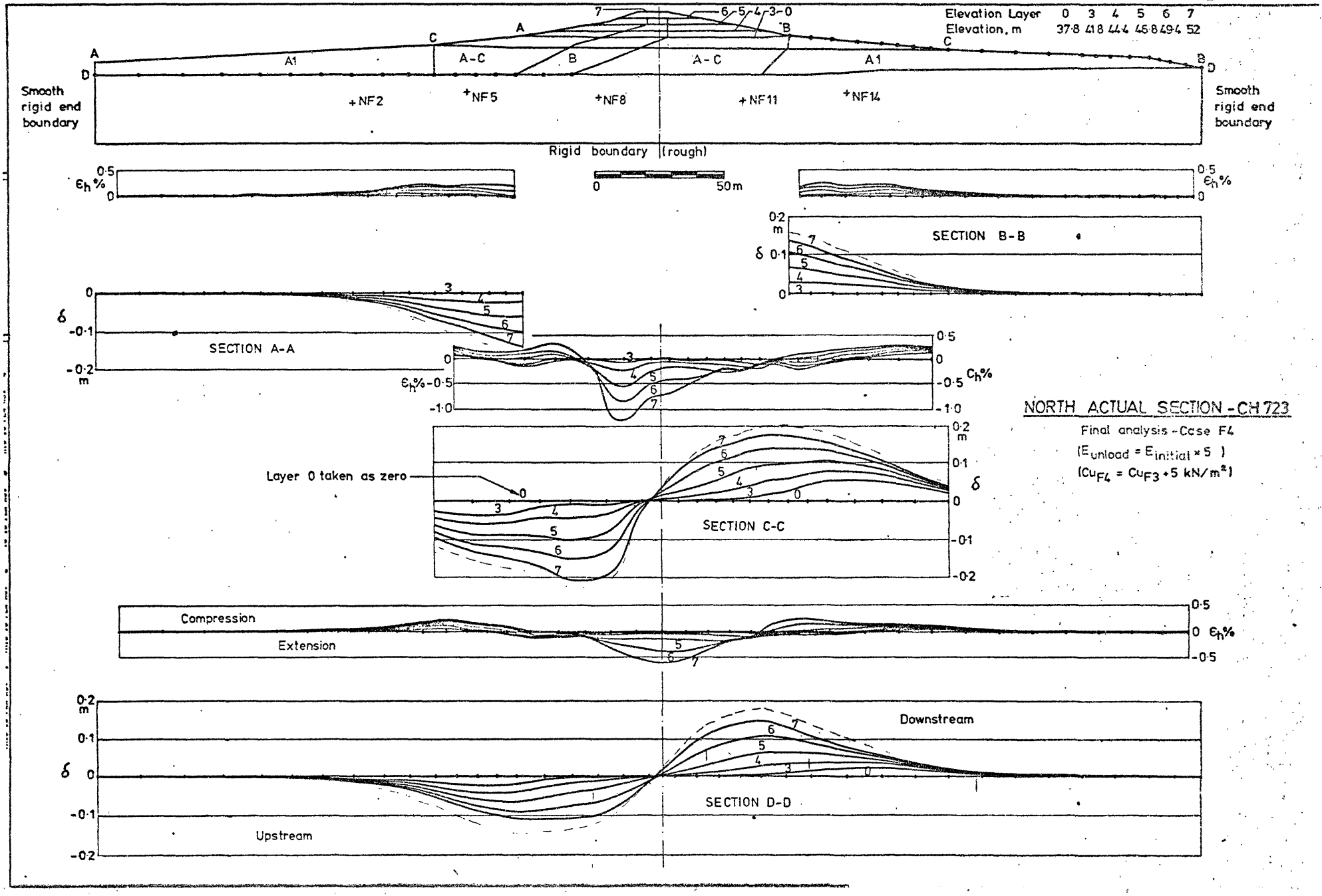
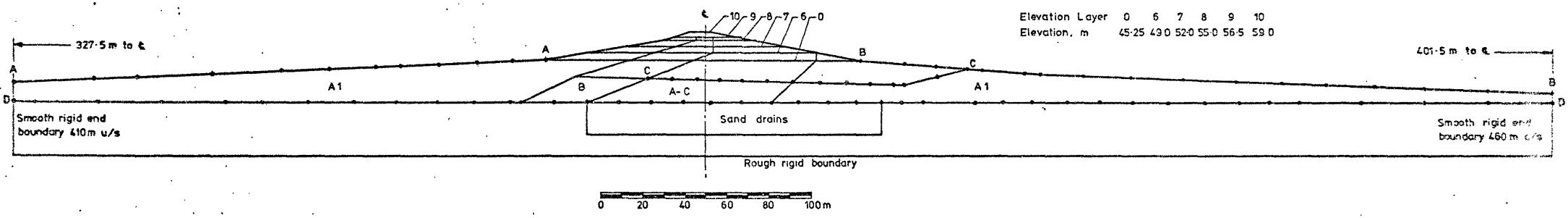
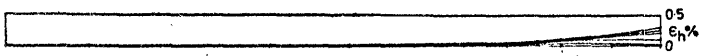
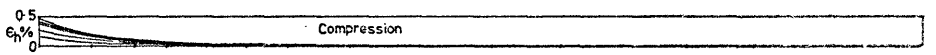

Elevation Layer 0 3 4 5 6 7
Elevation, m 37·8 41·8 44·4 45·8 49·4 52
A1
A-C
B
A-C
A1
Smooth rigid end boundary
+NF2
+NF5
+NF8
+NF11
+NF14
Smooth rigid end boundary
Rigid boundary (rough)
0
50m
SECTION B-B
SECTION A-A
SECTION C-C
NORTH ACTUAL SECTION - CH 723
Final analysis - Case F4
(Eunload = Einitial × 5)
(CuF4 = CuF3 + 5 kN/m²)
Layer 0 taken as zero
Compression
Extension
Downstream
Upstream
SECTION D-D

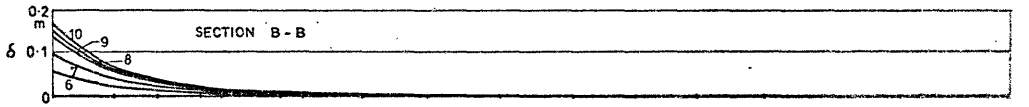
Fig. 7.42

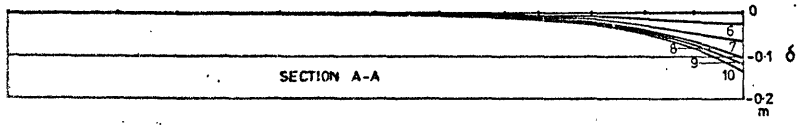
HORIZONTAL DISPLACMENTS AND STRAINS

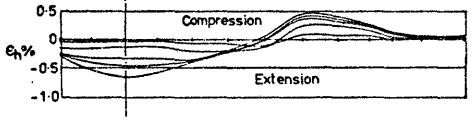


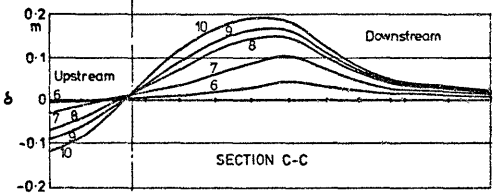




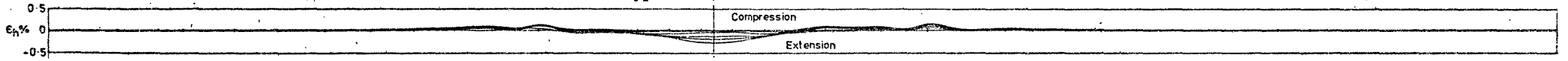








TYPICAL SECTION
Sand drain solution
CASE F5



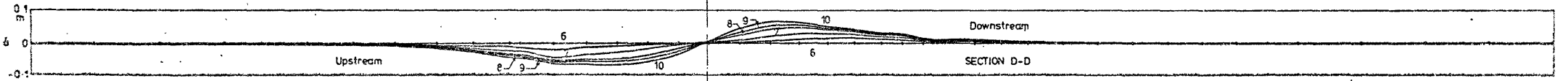


Fig. 7.43

CHAPTER 8

FINAL REVIEW OF ENGINEERING ANALYSIS OF EMBANKMENT DAMS

8.1 Introduction

In this chapter the current design procedure for embankment dams is examined with a view to highlighting those steps in the procedure in which finite element analysis may have an important role. The benefits of employing this method of analysis are discussed together with the problems encountered and the decisions to be made in its application when attempting to simulate real soil behaviour, and the construction sequence.

The designation "embankment dams" includes earth, earth-rock fill and rock fill dams and their foundations. An earth dam could be either "homogeneous" or "zoned" and in either type the difference between fill and foundation strengths could vary considerably. An earth-rock fill dam could have either a central or an inclined impervious clay core while a rock fill dam may include a concrete or asphalt slab resting on the upstream slope to act as the impervious membrane.

An embankment dam is subject during its life to the following loading conditions:-

1. During construction the dam is subject mainly to gravity loading due to its own weight. The fill is placed in layers of finite thickness which are compacted. The subsequent behaviour of the

material is influenced by the compaction effect, the conditions of placement and the duration of the construction period.

II During operation the dam is subject to several events, the timing of which vary and may overlap. One or more of the following events happen, possibly simultaneously:-

a) First impounding: the reservoir water level rises to its final height over a varying period of time, introducing an upstream water loading, seepage forces (the effect of which depend on the coefficient of permeability of the upstream slope of the dam), and saturation or wetting of the upstream rock fill shell (which produces changes in volume and material properties and an unknown redistribution of the stress field).

b) Equilibration of pore water pressure: this process starts when the reservoir is filled and continues until the water flow establishes a steady state between upstream and downstream water levels; the process may take centuries in the case of clay dams, Vaughan & Walbancke (1973).

c) Drawdown: the reservoir water level may fall at any time after first impounding. If the dam is a part of a power generation scheme, rapid drawdown and refilling may occur very frequently.

An ideal analysis should simulate each of these physical events as a continuous and correctly-timed process and should predict the changing stresses, strains, pore pressures, and general behaviour of all parts of a dam. This analysis should be able to deal with the available engineering data and assumptions, and from its results the designer should be able to judge whether his design criteria have been met. Such an analysis would be immensely complex, even if it could ever be achieved. Thus it is more realistic at this stage to consider and attempt "partial analyses" which are relevant to particular phases of embankment performance and to see whether useful results can be obtained. Only the construction phase will be discussed in this Chapter; the author did not examine other phases during the course of research and there is very little literature on the subject to review.

8.2 The design criteria and procedure

The function of a dam, namely the retention of water with acceptable leakage and without shear failure or sliding, leads to the three following design criteria:-

a) Stability: The design analysis should ensure an adequate reserve against shear failure or sliding during construction and operation, taking account of possible fluctuations in reservoir water level and the effect of earthquakes, where these pose a threat. Stability is often determined by the foundation

properties because the fill can be placed under conditions which can be controlled and which lead to it having desired properties.

b) Acceptable deformations: Deformations may become unacceptable without shear failure occurring. This is not usually a limiting condition but the design should ensure that free board remains adequate during operation and that no damage occurs to associated more rigid structures such as culverts, tunnels, draw-offs, access bridges, etc. Differential settlement along the crest of the dam and long term movements due to creep should also be acceptable.

c) Water tightness and internal and external erosion: The correct selection and zoning of materials, according to their permeability and the proper design of filter transitions, drains, cut-offs and blankets should ensure a self-sealing dam, free from internal and external erosion. The design must be able to predict where areas of tensile stress zones or steep stress gradients develop since these could result in the formation of cracks, either due to gravity loading during construction or by water loading or by reservoir seepage pressures. Moreover, cracks due to earthquake movements must be avoided.

The designer's task is to satisfy these criteria by

selecting the optimum dam shape and internal configuration (including drainage and protection measures) taking account of:-

a) The mechanical and consolidation properties of the foundation.

b) The available construction materials (and their properties) on and within reasonable reach of the site.

c) The geometry of the site and proposed dam height.

d) The required Factor of Safety against failure (which should include allowances for the uncertainties in the design and future events).

He must, in addition, recommend an instrumentation layout and a framework for monitoring and analysing the field data to check that the dam's performance is satisfactory during construction and operation.

The conventional design procedure for different dam types has been covered comprehensively by Vaughan (1974). The first step in the design procedure is to decide on a trial "shape" for the dam, and then to analyse that shape and determine whether it will satisfy the design criteria. Determining the optimum slopes of the dam involves trial and error using limit equilibrium methods (such as stability coefficients and/or simple multi-wedge techniques) in which the assumed shear strengths are less than the available shear strengths of the various materials. The reduction in shear strength can be based on an average 'Factor of

Safety' or an assessment of acceptable average strain.

The approximate form of the consolidation equation, i.e. based on Terzaghi's one-dimensional theory, and Laplace's seepage equation are employed to predict pore water pressures during construction and operation; these are used in the effective stress stability calculations. Simplified elasticity and plasticity solutions, Bishop (1952), are used to predict stresses which give guidance on such things as the pressure exerted by the core on the shoulders.

This conventional design procedure must rely heavily on experience (including information from case histories), intuition and engineering judgement when answering such questions as:-

a) Where is the best place for the core and what should be the optimum ratio of shoulder to core moduli to minimize arching and potential areas of cracking?

b) What is the best distribution of different fill materials in the cross-section to give a more even distribution of shear stresses in the foundation?

c) Does the construction require the use of sand drains or drainage blankets, and if so, where is the optimum place and how many are required?

d) What are the stress paths followed by soil elements within the dam and how do they differ from the stress paths followed in the laboratory tests? (From such

a comparison it may be possible to specify more appropriate tests which could yield more realistic parameters).

e) What are the measurements that should be obtained when monitoring the performance of the dam? Where should the instruments be placed to record the dam's characteristic behaviour and how should these field results be analysed?

8.3 The advantages and the role of the finite element method in design

By adding finite element analysis to his design procedure, the designer is far better placed to answer the questions listed above, since the method has the following important advantages over conventional procedures:-

a) In limit equilibrium methods a mechanism of behaviour at failure must be assumed and a backward analysis is followed while in finite element analysis the behaviour under working loads (and beyond, if required) is developed from the input information of material properties and geometry. The method is thus a forward analysis and this feature is of importance, particularly in the case of zoned dams where mobilization of strength in each material is difficult to assess, which means that the mechanism assumed for limit equilibrium could be very approximate.

b) Realistic stress-strain properties and boundary conditions can be handled, and stresses, strains and displacements are readily produced throughout the structure.

c) Consolidation and Seepage theory could be modelled in a more realistic manner (i.e. less approximation) and the coupled consolidation equations are currently under active research.

Simple finite element analyses of the trial cross-sections can be used at an early stage of the design to amplify the consequences of alternative design assumptions (including the type of dam). The method may be particularly useful in the design of dams which are to be raised after sometime in operation.

At the construction and operation stages the method of analysis may be used to check the performance of the dam in the light of changed circumstances revealed during construction, and field measurements of the actual behaviour of the dam. Thus the new concept of 'design as you build' is best supported.

The potential of the finite element method to "forward predict" unacceptable events from field observations is of particular importance. This is carried out by comparing measured and predicted values up to the current stage of construction and then extrapolating to forward

predict the behaviour during the next stage. An example of a forward prediction, in this case the pore water pressures under Empingham Main Dam, has been given by Vaughan (1975).

An important additional benefit of the method of analysis is the coupled use of a well-instrumented trial bank and a sound non-linear finite element programme. This is a relatively new technique which can be used to provide the strength and stress-strain properties of a foundation whose properties are not easily obtained in either laboratory or conventional in situ tests. A systematic back analysis technique is suggested and has been used during the course of this research (Chapter 6). The purpose of this technique is to deduce the in situ stress-strain curve using the measured principal strains and the calculated stresses in a non-linear finite element analysis. Its success arises from the finding that the stresses are relatively insensitive to stress-strain non-linearity. This is demonstrated in Figure (6.91) which shows that for three different stress-strain relationships, the maximum shear stresses do not vary appreciably. The method is an iterative one, but the process should succeed in two to three iterations provided that there are no abrupt changes in the strength and deformation properties. A summary of the steps in the method has been presented in Chapter 6.

Unfortunately field measurements of strains have

not received the attention they deserve. The value of the strain at a point provides more information than the value of displacements at a point. The strains can be related directly to stresses, but displacements cannot and it is the stresses which are of importance. Examination of a strain field provides immediately a better understanding of the behaviour than examination of a displacement field; thus areas of alarming volume change, passive, active and at rest conditions can be distinguished.

Finally, the finite element method is a good tool for parametric studies. The number of material parameters involved in the analysis of a dam is large and thus knowledge of the relative importance of these parameters is helpful. For a particular stage, some parameters are of greater importance than others, and finite element analysis will indicate which are the important ones.

8.4 Partial Analyses

Selection of material parameters is, of course, all-important when carrying out finite element analyses. Since soil behaviour is controlled by effective stresses these parameters should be in terms of effective stresses. However, when pore pressure and hence effective stress changes are a function of total stress changes only and not of consolidation or drainage, then total stress parameters can be used, (see Chapter 3).

As mentioned in the introduction to this chapter, partial step-by-step analysis rather than complete analysis of the dam's construction and operation phases is more feasible now (1975). In principle a step-by-step analysis of sufficient complexity should predict the complete behaviour of the dam. However, it is worth emphasising that increased complexity does not necessarily lead to results which are closer to the true solution. Also, over-simplified analysis may mislead. For every case, there must be 'critical' upper and lower limits of simplicity within which 'good' results should be obtained. These limits are obtained from experience with the method and understanding of the mechanism of the problem and the behaviour of the material.

In the remaining sections of this Chapter, the factors involved in partial analyses of construction stage are discussed and the relative importance of input data is assessed. Some analyses from the literature and from the author's work are presented in order to demonstrate the applicability of the finite element method in this field.

8.5 Analysis of construction phase

Most of the finite element analyses of embankment dams reported so far were carried out to simulate the events of the construction phase; the literature is rich with analysis of actual dams (about 40 in number) and these have been recently tabulated by Duncan (1974) and Eisenstein (1974). Most of the non-linear analyses used Kondner's

(1963) hyperbolic function to describe the non-linearity of the stress-strain curve and Janbu's (1963) exponential function to describe the dependency of the deformation modulus on the confining pressure, i.e. the family of stress-strain curves. However, the stress increments were related to the strain increment via the set of elastic equations as discussed in Chapter 3. The soil data was that of either conventional triaxial or oedometer tests, thus the stress path effects on the behaviour were not simulated.

Unfortunately, none of these analyses was employed as a design tool, nor forward predicted events for adding information to the design of dams under construction (i.e. none fell into Lambe's (1973) Class A predictions). The main use of the finite element method has been to compare actual measurements at existing dams with finite element predicted values of certain functions, such as stresses, strains and movements. The majority of the comparisons were with measured movements at certain points, especially vertical, rather than with patterns of behaviour. Little information has been given about stress prediction, except when comparison was made between tensile areas indicated by analysis and areas of cracks observed in the dam. Displays of the complete results are not found in the literature which is unfortunate since the educational value of these could be considerable.

Little can be gained, with respect to improvements

in design from those previous analyses apart from the fact that the finite element method can predict behaviour, the accuracy of such predictions depending on the quality of the input data. A design procedure which utilizes the great potential of the finite element method and which is an improvement on the current one has not been demonstrated yet.

The objective should be to use the finite element method as 'predictor-director' in a systematic design procedure. A 'predictor-director' approach is one in which the designer is able to use the predictions from an analysis to direct subsequent design analyses or processes. This is in contrast with the simple analysis which does not form part of a series of inter-related analyses (the examples in the literature fall into this category). The author has used the method as predictor-director, not in a design procedure, but in the systematic back analysis to derive in situ stress-strain properties, described in section 6.4.4.

8.5.1. Layered Analysis

A finite element analysis which simulates construction of the dam in layers will be named 'layered analysis', and not 'incremental analysis' as it is usually called in the literature; this is to avoid confusion with the incremental non-linear techniques for solving non-linear problems in which the weight due to one layer is added in several increments. The results of 'layered analyses' are generally compared with the results of 'single-lift' analyses, in which the dam loading and stiffness are

applied in one step.

The need to simulate the construction sequence in the finite element analysis of embankment dams has received some attention, e.g. Clough and Woodward (1967), Kulhawy, Duncan and Seed (1969), Pyrah (1971) and Naylor and Jones (1973). The findings of these workers can be discussed under the following two headings:-

A. Two-dimensional comparisons: Here the work of Clough and Woodward (1967) and Pyrah (1971) will be discussed. The former have analysed a "standard" homogeneous dam with rigid foundation and linear elastic material properties for both methods of analysis, i.e. 'single-lift' and 'layered'. The latter has analysed "Bishop"(1952) dam, a homogeneous, linear elastic material, which is resting on a flexible foundation.

The comparison between the two methods of analysis for the "standard" dam, showed that the three components of stress, vertical, horizontal and shear stress, are comparable for both 'layered' and 'single-lift' analyses. It is worth mentioning here that although the vertical stresses were identical in both cases, the shear stress showed some deviations, being slightly higher in the 'layered' analysis. The contours of vertical displacement were completely different for the two methods of analysis while the contours of the horizontal displacements were similar.

The great difference in the pattern of vertical displacement contours for both methods of analysis is mainly due to the definition of displacements, a matter which will be discussed later. To study the effect on the results of the number of layers needed for simulating the construction, the "standard" dam was analysed once with 7 layers and once with 14 layers; by comparing the settlements on the centre line at 2 points, it was shown that the results for 7 and 14 layers were similar and thus it was concluded that 7 layers was as good as 14. No attempt was made to see whether 3 layers, say, would give the same results as 7 layers.

Pyrah (1971) has compared the 'single-lift' and the 'layered' analysis solutions for stresses and displacements within the dam and its foundation. Within the dam near the centre line the vertical stresses were very similar, while the horizontal and shear stresses were much higher in the 'single-lift' analysis than the 'layered' analysis; in the latter these stresses tend to zero at the top. The deviation decreases from a maximum at the top to a negligable value at the mid-height of the dam. It is argued by Pyrah that the high compressive horizontal and shear stresses at the top of the dam in the 'single-lift' analysis are caused by a "beam action" due to the foundation settlements being larger at the centre of the dam than near

the toe, thus creating compressive strains within upper sections of the embankment. A large percentage of the settlements is caused by the bulk of the material forming the lower parts of the embankment and obviously these settlements cannot introduce stresses (or displacements) into any part of the embankment which does not exist when the loads are applied. The pattern and conclusions regarding settlement within the dam at the centre line are similar to those of Clough and Woodward. No other movements within the dam were compared.

Pyrah also found that the vertical, horizontal and shear stresses at the base of the embankment (i.e. the top of the foundation) were almost identical for both methods of analysis. The vertical settlements along the centre line within the foundation were reported to be identical for both methods of analysis. The horizontal displacements were not compared anywhere. Pyrah concluded that the foundation behaviour is unaffected by the method of analysis.

The two sets of conclusions are not contradictory but rather complementary in view of the different foundations considered; they may be summarised as follows:-

i. For dams resting on a rigid base only the vertical displacements differ with the method of analysis.

ii. For dams resting on a flexible foundation:-

a) Within the dam, horizontal and shear stresses and vertical settlement differ for both methods of analysis, especially at the top part of the dam.

b) The foundation stresses and settlements are independent of the method of analysis.

It is obvious that more comparisons should be made between both methods of analysis, especially with more critical functions, such as the maximum shear stresses, the principal stress ratios, the horizontal displacements and the shear strains, and it is necessary to concentrate on areas in the dam and its foundation away from the centre line, where the previous comparisons have been made. The use of a flexible foundation is often necessary in the case of embankment dams and is especially relevant to the type of embankment examined during the course of this work. The point of using a linear model to describe the material properties in this part of the study is in fact an advantage and by no means a draw-back, as will be explained later. The explanation for the difference in the vertical displacement patterns given by Clough and Woodward and the explanation given by Pyrah for the high values of compressive and shear stresses are satisfactory.

B. <u>One-dimensional analysis</u>: Here the work by Kulhawy, Duncan and Seed (1969) and Naylor and Jones (1973) is discussed. The purpose of their work was to provide an insight into the amount of error involved in the F.E. type of layering analysis by comparing their settlement results from F.E. analyses with an infinitesimal layer analysis, i.e. an 'exact' solution; they also attempted to determine the number of finite layers needed to achieve a solution close to the 'exact' one. For simplicity they used a one-dimensional model which mathematically represents either a soil column or a broad fill. The two works are very similar in analysis procedure and in their conclusions; they differ slightly in the assumptions made for material non-linearity, Kulhawy et al used Janbu's hyperbolic relation between deformation modulus and σ'_3 while Naylor and Jones used a linear relation between the stiffness $K(f(E,\nu))$ and σ_v (this, of course leads to a non-linear solution since stiffness is no longer an independent parameter).

Kulhawy Duncan and Seed compared the closed form solution of the infinitesimal analysis to the F.E. type layer analysis for different degrees of non-linearity and different numbers of layers. From their results it could be shown that for the same degree of non-linearity, the greater the number of layers the closer is the layered solution to that of the 'exact' one. Also, and most important in the author's view, the number of layers required

to achieve a solution close to the infinitesimal one reduced as the degree of non-linearity decreased until reaching the limit, when the material is linear, the layered solution coincided with the infinitesimal one, irrespective of the number of layers. No comparison was explicitly made with 'single-lift' analysis because a proper definition of the settlement was lacking.

In spite of using material non-linearity, which is different to that used by Kulhawy et al, Naylor and Jones arrived at the same conclusions and added a useful definition of the settlement. This definition has been used to interpret results quoted in this thesis and in the author's M.Sc. thesis (1972). They also demonstrated analytically that for linear material properties, the settlement computed at the base of the hypothetical layer (Naylor's definition of settlement) is independent of the number of layers, a result which stimulated further work by the author.

It is important here to comment on the way the writers dealt with the material non-linearity. Both groups used three different methods (which gave three different results for each case they considered); the parameters were based on either the state of stress before adding the new layer, the state of stress after adding the new layer or an average value; (For a one-dimensional analysis, stresses are independent of modulus of deformation and can be

calculated before determining non-constant deformation parameters). The parameters were then used in a non-iterative solution from which the results could not be compatible with the stress-strain curve. Thus their answers were dependent on the non-linear technique and the size of the load increment. This argument is supported by their results.

For comparisons between 'layered' and 'single-lift' analyses of non-linear materials a better non-linear technique, namely an iterative one or a multi-incremental method for each layer, is required to eliminate errors other than those due to layering. Avoiding the errors due to non-linearity also explains the author's comment that the use of a linear model in the two-dimensional analyses was an advantage.

Since the linear analysis in the one-dimensional case showed results independent of the number of layers and a better comparison was achieved using the average state of stress in the non-linear case, the author anticipated that if the non-linearity were to be handled by a better non-linear technique the answer to the non-linear problem would also be independent of the number of layers. This is in contrast to the conclusions of Kulhawy et al and Naylor and Jones that the solution for non-linear materials is dependent on the number of layers.

Therefore a sequence of F.E. analyses of this

one-dimensional case has been solved, using the same assumptions regarding non-linearity, using Naylor's definition for settlement and using the non-linear technique described in Chapter 2. They have confirmed the author's view, refer to figure (8.1). The finding that the results in the one dimensional linear and non-linear cases are both independent of construction sequence is due to the fact that the one dimensional continuum problem is statically determinate. (One dimensional means horizontally constrained, thus it is strictly statically determined as the horizontal shear stress is equal to zero) In contrast a two dimensional problem is statically indeterminate and it is a well known fact from structural engineering that stresses in statically indeterminate structures are dependent on their method of construction.

The choice of a one-dimensional problem by Kulhawy et al and by Naylor and Jones to study the effects of construction sequence was, therefore, inappropriate since a one-dimensional problem is, in fact, independent of construction sequence. Their conclusions, therefore, are invalid and reflect on the shortcomings of the non-linear techniques they employed.

From the summary given earlier of the conclusions reached by Pyrah (1971) and by Clough and Woodward (1967) it is evident that simulation of the construction sequence is necessary for accurately predicting stresses and deformations within a homogeneous fill. 'Layered' analyses

are even more necessary in dams in which the assumptions made by these workers are not met, i.e. in zoned dams, or those with materials having non-linear properties. However, the author wished to examine more closely Pyrah's conclusion that a single-lift analysis was sufficient for examining foundation behaviour. Comparisons have, therefore, been made of various stress and strain functions at points other than near the centreline in the foundation: the 'layered' and 'single-lift' analyses have used linear and non-linear material properties and the Empingham trial bank cross-section of Chapter 6. If a single-lift analysis could have been shown to be sufficient, this would have been of immense value since the behaviour of many dams, including Empingham, is controlled by their foundation.

The method adopted when performing the 'layered' analyses used in these comparisons is discussed subsequently. Linear behaviour was assumed initially and seven layers were used in the 'layered' analysis. The first comparison is between the maximum shear stresses at a depth of 1.5m below original ground level and the results are presented in figure (8.2). This figure shows that the 'layered' analysis predicts maximum shear stresses up to 50% higher than those found in a 'single-lift' analysis; this is obviously significant when examining stability, particularly at low factors of safety.

The second comparison is between the horizontal

strains at foundation level; the results shown in figure (8.3)indicate that the differences were less than 15%, which, in practice, is negligible. The third comparison is between predicted horizontal displacements at two sections remote from the dam centreline, figure (8.4). Again the differences are small but it is of interest to note that the differences increase with distance from the centreline.

To generalise conclusions regarding the differences in foundation behaviour found when using 'layered' and 'single-lift' analyses, non-linear behaviour was then assumed in identical situations. It must be emphasised that for the single-lift analysis it was ensured that the nominated non-linear stress-strain curve was followed accurately, i.e. that the non-linear technique was independent of the layering simulation; this was achieved by following either an incremental or iterative non-linear technique of the type described in Chapter 2; Figure (8.5) shows the compatibility of the 'layered' and 'single-lift' analyses, both following the nominated stress-strain curve with similar accuracy and so eliminating the errors due to the non-linearity.

Figures (8.6, 8.7, & 8.8) show the same comparisons as figures (8.2, 8.3, & 8.4) but with the non-linear properties assumed. The results shown in these figures confirm that a 'layered' analysis should be used whether soil behaviour is linear or non-linear, particularly when stresses

are being examined in linear materials and when both stresses and displacements are being examined in non-linear materials. The reason for the larger difference between displacements when non-linear properties were used is explained diagrammatically in figure (8,9); this shows that for the same magnitude of stress error the strain and thus the displacement errors are amplified by the non-linearity between stress and strain.

Thus it was concluded that while 'layered' analysis predicts different stresses and deformations in both the foundation and the fill, the effect of material non-linearity is only to amplify the differences in deformation.

It is of interest to note that Goodman and Brown (1963) proved theoretically that for the case of an infinite wedge there is a difference between stress and displacement in 'layered' and 'single-lift' analyses and the values of the stresses calculated in the 'layered' analysis are independent of the material properties. This conclusion does not conflict with the author's.

The differences in the stresses and horizontal displacements, predicted by 'layered' and 'single-lift' analyses at points in both the fill and foundation remote from the centreline, require explanation. It would appear that these differences result from the temporary discontinuity introduced at the top of each new layer. When a layer is added there is zero restraint at its top surface;

the restraint at this level, especially in the horizontal direction, increases with each additional layer placed above and reaches a maximum when the dam is complete. In contrast, at an equivalent level in a 'single-lift' analysis, the full restraint is present through-out the analysis, due to the pre-application of stiffness. Since deformations due to the weight of material below any horizontal plane through the dam will depend to some extent on the restraint to movement provided by the material above that plane, deformations in a 'layered' analysis will be higher than those predicted by a 'single-lift' analysis. Since the increasing restraint at any level in a 'layered' analysis takes the form of an increasing shear resistance, there will be a corresponding difference in shear stress distribution predicted by the two methods, 'single-lift' predicting lower shear stresses. On the centreline of a symmetrical dam, such as the one analysed by Pyrah, there is zero shear on horizontal planes so that this location is least affected by the method of analysis. In a one dimensional problem, as analysed by Kulhawy et al and by Naylor and Jones there is zero shear on horizontal planes, thus, following, the argument above, there can be no differences in predictions from'layered' and 'single-lift' analyses.

Having established the need to simulate the layering sequence it is necessary to examine the problems involved:-

1. Stiffness of the simulated layer: In the field the layers, which are generally 300mm thick, not only add weight to the underlying soils, but also modify the overall stiffness of the structure. It is impractical to include such small layers in the analysis, thus thicker layers are always used to simulate several actual layers. The question here is what value of stiffness should be given to the thick layer. In other words, what is the equivalent stiffness of one simulated layer added in one go to that of several layers added in steps (the equivalent stiffness should give the same deformation patterns in the underlying soils)? This problem has not been solved yet, but upper and lower limits are easy to establish. If a full stiffness is given to the layer according to its state of stress as it is modelled in one lift (assuming a perfect non-linear technique), the effect on the underlying part of the dam will be that of placing a slab of certain thickness and stiffness, and the resulting deformation will be in accordance with this confinement; this will provide a lower limit for deformation. The other extreme is to give the new layer no stiffness at all, thus the underlying part will take only load, no stiffness increase, and will deform freely; this will provide an upper limit. To explain this upper limit mathematically, assume that K is the stiffness of the dam up to the underside of the layer being placed, and δ the displacement vector and F is the load vector, thus:-

$$[K]\{\delta\} = \{F\}$$

By partial differentation.

$$\Delta[K]\{\delta\} + [K] \cdot \Delta\{\delta\} = \Delta\{F\}$$

$$\Delta\{\delta\} = [K]^{-1}\left(\Delta\{F\} - \Delta[K]\{\delta\}\right)$$

$$\Delta\{\delta\} = [K]^{-1}\Delta\{F\} - [K]^{-1}\Delta[K]\{\delta\}$$

Therefore, neglecting the stiffness of the new layer, $\Delta[K]$, is equivalent to ignoring the last term in the above equation and this must produce an upper limit.

2. Effect of the deformation on the geometry: In the analysis no account is taken of the influence on geometry of the soil compressibility. The modelled layer just placed will compress under its own weight and will settle further due to the compressibility of the soil underneath it. Thus, the volume of soil which is actually filled to achieve the level of a certain layer is larger than the volume which is based on the geometry between the two levels representing the layer in the f.e. idealization. To deal with this problem it is necessary to predict the settlement in a separate solution or to assume it for each layer and then to evaluate an equivalent unit weight according to the expected settlement. The value of the error here, if this effect is neglected, depends on the compressibility of the soil and thickness of the modelled layer, but may be significant in dams on soft foundations. This error could affect mainly the value of the mean stresses which in turn affect the strength in the drained case and the value of

pore water pressure in the undrained case, as mentioned in section 6.4.

3. Compaction stress: Due to heavy rolling machines, the layer just placed developes an overconsolidation state, (i.e. horizontal stress bigger than vertical stresses). The subsequent behaviour of this layer will be controlled by the state of stress developed during compaction. This is particularly true in the case of small dams, in which the development of σ_H due to compaction is more than that due to density and Poisson effect. The modelling of this effect is beyond the capability of the displacement approach of the finite element method, because it requires a predescribed stress boundary, unless a simulation of the dynamic loading is made. The technique used during the research, the dense liquid, which was described in Chapter 4, will predict an isotropic state of stress which may be a good approximation. An alternative model would have been the use of an anisotropic soil model for the layer just placed. The use of an anisotropic model for this effect is 'fictional', only being introduced to develop horizontal stresses larger than the vertical one. From the equations of cross anisotropy, it is possible to write (for broad fill)

$$\frac{\sigma_H}{\sigma_V} = \frac{n.\nu_V}{1-\nu_H} \qquad n = \frac{E_H}{Ev}$$

and thus σ_H will develop greater value than σ_V if:

$$n > \frac{1-\nu_H}{\nu_V}$$

for the particular case of $\nu_H = \nu_v = 0.5$ (i.e. incrompressibility, instropic conditions (n=1) gives an isotropic stress ($\sigma_H/\sigma_v = 1$). For σ_H to be bigger than (σ_v then n>1.)

8.5.2 Three-dimensional effects.

The question of whether or not it is necessary to take into account the third dimension in embankment dam analysis is examined by reviewing a number of comparative studies.

Lefebvre and Duncan (1971) and Lefebvre et al (1973) reported the results of 3-D analyses of an idealized dam resting in a valley with wall valley slopes of 1:1, 1:3, 1:6. They compared the results of these analyses at the maximum transverse and maximum longitudinal sections with the corresponding results of the 2-D analyses of those sections. Homogeneous, elastic linear material properties were used. 'Layered' analysis was performed to simulate the dam construction sequence. The foundation was taken as a rigid boundary. The difference between the 3-D and 2-D analyses at these locations was greatest for slopes steeper than 1:3; stresses from the 3-D being lower than those from the 2-D. This difference was attributed to a "cross valley arching", i.e. the dam tends to hang on the valley slopes. More details about their finding will not be repeated here.

Palmerton (1972) and Palmerton and Lefebvre (1972) analysed in 3-D a single dam with a central core on a flexible

foundation in a narrow valley of 1:1 valley wall slopes. Non-linear material properties were used. They compared their results with a 2-D analysis of the maximum transverse section. Their conclusions agreed with those of the previous investigations; they added that the introduction of a soft core increased the differences between the two solutions.

Eisenstein, Krishongya and Morgenstern (1972), with a view to studying the development of tension zones, examined the effects of 3-D idealization. The vertical settlements, horizontal stresses and horizontal strains along the crest of the dam derived from 2 and 3-D analysis of a homogeneous section were compared. They found that the differences between the 2 sets of calculations are not significant and that 2-D analysis in plane strain of the longitudinal cross section was good enough to investigate cracking. However, as soon as the core and shell possess different stiffnesses, significant deviations arise. This result confirms the findings of Palmerton (1972).

Eisenstein and Simons (1975) analysed a real dam in a deep valley in both 3-D and 2-D, and found that predictions were similar and compared favourably with the measured deformations in the plane that was used in the 2-D analysis. He concluded that 2-D analysis was sufficient. This is in conflict with the findings already discussed but may result from the fact that the plane selected by Eisenstein for comparison is shown by the results of the instrumentation to be one in which the behaviour was essentially two-dimensional.

The work discussed above is very useful for understanding the essential differences between the solutions for these idealized cases and proved that the 3-D F.E. method is applicable to truly 3-D situations such as curved axis dams. The main advantage of 3-D analysis is that it permits the engineer to examine the stress and displacement behaviour along any section through the dam, especially if the critical section is unknowingly not that at the centre of the valley. It is important to note that the average confining pressure was reported by Palmerton and Lefebvre (1972) to be up to 50% less at the lower part of the dam in a 3-D analysis. This has a significant effect on the pore water pressure development in the undrained case and on the shear strength in the drained case and on the prospects of hydraulic fracture, Vaughan (1975).

All the comparisons made so far have been for the 2-D planes representing the maximum transverse section. However, it can be anticipated that the greatest divergence between the two methods will occur on sections away from the centreline in either the passive or active zones.

In deciding whether to perform 2-D or 3-D analyses one must consider:-

(a) the availability of computer time and storage;

(b) the valley geometry;

(c) the position of the critical cross section in

relation to the valley centreline. If the critical cross section is close to the centreline or if the valley slopes are flat and the dam is relatively homogeneous a 2-D analysis is probably sufficient for analysis of the transverse section.

When it is sufficient to perform a 2-D analysis (or made necessary by costs) examination of the maximum longitudinal section is advantageous.

8.5.3. Soil Non-linearity

A number of aspects of soil behaviour are non-linear. Firstly, modulus of deformation is a function of $(\sigma_1-\sigma_3)$; secondly the modulus is a function of σ_3'; and thirdly soil shear strength is finite (and incorporation of a shear stress limit immediately makes an analysis non-linear). It is pertinent to pose the question: 'which of these facets of non-linearity predominate in their effects on the results of both undrained and drained analyses?'. If this question could be answered then most attention could be directed towards modelling the appropriate non-linearity.

In attempting to answer this question the author began by re-examining work by Bishop (1967) in which the latter compared the variation of $((\sigma_1-\sigma_3)/\gamma H)$, where H denotes the height of the dam and γ denotes the unit weight of the material, and (σ_1'/σ_3') along potential slip surfaces. Bishop used a linear model for both the fill and foundation. The

author conducted a finite element analysis using the geometry of the Empingham Trial Bank, linear material properties, and a deformation modulus for the foundation which increased with depth; the results of this analysis are presented in figure (8.10) and(8.11) in the form of contours of $(\sigma_1-\sigma_3)/\gamma H$ and (σ_1'/σ_3') and variation of these two functions along the same potential slip surface. These results confirmed Bishop's earlier predictions, namely that there is marked non-uniformity in each stress function along a potential slip surface; in the case of $(\sigma_1-\sigma_3)/\gamma H$ the function reaches a pronounced maximum over the middle portion of the surface whereas the non-uniformity in (σ_1'/σ_3') occurs at each end of the slip surface.

Unfortunately, the assumptions made regarding soil properties in Bishop's and the author's analysis are correct only for interpretation of the undrained case, since the modulus used was independent of the applied σ_3' and Poisson's Ratio was taken as 0.5 (.499 in the finite element analysis); thus only the distribution of $(\sigma_1-\sigma_3)/\gamma H$, which controls undrained behaviour, is strictly relevant. Anticipating that an analysis in which drained behaviour is correctly modelled (i.e. modulus is a function of σ_3' and Poisson's Ratio is less than 0.5) would yield a different distribution of (σ_1'/σ_3'), the stress function controlling drained behaviour, a further finite element calculation was made. In this calculation the same geometry was used, Poisson's Ratio was taken as 0.3 and Janbu's relation between

E and σ_3' was employed for the fill and foundation. The results of this analysis are plotted in figure (8.12); comparison with figure (8.11) shows a distinct difference in the contours of (σ_1'/σ_3'). The distribution of (σ_1'/σ_3') along a potential slip surface is far more uniform when drained behaviour is correctly modelled.

Two conclusions can be drawn directly from this investigation:-

(i) for undrained loading there is a concentration of shear stress on a potential slip surface which makes shear strength an important parameter. To ascertain just how critical a parameter is shear strength, further work was carried out. The results of the best fit between predicted and measured horizontal deformations in the Trial Bank (refer Chapter 6) were compared with two additional analyses. In the first additional analysis the shear strength was reduced by 15%; in the second, the slope of the stress-strain curve was increased by 25% throughout its length. The results can be compared in figures (8.13) and(8.14) which show clearly that shear strength predominates in controlling undrained behaviour, the change in deformation modulus made little practical difference.

(ii) for drained loading there is no significant concentration of (σ_1'/σ_3') and hence shear strength is not an important factor in controlling the behaviour. This could be

argued intuitively by the fact that an increment of loading is accompanied not only by an increase in (σ_1'/σ_3') but also an increase in $(\sigma_1' + \sigma_3')$ and hence in shear strength. Thus the behaviour is left to be controlled by the variation of E with σ_3' and the value of Poisson's Ratio.

Plasticity theory to model non-linear soil behaviour in earth dams has not been used to date. However its use is to be encouraged, especially to model materials such as normally consolidated clays since their behaviour is most conveniently expressed in terms of plasticity.

8.5.4 Progressive Failure

Progressive failure in soils will occur only if:-

(i) there is non-uniformity of mobilised shear strength along a potential slip surface. In the undrained saturated case this coincides with non-uniformity of shear stress. In the drained case it coincides with non-uniformity of principal stress ratio.

(ii) the soil exhibits brittle behaviour, i.e. a loss in strength after reaching a maximum value.

Both conditions are necessary in combination, Bishop (1967 and 1971). Additionally, Palmer and Rice (1972) have proved that there is a minimum volume of soil required to absorb the energy released by slip surface propagation.

The importance of progressive failure on the stability of dam slopes depends, inter alia, on the degree of non-uniformity of mobilised strength, the rate at which the relevant strength (drained or undrained) drops with increasing strain, and in certain cases, the residual strength.

At Empingham Trial Bank (Chapter 6) which was constructed with a material which was believed to be brittle in undrained loading, it was concluded that the effect of progressive failure on the stability of the slope was insignificant, since, despite large deformations, 'runaway' failure did not occur; this was attributed to the low rate of drop in strength with strain which was found by Maguire (1975).

The effect of progressive failure on the stability of dams built with granular materials under drained conditions is likely to be less critical than an undrained saturated situation in which the material has similar post-peak behaviour. This can be explained by reference to figures (8.10, & 8.12) which show that around a potential slip surface the non-uniformity of the principal stress ratio, which controls drained stability, is far less than the non-uniformity of the maximum shear stress, which controls undrained stability.

In materials showing a rapid drop in strength post-peak, it would be advantageous if the influence of

progressive failure on undrained stability of dam slopes could be allowed for. However, the uniqueness of a f.e. solution for a slope of material having a constitutive law which allows for strain-softening cannot be proved, because the material wil be unstable according to Drucker's (1959) definition. In addition, the strain-softening will be associated with slip surfaces and a continuum approach no longer applies unless the location of the slip surface is previously known and elements are concentrated around this plane to allow large strains to develop locally. Nevertheless, the solution obtained can not be proven to be unique because the over-all stiffness matrix of the structure may not be positive definite.

8.5.5 Anisotropy

The fact that soil behaviour is anisotropic, both as a result of geological history and stress path, has been introduced in Chapter 3. Up to the present time (1975) neither anisotropy of strength nor anisotropy of deformation parameters has been incorporated in the soil models used in the F.E. analysis of embankment dams.

The major problem in developing a model which simulates cross-anisotropy of deformation parameters, which is the simplest form of anisotropy, is the requirement for five deformation parameters, one of which it is not possible, at present, to measure (Atkinson, 1973). Limits to this

particular parameter have been established by Pickering (1971) using energy principles. The development of a cross-anisotropic model, using these limits, is to be encouraged since it could, (apart from representing a truly anisotropic material) predict three of the characteristics of soil behaviour which cannot be predicted by an isotropic model, viz

(i) volume change accompanying pure shear;

(ii) Poisson's ratio greater than 0.5 for certain stress paths (to be discussed subsequently); and

(iii) non-coincidence of the directions of principal strain increment and the causative principal stress increment.

In those soils problems in which behaviour is dominated by shear strength and which were discussed in the section on non-linearity, it is more important to cater for anisotropy of shear strength than for anisotropy of deformation parameters; this eliminates the problem of defining five deformation parameters.

8.5.6 Stress Path

Deformations in soils, which, as discussed previously, are controlled by effective stress changes, comprise both elastic and plastic strains. Plastic strains modify the soil's structure and hence its behaviour under

further loading; they result in the relation between deformations and effective stress being non-linear and they ensure that measured deformations will depend on:-

(i) the initial stresses and soil structure, and

(ii) the direction in which the soil is loaded, i.e. whether shear stresses, and in the case of drained loading, mean normal stresses, are increasing or reducing and whether principal stresses and/or principal stress increments are rotating.

This stress path dependency of soil behaviour was discussed briefly in Chapter 3. Both measurement of deformation parameters in the laboratory and the selection of appropriate parameters for analysis must take account of this characteristic. In fact, the two processes are inter-dependent, each relying on feedback from the other; thus, an ideal dam design procedure which takes full account of stress path dependency must be an iterative one, involving, for example, the following steps:-

1 Measure, or predict using geological history, the foundation in situ stresses.

11 Based on conventional laboratory test results or experience, assume deformation parameters for the construction materials and foundation, paying greater attention in non-homogeneous sections to getting their relative values correct than their absolute magnitude, because this tends to control the mechanism of behaviour.

III Calculate the stress changes, both magnitude and direction, which take place in the dam and foundation during construction.

IV Perform laboratory tests which follow most closely the calculated stress changes and measure deformation and strength parameters.

V Use the measured parameters in an appropriate F.E. analysis, the idealisation for which is established using the results from III.

Iteration with steps IV and V continues until there is compatibility between the calculated stress paths and those used in the laboratory.

In the following, this ideal process is considered in more detail. In particular, the influence of initial stresses and direction of loading on predicted behaviour is examined. The limitations imposed in the laboratory by the difficulty in performing controlled stress tests in which partial rotation of the principal stresses can be controlled is discussed together with potential problems presented in F.E. analysis by dilatant behaviour.

The initial stresses to be found in step I determine the consolidation stresses to be used for tests on foundation material in step IV and provide the starting point for the analysis in step V. In the analysis the distribution of initial stresses influences strongly the

location at which failure comences. For the case of K_o greater than one, local yield occurs first in the foundation beneath the toe of the dam; this is shown diagrammatically in figure (8.15) . In contrast, for K_o less than one, local yield probably occurs first in the foundation beneath the centre of the dam, refer figure (8.15).

The distribution of initial stresses also helps to determine the direction of loading at each point in the foundation. It is important to realise that in any foundation in which K_o is not equal to unity an increase in load on the surface will lead both to areas where there is an increase in shear stress and to areas where there is a reduction in shear stress (termed shear unloading). The extent and location of the areas of shear loading and shear unloading affect the deformation pattern, refer figure(6.79) and they are governed not only by the distribution of initial stresses but in embankment dams by the regularity (or irregularity) of the construction sequence and by the presence of berms.

The three situations leading to shear unloading during dam construction are examined in figure (8.16). In figure (8.16a) the case of K_o not equal to one is shown; with K_o less than one an applied load at the surface will lead to shear unloading of elements in the vicinity of the toe of the load, but to shear loading under the centre of the load, the reverse is true for K_o greater than one. The effect on the

deformation pattern of the change in direction of shear loading is to produce larger deformations at the toe for K_o greater than one than for K_o less than one. This arises since the non-linear behaviour of soils is not recoverable and a steeper stress-strain curve is found during shear unloading. For the case of an irregular construction sequence shown in figure (8.16(b)), the same element may be subject in turn to shear loading, shear unloading and shear reloading. At the element shown within the berm drawn in figure (8.16(c)), the placing of additional load increases the horizontal stress on the element with little change in vertical stress. This shear unloading leads to a more rigid response of the berm and a more uniform distribution of shear stresses in the foundation.

From these examples the importance of the direction of shear loading on deformation can be seen. In fact, modelling the effects of shear unloading is as important and similar to introducing non-homogeneous media, in that the existence of a stiffer modulus 'attracts' stresses and distributes the deformations more uniformly. It is essential, then, that the direction of shear loading is examined during the analysis and that the unloading-reloading stress-strain curve is defined at the outset, together with the first loading curve.

F.E. methods based on the tangential stiffness method cannot take account of the direction in which the

change of shear stress occurs. However, in the quasi Runge-Kutta method presented in Chapter 2 the direction is examined and the method can take account of the increased stiffness on unloading.

Failure to distinguish between shear loading and shear unloading and to model correctly the higher stiffness on unloading can produce an incorrect pattern of behaviour or can lead to a complete breakdown of the solution if unloading is from the failure state or close to it. This breakdown of the solution was demonstrated in an analysis of Empingham Main Dam which simulated an irregular construction sequence. Using a model which neglected the effects of shear unloading, the solution failed because areas under consideration were at failure and low modulus was ascribed to them. When a large increment of stress was applied to these areas very large numbers were encountered which caused complete instability of the solution. An example of an incorrect pattern of behaviour being predicted is provided by comparing analyses of Empingham Trial Bank, one in which shear unloading was neglected and the other in which it was correctly modelled. Differences in horizontal strain at foundation level of up to 120% were predicted as shown in figure (6.81).

The error due to ignoring shear unloading at low stress levels is small and probably can be tolerated.

In addition to the direction of shear loading, the

effect of the rotation of the principal stresses or their increments must be considered. Beneath the edge of each layer placed in a dam, there is rotation of the principal stresses. However, as demonstrated in Chapter 6, the placing of further layers in a regular construction sequence produces little or no additional rotation of the principal stresses at these points; the same would not, of course, be true in an irregular construction sequence.

This fact is of importance since it reduces to some extent the impact of not being able to simulate in the laboratory controlled partial rotation of the principal stresses, unless use is made of a hollow cylinder apparatus. Nevertheless this limitation in laboratory equipment may be particularly important in the case of soil elements on which reloading is accompanied by partial principal stress rotation, as occurs in the field. In the laboratory, the reload and unload curves determined without principal stress rotation are similar. It can be argued that near-coincidence of these two curves occurs because reloading stresses on every plane are similar to those produced on first loading, during which preferred orientation would have developed. Furthermore, it might be anticipated that rotation of the principal stresses through 90° would produce a reloading stress-strain curve parallel to the initial curve. There is an urgent need for a test programme to examine reload stress-strain curves for various principal stress rotations with a view to incorporating a relationship between rotation and

reload modulus in the analysis.

In addition to their starting point, to the direction in which shear loading is changing and to the degree of principal stress rotation, stress paths differ in another respect, namely the direction in which mean normal stress is changing. Under undrained conditions, changes in mean normal stress produce no change in effective stress in saturated soils. If principal stress rotation is ignored, there are, therefore, only two effective stress paths under these conditions, one for shear loading and one for shear unloading. Under drained conditions, there is a lack of data on deformations and volume changes produced by a reduction in the component of mean normal stress, particularly under anisotropic stress conditions.

Volume increases can be expected to accompany a reduction in mean normal effective stress. In addition, in conventional laboratory tests on medium dense and dense sands and rockfill, large volume increases accompany shear when the stress difference on the samples is increased beyond a certain limit. Direct interpretation of these results, assuming isotropy, yields a value for Poisson's Ratio in excess of 0,5, which is meaningless in an elastic model and which cannot be dealt with by an incremental elastic F.E. procedure, as was discussed in Chapter 3. Interpretation of the results using an anisotropic elastic model would, however, yield parameters which are acceptable

in that they satisfy the energy principles.

Closer examination of the stress paths followed in the conventional laboratory tests, in which dilatancy occurs, reveals that there are two distinct stages in the test, A - B and B - C in figure (8.17), both of which produce volume change. During the isotropic consolidation stage A - B, compressive volume strains occur; during stage B - C, when the shear stress is increasing, a point is reached beyond which expansive volume changes occur. The cumulative volume change measured at C after following the path A - B - C may be compressive or expansive, depending on the proximity of point C to the failure envelope and on the initial mean normal stress.

Laboratory tests on rock fill by El-Ruwayih (1975) and on sand by El-Sohby (1969) following the stress path, AC, i.e. along a line of constant stress ratio, R, have shown that the sign of the measured volume change depends on the magnitude of R. El-Ruwayeh conducted tests up to an R value of 3 (equivalent to ϕ'_m of 30°) and found that volume changes were compressive at all stages. El-Sohby found that up to an R of 4 there was no increase in volume; for an R of 4,5 he measured a large volume increase.

It is clearly important to determine which of these alternative stress paths, A - B - C and A - C, is appropriate in dams built with granular materials and hence to determine how frequently dilatant behaviour is encountered

and, by inference, how useful would be an anisotropic model for predicting such behaviour.

Using the Empingham Trial Bank cross section and material properties in which E' varied with σ_3', an F.E. analysis which simulated construction was carried out. The stress paths for 3 points were found and these are plotted in figure (8.18). The stress paths at these points approximately follow constant R lines. Since the maximum R value found for the points was 2.7, it can be inferred that dilatancy does not occur at these locations for the case examined, which preserves homogeneity.

It would appear, therefore, that by virtue of the stress paths followed, dilation is unlikely to occur widely in dams, and the use of an anisotropic model to deal with dilation alone is not warranted. Charles (1975) has reported the results from the instrumentation of two rockfill dams; these indicate that dilatancy has not taken place, so confirming the author's view.

8.6 Local failure and strength discontinuities

The discussion in section 8.5 has assumed a continuum which is homogeneous or regularly non-homogeneous (i.e. properties varying smoothly with depth), and which, in turn, produces solutions for stress, displacement and strain fields which are continuous. If continuity is maintained and the same model for material behaviour is

used, a change in the numerical value of the input porperties will only change the numerical value of the output; the predicted mechanism of behaviour will not change.

However, the introduction of a strength discontinuity in the form of a zone of reduced strength can have a marked influence on the mechanism of behaviour. This became apparent in the exercises which led to the conclusions reported in Chapter 7. A strength discontinuity is likely to control behaviour in those problems in which local failure occurs in the weak zone since strains will be concentrated in this zone leading to sliding, the formation of a geometrical discontinuity and subsequent multi-wedge behaviour.

If a strength discontinuity is shown to be present by site investigation, and this in itself is a major problem, then the discontinuity can be modelled by concentrating elements in its vicinity. Research is necessary to establish whether it is sufficient to place a random discontinuity to correctly predict behaviour.

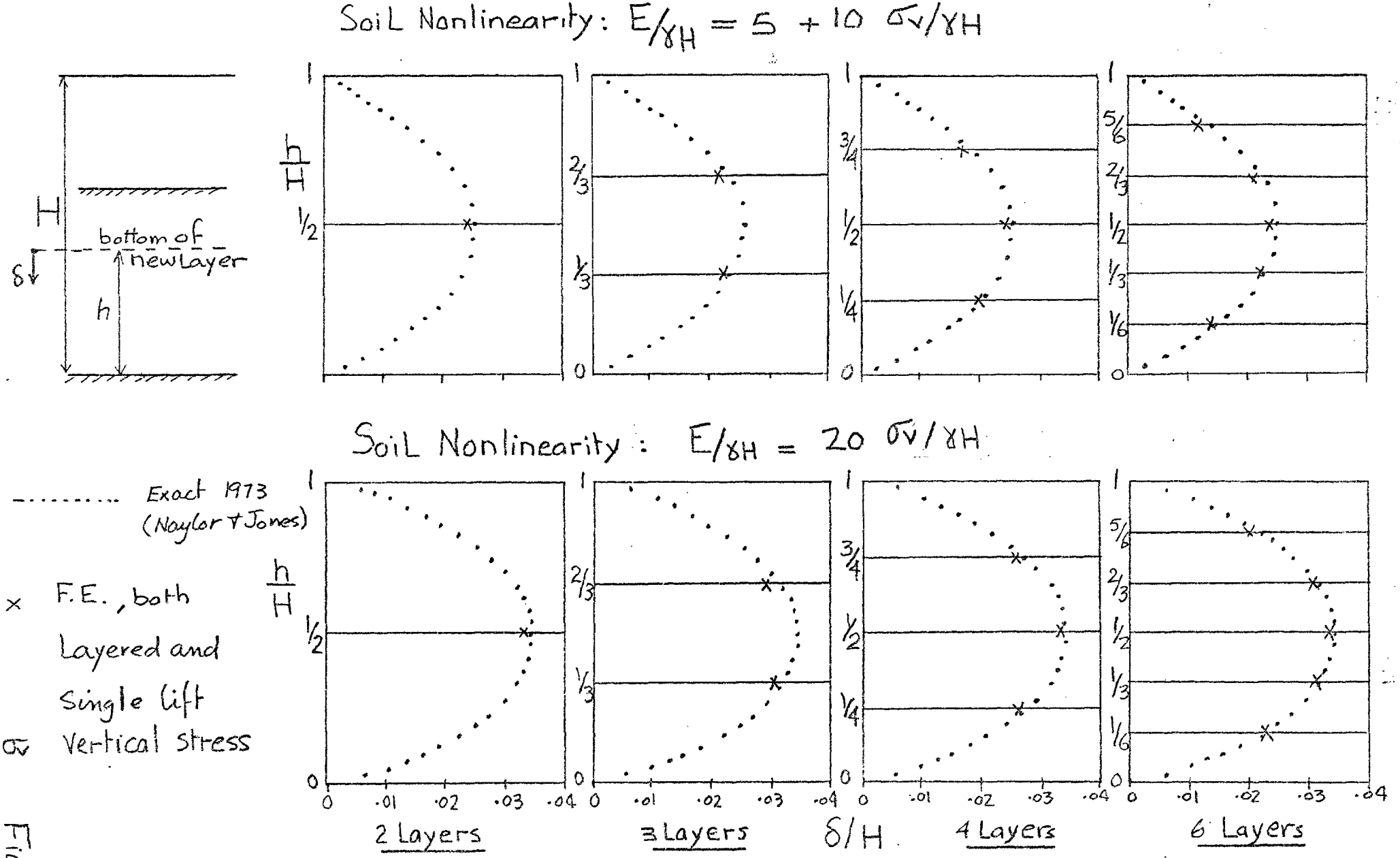


Fig. 8.1

ILLUSTRATION OF THE COINCIDENCE OF LAYERED AND SINGLE LIFT SOLUTIONS FOR NONLINEAR SOIL PROPERTIES DIMENSIONLESS FORM

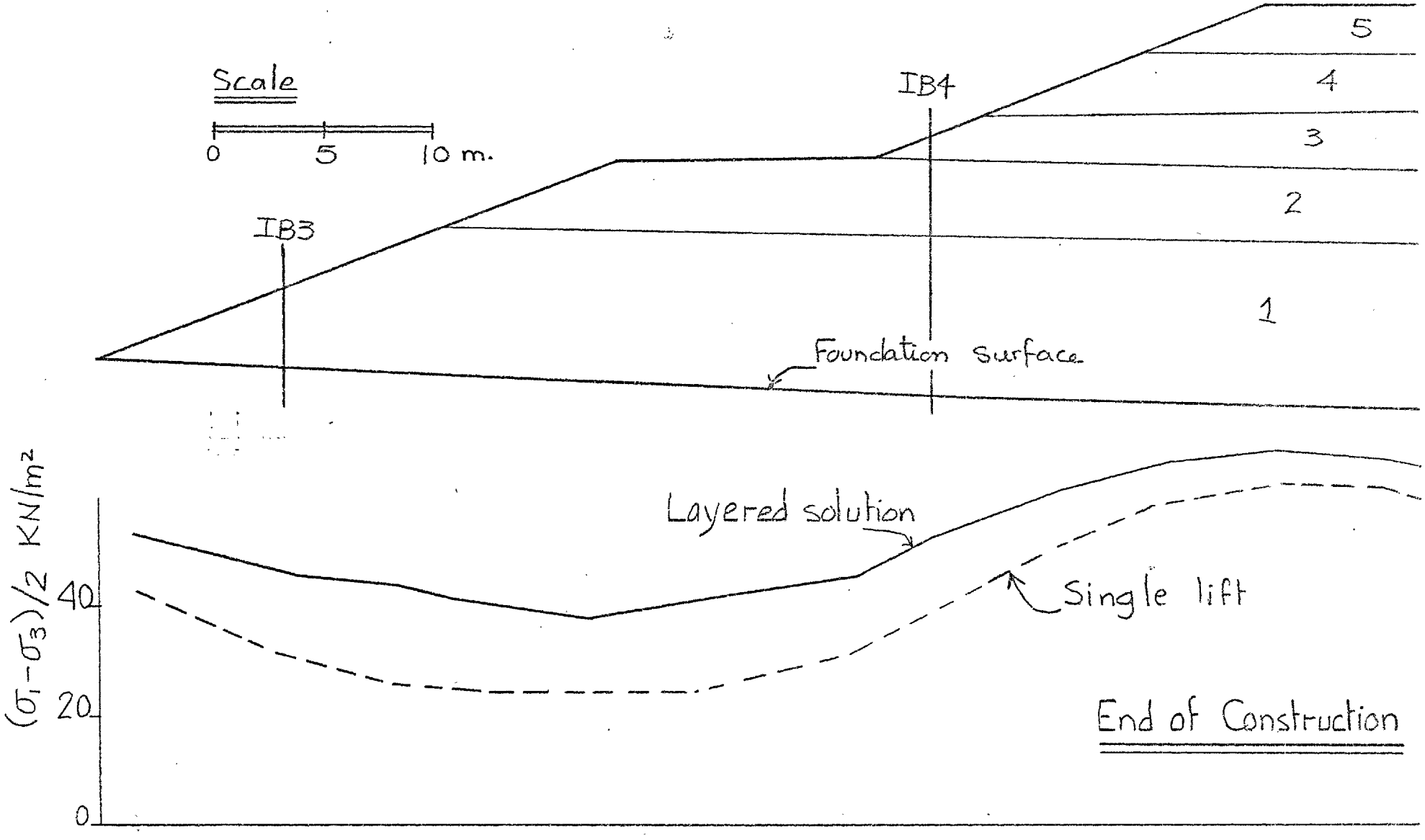


Fig. 8.2

MAX. SHEAR STRESSES AT 1.5 m. BELOW FOUNDATION SURFACE FOR LAYERED AND SINGLE LIFT SOLUTIONS - LINEAR ANALYSIS

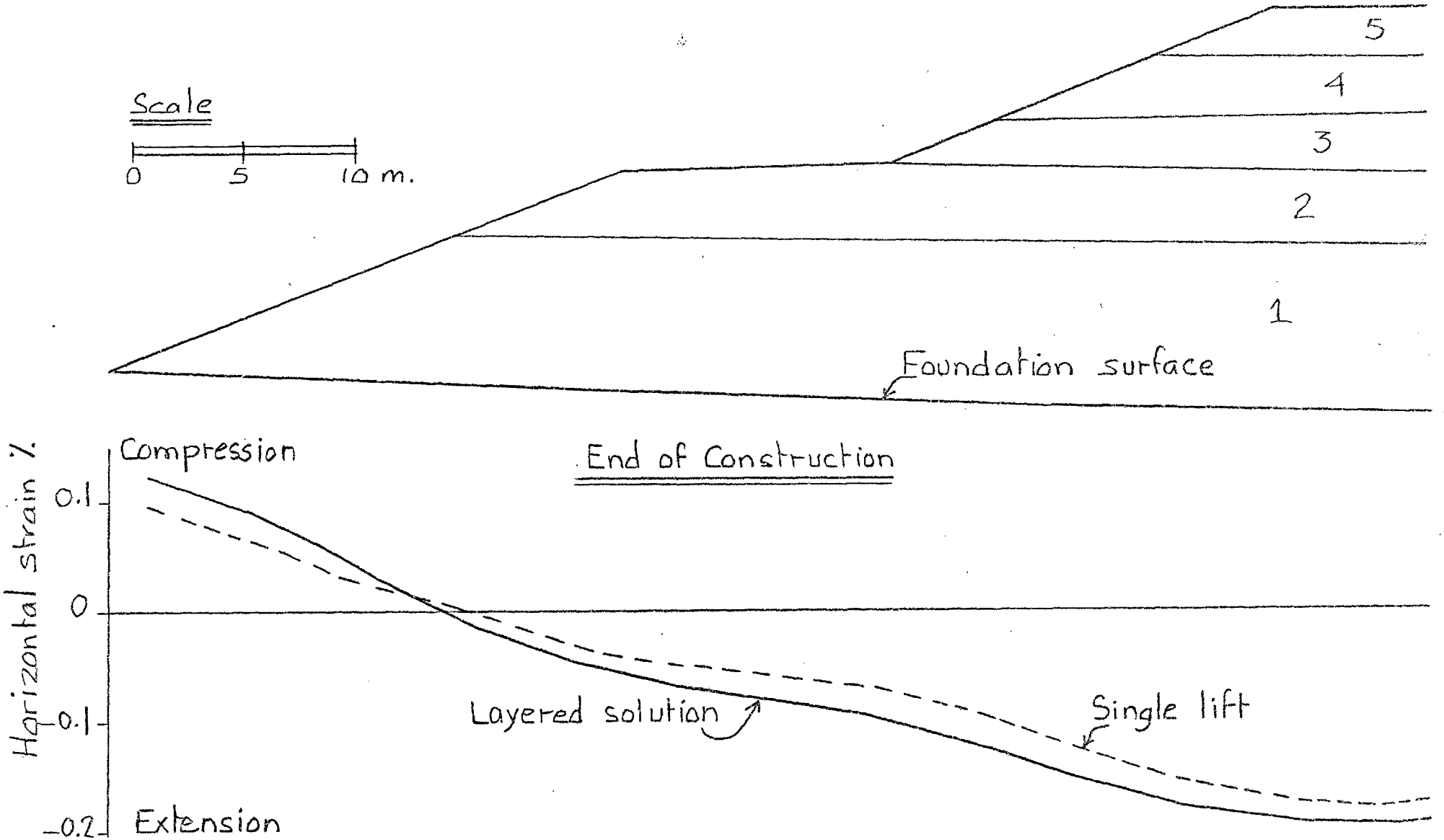
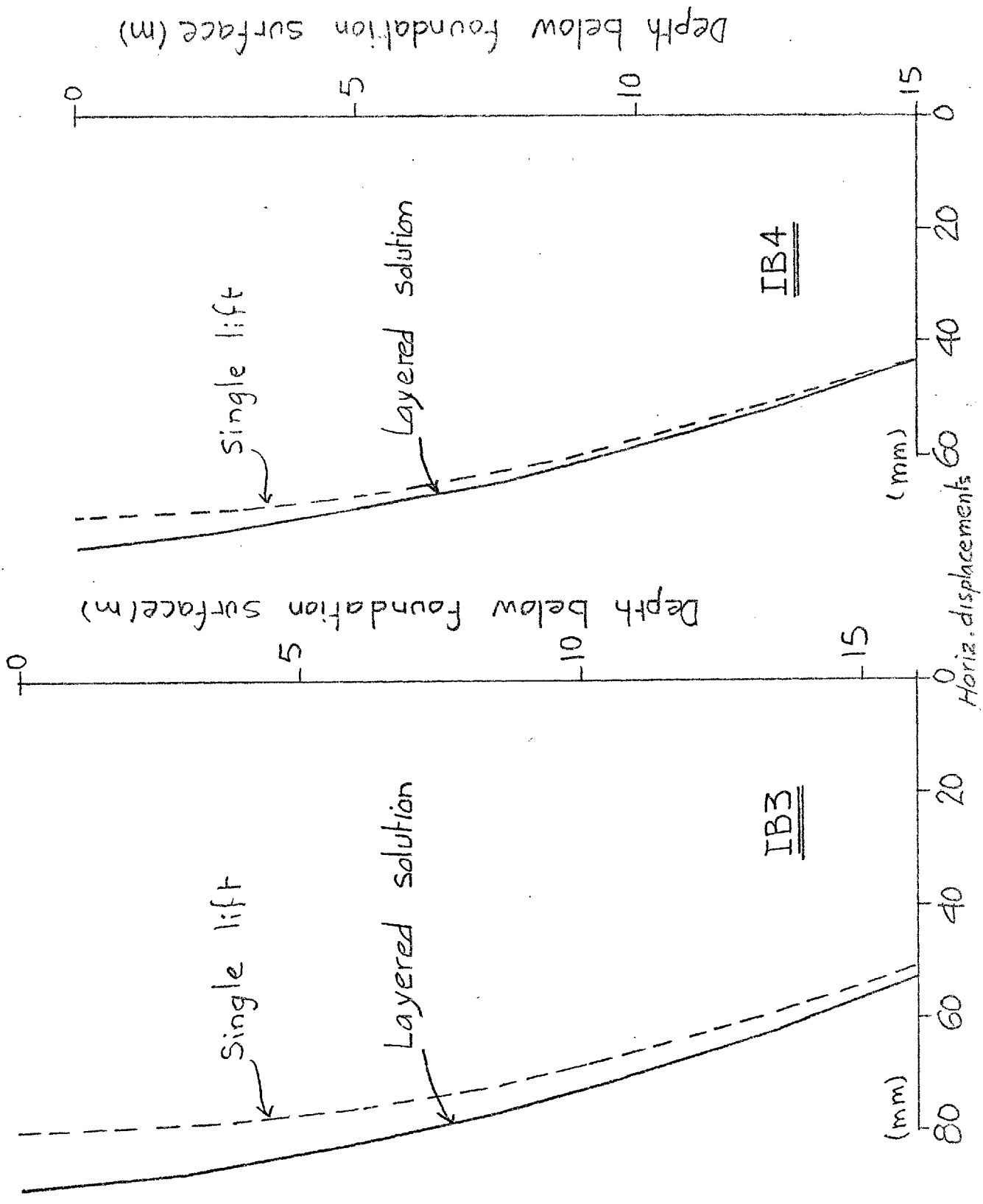


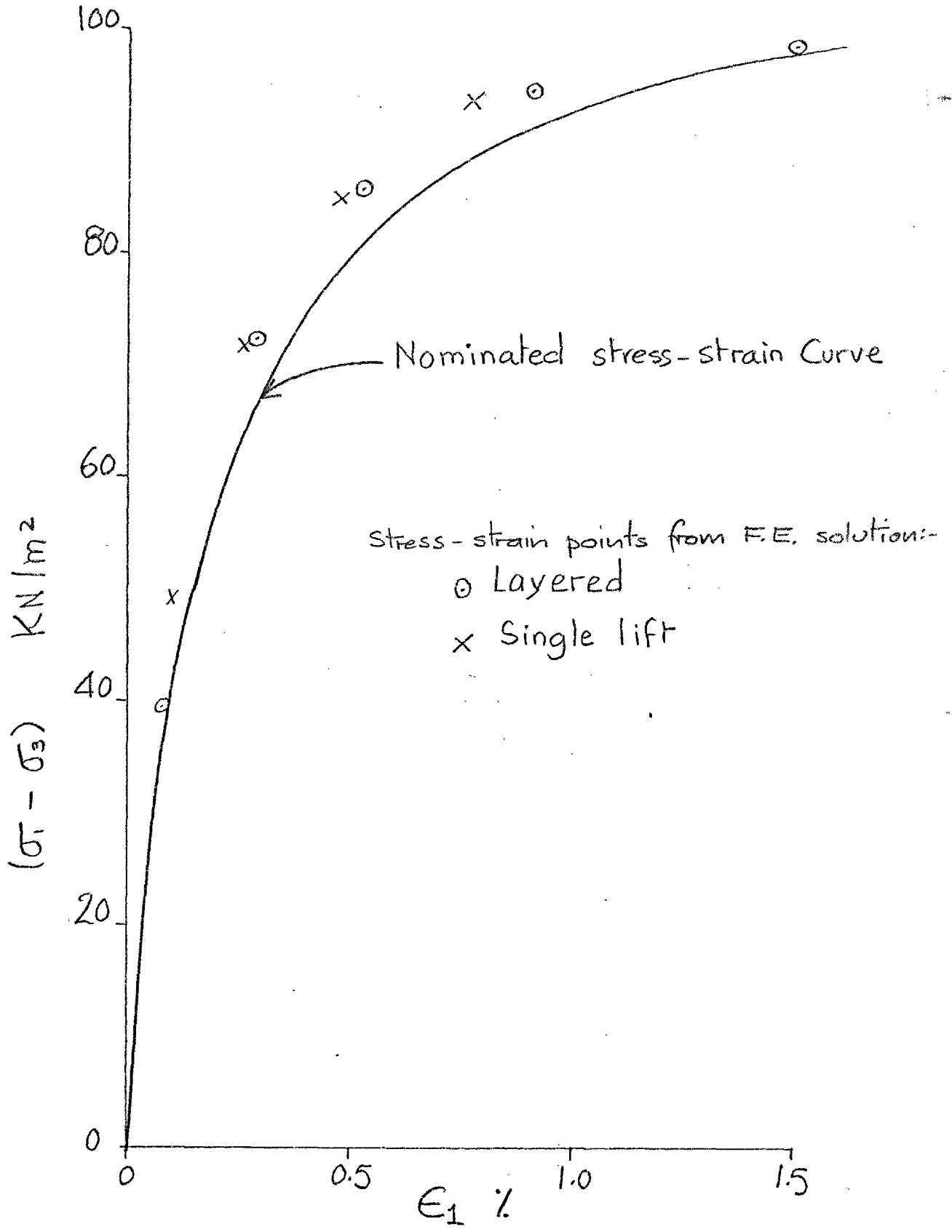
Fig. 8.3

HORIZONTAL STRAINS AT 1.5 m. BELOW FOUNDATION SURFACE FOR LAYERED AND SINGLE LIFT SOLUTIONS – LINEAR ANALYSIS



HORIZONTAL DISPLACEMENTS AT INCLINOMETERS IB3 & IB4 FOR LAYERED AND SINGLE LIFT. LINEAR ANALYSES.

Fig. 8.4



NONLINEAR STRESSES AND STRAINS FOR SINGLE AND LAYERED SOLUTIONS AT A POINT WITHIN THE LOCAL FAILURE ZONE

Fig. 8.5

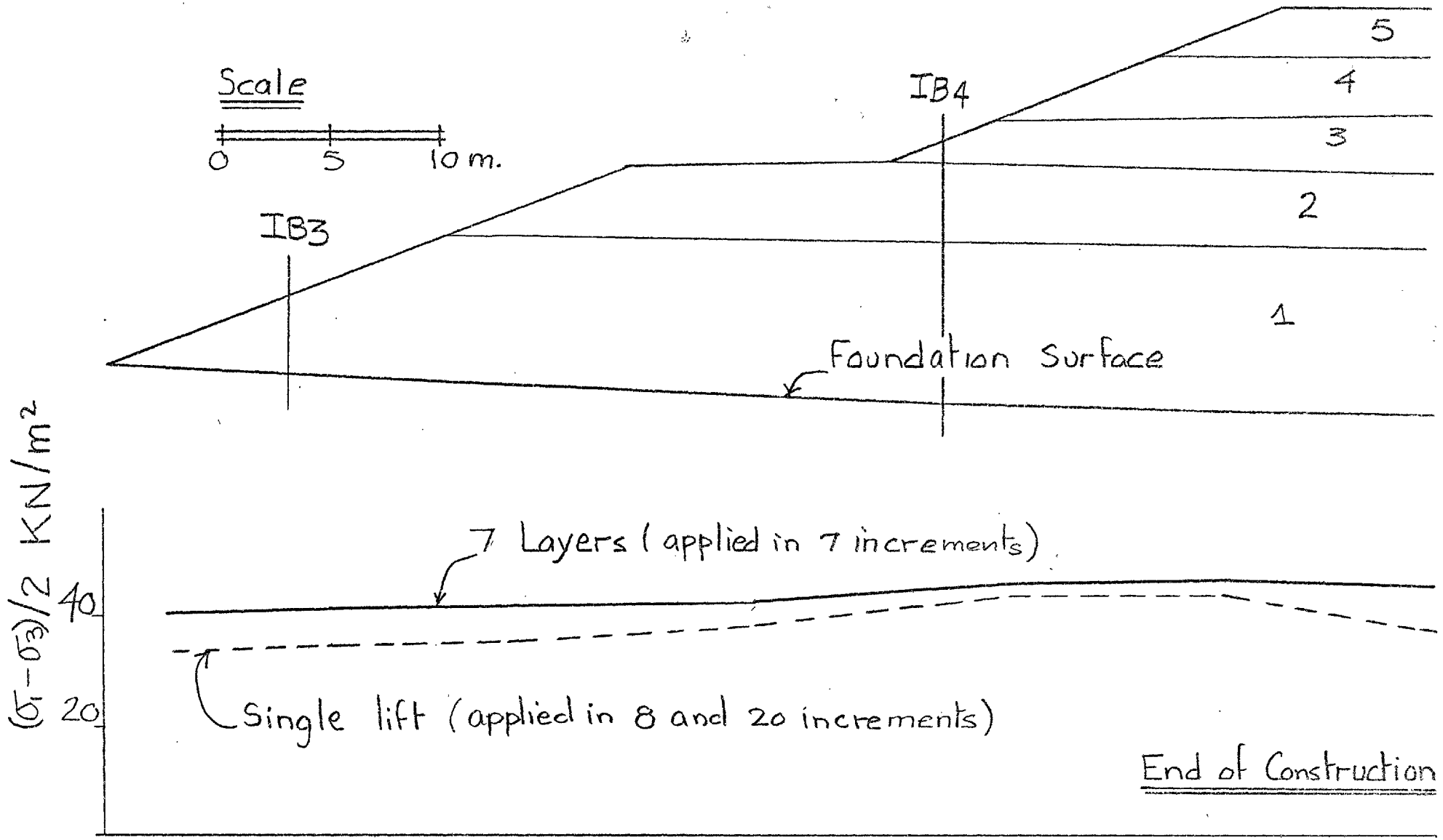


Fig. 8.6

MAX. SHEAR STRESSES AT 1.5 m. BELOW FOUNDATION SURFACE FOR LAYERED AND SINGLE LIFT SOLUTIONS _ NONLINEAR ANALYSIS

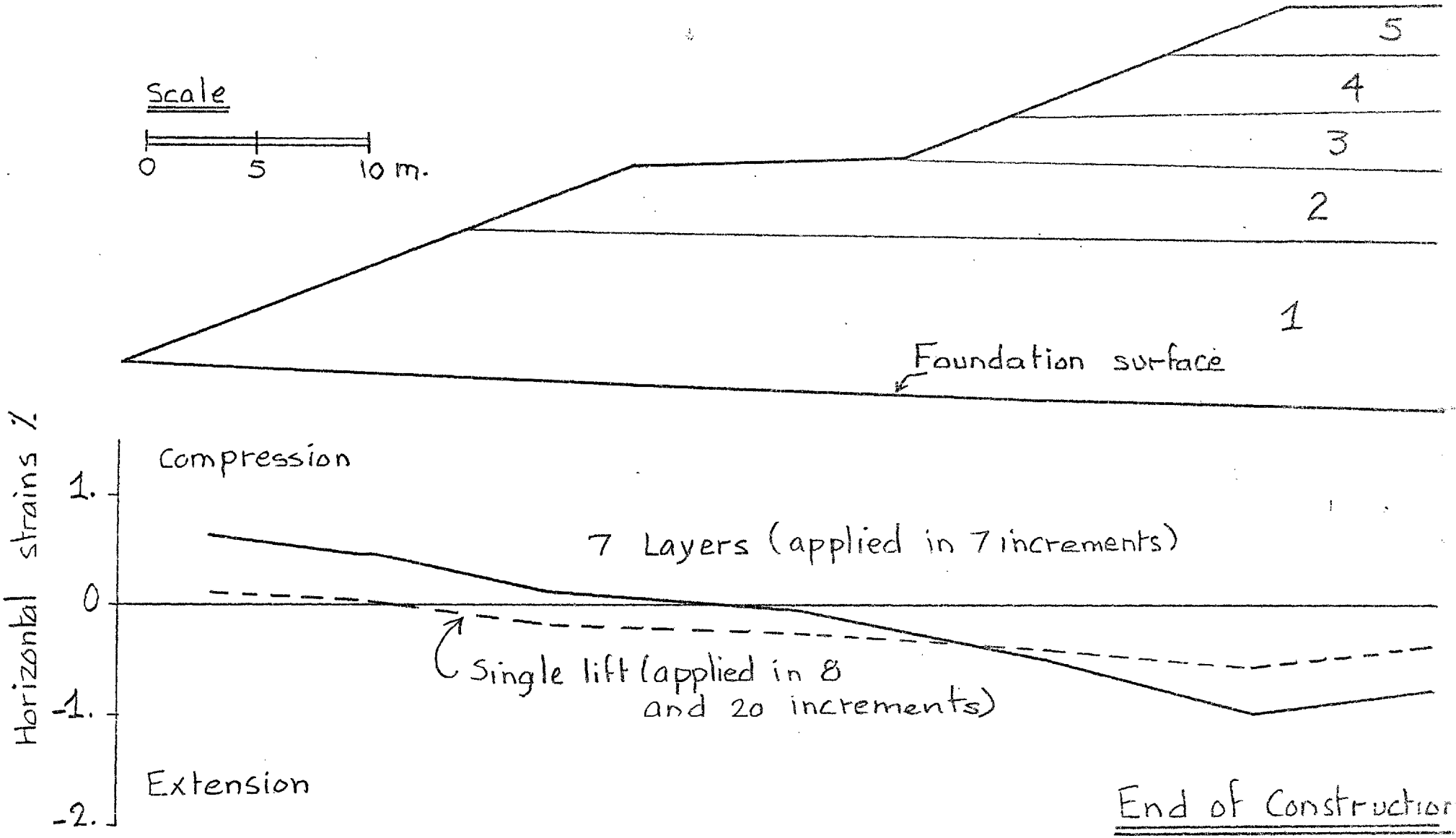
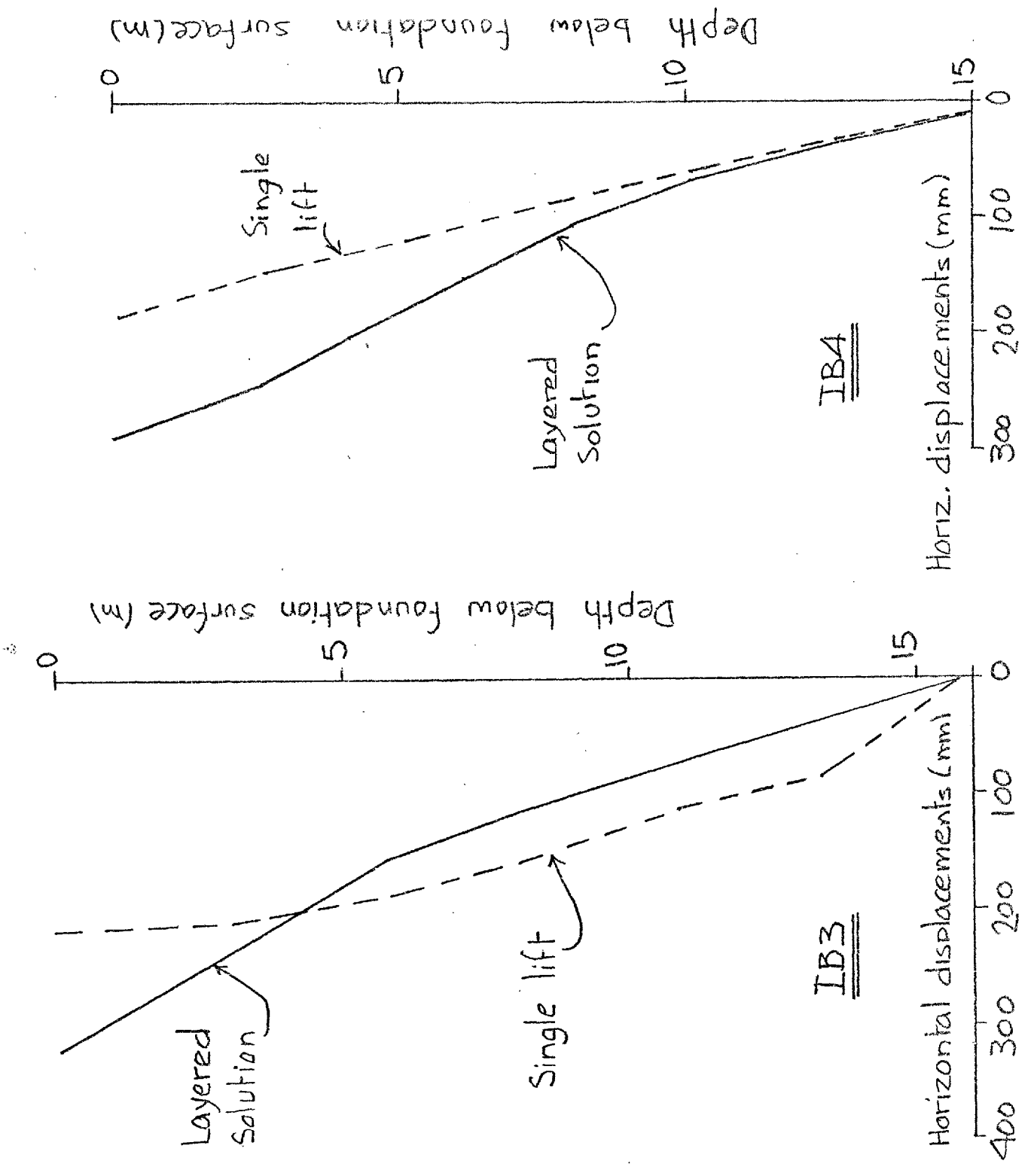


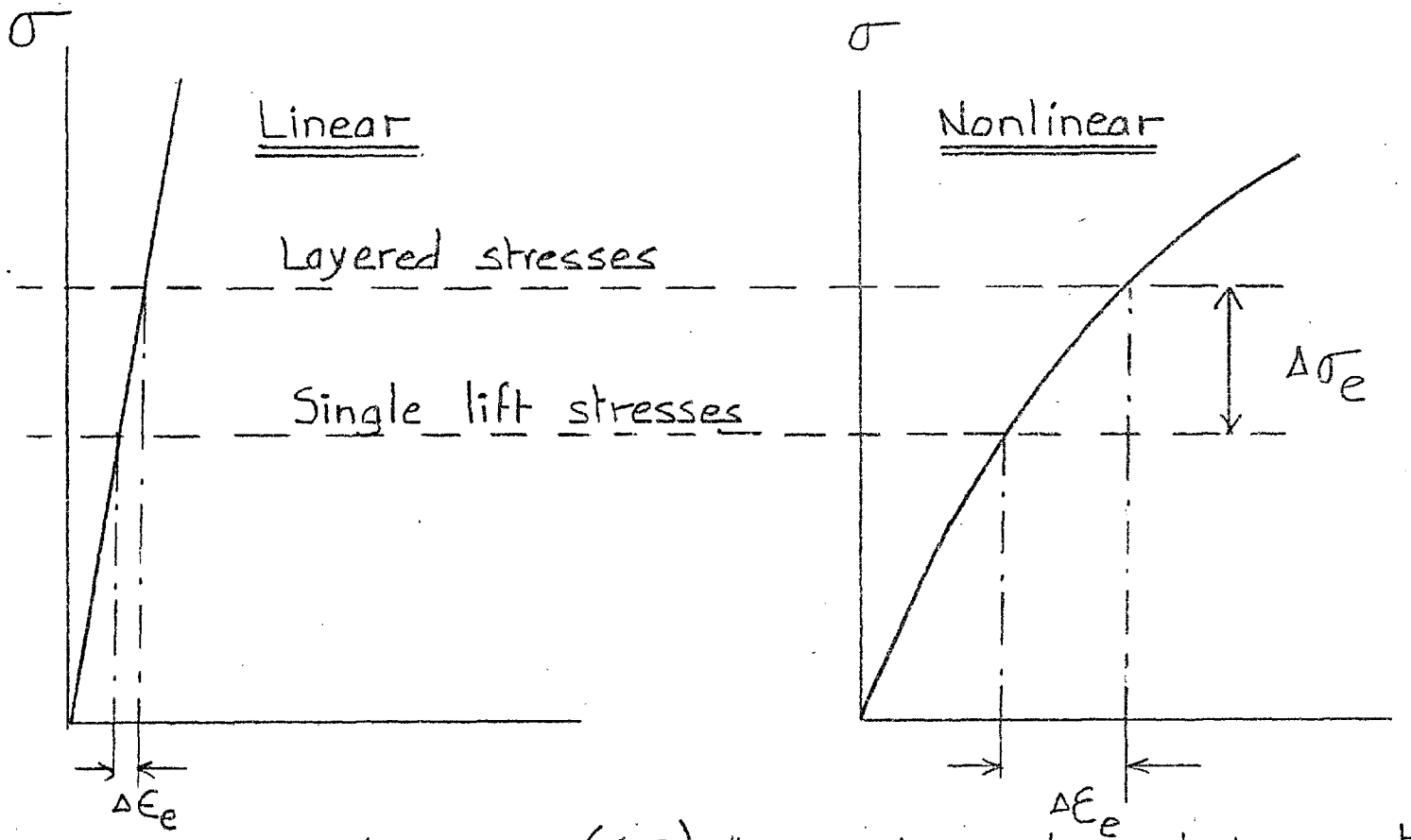
Fig. 8.7

HORIZONTAL STRAINS AT 1.5 m. BELOW FOUNDATION SURFACE FOR LAYERED AND SINGLE LIFT SOLUTIONS _ NONLINEAR ANALYSIS



HORIZONTAL DISPLACEMENTS AT INCLINOMETERS IB3 + IB4 FOR LAYERED AND SINGLE LIFT. NONLINEAR ANALYSES.

Fig. 8.8



For the same stress error ($\Delta\sigma_e$), the non-linear stress-strain assumption amplifies the strain error and hence the displacement error

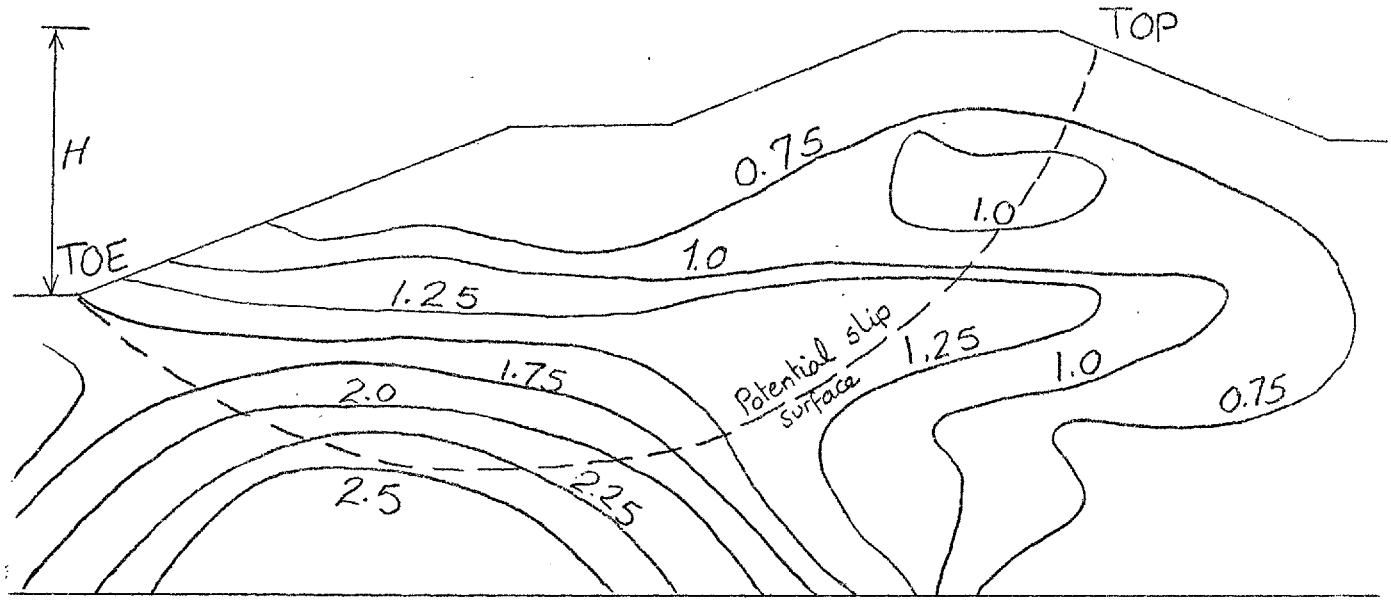
ILLUSTRATION OF THE ERRORS INVOLVED IN NONLINEAR AND LINEAR ANALYSES FOR SINGLE LIFT SOLUTION

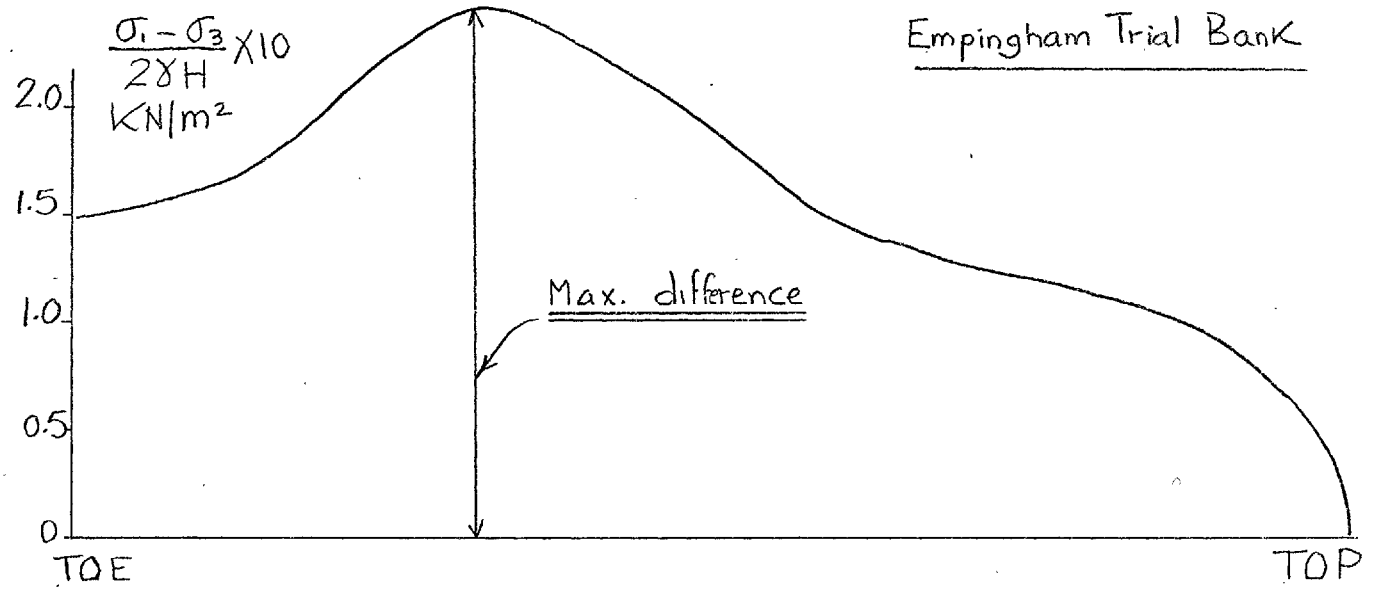
Fig. 8.9

Undrained Analysis

$\nu = 0.499$

E is independent of σ_3





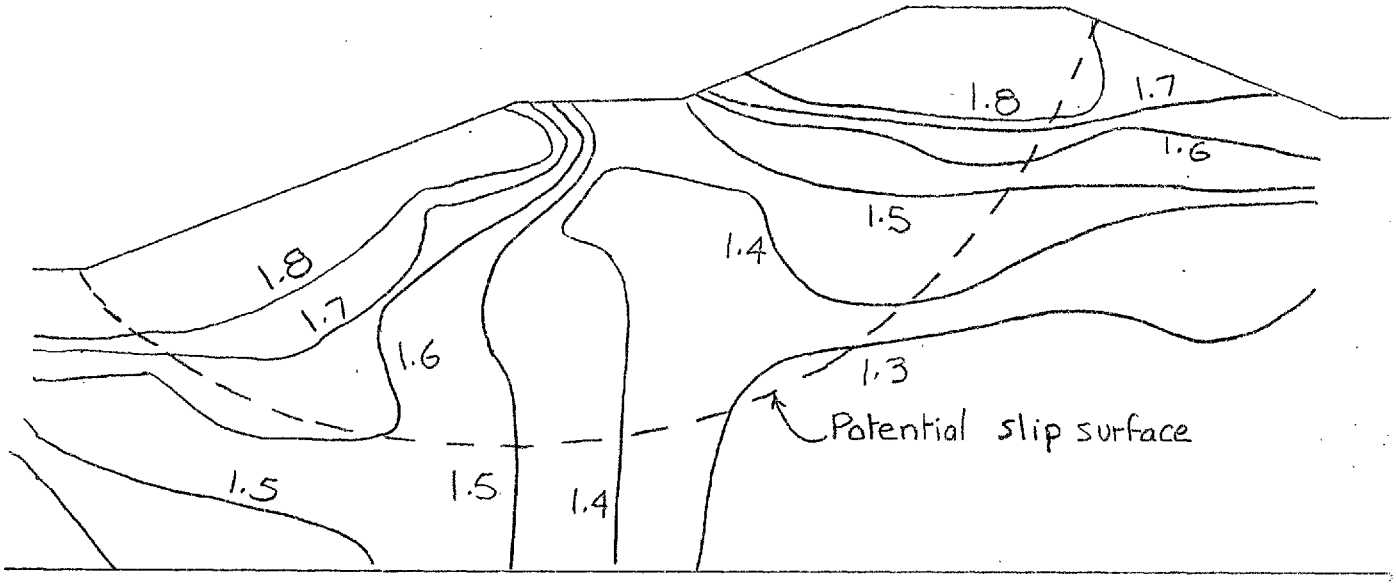
CONTOURS OF $[(\sigma_1 - \sigma_3)/2\gamma H]$ WITHIN EMPINGHAM TRIAL BANK AND ITS DISTRIBUTION ALONG POTENTIAL SLIP SURFACE LINEAR ANALYSIS

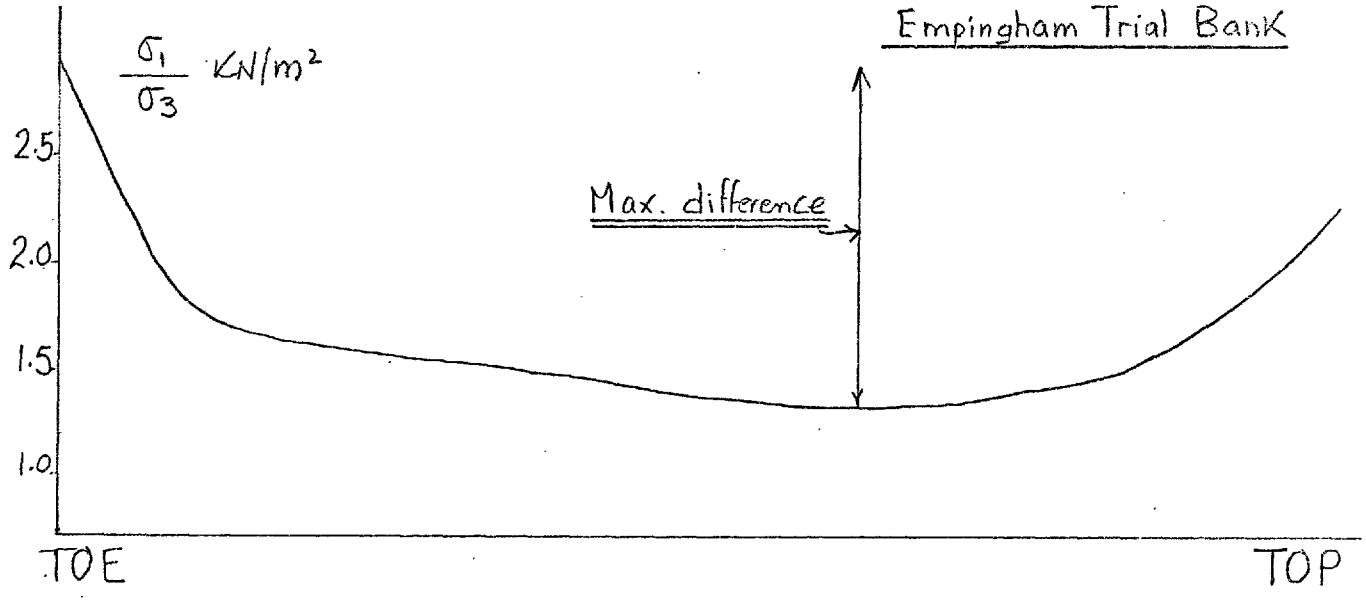
Fig. 8.10

"Undrained" Analysis

$\nu = 0.499$

E is independent of σ_3





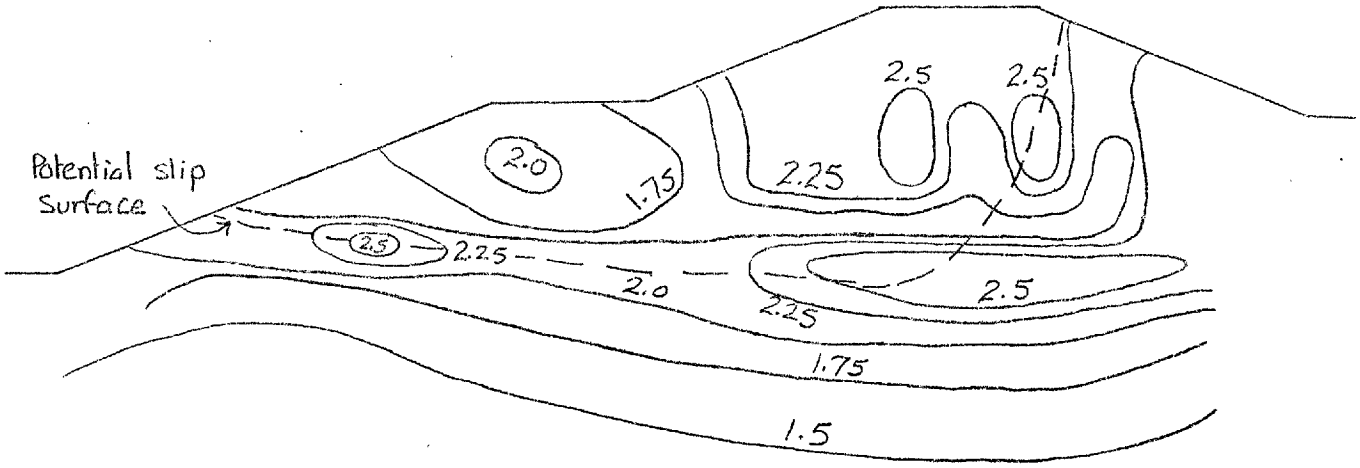
CONTOURS OF [σ_1/σ_3] WITHIN EMPINGHAM TRIAL BANK AND ITS DISTRIBUTION ALONG POTENTIAL SLIP SURFACE LINEAR ANALYSIS

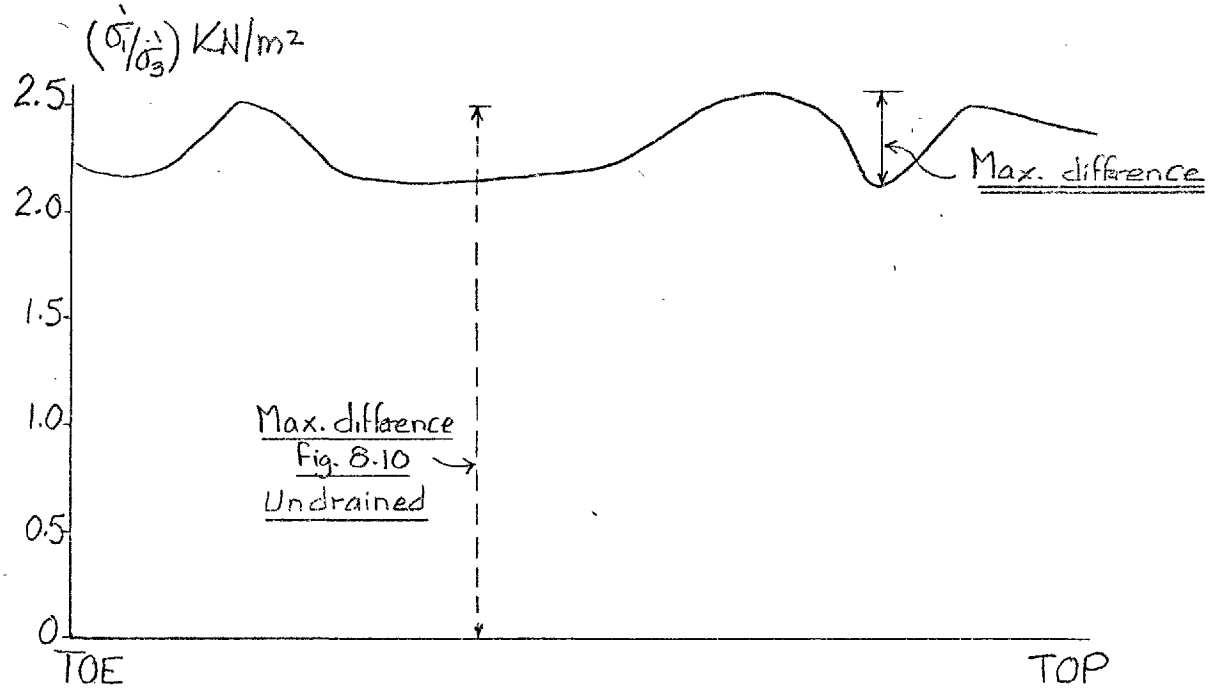
Fig. 8.11

Drained Analysis

$\nu = 0.25$

E is dependent on σ_3





CONTOURS OF $[\sigma_1'/\sigma_3']$ WITHIN EMPINGHAM TRIAL BANK AND ITS DISTRIBUTION ALONG POTENTIAL SLIP SURFACE LINEAR ANALYSIS

Fig. 8.12

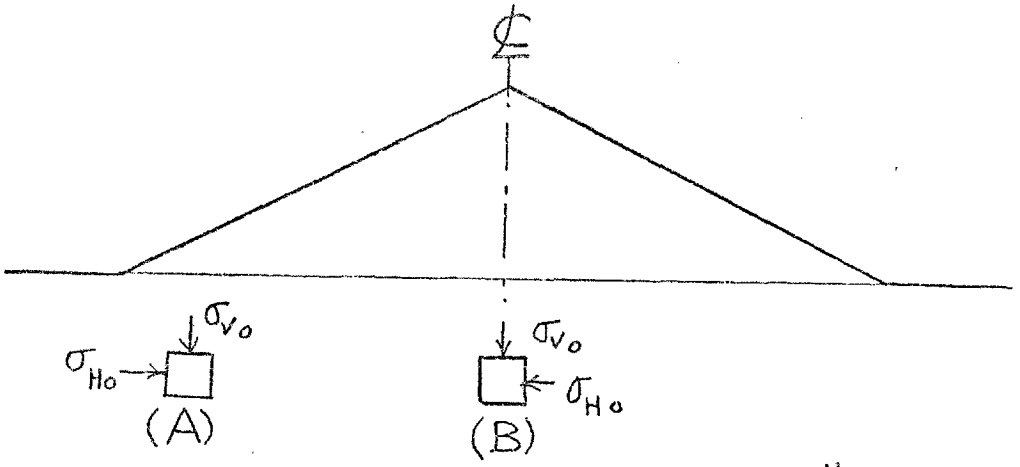
IMPORTANCE OF UNDRAINED SHEAR STRENGTH ON BEHAVIOUR - POINT I4

Fig. 8.13

IMPORTANCE OF UNDRAINED SHEAR STRENGTH ON BEHAVIOUR _ POINT I3

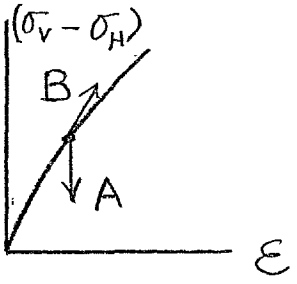
Fig. 8.14

EFFECT OF INITIAL STRESSES ON INITIATION OF LOCAL FAILURE



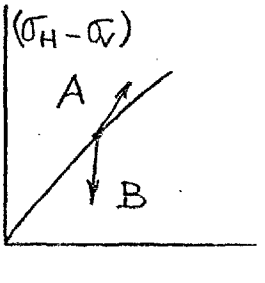
Applying the dam's own weight will increase $(\sigma_1 - \sigma_3)$ at (A) mainly due to an increase in σ_H and at (B) mainly due to an increase in σ_V.

IF $K_0 < 1$. (ie $\sigma_{V_0} > \sigma_{H_0}$)



The increase in σ_H at (A) will cause a decrease in shear stress and move the stress point away from failure, while an increase in σ_V at (B) will take the state of stress closer to failure and hence to local yield

IF $K_0 > 1$ (ie $\sigma_{V_0} < \sigma_{H_0}$)



The increase in σ_H at (A) will cause an increase in shear stress and move the stress point towards failure and local yield: while an increase in σ_V at (B) will take the state of stress away from failure.

Fig. 8.15

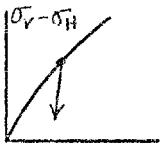
d) Anisotropic initial state of stress ($K \neq 1$)

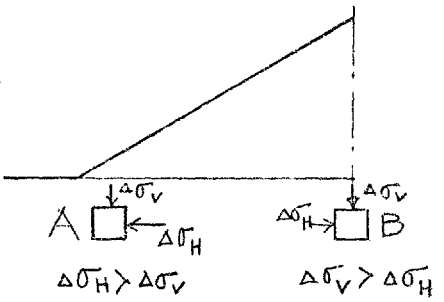
At (A): shear unloading occurs if

$K_o < 1$

due to increase

in $\Delta\sigma_H > \Delta\sigma_V$



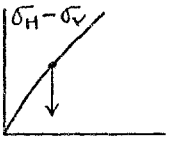


At (B): shear unloading occurs if

$K_o > 1$

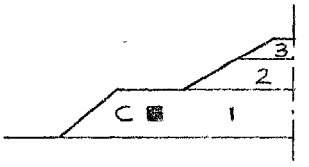
due to increase

in $\Delta\sigma_V > \Delta\sigma_V$



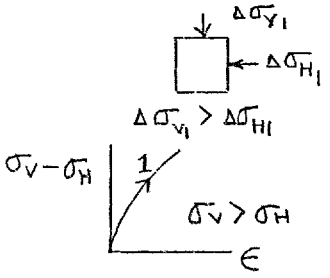
---

c) Use of berms

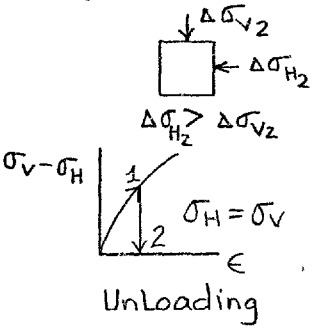


Consider point C inside the berm;

after Layer (1)

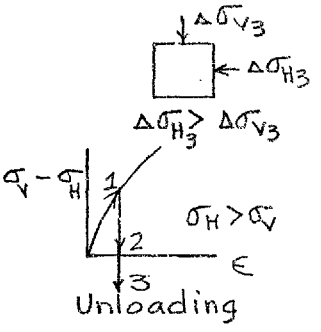


Layer (2)



Unloading

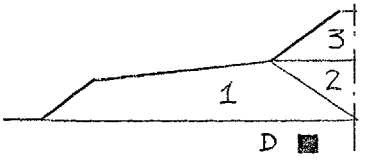
Layer (3)



Unloading

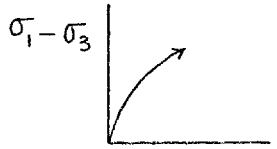
---

b) Irregular Construction Seauence



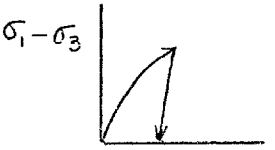
Consider point D in the foundation;

after Layer (1)



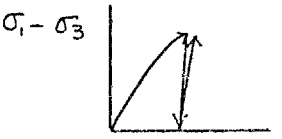
Loading

Layer (2)



Unloading

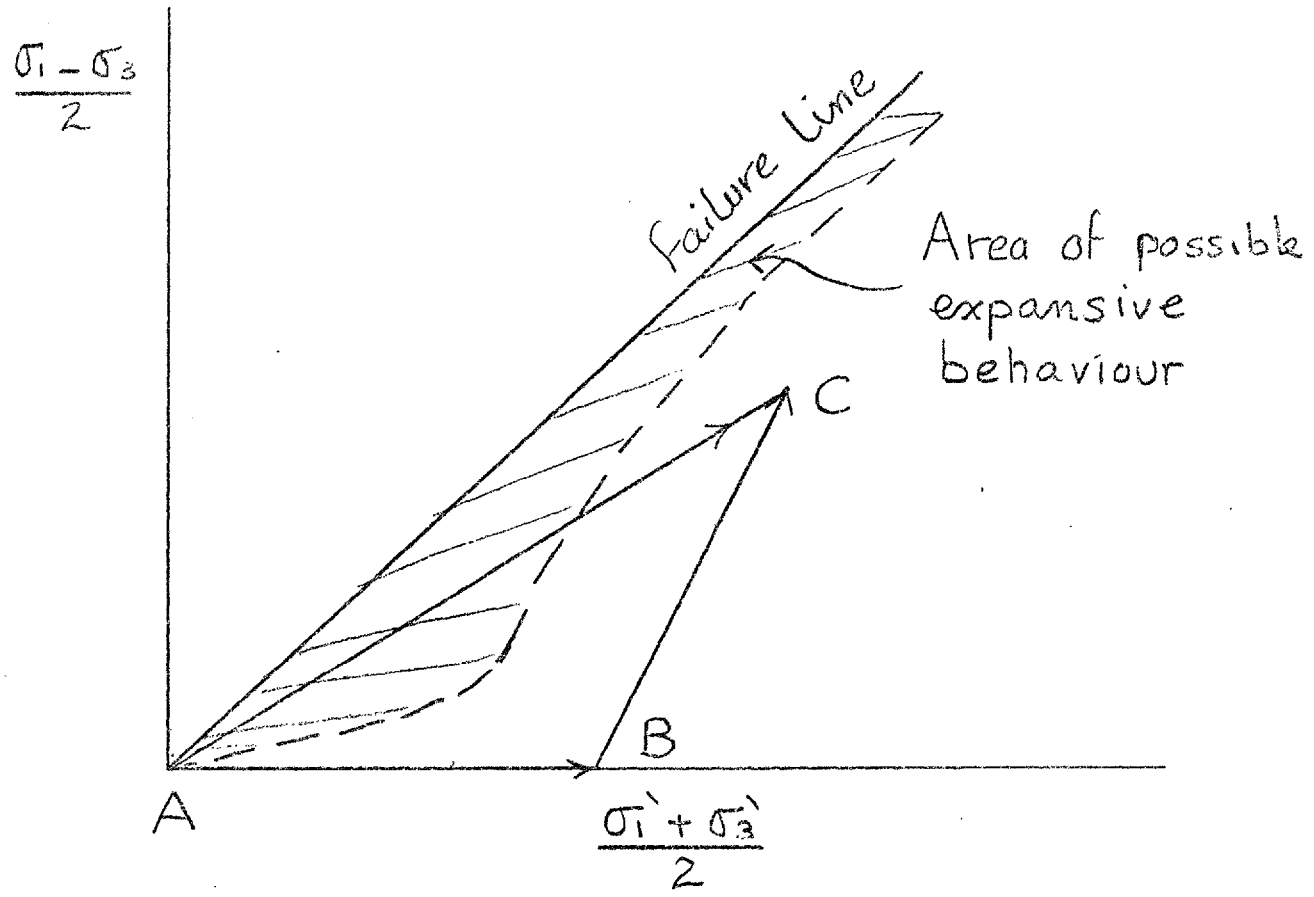
Layer (3)



Re-loading

SITUATIONS LEADING TO SHEAR UNLOADING AND RE-LOADING IN EMBANKMENT DAMS

Fig. 8.16



Triaxial Compression test (A-B-C)

Stage A-B : Isotropic compession stress produces only compressive strains

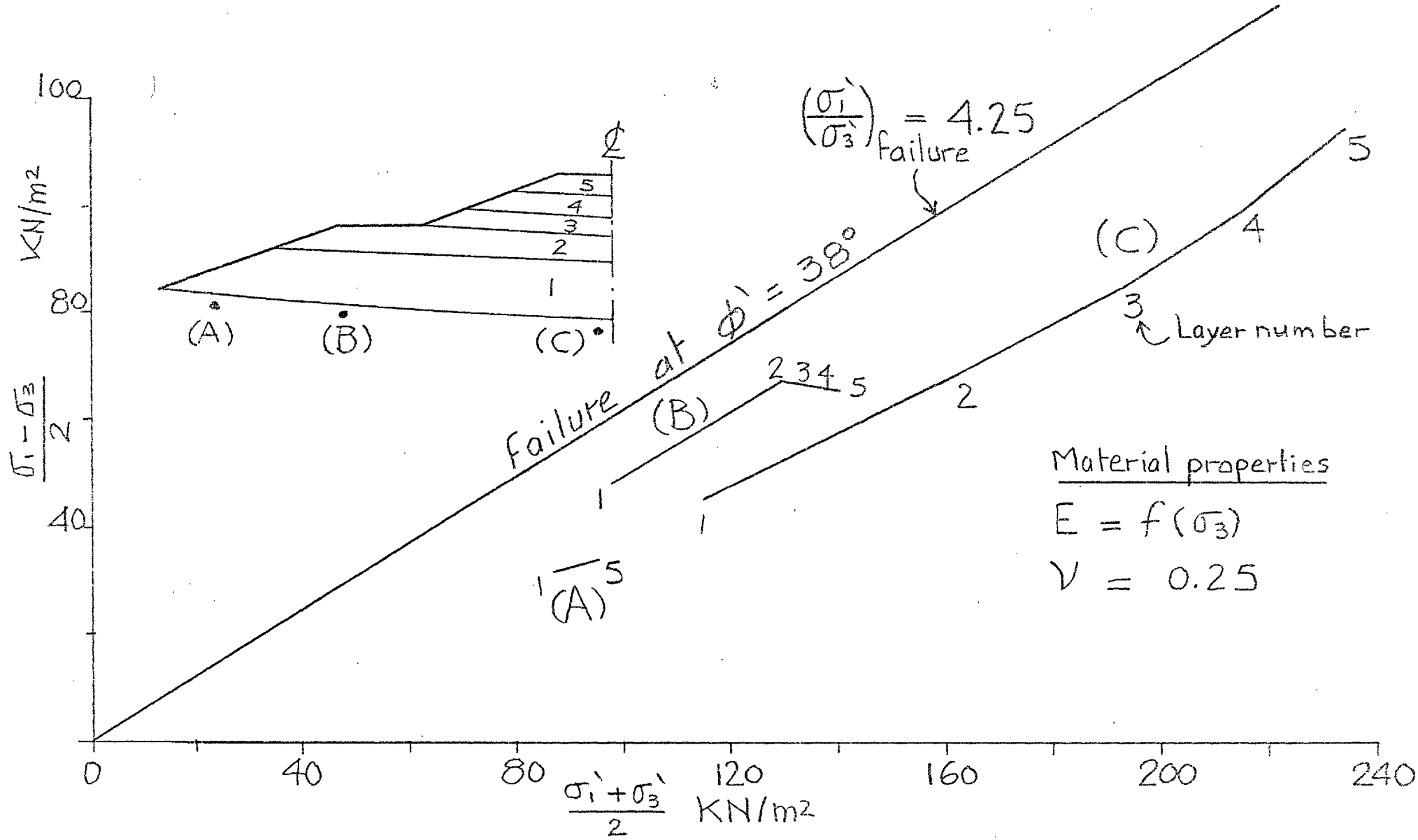
Stage B-C : Shearing by increasing σ_1' only, produces either compressive or/and expansive strains

Constant σ_1'/σ_3' test (A-C)

Volume change is only expansive if σ_1'/σ_3' exceeds certain value dependent on the relative density.

IMPORTANCE OF STRESS RATIO ON VOLUMETRIC BEHAVIOUR

Fig. 8.17



STRESS PATH FOR 3 POINTS UNDER AN EMBANKMENT BUILT IN 5 LAYERS FROM 'DRAINED' MATERIAL

Fig. 8.18

REFERENCES

AL-HUSSAINI M.M.T.& RADHAKRISHNAN N. (1972). Analysis of Plane Strain Tests using the finite element method. Applications of the finite element method in geotechnical engineering. Proceedings of the Symposium held at Vicksburg, Mississippi.

ARGYRIS J.H.& SCHARPF D.W. (1969). Methods of elasta-plastic analysis. ISD, ISSC symp. on Finite Element Tech., Stuttgart.

ATKINSON J.H. (1973). The deformation of undisturbed London clay. Ph.D. Thesis, Univ. of London.

BASU A.K. (1972). Private Communication.

BAZELEY G.P., CHEUNG Y.K., IRONS B.M. & ZIENKIEWICZ O.C. (1965). Triangular elements in bending-Conforming and non-conforming solutions. Proc. Conf. Matrix methods in struct. Mech., Air Force Inst. Techn. Wright Patterson A.F. Base Ohio, 1965.

BIOT M.A. (1941). General theory of three-dimensional consolidation. Jour. App. Phys., 12, 155-426 and 578.

BISHOP A.W. (1952). The stability of earth dams. Ph.D. Thesis, University of London.

BISHOP A.W. (1954). The use of pore pressure coefficients in practice Geot. Vol.4, pp.148-152.

BISHOP A.W. (1966 a). Soils and Soft Rocks as Engineering Materials Inaugural Lecture. Imperial College of Science and Technology, University of London.

BISHOP A.W. (1966b). The strength of soils as Engineering materials Sixth Rankin lecture. Geotechnique 10:2, pp.89-129.

BISHOP A.W. (1967). Progressive failure with special reference to the mechanism causing it. Proc. Geot. Conf., Oslo, 2, 142-150.

BISHOP A.W. (1971). The influence of progressive failure on the choice of the method of stability analysis. Geot. 21,2, 168-172.

BJERRUM L. (1967). Progressive failure in slopes of over consolidated plastic clay and clay shales. 3rd. Terzaghi Lecture, Proc. ASCE, 93, 3-49.

BOOTH A.D. (1966). Numerical methods. Butherworths Scientific Publications.

BROYDEN C.C. (1965). A class of methods for solving non-linear simultaneous equations. Math. Comp. 19, 577-593.

BROYDEN C.C. (1965). A class of methods for solving non-linear simultanous equations. Math. Comp. 19, 577-593.

BROYDON C.C. (1969). A new method of solving nonlinear simultaneous equations. Computer Journal 12, 94-100.

BROWN K.M. (1969). A quadratically convergent Newton like method based upon Gaussian elimination. SIAM J. Num. Anal., 6, 560-569.

CHANG C.Y. & DUNCAN J.M. (1970). Analysis of soil movement around a deep excavation. J. of SMFE Division, ASCE, Vol. 96, No.SM5 pp. 1655-1683.

CHARLES J.A. (1975). Strains developed in two rockfill dams during construction. Geotechnique, Vol. 25, No.2.

CHRISTIAN J.T. (1966). Plane strain deformation analysis of soil. Contract report No. 3-129 U.S. Army Engineers waterways experiment station, Vicksburg, Mississippi, December.

CLOUGH G.W. & DUNCAN J.M. (1969). Finite element analysis of Port Allen and old river locks. Contract report No. S-59-6. U.S. Army Engineering waterways experiment station, Vicksburg, Mississippi, Sept.

CLOUGH P.W. & WOODWARD R.J. (1967). Analysis of embankment stresses and deformations. J. of SMFE Division, ASCE, Vol.93, No.SM4. pp.529-549.

CRANDALL S.H. (1956). Engineering Analysis, McGraw-Hill, 1956.

CHRISTIAN J.T. & BOEHMER J.W. (1970). Plane Strain Consolidation by finite elements. J.of the SMFE Division, ASCE, Vol. 96, No.SM4.

D'APPOLONIA D.J. & LAMBE T.W. (1970). "Method for predicting intial settlement". J. of Soil Mechanics and Foundation Engineering, ASCE, SM2, Vol.96.

DAVACHI M.M. (1976). Ph.D. research results, unpublished.

DAVIDENKO D.F. (1953a), (1953b). On approximate solution of systems of nonlinear equations. UKrain Mat. Zurnal, 5, pp.196-206.

On a new method of numerical solution of nonlinear equations. DoKLady Akad. Nauk USSR (N.S) 88, 601-60

DAVIS E.H. (1968). Theories of plasticity and the failure of soil masses. Soil mechanics selected Topics. American Elserier Co., New-York. pp. 341-380.

De JOSSELIN de JONG G. (1964). Lower bound theorem and lack of normality of strain rate to yield surface for soils. IUTAM SYMP. on Rheology and soil mechanics, Grenoble, pp. 69-75.

DESAI C.S. (1971). "Nonlinear analysis using spline functions" J. of the Soil Mechanics and Foundations Division, ASCE, No.SM10, Vol.97, pp. 1461-1480.

DIBAJ M. & PENZIEN J. (1969). "Non-linear seismic response of earth structures". Report No. EERC 69-2, Earthquake Engineering Research Centre, College of Engineering, University of California, Berkeley, USA.

DOMASCHUK L. & WADE N.H. (1969). A study of bulk and shear moduli of a sand J. of SMFE Division, ASCE, Vol.95, No. SM2 pp.561-581.

DRUCKER D.C. (1950). Some implications of work hardening and ideal plasticity. Quarterly of applied mathematics, Vol.7, No.4, pp.411-418.

DRUCKER D.C.(1951). A more fundamental approach to plastic stress-strain relations. Proc. 1st. U.S. National Congress Applied Mechanics, Chicago, 1951.

DRUCKER D.C.(1953). Limit analysis of two and three dimensional soil mechanics problems. J. of mechanics and physics of solids. Vol. 1, pp. 217-226.

DRUCKER D.C. (1959). A definition of stable inelastic material. J. of applied mechanics. March. pp.101-106.

DRUCKER D.C., HENKEL D.J., GIBSON R.E. (1958). Soil mechanics and work hardening theories of Plasticity. Transaction, ASCE, Vol. 122, pp.338-346.

DRUCKER D.C. & PRAGER W. (1952). Soil mechanics and plastic analysis of limit design. Quarterly of applied mathematics. Vol. 10, No.2, pp. 157-165.

DUNCAN J.M. (1974). Notes for Program on Recent Developments in The design, Construction and Performance of Embankment Dams; Static finite Element Analyses. Civil Engineering Department, University of California, Berkeley.

DUNCAN J.M.& CHANG CY(1970)."Nonlinear analysis of stress and strain in soils", J. of the Soil Mechanics and Foundations Division ASCE, SM5, Vol.96, pp.1629-1653.

DUNLOP P. & DUNCAN J.M. (1970). Development of failure around excavated slopes. J. of the Soil Mechanics and Foundations division. SM2, ASCE, Vol.96.

EISENSTEIN Z., KRISHONGYA A. & MORGENSTERN N. (1972). An analysis of cracking in earth dams. Proc. of Symp. on Application of the FEM in Geotechnical Engrg. USAEWES, Vicksburg, Miss., USA, pp.431-454.

EISENSTEIN Z. (1974). State of the art paper: Embankment dams. Proceedings. Rio de Janeiro, Coordenacao dos Programas de Pos-Graduacao de EngenGaria Universidade Federal.

EISENSTEIN Z. & SIMONS J.V. (1975). Three-dimensional analysis of Mica dam. Proc. of the Numerical analysis of dams. Ed. Naylor, et al.

ELLISON, R.D. (1968). "Analytical study of mechanics of single pile". Ph.D. thesis, Carnegie-Mellon University, Pittsburgh, Penn., USA.

ELLISON R.D. & D'APPOLONIA E. & THIERS G.R. (1971). "Load-deformation mechanism for bored piles". J. of Soil Mechanics and Foundations Division, ASCE, SM4, Vol.97.

EL-RUWAYIH A. (1975). Stress-strain characteristics of rockfills, and of clays under high porewater tension. Ph.D. Thesis, Imperial College, Univ. of London.

EL-SOHBY A.A.K. (1969). Deformation of Sands Under Constant Stress Ratio. Proc. 7th. Int. Conf. Soil Mech., Mexico, Vol. 1, 111-119.

GALLAGHER R.H. & PADLOG J. & BIJLAARD P.B. (1962). Stress analysis of heated complex shapes. J. Am. Rocket Soc., 32, 700-707.

GOODMAN L.E. & BROWN C.B. (1963). Dead load stresses and the instability of slopes. J. of SMFE Division, ASCE, SM3.

GOPALAKRISHNAYYA,A.V. (1973). Analysis of cracking of earth dams. Ph.D. Thesis, the University of Alberta.

HAGMANN A.J. (1971). Predictions of stress and strain under drained loading conditions. M.I.T. Department of civil engineering report No. R71-3.

HAMZA M.M. (1972). Certain problems with nonlinear finite elements. Part I: Acceleration techniques. Part II: Studies on an earth dam. M.Sc. Thesis, University of Wales, Swansea.

HANSEN J.B. (1953). Earth pressure calculation. Danish Technical Press. Copenhagen, Denmark, pp.271.

HENKEL D.J. (1958). The correlation between deformation, pore water pressure and strength characteristics of saturated clays. Ph.D. Thesis, Imperial College, University of London.

HENKEL D.J. (1971). The relevance of laboratory measured parameters in field studies, Proc. Roscoe Mem. Symp., Cambridge, 669.

HENRICI P. (1962). Discrete Variable Methods in Ordinary differential equations. John Wiley, New York, 1962, Chapter 2 & 3.

HOUSEHOLDER A.S. (1953). Principles of numerical analysis. McGraw-Hill.

HWANG C.T., MORGENSTERN N.R. & MURRAY D.W. (1971). On solution of plane strain consolidation problems by finite element methods. Canadian Geotechnical Journal, Vol. 8, p.109-118.

IRONS B.M. (1963). Stress analysis by stiffnesses using numerical integration. Internal report, A.S.M. 622, Rolls Royce Ltd.

IRONS B.M. (1968). The technique of finite element analysis. Unpublished book.

IRONS B.M. (1970). A frontal solution program for finite element analysis. Int. J. Num. Meth. Engg. 2, 5-32.

IRONS B.M. (1971). A banded conjugate gradient solution. Internal report C/R/144/71 - Swansea.

IRONS B.M. (1973). Economisers for nonlinear finite element problems. Internal report Swansea, Feb.

IRONS B.M. & TREHARNE G. (1971). A bound theorem in eigen-values and its practical applications.. Wright-Patterson Conference, Ohio, USA.

IRONS B.M. (1973). Economic for nonlinear finite element problems. Private communication. To be published hopefully.

IRONS B.M., & ZIENKIEWICZ O.C. (1968). The isoparametric finite element system - a new concept in finite element

analysis. Proc. Conf. Recent Advances in stress Analysis, Royal Aero Soc.

JAEGER J.C. (1956). Plasticity, Fracture and flow. Methuen & Co. Ltd., London.

JANBU N. (1963). Soil compressibility as determined by Oedometer test and Triaxial tests. Proc. of the European Conference on Soil Mechanics and Foundation Engineering, Vol.1, Wiesbaden, Germany, p.19.

KAN D.K. (1972). Solution techniques for large finite element problems concerning creep and temperature transients in cooled gas turbine blades. Ph.D. Thesis, University of Wales, Swansea.

KING I.P. (1964). Finite element analysis of two-dimensional time-dependent stress problems. Dissertation presented to the University of California, Berkeley, in partial fulfilment of the requirements for the degree of Doctor of Philosophy.

KIZNER W. (1964). A numerical method for finding solutions of nonlinear equations. J. SIAM, 12, pp.424-428.

KLYUYEV V.V., & KOKOVKIN-SHERBAK N.I. (1965). On the minimization of the number of arithmetic operations for the solution of linear algebraic systems of equations. Technical report CS24, Computer Science department Stanford University.

KONDNER R.L. (1963). Hyperbolic stress-strain response: cohesive soils. J. of SMFE Division, ASCE, Vol.89, No.SM1.

KONDNER P.L., & ZELASKO, J.S.(1963). A hyperbolic stress-strain formulation for sands. Proc.2nd Pan American Conference on Soil Mech. and Found. Engg., Vol.1, pp. 289-324, Brazil.

KULHAWY F.H. & DUNCAN J.M. (1970). Nonlinear finite element analysis of stresses and movements in OLOVILLE dam. Report No. TE-70-2, University of California, Berkeley, Jan.

KULHAWY F.H., DUNCAN J.M. & SEED H.B. (1969). Finite element analysis of stresses and movements in embankments during construction. USAEWES Contract Report S-69-8- Vicksburg, Miss, USA.

LAMBE T.W. (1973). Predictions in soil engineering. Thirteenth Rankine Lecture. Geotechnique Vol.23.

LAMBE T.W. & WHITMAN R.V. (1969). "Soil mechanics", Wiley, New York.

LANCASTER P. (1966). Error analysis for Newton-Raphson method. Numer. Math, 9, 55-68.

LEFEBVRE G. & DUNCAN J.M. (1971). Three-dimensional finite element analysis of dams. Report No. TE 71-5, College of Engineering, office of research service, University of California.

LEFEBVRE G., DUNCAN J.M. & WILSON E.L. (1973). Three-dimensional finite element analysis of dams. J. of the SMFD, ASCE, Vol.99, SM7, pp.495-507.

LOVE A.E.H. (1927). "A treatise on the mathematical theory of elasticity". 4th. ed. New York, Dover, 1944. - Reprint of 1927 ed.

LU T.D. & SCOTT, R.F. (1972). "The distribution of stresses and developments of failure at the toe of a slope and around the tip of a crack". Proc. of the Conf. on the Application of the finite element method in Geotechnical Engineering, Vicksburg, Mississippi, USA.

LYNESS J. (1972). M.Sc. Thesis, University of Wales, Swansea.

MAGUIRE W.M. (1975). The undrained strength and stress strain behaviour of brecciated Upper Lias clay. Ph.D. Thesis, Imperial College, University of London.

MAKSIMOVIC M.M. (1971). "Cracking in dams with narrow central cores". M.Sc. thesis, Univ. of London, Imperial College.

MARCAL P.V. & KING I.P. (1967). Elastic-plastic analysis of two-dimensional stress systems by the finite element method. Int. J. Mech. Sci., 9, 3, 143-155.

MELOSH R.J. & BAMFORD (1969). Efficient solution of load-deflection equations. J. Struct. Div., Proc. ASCE, 95, ST4.

MITCHELL J.M. & GARDNER W.S. (1971). Analysis of load-bearing fills over soft subsoils. J. of SMFE Division. ASCE, Vol. 97, No.SM11. pp.1549-1571.

MURNAGHAN F.D. (1951). Finite deformation of an elastic solid. J. Wiley & Son, 1951.

NAYAK G.C. (1971). Plasticity and large deformation problems by the finite element method. Ph.D. Thesis, University of Wales, Swansea.

NAYAK G.C& ZIENKIEWICZ O.C. (1972). The 'alpha' constant stiffness method for the analysis of nonlinear problems. Int. J. Num. Method. Engg.

NAYLOR D.J. (1974). Stresses in nearly incompressible materials by finite elements with application to the calculation of excess pore pressures. Int. J. for Numerical methods in engineering. Vol 8, 443-460.

NAYLOR D.J. & HOOPER J.A. (1974). An effective stress finite element analysis to predict the short and long term behaviour of a piled-raft foundation on London clay. Proc. of the Conference of Settlement of Structures. Cambridge.

NAYLOR D.J. & JONES D.B. (1973). The predictions of settlement within broad layered fills. Geotechnique, Vol. 23.

NAYLOR D.J. & ZIENKIEWICZ O.C. (1971). Settlement analysis of a strip footing using a critical state soil model in conjunction with finite element . Proc. of the Symp. The interaction of structure and foundation, University of Birmingham.

OSTROWSKI A.M. (1966). Solution of equations and systems of equations. Academic Press (2nd ed.).

PALMER A.C. & RICE J.R. (1972). The growth of slip surfaces in the progressive failure of over-consolidated clay. Proc. Ray. Soc. Lond. A. 332, 527-548.

PALMERTON J.B. (1972). Application of three-dimensional finite element analysis. Proc. Application of the finite element method in Geotechnical Engineering. U.S. Army Engineers Waterways Experiment Station, Corps of Engineers, Vicksburg, Mississippi, USA.

PALMERTON J.B. & LEFEBVRE G. (1972). Three-dimensional behaviour of a central core dam. USAEWES, Research Report S-72-1, Vicksburg, Miss., USA.

POOROOSHASB H.S. & HOLUBEC I. & SHERBOURNE A.N. (1966) The yielding and flow of sand in triaxial compression. Part I, Canadian Geotechnical Journal 3, No.4, pp.179-190.

POOROOSHASB H.S. & HOLUBEC I. & SHERBOURNE A.N. (1967). The yielding and flow of sand in triaxial compression. Part 2 and 3. Canadian Geotechnical Journal No.4, pp. 376-397.

POPE G.G. (1965a) A discrete element method for analysis of plane elastic-plastic stress problems. Roy. Aero. Est. TR65028.

POPE G.G. (1965b). The application of the matrix displace-

ment method in plane elasto-plastic problem. Proc. Conf. on Matrix methods in struct. Mech. Wright Patterson Airforce Base, Ohio, pp.635-654.

PRANDTL L. (1920). Uber die Harte plastischer Korper. Nachrichten von der Koniglichen Gesellschaft der Wissenschaften zu Gottingen. Mathematisch - physikalische Klasse Berlin, S. 74-85.

PRZEMIENIECKI J.S. (1968). Theory of matrix structural analysis. McGraw-Hill.

PUGH R. (1976). Ph.D. Thesis, Imperial College, University of London.

PYRAH I.C. (1971). The calculation of deformation in earth structures using numerical methods. Ph.D. Thesis Imperial College, University of London.

RALL L.B. (1966). Convergence of the Newton process to multiple solutions. Numer. Math., 9, 23-37.

RALSTON A. (1965). A first course in numerical analysis McGraw-Hill Book Company.

RASHID Y.R. (1970). Three-dimensional analysis of elastic solids - II The computational problem. Int. J. Solids struct., 6, 1970.

ROSCOE K.H., ARTHUR J. & JAMES R. (1963). The determination of strain in soils by an x-ray method. Civil engineering and public work review. Vol.58, No.684, July (Part I) and Vol. 58, No.685, August (Part 2).

ROSCOE K.H. & BURLAND J.B. (1968). On the generalized stress-

strain behaviour of wet clay. Engineering plasticity. Ed. J. Heyman and F.A. Lecku, Cambridge University press. pp.535-609.

ROSCOE K.H., SCHOFIELD A.N. & WROTH C.P. (1958). On the Yielding of Soils. Geotechnique, 8, pp.22-53.

SAATY T.L. & BRAM J. (1964). Nonlinear Mathematics. McGraw-Hill Book Company, New York.

SCHOFIELD A.N. & WROTH C.P. (1968). Critical state soil mechanics. McGraw-Hill, London.

SKEMPTON A.W. (1954). The pore pressure parameters A and B. Geot., 4. pp 143-147.

SKEMPTON A.W. (1961). Horizontal stresses in an over-consolidated Eocene Clay. Proc. 5th, Int. Conf. of SMFE, Paris, 1, 351-357.

SMITH I.M. & KAY S. (1971). Stress analysis of contractive or dilative soil. J.SMFE Division Vol.97.

SODAH V.G. (1974). The stability of embankment dam fills of plastic clay. M.Phil.Thesis University of London, Imperial College.

SOKOLNIKOFF I.S. (1956). "Mathematical theory of elasticity". 2nd. Ed. McGraw-Hill, New York etc.

TAIG I.C. (1961). Structural analysis by the displacement method. English Electric Aviation Ltd., Report No. S.017.

TANG & HOEG (1968). Plane strain loading of a strain-hardening soil. Contract report No.5 to U.S. Corps of Engineers, M.I.T. March.

TERZAGHI K. (1943). Theoretical soil mechanics. John Wiley and Sons, New York, 1943,

TIMOSHENKO S.P. & GOODIER J.N. (1951). Theory of elasticity, 2nd ed. McGraw-Hill.

TIMOSHENKO S.P. & YOUNG D.H. (1965). Theory of Structures. 2nd ed. McGraw-Hill.

TRAUB J.F. (1964). Iterative methods for the solution of equations. Prentice-Hall, Inc., Englewood Cliffs, N.J. 215-230.

TRUESDELL C. (1966). "The elements of continuum mechanics". Springer-Verlag, Berlin. Heidelberg, New York.

VAUGHAN P.R. (1972a) Discussion, Proc. 5th European Conf. S.M. and F.E., Madrid, Vol.2, pp.72-75.

VAUGHAN P.R.(1972b) Report on the preliminary site investigation of Empingham dam site.

VAUGHAN P.R.(1974). M.Sc. Embankment dams course note, Imperial College, London University.

VAUGHAN P.R. (1975). Field Instrumentation and the behaviour of embankment dams. Simposio Sobre Instrumentacao de campo em engenharia de solus E. fundacoes. Coppe/UFRJ, Rio de Janeiro, November.

VAUGHAN P.R. & WALBANCKE H.J. (1973). Pore pressure changes and the delayed failure of cutting slopes in over-consolidated clay. Geotechnique, Vol. 23.

VAUGHAN P.R., WERNECK M.L.G. & HAMZA M.M. (1973). Discussion to sessions 3 and 4 Symp. on Field Instrumentation in Geotechnical Engineering, Butterworths London.

WASHIZU K. (1968). Variational methods in elasticity and plasticity. Pergamon Press.

WENDROFF B. (1966). Theoretical numerical analysis. Academic Press, 161-174.

WERNECK M.L.G. (1974). Field observations of the behaviour of the Upper Lias Clay at the Empingham Dam site. Ph.D. Thesis, Imperial College, University of London.

WONG H. (1971). "Analysis of braced excavation". Ph.D. Thesis, MIT at Cambridge, Massachussetts, USA.

WROTH C.P. (1971). Some aspects of the elastic behaviour of over-consolidated clay. Proc. Roscoe Mem. Symp. Cambridge, 347.

YAMADA Y. (1969). Recent Japanese developments in matrix displacement method for elastic-plastic problems. Proc. Japan -U.S., Seminar on Matrix Methods of Structural Analysis and Design, Tokyo, Alabama Univ.Press.

YAMADA Y. & YOSHIMURA N. & SAKURAI T. (1968). Plastic stress-strain matrix and its application for the solution of elastic-plastic problems by finite element method.

Int. J. Mech. Sci, 10, 343-354.

ZIENKIEWICZ O.C. (1971). The finite element method. McGraw-Hill.

ZIENKIEWICZ O.C. & NAYLOR D.J. (1971). The adaptation of critical state soil mechanics theory for use in finite elements. Proc. Roscoe Mem. Symp. Cambridge.

ZIENKIEWICZ O.C. & VALLIAPPAN S. & KING I.P. (1969). Elasto-plastic solutions of engineering problems; Initial stress finite element approach. Int. J. Num. Methods Engg, 1, 75-100.

APPENDIX

Flow chart of SAN2

In the following is given a brief description of the function of the SUBROUTINES appearing in the flow chart :-

GINPUT : Reads geometrical, material properties and boundary conditions. Store the input in the relevant disc and memory storage.

SHAPEF, SFR, AUX : Calculate shape function and its derivatives for each element using numerical integration and store it in disc file.

SINPUT : Reads the initial stresses and strains from cards or/and magnetic tape. Converts the initial stresses to nodal forces, and stores it in the memory

LINPUT : Reads the Loading pressures and forces Converts the loads into nodal forces and stores it in the memory.

ELSTIF, NLELAS : Calculate the stiffness matrix for each element according to it's state of stress and store it in disc file.

SOLVE : Assembles the overall stiffness matrix and reduces it by elimination.

BSUB : Obtains the displacement vector

SELECT : Selects the state of stress for the pilot solution.

RESID : Calculates the nodal forces corresponding to the total state of stress, and compares with the external applied loads.

STRAIN : Calculates strains from the displacements at the nodes.

STRESS : Calculates stresses from strains.

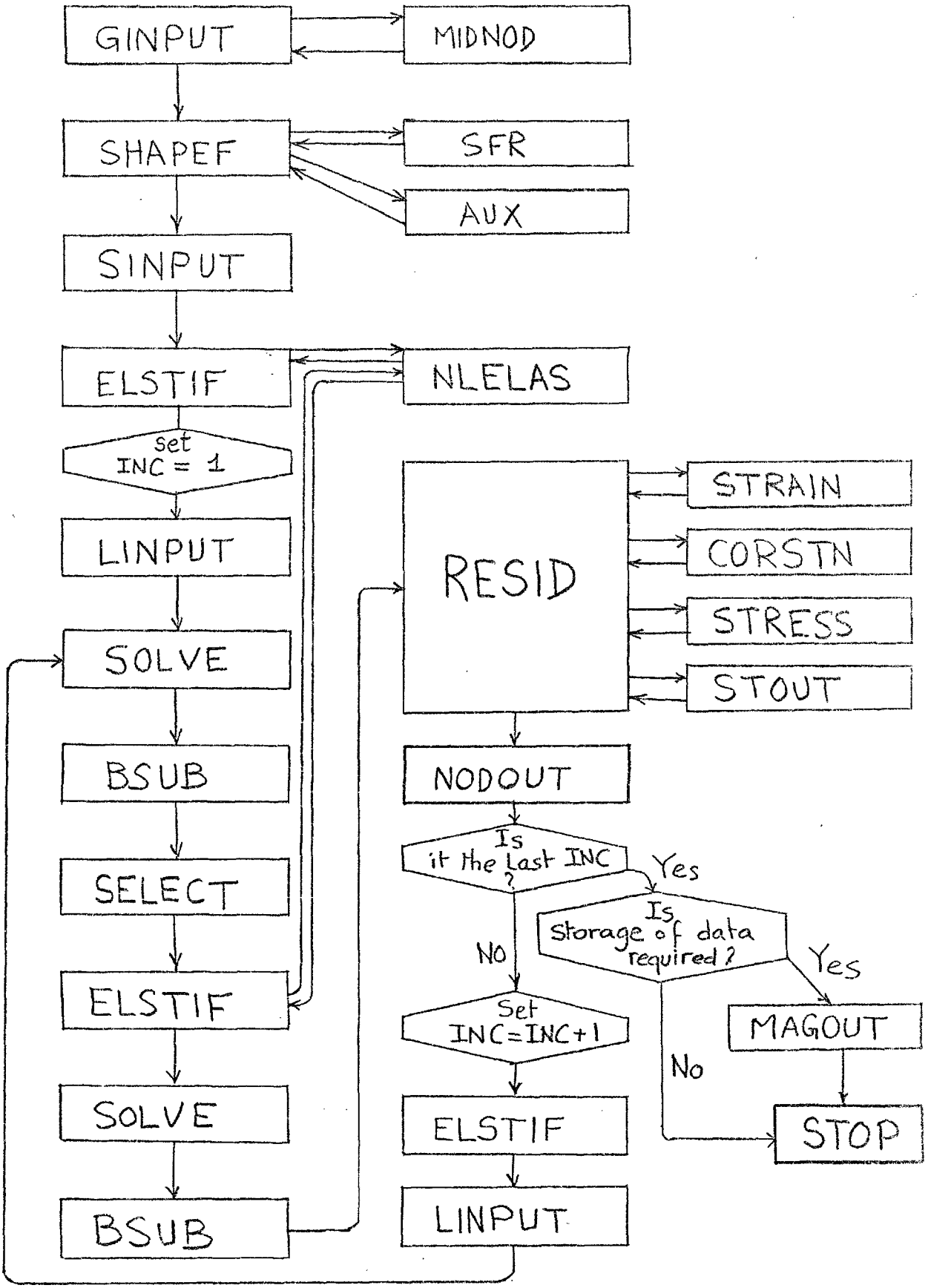
CORSTN : Corrects the values of strains due to the use of the dense liquid technique for layering analysis

NODOUT : Outputs the values of the residual forces and displacements at the nodes.

STOUT : Outputs stresses and strains at the required elements and points

MAGOUT : Stores the values of stresses and strains in disc file or magnetic tape for graphics and/or future reference.

Flow chart of SAN2



ACKNOWLEDGEMENTS

Empingham dam was constructed for the Anglian Water Authority (Welland & Nene Division), whose Consultants were T & C Hawksley. Part of the work included in the thesis was commissioned by them to assist in interpreting the field observations made during construction of the dam. Professor A.W. Bishop, Dr.P.R. Vaughan and Mr.J.M. McKenna acted as soil mechanics consultants. The permission of the Authority and the consultants to publish this data is gratefully acknowledged.

The work performed was conducted concurrently with other research by Dr.M.L. Werneck, who interpreted the field data, and by Dr. W.M. Maguire, who measured the strength and stress strain properties of the foundation clay in the laboratory. Their assistance and cooperation is gratefully acknowledged.

I am deeply indebted to Dr. P.R. Vaughan, my supervisor for his generous help in all directions, in particular, for those important discussions at weekends and after 6pm from which emerged many of the ideas for the research described in the thesis. Not only did he ensure that the analyses performed were correct in the engineering sense, but his persistence has eventually led me to describe them both in English and on engineering drawings.

I am also grateful to Professor A.W. Bishop for his overall guidance and for outlining my training programme

since 1971; to Professor B.M. Irons of Calgary for his patient teaching of the fundamentals of finite elements and for his guidance during the early development of nonlinear tehniques; to Mr.D.J. Naylor of Swansea for introducing and training me in the use of his programme; to my colleagues Dr.A.E. Skinner, Dr.R.J. Chandler, Dr.L. Wesley Messrs Ufuk Ergun, Yogi Sharma, Moustafa Ghamrawy and Mohamad Davachi for many helpful discussions.

My finite element training began while I was studying at Swansea for my second M.Sc., under the general and direct supervision of Professor O.C. Zienkiewicz. and Mr.D.J. Naylor respectively. This year has proved to be of immense value.

I would also like to thank the following friends of mine:
David Hight and Mark Baldwin for their help in preparing the manuscript and the former for his helpful discussions and suggestions. John Sammons, Nizar Rammadan and Georg Stut for their special help, Frank & Elizabeth Potter for their encouragement and for choosing me as Sub-warden for their Hall of Residence, and James Apted and Richard Pugh for help in data preparation and for making the tea on demand during unsocial hours.

Life during more social hours has been made brighter by the company of Messrs Evans, Senior and Junior, Spall, Gagg and Harris, and Mrs Eileen Gibbs, Barbara Price and Debbie Ratcliffe; who eventually accepted that research in

soil mechanics might not include laboratory testing.

I am very grateful to Valerie Collins who typed the manuscript so accurately and neatly and in such a good natured way and Peter Bell for his last minute help.

Final preparation of the thesis was undertaken while I held the position of Research Assistant which was sponsored by the Science Research Council.

Last, but by no means least, I should like to express my appreciation of the help given to me by some of the computer staff who accepted me as a member of the night shift and eventually as part of the hardware.